A novel microRNA signalling pathway in macrophages linking glucocorticoids and cellular metabolism

by

Sally Anne Clayton

A thesis submitted to the University of Birmingham for the degree of

DOCTOR OF PHILOSOPHY

Institute of Inflammation and Ageing

College of Medical and Dental Sciences

University of Birmingham

May 2020

UNIVERSITY OF BIRMINGHAM

University of Birmingham Research Archive

e-theses repository

Abstract

Glucocorticoids are frequently used to treat chronic inflammatory diseases due to their potent anti-inflammatory properties, but long-term use can cause severe side effects. We therefore require a better understanding of the mechanisms by which glucocorticoids achieve their desirable anti-inflammatory actions. This study aimed to investigate the role of a class of regulatory RNAs – microRNAs – in glucocorticoid function in macrophages, as this cell type represents a major target of glucocorticoids.

The microRNA miR-147b was upregulated by lipopolysaccharide and inhibited by glucocorticoid in macrophages, and was predicted to target metabolic pathways. The mitochondrial electron transport chain protein NDUFA4 was shown to be a functional target of miR-147b. NDUFA4 was strongly downregulated by toll-like receptor stimulation, and expression was partially rescued by glucocorticoid. Silencing of NDUFA4 enhanced the glycolytic shift that occurs upon macrophage inflammatory stimulation.

Glucocorticoids were shown to regulate macrophage metabolic processes, most notably the strong inhibition of glycolysis during lipopolysaccharide treatment. Clear differences in metabolic response were also demonstrated between mouse and human macrophages, which has translational implications for the field of immunometabolism.

This work identified a pathway linking glucocorticoid action to the regulation of macrophage metabolism through the action of miR-147b, which could impact cellular function and glucocorticoid efficacy.

Dedication

To Tim Clayton

2nd June 1955 – 29th Jan 2020

I know that you are so proud

Acknowledgements

It's safe to say that the past 3 years have been full of ups and downs, and it's definitely a journey that I wouldn't have been able to complete on my own. My first thanks have to go to my supervisor and mentor Prof Andy Clark, who has believed in me probably more than I have in myself, and has been consistently encouraging and gracious. It's been a privilege to work with him, as well as to learn together as we've taken the plunge into the murky waters of metabolism. While not entirely of our own volition, this has thankfully been an interesting road and one that will hopefully bear fruit. I am also very grateful for the time that he put in to read all of my lengthy thesis chapters through multiple iterations. I would also like to thank the rest of the Clark group, in particular Tina and Kali for keeping me sane at the start and end of my project, and John for helping to keep me *in*sane just the right amount, and being a continual presence and source of many laughs. Thanks also to Kalvin for being good company on many a late night in the lab, and always being up for a good chat or some eclectic music. I'd also like to thank my co-supervisors Dr Simon Jones, Dr Mariola Kurowska-Stolarska, and Dr Dan Tennant for their helpful advice and guidance along the way.

My next thanks go to my family, who are eternally supportive and proud, even if I did give my Dad nightmares about losing my entire thesis. Thank you to my Mum for convincing me that I had made the right decision (as she does in every big decision I make in my life!), and always being on the end of the phone when I need last minute advice. Finally a big thank you goes to Sean for supporting me both financially and emotionally throughout these years; for always knowing when I'm grumpy and in need of a hug or just some wine and chocolate; and eventually learning that just saying "don't stress" is not appropriate advice.

Contents

List of Figures

7)   Discussion

Supplementary Material

List of Tables

Abbreviations

11β-HSD	11-beta-hydroxysteroid dehydrogenase
ALL	acute lymphoblastic leukaemia
BMDM	bone marrow-derived macrophage
CoQ	coenzyme Q / ubiquinone
DAMP	damage-associated molecular pattern
DC	dendritic cell
ELISA	enzyme-linked immunosorbant assay
ETC	electron transport chain
FCS	fetal calf serum
GC	glucocorticoid
GC-MS	gas chromatography-mass spectrometry
GM-CSF	granulocyte-macrophage colony stimulating factor
GR	glucocorticoid receptor
HIF-1α	hypoxia-inducible factor 1 alpha
HK2	hexokinase 2
IFN	interferon
IFNAR	type I interferon receptor
IL-x	interleukin x (e.g. IL-10)
iNOS	inducible nitric oxide synthase
LPS	lipopolysaccharide
M-CSF (CSF-1)	macrophage colony stimulating factor
miRNA	microRNA
MoDM	monocyte-derived macrophage
mROS	mitochondrial reactive oxygen species
NF-κB	nuclear factor kappa-light-chain-enhancer of activated B cells
NO	nitric oxide
OA	osteoarthritis
PAMP	pathogen-associated molecular pattern
PBMC	peripheral blood mononuclear cell
PFKFB3	6-phosphofructo-2-kinase/fructose-2,6-bisphosphatase isoform 3
PHD	prolyl hydroxylase
pmf	proton motive force
PRR	patter recognition receptor
RA	rheumatoid arthritis
RET	reverse electron transport
ROS	reactive oxygen species
SLE	systemic lupus erythematosus
TCA cycle	tricarboxylic acid cycle
TLR	toll-like receptor
TNFα	tumour necrosis factor alpha

Chapter 1) INTRODUCTION

1.1 The immune system – innate vs. adaptive

The mammalian immune system is a highly complex and dynamic system of cellular and acellular components that serves a multitude of purposes. One of the major functions of the immune system is protection of the host from pathogens, but it also mediates wound healing and contributes to maintenance of tissue function and physiological homeostasis. Unlike more primitive organisms, mammals possess a two-armed immune system, comprising innate and adaptive branches, which are highly interconnected (11).

The innate immune system is composed of myeloid cells - the first-responders to infection. Circulating protein components called complement are also important for initial pathogen detection and neutralisation, and these proteins activate immune cells and directly mediate pathogen killing. Innate immune cells recognise conserved features of invading pathogens or products of tissue injury, and act quickly to combat spread of the pathogenic organism or to initiate wound repair. The cells that make up the innate immune system are monocytes, macrophages and dendritic cells – which are highly heterogeneous and carry out phagocytosis and antigen presentation; granulocytes (neutrophils, basophils and eosinophils) – which are characterised by lobed nuclei and cytoplasmic granules containing antimicrobial enzymes and toxins that can be released upon stimulation; and mast cells – which release histamine (11). Defects in innate immune function can have severe consequences, for example due to the importance of macrophages in the development of many organs (12). Loss of innate immune components also results in severe susceptibility to infection, which can be life-threatening (11).

If an infection is not cleared by the innate system, the adaptive immune system mounts a highly specific and specialised response. The cells of the adaptive immune system are the lymphocytes (B cells and T cells), which respond to native or processed antigens respectively, and function to regulate other immune cells, kill infected cells or produce antibodies. A unique and important feature of the adaptive immune system is that it maintains an immunological memory of previously encountered infections, such that a secondary encounter results in a rapid and specific immune response that clears the infection with minimal host damage. This memory forms the basis of vaccination. Similarly to loss of innate immune function, deficiency in components of the adaptive immune system can have catastrophic consequences. These are exacerbated due to the highly interdependent nature of immune signalling, by which dysfunction of one system has knock-on effects by resulting in failure to activate other systems. An example of the severity of adaptive immune dysfunction is shown by the loss of CD4 T cells that occurs due to infection with human immunodeficiency virus (HIV). This can result in the development of acquired immune deficiency syndrome (AIDS), the sufferers of which are highly at risk of opportunistic infections that are most often fatal (11).

Cross-talk between cell types of both branches of the immune system, as well as between immune cells and non-haematopoietic cells, is vital for proper immune function and organismal homeostasis. Despite this, I shall focus in detail on a single cell type, the macrophage, as my project was based around understanding the molecular mechanisms of macrophage regulation. I shall discuss how the actions of this cell type impact upon other cells in contexts of health and disease where appropriate.

1.2 Macrophages

Macrophages are mononuclear cells of the innate immune system, so-named due to their great capacity for phagocytosis. These cells play a vital role in immune surveillance and the orchestration of the inflammatory response, as well as in maintenance of tissue homeostasis and resolution of inflammation (12). Macrophages are a highly plastic and diverse cell type that can perform a wide range of functions in response to physiological and environmental cues. Macrophage responses are highly specialised depending on the nature of the stimulant, and a major function is the production of cytokines and chemokines, driving further recruitment of immune cells and the activation of multiple cell types. Macrophages also carry out phagocytosis of pathogens, and are capable of presenting antigen to activate the adaptive immune system (3, 11, 13). Roles of macrophages in development, repair and tissue homeostasis are also many and varied, and include phagocytosis of apoptotic cells (efferocytosis) and stimulation of angiogenesis (12).

1.2.1 Macrophage origins and development

Macrophages can be found within every tissue of the body, where they display specialised features and gene expression patterns that allow them to carry out tissue-specific functions (14). For example, the resident macrophages of the central nervous system – microglia – produce growth factors that maintain neuronal integrity, and also act to remove dead neurons; while resident liver macrophages – Kupffer cells – recycle aged erythrocytes (15). Until recently, tissue macrophages were thought to be terminally differentiated and develop from bone marrow-derived circulating monocytes, which migrate into peripheral tissue in response to microenvironmental signals. However due to extensive study using such techniques as parabiosis, adoptive transfer and fate mapping, it is now known that the

majority of tissue-resident macrophage populations are established prior to birth, derived from extra- and intra-embryonic precursors originating in the yolk sac or fetal liver (16). These cells maintain their populations independently from bone marrow precursors due to a low-level capacity for self-renewal (16-18). The precise contribution of each precursor type to each tissue population is still an active area of investigation, and different niches show differing degrees of steady state monocyte-derived macrophage contribution (16). Upon loss of tissue-resident macrophages, monocyte-derived macrophages are able to replenish the populations and adopt many of the characteristics and functions of the original residents, indicating that the local microenvironment plays a key role in driving macrophage gene expression. It has been reported that these repopulating cells fail to completely recapitulate the original tissue macrophage gene expression profile, which could have implications for tissue function and homeostasis (16, 19). However other reports describe that the new monocyte-derived cells are indistinguishable from yolk sac or liver-derived cells in the same niche (3, 20). It is important to note that these studies have been almost exclusively carried out in mouse due to the relative ease of manipulation, and it is unclear how closely the human system mirrors these discoveries (3).

The generation of monocytes and macrophage in the adult begins in the bone marrow, which is the major site of haematopoiesis after birth. **Figure 1.1** depicts the fate of the haematopoietic stem cell (HSC) through progressive stages of differentiation, accompanied by gradual loss of developmental potential (3). Circulating monocytes are generally classed as being "classical", which are also described as inflammatory monocytes and are characterised as Ly6C+ CCR2+ in mouse, and CD14hi CD16neg in human; or "non-classical"/ "patrolling", which are Ly6Cneg CCR2neg in mouse and CD14lo CD16hi in human (21). Non-classical

monocytes patrol endothelial cell barriers and maintain vessel integrity, while classical monocytes are thought to be the main subset that are recruited to sites of infection or injury due to high expression of the chemokine receptor CCR2 (however non-classical monocytes have been implicated in inflammatory disease development in certain models of rheumatoid arthritis) (3, 21-23). Large influx of monocytes into tissue is generally associated with their differentiation into pro-inflammatory macrophages and has been implicated in the pathogenesis of inflammatory diseases (to be discussed) (23). Human monocytes can additionally fall into an "intermediate" class (CD14hi CD16+), which have been shown to possess enhanced antigen presentation and pro-angiogenic capacity (24). It is unclear whether these cells represent a transition phase from classical to non-classical phenotype, as it has been shown in mouse that Ly6C- cells can arise from Ly6C+ monocytes (18, 23).

1.2.2 Macrophage signalling networks

As sentinels of the innate immune system, macrophages are able to recognise and response to a plethora of signals, broadly grouped into pathogen-associated molecular patters (PAMPs) and damage-associated molecular patterns (DAMPs). Recognition occurs through the activation of pattern recognition receptors (PRRs), resulting in coordinated activation of signalling cascades that produce functional effects tailored to the specific insult (11). I will focus here on some of the key pathways involved in the macrophage inflammatory response to infection, which have direct relevance to this project.
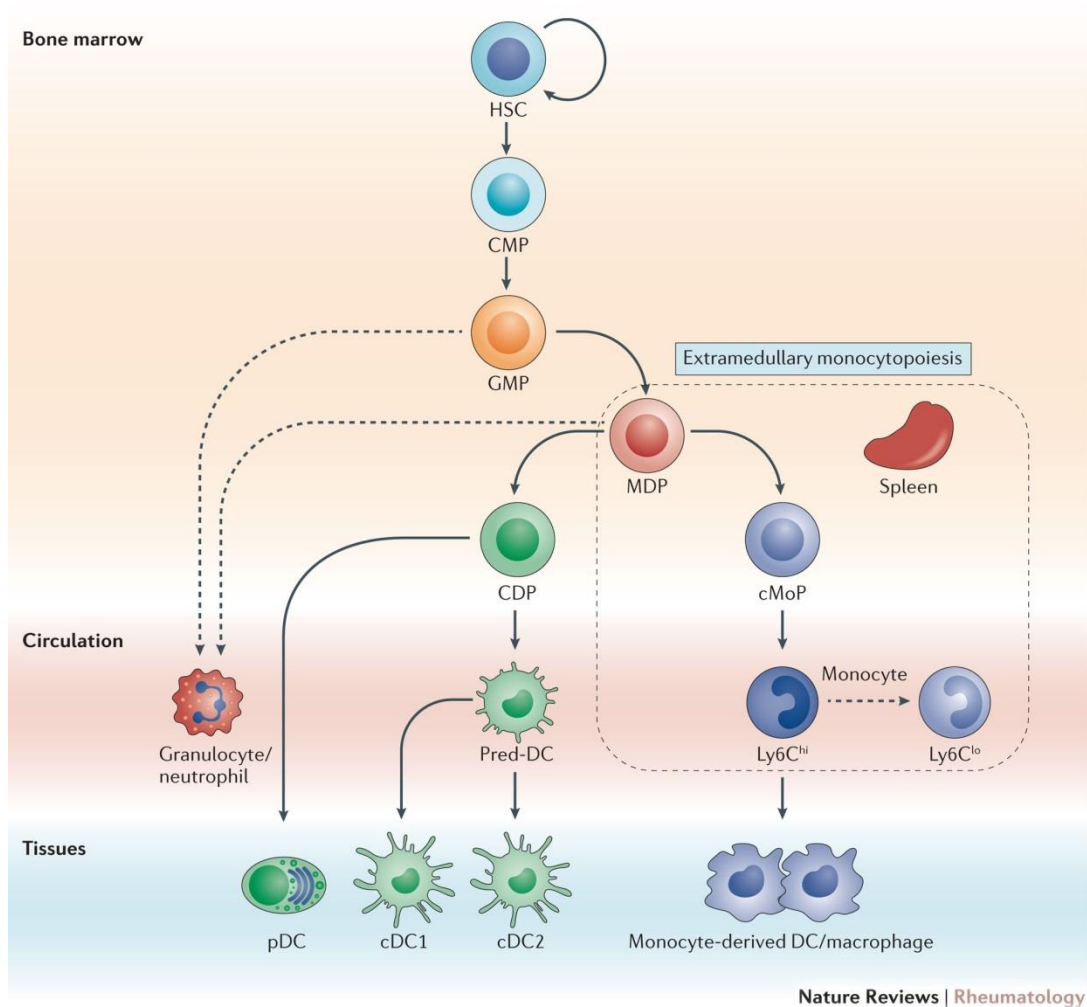
Figure 1.1) Macrophage development during adult murine myelopoiesis

Taken from Udalova *et al* 2016 (3)

The major site of postnatal haematopoiesis is the bone marrow, which contains a population of multi-potent, self-renewing haematopoietic stem cells (HSCs). Production of myeloid cells involves progressive lineage-restriction, beginning with differentiation into the common myeloid progenitor (CMP), which has lost capacity for lymphocyte development. The granulocyte-macrophage progenitor (GMP) can generate granulocytes such as eosinophils, basophils and neutrophils (through additional precursors not shown), or give rise to the monocyte and dendritic cell progenitor (MDP), which in turn produces the common dendritic cell progenitor (CDP) and the common monocyte progenitor (cMoP). In mice, monocytes are generated with a classical Ly6Chi phenotype, and these are thought to be able to convert to non-classical Ly6Clo monocytes, which carry out patrolling functions and maintain endothelial integrity. Translocation of monocytes from the circulation into the tissue most often results in differentiation into monocyte-derived macrophages or dendritic cells (DC). These are highly plastic and heterogeneous, and are distinct from the prenatally-derived tissue resident macrophages. Subsets of DCs are also shown, consisting of plasmacytoid (pDC) and conventional (cDC1 and cDC2) DCs.

A major class of PRRs is the Toll-like receptor family (TLR), which are membrane-spanning receptors that transduce signals from a variety of pathogen components into the cell, and which share homology with the interleukin-1 receptor (IL-1R) (5). Table 1.1 summarises our knowledge of mouse and human TLRs and their ligands, and **Figure 1.2** illustrates some of the molecular pathways that they signal through.

Table 1.1) Toll-like receptors and their ligands (*Adapted from (5))*

Toll-like receptor	Origin of ligand	Ligand	Localisation
TLR1*	Bacteria	Triacyl lipoprotein (e.g. Pam3CSK4)	Plasma membrane
TLR2	Bacteria, viruses, parasites	Lipoprotein, peptidoglycan	Plasma membrane
TLR3	Virus	dsRNA (e.g. polyI:C)	Endolysosome
TLR4	Bacteria, viruses, self	LPS	Plasma membrane
TLR5	Bacteria	Flagellin	Plasma membrane
TLR6*	Bacteria, viruses	Diacyl lipoprotein	Plasma membrane
TLR7 TLR8 (human)	Virus, bacteria, self	ssRNA	Endolysosome
TLR9	Virus, bacteria, protozoa, self	Unmethylated CpG-DNA	Endolysosome
TLR10* (human)	Unknown	Unknown	Endolysosome
TLR11	Protozoa	Profilin-like molecule	Plasma membrane

*Interacts with TLR2 (TLR10 negatively regulates TLR2 (7))

A major regulator of inflammatory gene expression downstream of TLR activation is NF-κB. This transcription factor is held in the cytoplasm of stimulus-naïve cells by interaction with members of the IκB protein family. Signalling through the MyD88 adapter protein in response to TLR engagement results in the activation of the multiprotein IKK complex, via the actions of the death domain-containing IRAK proteins, the RING-domain E3 ubiquitin ligase TRAF6 and the TAK1 kinase complex (**Figure 1.2**). IKK rapidly phosphorylates specific serine residues of IκB, which is then polyubiquitinated and degraded by the proteasome. This allows NF-κB to translocate to the nucleus and bind to κB sites within enhancer and promoter regions of target genes, which include multiple cytokines and chemokines. The TRIF adapter protein can also activate NF-κB by directly binding TRAF6 and causing IKK activation (25).
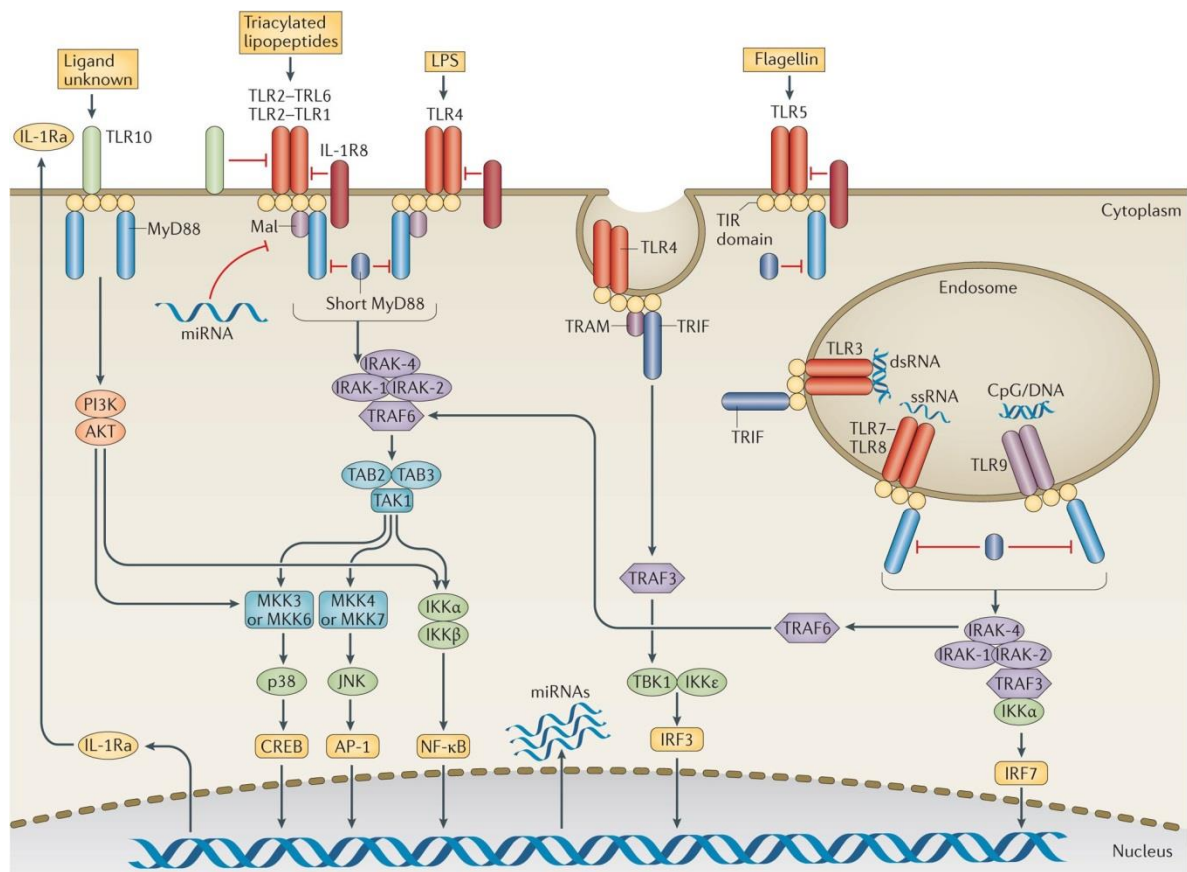
Nature Reviews | Rheumatology

Figure 1.2) Toll like receptor signalling

Taken from Joosten *et al* 2016 (1)

Toll like receptors (TLRs) responsible for detection of pathogens and tissue damage. TLRs act as homodimers or heterodimers and signal from the plasma membrane or the endosome in response to the indicated ligands through adaptor proteins MyD88 and TRIF.

MyD88 recruits and activates the IL-1R-activating kinases (IRAKs), resulting in subsequent activation of the ubiquitin ligase TRAF6. Ubiquitination by TRAF6 activates a complex consisting of the TAK1 kinase and TAK-binding proteins (TABs). TAK1 activates MAPK and NF-κB signalling through the phosphorylation of IκB kinase (IKK)-β and MAP kinase kinases (MKK), resulting in inflammatory gene transcription. MyD88 signalling from the endosome can also result in type I interferon production by activation of IRF7 through a complex of IRAKs, TRAF3 and IKK-α.

TLR3 and TLR4 can signal through the TRIF adapter protein, which activates the two E3 ubiquitin ligases TRAF3 and TRAF6. TRAF3 activates the two kinases TBK1 and IKK-ε, which in turn phosphorylate IRF3. This can then translocate to the nucleus and drive expression of type I interferons (5).

TLR10 has no known ligand, and negatively regulates signalling from TLR2, as well as bringing about production of the IL-1 receptor antagonist IL-1Ra through PI3K/Akt pathway activation. Mouse TLR10 is thought to be non-function due to disruption by an endogenous retrovirus (7).

Another important signalling pathway that is activated upon TLR engagement is the mitogen-activated protein kinase (MAPK) cascade, involving sequential phosphorylation steps to activate kinases including p38, JNK and ERK. Similarly to the IKK complex, these kinases are activated via the ubiquitin ligase activity of TRAF6 and the kinase TAK1. The MAPK phosphorylation cascade results in the activation of transcription factors such as AP-1, leading to coordinated inflammatory gene expression (25, 26).

The activation of PRRs associated with detection of viral PAMPs results in the production of interferons, a family of cytokines that coordinate responses to viral infection, including regulation of both the innate and adaptive immune systems (27). Type I interferons (IFNα and β), produced by infected cells, bind to the heterodimeric type I interferon receptor (IFNAR), which can be found on the surface of all nucleated cells. IFNAR activation stimulates a signalling cascade that culminates in the expression of cell type-specific sets of genes known as interferon-stimulated genes (ISGs), which encode a broad array of anti-viral and pro-inflammatory mediators (28). Upon binding to their receptors, IFNs activate members of the Janus kinase (JAK) family (IFNAR activates JAK1 and TYK2), which associate with the cytoplasmic domains of the receptors. Activated JAKs phosphorylate the interferon receptors, forming binding sites for the signal transducer and activator of transcription (STAT) proteins, which are then themselves phosphorylated by JAKs on specific tyrosine residues (29, 30). Phosphorylated STAT1 and STAT2 heterodimerise, and along with the IFN regulatory factor IRF9 are transported to the nucleus. Here the complex binds to IFN-stimulated regulatory elements (ISREs) upstream of ISGs, and stimulates transcription. Alternatively, homodimers of STAT1 activated by the type II interferon IFNγ recognise GAS elements, also resulting in expression of anti-viral genes (30). The functions of ISGs vary greatly, and include direct

inhibition of viral survival or replication; and increasing cellular sensitivity to further pathogen encounter (30).

The most commonly studied toll-like receptor is TLR4, which is expressed on the cell surface and recognises the Gram negative bacterial outer membrane component lipopolysaccharide (LPS) (also known as endotoxin), as well as viral envelope components and certain DAMPs (5). LPS encompasses a range of structurally related molecules, comprised of a highly variable polysaccharide region and a phospholipid region (lipid A), which anchors the molecule into the bacterial membrane and can be composed of a variable number of fatty acid chains (11, 31). Unlike other TLRs, TLR4 can signal through both MyD88 and TRIF adapter proteins. This generates a broad immune response to infection, which includes the expression of type I interferon (IFNβ) through TBK1 signalling to the transcription factor IRF3 (**Figure 1.2**) (5). This IFNβ can then act in a paracrine and autocrine fashion to stimulate IFNAR, as described above. The CD14 surface marker commonly used to identify macrophages and monocytes is an accessory protein of TLR4 (11).

1.2.3 Macrophage polarisation

As mentioned, macrophages are highly plastic cells that are capable of carrying out a wide variety of functions in response to a range of stimuli. The acquisition of a defined set of features in order to execute a particular function is described as cellular polarisation (or activation if as a response to an acute stimulus such as a TLR agonist). The macrophage field has historically described macrophages in terms of two major polarisation states: classical and alternative (32), which are also known as M1 and M2 respectively, in order to mirror the nomenclature of T helper subsets (33). *In vitro,* these polarisation states are typically achieved

through treatment with the Th1 cytokine interferon-γ (IFNγ) and/or TLR agonists such as LPS for M1 activation; or with the Th2-related cytokines IL-4 or IL-13 for M2 activation, although alternative treatments can be used to achieve similar (though not identical) polarisation (**Figure 1.3**) (32, 34). One of the first features used to distinguish these two subtypes was the metabolism of arginine: M1 macrophages utilise this amino acid for the production of nitric oxide, while M2 macrophages express the enzyme arginase for conversion of arginine into ornithine (33, 35) – *discussed in more detail in Sections 1.6 & 1.7.*

In general terms, classical M1 macrophages are considered to be pro-inflammatory - producing large amounts of inflammatory cytokines such as TNFα and interleukin-1β (IL-1β); capable of phagocytosing bacteria; and expressing high levels of co-stimulatory molecules and MHC class II for adaptive immune activation. Conversely, alternative M2 macrophages are described as being anti-inflammatory/pro-resolution, involved in wound healing and anti-parasite responses. These cells express scavenger receptors; produce the cytokines interleukin-10 (IL-10) and TGFβ that are associated with inhibition of inflammation; and produce chemokines that recruit Th2 cells and Tregs (3, 12). **Figure 1.3** summarises macrophage M1/M2 polarisation and some of their defining characteristics. It should be noted that the majority of the work in defining these populations has been carried out in mouse macrophages. Some of these characteristics do not hold true for human cells, and much less is known about macrophage classes in other species (32). It is also worth noting that many of the markers used to characterise these populations are not binary in their expression, but instead the relative degrees of expression of several markers separates the two populations.
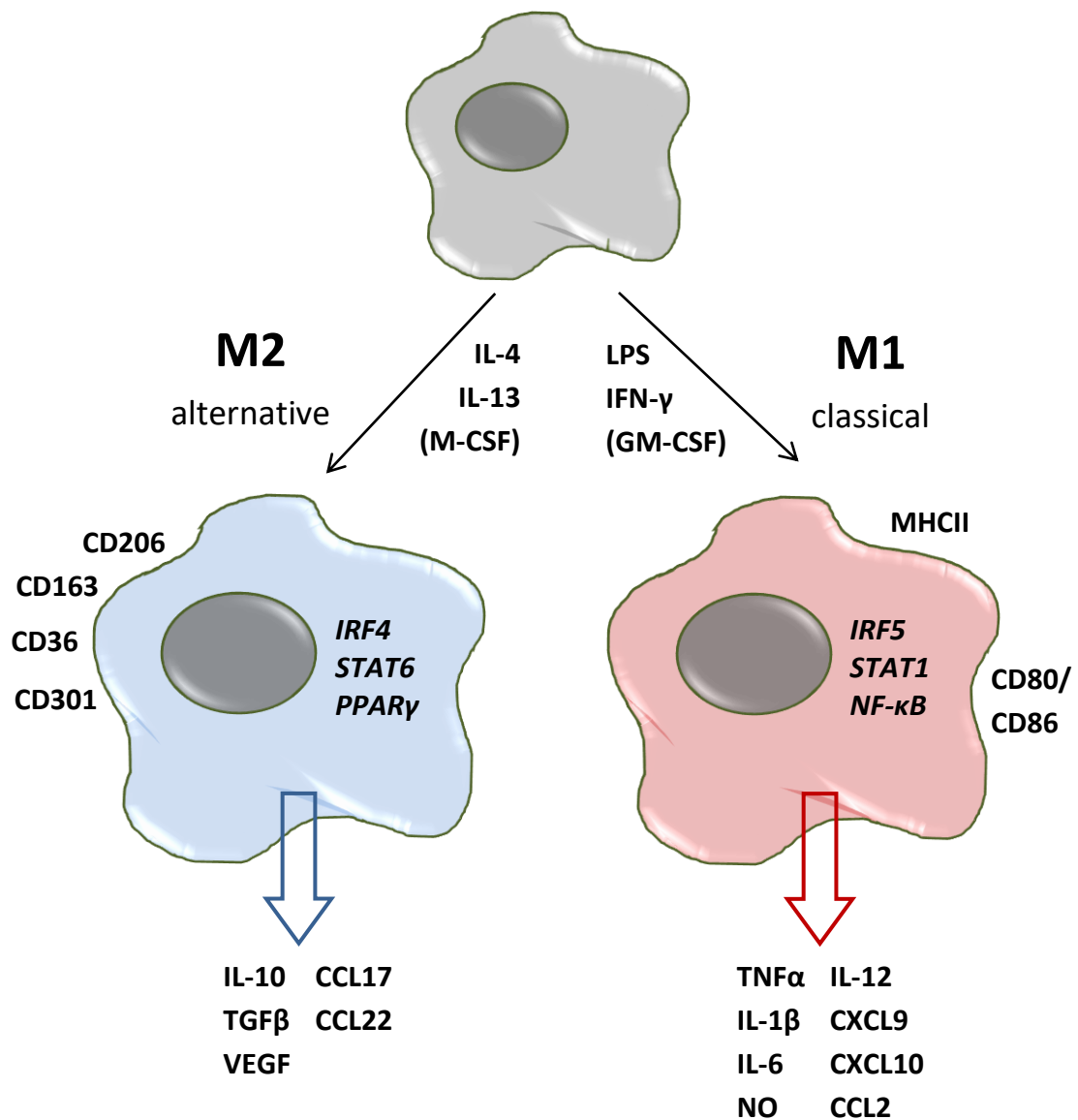
Figure 1.3) M1/M2 macrophage polarisation

In vitro polarisation of macrophages from M0 unstimulated cells (grey) to M1 (classical) or M2 (alternative) phenotypes. Indicated are the stimuli typically used for polarisation; major transcription factors involved in driving the phenotypes; characteristic surface marker expression; and examples of bioactive mediator production, including cytokine profile.

Despite the focus on these macrophage subtypes within the literature for many years, it has become increasingly evident that this dichotomy is a substantial oversimplification of macrophage phenotype and function in both healthy and diseased states *in vivo*. In fact, even during the first use of the terms M1 and M2 to distinguish between Th1 and Th2 cytokine-related macrophage responses, the authors commented that there likely exists a "continuum of phenotypes" between the two classes (33). The oversimplification is clear from the great diversity described between resident macrophage populations from different tissues, as well as upon the study of macrophages activated by stimuli other than the conventional M1/M2 polarisation signals, or studied *ex vivo* (14, 36).

In 2008, Mosser *et al* postulated a spectrum model of macrophage activation, in which cells can display varying degrees of characteristics associated with three major themes of macrophage function: host defence, wound healing, and immune regulation (36). Subsequently, Xue *et al* performed detailed transcriptional analysis of human macrophages treated with 28 different stimuli, using the results to describe a macrophage polarisation spectrum based on hierarchical clustering. This helped to identify transcription factors that were associated with particular activation programmes, and highlighted similarities as well as differences between individual polarisation states (37). While this impressive undertaking enhances our understanding of macrophage responses to individual stimuli or limited combinations of signals, and supports the spectrum theory that many have proposed, macrophages *in vivo* are exposed to highly complex cocktails of growth factors, cytokines, hormones, metabolites and PRR agonists, and we are still some way from fully understanding how these combine to dictate macrophage behaviour. We also know that transcriptional

changes do not always correlate with protein and functional alterations, which somewhat limits the utility of transcriptome-based approaches.

In addition to being over-simplified, the assignment of a fixed classification onto an individual macrophage or macrophage population is also impractical due to the temporal plasticity of macrophages, which will usually switch off pro-inflammatory gene expression after an insult and obtain more "regulatory"/"resolution" characteristics in order to prevent tissue damage (38, 39). Therefore the timings of macrophage treatment and analysis are important variables to consider during experimentation. The over-reliance on the M1/M2 paradigm also does not fit with our understanding of the different origins of tissue macrophages, since M1/M2 phenotypes have been characterised predominantly in bone marrow-derived cells, which we now know do not represent the majority of resident macrophages (16).

In summary, while the segregation of macrophage function into discrete categories is useful for the experimental characterisation of these cells in response to treatments or perturbations, it should be borne in mind that this does not reflect the true heterogeneity of macrophages, and researchers should be careful not be get bogged down in the conventional definitions of these cell types.

There are several different *in vitro* model systems that are used for the study of macrophage function. Primary macrophages can be differentiated *in vitro* from mouse bone marrow (BMDMs) or human circulating monocytes (MoDMs), generally using macrophage colony stimulating factor (M-CSF) (*see Chapter 2*). The use of these models has its limitations, in part that they do not properly represent tissue macrophages that arise prenatally.

Alternative primary cell sources are the mouse peritoneal cavity, which has a resident macrophage population that can be extracted for study (40); or alveolar macrophages extracted by bronchoalveolar lavage (41), although these yield comparatively low cell numbers. Once terminally differentiated, all of these primary cell types are relatively non-proliferative and cannot be maintained in culture long term, therefore the use of immortalised cell lines is also common. The most widely-used of these are RAW264.7 - a mouse macrophage-like cell line, and THP-1 – a human monocyte-like cell line that may be induced to form an inflammatory macrophage-like population using phorbol-12-myristate-13-acetate (PMA). Neither of these cell types (in particular THP-1) fully recapitulates the primary macrophage, however, so results should be interpreted cautiously (42, 43).

1.2.4 Macrophages in disease

Macrophage activity has been linked to the development and progression of many different diseases, including those of obvious immune origin as well as those with more concealed inflammatory involvement. An example of the latter is the association of macrophages with obesity. Under homeostatic conditions, adipose tissue contains a large number of macrophages that support adipocyte function and maintain insulin sensitivity e.g. through IL-10 production (12). Upon nutrient excess, stressed adipocytes release chemokines that recruit CCR2+ monocytes into the tissue. These monocytes differentiate into pro-inflammatory macrophages, and the resulting chronic low-level inflammation promotes insulin resistance - a common complication of obesity (12).

The contribution of macrophages to chronic inflammatory disease is well-established, as these cells are central orchestrators of inflammation through the recruitment, activation and maintenance of multiple immune cell subtypes. The importance of macrophages in the

pathogenesis of rheumatoid arthritis (RA) is demonstrated by the great success of anti-TNFα therapy, which revolutionised RA treatment, as macrophages are the major producers of TNFα within the synovium (44-47). Macrophage production of inflammatory cytokines such as TNFα and IL-1β in the synovium results in activation and apoptosis of chondrocytes, as well as activation of synovial fibroblasts, which themselves produce matrix-degrading enzymes, angiogenesis-promoting factors, and osteoclast-activating factors. The combination of these effects results in joint destruction and disability (48). The involvement of antigen presenting cells in RA development is also highlighted by the strong genetic association of the disease with a variant of MHCII HLR-DRB1, termed the "shared epitope" (48, 49). Macrophages are able to present autoantigen to T cells, facilitating the production of autoantibodies that subsequently further activate fibroblasts, macrophages and osteoclasts through the formation of immune complexes (50, 51).

The precise contribution of different macrophage populations to disease processes in RA is still incompletely understood. Recent work described a newly-identified resident population of macrophages that form a tight barrier layer in the synovial lining, associating with lining layer fibroblasts and forming tight junctions similar to epithelial cells. This macrophage barrier was disrupted during active RA, and perturbation of these macrophages exacerbated disease severity (52). In the K/B×N mouse model of resolving arthritis it has been reported that the same infiltrating monocyte-derived macrophages that obtain a pro-inflammatory phenotype and drive disease are also responsible for disease resolution. This is achieved through macrophage reprogramming, for example loss of MHCII expression and upregulation of scavenger receptors (22). It is still yet to be understood whether this holds true in other models of RA or in patients (51). Disease in the K/B×N model has been shown to

be driven by the recruitment of non-classical monocytes, in contrast to the role of classical monocytes in collagen-induced arthritis models, and depletion of Ly6C+ monocytes after disease initiation in the latter model was able to reduce disease severity (3).

These examples highlight the fact that it is important to consider all aspects of macrophage function when studying disease processes. Macrophages may help to prevent disease development; contribute to its initiation or progression; or assist in disease resolution. These are important distinctions that require a better understanding in individual tissue and disease contexts in order to best tackle the prospect of targeting macrophages for disease treatment (53).

I have highlighted merely a few examples of the many different diseases with known macrophage involvement. Others include: fibrosis, in which prolonged stimulation of myofibroblasts by macrophage-derived TGFβ contributes to the excessive and pathogenic wound healing response (54); atherosclerosis, in which macrophages ingest cholesterol and contribute to unstable plaque formation (55); and cancer, in which resident or monocyte-derived macrophages can either mediate anti-tumour immunity or promote tumour expansion and metastasis (55).

1.3 Glucocorticoids

Glucocorticoids (GCs) are a group of steroid hormones that have varied roles in development and homeostasis. They are commonly used in the treatment of chronic inflammatory disorders and to prevent organ transplant rejection, due to their broad and effective anti-inflammatory actions. They are also used for the treatment of haematological malignancies due to their anti-proliferative and apoptosis-inducing effects in these diseases (56, 57). The first clinical use of GCs was in the successful treatment of RA in 1948 by Phillip

Hench, thanks to the pioneering work of Kendall and Reichstein on the isolation and synthesis of the endogenous GC hormone cortisol. This work was awarded the Nobel Prize for Physiology or Medicine in 1950, following rapid clinical application of cortisol for a number of inflammatory conditions (56, 58).

1.3.1 Cortisol synthesis and regulation

Cortisol is produced by the adrenal cortex and regulated by the hypothalamic-pituitary-adrenal (HPA) axis. It regulates a wide variety of physiological and cellular processes, including development of the lungs, CNS and immune system; metabolism and inflammation; and circadian rhythm effects. Normal cellular and physiological function is maintained by the tight regulation of GC availability. Cortisol synthesis and release are subject to negative feedback regulation through the control of adrenocorticotropic hormone (ACTH) release from the pituitary gland, and corticotropin-releasing hormone (CRH) release from the hypothalamus (59). Local concentrations of active GC are further controlled by tissue-specific expression of two forms of the enzyme 11-beta-hydroxysteroid dehydrogenase (11β-HSD), which regulate interconversion between the active cortisol and its inactive form cortisone (**Figure 1.4**) (56, 60). 11β-HSD1 catalyses the production of active cortisol from cortisone, and is expressed in multiple different cell types, including macrophages. 11β-HSD2 mediates the opposite reaction and is predominantly expressed in the kidney (60). An additional level of control is afforded by circulating corticosteroid-binding globulin (CBG), which buffers free cortisol in the blood (**Figure 1.4**) (61).

Disruption of these regulatory mechanisms can lead to the development of a number of side effects due to the broad activity of GCs. These symptoms are observed in patients with Cushing's syndrome, a rare disorder characterised by chronic elevation of endogenous GCs

(62). Such complications can also manifest as side effects of prolonged or high dose therapeutic GC use. These side effects can be severe and even life-threatening, affecting a range of tissues and organs, and include osteoporosis, hypertension, diabetes mellitus, muscle and skin atrophy, and increased susceptibility to infection (56). Synthetic GCs differ in their susceptibility to inactivation by 11β-HSD2, which can cause elevated local availability upon clinical administration. This is beneficial for the treatment of chronic inflammation, but can also exacerbate the development of side effects (63). The clinical potency of different GCs is dependent upon several different factors, including their rate of metabolism and affinity for the GC receptor (64-66).

1.3.2 The glucocorticoid receptor and molecular action

Glucocorticoids carry out their actions by binding to the glucocorticoid receptor (GR), a nuclear hormone receptor encoded by the *NR3C1* gene. GR is maintained in an inactive form in the cytoplasm by association with chaperone proteins, including Hsp90 and FKBP5 (58, 67). This protein complex masks the nuclear localisation sequence (NLS) of GR, thereby blocking nuclear entry, but is also necessary for maintaining GR in a conformation capable of binding ligand (68). GCs can freely diffuse across the plasma membrane due to their lipophilic properties, and binding of the GC to the cytoplasmic GR results in a conformational change in the receptor, unmasking the NLS. Nuclear translocation is mediated by the importin-β family of nuclear transporters (69). The specific actions of the GR are complicated by the existence of different splicing variants, which vary in their functional abilities, as well as by multiple possible post-translational modifications of the receptor (67, 70).

A full understanding of the mechanisms by which the GC/GR complex brings about its biological effects is still lacking. A major function of GR occurs through specific recognition of

target genes, but the lists of targeted genes are extensive and cell type-specific (56). Direct DNA recognition involves receptor homodimerization, mediated by the region of the GR termed the D-loop. These homodimers recognise and bind glucocorticoid response elements (GREs) in target gene promoters via the DNA-binding domain (**Figure 1.4**), and the N-terminal domain then mediates transcriptional regulation. Activation of gene expression from GREs occurs through the recruitment of co-activator proteins, which can include histone acetyltransferases or chromatin remodelling complexes. Conversely, inhibition of gene expression can be mediated through the recruitment of histone deacetylases or other co-repressor proteins (58, 63, 71). A consensus GRE sequence was determined as an inverted repeat of the core sequence AGAACA. Many different factors affect the precise outcome of GC/GR binding to DNA, including the exact sequence of the binding site and the presence of additional transcription factor binding sites. The accessibility of individual DNA sequences to GR binding is also regulated in a cell type-specific manner (56).

Alternative mechanisms of action of the GC/GR complex include interaction with other transcription factors such as AP-1 and NF-κB, enabling GR to alter gene expression without direct chromatin binding (**Figure 1.4**). This is possible without receptor homodimerisation, shown by the partial functionality in a mouse model bearing a mutation in the D-loop region of the GR. GC was still able to mediate inhibition of NF-κB activity and pro-inflammatory cytokine production in these mice (56, 63, 72). GC/GR is also capable of functioning outside the nucleus, where its actions occur rapidly in response to GC administration. One example is seen in the GC-mediated impairment of insulin signalling in skeletal muscle, which involves binding of the activated GR to the regulatory subunit of PI3K, blocking its activation and downstream signalling in the insulin pathway (57).

Nature Reviews | Immunology
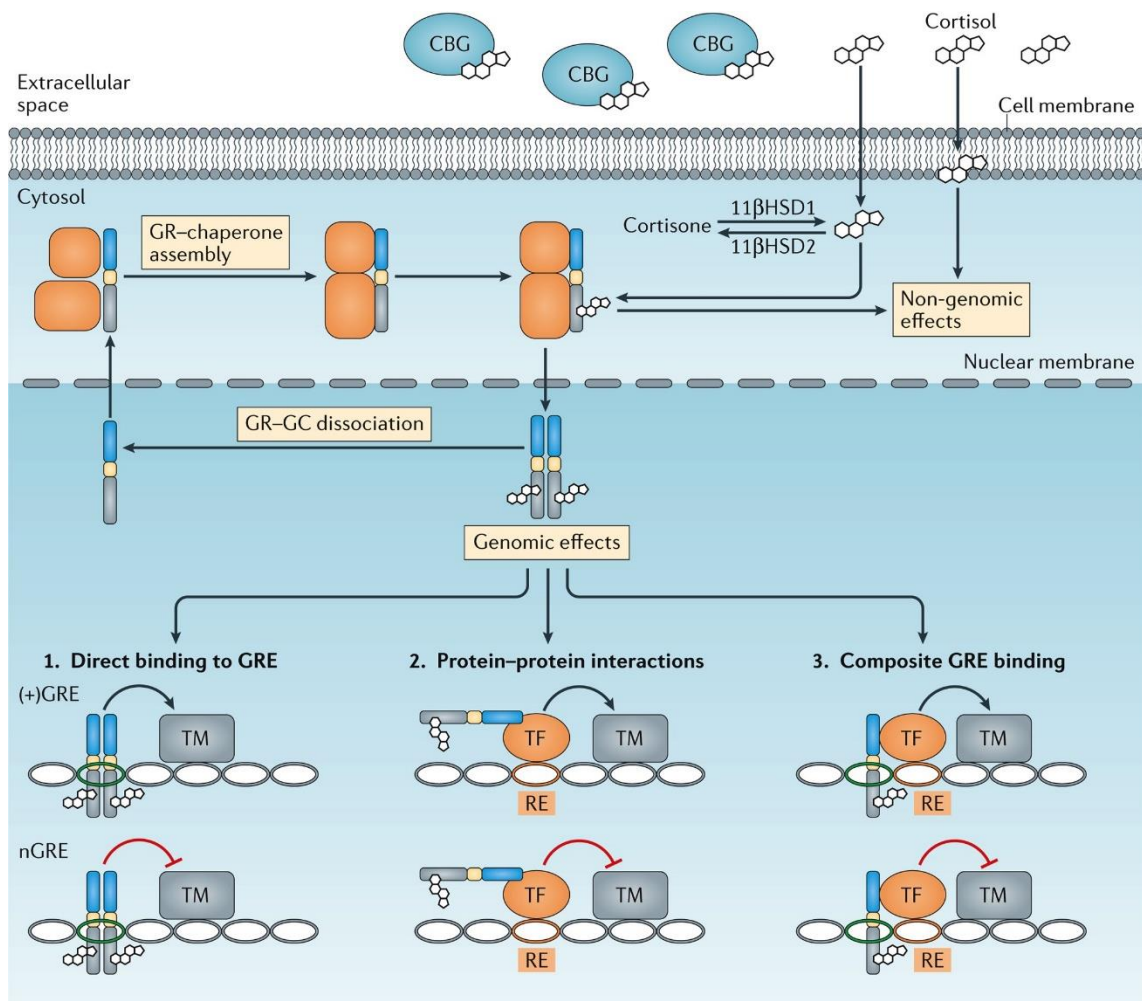
Figure 1.4) Mechanisms of action of glucocorticoids

Taken from Cain & Cidlowski 2017 (8)

Endogenous regulation of the glucocorticoid hormone cortisol occurs by binding to circulating corticosteroid-binding globin (CBG), and by conversion to and from the inactive cortisone by 11β-HSD enzymes. As well a mediating some non-genomic effects, cortisol acts by binding to the glucocorticoid receptor (GR), which dimerises and translocates into the nucleus. Genomic effects of activated GR occur by several possible mechanisms. 1) Direct binding to positive or negative glucocorticoid response elements (GRE) leads to activation of repression of transcriptional machinery (TM) respectively; 2) Tethering to transcription factors (TF) without direct DNA binding can have activating or repressive effects on genes expression; 3) A combination of the first two mechanisms, in which GR binds to both DNA and other proteins where GRE and other response elements (RE) are present (e.g. GR commonly interacts with the TF AP-1 at composite elements).

Much of the historical literature surrounding the effort to dissociate the beneficial actions from the unwanted effects of GCs have focused on the disparate effects of DNA-binding-proficient and -deficient GR, with an aim to develop specific ligands that can activate one of these mechanisms and not the other (56). These studies are based on the rationale that the anti-inflammatory effects are mediated by transrepression, without direct DNA binding - for example by tethering to transcription factors; while GC side effects are driven by direct transactivation (56, 72). More recently these conclusions have been overturned for a number of reasons, including the discovery of numerous GR-mediated transactivation pathways that have profound anti-inflammatory functions, for example expression of the MAPK phosphatase DUSP1 (56, 73, 74).

1.3.3 Anti-inflammatory actions of GCs

Glucocorticoids mediate broad anti-inflammatory effects, and act upon cells of both the innate and adaptive immune systems, as well as non-haematopoietic cells e.g. vascular endothelial cells and fibroblasts (56, 71). GCs induce apoptosis of B and T cells, as well as inhibiting differentiation, activation and immunoglobulin production of the former; and inhibiting inflammatory cytokine production by the latter (71). GCs inhibit differentiation and migration of dendritic cells (DCs), and suppress their ability to activate T cells, further contributing to the downregulation of lymphocyte responses. GCs also have a variety of effects on granulocytes, including the surprising action of promoting neutrophil survival, explaining why GCs are ineffective against neutrophilic inflammation (71). I will focus in more detail on the effects of GCs in macrophages, since a major function of these steroids is the inhibition of macrophage inflammatory cytokine production.

As mentioned above, the activated GR is able to associate with other transcription factors at their target promoters and modulate their activity, including the central regulator of inflammation NF-κB. GR associates with the p65 subunit of NF-κB, resulting in inhibition of RNA polymerase II activity at NF-κB-regulated genes (75). The resulting inhibition of inflammatory cytokine transcription is a major contributor to the anti-inflammatory actions of GCs (67, 72, 73). GC may also have cell type-specific effects on NF-κB activity, including through increasing expression of the NF-κB inhibitor IκBα (58, 73, 76).

Another principal method of GC action in macrophages is the downregulation of MAPK signalling through reduced phosphorylation of p38 and JNK, which are key inflammatory drivers. This occurs through upregulation of the dual-specificity phosphatase 1 (DUSP1), which is capable of dephosphorylating both threonine and tyrosine residues, and functions as a negative feedback regulator to turn off MAPK signalling in response to pro-inflammatory stimuli. GCs enhance and sustain DUSP1 expression, resulting in a broad reduction in inflammatory mediator production (38, 74). As well as regulating inflammatory gene transcription, the inhibition of MAPK signalling can control mRNA stability. Tristetraprolin (TTP) is an important immunoregulator that functions by destabilising the mRNA of a wide array of inflammatory mediators. TTP activity is inhibited by MAP kinases, therefore GC-mediated reduction in MAPK activity enhances TTP function and results in rapid downregulation of cytokine production (73).

There are numerous other mechanisms and proteins involved in the ability of GCs to inhibit inflammatory processes. GRIP1 is a co-regulator that associates with the GR and facilitates transrepression at target genes (71). Glucocorticoid-induced leucine zipper (GILZ), which is most well-studied in lymphocytes, interacts with and inhibits multiple proteins,

including NF-κB p65 (77). The contributions of these processes have been demonstrated in mouse models of many different inflammatory diseases, due to the use of GCs for multiple clinical manifestations (63, 71, 77). All of the above mentioned mechanisms and more contribute to the broad and potent anti-inflammatory functions of these steroids, and are the reasons that they continue to feature heavily in therapeutic regimes over 70 years on from their first clinical use.

1.3.4 Effects of GCs on systemic metabolism

Glucocorticoids are so-called because of their importance in the regulation of glucose metabolism, and they also regulate other metabolic processes including fatty acid metabolism and appetite (78). This is evident in conditions of GC dysregulation, such as Cushing's disease (GC excess) and Addison's disease (GC insufficiency), which are characterised by numerous metabolic symptoms (79). Many of the side effects of therapeutic GC use also result from actions of the drug on metabolic tissues; including the development of diabetes and muscle atrophy (64).

The principle roles of endogenous cortisol include the mobilisation of energy substrates in response to stress, and the redistribution of these substrates throughout the body. Amongst other complex functions, these effects are achieved through actions of the hormone on the liver, skeletal muscle and adipose tissue, which are important energy-storing organs; as well as interactions with pancreatic insulin secretion and insulin signalling. Interrogation of the direct effects of GCs on systemic metabolism is complicated by the multiple feedback systems involved in GC signalling and energy homeostasis, and the cross-talk between different hormonal axes (80).

The Liver

Glucocorticoids co-ordinately regulate gene transcription from liver-specific promoters in order to upregulate gluconeogenesis in liver cells. Gluconeogenesis is essentially the opposite of glycolysis, with many enzymes able to function in both pathways, and results in the synthesis of glucose, which is released into the circulation to supply tissues such as the brain during nutrient deprivation (79). Amongst many enzymes upregulated by GCs in this context is glucose 6-phosphatase, which catalyses the reverse reaction to hexokinase, and also controls glucose release from hepatocytes (79). These hepatic actions greatly contribute to the development of hyperglycaemia during chronic GC exposure (81). Interestingly, loss of expression of the GC-activating enzyme 11β-HSD1 in hepatocarcinoma cells was shown to increase cancer survival due to unrestrained glycolysis. This could be circumvented by treatment with dexamethasone, which does not require local enzymatic activation, and which inhibited tumour growth through upregulation of gluconeogenesis (82).

The Pancreas

Glucocorticoids suppress pancreatic β-cell development *in utero*, and in adults acute GC administration inhibits the secretion of insulin, also contributing to hyperglycaemia and diabetes development (79). The decrease in glucose-stimulated insulin secretion is in part due to degradation of the β-cell glucose transporter GLUT2, causing defective glucose signalling (83). GCs can also induce β-cell apoptosis by activation of the unfolded protein response and ER stress (79). However chronic GC exposure can result in a compensatory increase in insulin production, which can lead to hyperinsulinaemia (84). A chronic effect of GCs on pancreatic α-cells may also contribute to glucose intolerance and diabetes development. Increases in α-cell mass and glucagon production have been reported upon GC administration, further

stimulating hepatic gluconeogenesis as well as elevating blood glucose through glycogenolysis (84).

Skeletal Muscle

Skeletal muscle is a major storage organ for glucose in the form of glycogen, and is a key target of insulin signalling. GCs strongly impair skeletal muscle insulin sensitivity, resulting in reduced uptake of circulating glucose (84). GCs regulate surface expression of the GLUT4 glucose transporter in skeletal muscle by decreasing receptor translocation from intracellular stores in response to insulin (85). GCs also reduce muscle glucose storage by antagonising the stimulatory effect of insulin on glycogen synthase activity (86).

Glucocorticoids can induce muscle atrophy through increased protein breakdown. They have been shown to increase expression of ubiquitin-proteasome pathway components, giving an enhanced capacity for protein degradation (64). GCs also stimulate expression of glutamine synthetase (GS) (aka glutamate-ammonia ligase/GLUL), which catalyses the production of glutamine from glutamate and ammonia, thereby capturing the intracellular ammonia released by protein breakdown. Glutamine is exported from muscle cells at high rates during GC treatment (87).

Adipose Tissue

Glucocorticoids are required for adipocyte differentiation, and they induce expression of lipolysis genes in adipocytes *in vitro*, although similar studies *in vivo* have provided mixed results (79). Acute GC action causes release of fatty acids from adipose tissue, and chronic GC exposure can result in abdominal obesity due to redistribution of lipids from peripheral to central adipose tissue, as displayed in Cushing's syndrome. Increased central fat depots are linked to a greater risk of insulin resistance, further demonstrating the complex interplay of GC action in different tissues, which culminates in loss of metabolic homeostasis during long

term exposure (80, 88). GC signalling is also implicated in the development and regulation of brown adipose tissue, which carries out thermogenesis through the expression of the uncoupling protein UCP1. Studies indicate that GCs cause decreased expression of UCP1 in brown adipose tissue and a resulting loss of thermogenic capacity (88).

There are many other reported mechanisms of GC action in the regulation of glucose, protein and fatty acid metabolism in the above mentioned tissues as well as others. Interestingly, the ocular side effects of therapeutic GCs also have a metabolic basis, as cataracts can result from increased ocular glucose concentrations brought about by the stimulation of gluconeogenesis (64).

1.4 microRNAs

MicroRNAs (miRNAs) are short RNA species, 19-22 nucleotides in length, which mediate post-transcriptional gene regulation by sequence-specific recognition of complementary target sites within mRNAs (89-91). Each miRNA is capable of potentially targeting up to hundreds of different genes, and it is now accepted that almost every cellular process is under the regulation of miRNAs, with large numbers of miRNA target sites being conserved across multiple species (89, 90).

RNA-induced silencing was first described in the early 20th century as a mediator of anti-viral immunity in plants (92). The first true microRNA was not discovered until 1993, during the study of developmental timing mutants of the microscopic worm *C. elegans.* The genes *lin-4* and *lin-14* were shown to have opposing effects on development, and it was identified that *lin-4* encodes a short RNA species that post-transcriptionally regulates *lin-14* through RNA duplex formation (93). The first mammalian microRNA was identified in 2000, when homologues of another *C. elegans* microRNA, *let-7*, were described in a number of

animal species, including humans. This was followed by rapid expansion of the field, and today thousands of miRNAs have been described (93).

1.4.1 miRNA biogenesis and miRISC

MiRNAs are generally transcribed from the genome by RNA polymerase II. They can be expressed from within protein-coding genes (generally from introns or 3'UTRs); from miRNA clusters, where multiple miRNAs are regulated in tandem; or as single miRNAs within noncoding regions (94, 95). A miRNA is synthesised as an initial extended transcript called a primary miRNA (pri-mirna), which undergoes a first round of processing by the RNase III enzyme Drosha and associated protein DGCR8, to form the 70nt precursor miRNA (pre-mirna) (**Figure 1.5**). After export from the nucleus, a second round of cleavage is performed by the RNase enzyme Dicer, resulting in the mature miRNA as a bulged duplex of around 21nts (**Figure 1.5**) (95, 96).

The miRNA functions as part of an RNA-Induced Silencing Complex (RISC), the two main protein components of which are the Argonaute protein (AGO), and GW182 (90). The mammalian Argonaute family has 4 members (AGO1-4), any of which can function in the miRNA-mediated silencing pathway (91, 96, 97). GW182 was originally found to localise within processing (P) bodies – cytoplasmic foci rich in RNA turn-over machinery – and GW182 was later found to interact with AGO proteins and play a key role in miRNA function (96, 98). The mature miRNA is loaded onto the AGO protein and the passenger strand is removed and degraded, resulting in the final active complex containing a single-stranded miRNA species complementary to a portion of the target gene (95, 96). MicroRNA target sites are predominantly located within the 3' untranslated region (3'UTR) of target mRNA. MicroRNAs have also been shown to regulate genes by targeting their 5'UTR or coding regions, although this is thought to be rare and is relatively poorly understood (99, 100).
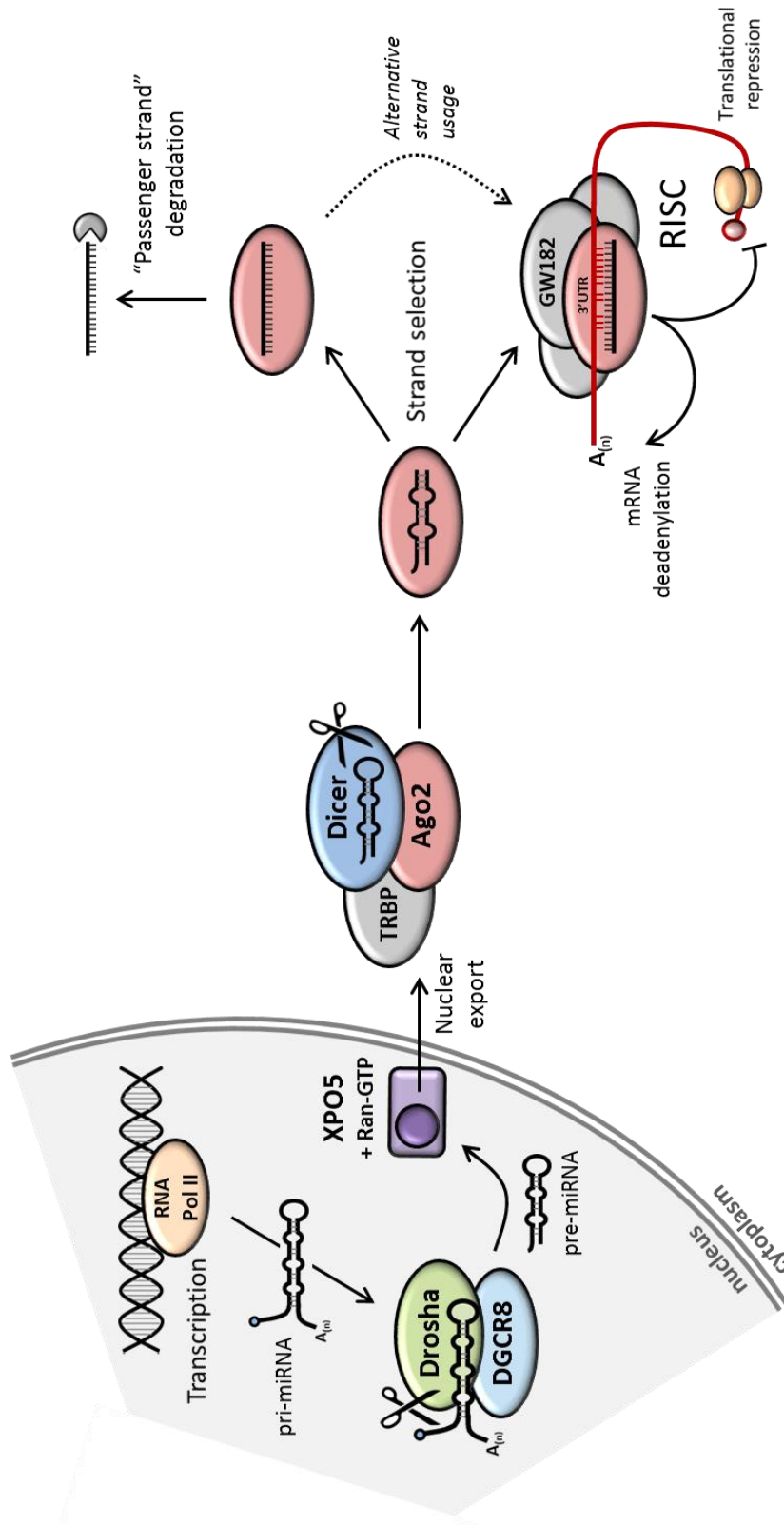
Figure 1.5) microRNA biogenesis and miRISC assembly - Produced for Clayton *et al* 2018 (2)

MicroRNAs are transcribed from the genome to create primary (pri-)miRNAs. The first round of cleavage occurs in the nucleus, carried out by the RNase III enzyme Drosha and associated factor Pasha/DGCR8, resulting in the shorter precursor (pre-)miRNA. Nuclear export is mediated by Exportin 5 (XPO5) and Ran-GTP. The second cleavage occurs in the cytoplasm by the RNase III enzyme Dicer as part of a protein complex that produces the mature miRNA. Strand selection results in release of one of the two miRNA strands, which is degraded. The retained strand is loaded onto Argonaute protein (e.g. Ago2), and forms the RNA-induced Silencing Complex (RISC) along with other proteins such as GW182. Silencing can occur by promoting deadenylation and mRNA degradation, or translational repression.

MicroRNA-mediated silencing in mammals differs from RNA interference (RNAi) due to the extent of sequence complementarity between miRNA and target, and consequently different silencing mechanisms are employed (91). RNAi occurs when sequence match is perfect or near-perfect, resulting in endonucleolytic cleavage of the target transcript by the RNase H domain of AGO2 (91, 97, 101, 102). This is the mechanism largely employed by plant miRNAs, which show high percentage match to targets (91). The vast majority of animal miRNAs show only partial complementarity to target mRNAs, and the vital region for the repressive interaction is termed the seed region. The basic seed region corresponds to miRNA positions 2 to 7, and this is termed the "6mer". Other types of seed match have also been widely described, including additional pairing to the 8th nucleotide, and/or presence of an A opposite miRNA position 1 (89, 103). The importance of pairing to the seed sequence has been extensively demonstrated by mutational studies (103).

1.4.2 Mechanisms of miRNA-induced silencing

The consequence of the association of miRISC (miRNA loaded into RISC) with the target site within the mRNA is either translational repression or enhanced mRNA degradation (or both effects sequentially). Translational repression was initially considered to be the major mechanism leading to reduced protein expression, and this repression occurs rapidly in response to miRNA engagement. Evidence suggests that miRISC inhibits translational initiation, as the inclusion of internal ribosome entry sites in target mRNA can circumvent miRNA effects (89, 104). However it has more recently been shown that translational repression can precede mRNA destabilisation, and that degradation of the mRNA plays the more substantial role in miRNA-mediated silencing (90, 91, 105).

Many of the mechanisms reported for the action of miRISC centre around the protein GW182, which has been described as a "hub protein", recruiting several other factors to the target mRNA (91). One of the major functions of this protein is the recruitment of deadenylase complexes. The CCR4–NOT deadenylase complex, which is found within the P bodies along with GW182, is thought to be the most functionally important in miRNA-mediated silencing (91, 106). This complex removes the poly(A) tail of the mRNA, leading to mRNA de-capping (removal of the 5' m(7)G cap), followed by accelerated degradation via 5'-3' exonuclease activity (91, 107). RISC further assists in these final steps by recruiting activators of de-capping e.g. DCP1 (91).

GW182 also plays a vital role in translational inhibition by binding to poly(A) binding protein (PABP), preventing association of PABP with the translation initiation factor eIF4G through competition for the same binding domain, thereby inhibiting mRNA circularisation and ribosome recruitment (108). PABP has also been implicated in assisting recruitment of CCR4–NOT complexes (108). Another proposed mechanism of translational repression by RISC is through the displacement of eIF4A, an RNA helicase that is necessary for ribosome recruitment and initial ribosome scanning (109).

Many other proteins are reportedly involved in miRNA-mediated mRNA silencing, either through direct interaction with AGO or GW182, or by recruitment through other factors. It has also been suggested that stalling of mRNAs on active polysomes may be a useful function of miRNAs to enable rapid up- or down-regulation of protein production (102). It is likely that a combination of these mechanisms contributes to the final outcome, and that the precise functionality depends upon specific features of both miRNA and mRNA, as well as the relative abundance of proteins present.

1.4.3 miRNAs in immune regulation

Immune responses involve complex signalling cascades that culminate in coordinated expression of suites of genes. MicroRNA-mediated gene targeting can result in coordinated regulation of whole pathways by the targeting of several different components, therefore miRNAs represent an efficient method of pathway regulation in immune cells. Both innate and adaptive immune signalling are subject to miRNA-mediated fine tuning. MiRNAs are vital for the proper development and functioning of T cells, as demonstrated by T cell lineage-specific deletion of the miRNA processing enzyme Dicer. This leads to a block in CD8+ T cell differentiation, impaired CD4+ T cell proliferation and dysregulated cytokine production (110). MiRNAs are central in early B cell development, as well as the regulation of class switching, and maturation to antibody-producing plasma cells (111, 112).

Multiple miRNAs have been described to regulate immune function and to contribute to pathology in chronic inflammatory diseases, and miRNA targeting has been successful in preventing or alleviating disease in mouse models of chronic inflammation (113-115). MiRNA-mRNA interaction results in specific downregulation of the target gene, however on a pathway level miRNAs can either decrease or increase pathway signalling by targeting either positive or negative regulators, respectively.

Three particular miRNAs have received the majority of attention in the area of immunology due to their dysregulation in multiple cell types in several inflammatory diseases, and they have been widely studied in regard to the control of macrophage responses to TLR engagement. These miRNAs are: miR-146a, miR-21 and miR-155 (116, 117). Collectively they act as prime examples of both positive and negative regulation of inflammatory signalling, as while miR-155 is generally described to play a pro-inflammatory role by targeting negative

regulators of TLR signalling, miR-146a and miR-21 have been linked to the downregulation of macrophage inflammatory signalling and the switch to a pro-resolution phenotype (116, 117). MiR-155 and miR-21 have also been linked to cancer development or progression, and are therefore termed oncomirs (oncogenic miRNAs) (118). *These miRNAs shall be introduced in more detail in Chapter 3.*

1.4.4 miRNAs in therapy

MicroRNAs represent a new avenue for therapy, and the ability of miRNAs to regulate a large number of target genes, spanning multiple cellular pathways, could prove beneficial. RNA-based therapies offer several advantages over conventional small molecule drugs, including adaptability and ease of synthesis. However, several challenges must be overcome before RNA therapeutics can be developed for a wide range of diseases. Nucleic acids are poorly cell permeable and have unsuitable pharmacokinetic properties due to their negative charge and high molecular weight. Delivery is also restricted by the cellular RNA-detecting defence mechanisms that activate innate immune signalling or apoptotic pathways (119, 120). Despite these challenges, the technology to enable successful delivery of RNA therapeutics to target tissues is rapidly progressing, and several oligonucleotide therapies have been approved by the US FDA (121).

The liver is the simplest organ to target with RNA therapies due to scavenger receptor-mediated oligonucleotide clearance (122). The first miRNA-targeted therapy to enter clinical trials was an anti-miR-122 LNA for the treatment of hepatitis C infection in the liver (123). MiR-155 is another major focus for therapeutic intervention due to its key role in oncogenic and inflammatory processes. The miRNA-focused pharmaceutical company miRagen is developing inhibitors of miR-155 for two main disease areas: haematological malignancies, such as

lymphomas, where their LNA-based antogimiRs inhibit immune cell proliferation and function and are undergoing phase I clinical trials (124, 125); and neuroinflammation, as miR-155 was found to be elevated in the spinal cord of patients with ALS, and is associated with microglial activation (125, 126). Despite these developments, there are currently no miRNA-directed therapeutics that have entered clinical trials for the treatment of inflammatory diseases (115).

1.4.5 miRNAs and glucocorticoids

Extensive cross-talk exists between glucocorticoid signalling and microRNAs, resulting in a variety of physiological effects in multiple tissues throughout the body (2). **Figure 1.6** summarises some of the best-studied areas that are subject to miRNA-GC crosstalk, and demonstrates that the same miRNA can interact with GC signalling in different cell types. For example, miR-124 has been shown to target the GR receptor gene *NR3C1* in lymphocytes and neurons, and is associated with GC resistance in both cell types (127, 128). In lymphocytes, the outcome is a reduction in GC-induced apoptosis, and elevated miR-124 expression is associated with poor response to GC therapy in acute lymphoblastic leukaemia (ALL) patients (129). MiR-124 action in the brain is linked to depressive behaviour and reduced resistance to stress, as GC signalling is vital for stress resilience (130-132).

I have previously published a review of the literature surrounding miRNA and GC interaction (2), and do not have space here to address all of the areas in which this cross-talk occurs. I will therefore focus briefly on the contribution of miRNA action to the anti-inflammatory effects of GCs, which has most relevance to this project.
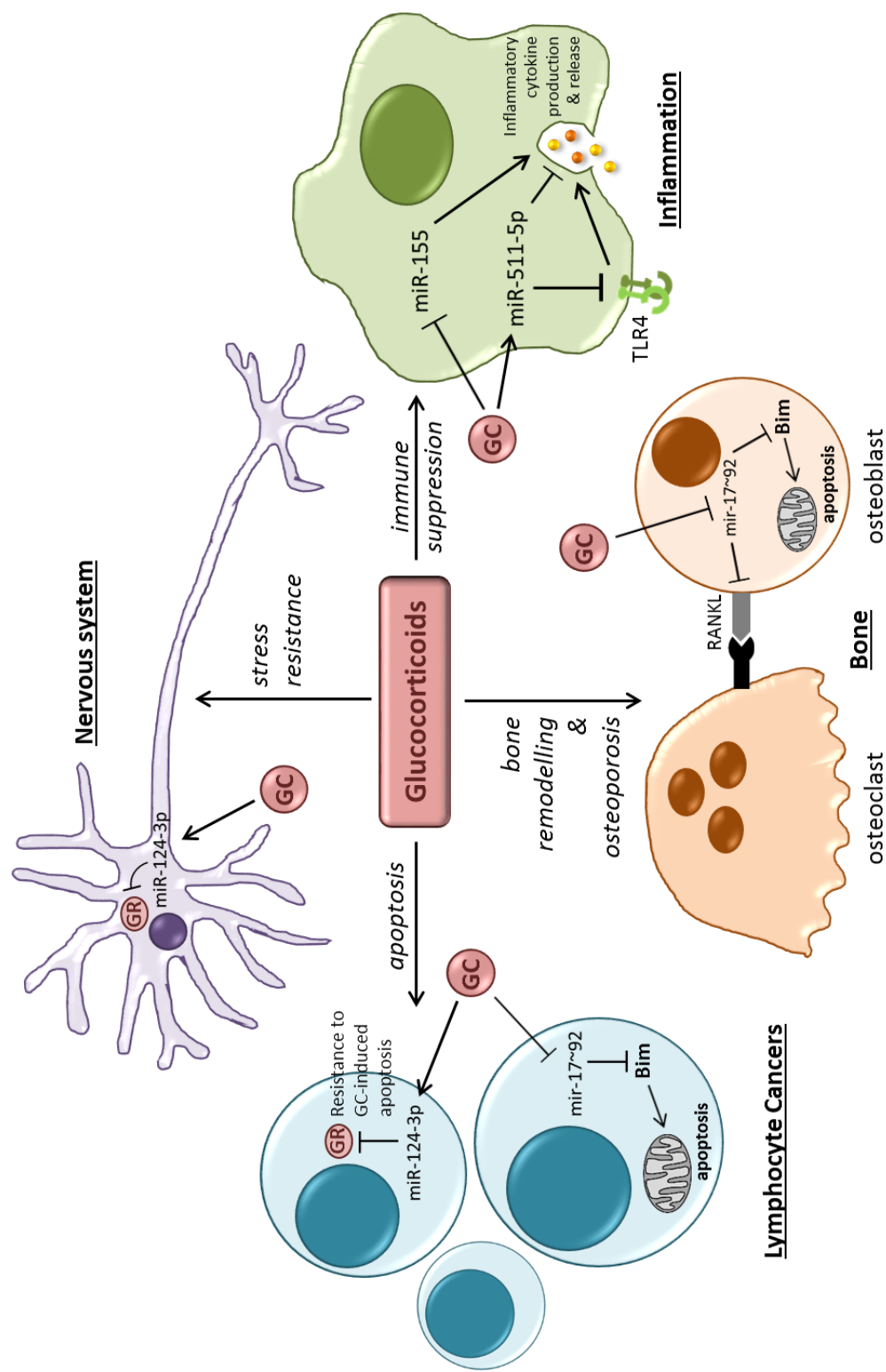
Figure 1.6) Glucocorticoids and microRNAs – tissue-specific interactions

Examples of some of the main mechanisms of miRNA-mediated regulation of GC action in the contexts of bone remodelling, immune suppression, cancer apoptosis and neuronal response to stress

The miRNA miR-155 plays a central role in the regulation of both adaptive immunity and the innate inflammatory response. This miRNA was found to be inhibited by GCs in mouse and human macrophages, which was dependent on NF-kB function (133). Transfection with a miR-155 mimic reduced the anti-inflammatory effects of GCs with regard to cytokine and NO production, implicating miR-155 inhibition in the functional effects of GCs. Inhibition of miR-155 augmented the anti-inflammatory effect of low dose dexamethasone on cytokine production, suggesting a possible approach for complementing GC therapy with miR-155 inhibition to minimise GC off target effects (133). GCs also downregulate miRNA-155 in T cells (134, 135), and in the liver (136).

MiRNA-511 is induced by a number of anti-inflammatory or pro-resolution stimuli, including GCs, IL-4 and TGFβ (137, 138). This miRNA is co-transcribed from within an intron of the *Mrc1* gene, which encodes the C-type mannose receptor CD206 that is associated with alternatively activated macrophages. miR-511-5p targets the 3'UTR of TLR4 in human monocytes, reducing receptor levels and decreasing the production of pro-inflammatory cytokines upon LPS challenge (137). This could contribute to the pro-resolution macrophage phenotype induced by IL-4, as well as the induction of endotoxin tolerance by GCs, a state in which cells become refractory to subsequent stimulation after an initial inflammatory challenge. MiR-511-5p has also been shown to target the M1-associated cytokine IL-12β (137).

The regulation of additional miRNAs has been associated with the anti-inflammatory function of GCs, including miR-101, which targets the key regulatory phosphatase DUSP1 (139); and miR-98, which targets the TNF receptor TNFR2 and the cytokine IL-13, contributing to the efficacy of GCs for the treatment of allergic airway inflammation (134, 140). Suppression

of the miR-17~92 cluster is implicated in the apoptotic effect of GCs in lymphocytes, as members of this cluster target the pro-apoptotic protein Bim (141-144).

1.4.6 miRNAs and metabolism

MicroRNAs have been shown to regulate cellular metabolic processes through the direct targeting of metabolic components or metabolism-related signalling pathways. The miR-125 family has been demonstrated to have metabolism-regulating effects related to inflammation. Downregulation of miR-125a was shown to cause increased glycolytic rate and decreased oxidative respiration in endothelial cells. This was linked to the elevated vessel branching and network formation that contributes to the hypoxic environment and leukocyte infiltration in psoriatic arthritis (145). MiR-125b is induced by LPS in human monocytes, and its expression was shown to cause a decrease in oxidative respiration and an increase in mitochondrial fusion in THP-1 cells, in part through the targeting of mitochondrial fission protein MTP18 (146).

MiRNAs can also directly target components of the electron transport chain, altering mitochondrial function. MiR-338 is highly expressed in the brain, and was found to target nuclear-encoded subunits of complex IV and ATP synthase in neuronal axons, which are enriched in mitochondria. This resulted in decreased ATP production, an increase in reactive oxygen species, and impaired axonal growth (147). MiR-210 expression is strongly induced by hypoxia, and this miRNA facilitates the downregulation of oxidative metabolism by targeting iron-sulphur cluster assembly proteins that are required for electron transport chain function (148).

MiRNAs have also been found to localise to mitochondria (termed mitomiRs), but the precise function of these miRNAs is incompletely understood. It is also currently unknown how these miRNAs are imported into the mitochondrion, or how many of them are encoded from the mitochondrial genome itself, which has been shown to produce non-coding RNAs (149). However, miR-181a-5p was recently reported to target mitochondrially-encoded electron transport chain subunits mt-CYB (complex III) and mt-CO2 (complex IV) in liver cancer (150).

This is in no way an exhaustive list of metabolic miRNA action. Due to the potential for each miRNA to target numerous genes, and the interactions between multiple signalling pathways and metabolic regulation, it is likely that the number of miRNAs connected to metabolism is greater than the current literature describes. Like most miRNA function, these effects are also likely to be highly cell type-specific.

1.5 Introduction to metabolism

The field of immunometabolism has been growing in popularity and recognition over the past decade, and it is now widely appreciated that immune cell metabolic status is closely linked to cellular phenotype and function. Specific metabolic pathways have be implicated in controlling the differentiation or activation of immune cell subtypes, and many aspects of metabolic machinery have been shown to play immunoregulatory roles. There is ample evidence of the existence of a two-way relationship between immune signalling and metabolic regulation, with each able to drive changes in the other (151). Resident or infiltrating immune cells have also been linked to metabolic syndromes such as obesity and diabetes, *as discussed in Section 1.2*. This is broadly classed as "metaflammation", and demonstrates how immune cells are able to influence systemic metabolism (152).

I shall begin this section by introducing some of the main cellular metabolic pathways that are of relevance to my project and the field immunometabolism in general; including how they are interlinked and some of the ways in which they are regulated in normal and pathological situations. I will then continue by describing how these pathways are connected to macrophage function.

1.5.1 Glycolysis

Glycolysis is the process of glucose metabolism through a multi-step pathway that occurs in the cell cytoplasm, generating the major products of pyruvate, ATP, and reducing equivalents of NADH (**Figure 1.7**) (153). This pathway is seen as relatively inefficient for energy production, producing only net two molecules of ATP per glucose molecule, whereas oxidative phosphorylation in the mitochondria can produce up to 36 (151). However, glycolysis can

achieve this ATP production more rapidly and can be quickly upregulated upon demand, making this pathway beneficial when competition for resources is high or when cells need to adapt quickly to an environmental change (154). Glycolysis also plays a central role in feeding glucose-derived carbon into other metabolic pathways for the production of biosynthetic intermediates, and it is the only ATP-generating process that can occur in the absence of oxygen (153).

The pyruvate produced from glycolysis has different potential fates depending on cellular demands and environmental conditions. When oxygen is plentiful, pyruvate can be converted to acetyl-CoA and enters the TCA cycle (discussed below) to power mitochondrial ATP production and biosynthetic pathways. Alternatively, as occurs during oxygen deprivation (hypoxia), glycolysis-derived pyruvate is converted into lactate within the cytoplasm by the enzyme lactate dehydrogenase (LDH). This process utilises NADH, regenerating oxidised NAD+ and allowing continuation of glycolytic flux (153, 154). This is particularly important when high rates of glycolysis result in saturation of the malate-aspartate shuttle – a mitochondrial antiporter that normally serves to restore redox balance by transferring net NADH from the cytosol to the mitochondria for oxidation (155). In addition to facilitating continued ATP generation by glycolysis, the recovery of the NAD+/NADH ratio through the action of LDH is important for the many enzymes that require oxidised NAD+ as a co-factor, including deacetylases (sirtuins) that regulate gene transcription (155).
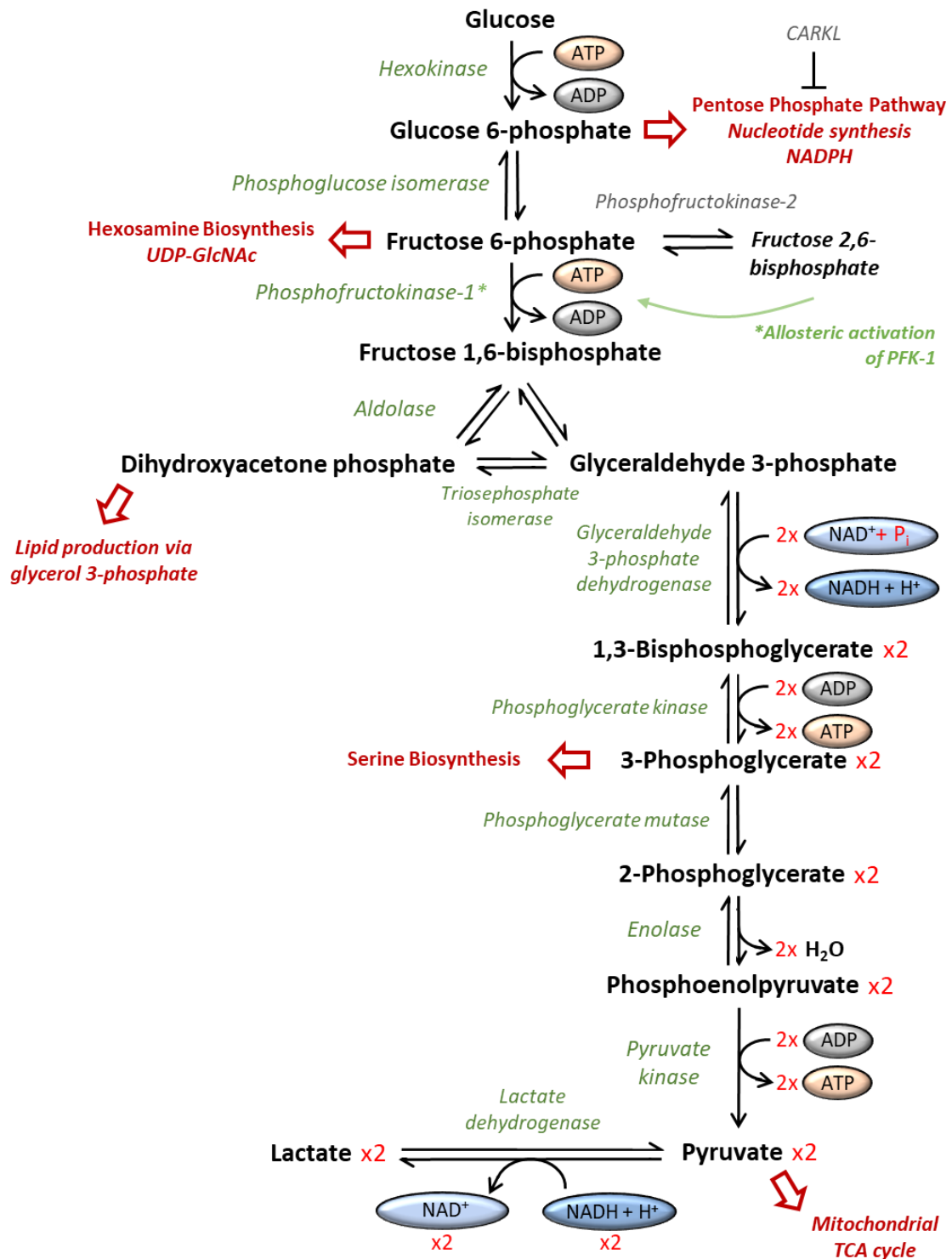
Figure 1.7) Glycolysis pathway

Schematic of the glycolytic metabolism of glucose, as well as branching pathways and regulation points relevant to macrophage metabolic control. Key enzymes and reaction products are annotated.

If lactate levels are allowed to build up within the cell, the accompanying drop in pH results in metabolic dysfunction and ultimately cell death (156). Therefore lactate must be exported from the cell, and this occurs through the action of the SLC16A family of monocarboxylate transporters. The MCT4 isoform is the most abundantly expressed in many cells that show high glycolytic rates, such as white skeletal muscle; while MCT1 is employed by activated T cells (157). Since lactate represents only a partially metabolised fuel source, it is becoming increasingly evident that cells can take up lactate from the circulation or surrounding microenvironment to use as a fuel. For example, lactate released by astrocytes in the brain is taken up and metabolised by neurons (157); and cancer cells that reside within less hypoxic regions take up extracellular lactate via the transporter MCT1 (158).

Due to the role of this pathway in the rapid response of cells to increased energetic and biosynthetic demands, the regulation of glycolysis is key for cell survival and function, and pathway flux is tightly controlled at multiple stages. Tanner *et al* systematically evaluated the contribution of each step of the glycolytic pathway to overall flux control. This study identified four key rate-limiting steps of glycolysis: glucose import, hexokinase, phosphofructokinase, and lactate export. The genes controlling these steps were found to be consistently upregulated in tumours, which rely on high glycolytic rates for survival and proliferation (159).

The phosphorylation of fructose 6-phosphate to fructose 1,6-bisphosphate (F1,6BP), catalysed by 6-phosphofructo-1-kinase (aka phosphofructokinase-1: PFK1), is an important control point for glycolysis, and increasing the expression of this enzyme has been shown to increase glycolytic rate (159). PFK1 is also subject to allosteric regulation by the alternatively phosphorylated sugar: fructose 2,6-bisphosphate (F2,6BP), which strongly enhances catalytic activity of PFK1 and therefore glycolytic flux (160). F2,6BP is produced by the bifunctional

enzyme 6-phosphofructo-2-kinase/fructose-2,6-bisphosphatase (phosphofructokinase-2: PFK2 or PFKFB) (**Figure 1.7**). The mammalian genome encodes four different isoforms of this enzyme, which vary in their ratios of kinase:phosphatase activity (159, 160). Increasing expression of the isoform with the highest kinase activity (PFKFB3 or uPFK2) can enhance glycolytic lactate secretion to a similar extent to overexpression of PFK1 (159).

An important early commitment step in glycolysis is phosphorylation of glucose by hexokinase, which traps the glucose within the cell (161). The hexokinase-2 (HK2) isoform is the predominant form expressed by highly glycolytic cancer cells. This isoform has a high affinity for glucose, and interaction with the outside of mitochondria via the voltage-dependent anion channel (VDAC) positions the enzyme close to the mitochondrial ATP synthase, allowing rapid binding of ATP for glucose phosphorylation (161). The importance of PFK1 and HK activity in the control of glycolysis makes sense conceptually, as these are the two steps within the pathway that consume ATP. It would be potentially detrimental to the cell to commit ATP to the phosphorylation of glucose if the pathway could not be adequately completed to regenerate this ATP. Hence it was observed that excessive overexpression of HK2 actually decreased glycolytic flux due to ATP depletion (159). This also explains why HK isoforms 1, 2 and 3 are subject to strong product inhibition by glucose 6-phosphate (162).

The remaining steps shown by Tanner *et al* to enhance glycolytic flux are performed by the transporters GLUT1/3/5 for the uptake of glucose, and MCT (in this case MCT4) for lactate export (159). Competition for glucose in the microenvironment can be fierce, particularly in a tumour, where demand by multiple cells types is high. Elevated expression of glucose transporters is vital for the survival of glycolytic cells in these environments, and it has been shown that overexpression of GLUT1 in cancer cells helps them to evade anti-tumour

immune activity by outcompeting tumour-infiltrating T cells for glucose (163). Similarly, high expression of lactate transporters is a hallmark of cancer cells, and inhibition of MCT1 in B cell lymphoma lines prevented proliferation and caused cell death (156).

While the study by Tanner *et al* identified four of the main players in glycolytic regulation, the level of control afforded by each enzyme is dependent upon the relative expression and activity of that enzyme in any given context. This means that other steps may gain considerable flux control in different cell types or conditions (159). Additional glycolytic enzymes that have been reported to control pathway flux in various contexts include pyruvate kinase, in particular the PKM2 isoform, which is subject to allosteric activation and is also regulated by dimerization state (164, 165); and glyceraldehyde 3-phosphate dehydrogenase (GAPDH), which is limiting in some cancer cells (166). The direct enzymatic regulation of many of these enzymes allows for the rapid modulation of pathway flux that gives glycolysis its central role in the cellular response to stimuli. Glycolytic enzymes are also subject to tight transcriptional regulation, for example through HIF-1α (*to be discussed in Section 1.6*) (167).

1.5.2 The Warburg Effect

The Warburg effect was originally observed in aggressively proliferating cancer cells by Otto Warburg in the 1920s. This term describes a phenomenon of aerobic glycolysis, in which cells consume large amounts of glucose that is converted to lactate instead of being oxidised in the mitochondria, despite the presence of adequate oxygen (168). In 2011, Hanahan and Weinburg added the reprogramming of energy metabolism to the core underlying hallmarks of cancer cells, as it had become apparent that aerobic glycolysis is critical for fuelling many of the aggressive properties of tumours (169). In these cells the Warburg effect is thought necessary to fuel proliferation. As well as being a rapid and controllable source of ATP

production, glucose acts as an important carbon source for the generation of biosynthetic intermediates required for anabolic processes of DNA, protein and lipid synthesis, which are vital for cell growth and division (167). This occurs through the diversion of glycolytic intermediates into branching pathways such as the pentose phosphate pathway (153). While the majority of the literature surrounding the Warburg effect is focused on cancer, aerobic glycolysis is not specific to cancer cells. High rates of aerobic glycolysis have now been shown to drive important phenotypes of immune cells; including effector T cells and pro-inflammatory macrophages (170).

1.5.3 The pentose phosphate pathway

The pentose phosphate pathway (PPP) branches off glycolysis at glucose 6-phosphate (**Figure 1.7**), catalysed by glucose 6-phosphate dehydrogenase (153). This pathway is key for the synthesis of ribose 5-phosphate, the backbone for DNA and RNA production; hence its importance for rapidly proliferating cells (171). The PPP is also a major source of NADPH, which can play a variety of roles, dependent upon cellular demands. These roles include the production of fatty acids and cholesterol, as well as aiding cell survival in conditions of oxidative stress through the synthesis of glutathione, an important anti-oxidant (171). NADPH can also be used for the generation of nitric oxide (NO) by nitric oxide synthase, and of the superoxide anion ($O_2 \bullet -$) through the enzyme NADPH oxidase. Flux through the PPP is regulated by the rate of glucose 6-phosphate production from glycolysis, as well as through regulated expression of glucose 6-phosphate dehydrogenase and 6-phosphogluconate dehydrogenase enzymes (153).

Additional pathways that branch from glycolysis include the hexosamine biosynthesis pathway, which utilises fructose 6-phosphate to synthesise amino sugars used for the glycosylation of proteins and lipids (153, 172); and the serine biosynthesis pathway, in which the glycolytic intermediate 3-phosphoglycerate is used for the production of serine, which is also ultimately used for the synthesis of glycine and cysteine (**Figure 1.7**) (153).

1.5.4 The TCA cycle and oxidative phosphorylation

Mitochondria are professional energy-generating organelles, which coordinate oxidation of substrates from numerous sources for the production of ATP. A double-membraned structure that contains its own self-replicating DNA, the mitochondrion evolved from endosymbiosis of α-proteobacteria, though the precise stage at which this occurred in eukaryotic evolution is still a topic of debate (173, 174). The number of protein-coding genes, as well as ribosomal components and tRNAs encoded by the mitochondrial DNA differs greatly between eukaryotic species, but in all cases the mitochondria also rely on nuclear-encoded components for their propagation and functioning (173). Human mitochondria encode a total of 37 genes, including 13 that are essential for the process of oxidative phosphorylation (153).

The tricarboxylic acid (TCA) cycle (**Figure 1.8**); otherwise known as the Krebs' cycle or citric acid cycle; was first described by German/British biochemist Hans Krebs, who in his early career was assistant to Professor Otto Warburg, and who received the 1953 Nobel Prize for his pioneering work on cellular metabolism (175). He described a cycle of reversible and irreversible enzymatic reactions that consumed and regenerated citric acid, explaining the observed experimental phenomenon that the addition of citrate could sustain respiration of pigeon heart tissue (176). The TCA cycle takes place in the mitochondrial matrix, utilising carbon from a variety of carbohydrate, fatty acid and protein substrates. The cycle results in

the reduction of NAD+ and FAD to produce NADH and FADH$_2$ (**Figure 1.8**), and this reducing power is fed into the electron transport chain to generate ATP via the process of oxidative phosphorylation (**Figure 1.9**). The TCA cycle and oxidative phosphorylation are further intimately linked by TCA cycle enzyme succinate dehydrogenase, which also acts as complex II of the electron transport chain (177).

In addition to the branching pathways from glycolysis described above, the TCA cycle is important for the biosynthetic production of macromolecules, and its metabolites also play a number of signalling roles. One example is the TCA cycle intermediate citrate, which can be exported from the mitochondrion via the citrate/malate exchange carrier (153). One fate of cytosolic citrate is conversion to oxaloacetate and acetyl-CoA, the latter of which is used for the synthesis of nucleotides and lipids. Alternatively, citrate is a substrate for the cytosolic isoform of isocitrate dehydrogenase (IDH1), which generates NADPH for fatty acid synthesis and anti-oxidant functions (153). Citrate is also an important metabolite for the immunometabolic control of pro-inflammatory macrophages, as will be discussed later. The TCA cycle is controlled through allosteric regulation of many of the pathway enzymes, as well as at the level of substrate availability, with entry and exit of carbon from the cycle requiring exquisite coordination.
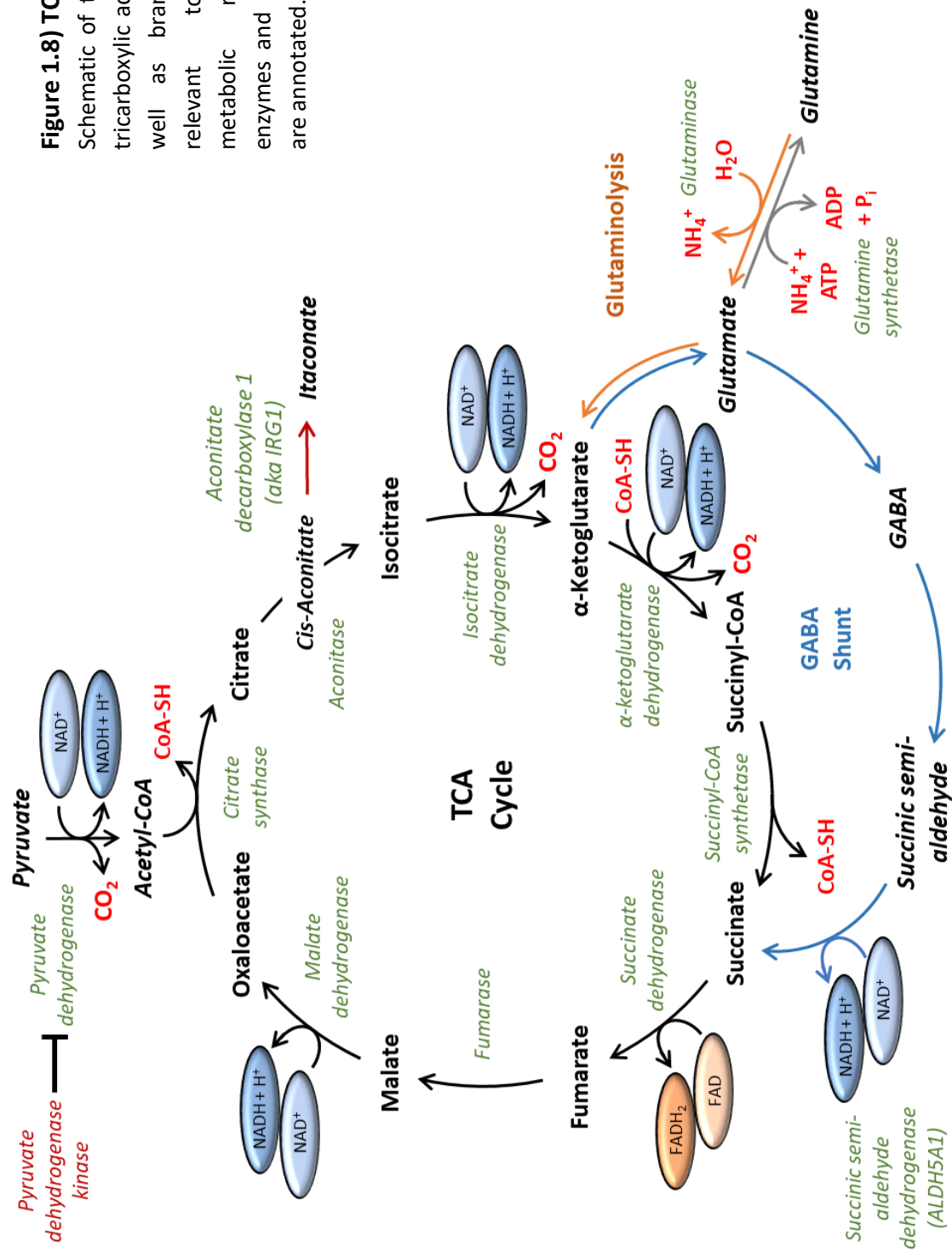
Figure 1.8) TCA cycle
Schematic of the mitochondrial tricarboxylic acid (TCA) cycle, as well as branching pathways relevant to macrophage metabolic regulation. Key enzymes and reaction products are annotated.

The electron transport chain (ETC) is a series of protein complexes that sit within the inner mitochondrial membrane, which couple the transport of electrons between the complexes to the pumping of protons across the membrane to the intermembrane space (**Figure 1.9**). This establishes an electrochemical gradient, referred to as the proton motive force (pmf), which is utilised by ATP synthase to convert ADP and inorganic phosphate into ATP (177). This is the chemiosmotic theory of ATP production described by Peter Mitchell in the 1960s (178). The intricate workings of ATP synthase were elucidated by John Walker and Paul Boyer, who shared the 1997 Nobel Prize for their work, which included a high resolution crystal structure of the catalytic domain of the complex which took 10 years to achieve (179).

There are four protein complexes responsible for electron transport within the respiratory chain (**Figure 1.9**). Complex I (NADH dehydrogenase) accepts electrons from NADH generated by glycolysis or the TCA cycle, and passes them to the electron carrier coenzyme Q (CoQ/ubiquinone) within the inner mitochondrial membrane. Reduced CoQ is oxidised by complex III (CoQ-cytochrome c oxidoreductase/cytochrome bc_1 complex), which passes electrons down the chain to cytochrome c. This is oxidised by complex IV (cytochrome c oxidase), and the electrons pass to the "final electron acceptor" – a molecule of oxygen (153). An alternative entry site for electrons is complex II (succinate dehydrogenase), which accepts electrons from $FADH_2$ generated by succinate oxidation, and feeds these electrons down the chain via CoQ. Complexes I, III and IV are responsible for electron-coupled pumping of protons to create the electrochemical gradient (153).
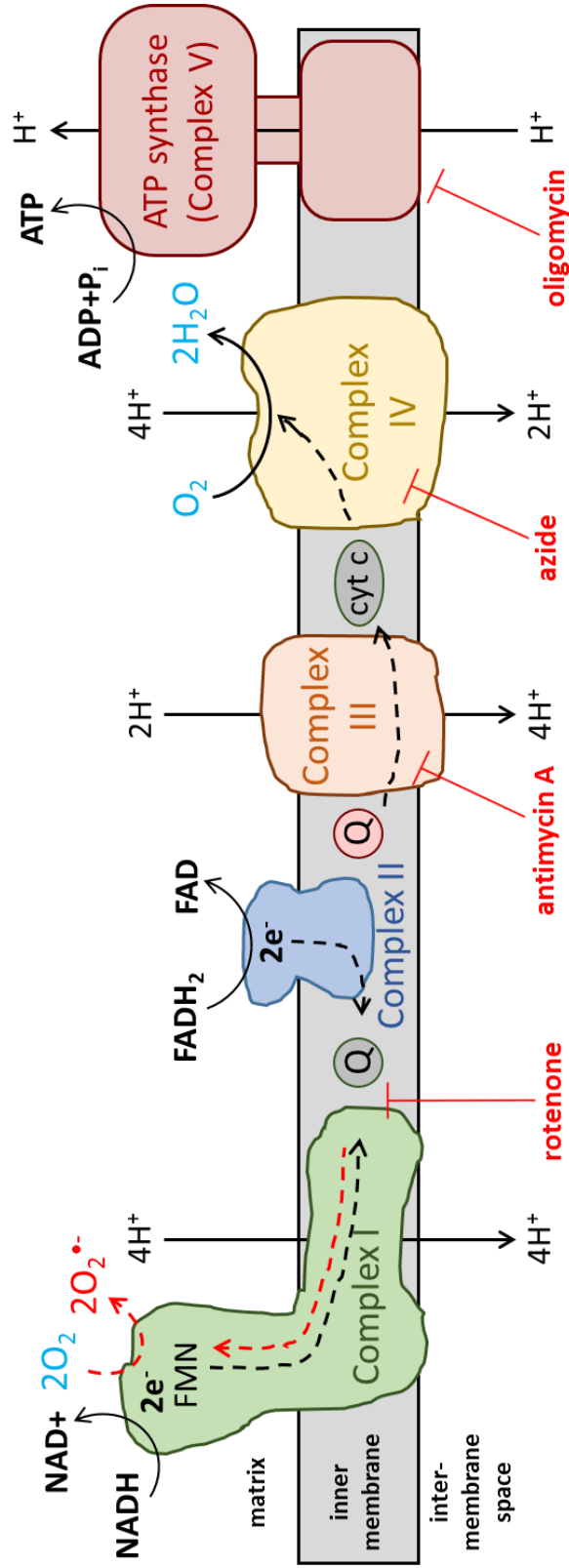
Figure 1.9) Mitochondrial electron transport chain

The electron transport chain (ETC) within the inner mitochondrial membrane passes electrons through complexes I to IV and electron carriers CoQ and cytochrome c. Protons are pumped across the membrane by complexes I, III and IV to generate the proton motive force (pmf). Protons pass back through complex V (ATP synthase) to generate ATP. Black dashed arrows represent forward electron transport from NADH and FADH$_2$, resulting in ultimate conversion of molecular oxygen to water. Red dashed arrows represent reverse electron transport (RET) through complex I to generate superoxide. The sites of inhibition by toxins commonly used to study mitochondrial respiration are shown.

Mitochondria have many other roles in addition to ATP production, including the regulation of apoptosis, calcium homeostasis and reactive oxygen species generation (177). Mitochondrial dysfunction has been linked to cellular senescence and ageing; as well as to a host of diseases. Mutation of mitochondrial proteins typically lead to manifestations in the brain and skeletal muscle, as these organs are heavily depend on mitochondrial respiration, and these disorders can be extremely severe (180, 181). Changes in mitochondria function are also associated with more common conditions, including neurodegenerative diseases such as Alzheimer's and Parkinson's diseases (177, 182); and inflammatory diseases such as RA (183, 184). Mitophagy is the cell intrinsic process of degrading dysfunctional mitochondria and recycling of resulting biosynthetic substrates. The balance of mitochondrial biogenesis and mitophagy controls cellular mitochondrial content, and prevents the accumulation of defective mitochondria that can cause disease (177). The opposing processes of fusion and fission also regulate mitochondrial function and cellular distribution. Mutations in the genes controlling these processes have been linked to neurodegenerative diseases (180). Mitochondria therefore act as important intracellular hubs for energy generation and signalling, and while much of their functionality and many links to disease have been described, there are still many complexities yet to be elucidated.

1.5.5 Nutrient sensing

The ability to sense and react to nutrient and energy status is an important intrinsic capability of all cells. This is important for growth and development, as well as for maintaining organismal homeostasis. On a whole organism level, nutrient availability is controlled at the level of food intake by hormones such as leptin, and through specialised nutrient-storing organs such as the liver and adipose tissue (185). However an individual cell must also control

allocation of resources and energy production. Since the cells of the immune system must respond to numerous signals in a timely and appropriate manner, management of anabolic and catabolic processes and the regulation of energy production are vital for the immune response. Several nutrient sensing pathways have been shown to be critical in regulating macrophage polarisation and response to stimulus, including mTOR, AMPK and PPARs, and they do so in a large part by controlling metabolic gene expression and pathway flux (186-189). Dysregulation or over-activation of these pathways can lead to loss of immune homeostasis and can drive diseases such as atherosclerosis, obesity and diabetes (185).

The serine/threonine kinase mTOR is a key nutrient sensor that coordinates metabolic changes in response to cellular availability of amino acids, glucose, lipids and ATP. In general mTOR promotes glycolysis, oxidative respiration and anabolic processes whilst inhibiting autophagy, due to an abundance of substrates. mTOR complexes I and II (mTORCI & mTORC2) are activated by multiple extracellular signals in macrophages, including TLR agonists and IL-4; and these complexes stimulate a global increase in protein production by regulating translation factors, as well as carrying out more targeted gene regulation (188).

In contrast to mTOR, AMP-activated protein kinase (AMPK) promotes catabolic process due to its role in sensing energy deprivation. As the name suggests, this kinase is activated by a high AMP/ATP ratio, and it regulates a multitude of pathways, including inducing fatty acid oxidation. AMPK inhibits mTOR complexes, preventing anabolic processes when energy is scarce, and promotes mitochondrial biogenesis and expression of genes for oxidative metabolism (187, 189).

Peroxisome Proliferator Activated Receptors (PPARs), of which 3 types have been described (α, δ/β and γ) act as sensors of fatty acids. These are nuclear receptors that regulate expression of genes controlling multiple aspects of lipid metabolism, including uptake, storage and oxidation (186).

1.6 Macrophage metabolism

All of the metabolic pathways discussed in Section 1.5 have been shown to play important roles in the regulation of immune cell responses. Of particular relevance to my project is the metabolic control of macrophages. Much of the work that has been carried out on macrophage metabolism has focused on the two classes of polarised macrophage that are commonly referred to in the literature – M1 (classical) and M2 (alternative) (**Figure 1.3**). These phenotypes have been shown to be driven by different metabolic profiles.

An important caveat of this overview of macrophage immunometabolism is that the vast majority of research in this area has been carried out in murine bone marrow-derived macrophages (BMDMs). As I shall discuss further in Chapter 5, there are fundamental differences between the inflammatory and metabolic responses of mouse and human macrophages. Here I shall summarise the main dogma within the field of macrophage metabolism, and I will highlight aspects which may differ in human macrophages as they become relevant throughout the thesis.

1.6.1 "M1" macrophage metabolism

Classically activated (M1/M(LPS+IFNγ)) macrophages produce large quantities of pro-inflammatory cytokines such as TNFα and IL-1β (190). They also generate reactive oxygen species (ROS) and nitric oxide (NO) to assist in the killing of microorganisms. This phenotype

has been shown to be dependent upon a highly glycolytic metabolism, which results in the aerobic production of lactate as described by the Warburg effect (160, 191). It has been known for decades that macrophages stimulated with LPS show high rates of glucose uptake and increase expression of the glucose transporter GLUT1 (192, 193). This also occurs upon stimulation with alternative TLR agonists, as well as in monocyte-derived dendritic cells (MoDCs, differentiated with GM-CSF) upon TLR activation (160, 194). However it is only more recently that the implications of these observations have been investigated in greater detail. The purpose of glycolytic metabolism in pro-inflammatory macrophages appears to be many-fold; and is still incompletely understood.

2-deoxyglucose (2-DG) is a glucose analogue that enters the glycolytic pathway through phosphorylation by hexokinase, and inhibits downstream glycolysis by acting as a competitive inhibitor of phosphoglucose isomerase (195). In LPS-stimulated mouse macrophages 2-DG was shown to greatly reduce production of the pro-inflammatory cytokine IL-1β, as well as expression of monocyte chemoattractant CCL2 and the anti-inflammatory cytokine IL-10 (190, 191). In macrophages differentiated from patients with coronary artery disease, inhibition of glucose metabolism using 2-DG prevented ROS generation and downregulated expression of IL-1β and IL-6 (196). However, 2-DG has been shown to have inhibitory effects on mitochondrial metabolism as well as glycolytic, consistent with the inability of this analogue to be oxidised by the mitochondria via pyruvate entering the TCA cycle. These mitochondrial deficits could therefore contribute to the effects seen in these studies (197, 198).

The increased glycolytic flux in inflammatory macrophages not only allows rapid and controllable production of ATP, but also drives the pentose phosphate pathway for the

production of NADPH and nucleotides. NADPH is necessary for the antimicrobial production of ROS and NO in these phagocytes (199). PPP flux is inhibited by carbohydrate kinase-like protein (CARKL; aka sedoheptulose kinase/Shpk), and downregulation of this enzyme is required for M1 polarisation (199, 200). While TNFα production in stimulated macrophages was reportedly not affected by 2-DG treatment (191, 196), upregulation of CARKL or pharmacological inhibition of the rate limiting enzyme of the PPP (glucose 6-phosphate dehydrogenase) significantly inhibited expression of both IL-6 and TNFα, in addition to IL-1β and CCL2 (200). Interestingly, inhibition of lactate dehydrogenase by the pyruvate analogue oxamate, preventing conversion of pyruvate to lactate, also reduced TNFα and IL-6 production in this study (200). This suggests that redox control through the regeneration of NAD+ helps to regulate the expression of important cytokines during the macrophage inflammatory response (199).

As well as ultimately being converted to lactate, glucose metabolism in pro-inflammatory macrophages fuels the TCA cycle, which plays important signalling and catabolic roles in these cells. The TCA cycle is described as being reprogrammed in M1 macrophages, resulting in precisely controlled accumulation of certain TCA cycle intermediates (151). One of these accumulating intermediates is succinate, which regulates IL-1β production through the activation of the transcription factor HIF-1α (191). An additional role for succinate is through its export from the cell, allowing it to mediate intercellular signalling via the G protein-coupled receptor GPR91 (SUCNR1). Extracellular succinate signalling promotes inflammatory macrophage infiltration and glucose intolerance within adipose tissue in mouse models of obesity (201), as well as contributing to activated and inflammatory properties of synovial fibroblasts and endothelial cells in RA (202, 203). Succinate has also been shown to inhibit

expression of the anti-inflammatory cytokine IL-10, though the mechanism for this isn't known (204).

HIF-1α

Hypoxia-inducible factor 1 (HIF-1) is a heterodimeric transcription factor responsible for the regulation of genes important for adaptation to a low oxygen environment – termed hypoxia – including a number of metabolic genes. HIF is comprised of a constitutively expressed HIF-1β subunit (aka ARNT) and a hypoxia-dependent HIF-1α subunit (205). Under conditions of normoxia, HIF-1α is hydroxylated on two conserved proline residues by a family of prolyl hydroxylase (PHD) enzymes. This allows interaction of HIF-1α with the E3 ubiquitin ligase von Hippel-Lindau (pVHL) through hydrogen bond formation, and consequently HIF-1α is ubiquitinated and degraded by the proteasome. The proline hydroxylation reaction requires molecular oxygen and α-ketoglutarate, as well as cofactors Fe^{2+} and ascorbate, and produces succinate and CO_2. The requirement for oxygen for this reaction acts as the hypoxia sensor for stabilisation of the HIF-1α subunit, as a low oxygen partial pressure (pO_2) hinders the hydroxylation reaction, preventing the interaction with pVHL and HIF-1α ubiquitination (205, 206).

LPS stimulation of macrophages induces a state known as "pseudohypoxia", in which HIF-1α is active in the absence of a fall in pO_2 (160, 207). Activity of this transcription factor is implicated in the increased glycolytic rate of LPS-treated macrophages, as HIF-1α drives expression of a number of key rate-limiting genes in glycolysis, including GLUT-1, HK2, PFK-1 and PFKFB3 (208, 209). Loss of HIF-1α impairs glycolytic capacity and ATP production, and reduces NO production and phagocytosis, resulting in defective microbial killing. Therefore

HIF-1α deletion can alleviate chronic inflammation and protect against LPS-induced sepsis (207, 210-212). HIF-1α activity and glycolysis are also required for macrophage migration, impacting inflammation and tumour surveillance *in vivo.* This was associated with the requirement for rapid cytosolic ATP delivery to fuel cytoskeletal rearrangements (213). HIF-1α expression is also enhanced by activity of mTORC1, linking nutrient sensing to the activity of this transcription factor (187).

LPS stimulation results in upregulation of *HIF1A* mRNA through NF-κB activation (214, 215). The pseudohypoxic stabilisation of HIF-1α protein that occurs in inflammatory macrophages has been linked to the accumulation of succinate from the TCA cycle, as succinate prevents HIF-1α degradation through inhibition of PHD enzymes (191). This was originally hypothesised to be through direct product inhibition of these enzymes, however it has since been reported that a major contributing factor is succinate-driven reactive oxygen species production (*to be discussed in Section 1.7*) (190, 191). ROS have been shown to promote HIF-1α stabilisation via multiple mechanisms, including the inhibition of PHD activity through direct oxidation of cysteine residues, and through oxidation of the essential cofactor Fe^{2+} to Fe^{3+} (206, 208, 216). Further cross-talk between metabolic pathways and HIF-1α exists by the action of the glycolytic enzyme pyruvate kinase type M2 (PKM2), which forms enzymatically-inactive dimers upon LPS stimulation that translocate to the nucleus and enhance the transactivation of HIF-1α-dependent genes (164).

Another well-documented metabolic characteristic of (mouse) M1 macrophages is a strongly suppressed capacity for oxidative phosphorylation. It has been reported that the mitochondrial machinery of classically-activated macrophages is re-purposed for the

production of ROS from the ETC instead of ATP generation (190), thus the increased glycolytic rate is necessary to fulfil the cellular ATP requirements. This repurposing is dependent upon the activity of succinate dehydrogenase (SDH), which oxidises the accumulated succinate from the TCA cycle and contributes to an elevated mitochondrial membrane potential. This allows ROS production by transfer of electrons to molecular oxygen via reverse electron transport – *to be discussed in more detail in Section 1.7*. Inhibition of succinate dehydrogenase activity promoted an anti-inflammatory gene signature in mouse BMDMs (190, 204).

A second regulatory point of the TCA cycle in M1 macrophages is the decreased expression and activity of isocitrate dehydrogenase (IDH), resulting in an accumulation of citrate (172, 191). Through its conversion to acetyl-CoA in the cysosol, citrate is an important substrate for the synthesis of fatty acids, phospholipids and cholesterol (153). This is key for the production of the inflammatory signalling lipid molecules prostaglandins; as well as membrane synthesis for maintenance of the plasma membrane and endoplasmic reticulum (217, 218). The metabolism of citrate by IDH also produces NADPH, allowing generation of NO and ROS (217). Expression of the mitochondrial citrate carrier (CIC) is increased by LPS stimulation and is necessary for the use of citrate in these pathways (190).

Itaconate

Citrate is also important for the synthesis of itaconic acid/itaconate in inflammatory macrophages, and this is one of the most highly differentially expressed metabolites between M1 and M2 polarisation states (172). Itaconate is produced from cis-aconitate by the enzyme aconitate decarboxylase 1 (ACOD1), also known as immune-responsive gene 1 protein (IRG1) (**Figure 1.8**). The expression of this gene is highly induced by inflammatory stimuli including TLR agonists and type I interferons (219). The first described function of itaconate was its

direct anti-microbial action through the inhibition of the bacterial glyoxylate shunt enzyme isocitrate lyase (220).

More recently, itaconate has been shown to have important anti-inflammatory and anti-oxidant properties through a number of mechanisms (221). One such mechanism is the indirect activation of the key transcription factor Nrf2, resulting in a suite of anti-inflammatory gene expression and increased synthesis of the anti-oxidant glutathione (219, 222). Itaconate is able to directly alkylate proteins by acting as an electrophile (222), and the activation of Nrf2 occurs through alkylation of the protein KEAP1, inhibiting association of KEAP1 with Nrf2 and preventing the stimulation of Nrf2 degradation (219). Itaconate also modifies cysteine residues of glycolytic enzymes such as GAPDH, inhibiting the glycolytic flux necessary for many pro-inflammatory functions (219, 223).

The anti-inflammatory effects of itaconate have also been attributed to inhibition of succinate dehydrogenase activity, as itaconate is structurally similar to malate, a potent SDH inhibitor (224). *Irg*-KO BMDMs showed increased LPS-induced production of multiple inflammatory mediators, including NO, IL-1β, IL-6, IL-12p70 (but not TNFα), as well as increased *Hif-1α* expression. Strikingly, Lampropoulou *et al* showed that KO of *Irg1* completely abolished the decrease in oxidative respiration seen in mouse macrophages upon LPS stimulation, and oxygen consumption was enhanced with LPS treatment in these cells (225). A negative feedback loop involving interferon signalling and itaconate has been reported. Full induction of *Irg1* expression was shown to require signalling through the type I interferon receptor, but exogenously supplied itaconate was found to inhibit expression of IFN-β (219,

226). *In vivo,* loss of itaconate synthesis through *Irg1* deletion resulted in a fatal inflammatory response to *M. tuberculosis* infection (227).

Due to its induction by inflammatory stimuli and strong anti-inflammatory properties, itaconate is a key player in the induction of tolerance in myeloid cells, and has been linked to the overwhelming immune paralysis that occurs during sepsis (228). Conversely, the induction of trained immunity – a phenomenon in which certain immune stimuli induce a state of hyper-responsiveness in myeloid cells – involves the suppression of itaconate activity. β-glucan was found to inhibit *Irg1* expression, allowing continued activity of SDH and resulting in an elevated secondary response to inflammatory stimulus (229).

These and other data show that itaconate functions as a negative feedback regulator to inhibit inflammatory signalling after an initial pro-inflammatory response (219, 225, 230). Itanonate has also been described to have pro-tumour properties, and to suppress viral replication in neuronal cells (230).

Due to the removal of carbon from the TCA cycle for increased production of itaconate and fatty acids; and the decreased entry of pyruvate into the TCA cycle owing to preferential lactate production, TCA cycle intermediates must be replenished from other sources – a process known as anaplerosis (153). Succinate is replenished through the breakdown of glutamine (glutaminolysis) as well as contribution from the GABA shunt (**Figure 1.8**). This is facilitated by upregulation of the glutamine transporter (Slc3a2) in pro-inflammatory macrophages (191). Glutamine has been reported to be required for NO synthesis in M1 macrophages (231), however Jha *et al* reported minimal defects in M1 signatures upon glutamine deprivation (172). The aspartate-arginosuccinate shunt connects the TCA cycle with

the urea cycle and replenishes TCA cycle malate in LPS-stimulated macrophages. This pathway also helps to maintain production of NO through generation of arginine, the substrate for nitric oxide synthase (NOS)-mediated NO production (153, 172).

Interferons have been shown to regulate multiple metabolic processes, which likely contribute to their immune function (232). While macrophages are typically treated with the type II interferon IFNγ in order to induce M1 programming *in vitro*, which contributes to the metabolic phenotype thus far described, type I interferons also elicit metabolic reprogramming. In addition to the reported role of IFNAR in *Irg1* induction, feedback signalling through this receptor to HIF-1α was shown to be vital for the metabolic shift to glycolysis upon treatment of DCs with the TLR3 agonist poly(I:C), consistent with the reduced anti-viral capacity of cells lacking IFNAR (233). Type I interferons have also been reported to inhibit cholesterol and fatty acid biosynthesis, which are vital for viral replication (232). As well as regulating metabolic processes themselves, the production of interferons is also regulated by cellular metabolic status, mediated by the mTOR complexes, demonstrating the two-way communication that appears to be characteristic of immune signalling and metabolic pathways (232).

1.6.2 "M2" macrophage metabolism

Alternatively activated macrophages (M2/M(IL-4)) promote resolution of inflammation, wound healing and anti-helminth immunity. They express Th2 and Treg-promoting factors; show surface expression of scavenger receptors; and metabolise arginine via arginase to produce polyamines and proline (12). This discrepancy in arginine metabolism is one of the earliest described metabolic distinctions between classical and alternative macrophages, and is commonly used as a marker of macrophage phenotype (33, 35).

In comparison to the decreased mitochondrial metabolism described for M1 mouse macrophages, M2 macrophages are driven by high rates of oxidative phosphorylation and an intact TCA cycle (218). One way in which oxidative metabolism is promoted in these cells is through high activity of AMPK, which regulates multiple signalling pathways including HIF-1 and mTOR, with an overall anti-inflammatory outcome (187). Oxidative respiration is vital for the M2 phenotype, and capacity for mitochondrial respiration has been shown to determine whether a macrophage can be repolarised to an anti-inflammatory state. This may have important implications for translational immunology, as the repurposing of macrophages has been suggested as a treatment option for inflammatory conditions (234).

Whilst glycolysis is typically seen as a defining characteristic of M1 macrophages, glucose metabolism is also increased by IL-4 stimulation, compared with M0 (unstimulated) cells. Glycolysis in M2 cells was found to be driven by a signalling cascade involving M-CSF, STAT6, mTORC2 and IRF4. Much of the glucose-derived pyruvate in these cells enters the mitochondria and helps to fuel high rates of oxidative metabolism (235). This is facilitated by the upregulation of CARKL kinase by IL-4, thereby inhibiting flux through the PPP (200). 2-DG has previously been shown to impair IL-4-mediated M2 polarisation, however more recently it was demonstrated that this effect is in fact due to the actions of 2-DG on oxidative metabolism rather than glycolysis, resulting in reduced ATP levels and impaired JAK-STAT6 signalling. The authors showed that glycolysis was dispensable for M2 polarisation as long as oxidative metabolism wasn't compromised (198). Despite the observed increase in glycolytic capacity in M2 compared with M0 macrophages, IL-4-stimuated cells retain expression of the PFKFB1 isoform of PFK-2, which has relatively low kinase activity, in contrast to M1 macrophages in which a key event is the switch to PFKFB3 (160).

Fatty acid oxidation (FAO) is strongly induced by IL-4, and has been described as being vital for M2 macrophage polarisation. IL-4-treated macrophages increase expression of genes associated with fatty acid uptake and oxidation, which helps to fuel mitochondrial ATP production (236). This is achieved by STAT6-mediated activation of PPARs γ and δ, as well as the PPARγ co-activator PGC-1β. Genetic ablation of PPARγ, silencing of PGC-1β, or inhibition of the key mitochondrial fatty acid transporter CPT1 with etomoxir have all been shown to inhibit expression of M2-associated markers and anti-inflammatory function (186, 236, 237). Uptake of lipoproteins via CD36 and delivery of triacylglycerol to lysosomes fuels lipolysis in these cells, and were found to be necessary for efficient parasite clearance *in vivo* (236).

Whilst many studies have quoted the necessity for FAO for M(IL-4) macrophage activation, this has more recently been brought into question. The use of etomoxir should be approached with caution, as high concentrations of this drug (>5μM) have been shown to induce effects independent of CPT1 inhibition, including inhibition of complex I, induction of oxidative stress, and Coenzyme A depletion (238, 239). The deletion of *Cpt1* or *Cpt2* did not prevent M2 polarisation, indicating that FAO is dispensable. The Coenzyme A depletion caused by excessive etomoxir was found to be responsible for the polarisation defects previously attributed to FAO inhibition (238). It has also been demonstrated that human monocyte-derived macrophages show only modest upregulation of oxidative phosphorylation and FAO upon IL-4 treatment, and inhibition of FAO in this context did not prevent M2 gene expression or anti-inflammatory function (189).

Glutamine is another important fuel for M2 macrophages, and these cells derive much of their TCA cycle carbon from glutamine. Deprivation of this amino acid was shown to greatly impair the M2 gene expression signature (e.g. *Cd206*, *Ccl22*, *Irf4, Arg1*), as well as TCA cycle

gene expression (172, 240). Production of the TCA cycle intermediate α-ketoglutarate via glutaminolysis was found to be necessary for elevation of oxidative respiration in response to IL-4. This occurs through reversal of inhibitory histone methylation at M2-associated genes, and the ratio of α-ketoglutarate to succinate abundance regulates M1/M2 polarisation through epigenetic modulation (240).

In addition, glutamine is a key substrate for the production of UDP-N-acetyl-glucosamine (UDP-GlnNAc) (172). Glucosamine synthesis through the hexosamine biosynthesis pathway utilises glucose and glutamine as carbon and nitrogen sources, respectively. The added acetate to create N-acetyl-glucosamine is derived from fatty acid metabolism, and the UDP stems from nucleotide metabolism, therefore this pathway combines metabolism from all major classes of macromolecule. UDP-GlnNAc is a vital substrate for *O*-glycosylation of intracellular proteins and *N*-glycosylation of extracellular proteins, and this molecule serves as an important link between metabolism and signalling, for example *O*-glycosylation of PFK-1 alters its enzymatic activity and regulates glycolytic flux (231). UDP-GlnNAc is essential for glycosylation of M2-specific mannose receptors e.g. CD206, thus its depletion impairs M2 function (172).

In the field of cancer immunology, the enzyme glutamine synthetase (GS/GLUL) has gained attention for its requirement for the M2 characteristics of tumour-associated macrophages (TAMs). Expression of this enzyme is induced by M2-like stimuli such as IL-4 and IL-10, and its inhibition causes decreased expression of typical M2 marker genes, and suppression of tumour-promoting capabilities of TAMs (241). The inhibition of GS also promotes an inflammatory response in microglial cells, pointing to a more universal role for this enzyme in myeloid cell anti-inflammatory action (242).

While not considered a prototypical M2-polarising cytokine, IL-10 has anti-inflammatory properties and induces an M2-like phenotype with many overlapping characteristics to IL-4/IL-13 polarisation (243). Alterations in metabolism have been shown to underpin the anti-inflammatory actions of IL-10, including inhibition of the glycolytic shift and rescue of basal and maximal oxidative respiration in response to LPS (244). Other key finding are the inhibition of mitochondrial ROS production by IL-10; and the induction of mitophagy, allowing degradation of dysfunctional mitochondria and maintenance of mitochondrial integrity. The mechanism for this was found to be through increased expression of DDIT4, a negative regulator of mTOR, thereby preventing the inhibition of autophagy by mTORC1 (244).

As discussed in Section 1.2, the M1/M2 dichotomy is an over-simplification of the complexity of macrophage function, and the intricacies of macrophage metabolism can be demonstrated in certain *in vivo* situations. In the study of tumour-associated macrophages (TAMs), is has been shown that hypoxic areas of a tumour drive the expression of HIF-1α in infiltrating macrophages. In contrast to the reported role of HIF-1α in M1 function seen during *in vitro* macrophage polarisation with LPS (191), TAM expression of HIF-1α has been associated with an M2-like phenotype, promoting tumour survival through suppression of T cell effector activity and stimulation of dysregulated angiogenesis (231). In adipose tissue, excess fatty acids associated with obesity result in an inflammatory phenotype in infiltrating and tissue resident macrophages, which contributes to insulin resistance. This is contrary to the association of fatty acid uptake and oxidation with anti-inflammatory function as described for IL-4-mediated polarisation. Short chain saturated fats have also been shown to activate TLRs (189). Therefore while the M1/M2 paradigm is useful for the segregation of inflammatory

vs homeostatic function, this oversimplified view may be misleading, and detailed study of *in vivo* or *ex vivo* metabolic function in specific tissues or disease states will likely be necessary to take the field forward.

Despite the over-simplification, the contrast in metabolic phenotype between M1 and M2 macrophages highlights the importance of metabolic control for the function of these cells. Many of the studies mentioned above have demonstrated that specific targeting of metabolic components can have profound effects on aspects of macrophage behaviour, which has important therapeutic implications.

1.7 Reactive Oxygen Species and Nitric Oxide

1.7.1 Reactive oxygen species

Cellular reactive oxygen species (ROS) are generated by a variety of mechanisms, and it is now known that their synthesis is highly regulated, contributing to multiple areas of cell signalling and the immune response. In the field of macrophage biology, the most widely studied sources of ROS are phagosomal NADPH oxidase, and the mitochondrial ETC (245). Several other sources contribute smaller amounts of ROS, including peroxisomes and the endoplasmic reticulum (175), and other mitochondrial sources such as monoamine oxidases can also generate significant ROS (246, 247), but I shall not focus on these.

Phagocytes utilise ROS for direct microbial killing by release into the phagosome. NADPH oxidase is a membrane-bound enzyme that makes use of NADPH for the production of superoxide radicals ($O_2^{\bullet-}$). The enzyme is assembled upon activation of phagocytosis-associated receptors such as Fcγ receptors and CD11b, and the active site faces the extracellular compartment, allowing superoxide to be produced within phagosomes (248).

Macrophages highly express DNA repair enzymes and free radical scavengers, allowing them to survive oxidative bursts (245).

The other major source of ROS is the mitochondrion, which can generate superoxide, hydrogen peroxide (H_2O_2) and the hydroxyl free radical ($\bullet OH$), collectively termed mitochondrial ROS (mROS) (249). Superoxide is generated by the electron transport chain by the transfer of an electron to molecular oxygen. Important determinants of both mechanism and rate of superoxide generation include the following: proton motive force (pmf) across the inner mitochondrial membrane; concentration of electron donor NADH; reduction status of CoQ electron acceptor; and local oxygen concentration (250).

One mechanism of superoxide generation is by forward transport of electrons from a fully reduced flavin monoucleotide (FMN) group in complex I (CI) to oxygen. The CI inhibitor rotenone can increase ROS production by this mechanism, by preventing transfer of electrons from CI to CoQ, maintaining a reduced FMN site (250, 251). CI receives electrons from reduced NADH, therefore the generation of superoxide by this method is favoured by a high NADH/NAD+ ratio (190, 250).

An alternative mechanism of superoxide production at CI is through the process of reverse electron transport (RET). During this process electrons travel in the reverse direction through CI from CoQ to the FMN group and either back to NAD+ or to reduce oxygen (**Figure 1.9**) (250, 251). This is driven by a high pmf, along with a large pool of reduced CoQ (251). RET can therefore be induced by an accumulation of succinate, since the oxidation of succinate by complex II (SDH/CII) drives reduction of CoQ and an increased pmf through proton pumping by CIII and CIV. This has been shown to occur during ischaemia-reperfusion injury, where

accumulation of succinate during ischaemia results in mROS production upon reperfusion, which is responsible for early tissue damage (251). This is also the proposed mechanism for the production of mROS in inflammatory macrophages, explaining the dependence on SDH activity described by Mills *et al* (204). Interestingly, it has been shown that while stimulation of cell surface TLRs (1,2&4) induces mROS production in BMDMs and RAW264.7 cells, no induction is seen by stimulation of endosomal TLRs (3,7,8&9), which are associated with the induction of an antiviral immune response (252).

Complex III has also been cited as a site of mROS production. This occurs in the presence of antimycin, which blocks one of the Q sites in CIII, resulting in interation of oxygen with the highly reactive ubisemiquinone at the other site. However in physiological contexts CIII-derived superoxide has been suggested to be insignificant compared with that derived from CI (250).

In addition to promoting HIF-1α stabilisation, as described in Section 1.6, ROS have been shown to enhance MAPK signalling. This occurs through oxidation of cysteine residues of MAPK phosphatases, inhibiting their activity and increasing MAPK phosphorylation (253). Scavenging of mROS in PBMCs reduced LPS-induced production of cytokines associated with MAPK signalling (TNF-α, IL-10 and IL-6); and mROS were also implicated in the elevated expression of IL-6 in patients with TNF receptor-associated periodic syndrome (TRAPS) (254). ROS can also activate the NLRP3 inflammasome, resulting in release of the mature forms of IL-1β and IL-18 (190, 255). As well as contributing to intracellular signalling, mROS engage in direct bacterial killing similarly to NADPH oxidase-derived ROS. This is accomplished by the recruitment of mitochondria to the phagosome, allowing mROS to accumulate to high concentrations. This recruitment is mediated by interaction between the TLR signalling

adaptor TRAF6 and the mitochondrial protein ECSIT (252). Extracellular ROS can also act as paracrine and autocrine signals (245).

1.7.2 Nitric oxide

Nitric oxide (NO/•NO) is a free radical species that is produced by nitric oxide synthase (NOS) enzymes, utilising arginine, NADPH and oxygen (256). Hibbs *et al* made the discovery that deimination of L-arginine to produce nitrite (NO_2^-) is an important part of the effector function of stimulated macrophages (257). Nitrite is the stable oxidation product of NO and can be used as a readout of NO production, utilising the Griess reaction. In mouse macrophages, NO is produced in response to LPS or cytokines through expression of inducible nitric oxide synthase (iNOS) (256, 258). Similarly to ROS, this NO has direct bactericidal effects, and contributes to macrophage-mediated tumour cell killing (258). NO is now also known to be a key contributor to macrophage metabolic reprogramming (234).

Low levels of NO specifically and reversibly inhibit the activity of cytochrome c oxidase by competing with molecular oxygen, thereby decreasing oxidative respiration. NO interacts with the reduced heme iron (Fe^{2+}) of cytochrome a3 and the copper centre CuB, which constitute the oxygen binding site of CIV. NO can associate with and dissociate from CIV rapidly, hence the reversible nature of the inhibition (259). High levels or prolonged exposure of mitochondria to NO can also irreversibly inhibit other ETC complexes, for example by displacement of the iron centre of CII, or direct S-nitrosylation at CI (259, 260). The latter effect was found to be dependent upon depletion of the pool of reduced glutathione, which continuously counteracts the repressive action of NO at CI (260). NO can be converted to a number of alternative reactive nitrogen species (RNS), which also have inhibitory effects on respiration (259). Peroxynitrite ($ONOO^-$) is formed by the reaction of NO with superoxide, and

is a potent oxidant that can lead to DNA damage and lipid peroxidation. Peroxynitrite is thought to mediate some of the irreversible effects on mitochondrial respiration that occur following NO generation, including inhibition of CI and CII, as well as the TCA cycle enzyme aconitase. Peroxynitrite-mediated effects are thought to occur by nitrosylation of protein thiols, as well as thiol crosslinking, resulting in protein modification and loss of iron from iron-sulphur centres (259).

Metabolic reprogramming of macrophages by NO is thought to occur through inhibition of CIV, as well as CI inhibition if the pool of reduced glutathione is diminished. NO has also been implicated in the reduced expression of several CI subunits in response to LPS+IFNγ (209). When NO production is prevented, e.g. by the iNOS inhibitor 1400W or knock out of the iNOS-encoding gene (*Nos2*), oxidative respiration can be partially rescued in LPS+IFNγ stimulated macrophages (209, 234). This enabled improved repolarisation of M1 cells to an M2 phenotype upon IL-4 treatment, implicating NO activity in the irreversible nature of inflammatory polarisation in mouse macrophages. However NO was shown not to be required for polarisation to M1 in the first instance, shown by LPS+IFNγ treatment of *Nos2*-KO BMDMs (234). It has also been shown that the decrease in oxygen consumption induced by stimulation of macrophages with IFNγ alone is not rescued by inhibition of NO production (197). Therefore the role of NO in the metabolic changes seen in inflammatory macrophages still needs further investigation, and is likely not the only mechanism responsible for respiratory inhibition in these cells.

The relationship between NO and HIF-1α signalling is complex. NO has been shown to increase HIF-1α activity, both through inducing protein synthesis (261), and through direct nitrosation of HIF-1α protein leading to increased interaction with its coactivator p300 (262).

As HIF-1α is a key driver in both metabolic and inflammatory changes of activated macrophages, this could be another mechanism of regulation of these factors by NO. However, instead of increasing the production of the HIF-1α target IL-1β, NO has been found to decrease the release of mature IL-1β, due to nitrosylation of NLRP3 and inhibition of inflammasome assembly. This effect may have a role in reducing IL-1β-mediated tissue damage during chronic infection (263).

A major complication in understanding the role of NO in macrophage inflammatory responses is the difference in its production between species, most relevantly between mouse and human (264). NO production by human monocytes and macrophages has been historically controversial, with some researchers stating that induction of NO synthesis can be seen *in vivo* but not *in vitro* (35, 265). The nature of the inflammatory stimulus has also been described as an important factor, with LPS alone or the typical M1-inducing stimulus of LPS+IFN-γ not leading to detectable production in many cases, but other stimuli such as live bacteria or immune complexes able to induce NO synthesis (266, 267). It has been reported that PBMCs from RA patients display elevated NOS activity and could be stimulated to produce nitrite by LPS and/or IFNγ, while healthy controls could not (268). NO has also been linked to other inflammatory or infectious diseases, including atherosclerosis and tuberculosis (35, 266, 267).

The origin of the macrophage being studied is also a potential confounding factor for direct comparison of NO production and metabolic phenotype. For example, tissue macrophages and monocyte-derived macrophages originate from different stem cell populations, and *in vitro* differentiation may alter gene expression and responses to inflammatory challenge (35). Strikingly, dramatic differences in metabolic response to stimulus have been reported even between cells derived from the same species. A comparison

of mouse BMDMs and peritoneal macrophages (a monocyte-derived cell that differentiates *in vivo*) revealed that the latter actually showed increased oxidative respiration in response to LPS treatment. This was linked to lower iNOS levels and greater arginase expression in peritoneal macrophages, implicating lack of NO signalling in the differential respiratory phenotype. This effect was despite the fact that the two macrophage types show around 90% similarity in global gene expression upon LPS stimulation (269). Different strains of mice also show varying propensities to express iNOS or arginase in response to stimuli, and this was exploited relatively early in the history of this field to examine M1 vs M2 macrophage responses (33).

What can be said for certain is that NO production by human monocyte-derived macrophages is not consistently observed, and the production that has been reported is to a much lesser degree than that produced by mouse macrophages (266). This would suggest that NO is not responsible for the metabolic adaptations of human macrophages, and that results obtained in mouse BMDMs are not directly translatable.

1.8 Hypotheses and Aims

Hypothesis 1: Glucocorticoids carry out their anti-inflammatory actions in macrophages at least in part through the regulation of microRNA species.

Chapter 3 Aims:

- To identify microRNA species regulated by glucocorticoid treatment of macrophages and characterise their regulation

Chapter 4 Aims:

- To identify potential targets of miRNA-147b and validate their functional targeting in macrophages
- To investigate the regulation of these targets in response to inflammatory stimuli and glucocorticoids

Based upon the findings from my first two results chapters I developed additional hypotheses:

Hypothesis 2:

a) Glucocorticoids regulate macrophage metabolism
b) This metabolic regulation contributes to the anti-inflammatory action of the steroids

Hypothesis 3: miR-147b alters macrophage metabolism through the targeting of mitochondrial protein NDUFA4

Chapter 5 Aims:

- To identify metabolic effects of glucocorticoid treatment of macrophages
- To investigate the mechanisms of this metabolic regulation

Chapter 6 Aims:

- To determine the effects of NDUFA4 regulation on macrophage metabolism
- To determine the effects of NDUFA4 regulation on macrophage inflammatory function

Chapter 2) MATERIALS AND METHODS

Materials

2.1 Cell Culture

Table 2.1.1) Cell culture general reagents

Reagent	Supplier	Cat #	Cell type
RPMI1640 Med 1X w/L-Glutamine 500 ml (contains phenol red and sodium bicarbonate)	Gibco (ThermoFisher)	21875034	Human mφ
RPMI-1640 Medium With L-glutamine and sodium bicarbonate, liquid, sterile-filtered, suitable for cell culture	Sigma Aldrich	R8758-500ML	Mouse mφ
Fetal bovine serum (FBS) *Referred to as FCS*	Biosera	FB-1001	Human mφ Mouse mφ HEK293 RAW264.7
Penicillin. Streptomycin Soln. 10000units 100ml	Gibco (ThermoFisher)	15140122	Mouse mφ HEK293 RAW264.7
Cell Dissociation Buffer, enzyme-free, PBS	Gibco (ThermoFisher)	13151014	Human mφ Mouse mφ RAW264.7
Phosphate buffered saline (PBS) tablets 1 tablet per 500ml distilled water	Gibco (ThermoFisher)	18912014	Human mφ Mouse mφ HEK293 RAW264.7
DMEM High Glucose 500 ml	Sigma Aldrich	D5796-500ML	HEK293 RAW264.7
Trypsin-EDTA solution (10x)	Sigma Aldrich	T4174-100ML	HEK293

Table 2.1.2) Cell culture plasticware

Item	Supplier	Cat #	Cell type
TC Dishes 100mm (20-sleeve)	Corning	BC153	Human mφ Mouse mφ
Costar Multiple Well Cell Culture Plates (6-well, 12-well, 24-well, 48-well, 96-well)	Corning	3335; 3336; 3337; 3338	Human mφ Mouse mφ HEK293 RAW264.7
Corning TC Flask 75cm2 canted neck vented cap (100**)**	Corning	BC301	HEK293 RAW264.7
Cell lifter	Fisher Scientific	08-100-240	Human mφ Mouse mφ
Cell scraper	Starstedt	83.1830	RAW264.7

Table 2.1.3) Human monocyte isolation

Reagent	Supplier	Cat #
Ficoll-Paque PLUS	VWR	17144003
Percoll(R) PLUS	Sigma Aldrich	GE17-5445-01
***RosetteSep Human Monocyte Enrichment Cocktail** (5x2ml)	Stemcell	15068

EasySep Human Monocyte Enrichment Kit (sample kit)	Stemcell	19059
Ethylenediaminetetraacetic acid disodium salt solution (EDTA)	Sigma Aldrich	E7889-100ML

*Chosen reagent after comparison of isolation protocols

Table 2.1.4) Cytokines, stimulants and inhibitors

Reagent	Supplier	Cat #	Stock concentration	Final concentration
M-CSF used for both mouse and human	Gifted (2016 – Feb 2018)	N/A	100µg/ml	50ng/ml
Recombinant human M-CSF used for both mouse and human	Peprotech (Feb 2018 onwards)	300-25	100µg/ml	50ng/ml
LPS (E. coli, Serotype EH100 (Ra) (TLRgrade™))	Enzo Life Sciences	ALX-581-010-L002	1mg/ml	10ng/ml
Dexamethasone (powder, γ-irradiated, BioXtra, suitable for cell culture, ≥80% (HPLC))	Sigma Aldrich	D8893-1MG	1mM	100nM
Recombinant human IFN-β (cross-reacts with mouse)	Peprotech	300-02BC	1mg/ml	10ng/ml
Ruxolitinib	Selleck	S1378	10mM	1µM
TLR agonist kit	Invivogen	tlrl-kit1hw	-	See Figure 4.6
Pam3CSK4		tlrl-pms	1mg/ml	1µg/ml
Poly (I:C) HMW		tlrl-pic	1mg/ml	10 µg/ml
Cycloheximide	Sigma Aldrich	01810	100mg/ml	5µg/ml

2.2 Flow Cytometry

Table 2.2.1) Flow cytometry antibodies for monocyte/macrophage characterisation

Target	Fluorochrome	Supplier	Clone	Cat #	Dilution
CD14 (human)	PE	Biolegend	63D3	367104	1/100
Isotype	PE		MOPC-21	400113	1/20
CD163 (human)	FITC	BD	GHI/61	563697	1/20
Isotype	FITC		MOPC-21	554679	1/20
CD64 (human)	PerCP-eFluor710	eBioscience	10.1	46-0649-41	1/20
Isotype	PerCP-eFluor710		P3.6.2.8.1	46-4714-80	1/20
CD206 (human)	APC	Biolegend	15-2	321110	1/20
Isotype	APC		MOPC-21	400119	1/20
CD16 (human)	APC-eFluor780	eBioscience	eBioCB16	47-0168-41	1/20
Isotype	APC-eFluor780		P3.6.2.8.1	47-4714-80	1/20
Fixable Viability Dye	eFluor780		-	65-0865	1/1000
Fixation Buffer	-	Biolegend	-	420801	-

Table 2.2.2) Mitochondrial staining reagents

Reagent	Supplier	Cat #
MitoTracker™ Green FM	Invitrogen (ThermoFisher)	M7514
MitoTracker™ Red CMXRos		M7512
MitoSOX™ Red Mitochondrial Superoxide Indicator	ThermoFisher	M36008
HBSS + calcium + magnesium, no phenol red	Gibco (ThermoFisher)	14025050

2.3 Transfections

Table 2.3.1) General transfection reagents

Item	Supplier	Cat #
Opti-MEM I Reduced Serum Medium	Gibco (ThermoFisher)	31985070
TransIT-TKO Transfection Reagent	Geneflow (Mirus)	Geneflow - E7-0106; Mirus - MIR 2150
***TransIT-X2 Transfection Reagent**	Geneflow (Mirus)	Geneflow - E7-0176; Mirus - MIR 6004
5X siRNA Buffer - 100ml	Dharmacon	B-002000-UB-100
miRIDIAN hairpin inhibitor Dy547 labelled control (transfection efficiency control)	Dharmacon	IP-004500-01-05

*Chosen reagent after comparison of transfection protocols

Table 2.3.2) miRNA mimics

Item	Supplier	Cat #
miRIDIAN miRNA mimic Negative Control #1		CN-001000-01-05
miRIDIAN miRNA mimic Negative Control #2	Dharmacon	CN-002000-01-05
miRIDIAN miRNA mimic hsa-miR-147b		C-301239-01-0005

Table 2.3.3) miRNA inhibitors

Item	Supplier	Cat #
miScript Inhibitor Neg. Control		1027271
Anti-hsa-miR-155-5p miScript miRNA Inhibitor		MIN0000646
Anti-hsa-miR-147b miScript miRNA Inhibitor		MIN0004928
***Negative control A miRCURY LNA miRNA Power Inhibitor Control,** Power Inhibitor / PS, 1 nmol, no label (YI00199006-DCA)	Qiagen	339135
***hsa-miR-147b miRCURY LNA miRNA Power Inhibitor,** Power Inhibitor / PS, 1 nmol, no label (YI04100977-DCA)		399130

Table 2.3.4) siRNAs

Item	Supplier	Cat #	Sequence
ON-TARGETplus Non-targeting Pool		D-001810-10-05	UGGUUUACAUGUCGACUAA UGGUUUACAUGUUGUGUGA UGGUUUACAUGUUUUCUGA UGGUUUACAUGUUUUCCUA
SMARTpool: ON-TARGETplus NDUFA4 siRNA – Human (Upgraded to individual siRNAs)		L-019200-01-0005	09: CCGCACAAUUUUCCACUUA 10: GUGUAUAGACUGUUGGUAA 11: AAGUAAAUUGGGAAGGAUA 12: CUUCACUAGAGCAUACAUA
ON-TARGETplus Non-targeting siRNA #1	Dharmacon	D-001810-01-05	UGGUUUACAUGUCGACUAA
siGENOME Non-Targeting siRNA #1		D-001210-01-05	UAGCGACUAAACACAUCAA
siGENOME Non-Targeting siRNA #2		D-001210-02-05	UAAGGCAUGAAGAGAUAC
siGENOME Non-Targeting siRNA #3		D-001210-03-05	AUGUAUUGGCCUGUAUUAG
Set of 4 Upgrade: siGENOME NDUFA4 siRNA - Human		MU-019200-00-0002	01: GAUCAUCGGUCAGGCCAAG; 02: CACUGUAUCUCUUGCGUCU; 03: GUUUGUUGGGACAGAAAUA 04: AGGAACGUCCAGAUUUCUA

2.4 RNA isolation and RT-qPCR

Table 2.4.1) RNA isolation, cDNA synthesis and RT-qPCR general reagents

Item	Supplier	Cat #
*Total RNA Purification Plus Kit	Norgen (Geneflow)	48400 (P4-0016)
miRNeasy Mini Kit	Qiagen	217004
RNeasy Mini Kit	Qiagen	74106
Quick-RNA Miniprep	Zymo Research	R1054
miScript II RT Kit	Qiagen	218161
miScript SYBR Green	Qiagen	218075
SYBR TB Green Premix Ex Taq	Takara	RR820W

*Chosen kit after comparison of isolation protocols

Table 2.4.2) miRNA primers

Target	Item	Supplier	Cat #
RNU6-6P RNA, U6 small nuclear 6, pseudogene	Hs_RNU6-2_11 miScript Primer Assay		MS00033740
mmu-miR-155-5p	Mm_miR-155_1 miScript Primer Assay		MS00001701
hsa-miR-155-5p	Hs_miR-155_2 miScript Primer Assay		MS00031486
mmu-miR-146a-5p	Mm_miR-146_1 miScript Primer Assay		MS00001638
hsa-miR-146a-5p	Hs_miR-146a_1 miScript Primer Assay	Qiagen	MS00003535
mmu-miR-21a-5p	Mm_miR-21_2 miScript Primer Assay		MS00011487
hsa-miR-21-5p	Hs_miR-21_2 miScript Primer Assay		MS00009079
mmu-miR-147-3p	Mm_miR-147_2 miScript Primer Assay		MS00032333
hsa-miR-147b-3p	Hs_miR-147b_1 miScript Primer Assay		MS00008729

Table 2.4.3) mRNA primers - DNA oligonucleotide primers supplied by Eurofins Genomics

Gene	Species	Fwd primer sequence	Rev primer sequence
UBC	Human	CGGGATTTGGGTCGCAGTTCTTG	CGATGGTGTCACTGGGCTCAAC
pri-mir-147b (C15orf48)	Human	GCACAAACTAGATTCTGGACACCA	AAGCACAAACTTTTAGACAGTGC
NDUFA4	Human	AAGCATCCGAGCTTGATCCC	ACAATGCCAGACGCAAGAGA
LONP1	Human	CGGGAAGATCATCCAGTGTT	ACGTCCAGGTAGTGGTCCAG
SDHD	Human	CATACACTTGTCACCGAGCCA	AACTTGTCCAAGGCCCCAGTG
ALDH5A1	Human	CAGTCATCACCCCGTGGAAT	GGCTTCACCACGACAGTACA
SLC2A1 (Glut1)	Human	GAACTCTTCAGCCAGGGTCC	ACCACACAGTTGCTCCACAT
HK2	Human	CCTGAGGACATCATGCGAGG	CAAAGTCCCCTCTCCTCTGGA
PFKFB3	Human	GCGATGCCCTTCAGGAAAGC	TACTCCCCGACGTTGAACAC
HIF-1A	Human	GTTTACTAAAGGACAAGTCAC	TTCTGTTTGTTGAAGGGAG
SLC16A3 (MCT4)	Human	CCAAGCCGCAAGGTTACAAG	CACCCACCCTCCCATTAAAGTC
NDUFA4L2 (set 1)	Human	TTCTACCGGCAGATCAAAAGACA	GGGCGAGTCGCAGCAA
NDUFA4L2 (set 2)	Human	CAAAAGACATCCGGGGATCA	GCGAGTCGCAGCAAGTAAAG
β-2-microglobin	Mouse	CTGCTACGTAACACAGTTCCACCC	CATGATGCTTGATCACATGTCTCG
Tnfa	Mouse	CAGAAAGCATGATCCGCGAC	TCTGAGTGTGAGGGTCTGGG
Rpl13a	Mouse	GCGGATGAATACCAACCCCT	CCACCATCCGCTTTTTCTTGT
Ndufa4	Mouse	AGATGTCAGCTGGGACAGAAA	GTGCGGATGGCTTCTGAAAG

2.5 Western Blotting

Table 2.5.1) RIPA Buffer composition

NaCl	1M
NP-40 (Igepal)	1%
Sodium Deoxycholate	0.5%
SDS	0.1%
Tris HCl (pH8)	50mM

Table 2.5.2) 5X Loading Dye composition

Bromophenol blue	0.6mg/ml
SDS	4%
glycerol	30%
B-mercaptoethanol	16%
Tris (pH6.8)	0.25M

Table 2.5.3) Western blotting general reagents

Item	Supplier	Cat #
cOmplete(TM), Mini Protease Inhibitor Cocktail	Roche	04 693 124 001
Phostop 20 tablets	Roche	04 906 837 001
Qiashredder	Qiagen	79656
Pierce™ BCA Protein Assay	ThermoFisher	23225
Criterion TGX Protein Gel, 12+2 well, 45ul (4-20%)	BioRad	5678093
SDS PAGE Tank Buffer (10 X) Tris-Glycine SDS	Geneflow	B9-0032
Trans-Blot Turbo Transfer Pack, PVDF, 8.5 x 13.5 cm, 10 pack	BioRad	1704157
Tween-20	ThermoFisher	10113103
Anti- rabbit lgG, HRP linked	NEB	7074SNEB
Anti-mouse lgG, HRP linked		7076SNEB
ECL Western Blotting Reagent	GE Healthcare	RPN2106
ReBlot Plus 10X mild Antibody stripping solution	Sigma Aldrich	2502
BLUeye Pre-Stained Protein Ladder 10-245kDa	Geneflow	S6-0024

Table 2.5.4) Western blotting primary antibodies

Target	Supplier	Cat #	Host Species	Species used for	Dilution	Dilute in:
NDUFA4	ThermoFisher	PA5-50068	Rabbit	Human	1/5000	5% Milk
NDUFA4	Stratech (Bioworld Technology)	BS3883-BTW	Rabbit	Mouse	1/800	5% Milk
SDHA	Abcam	ab14715	Mouse	Human	1/2000	5% Milk
α-tubulin	Sigma Aldrich	T9026 (DM1A)	Mouse	Human	1/2000	5% Milk
β-actin	Sigma Aldrich	A1978	Mouse	Mouse (also compatible with human)	1/5000	5% Milk
HIF-1α*	BD	610959	Mouse	Human	1/500	**1% Milk**

Pro-IL-1β	Chemicon	AB2144P[#]	Rabbit	Human	1/200	5% Milk
MT-CO1**	Abcam	ab14705	Mouse	Human	1/1000	5% Milk
COXIV-1	Abcam	ab14744	Mouse	Human	1/1000 (1ug/ml)	5% Milk
NDUFA4L2	Abcam	ab74138	Rabbit	Human	1/1000	5% Milk
NDUFA4L2	Proteintech	66050-1-Ig	Mouse	Human	1/1000	5% Milk
C15orf48	Abcam	ab128382	Rabbit	Human	1/1000	5% Milk

*Harvest samples in 1x loading dye instead of RIPA; **Do not boil samples before loading; [#] Out of production

2.6 Luciferase Assay (& cloning)

Table 2.6.1) Luciferase Assay and Cloning Reagents

Reagent	*Supplier*	*Cat #*
pmirGLO Dual-Luciferase miRNA Target Expression Vector	Promega (supplied by MKS)	E1330
Alpha-Select Silver Efficiency Competent Cells	Bioline	BIO-85026
LB Agar	Sigma	L2897-1KG
LB Broth		L3022-1KG
Ampicillin		
QIAprep Spin Miniprep Kit	Qiagen	27104
Plasmid Plus Maxi kit		12963
QIAquick PCR Purification Kit		28104
Human Genomic DNA from human blood (buffy coat)	Roche	11691112001
Phusion Hot start ll High-fidelity DNA polymerase	ThermoFisher	F549S
dATP, dCTP, dGTP, dTTP	Promega	U1330
UltraPure Agarose	Invitrogen	16500100
UltraPure 10X TBE Buffer		15581044
HyperLadder 1kb	Bioline	BIO-33025
HyperLadder 100bp		BIO-33029
NotI-HF	NEB	R0189S
SalI		R0138S
BamHI		R0136S
SacII		R0157S
Antarctic phosphatase		M0289S
Vent DNA Polymerase		M0254S
T4 DNA Ligase	Promega	M1804
QuikChange II Site-Directed Mutagenesis Kit	Agilent	200523
Dual Luciferase Reporter Assay	Promega	E1910
96 well assay plates – white, clear bottom	Costar	CLS3610

Table 2.6.2) Cloning primers

Purpose	*Fwd primer sequence*	*Rev primer sequence*	*Annealing temperature*
NDUFA4 3'UTR amplification from human cDNA	AAGGTCGACCTAAATGAAATGTTTCACTATAACGCTGC	AAGGCGGCCGCCTAATTTCTTAATGTAGCATTTATTTGGAG	58°C
Site-directed mutagenesis PCR for NDUFA4 mutB	GCCACATCCGC<u>GGG</u>ATTTTCCACTTAACCAGG	CCTGGTTAAGTGGAAAAT<u>CCC</u>GCGGATGTGGC	55°C

Mutation underlined

2.7 Seahorse

Table 2.7.1) Seahorse assay reagents

Item	Supplier	Cat #	Assay type
Seahorse XFe96 FluxPak (18 cartidges, 20 plates, 500ml calibrant)	Agilent	102416-100	All
Seahorse XF Base Medium		102353-100	Mito/Glyco stress test
Seahorse XF DMEM medium, w/HEPES, w/o phenol red, pH 7.4		103575-100	ATP rate assay
Seahorse XF Plasma Membrane Permeabilizer		102504-100	Respiratory chain assay
Bovine Serum Albumin Fraction V heat shock, fatty acid free (Roche)	Sigma Aldrich	3117057001	Respiratory chain assay
D-Glucose		G7021-1KG	Mito/Glyco stress test ATP rate assay
Glutamine		G7513	Mito/Glyco stress test ATP rate assay
Sodium pyruvate		P5280-100G	Mito/Glyco stress test ATP rate assay
2-Deoxy-D-Glucose >= 98% (GC) Crystalline		D8375-5G	Mito/Glyco stress test ATP rate assay
Antimycin A		A8674	Mito/Glyco stress test ATP rate assay Respiratory chain assay
Oligomycin A	Cayman Chemical Company	11342	Mito/Glyco stress test ATP rate assay Respiratory chain assay
FCCP		15218	Mito/Glyco stress test
Rotenone		83-79-4	Mito/Glyco stress test ATP rate assay Respiratory chain assay
Sodium Azide	Sigma Aldrich	S2002-25G	Respiratory chain assay
Adenosine 5'-diphosphate monopotassium		A5285-5X1G	Respiratory chain assay
DL-Malic acid		M0875-100G	Respiratory chain assay
Succinic acid		S3674-100G	Respiratory chain assay
Tetramethylhydroquinone (Duroquinol)	Sigma Aldrich (Combi-Blocks)	COM448666887-100MG	Respiratory chain assay
L-Ascorbic acid Bioxtra, crystalline	Sigma Aldrich	A5960-25G	Respiratory chain assay
TMPD (N,N,N',N'-tetramethyl-p-*phenylenediamin)		T7394-5G	Respiratory chain assay
Calcein AM Viability Dye UltraPure Grade; 20 x 50ug	eBioscience (ThermoFisher)	65-0853-78	Mito/Glyco stress test ATP rate assay
Quant-iT™ PicoGreen™ dsDNA Reagent	ThermoFisher	41116133	Respiratory chain assay
TE buffer pH7.4 Molecular Biology Grade		BP2476-500	Respiratory chain assay

Table 2.7.2) Seahorse MAS Buffer composition

Constituent	Final concentration	Supplier	Cat #
Sucrose	70mM	Sigma Aldrich	S0389-1KG
Mannitol	220mM		M4125-100G
Potassium phosphate monobasic (KH_2PO_4)	10mM		P5655-500G
MgCl2	5mM	Sigma Aldrich	M8266-100G
HEPES	2mM		H3375-100G
EGTA	1mM		E4378-25G

2.8 GC-MS

Table 2.8) GC-MS metabolite extraction and derivatisation

Reagent	Supplier	Cat #
Methanol	ThermoFisher	M/4058/17
D6-glutaric acid (Pentanedioic-d6 acid)	C/D/N Isotopes Inc	D-5227
Chloroform	ThermoFisher	C/4966/17
Methoxyamine hydrochloride (MeOX)	Sigma Aldrich	226904-5G
Pierce™ Pyridine, LC-MS Grade	ThermoFisher	25104
N-(t-butyldimethylsilyl)-N-methyltrifluoroacetamide (MTBSTFA)	Restek	35610

2.9 ELISA and Luminex

Table 2.9) Enzyme-Linked Immunosorbent Assay (ELISA) and Luminex reagents

Reagent	Supplier	Cat #
Purified Mouse Anti-Human TNF (MAb1)	BD	551220
Biotin Mouse Anti-Human TNF (MAb11)		554511
Streptavidin-HRP	Biotechne	DY998
Human IL-6 DuoSet ELISA		DY206
Human IL-10 ELISA Ready-SET-Go! Kit	Invitrogen	88-7106-88
TMB Substrate Kit	ThermoFisher	34021
Tween-20		10113103
Bovine Serum Albumin (biotechnology grade)	VWR	0332-100GP
Human magnetic luminex assay - Config: d9XQWJaA	Biotechne (R&D)	LXSAHM

Methods

2.10 Macrophage Isolation and Culture

Mouse bone marrow-derived macrophages (BMDMs) were isolated from hind legs of C57BL/6 wild type mice. Bones were cleaned of muscle tissue, cut at both ends and centrigued (4000rpm, 3min) inside a pierced eppendorf within a second tube (both sterile). Bone marrow from each mouse was resuspended in 50ml RPMI + 10% HI-FCS + 1% Pen/Strep with 50ng/ml M-CSF and seeded into five 10cm dishes. Cells were cultured as shown in **Figure 2.1**.

Human monocytes were isolated from leukapheresis blood cones from the National Blood and Transplant Service. For optimum monocyte isolation, three protocols were compared – StemCell EasySep Human Monocyte Isolation Kit (negative selection via magnetic beads); StemCell RosetteSep Human Monocyte Enrichment Cocktail (negative selection via antibody-mediated complexing with red blood cells); and Percoll density centrifugation. See Table 2.10.1 for a comparsion of resulting cell numbers, and **Figure 2.3** for results of flow cytometry and morphology comparisons. The RosetteSep protocol was selected for future use due to high yield and viability; comparable staining and morphology; low cost; and ease of application.

Table 2.10.1) Monocyte isolation protocol comparison

	EasySep	*RosetteSep*	*Percoll*
% of cone processed	20%	50%	30%
# monocytes obtained	22.11 x 10^6	161.3 x 10^6	25.0 x 10^6
Normalised monocyte count (#/% cone)	1.11 x 10^6	3.23 x 10^6	0.83 x 10^6
# macrophages at Day 7 (viable)	10.5 x 10^6	45.4 x 10^6	10.27 x 10^6
% viability at Day 7	77%	93%	97%
Normalised macrophage count (#/% cone)	**0.525 x 10^6**	**0.908 x 10^6**	**0.342 x 10^6**

Human monocytes were isolated according to the following protocol (RosetteSep Human Monocyte Negative Selection):

Drain blood into a 50ml tube. Add sterile filtered EDTA to 1mM final concentration. Cone blood: add 75µl StemCell RosetteSep human monocyte isolation cocktail per ml of blood. Whole peripheral blood: add 50µl per ml of blood. Mix gently by swirling. Incubate at room temperature for 20mins. Dilute blood with PBS + 2% HI-FCS + 1mM EDTA and mix gently: cone blood roughly 1 in 4, whole blood 1 in 2. Layer onto an equal volume of Ficoll Paque in an appropriate number of 50ml tubes by trickling the diluted blood down the side of the tube. Centrifuge at 1200g for 30min - 0 brake, 1 acceleration. Remove and discard top layer to reduce platelet contamination. Collect interface cell layer (=enriched monocytes). Pool cells and top up to 40ml with sterile PBS + 2% HI-FCS + 1mM EDTA to wash. Pellet cells (300g, 10min). Discard supernatant and repeat wash until supernatant is transparent (clear of Ficoll). Resuspend pellet in RPMI + 5% HI-FCS. Count cells with trypan blue. Seed monocytes for differentiation with 50ng/ml M-CSF into 10cm dishes at 10-15x10^6 cells/dish (depending on total monocyte count), or into 12 well plates for transfection experiments (see Table 2.10.2). See Figure 2.1 for cell culture workflow.

For primary cell harvesting, cells were PBS-washed, incubated with cell dissociation buffer (10-15mins at 37°C), lifted with a cell lifter, counted and seeded for experiments (see Table 2.10.2). Mouse macrophages were seeded on Day 7 in RPMI + 10% HI-FCS + 1% Pen/Strep. Human macrophages were seeded on Day 6 in RPMI + 5% HI-FCS + 50ng/ml M-CSF.

RAW264.7 and HEK293 cells were cultured in flasks in DMEM +10% HI-FCS +1% Pen/Strep and split roughly twice/week. RAW264.7 cells were harvested with cell dissociation buffer and cell scrapers. HEK293 cells were harvested with 1x trypsin.

Table 2.10.2) Cell seeding

Species	Culture plate	Cell # per well
Mouse	12 well	1 x 10^6
	6 well	2.5 x 10^6
Human	12 well	0.5 x 10^6
	6 well	1 x 10^6
	12 well (for transfection)	0.6 x 10^6 (seeded at Day 0)
RAW264.7	6 well	2.5 x 10^6
HEK293	24 well	0.1 x 10^6

2.10.1 Cell culture stimulations

Cells for stimulation were seeded one day prior to stimulation. Treatments were added as detailed in Table 2.1.4. Master mixes were prepared and stimulations carried out by replacing total culture medium. All stimulants were added simultaneously unless otherwise stated. Stimulation medium did not contain M-CSF, and was not removed until the time of harvest or assay. Mock treatment included suitable vehicle controls for all relevant conditions.
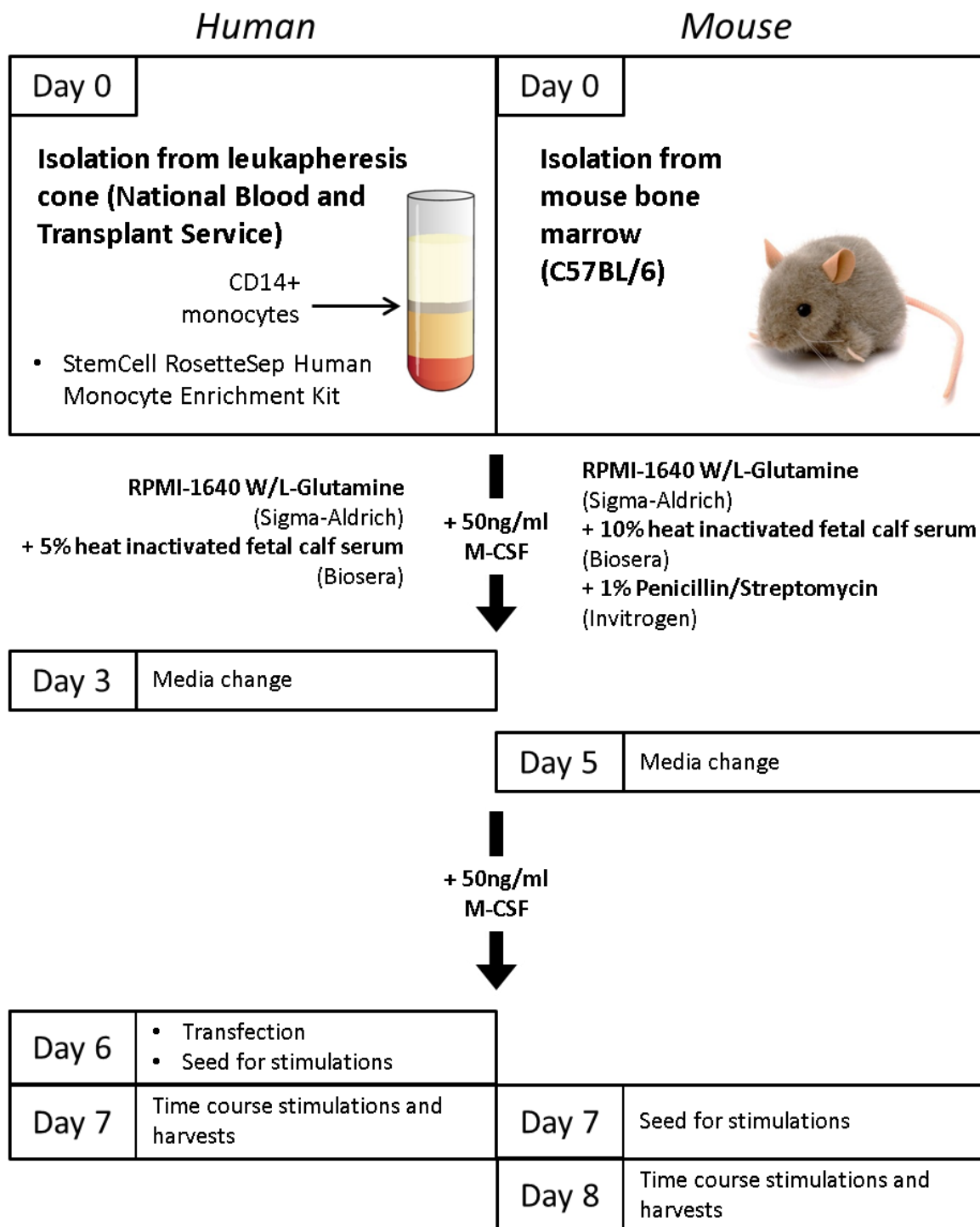
Figure 2.1) Primary macrophage cell culture workflow

2.11 Flow cytometry

2.11.1 Monocyte/Macrophage characterisation

Cells were harvested as described above, counted with typan blue and 100,000 live cells were aliquotted per sample. Fixable viability dye (FVD) was diluted 1/1000 in PBS +2% HI-FCS +1mM EDTA (FACS buffer). All samples (except unstained and single colour controls) were stained with FVD, 20-30min on ice in the dark. Cells were washed with FACS buffer and pelletted (400g, 5min). Antibodies were diluted in FACS buffer as indicated in Table 2.2.1. Cells were stained in antibody mix for 30min on ice in the dark. Cells were washed with FACS buffer, resuspended in fixation buffer and fixed, 20min at room temp in the dark. Cells were washed with FACS buffer twice, pelletted and stored at 4°C over night in foil. Stained cells were run on a BD LSRFortessa X-20 and results analysed using FlowJo v10 – see **Figure 2.2** for gating strategy and **Figure 2.3** for characterisation results. Gating for positive staining was based on isotype control staining – see **Supplementary Figure S1**.
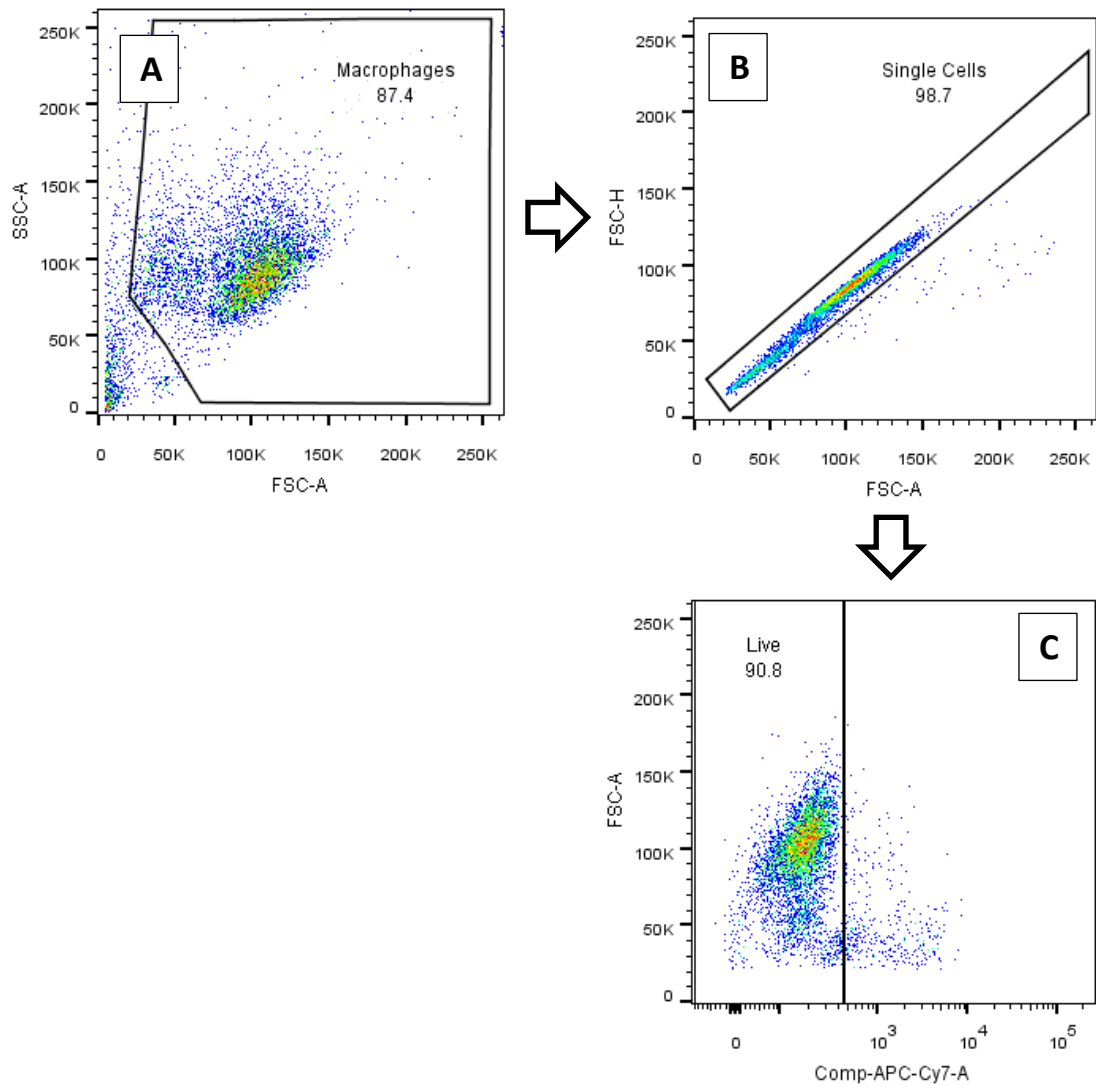
Figure 2.2) Flow cytometry gating strategy for *in vitro* cultured macrophages

Panel A: cell debris excluded; Panel B: doublets excluded; Panel C: dead cells excluded (positive for fixable viability dye)

A
<u>Day 0</u>

EasySep

<u>CD14</u> **86.3%**   <u>CD163</u>   **77.5%**   <u>CD64</u>   **86.1%**   <u>CD206</u>   **2.47%**

RosetteSep

<u>CD14</u>   **85.8%**   <u>CD163</u>   **74.5%**   <u>CD64</u>   **78.3%**   <u>CD206</u>   **1.51%**

B
<u>Day 6</u>

EasySep

<u>CD14</u>   **99.2%**   <u>CD163</u>   **93.7%**   <u>CD64</u>   **95.0%**   <u>CD206</u>   **99.2%**   <u>CD16</u>   **83.4%**

RosetteSep

<u>CD14</u>   **98.6%**   <u>CD163</u>   **96.8%**   <u>CD64</u>   **97.3%**   <u>CD206</u>   **98.9%**   <u>CD16</u>   **84.6%**

Percoll

<u>CD14</u>   **98.8%**   <u>CD163</u>   **95.2%**   <u>CD64</u>   **96.6%**   <u>CD206</u>   **98.2%**   <u>CD16</u>   **83.2%**
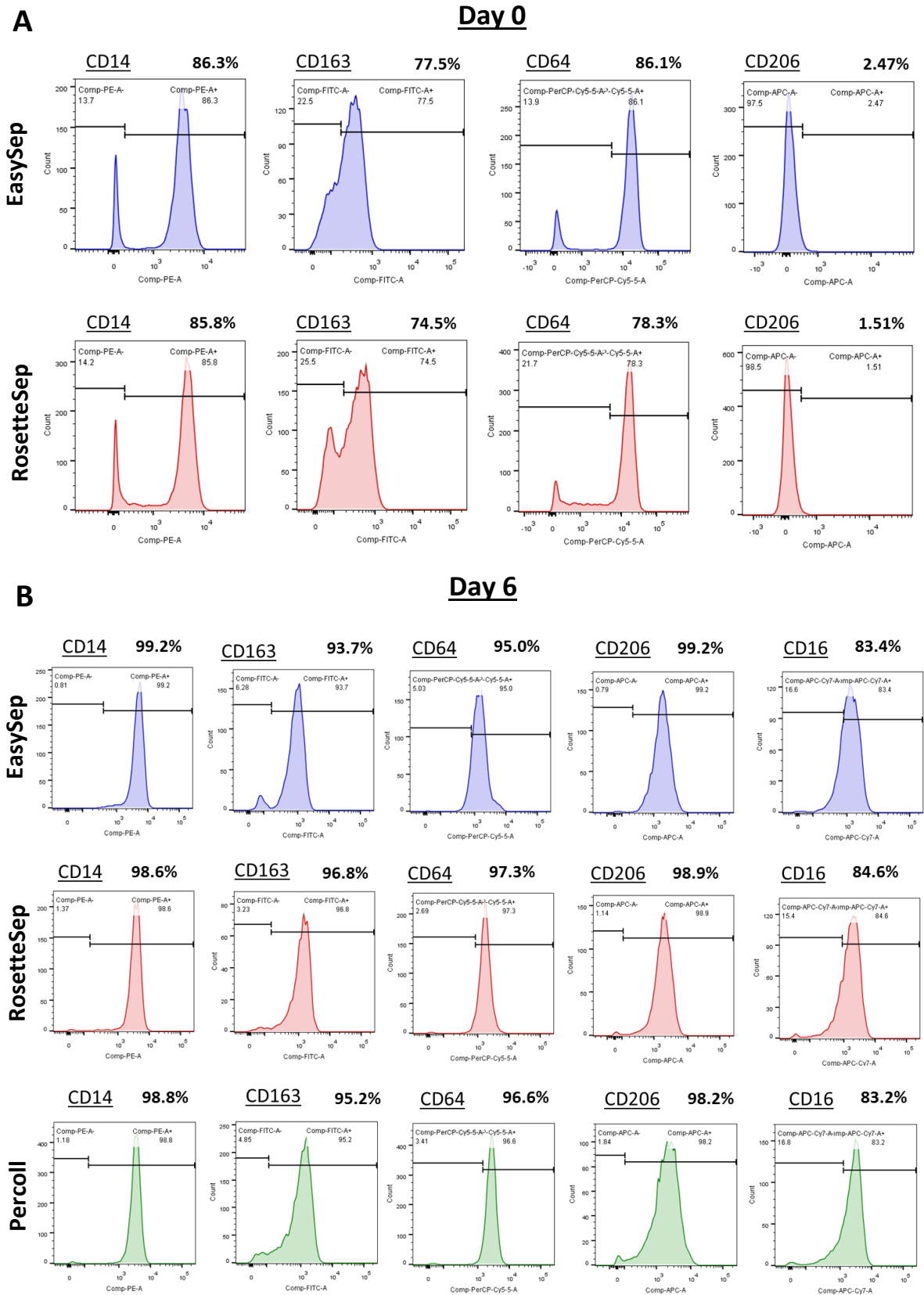
Figure 2.3 continues overleaf

C

Day 8
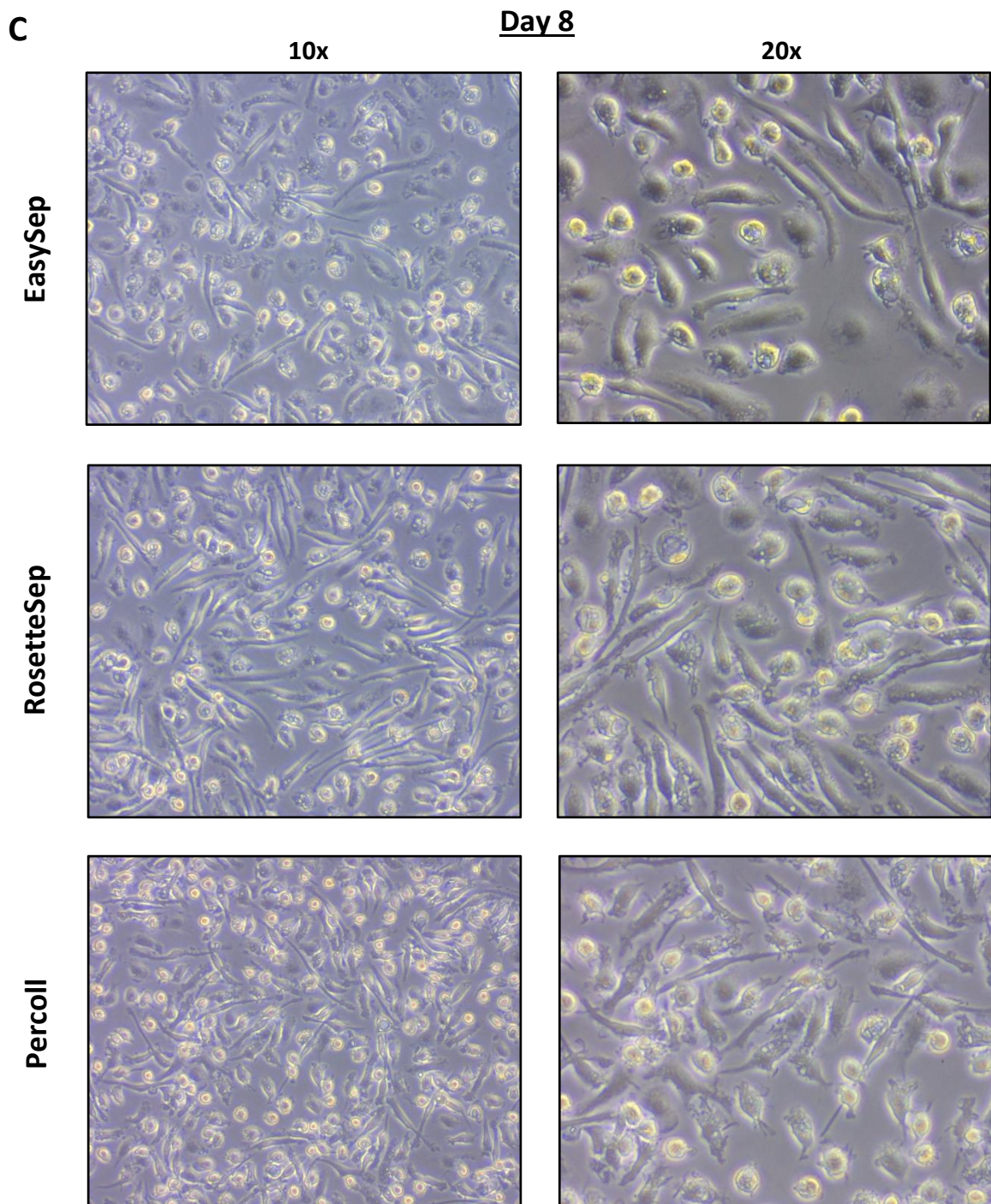
Figure 2.3) Monocyte Isolation Kit Comparison

Human monocytes were isolated using the indicated techniques. Cells were stained for characteristic monocyte/macrophage markers **A)** directly after isolation (Day 0) or **B)** after 6 days of differentiation with 50ng/ml M-CSF (Day 6). See **Supplementary Figure S1** for isotype control staining.

C) Cells were harvested on day 6 and seeded into 12 well culture plates at 0.5x10^6cells/well with 50ng/ml M-CSF. On Day 8 brightfield microscopy images were taken (10x and 20x) to compare cell morphology.

2.11.2 MitoTracker and MitoSox staining

Staining was performed in 12 well culture plates (0.5x10^{6}cells/well) immediately following the stimulation period. Cells were washed with PBS and stained for 20min at 37°C according to Table 2.11. Staining medium was removed and cells washed twice with PBS, followed by harvesting as described above. Cells were stained with 1/1000 FVD, 30min on ice in the dark, washed with FACS buffer (PBS +2% HI-FCS +1mM EDTA) and resuspended in FACS buffer for analysis on BD Fortessa. Initial gating as indicted in **Figure 2.2**. See **Figure 2.4** for MitoTracker concentration optmisation. For controls, FCCP (5µM final), rotenone (1µM final) or antimycin A (1µM) were spiked into wells for the final hour of 24h LPS stimulation.

Table 2.11) Mitochondrial staining

Stain	Staining concentration	Staining Buffer
MitoTracker Green	150nM	RPMI medium
MitoTracker Red CMXRos	200nM	RPMI medium
MitoSOX	5µM	HBSS + calcium + magnesium (no phenol red)
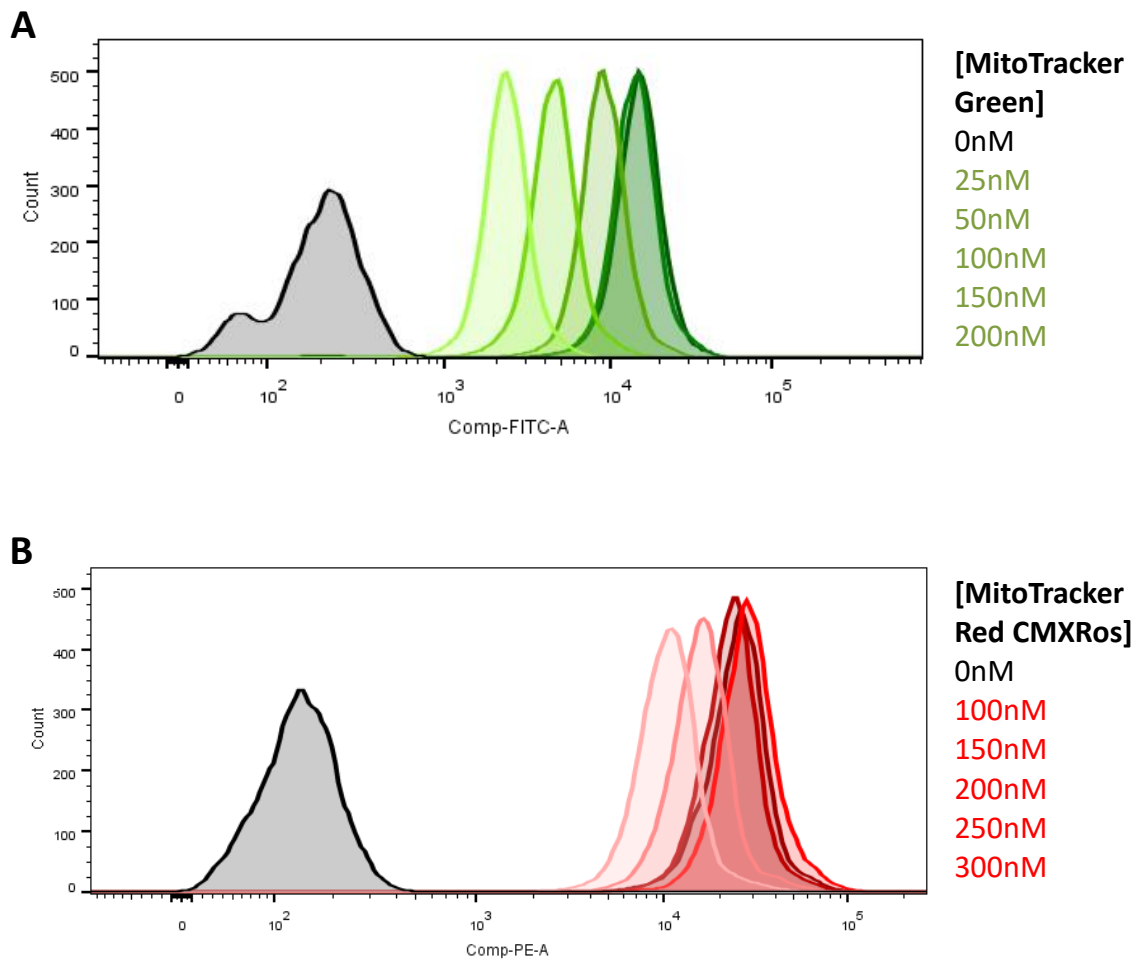
Figure 2.4) MitoTracker dose testing

Unstimulated human monocytes were stained with the indicated concentrations of **A)** MitoTracker Green or **B)** MitoTracker Red CMXRos to determine the saturation point.

2.12 Transfections

Transfections were performed of primary human monocyte-derived macrophages for delivery of miRNA mimics, miRNA inhibitors and siRNAs. Transfection reagents were compared for their suitablity in primary macrophages (discussed in Chapter 4).

Cells were seeded on Day 0 as described in Table 2.10.2. On Day 6, media were changed to 0.5ml/well RPMI +5% HI-FCS +2ng/ml M-CSF. RNA for transfection was diluted in 1XsiRNA dilution buffer in sterile nuclease-free water. Transfection mixes were made up as below using sterile filter tips and incubated at room temperature for the given times. 100µl of transfection mix was added dropwise to the cells and plates swirled to mix. (12wp = 12 well plate)

*For **TransIT-TKO** (per 12wp well reaction):* **80µl** Opti-MEM medium (no FCS)
Incubation: **30min** **5µl** TransIT-TKO reagent
  15µl diluted RNA

*For **TransIT-X2** (per 12wp well reaction):* **82.2µl** Opti-MEM medium (no FCS)
Incubation: **30min** **2.8µl** TransIT-TKO reagent
  15µl diluted RNA

*For **Lipofectamine 3000** (per 12wp well reaction):*
Combine tubes and incubate for **15min**

First tube: **48µl** Opti-MEM medium (no FCS)
  2µl TransIT-TKO reagent
Second tube: **35µl** Opti-MEM medium (no FCS)
  15µl diluted RNA

General transfection efficiency was assessed for each donor using a fluorescently-labelled oligo RNA (Dy547: absorbance/emission =557/570 nm), analysed by flow cytometry 1 day post transfection. See **Figure 2.5** for transfection efficiency comparison. See individual figure

legends for timings of harvests post transfection. **Figure 2.6** depicts the RNA modifications present in the miRCURY LNA miRNA Power Inhibitors (Qiagen) (*discussed in Chapter 4*).

2.13 RNA isolation

To enable reliable measurement of miRNA and mRNA expression, commercially available RNA isolation kits were compared. MiRNA-155 and TNF-α mature mRNA were measured, as both are known to be induced by LPS in macrophages. **Figure 2.7** shows the comparison results for Norgen Total RNA Purification Plus kit and Qiagen miRNeasy kit, which gave comparable results. The latter is specifically designed for miRNA detection and employs phenol-chloroform extraction. Qiagen RNeasy Mini Kit and Zymo Quick-RNA Miniprep kits were also tested (data not shown), but neither gave superior results to Norgen. The Norgen Total RNA Purification Plus kit was chosen to take forward, as the kit is cheaper and the protocol quicker than the miRNeasy kit.
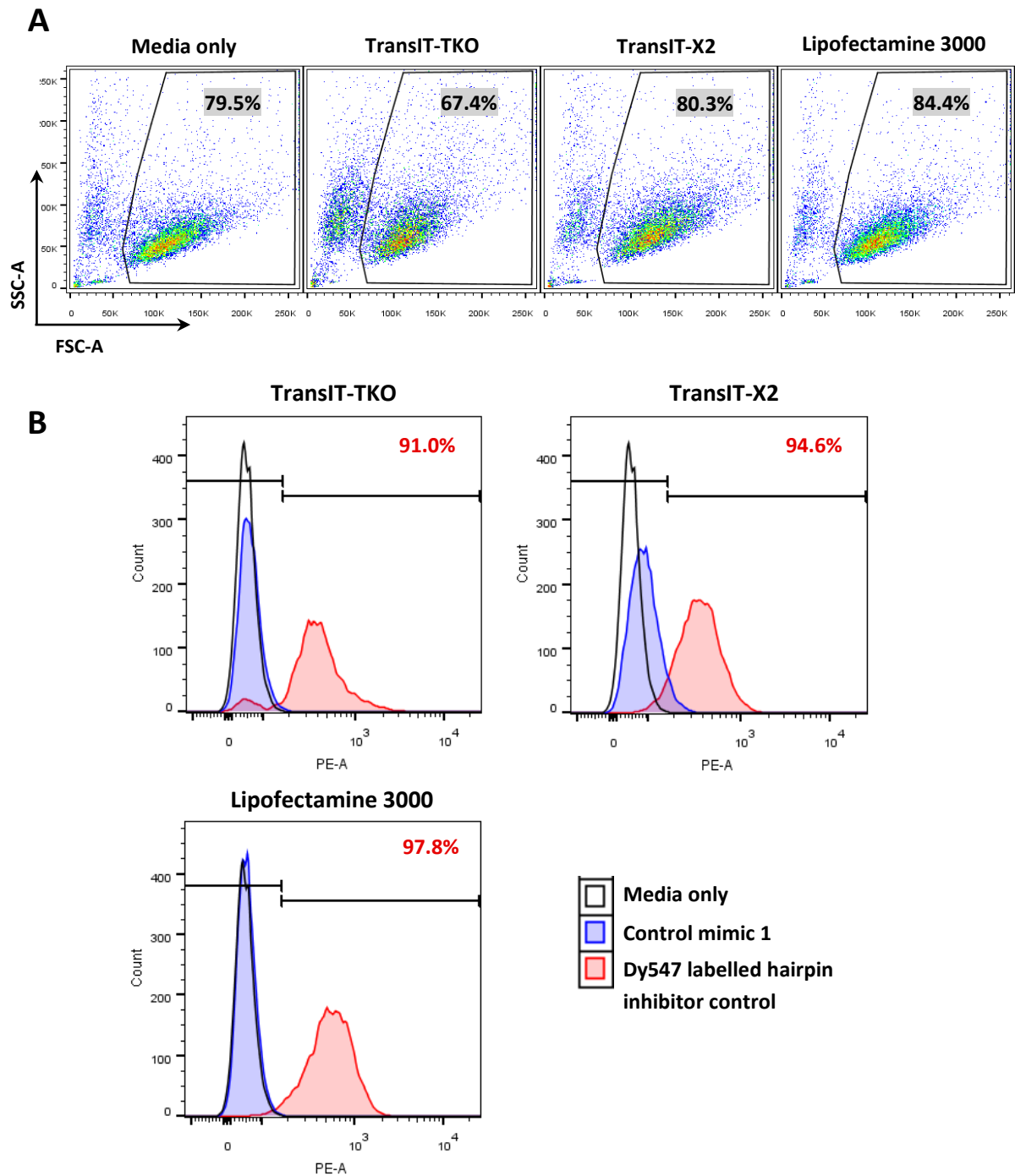
Figure 2.5) Transfection reagent comparison flow cytometry

Human monocyte-derived macrophages transfected with 2nM control mimic 1 or Dy547 labelled hairpin inhibitor control using the indicated transfection reagents, or treated with Opti-MEM (Media only).

A) Cell morphology assessed by forward scatter (FSC) and side scatter (SSC) in media only or control mimic transfected cells. **B)** Transfection efficiency assessed in Dy547 inhibitor-transfected single cells compared with control mimic or media only.
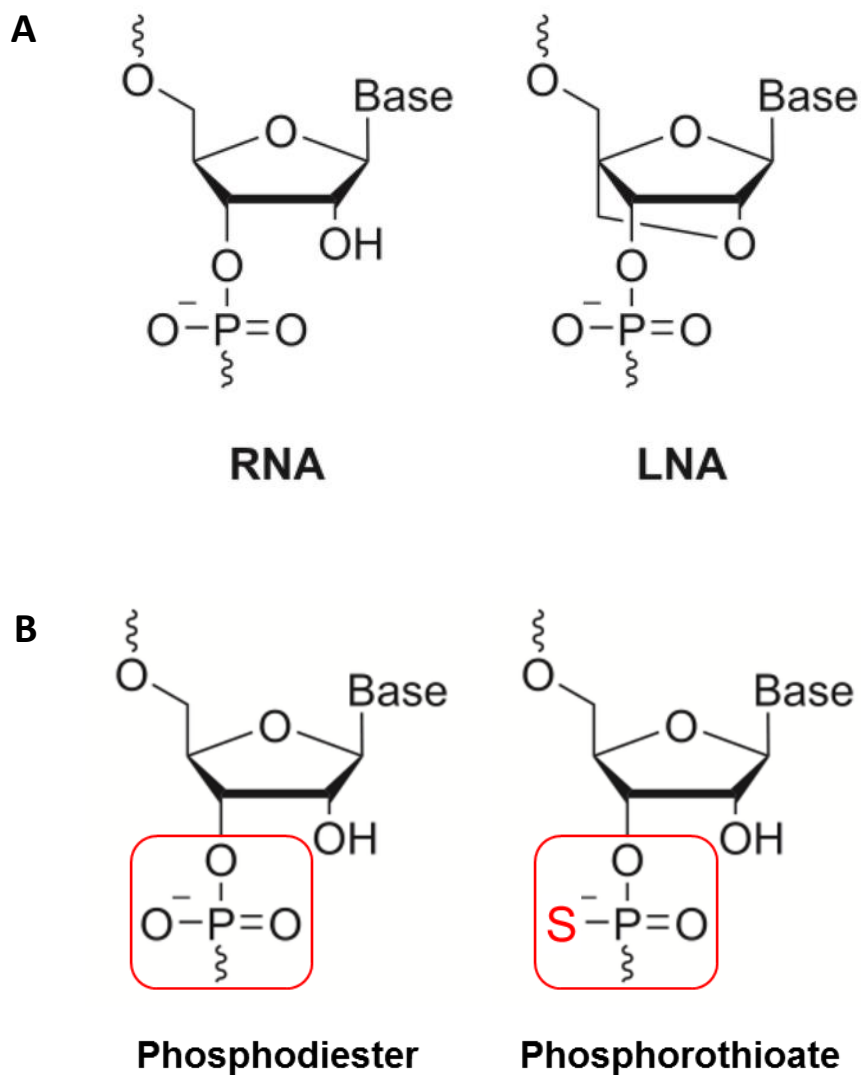
Figure 2.6) Nucleotide modifications of miRCURY LNA miRNA Power Inhibitors

A) Taken from Astakhova 2014 (9). Structure of a locked nucleic acid (LNA) nucleotide compared with a standard RNA nucleotide. LNA formed by a 2'-O -> 4'-C methyl linkage

B) Adapted from Astakhova 2014 (9). Structure of a phosphorothioate (PS)-modified RNA nucleotide compared with a standard phosphodiester (PO) RNA nucleotide
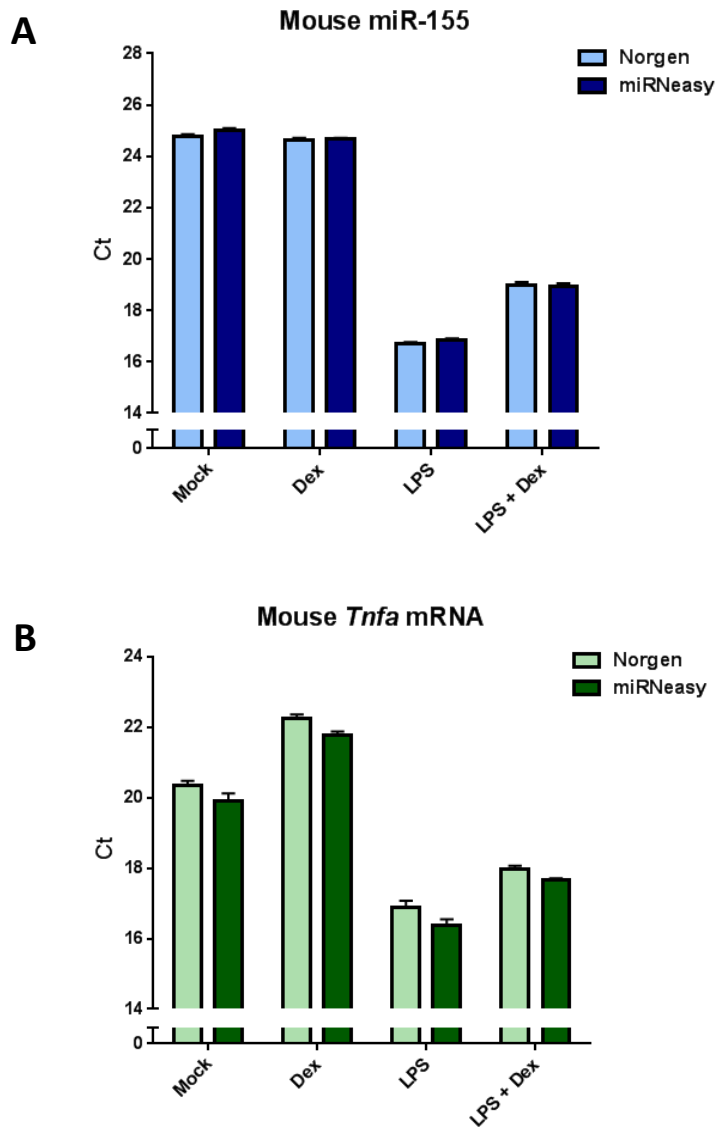
Figure 2.7) Comparison of RNA isolation kits for miRNA and mRNA detection
RAW264.7 cells were stimulated with Dex (100nM), LPS (10ng/ml) or a combination of the two for 24h. RNA was isolated with Norgen Total RNA Purification Plus kit or Qiagen miRNeasy kit. RT-qPCR was used to detect expression of **A)** mmu-miR-155 and **B)** mouse mature TNF-α mRNA. Data presented as raw Ct values; n=1 (mean+SD of technical replicates).

RNA was isolated according to the following protocol (Norgen Total RNA Purification Plus):

Add ethanol to wash solution A as directed by manufucturer. Add 400µl β-mercaptoethanol (β-ME) to a fresh bottle of lysis buffer RL (10µl per ml) (β-ME inactivates RNases, preventing sample degradation). Remove medium from cultured cells and freeze for cytokine analysis. Wash cells with PBS and lyse using 350µl/well buffer RL +β-ME (for a 12wp). Freeze lysate at -80°C or process immediately. Transfer lysate to a gDNA removal column and centrifuge (14,000g, 1min). **Keep flow-through from this step.** Add 60µl 100% ethanol per 100µl of flow-through and mix thoroughly by pipetting. Transfer sample to an RNA purification column and centrifuge (3500g, 1min). Discard flow-through. Wash column 3 times with 400µl Wash Solution A (+ethanol) per wash, centrifuge (14,000g, 1min) after each wash and discard flow-through. After the third wash dry the column by centrifuging again (14,000g, 2min). Add 30µl Elution Solution A to each column and elute by centrifuging (200g, 2min followed by 14,000g, 1min).

RNA concentration was measured by Nanodrop (Thermo Scientific) and purity assessed by 260/280 and 260/230 ratios. Ratio values >1.5 were considered adequate for downstream analysis.

2.14 cDNA synthesis and RT-qPCR

See **Figure 2.8** for schematic of cDNA synthesis and RT-qPCR for miRNA detection. cDNA was synthesised using Qiagen miScript Reverse Transcriptase kit using 250ng RNA per reaction.

Table 2.14.1) cDNA synthesis reaction mix setup

Reagent	*Volume for 1 reaction*
5x miScript buffer (**HiFlex**)	4 µl
10x miScript Nucleics mix	2 µl
miScript Reverse transcriptase	1 µl
RNA template (250ng)	X µl
RNase-free water	to 20µl

Reaction mixes were incubated in a thermocycler (BioRad) at 37°C for 60min, followed by 95°C for 5min for enzyme inactivation. cDNA was diluted to 100µl using nuclease-free water.

RT-qPCRs were run on a Biorad CFX384. MicroRNAs were detected using Qiagen miScript SYBR green master mix and Qiagen miScript Primer assays, utilising the proprietary universal reverse primer and miRNA-specific forward primer. MiRNA RT-qPCR was run using the following parameters: 95°C 15min (94°C 15sec; 55°C 30sec; 70°C 30sec)x40.

Messenger RNAs were detected using Takara SYBR TB Green and oligonucleotide primers from Eurofins (see Table 2.4.3), run using the following parameters: 95°C 30sec (95°C 10sec; 59°C 30sec; 78°C 20sec)x40. ΔΔCt values were calculated by normalising to the relevant housekeeping gene (RNU6-2 for miRNAs; as specified for mRNAs), and relative to the control condition indicated in the figure legends.

miRNA cDNA synthesis:
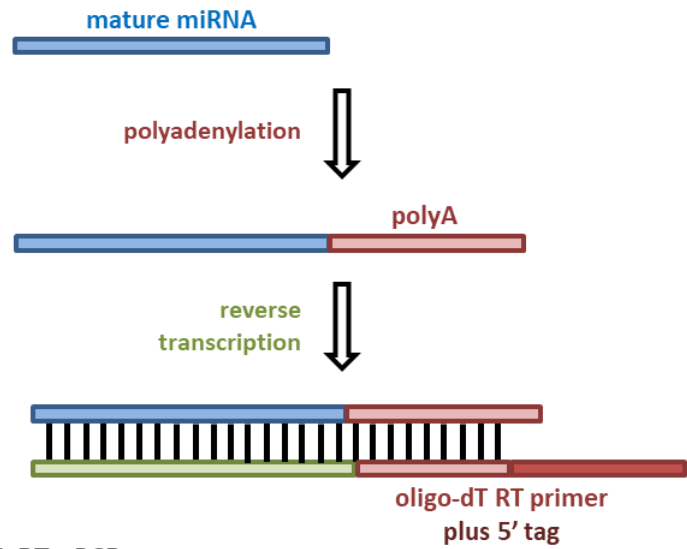
miRNA RT-qPCR:
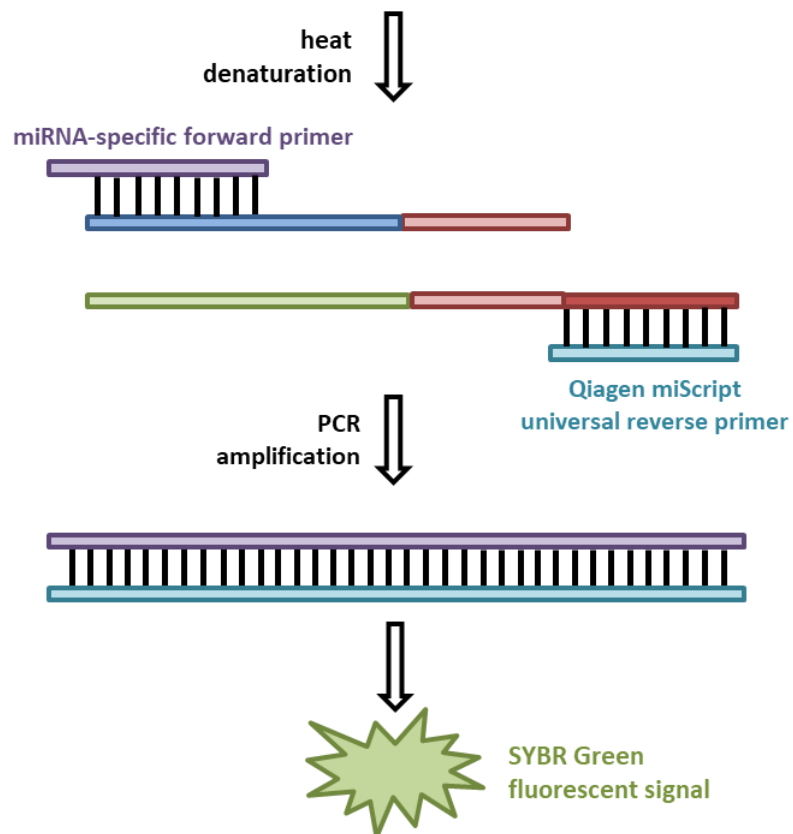
Figure 2.8) microRNA reverse transcription and RT-qPCR workflow

Adapted from Kramer *et al* 2011 (6), utilising product details from Qiagen

Depiction of cDNA synthesis and RT-qPCR workflow for the detection of microRNAs using Qiagen miScript kit.

Table 2.14.2) RT-qPCR reaction mix setup

Reagent	miRNA RT-qPCR	mRNA RT-qPCR
SYBR Green	2.5µl	3µl
Fwd primer / miRNA specific primer	0.5µl	0.3µl
Rev primer / universal primer	0.5µl	0.3µl
cDNA	1.5µl	2.4µl

See **Figures 2.9** and **2.10** for RT-qPCR housekeeping gene tests. β-2-microglobin (*β2M*) forms part of the MHC class I molecule and is a commonly used housekeeper as is expressed from all nucleated cells. However this gene was found to be upregulated by LPS stimulation at later time points in both mouse and human macrophages (**Figure 2.9A & 2.10A**). *Rpl13a* was chosen as a suitable housekeeping gene in mouse macrophages (**Figure 2.9B**) (chosen over *Tbp* due to a cleaner melt curve – **Figure 2.9C**). *UBC* was chosen as a suitable housekeeping gene in human macrophages (**Figure 2.10B**).

2.15 Bioinformatics

2.15.1 Microarray analysis

Analysis of previously generated microarray data was performed using Partek Genomics Suite v6.6 (2016). Raw data were log-transformed and subjected to analysis of variance (ANOVA) statistical analysis for comparison of LPS vs LPS+Dex treated samples. Gene lists were compiled with the following conditions: p value with false discovery rate (FDV) < 0.05; Fold change >2 or <-2. MicroRNA-related probes were annotated within lists of significantly altered genes using Ensembl BioMart data mining tool. Data that were normalised for input and technical variation were extracted for these probe sets and analysed using GraphPad Prism for comparison of all conditions.
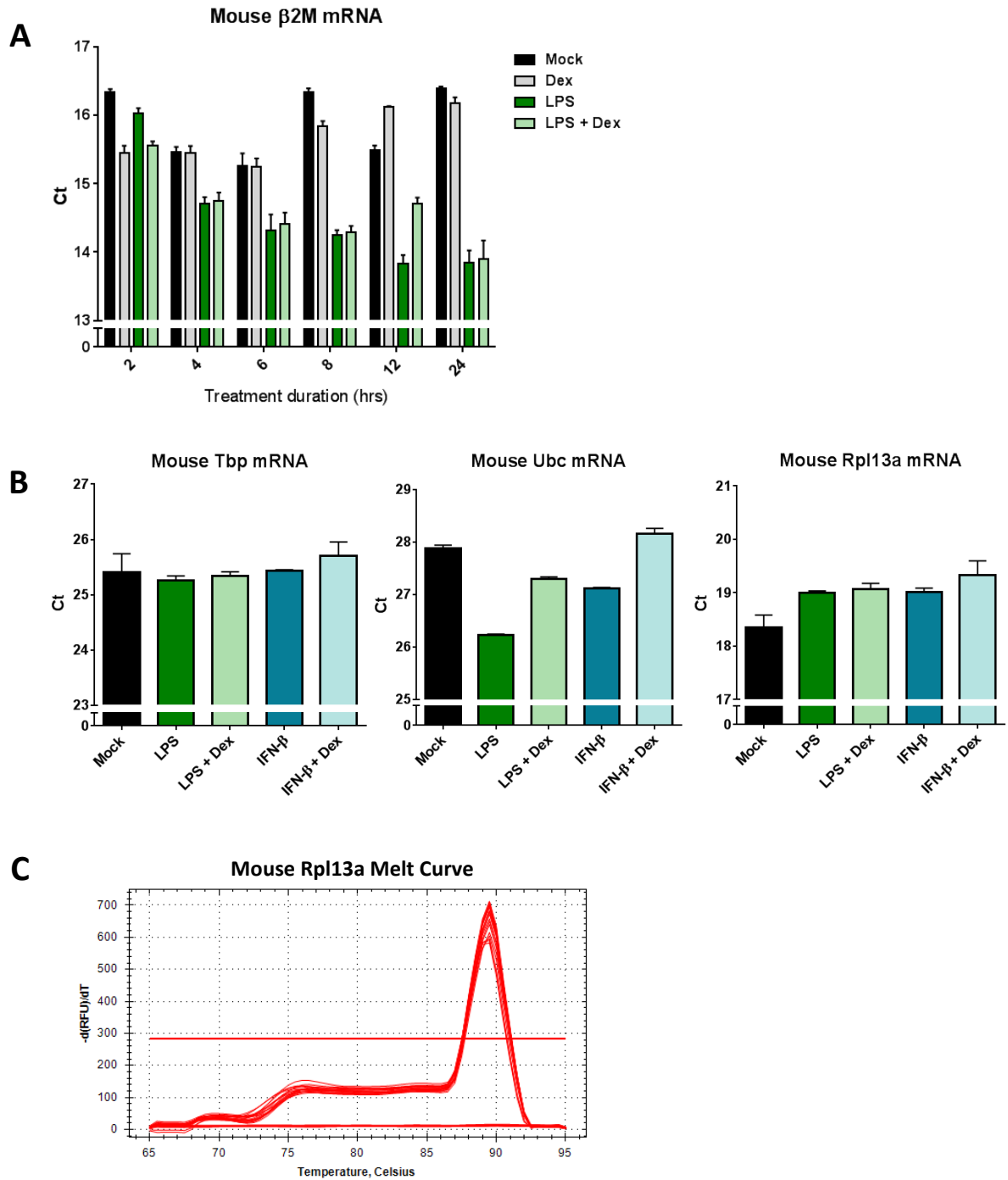
Figure 2.9) Mouse RT-qPCR housekeeping gene optimisation

Several genes were tested by RT-qPCR for stable expression in cDNA from mouse bone marrow-derived macrophages stimulated with LPS (10ng/ml) and Dex (100nM) for **A)** the indicated time course; or **B)** 24h; Presented as raw Ct values; n=1 (mean+SD of technical replicates).

C) Melt curve of chosen housekeeping gene (*Rpl13a*) taken from BioRad CFX Manager software.
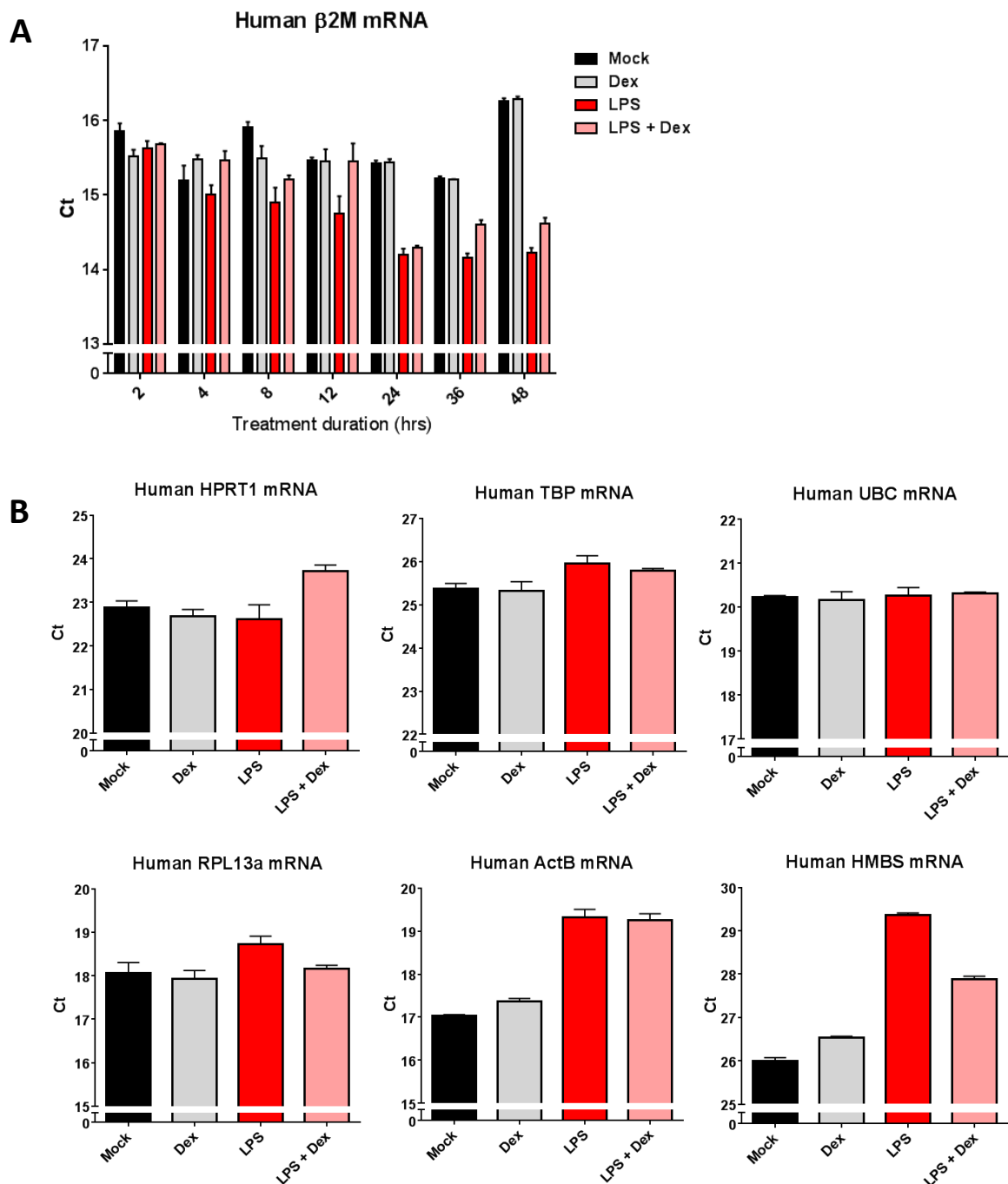
Figure 2.10) Human RT-qPCR housekeeping gene optimisation

Several genes were tested by RT-qPCR for stable expression in cDNA from human monocyte-derived macrophages stimulated with LPS (10ng/ml) and Dex (100nM) for **A)** the indicated time course; or **B)** 36h; Presented as raw Ct values; n=1 (mean+SD of technical replicates).

2.15.2 MicroRNA target prediction and pathway analysis

Predicted targets of miR-147b were assessed using Targetscan7.1; miRTarBase; miRDB; and miRanda (microRNA.org) online tools, and the results compared for common genes. The miRanda tool provided a list of >2000 potential targets, however the scoring for the majority was very low (|score|<0.1, where the top predicted target scored of -1.3). Only the top 500 genes were used for the comparison.

Gene Ontology enrichment analysis of the combined results from Targetscan7.1, miRTarBase and miRDB (replicates removed) was performed using DAVID functional annotation bioinformatics tool (https://david.ncifcrf.gov/) (270, 271). Third tier Gene Ontology Biological Process terms were visualised using CirGO tool by John O'Neill (https://github.com/IrinaVKuznetsova/CirGO.git) (272).

2.16 Western Blotting

Cells were lysed in RIPA buffer containing protease and phosphatase inhibitors and lysate was shredded by Qiashredder. Protein was quantified using Pierce BCA Protein Assay. Western blots were performed using 4-20% Criterion TGX Protein Gels and Trans-Blot Turbo Transfer PVDF membrane. 25µg of protein was loaded per sample unless otherwise stated. Blots were blocked with 5% milk in Tris buffered saline plus 0.1% Tween-20 (TBS-T), 1h at room temperature. Primary antibodies were applied overnight at 4°C using dilutions indicated in Table 2.5.4, followed by 3x 5min washes with TBS-T. Secondary antibodies (HRP-linked) were applied at 1/2000 in TBS-T +5% milk, 1h at room temperature, followed by 3x 5min washes with TBS-T. Blots were imaged using ECL reagent and BioRad ChemiDoc MP Imaging System. Quantification of Western blots was performed using ImageJ software, normalised to housekeeping protein and presented relative to the indicated control.

2.17 Luciferase Assay

2.17.1 Luciferase assay plasmid cloning

Validation of miRNA targeting by luciferase reporter gene assay required cloning of the 3'UTR of the target gene of interest (NDUFA4) into the pmirGLO Dual-Luciferase miRNA Target Expression Vector (Promega) (**Figure 2.9A**). NDUFA4 3'UTR was amplified from commercially obtained human genomic DNA and cloned into the multiple cloning site downstream of the Firefly luciferase gene using SalI and NotI restriction enzymes.

NDUFA4 amplification PCR cycling parameters: 98°C 30sec (98°C 10sec; 58°C 30sec; 72°C 60sec)x35; 72°C 5min

I also created a vector containing the NDUFA4 3'UTR with a mutation in the seed sequence of the predicted miRNA binding site. The ImiRP computational biology tool (imirp.org) is an online program that predicts generation of novel miRNA binding sites during sequence alteration, and provides lists of tolerated mutations (273). I used this tool to plan mutation of the miR-147b predicted target site within the human NDUFA4 3'UTR. **Figure 2.9B** shows the resulting legitimate mutations that did not create alternative miRNA sites. I selected mutation B (mutB), as this mutates the early seed sequence residues (bases 2-4) (described to be the most crucial for miRNA-mediated repression (274)), and creates a SacII restriction site that can be used for cloning validation. This vector was created from the completed pmirGLO NDUFA4 WT using QuikChange II Site-Directed Mutagenesis Kit (Agilent) according to the manufacturer's instructions.

Site-directed mutagenesis PCR cycling parameters: 95°C 30sec [95°C 30sec; 55°C 60sec; 68°C 9min(1min/kb plasmid)]x16
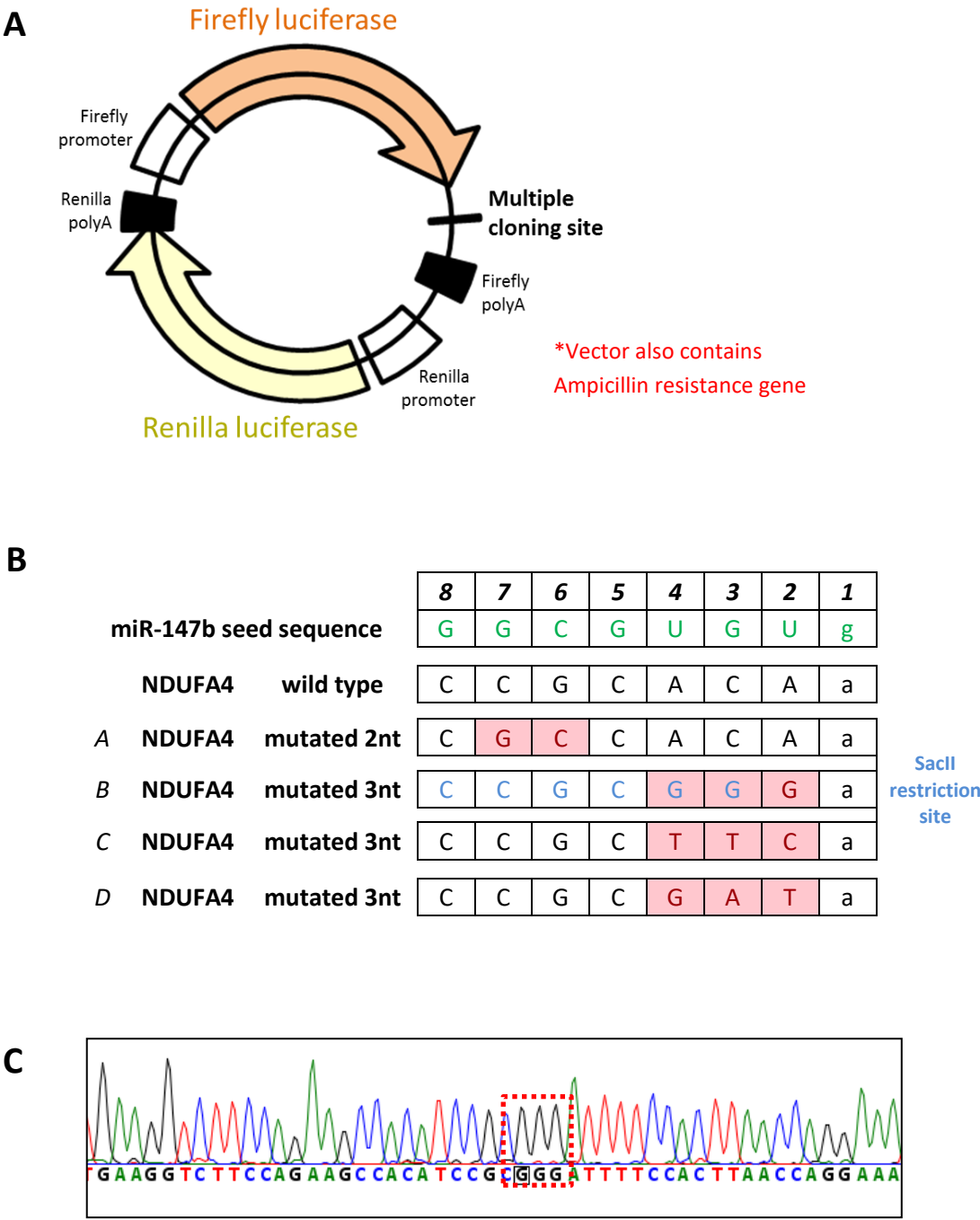
Figure 2.11) Luciferase Assay Plasmids

A) Simplified vector map of unmodified pmirGLO Dual-Luciferase miRNA Target Expression Vector (7.35kb).

B) Results from ImiRP - valid mutations of miR-147b predicted target site within human NDUFA4 3'UTR (highlighted in red) that do not create alternative miRNA binding sites. Novel SacII restriction site in mutation B shown in blue.

C) Section from sequencing results from pmirGLO NDUFA4 3'UTR mutB following site-directed mutagenesis cloning. Mutation of miR-147b predicted target site seed match is highlighted.

Plasmid preparation and cloning were performed by standard methods (Sambrook *et al* Molecular Cloning: a laboratory manual) using reagents listed in Table 2.6.1 and primers listed in Table 2.6.2. Site-directed mutagenesis primers were designed according to Quickchange II SDM kit guidelines. Mini preps were validated by colony PCR and restriction digest. Final maxi preps were validated by colony PCR, restriction digest and sequencing by Eurofins Genomics TubeSeq service (**Figure 2.9C**). All purified DNA preps were quantified by Nanodrop.

2.17.2 Dual luciferase assay

HEK293 cells were seeded at 100,000 cells/well into 24 well plates. After 24h, medium was changed to DMEM +10% FCS (no Pen/Strep) and cells were co-transfected with 20nM control mimic or miR-147b mimic along with 0.5µg/well pmirGLO plasmid DNA (unmodified/ NDUFA4 WT/ NDUFA4 mut) using TransIT-X2 reagent according to Section 2.12. One day post transfection cells were washed with PBS and lysed with 100µl/well 1X passive lysis buffer (Promega Dual Luciferase Assay kit) on plate shaker for 20min. Samples were diluted 1/10 in nuclease-free water and 10µl of sample added to 96 well assay plate. LARII Firefly luciferase substrate was added (100µl/well) by multichannel and briefly mixed by pipetting, followed by immediate reading of luminescence signal using a BioTek Synergy HT plate reader - end-point luminescence read, integration time = 0.1sec. After the initial read, 100µl/well 1X Stop&Glo reagent was added by multichannel, mixed briefly and read using the same parameters. This reagent stops Firefly luciferase activity and provides substrate for Renilla luciferase - used for normalisation. Measurements were performed in triplicate.

2.18 Cycloheximide Chase

Cycloheximide concentration was tested by stimulating cells with LPS (10ng/ml) +/- 5μg/ml cycloheximide and harvesting conditioned medium for cytokine measurements. Human TNFα was measured by ELISA (**Figure 2.12**). For chase experiments, cells were seeded into 12 well plates according to Table 2.10.2. The protein of interest (NDUFA4) is downregulated from 12 hours of LPS treatment onwards, however treatment of the cells with cycloheximide for this long would likely be toxic. Therefore cells were Mock treated or LPS treated in 0.75ml/well stimulation medium, and 0.25ml medium + 20μg/ml cycloheximide was spiked in after 12 hours to give a final concentration of 5μg/ml. Cells were then harvested for protein at various time points for the following 12 hours, and western blotting was performed as previously described.
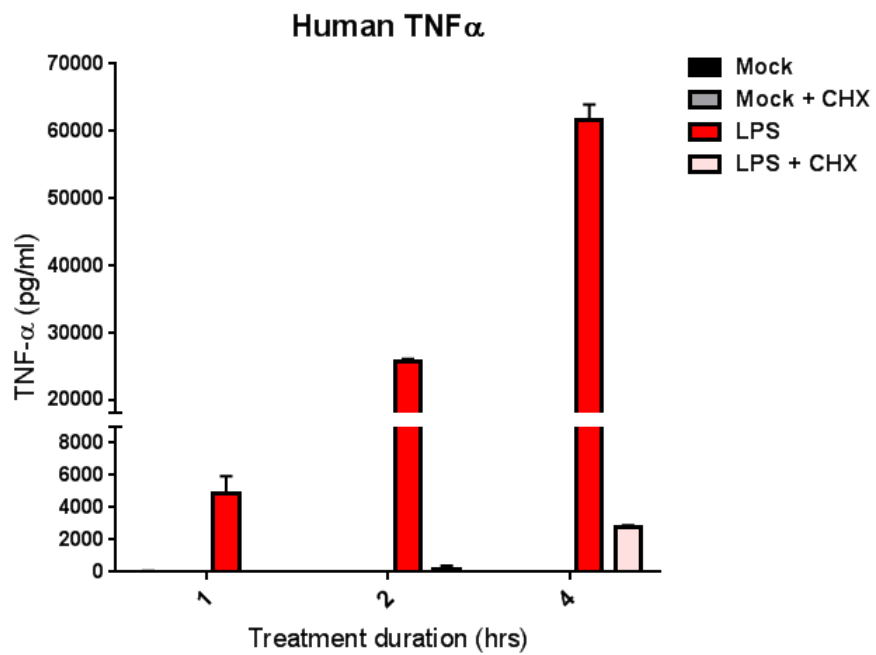
Figure 2.12) Cycloheximide Test

Human monocyte-derived macrophages were stimulated with LPS (10ng/ml) and cycloheximide (5μg/ml) for the indicated times. TNF-α was measured in conditioned medium by ELISA; n=1 (mean+SD of technical replicates).

2.19 Seahorse Assays

All Seahorse assays were carried out using an Agilent Seahorse XFe96 Extracellular Flux analyser. Cells were seeded with 4-6 replicate wells per condition, avoiding the use of outside wells due to positional effects. After seeding, plates were left at room temperature for roughly 1hour to ensure uniform adherence, as per Seahorse protocol.

For intact cell assays (Mito+Glyco stress test and ATP rate assay) an appropriate number of human monocyte-derived macrophages was determined to be 50,000 cells/well based on a Mito Stress test giving OCR values between 50 and 200pmol/min. A density of 75,000 cells/well gave comparable values for mouse BMDMs. Results from these assays were normalised using calcein-AM viability dye. Whilst other viability dyes read out cellular redox potential, which is sensitive to metabolic alterations, calcein-AM relies on cytosolic esterase activity. Calcein-AM is a membrane permeable, non-fluorescent molecule that is converted to fluorescent calcein in the cytosol of living cells (275). This technique controls for variations in cell seeding density and cell death. Measurements were made using a Labsystems Fluoroskan Ascent 96-well plate reader.

2.19.1 Mito+Glyco Stress Test

The Mito and Glyco stress tests are used to assess mitochondrial and glycolytic metabolic parameters by injecting a series of fuels/toxins that force cellular metabolism to its extremes. I used a combined version of these assays as described by Van den Bossche *et al*, such that both types of metabolism could be assessed in the same assay well (276). See **Figures 2.13 & 2.14** for calculation of parameters from Mito+Glyco stress test Seahorse plots. FCCP concentration was titrated for the optimised cell number using a standard Mito Stress test and stepwise FCCP injection (**Figure 2.15**).
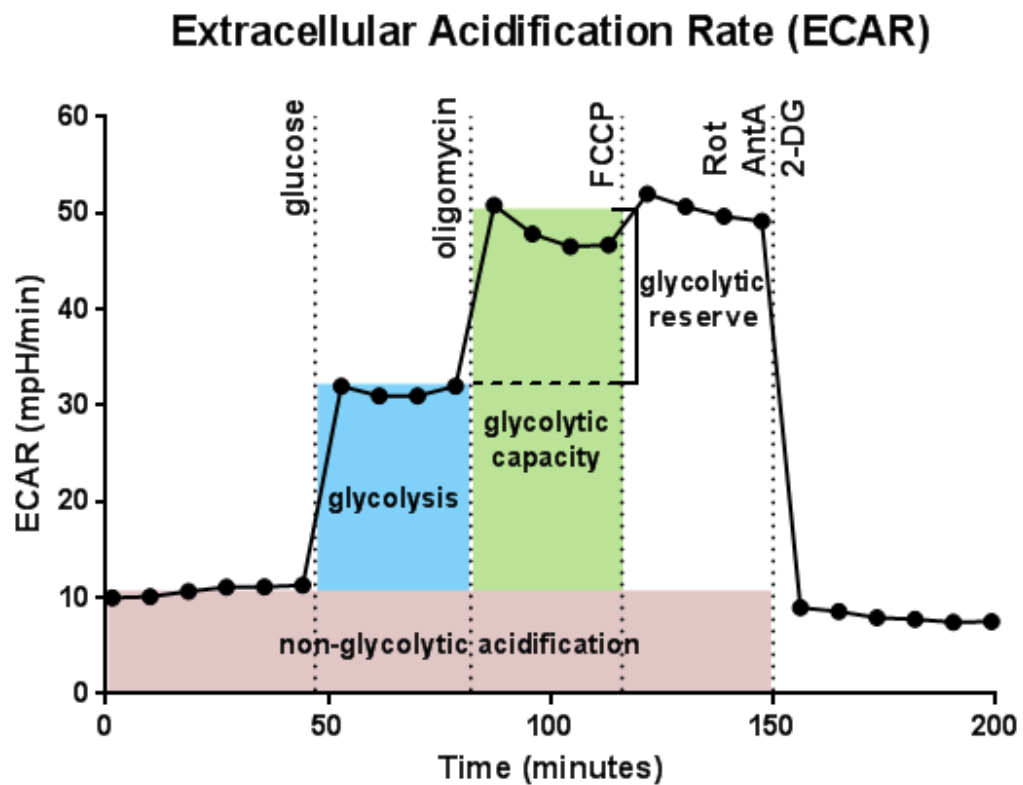
Glycolysis	max rate before oligomycin injection	MINUS	last rate before glucose injection
Glycolytic capacity	max rate before FCCP injection	MINUS	last rate before glucose injection
Glycolytic reserve	glycolytic capacity	MINUS	glycolysis
Non-glycolytic acidification	last rate before glucose injection		

Figure 2.13) Seahorse Mito+Glyco Stress Test injections and parameter calculations - ECAR

Schematic showing an example ECAR Mito+Glyco Stress Test Seahorse plot with areas indicating the metabolic parameters calculated as specified in the table

Oxygen Consumption Rate (OCR)
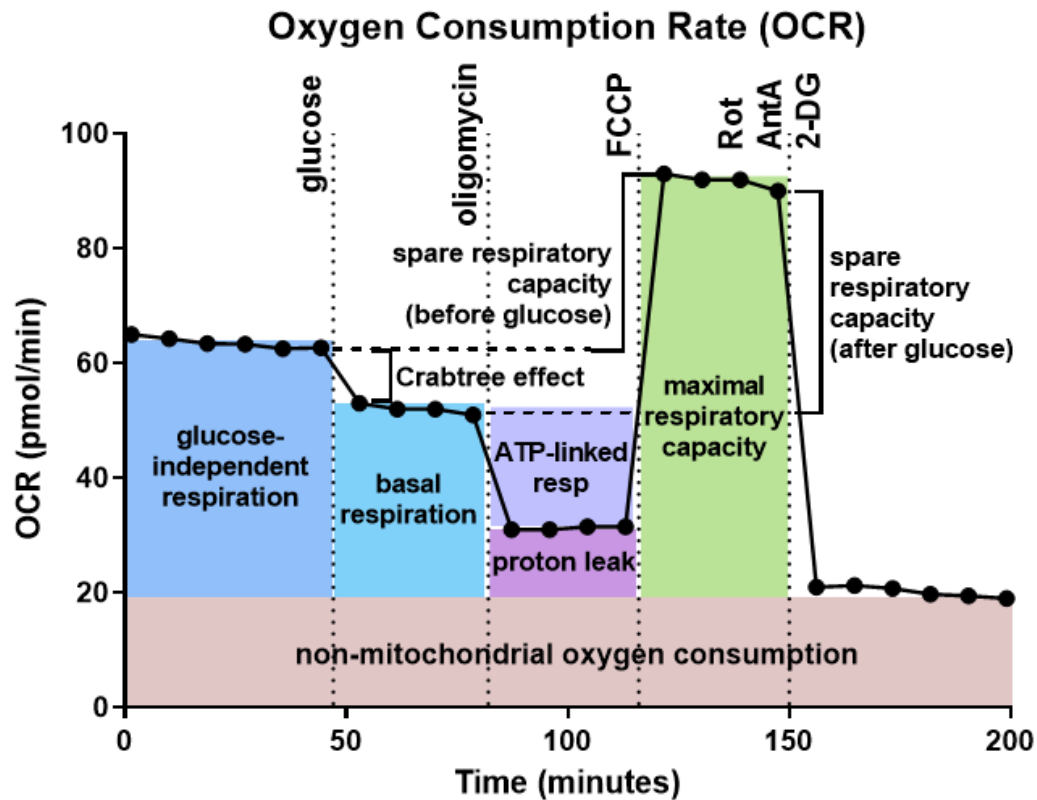
Basal Respiration (plus glucose)	last measurement before oligomycin	MINUS	non-mitochondrial oxygen consumption
Spare Respiratory Capacity (before glucose)	maximal respiration rate	MINUS	glucose-independent respiration rate
Spare Respiratory Capacity (after glucose)	maximal respiration rate	MINUS	basal respiration rate (after glucose injection)
Maximal Respiratory Capacity	maximal respiration rate	MINUS	non-mitochondrial oxygen consumption
Proton Leak	minimum rate after oligomycin injection	MINUS	non-mitochondrial oxygen consumption
Glucose-independent respiration	last measurement before glucose injection	MINUS	non-mitochondrial oxygen consumption
ATP-linked respiration	basal respiration rate (+/- glucose)	MINUS	proton leak
Crabtree effect	glucose-independent respiration	MINUS	basal respiration (plus glucose)

Figure 2.14) Seahorse Mito+Glyco Stress Test injections and parameter calculations - OCR

Schematic showing an example OCR Mito+Glyco Stress Test Seahorse plot with areas indicating the metabolic parameters calculated as specified in the table
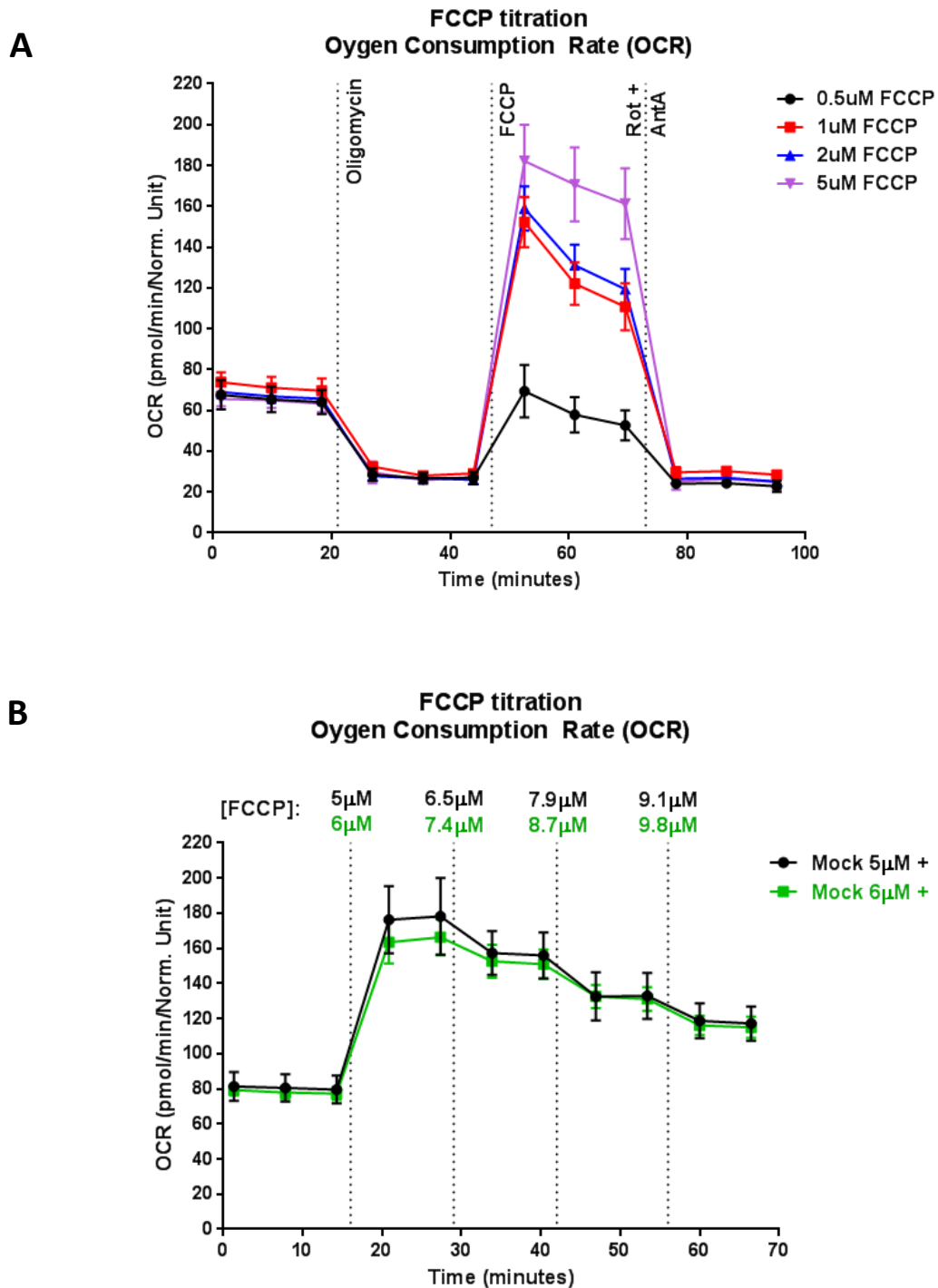
Figure 2.15) Seahorse FCCP titration

Human monocyte-derived macrophages were seeded at 50,000 cells per well in 96-well Seahorse XFe culture plate. **A)** Seahorse trace showing real-time OCR from Mito stress test, including titration of FCCP concentration; **B)** Seahorse trace showing real-time OCR from stepwise injection of FCCP to give the indicated final concentrations.

n=1 (mean+SD of technical replicates)

Table 2.19.1) Seahorse Mito+Glyco stress test

	Reagent	Final concentration	
		Human	Mouse
Assay medium	Seahorse XF Base Medium		
	Glutamine	2mM	2mM
Injection A (20μl)	Glucose	10mM	10mM
Injection B (22μl)	Oligomycin	1μM	3μM
Injection C (25μl)	FCCP	5μM	0.5μM
	Sodium Pyruvate	1mM	1mM
Injection D (28μl)	Rotenone	100nM	100nM
	Antimycin A	1μM	1μM
	2-deoxyglucose	20mM	20mM

2.19.2 ATP rate assay

The Seahorse ATP rate assay is used to determine the rates of mitochondrial and glycolytic ATP production, and involves inhibition of mitochondrial ATP synthase (complex V) using oligomycin, followed by inhibition of complexes I and III with rotenone and antimycin A respectively. I also added a final injection to inhibit glycolysis with 2-deoxyglucose (2-DG) in this assay to confirm that the ECAR reading was responding correctly, since in my cell system ECAR is not affected by mitochondrial inhibition.

ATP production rates were calculated using the Seahorse ATP assay report generator, which utilises the formulae described by Romero *et al* (277). These calculations use a theoretical P/O ratio (number of molecules of ATP produced per atom of oxygen that is reduced by a pair of electrons) of 2.75, based on oxidation of a mixture of fuels external and internal to the cell.

Table 2.19.2) Seahorse ATP rate assay

	Reagent	Final concentration
Assay medium	Seahorse XF DMEM medium w/HEPES, w/o phenol red, pH 7.4	
	Glutamine	2mM
	Glucose	10mM
	Sodium Pyruvate	1mM
Injection A (20μl)	Oligomycin	1μM
Injection B (22μl)	Rotenone	100nM
	Antimycin A	1μM
Injection C (25μl)	2-deoxyglucose	20mM

Mito+Glyco stress test & ATP rate assay were performed according to the following protocol:

Harvest cells on Day 6 of differentiation, seed into Seahorse XFe96 culture plate at 50,000 cells/well in RPMI +5% FCS +50ng/ml M-CSF, leave plate at room temperature for 1hours, then incubate overnight at 37°C. Stimulate cells in Seahorse plate in RPMI +5% FCS for 24h or as desired. Hydrate Seahorse XFe96 cartridge using 200µl/well sterile distilled water. Incubate cartridge and Seahorse Calibrant Solution overnight at 37°C (no added CO_2). Turn on Seahorse machine.

On the day of assay, replace the water in the cartridge with the pre-warmed Calibrant Solution and incubate at 37°C (no added CO_2) for at least 1h. Add the necessary fuels to 30-35ml Seahorse medium (Tables 2.19.1 & 2.19.2), adjust to pH7.4 and sterile filter. Wash stimulated cells with basal Seahorse medium to remove buffered medium, add 180µl/well pH7.4 Seahorse medium + fuels, and incubate at 37°C (no added CO_2) for 1h before running assay. Make up injection port mixes using Seahorse medium +fuels and adjust to pH7.4 (NB/ injection mixes must be made up at 10X desired final concentration). Add the indicated volumes of injection mixes to the Seahorse cassette ports (Table 2.19.1/2), being careful not to create air bubbles or jolt the cartridge (NB/ if a port is to be used for injection, every well of that port must be filled in the cassette). Calibrate the cartridge (~20mins) and insert the cell plate when directed.

Normalisation: Immediately following assay completion, remove assay medium and add 200µl/well 1µM calcein-AM in PBS. Incubate at 37°C for 30-45min and measure on plate reader (ex:490nm em:515nm). Subtract background reading and calculate a ratio of readings from all wells containing cells (such that the average =1). Input values into Wave software.

2.19.3 Respiratory chain complex activity assay

For measurement of respiration driven from each ETC complex, cells were permeabilised and supplied with complex-specific fuels (Table 2.19.3). Pyruvate+malate drive NADH production, which feeds electrons to complex I. Succinate is oxidised by complex II (succinate dehydrogenase), and electrons pass to this complex via $FADH_2$. Rotenone is included in this reaction to inhibit complex I-mediated respiration. Tetramethylhydroquinone (duroquinol) mimics reduced coenzyme A (ubiquinone), passing electrons to complex III. TMPD (*N,N,N',N'*-tetramethyl-p-phenylenediamine, also called Wurster's blue) donates electrons to cytochrome c, which is oxidised by complex IV. Ascorbate is used as a reducing agent in this reaction to prevent spontaneous oxidation of TMPD (ascorbate should be added before TMPD). BSA is included in the assay medium to maintain mitochondrial coupling after permeabilisation. See **Figure 2.16** for individual complex Seahorse plots. Cell number was titrated (data not shown) and 30,000 cells/well was found to be optimal.

Protocol was carried out according to Salabei *et al* using Agilent plasma membrane permeabiliser and injections as described in Table 2.19.3 (278). Note that assay medium must be added immediately before running on the machine due to use of membrane permeabiliser. Injection mixes must be made up in BSA-free assay medium to avoid bubbles in injection ports.
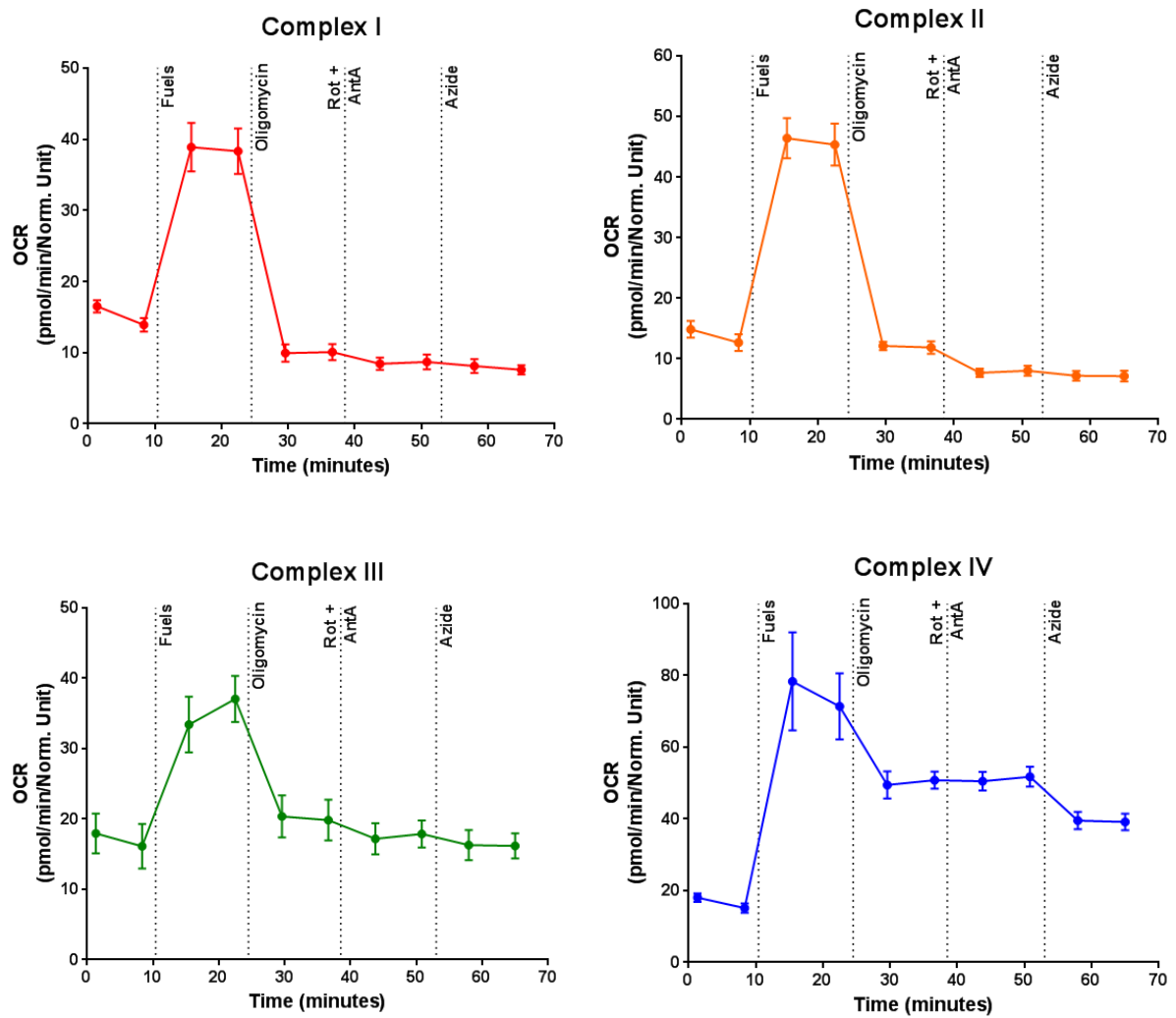
Figure 2.16) Seahorse respiratory chain assay optimisation

Human monocyte-derived macrophages were seeded at 30,000 cells per well in 96-well Seahorse XFe culture plate and permeabilised using Agilent plasma membrane permeabiliser immediately before assay (1nM). Respiration initiating from the indicated respiratory chain complex was measured by Seahorse XFe flux analyser using the fuels described in the text, and normalised to PicoGreen assay ratio; n=1 (mean+SD of technical replicates).

Normalisation: Due to cell permeabilisation in this assay, a viability dye couldn't be used for normalisation. Salabei *et al* suggest performing protein quantification for normalisation (BCA assay or equivalent), however this required washing of the plate due to the presence of BSA in the assay medium, which resulted in loss of cells. I optimised the use of a DNA quantification assay instead, which should not be affected by the assay conditions. I used PicoGreen fluorescent dsDNA dye for respiratory chain assay normalisation.

Immediately following assay completion, medium was removed and replaced with 200µl/well 1/400 PicoGreen in TE buffer, incubated at room temperature in the dark for 30min and measured on a Labsystems Fluoroskan Ascent plate reader (ex:485nm, em:528nm).

Complex-specific activity was calculated as the average of measurements after fuel injection, minus final measurement after inhibition.

Table 2.19.3) Seahorse respiratory chain complex activity assay

	Reagent	*Final concentration*
Assay medium	**MAS buffer**	
	ADP	1mM
	BSA	4mg/ml
	Plasma Membrane Permeabilizer	1nM
Injection A (20µl)	**Complex-specific fuels**	
Complex I	Pyruvate	5mM
	Malate	2.5mM
Complex II	Succinate	10mM
	Rotenone	1µM
Complex III	Tetramethylhydroquinone (Duroquinol)	0.5mM
Complex IV	TMPD	500mM
	Ascorbate	200mM
Injection B (22µl)	Oligomycin	1µM
Injection C (25µl)	Rotenone	1µM
	Antimycin A	1µM
Injection D (28µl)	Sodium Azide	20mM

2.20 GC-MS

Gas chromatography-mass spectrometry (GC-MS) was performed on conditioned medium (100µl/sample) from 5 donors stimulated in 6well plates for 24h.

Polar metabolites were extracted using the following protocol:

Precipitate protein by adding 4 volumes of ice cold 8:2:2 isopropanol:acetonitrile:water, shake at high speed on ice for 15min. Centrifuge at high speed, 4°C 10min. Transfer 400µl of supernatant to a fresh tube. Add 500µl of ice cold MS-grade methanol and 200µl of D6-Glutaric acid internal standard working solution (2.5µg/ml in water). Vortex and shake at high speed on ice for 15min. Add 500µl chilled chloroform using a glass syringe. Vortex and shake at high speed on ice for 15min. Centrifuge at high speed, 4°C 10min. Transfer top layer (polar metabolites) in a fresh tube. Vacuum dry and store at -80°C until further processing.

Derivatisation: N-(t-butyldimethylsilyl)-N-methyltrifluoroacetamide (MTBSTFA) was used for silylation of acidic functional groups to decrease polarity and increase volatility.

Derivatisation was performed using the following protocol (including derivatisation blank):

Add 40µl Methoxyamine hydrochloride [MeOX] solution in pyridine (20mg/ml). Vortex vigorously and incubate for 1h at 60°C. Add 60µl MTBSTFA, vortex vigorously and incubate for 1h at 60°C. Centrifuge at high speed, 4°C 10min. Transfer to glass vials with micro-inserts and cap immediately. Store at -20°C or analyse immediately.

Data acquisition and processing were performed by Alpesh Thakker. Data acquisition was performed using an Agilent 6890GC and Agilent 5975C MS. Data processing was performed using MetaboliteDetector (279).

2.21 Enzyme-Linked Immunosorbent Assays (ELISA) and Luminex

2.21.1 ELISA

Cytokine ELISAs were performed on conditioned medium samples from cell stimulations collected at time of cell harvest and frozen until analysis. Human IL-10 and IL-6 ELISAs were performed according to manufacturer's protocols. Samples were diluted as in Table 2.21. Readings were taken on a BioTek Synergy HT 96-well plate reader. Standard curves were fitted using nonlinear regression and sample concentrations calculated from the curve equation in GraphPad Prism v6.

Table 2.21) ELISA sample dilution

Target	Dilution factor	
	Unstimulated	LPS
Human IL-10	1	20
Human TNFα	1	20
Human IL-6	1	40

Human TNFα ELISA was performed using the following protocol:

Dilute capture antibody 1/125 in PBS (4µg/ml) and coat 96-well plate with 50µl/well overnight at 4°C. Wash plate 3x with PBS-T (PBS +0.005% Tween-20). Block plate with 100µl/well 2% BSA in PBS. Incubate, 1h at room temperature. Make a 3-fold serial dilution of TNFα standard (10,000pg/ml to 13.71pg/ml) in PBS+0.5% BSA by first diluting master stock 1/1000. Dilute samples in PBS+0.5% BSA. Wash plate 3x with PBS-T. Add 50µl/well of standard or sample, each in triplicate. Incubate for 2h at room temperature or 4°C overnight. Wash plate 3x with PBS-T. Dilute biotylated TNFα detection antibody 1/000 in PBS+0.5%BSA. Add 50µl/well and incubate, 1h at room temperature. Wash plate 3x with PBS-T. Dilute Avidin-HRP as instructed by manufacturer and add 50µl/well. Incubate, 45min at room temperature. Wash plate 5-6x with PBS-T, incubating for a minute during each wash. Combine TMB reagents 1:1 and add 50µl/well. Incubate on plate rocker in the dark for 15mins or until bottom

standard is just starting to turn blue. Add 50µl/well 2N HCl to stop the reaction. Read at 450nm.

2.21.2 Luminex

Luminex assay was performed on conditioned medium from Donor 46 according to manufacturer's protocol, with the exception that volumes were halved to allow two plates to be performed. Samples were diluted 1/2, 1/20 and 1/50.

2.22 NDUFA4 patients

NDUFA4-associated Leigh syndrome patients (3 individuals) were recruited by Dr Robert Pitceathly at the Queen Square Centre for Neuromuscular Diseases, University College London. Blood samples were collected at UCL and transported to the University of Birmingham for processing. Cells were isolated as described in Section 2.10. Controls samples were collected at the University of Birmingham and processed alongside patient samples. See (280) for genetic and clinical patient details.

2.23 Ethics

Healthy leukapheresis blood cones were obtained from the National Blood and Transplant Service under ethical approval code ERN_16-0191. Peripheral blood samples from patients with NDUFA4 mutations were obtained under Material Transfer Agreement with University College London. The study was approved by the Queen Square Research Ethics Committee, London (09/H0716/76). Informed consent was obtained from all participants.

2.24 Statistics

Statistical analyses were carried out using GraphPad Prism v6. Statistical tests and corrections utilised are indicated in figure legends. * $p < 0.05$; ** $p < 0.01$; *** $p < 0.001$; **** $p < 0.0001$.

Chapter 3) Glucocorticoids regulate microRNA expression in macrophages

3.1 Introduction

3.1.1 MiRNAs in inflammation

As discussed in chapter 1, miRNAs are capable of targeting a myriad of genes, and are vital regulators of both adaptive and innate immune responses. In this chapter I aimed to characterise the regulation of miRNAs by the anti-inflammatory glucocorticoid steroid hormone in macrophages, and I therefore focused on known regulators of macrophage inflammatory responses, which have been linked to the functions of GCs in certain contexts.

miR-146a

MicroRNA-146a was one of the first miRNAs to be linked to innate immune signalling, found to be upregulated after TLR stimulation through the action of NF-κB (281). This miRNA is an important negative regulator of the NF-κB signalling pathway, contributing to the induction of endotoxin tolerance in innate immune cells (282). This phenomenon describes a state of hyporesponsiveness following an initial inflammatory challenge (such as TLR4 activation by LPS) and serves to prevent excessive production of pro-inflammatory cytokines that could cause tissue damage. While the mechanisms underlying endotoxin tolerance are complex, Nahid *et al* demonstrated that miR-146a inhibition diminished the tolerising effect of LPS in the human monocytic cell line THP1 (282). The negative feedback shown by this miRNA is mediated through the direct targeting of two upstream regulators of the NF-κB pathway: IRAK1 and TRAF6, both of which contain multiple predicted target sites for miR-146a in their 3'UTRs (281, 283). These two genes encode important adapter proteins required for signal transduction downstream from TLRs and IL-1R (**Figure 1.2**).

NF-κB signalling is also important in adaptive immune cells, and miR-146a is upregulated in T cells upon T cell receptor activation (284). Consistent with its reported roles in both innate and adaptive immune responses, miR-146a-/- mice show increased autoimmunity, characterised by excessive myeloid cell proliferation and loss of peripheral T cell tolerance (283). Peripheral blood mononuclear cells (PBMCs) from patients with the autoimmune condition systemic lupus erythematosus (SLE) show decreased expression of miR-146a, and expression levels negatively correlate with disease severity (284). In contrast, miR-146a is upregulated in multiple cell types in RA and its expression positively correlates with TNFα levels and disease activity score (285, 286). This expression is likely induced by the highly inflammatory environment, and its consistent elevation in plasma of RA patients makes it an interesting potential biomarker of disease. It would also be of interest to understand why the high levels of miR-146a fail to curb the expression of pro-inflammatory cytokines in these patients (284).

Feng *et al* showed that miR-146a is elevated in CD4+ T cells in a mouse model of acute asthma, and that the expression is inhibited by treatment with dexamethasone (287). However Tsitsiou *et al* reported a decrease in miR-146a expression in circulating CD4+ and CD8+ T cells from asthma patients compared with controls (288).

The work on miR-146a identified miRNAs as crucial effectors in negative feedback mechanisms, which are critical for the prevention of serious diseases associated with dysregulated inflammatory responses.

miR-21

MiR-21 is well-studied as an oncogenic miRNA, and is a key player in the link between inflammation and cancer through the targeting of tumour suppressor PTEN in response to inflammatory stimuli (289). Like miR-146a, miR-21 has been shown to mediate negative feedback of TLR signalling. PDCD4 is another tumour suppressor that has been validated as a target of miR-21. This protein functions in response to cytokine signalling to activate inflammatory NF-κB activity, and concurrently to inhibit expression of the anti-inflammatory cytokine IL-10. Downregulation of PDCD4 by miR-21 is therefore thought to contribute to the phenotypic switch of macrophages from pro-inflammatory to pro-resolution function (290). MiR-21 also inhibits immune signalling through the direct targeting of IL-12p35, a cytokine that promotes Th1 differentiation (291). The upregulation of miR-21 in airway macrophages during allergic airway inflammation has therefore been linked to increases in Th2 differentiation that contribute to the disease, and inhibition of miR-21 was found to suppress airway inflammation (291, 292). MiR-21 expression in bronchial epithelial cells was lower in asthma patients treated with inhaled corticosteroids, compared with non-treated patients (293).

miR-155

MicroRNA-155 is one of the best studied miRNAs in the fields of both immunology and oncology. It is expressed from the *BIC* transcript, an RNA species derived from the integration site of avian leukosis virus, which causes B cell lymphoma in chickens (294). The lack of extensive open reading frame and prediction of organised secondary structure in the BIC RNA hinted to a non-translational role, and there was growing evidence for the role of non-coding RNAs in growth and development at this time (295). BIC was also seen to be overexpressed in

human lymphomas, and the explosion of the field of miRNAs in the early 2000s lead to the annotation of miR-155 within this transcript (296). MiR-155 was consequently one of the first described oncomirs, and has become the focus for development of some of the first miRNA-directed therapeutics (115, 124, 125).

MiR-155 is important for functional immune homeostasis, hence its dysregulation contributes to lymphocyte malignancies (124, 296). Mice lacking the *BIC* transcript are unable to mount a protective vaccine response against *Salmonella typhimurium*, with T cells in these mice showing a bias towards Th2 differentiation (297). A role for miR-155 in the innate immune response was identified by Taganov *et al* during a screen for miRNAs induced by TLR4 stimulation in THP1 cells (281). The group went on to determine that miR-155 can be induced by a variety of stimuli, including other TLR agonists and interferon (298). A strong pro-inflammatory role has been reported for miR-155, through the direct targeting of multiple anti-inflammatory mediators, including suppressor of cytokine signalling 1 (SOCS1) (299) and Src homology 2-containing inositol phosphatase 1 (SHIP1) (300, 301). Repression of these targets results in expansion of myeloid cell compartments and increased production of pro-inflammatory mediators (300, 302). MiR-155 is overexpressed in synovial macrophages and fibroblasts during RA, and causes elevated expression of chemokines and chemokine receptors, contributing to the inflammatory state (285, 303, 304). miR-155-/- mice are resistant to collagen-induced arthritis, and show lack of synovial inflammation and bone destruction upon collagen injection (301).

In additional to these pro-inflammatory functions, miR-155 has been reported to display anti-inflammatory function by negatively regulating NF-κB activation (117). Silencing

of miR-155 resulted in upregulated expression of pro-inflammatory cytokines in monocyte-derived dendritic cells, including IL-1β. MiR-155 was found to target TAB2, a component of the TRAF6 protein complex that activates p38 MAPK and NF-κB signalling downstream of PRRs (**Figure 1.2**) (305). Xiao *et al* identified additional direct targets of miR-155, including the IκB kinase IKK-ε, and miR-155 upregulation in gastric epithelial cells inhibited IL-8 production (114). These contradictory roles of miR-155 in both promoting and attenuating inflammatory signalling demonstrate the complexity of miRNA action. Specific responses are likely to be both cell type and context-dependent, complicating the therapeutic harnessing of miRNAs, and highlighting the importance of *in vivo* study of cellular responses in biologically relevant systems.

As discussed in Chapter 1, miR-155 is regulated by GCs, which inhibit LPS-induced expression of miR-155 in human and mouse macrophages (133), and I sought to replicate this in my experiments. The study by Zheng *et al* implicated miR-155 inhibition in the functional effects of GCs (133).

3.1.2 miRNA-147

The murine miRNA miR-147 has also been associated with inflammatory signalling. Liu *et al* reported that miR-147 is derived from the 3'UTR of the *NMES1* transcript (aka AA467197 in mouse, *C15orf48* in human) (10). This gene has been shown to express a short protein product, but no precise function for this protein has been determined. Additional links between this gene and inflammation have been made in IL-1β-treated astrocytes and in virally-infected cells, where is it shown to be upregulated (306-308). Methylation of the *C15orf48/NMES1* locus has been reported in colon cancer and cervical carcinoma, and associated with poor prognosis in esophageal squamous cell carcinoma (309-312).

Liu *et al* found that expression of miR-147 in mouse macrophages is induced by activation of TLR4 by LPS; TLR2 by PAM3CSK4; and TLR3 by poly(I:C). Full expression is driven by both MyD88 and TRIF pathway signalling through the action of NF-κB and STAT1 transcription factors. The authors reported that miR-147 is a negative regulator of macrophage inflammatory responses, as a miR-147 mimic inhibited the TLR-induced production of TNFα and IL-6 from mouse peritoneal macrophages (10). Consistent with its upregulation by TLR activation, miR-147 was found to be more highly expressed in M1 macrophages (LPS+IFNγ-induced) than M2 macrophages (IL-4-induced) (313). Contrary to the proposed anti-inflammatory role of miR-147, however, are the results of a study of periodontitis in rat models, in which miR-147 was found to be elevated. Inhibition of miR-147 in this model lead to a decrease in expression of the pro-inflammatory cytokines TNFα and IL-12, as well as the gene encoding iNOS (*Nos2*), which synthesises the inflammatory mediator NO (314).

MiR-147 has also been associated with viral infection, consistent with its induction by TLR3 activation and IRF3 signalling, and was found to be upregulated in mouse lung tissue upon viral infection (315). Conversely, miR-147 was strongly repressed in porcine alveolar macrophages upon infection with Porcine Reproductive and Respiratory Syndrome Virus, and overexpression with a miR-147 mimic inhibited viral replication (316). MiR-147 was shown by 3'UTR luciferase assay to target a number of genes in this study, including GM-CSF and STAT6 (316).

The human homologue of mouse miR-147 (miR-147b) has an identical sequence to the mouse miRNA, and expression changes of miR-147b have been linked to various types of cancer. Several groups have reported decreased expression in colorectal cancer, and

overexpression was shown to reduce proliferation, migration and chemotherapy resistance in colorectal cancer and hepatocellular carcinoma (317-319). The mechanism of tumour suppression by miR-147b have been reported as an inhibition of the epithelial-to-mesenchymal transition that is associated with aggressive and invasive cancers; through decreased Akt phosphorylation, and inhibition of c-Myc and β-catenin expression (318, 320). Conversely, elevated miR-147b levels were associated with increased resistance to chemotherapy and poor prognosis in small cell lung cancer (321). The identification of circulating miRNAs that could be prognostic for disease progression or response to therapy could allow better stratification and more effective disease treatment. However, the specific role of this miRNA in tumours appears to be highly dependent upon tissue type and tumour status, highlighting the need for thorough investigation in different cell types (322).

MiR-147b has been linked to the miRNA miR-210, as the pair share an identical seed sequence. MiR-147b and miR-210 were found to show similar targeting in luciferase studies, further demonstrating the importance of the seed region, as these miRNAs share no other sequence match. While miR-147b is induced by LPS and TNFα, miR-210 is induced by hypoxia, implying that these miRNAs may play similar roles but in response to different environmental cues (323).

The only report of miR-147 regulation by GCs to my knowledge is a study by Shen *et al*, which looked at miRNA regulation in muscle tissue during dexamethasone-induced muscle atrophy. MiR-147 was found to be significantly decreased in mouse myoblast cells upon Dex treatment, along with several other miRNAs, however the authors did not investigate the mechanisms by which these miRNA may contribute to GC action in these cells (324).

The miRNAs mentioned in this section all have established roles in immune regulation, in particular the macrophage response to TLR activation. Although the regulation of these miRNAs by GCs in some systems has been suggested, this has not been extensively demonstrated, and merits further investigation. Many of the major immunoregulatory effects of GCs occur through their action in macrophages, therefore my aim was to examine the regulation of these inflammation-associated miRNAs by GCs in this cell type.

Results

3.2 The regulation of inflammation-associated miRNAs by glucocorticoids

The expression of the three major immune regulatory miRNAs discussed above – miR-155, miR-146a and miR-21 – was measured in macrophages in response to TLR4 stimulation by LPS, in the presence or absence of the synthetic glucocorticoid dexamethasone (Dex). This glucocorticoid was used as it is a highly potent activator of the glucocorticoid receptor, with minimal mineralocorticoid activity. It does not require local activation through 11β-HSD activity, and it is frequently used therapeutically (63, 66). MiR-155 was strongly upregulated by LPS in mouse bone marrow-derived macrophages (BMDMs) (**Figure 3.1A**), and also upregulated in human monocyte-derived macrophages (MoDMs) (**Figure 3.1B**), consistent with previous findings from THP1 cells (281). The LPS-induced expression of miR-155 showed significant inhibition by Dex across the whole time course examined, in both species. This replicates the work by Zheng *et al*, and gave me confidence in my experimental design (133).
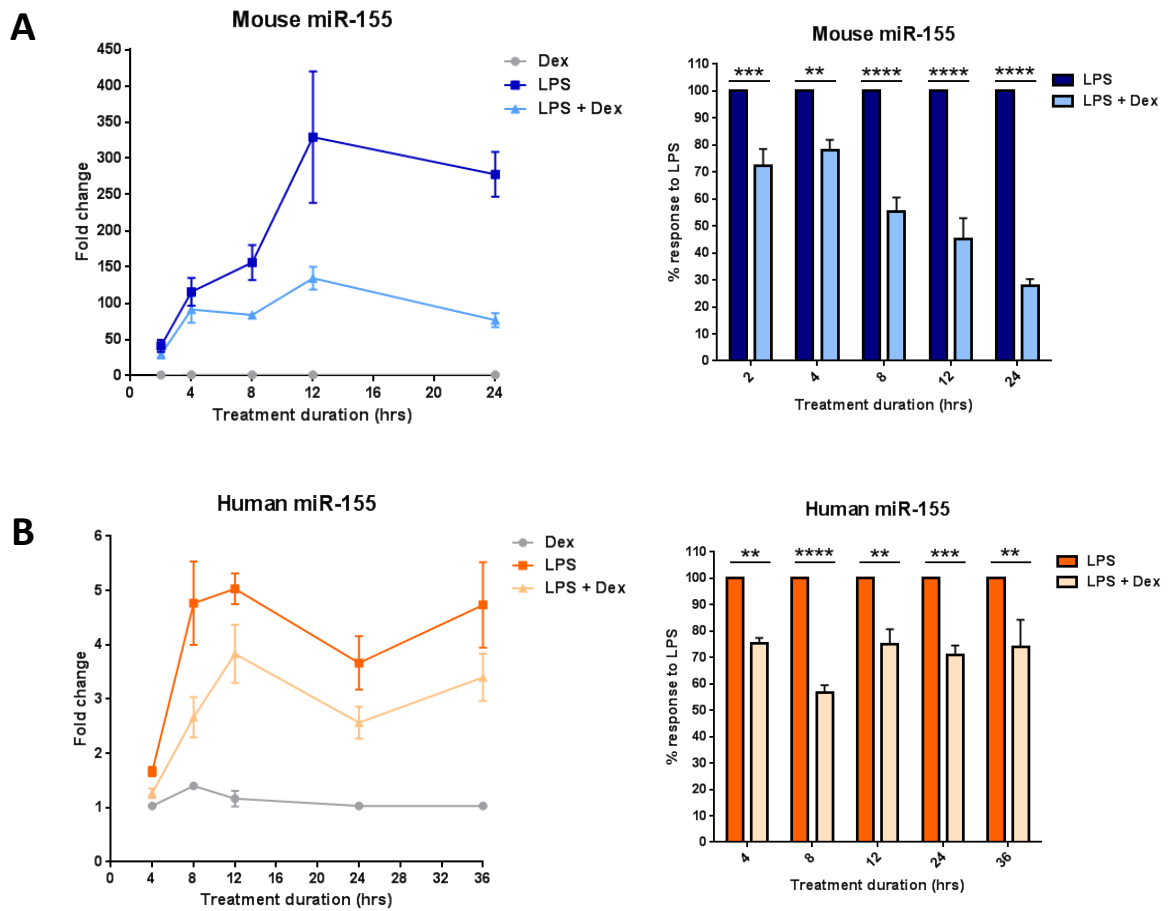
Figure 3.1) Regulation of miRNA-155 by glucocorticoids in macrophages

A) WT mouse BMDMs and **B)** human monocyte-derived macrophages were stimulated with LPS (10ng/ml), Dex (100nM) or a combination of the two for the indicated times. **A)** mmu-miR-155 or **B)** hsa-miR-155 were detected by RT-qPCR. Expressed as fold change (2^-ΔΔCt) normalised to RNU6-2, relative to time-matched mock treated control; also as % response to LPS at each time point to demonstrate effect of Dex; all n=3; Two-way ANOVA with Sidak correction for multiple comparisons. Data presented as mean +/-SEM.

The induction of miR-146a by LPS in mouse BMDMs was to a much lesser degree than that of miR-155 (**Figure 3.2**). Consistent with its role in the negative regulation of TLR pathway signalling, miR-146a was upregulated late in the time course of stimulation in mouse macrophages. This miRNA showed no significant inhibition by Dex (**Figure 3.2**). Human miR-146a showed only minor upregulation by LPS, in contrast to published work (281, 282). This may be due to difference between primary macrophages and the monocytic cell line THP1 that was used in these studies (281, 282). The addition of dexamethasone resulted in significantly higher expression of human miR-146a in the LPS+Dex samples relative to LPS alone at later time points, but since the fold induction was less than 2 it is unclear whether this would have biological relevance (**Figure 3.2B**).

In contrast to the reports of Sheedy *et al* (290), the expression of miR-21 was not significantly induced by LPS in mouse macrophages, and was slightly inhibited in human macrophages (significant relative to mock at 36h – statistics not shown) (**Figure 3.3**). The discrepancy of these data with previous reports may be due to different concentrations of LPS used (100ng/ml used by Sheedy *et al*) (290). In comparison to LPS treatment alone, the addition of Dex significantly increased the expression of miR-21, but this occurred only at select time points and the magnitude of response was not great (**Figure 3.3**).
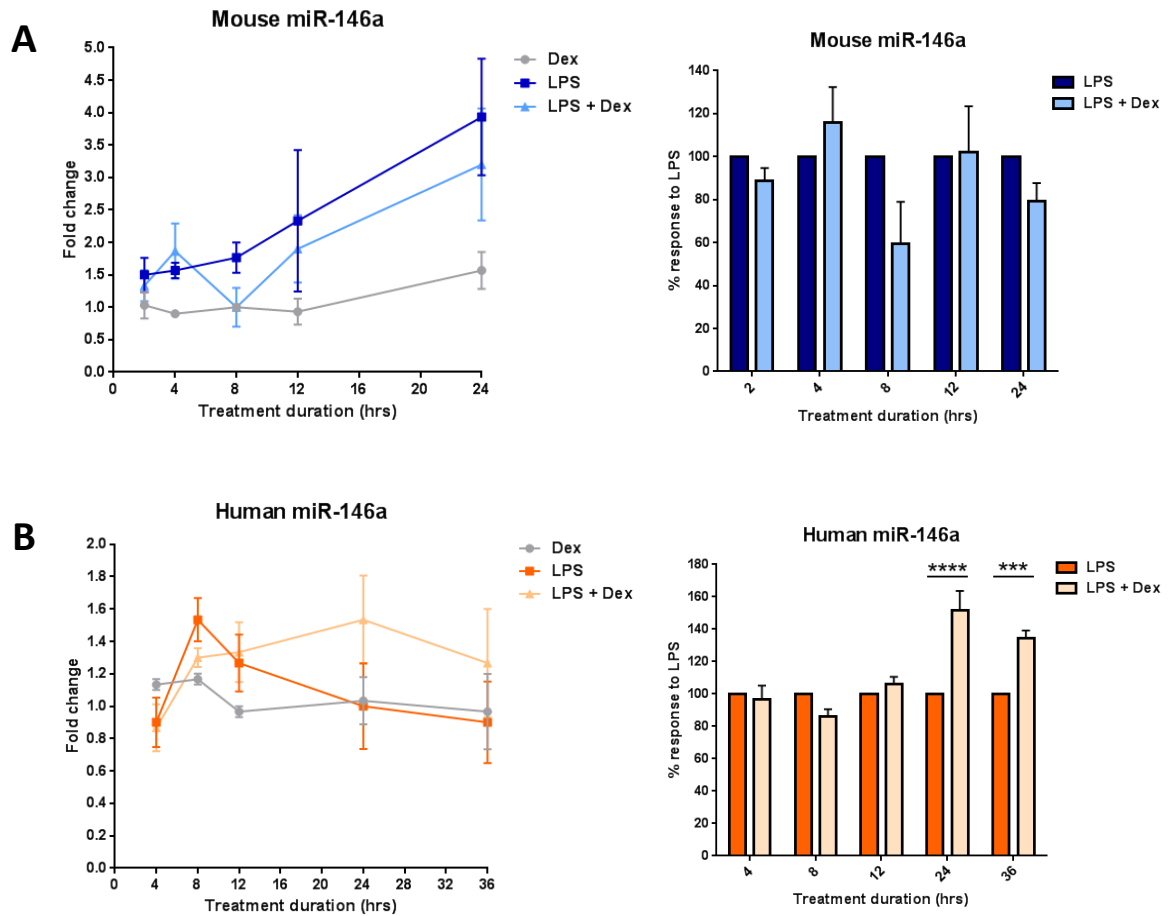
Figure 3.2) Regulation of miRNA-146a by glucocorticoids in macrophages

A) WT mouse BMDMs and **B)** human monocyte-derived macrophages were stimulated with LPS (10ng/ml), Dex (100nM) or a combination of the two for the indicated times. **A)** mmu-miR-146a or **B)** hsa-miR-146a were detected by RT-qPCR. Expressed as fold change (2^-ΔΔCt) normalised to RNU6-2, relative to time-matched mock treated control; also as % response to LPS at each time point to demonstrate effect of Dex; all n=3; Two-way ANOVA with Sidak correction for multiple comparisons. Data presented as mean +/-SEM.
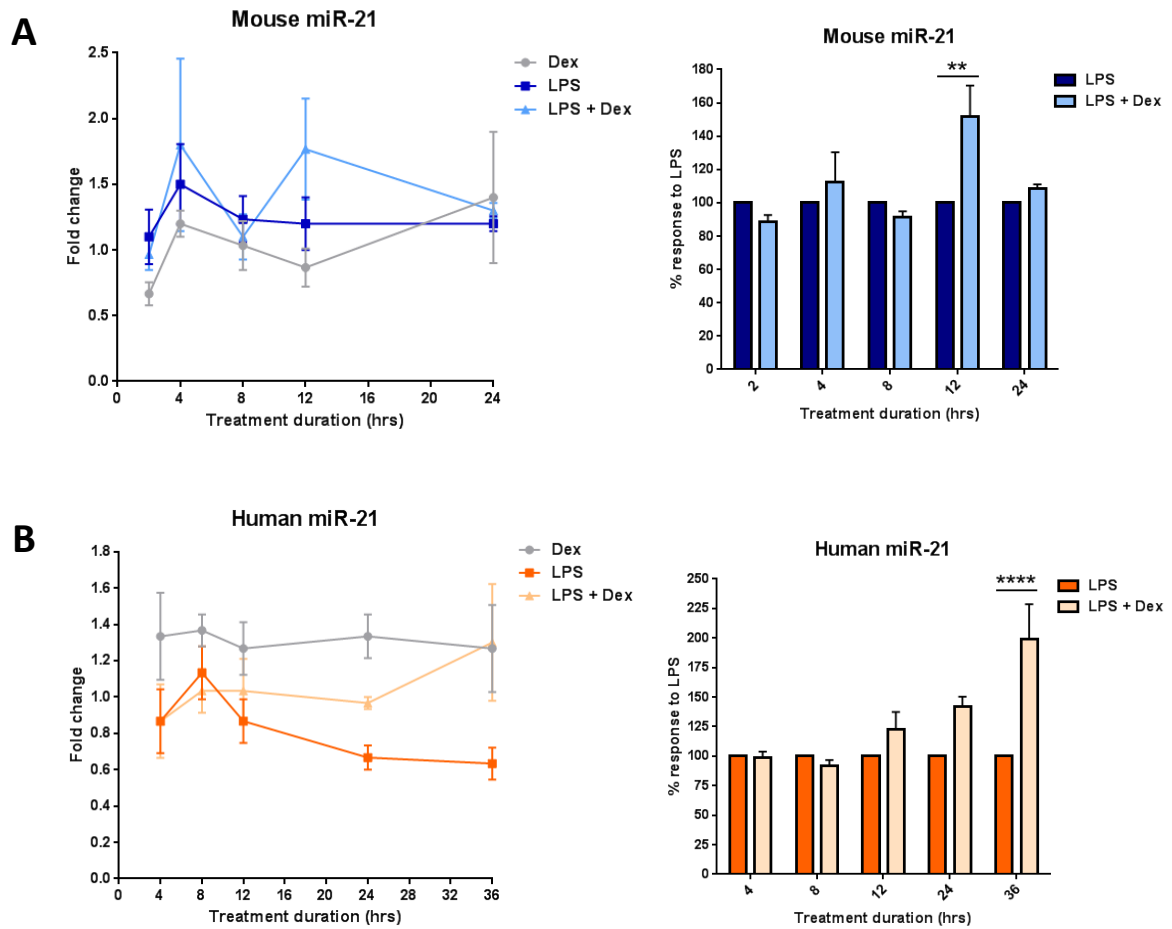
Figure 3.3) Regulation of miRNA-21 by glucocorticoids in macrophages

A) WT mouse BMDMs and **B)** human monocyte-derived macrophages were stimulated with LPS (10ng/ml), Dex (100nM) or a combination of the two for the indicated times. **A)** mmu-miR-21 or **B)** hsa-miR-21 were detected by RT-qPCR. Expressed as fold change ($2^{-\Delta\Delta Ct}$) normalised to RNU6-2, relative to time-matched mock treated control; also as % response to LPS at each time point to demonstrate effect of Dex; all n=3; Two-way ANOVA with Sidak correction for multiple comparisons. Data presented as mean +/-SEM.

3.3 MiR-147(b) as a novel target of glucocorticoids in macrophages

In order to identify uncharacterised miRNA targets of GCs, I carried out analysis of microarray data that had previously been generated by the Clark group from LPS and dexamethasone-treated mouse BMDMs. I created lists of genes that were differentially expressed between LPS and LPS+Dex conditions using Partek Genomics Suite. The microarray had not been carried out to detect non-coding RNAs, therefore the probe set used was not specific for miRNAs. The online tool Ensembl BioMart allows annotation of probes that are known to be associated with miRNA-containing genomic regions, so I applied this analysis to the differentially expressed gene lists. Only two of these probes were annotated to be associated with a miRNA - the miRNAs being miR-147 and miR-29c (**Figure 3.4A**). Examination of the raw data showed that the miR-147-associated transcript was strongly upregulated by LPS and significantly inhibited by Dex, while the miR-29c-associated transcript was slightly inhibited by LPS and upregulated by Dex (**Figure 3.4B**).

The miR-29 family has been linked to both oncogenic and tumour-suppressive actions in multiple cancer types, including haematological malignancies. These miRNAs have been described as key regulators of adaptive immunity by controlling T cell polarisation; and at least 50 genes have been validated as targets of this miRNA family in various cell types. These targets include IFNγ and the Th1-associated transcription factor T-bet, as well as DNA methyltransferases DNMT3A/B (325, 326). MiR-29b and miR-29c have previously been shown to be upregulated by dexamethasone in plasmacytoid dendritic cells, and were reported to contribute to Dex-induced apoptosis through targeting of anti-apoptotic Bcl-2 (327).

A

Probe ID	Gene Name	Annotated miRNA (BioMart)	p-value (Treatment)	p-value (4h LPS vs. 4h LPS + Dex)	Ratio (4h LPS vs. 4h LPS + Dex)	Fold-Change (4h LPS vs. 4h LPS + Dex)
A_55_P2 137049	AA467197	**miR-147**	9.22098E-28	2.97536E-07	2.34398	2.34398
A_30_P0 1023491	chr1:1968435 92-196865102_F	**miR-29c**	1.76505E-07	0.0001145 94	0.415046	-2.40937

B
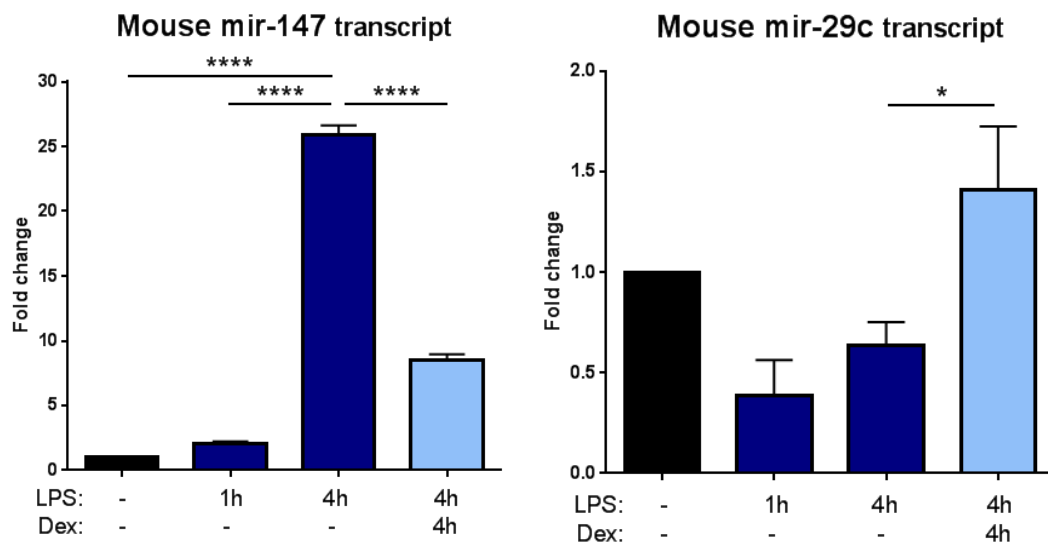
Figure 3.4) Identification of glucocorticoid-regulated microRNAs by microarray analysis
A) MicroRNAs significantly altered by Dex treatment of LPS-stimulated mouse BDMDs were identified by analysis of previously-generated microarray data using Partek Genomics Suite and Ensembl BioMart (Agilent SurePrint G3 GE 8x60k probeset). Table shows results from Partek analysis.
B) Raw data corrected for input variation were normalised to unstimulated condition and subjected to One-way ANOVA with Dunnett's correction for multiple comparisons, compared with 4h LPS treatment only, using GraphPad Prism; n=3. Data presented as mean +SEM.

In contrast, miR-147 is a fairly poorly studied miRNA with few validated target genes. miR-147 has only been associated with GC action in muscle cells, and no specific function was described in these cells (324). I therefore used RT-qPCR to confirm the microarray results, as well as the results of Liu *et al,* that miR-147 is strongly induced by LPS in mouse BMDMs (**Figure 3.5A**) (10). I also showed that the human homologue, miR-147b, was upregulated in response to TLR4 activation (**Figure 3.5B**), which was not reported by Liu *et al* (10). The RT-qPCR also confirmed the microarray results that induction of mouse miR-147 by LPS was strongly and significantly inhibited by GC. The same was true of human miR-147b (**Figure 3.5**). In order to rule out the possibility that this regulation occurs at a downstream miRNA processing step, I measured the expression of the primary miRNA transcript (pri-mir-147b), derived from the *C15orf48* gene locus, in samples from LPS+/-Dex-treated human macrophages. The primers used target the 3'UTR of the *C15orf48* gene, flanking the miR-147b sequence. The results show an identical expression profile to the mature miR-147b, confirming that regulation indeed occurs at the level of the precursor transcript (**Figure 3.5C**). This was expected given the microarray result, which also shows expression of the primary *C15orf48* transcript (**Figure 3.4**).
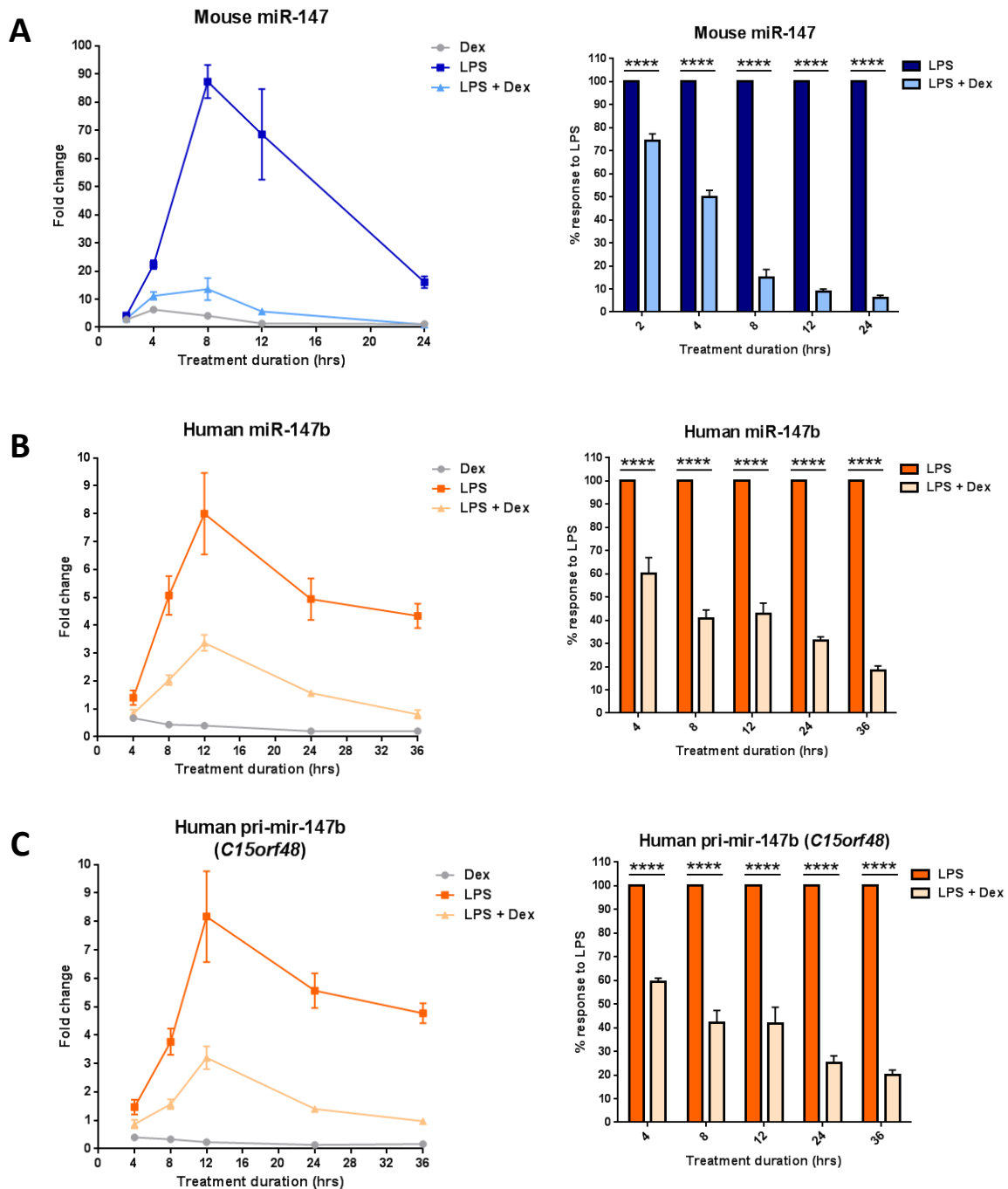
Figure 3.5) miR-147(b) as a novel target of glucocorticoids in macrophages

A) WT mouse BMDMs or **B&C)** human monocyte-derived macrophages were stimulated with LPS (10ng/ml), Dex (100nM) or a combination of the two for the indicated times. **A)** mmu-miR-147; **B)** hsa-miR147b and **C)** pri-mir-147b (*C15orf48*) were detected by RT-qPCR. Expressed as fold change ($2^{\wedge}$-ΔΔCt) normalised to RNU6-2 (**A&B**) or UBC (**C**), relative to time-matched mock treated control; also as % response to LPS at each time point to demonstrate effect of Dex; all n=3; Two-way ANOVA with Sidak correction for multiple comparisons. Data presented as mean +/-SEM.

3.4 Differential regulation of miRNAs through type I interferon signalling

As discussed in Chapter 1, macrophage responses to LPS are partially dependent upon TBK and IRF3-mediated production of interferon β (IFNβ) (**Figure 1.2**), which drives an autocrine/paracrine feedback loop by binding to its receptors on the cell surface. The resulting activation of STAT1 and/or STAT2 transcription factors by the Janus kinases JAK1 and TYK2 contribute to a second wave of transcriptional activation that can be blocked by Janus kinase inhibitors. Amongst the secondary, IFNβ-induced genes are both pro-inflammatory and anti-viral mediators (5, 30). It has been suggested that GCs inhibit IFNβ-mediated JAK-STAT signalling (328-330). Researchers in the Clark group had also uncovered evidence that GCs can disrupt the IFNβ-mediated feedback loop in LPS-stimulated macrophages, as Dex was found to dose-dependently inhibit IFNβ protein expression in mouse BMDMs (**Figure 3.6**). Given the relatively slow induction of miR-147 in response to LPS (peaking at 8-12h), I wondered whether this could be a secondary, IFNβ-dependent process.

In mouse BMDMs, miR-147 was strongly induced by LPS and significantly inhibited by dexamethasone, as shown previously (**Figure 3.7A**). Expression of miR-147 was also strongly induced by treatment of macrophages with IFNβ alone, the response being evident earlier than that of LPS. However in this case the induction was not inhibited by Dex, but actually augmented at some time points. LPS-induced expression of miR-147 was strongly reduced by the JAK inhibitor Ruxolitinib (**Figure 3.7B**). This suggests that LPS may induce the expression of miR-147 in mouse BMDMs at least partly via IFNβ, and that Dex might inhibit miR-147 expression by blocking IFNβ biosynthesis.
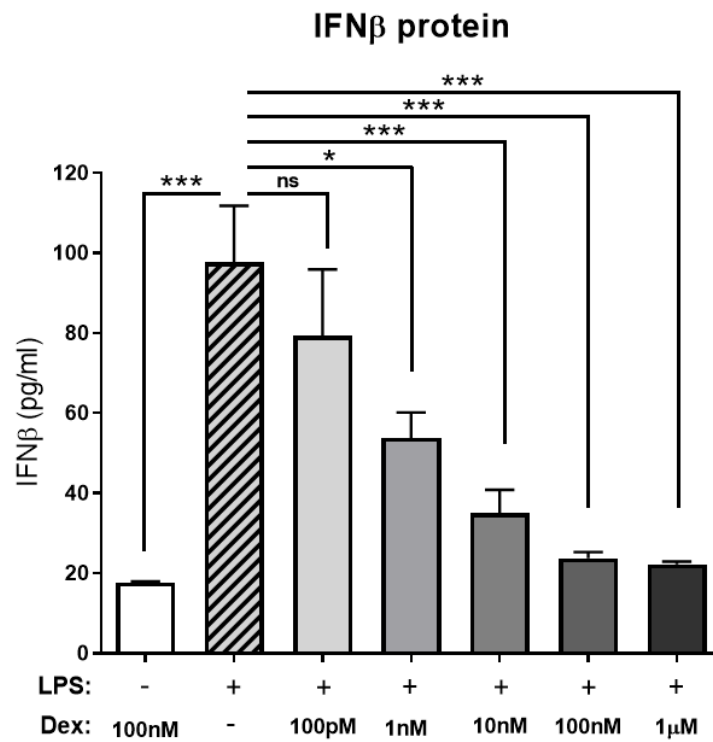
Figure 3.6) Interferon-β is dose-dependently inhibited by dexamethasone in mouse BMDMs

Data generated by Tina Tang

WT mouse BMDMs were stimulated with LPS (10ng/ml) and the indicated concentrations of Dex for 8h. IFNβ was measured in conditioned medium by Luminex; n=3; One-way ANOVA with Dunnett's correction for multiple comparisons, compared with LPS stimulation alone. Data presented as mean +SEM.

A
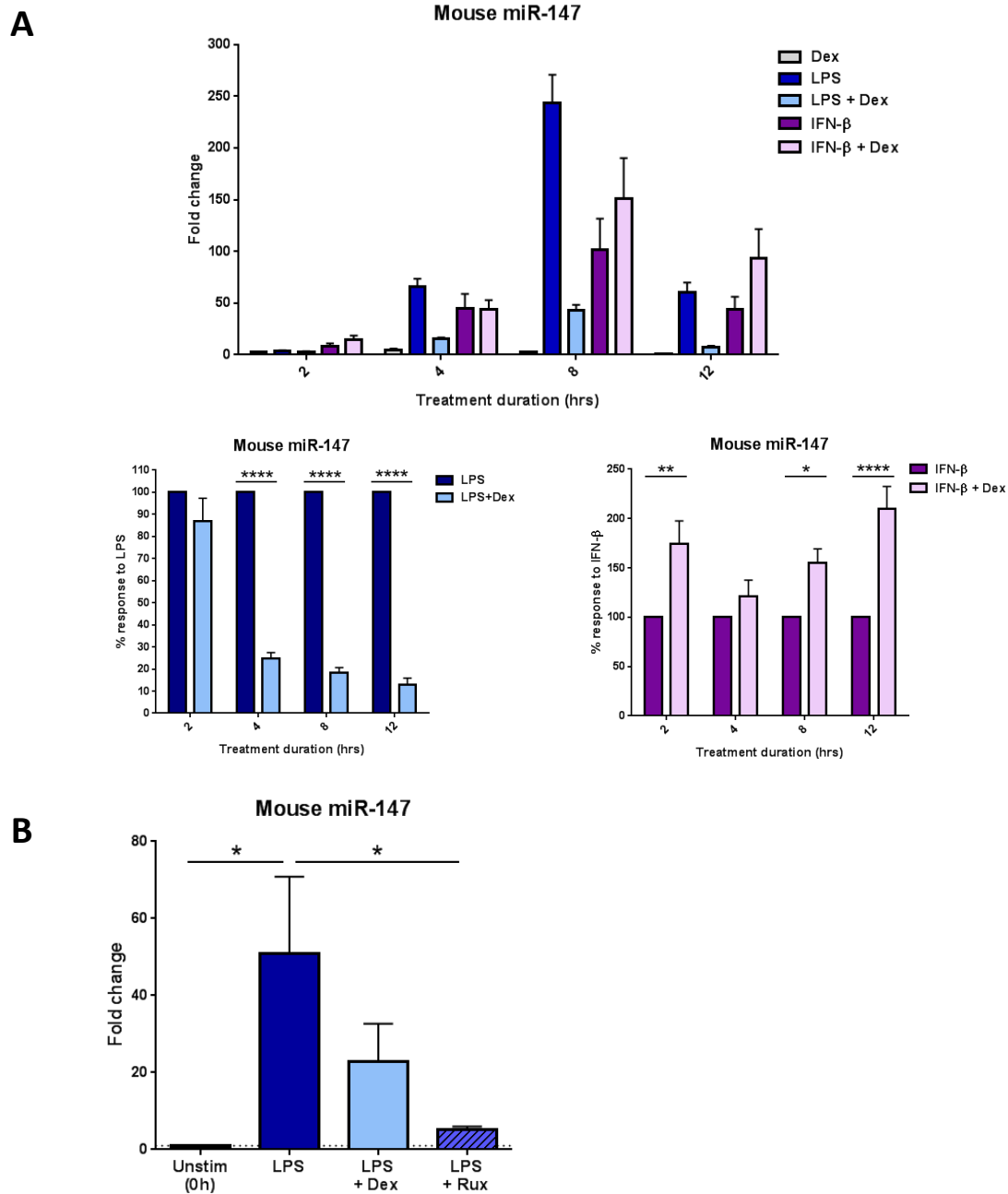
Figure 3.7) Upregulation of mouse miR-147 occurs through IFN-β/Jak/STAT signalling

A) WT mouse BMDMs were stimulated with Dex (100nM), LPS (10ng/ml), IFN-β (10ng/ml) or the combinations shown for the indicated times. Mmu-miR-147 was detected by RT-qPCR. Expressed as fold change (2^-ΔΔCt) normalised to RNU6-2, relative to time-matched mock treated control; also as % response to LPS or IFN-β at each time point; n=6; Two-way ANOVA with Sidak correction for multiple comparisons. Data presented as mean +SEM.

B) WT mouse BMDMs were stimulated with LPS (10ng/ml) in the presence or absence of Dex (100nM) or Rux (1μM) for 8h. Mmu-miR-147 was detected by RT-qPCR. Normalised to RNU6-2 and expressed as fold change relative to unstimulated (0h); n=3; One-way ANOVA with Dunnett's correction for multiple comparisons, relative to LPS only. Data presented as mean +SEM.

In human MoDMs the expression of miR-147b was not significantly induced by IFNβ alone (**Figure 3.8**). As previously shown, the induction of miR-147b by LPS was sensitive to Dex, but it was not significantly inhibited by Ruxolitinib (**Figure 3.8B**). Therefore LPS-induced expression of miR-147b in human macrophages does not appear to be governed by an IFNβ-mediated feedback loop.

O'Connell *et al* reported that miR-155 can be induced in mouse BMDMs by agonists relevant to viral infection, including the TLR3 agonist poly(I:C), and IFNβ (298). In contrast to miR-147, I found that mouse miR-155 is much more weakly induced by IFNβ treatment than LPS treatment, and IFNβ-induced expression was also subject to strong inhibition by GC (**Figure 3.9A**). Human miR-155 showed weak induction by IFNβ at later time points, which was inhibited by Dex (**Figure 3.9B**). These results indicate that the major production of miR-155 in response to LPS is mediated through primary signalling rather than secondary signalling through the interferon receptor.
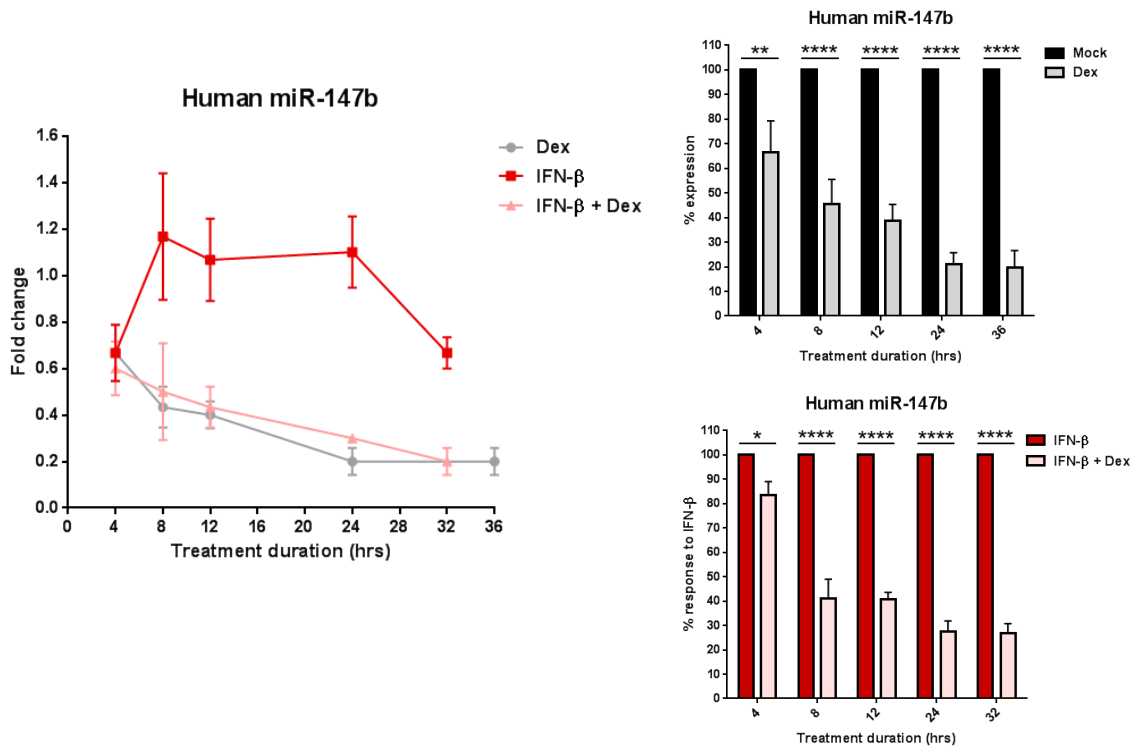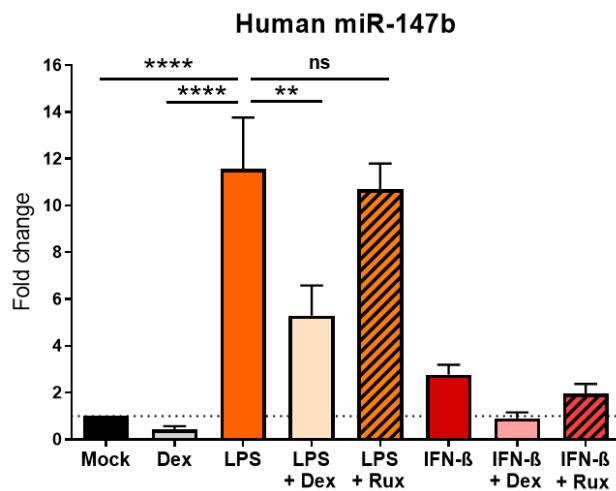
Figure 3.8) Human miR-147b is not regulated by IFN-β/Jak/STAT signalling

A) Human monocyte-derived macrophages were stimulated with Dex (100nM), IFN-β (10ng/ml) or a combination of the two for the indicated times. Hsa-miR-147b was detected by RT-qPCR. Expressed as fold change ($2^{-\Delta\Delta Ct}$) normalised to RNU6-2, relative to time-matched mock treated control; also as % response to Mock or IFN-β at each time point; n=3; Two-way ANOVA with Sidak correction for multiple comparisons. Data presented as mean +/-SEM.

B) Human monocyte-derived macrophages were stimulated with the indicated combinations of LPS (10ng/ml), Dex (100nM), IFN-β (10ng/ml) and Ruxolitinib (Rux, 1μM) for 12 hours. Hsa-miR-147b was detected by RT-qPCR. Expressed as fold change ($2^{-\Delta\Delta Ct}$) normalised to RNU6-2, relative to mock treated control; n=3; One-way ANOVA with Dunnett's correction for multiple comparisons, relative to LPS alone (statistical comparisons to IFNβ stimulations not shown). Data presented as mean +SEM.
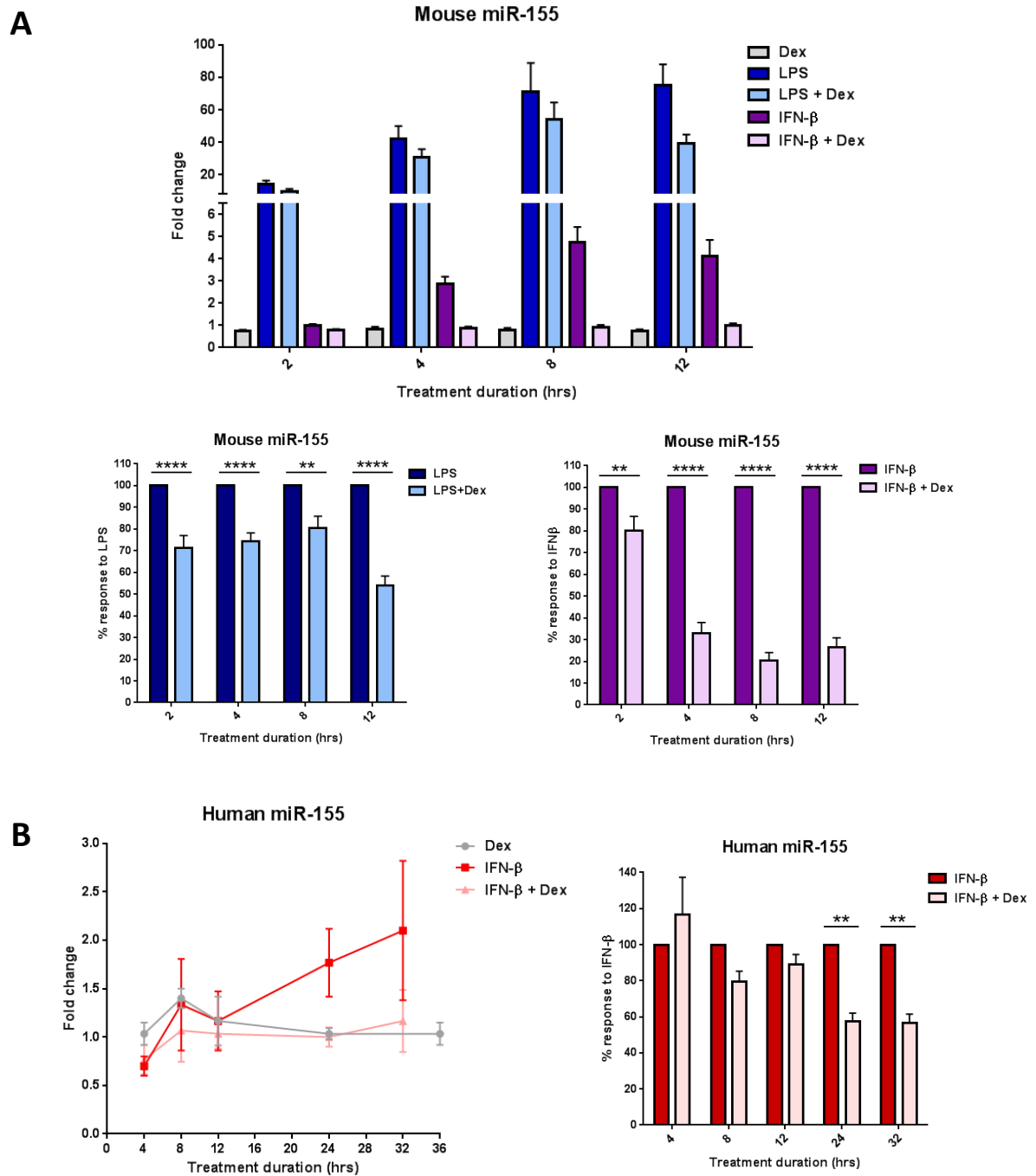
Figure 3.9) IFN-β-induced expression of miR-155 is sensitive to glucocorticoid inhibition
A) WT mouse BMDMs or **B)** human monocyte-derived macrophages, were stimulated with Dex (100nM), LPS (10ng/ml), IFN-β (10ng/ml) or the combinations shown for the indicated times. **A)** Mmu-miR-155 or **B)** hsa-miR-155 were detected by RT-qPCR. Expressed as fold change (2^-ΔΔCt) normalised to RNU6-2, relative to time-matched mock treated control; also as % response to LPS or IFN-β at each time point; **A)** n=6; **B)** n=3; Two-way ANOVA with Sidak correction for multiple comparisons. Data presented as mean +/-SEM.

3.5 Discussion

My investigation into the effects of glucocorticoids on a few established inflammation-associated miRNAs demonstrates that global miRNA processing in macrophages is not affected by GCs, due to the miRNA-specific responses. Table 3.1 summarises the effects of LPS and dexamethasone on the miRNAs studied in this chapter in both mouse and human macrophages. The number of arrows approximately indicates the relative magnitude of each response.

Table 3.1) Regulation of miRNA expression by LPS and Dex in macrophages

miRNA	Mouse BMDM		Human MoDM	
	Effect of LPS (rel to Mock)	Effect of Dex (rel to LPS alone)	Effect of LPS (rel to Mock)	Effect of Dex (rel to LPS alone)
miR-155	↑↑↑↑	↓↓↓	↑↑	↓↓
miR-146a	↑	-	↑	↑
miR-21	-	↑	↓	↑
miR-147(b)	↑↑↑	↓↓↓↓	↑↑	↓↓↓
miR-29c (microarray results only)	↓	↑↑	No data	No data

MiR-155 expression was significantly inhibited by Dex, as previously reported (133). This likely contributes to the broad anti-inflammatory properties of GCs and their efficacy in diseases such as RA, since miR-155 has been shown to control B cell antibody production, Th17 cell differentiation and inflammatory macrophage and DC function (116, 301). My results also supported the previously reported induction of miR-155 by IFNβ, which contributes to further type I interferon production and anti-viral immunity through targeting of SOCS1 (298, 299). The greater response of miR-155 to LPS than to IFNβ suggests that this miRNA acts as an early mediator of anti-pathogen responses, and the inhibition of miR-155 may contribute to the suppression of IFNβ production by GCs.

Despite report of the regulation of miR-146a by GCs in CD4+ T cells *in vivo* (287), my results showed no significant effect of Dex on miR-146a in mouse macrophages. Since expression of miR-146a was still increasing towards the end of the time course in my experiments, I cannot rule out an effect of GCs after longer stimulation. The addition of Dex appeared to increase and prolong the expression of miR-146a compared with LPS alone in human macrophages. While many of the outcomes of GC treatment are in opposition to the effects of inflammatory stimuli such as TLR activation, mediated for example through inhibition of transcription factor activity or downregulation of MAPK signalling (discussed in Section 1.3.3), GC action has also been demonstrated to synergise with pro-inflammatory signals. One example is sphingosine kinase 1 (SphK1), which is greatly induced by the combination of TLR agonist and Dex, with potential therapeutically beneficial effects in acute lung injury. This was shown to involve direct binding of the dimerised GR at the *SphK1* gene (331). Glucocorticoids also synergise with IL-6 signalling through interactions between the GR and STAT3 (332). Interestingly, STAT3 has also been found to associate with the promoter of miR-146a and drive its expression in hepatocellular carcinoma cells (333). Due to the late timing of the upregulation of miR-146a by Dex, an alternative explanation is that the GC inhibits a feedback mechanism that would otherwise act to turn off expression of the miRNA after initial induction by LPS. The increase of human miR-146a could contribute to the anti-inflammatory effects of GCs, since miR-146a targets positive upstream regulators of NF-κB signalling. However, the therapeutic implications of this effect are unclear, both due to the small magnitude of the effect in my results, and the complexities of the role of miR-146a in inflammatory diseases (discussed in Section 3.1.1).

In addition to the potential difference between primary macrophages and THP1 cells as discussed, the lack of a strong induction by LPS in this experiment compared with published

reports may relate to the variable constituents and contaminants of LPS preparations. Taganov *et al* showed a smaller fold induction of miR-146a when using ultrapure LPS, compared with crude preparations. The authors suggested that other bacterial cell wall components could be responsible for this difference, since the lipoprotein mimic Pam3CSK4 was also able to induce miR-146a (281). LPS is also highly heterogeneous, consisting of multiple different chain lengths and antigens, which serve to increase bacterial diversity (334), so different preparations of LPS may result in different magnitudes of response depending upon individual constituents.

The expression of miR-21 in my experiments did not replicate previously published work (290), as I saw little/no induction by LPS. Despite this, the addition of GC significantly elevated expression at certain time points. This is consistent with the role of miR-21 in promoting a pro-resolution macrophage phenotype, and negative regulation of the inflammatory cytokine IL-12, which is strongly inhibited by GCs (290, 291, 335). However, the reported role of miR-21 in allergic inflammation in asthma, and the effective use of GCs in the treatment of airway inflammation, are contrary to the results reported here (292, 293). This may be a result of differences in regulation between airway macrophages and monocyte-derived macrophages; or may be an oversimplification of the *in vitro* GC treatment, in comparison to an *in vivo* setting where the cells will be subject to a complex microenvironment. We must also consider the difference in stimulation between LPS, which mimics a bacterial infection and elicits a type 1 inflammatory response, and an allergic type 2-dominated stimulus. The fact that I did not see a convincing upregulation upon LPS stimulation; coupled with the fact that Dex only elicited a significant response at certain time points; meant that I decided not to investigate this miRNA further.

The use of existing microarray data allowed identification of novel targets of GCs in macrophages, however this was limited by a reliance upon annotation of probe IDs due to the microarray not being focused toward miRNAs. The fact that I did not pick up miR-155 in this data set, despite the demonstrated inhibition of this miRNA by Dex, may be due to lack of annotation of miR-155 within this probe set. Alternatively this transcript may not have reached significance at the early time point assessed in the microarray (4h). Despite identifying two differentially-expressed miRNA-associated transcripts (**Figure 3.4**), I focused on miR-147, as this is much less-studied than miR-29c, the latter of which having already been linked to GC regulation (327).

The expression of miR-147(b) showed clear induction by LPS and a dramatic downregulation by the addition of Dex across much of the time course, in both mouse and human macrophages. The results in mouse macrophages show that miR-147 is a secondary response gene in relation to LPS signalling, dependent upon signalling through the JAK/STAT pathway, most likely due to autocrine actions of IFNβ (**Figure 3.10**). This is consistent with the results of Liu *et al*, who carried out cycloheximide-mediated translational repression, and showed that *de novo* protein synthesis was required for miR-147 induction (10). The role of interferon signalling in the induction of miR-147 gives clues about the potential role of this miRNA in macrophages, since interferon signalling regulates responses to viral infection and has potent immunomodulatory effects (30, 336). This supports the findings that miR-147 is induced by viral infection of mice (315), and by TLR3 activation (10). Interferons are also known to regulate immune cell metabolism, as discussed in Chapter 1 (232).

The insensitivity of interferon-induced miR-147 expression to GC inhibition in BMDMs suggests that the GC action occurs upstream of the interferon receptor. This is supported by

the finding that GCs strongly suppress LPS-induced expression of IFNβ (**Figure 3.6**). The role of GCs in inhibiting interferon production is also demonstrated by their efficacy in the treatment of SLE. This is a complex autoimmune condition with a broad range of manifestations, which is driven in a large part by interferons (337). GCs remain one of the most commonly used treatments for SLE, with up to 88% of patients being treated with these steroids (337). The 2019 EULAR recommendations for the management of SLE still acknowledge that steroids are useful for rapid symptom relief, but that long term use should be avoided, which was demonstrated in a long-term study on the adverse effects of GC therapy in SLE patients published in 2018 (338, 339). These recent publications confirm the need for a replacement for GCs in the management of inflammatory conditions; highlighting that this is still a real and on-going issue, and that the highly effective anti-inflammatory properties of GCs have not been replicated by more modern and targeted therapeutics.

The contrasting results in human macrophages with respect to the role of IFNβ and JAK signalling in miR-147b expression highlight a difference in regulation of the miRNA between the two species, despite complete sequence conservation (**Figure 3.10**). This may indicate a divergence in function for the miRNA, which may not be involved in the anti-viral immune response in human macrophages. Species differences in the regulation of miR-147 were already evident from the literature (*see Section 3.1.2*), since porcine miR-147 is downregulated upon viral infection (316). These differences would potentially complicate any *in vivo* work requiring the use of mouse models to dissect the regulation and roles of miR-147 in the context of disease, as results would not necessarily be directly applicable to humans. This is always a consideration when working with animal models, which is why fundamental *in vitro* work such as performed here is important to identify any potential confounding factors for the translation of findings in different species. Alternatively, the differences in miRNA

regulation highlighted here could be a result of the different sources of macrophages (bone marrow vs. monocyte-derived), similarly to the differences in metabolic regulation and NO production discussed in Chapter 1 (269).

Despite the regulatory differences with regard to interferon signalling, both mouse and human miR-147(b) were strongly inhibited by glucocorticoid. This miRNA showed the most robust response to Dex of all of those examined here. This finding; as well as the fact that miR-147(b) is a relatively poorly studied miRNA, particularly in an immune context; lead to my decision to focus on this miRNA, and to continue investigation into its role in macrophages. I can conclude from this chapter that glucocorticoids regulate the expression of select miRNAs, and that miRNA-147(b) is a novel target of glucocorticoids in macrophages.
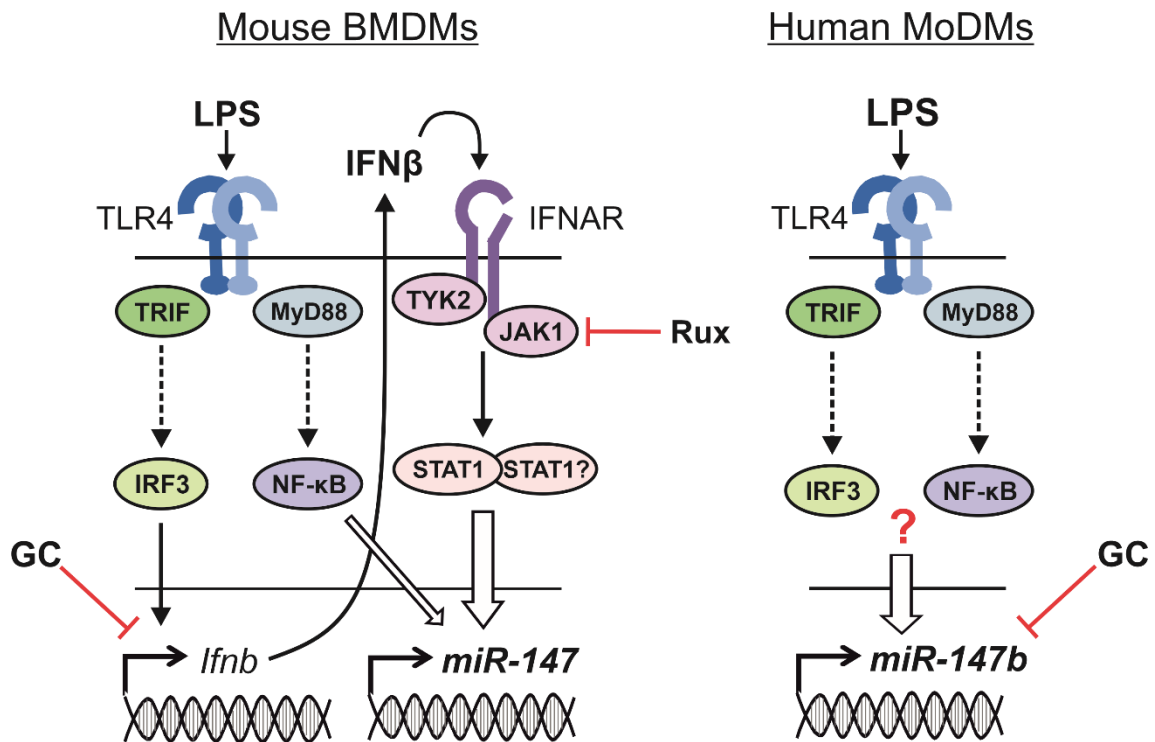
Figure 3.10) Model of miR-147(b) regulation by LPS and IFN-β in mouse and human macrophages

Based upon results from Chapter 3 as well as data from Liu et al (10).

Full expression of miR-147 in mouse BMDMs requires signalling through both TRIF and MyD88, as well as *de novo* protein synthesis, which most likely represents IFNβ synthesis. Autocrine/paracrine IFNβ signalling occurs through the type I interferon receptor (IFNAR), which signals through TYK2 and JAK1 to activate STAT transcription factors. STAT1 homodimers likely mediate miR-147 transcriptional activation by recognition of GAS elements, and the majority of miR-147 expression can be prevented by JAK inhibition by Ruxolitinib (Rux). NF-κB may play a minor role in miR-147 expression. Glucocorticoid-mediated inhibition of miR-147 expression can be circumvented by direct treatment with IFNβ, therefore GC action likely occurs through inhibition of interferon synthesis.

In human monocyte-derived macrophages (MoDMs), miR-147b expression is not induced by direct IFNβ treatment, and is not sensitive to JAK inhibition. The precise mechanism of miR-147b induction downstream of TLR4 is yet to be determined, but this induction is sensitive to glucocorticoid-mediated inhibition.

Chapter 4) Gene targets of microRNA-147(b) and their regulation in response to pro- and anti-inflammatory stimuli

4.1 Introduction

I have established that miR-147(b) is regulated by glucocorticoids in macrophages, however, the precise function of this miRNA is not understood, and gene targets are yet to be fully validated. The study by Liu *et al* identified miR-147 as a player in TLR signalling (10), and my finding that it is strongly regulated by the anti-inflammatory glucocorticoid supports the hypothesis that miR-147(b) has a role in regulating macrophage responses to pro- and anti-inflammatory signals.

Therefore the aims of this chapter were to identify and validate targets of miR-147(b), and investigate the regulation of these targets in response to macrophage inflammatory challenge. This will greatly enhance our understanding of the role of miR-147(b) - how this miRNA mediates the immunomodulatory effects of inhibiting TNFα and IL-6 production described by Liu *et al* (10), and how the regulation of miR-147(b) may contribute to glucocorticoid action.

4.1.1 NDUFA4 - localisation and metabolic function

As shall be discussed in detail in Section 4.2, the gene *NDUFA4* (mouse homologue *Ndufa4*) is a high-scoring predicted target of miR-147(b) that subsequently became of interest throughout the remainder of this project.

NDUFA4 (NADH Dehydrogenase (Ubiquinone) 1 Alpha Subcomplex 4) is a genomically-encoded component of the mitochondrial electron transport chain (ETC). Although only 81

amino acids in length, this small protein has been a source of debate in the mitochondrial field over the past few years, due to disagreements over its precise localisation and function. NDUFA4 was originally classified as an accessory subunit of NADH dehydrogenase (complex I) by John Walker and colleagues in the early 2000s, and the gene was therefore named after this complex (340, 341). However, it has more recently been described as belonging to cytochrome c oxidase (COX, CIV) and reported to be necessary for maximal COX activity (342). These claims were made based on a number of observations, including the following:

- Blue native gel electrophoresis showed that NDUFA4 co-migrated with CIV or the supercomplex I+III$_2$+IV, but not with complex I (CI) alone

- Co-immunoprecipitation studies showed that endogenous NDUFA4 could be pulled down using antibodies against CIV, but not by those targeting CI

- CIV activity was measured by spectrophotometry in isolated mitochondria from NDUFA4-KD cells. NDUFA4 silencing reduced the activity of CIV relative to citrate synthase. This could be rescued by overexpression of exogenous NDUFA4

- The authors also analysed the phylogenetic homology of NDUFA4 to determine its evolutionary development and loss, with the results arguing for a role in CIV rather than CI (342).

This proposed role for NDUFA4 in CIV was not initially accepted. In response, Kadenbach pointed out that numerous published crystal structures of cytochrome c oxidase lack a 14th subunit corresponding to NDUFA4, and instead suggested a potential role for this protein as a supercomplex assembly factor, which would explain its apparent association with both CI and CIV (343). This would also explain the need for using mild, non-ionic detergents, such as digitonin, for maintenance of the interaction between NDUFA4 and CIV during

isolation, since supercomplex associations are also disrupted by more harsh detergent extraction (e.g. sodium cholate or *n*-dodecyl β-D-maltoside (DDM)). Supercomplexes are relatively recently described phenomena that involve specific and stoichiometrically-defined groups of ETC complexes and electron carriers. One such supercomplex is the "respirasome", consisting of complexes I+III$_2$+IV, along with ubiquinone and cytochrome c electron carriers, such that the isolated supercomplex can transfer electrons from NADH to oxygen (344). The assembly of supercomplexes is thought to increase the efficiency of electron transfer between the individual complexes, reducing production of ROS by the ETC. Supercomplexes may also function to coordinate the regulation of individual complex assembly or expression, for example CIII and CIV have been shown to be required for full stability of CI in the inner mitochondrial membrane (344).

Despite the initial resistance to the re-assignment of NDUFA4, additional support for the role of this protein in CIV came in late 2018, when the crystal structure of a 14-subunit cytochrome c oxidase was published by Zong *et al* (345). This included the transmembrane position of NDUFA4, which was shown to span the inner mitochondrial membrane as part of CIV, and also to associate with a molecule of cardiolipin within this membrane. Cardiolipin, a specialised mitochondrial phospholipid that supports membrane structure, dynamics and protein function (346), is displaced by the cholic acid salts used in the crystallisation buffers for previous CIV crystal structure determination, and this may explain the loss of NDUFA4 in these structures. The authors also note that the previous structures appeared as dimers, whereas CIV does not dimerise when present in supercomplexes. The loss of NDUFA4 may have allowed for this potentially non-physiological dimerization, since NDUFA4 in the monomeric structure sits precisely at the dimerization interface of the historical structures

(345). In a study utilising cross-linking mass spectrometry to analyse mitochondrial protein interactions, Liu *et al* found that NDUFA4 cross-linked to components of complexes III, IV and V in intact mitochondria. Upon salt treatment, however, NDUFA4 appeared to relocate, and could then be found to cross-link to a different set of proteins, including many CI subunits (347). This work highlights the difficulties in measurement of mitochondrial protein networks, and supports previous data indicating that NDUFA4 is particularly susceptible to disruption.

Based on the accumulated data since 2012, it has been suggested that the *NDUFA4* gene be renamed *COXFA4* due to its localisation within cytochrome c oxidase (348). However I shall continue to refer to it as *NDUFA4* in order to remain consistent with the literature.

4.1.2 NDUFA4 in disease

The most striking links of NDUFA4 to disease occur when mutations within the gene result in complete loss of functional protein. Leigh syndrome is a class of paediatric-onset neurological diseases caused by mitochondrial dysfunction, which can often result in early childhood mortality. The general characteristics of Leigh syndrome include developmental delay; dystonia (spasms); and lactic acidosis, which indicates a metabolic component (181). There have been more than 75 genes linked to Leigh syndrome, the majority of which encode components of CI, but several CIV subunit mutations have also been shown to cause the disease, as well as other factors affecting mitochondrial function such as mitochondrial translation and DNA maintenance (181). A mutation within the *NDUFA4* gene was found to be associated with a form of familial Leigh syndrome, though the requirement for mutation of both alleles for the disease to manifest makes this a rare cause of the condition. These patients present with a range of neuromuscular symptoms that vary in severity, and while two known

affected individuals died in early age (8 and 26 years), the symptom onset is reportedly later than other known forms of nuclear COX deficiency (280).

In one such family affected by NDUFA4-associated Leigh syndrome, the mutation was found to occur at a splice donor site within the *NDUFA4* gene, causing a frame shift in the resultant transcript and introducing a premature stop codon. As a result there is no detectable expression of NDUFA4 protein in muscle tissue or cultured skin fibroblasts from the homozygous family members, whereas protein is present in the heterozygous relatives, who do not suffer symptoms of the disease (280). *In vitro* analysis of ETC complex activity in muscle cells from these patients showed a decrease in CIV activity, with no loss of CI activity. The authors also further support the findings of Balsa *et al* by providing additional evidence for the localisation of NDUFA4 protein within CIV through native gel electrophoresis (280, 342).

The loss of NDUFA4 expression has also been linked to disease development in the Cohen rat model of diet-induced diabetes. This is caused by the deletion of the entire third exon of the *Ndufa4* gene in this rat strain (349). Whilst there was no detected effect of NDUFA4 loss on basal mitochondrial function, the rats carrying the mutation showed an inability to increase CI activity and ATP production in metabolic tissues in response to a high sugar, diabetogenic diet. These rats were also unable to increase expression of anti-oxidant superoxide dismutase (SOD) enzymes in the pancreas when subjected to a diabetogenic diet. This could lead to excessive oxidative stress, resulting in impaired pancreatic function and bringing about the diabetic phenotype (349).

Genetic association studies and mRNA expression data have linked the *NDUFA4* gene to Alzheimer's disease. Chang *et al* found that *NDUFA4* mRNA was downregulated in total

blood of Alzheimer's disease patients, associated with an increased expression of certain miRNAs predicted to target the gene (miR-26a and miR-26b) (350). Bi *et al* investigated the genetic association of CIV subunits with Alzheimer's disease, and found variants in *NDUFA4* (and others) to be linked to the disease (351). Quantitative proteomics revealed a decrease in expression of NDUFA4 protein in brain tissue of both early and late onset Alzheimer's disease patients compared with controls, as well as decreases in several other respiratory chain subunits (182). These data suggest that there may be a link between downregulation of NDUFA4 expression and the mitochondrial dysfunction that is a key feature of neurodegenerative diseases such as Alzheimer's. This is consistent with the finding that alterations in the *NDUFA4* locus are associated with congenital cerebellar malformation, and that *NDUFA4* overexpression enhanced neuronal growth factor production and inhibited neuronal apoptosis (352).

There has been very little reported about the role of NDUFA4 in immune cell function and inflammatory disease. However, a study to identify biomarkers of responsiveness to abatacept plus methotrexate dual therapy in RA patients found that several ETC proteins were differentially expressed between responders and non-responders (353). Pre-therapy expression of *NDUFA4* in whole blood RNA (as well as other subunits of complexes I, IV and V) was significantly lower in the group that responded to the therapy, indicating a potential role for the mitochondrial ETC in the action of abatacept, and a functional consequence for the regulation of *NDUFA4* expression levels in immune cells (353). Abatacept is a fusion of the extracellular domain of CTLA-4 and the Fc portion of IgG1, and functions by binding to CD80 and CD86 co-stimulatory molecules on antigen presenting cells, preventing interaction with CD28 on T cells (354). While the major therapeutic mechanism of abatacept is considered to

be the inhibition of T-cell activation, the drug has been shown to have additional effects on other cell types, which may contribute to therapeutic efficacy (354).

There has been recent interest in the study of NDUFA4 expression and regulation in the cancer field, resulting in growing evidence for its role in regulating cell behaviour, as discussed below.

4.1.3 NDUFA4 regulation and cellular function

NDUFA4 has been reported to have oncogenic properties in several types of cancer, with overexpression leading to increased proliferation, apoptosis resistance and invasive or migratory capacity in colorectal cancer (319); gastric cancer (351); and lung cancer (355). Several mechanisms for NDUFA4 regulation have been proposed based on the action of non-coding RNAs in these tumours. For example, miR-7 is a known tumour suppressor in lung cancer, and this capacity has been linked to the silencing of NDUFA4 and a resulting decrease in Akt and Erk phosphorylation (355). Also relevant to lung cancer, miR-210 is a hypoxia-induced miRNA that is upregulated at late stages of non-small cell lung cancer. This miRNA, which shares a seed sequence with miR-147b, has been shown by luciferase assay to target *NDUFA4*, though the impact of this regulation was not assessed (323, 356).

MiRNA-147b has been shown to reduce NDUFA4 mRNA and protein expression in colorectal cancer cells (319). As discussed in section 3.1.2, miR-147b has tumour suppressive properties in this cancer type, in part through the inhibition of Akt phosphorylation (320), as described above for miR-7 (355). Cui *et al* report that inhibition of miR-147b increases cellular glucose uptake and lactate production in colorectal cancer cells. This effect could be reversed by addition of an NDUFA4-targeting siRNA, suggesting that the stimulatory effect on

glycolysis-associated carbon flux is mediated by an increase in NDUFA4 expression (319). The effects of synthetic inhibition of miR-147b in these cells are replicated by the action of the endogenous long non-coding RNA (lncRNA) MAFG-AS1. This lncRNA is believed to antagonise miR-147b activity through a sponging effect, whereby sequence complementarity between the two RNA species results in their interaction, in competition with the mRNA of *NDUFA4* (319). This phenomenon is described by the hypothesis of "competing endogenous RNA", which has also been reported to occur between miRNAs and protein-coding mRNAs, resulting in changes to the regulation of alternative target mRNAs (357).

Li *et al* also report that NDUFA4 is regulated by lncRNA and miRNA action in gastric cancer cells, with MIF-AS1 lncRNA antagonising the repressive effects of miR-212-5p on NDUFA4 expression (351). However, unlike the stimulation of glycolysis that was reported in colorectal cancer (319), rescue of NDUFA4 expression in gastric cancer was shown to increase oxygen consumption and ATP synthase activity (351). Other ETC components (COX6C, COX5B and NDUFA8) were also shown to be elevated by overexpression of either NDUFA4 or MIF-AS1, suggesting that more widespread changes in ETC architecture can be brought about by altering individual components, including NDUFA4 (351).

Hypoxia is a common feature of tumours, due to dysregulated angiogenesis and poor oxygen delivery (358). Hypoxia has been shown to cause a dramatic downregulation of NDUFA4 at the protein level but not at the transcript level in the HeLa adenocarcinoma cell line (359). This may be related to induction of the NDUFA4-targeting miRNA miR-210 in hypoxia (323), although this was not investigated in this context (359).

As mentioned above, there has been little investigation into the role of NDUFA4 in immune cells, and NDUFA4 expression and regulation have not been assessed directly in macrophages. This chapter addresses the targeting of NDUFA4 by the glucocorticoid-regulated miR-147b in primary macrophages, as well the response of NDUFA4 to inflammatory challenge. I also investigated other potential targets of miR-147(b). Cui *et al* published a validation of NDUFA4 as a target of miR-147b while I was working on this project, however these experiments were performed in a transformed colorectal cancer cell line, so may not be directly translatable to haematopoietic cells (319). Furthermore, the concentrations of miRNA mimic and inhibitor used in these experiments were not stated, so a non-physiological response due to excessive overexpression cannot be ruled out. However, these results do give credence to my selection of NDUFA4 to study as a potentially interesting target of miR-147(b), and indicate that this regulatory axis is likely to exist in multiple cell types.

Results

4.2 miRNA-147b is predicted to target metabolic genes

MicroRNAs carry out their gene-repressive actions by binding to target sequences within mRNA species. These interactions are based on Watson-Crick base pairing, which allows potential miRNA-mRNA interactions to be predicted based on sequence. Several miRNA target prediction tools are available online, and each tool gives a slightly different weighting to a number of parameters that are used for prediction. The key factor for prediction is sequence match to the miRNA seed region (nucleotides 2-7/8), but other parameters include additional sequence pairing 3' of the seed region and accessibility of the site to the silencing machinery (103). Because of the differences in prediction weighting, I used several available tools to

predict targets of human miR-147b, and compared the resulting gene lists (Targetscan7.1; miRTarBase; miRDB; miRanda). The number of common predicted targets between the different tools is shown in **Figure 4.1A**. It is clear that there are very few commonly predicted targets, even within the 500 top targets predicted by miRanda. This suggests that we are still yet to fully understand the precise requirements for successful gene silencing by miRNAs. Target prediction is also complicated by potential cell type-specific targeting, since these prediction sites do not take cell type into account. Only one gene was predicted as a target of human miR-147b by all four tools. That gene was *NDUFA4*, and **Figure 4.1B** depicts the sequence match of miR-147b to the putative target site within the 3'UTR of this gene. The target site is also conserved in the mouse *Ndufa4* 3'UTR, and this species conservation is particularly pertinent when considering the functional impact of the predicted target site, since the percentage of overall conservation between these 3'UTRs is low (13%). The conservation contributes to the high scoring for *NDUFA4* in the prediction algorithms, and this gene is the highest scoring predicted target from each of the sites.

A

B

Human Target Alignment   *seed interaction*

```
3' A U C G U C U U C - G U A A A G G C G U G U G 5' hsa-miR-147b
      I I I I I I    I I     I I I I I I I I
5' U U C C A G A A G C C A C A U C C G C A C A A 3' NDUFA4
```

Mouse Target Alignment   *seed interaction*

```
3' A U C G U C U U C G U A A A G G C G U G U G 5' mmu-miR-147
      I I I I I I I        I I I I I I I I
5' U U U C A G A A G C - C A U C C G C A C A A 3' Ndufa4
```
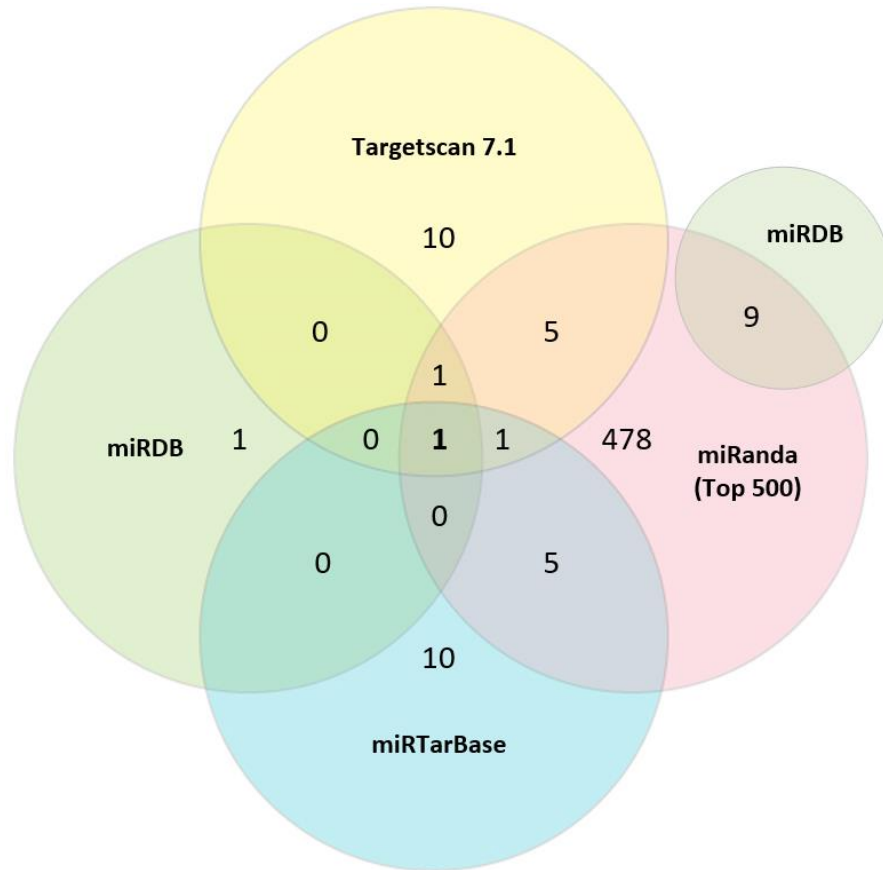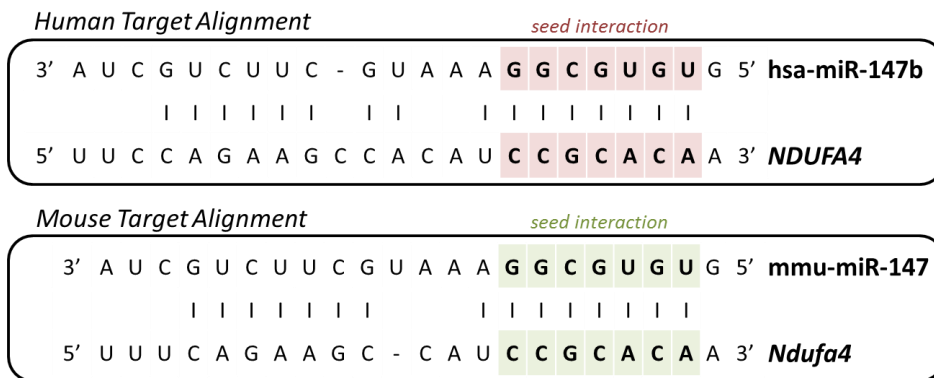
Figure 4.1) miR-147b target prediction

Potential targets of hsa-miR-147b were predicted using online tools: Targetscan7.1; miRanda (microRNA.org); miRDB and miRTarBase. **A)** Resulting lists of predicted targets were compared for common genes. Total target prediction numbers: Targetscan7.1: 18; miRDB: 12; miRTarBase: 17; miRanda: 2,012 (comparisons were carried out with the top 500 of these targets).

NDUFA4 was the only gene common to all prediction tools. **B)** Human *NDUFA4* and mouse *Ndufa4* 3'UTR predicted target site match to the miR-147(b) sequence.

In order to assess the overall cellular impact of miR-147b, I carried out Gene Ontology (GO) enrichment analysis of the combined gene lists from Targetscan7.1, miRTarBase and miRDB, using DAVID functional annotation bioinformatics tool (270, 271). The enrichment of third tier Biological Process terms is shown in **Figure 4.2**, and the allocation of all predicted targets into each of these processes is shown in Supplementary Table S1. Amongst the significantly enriched terms are several that relate to metabolic processes, including 'energy derivation by oxidation of organic compounds' and 'electron transport chain'. These results indicate that miR-147b may contribute to macrophage metabolic regulation in response to TLR activation. This is also of particular interest when considering *NDUFA4* as the highest scoring predicted target, since this gene encodes a component of the mitochondrial electron transport chain. Based on these results, *NDUFA4* was the obvious candidate to investigate as a target of miR-147b.

GO Biological process_3	P Value	Fold Enrichment	# Genes
regulation of cellular component size	0.009	5.9	5
energy derivation by oxidation of organic compounds	0.025	6.1	4
regulation of anatomical structure size	0.026	4.3	5
electron transport chain	0.028	11.3	3
regulation of signal transduction	0.044	1.8	12
phosphorus metabolic process	0.045	1.8	13
protein complex biogenesis	0.048	2.3	8
generation of precursor metabolites and energy	0.058	4.4	4
cellular component assembly	0.075	1.8	11
cell projection organization	0.080	2.2	7
pattern specification process	0.081	3.8	4
regulation of cell communication	0.082	1.7	12

Figure 4.2) miR-147b predicted target pathway analysis

CirGO image produced by John D O'Neil

Predicted targets of hsa-miR-147b from Targetscan7.1, miRDB and miRTarBase (replicates removed) subjected to gene enrichment analysis using DAVID functional annotation bioinformatics tool (https://david.ncifcrf.gov/). Third tier Gene Ontology Biological Process terms were visualised using CirGO visualisation tool (https://github.com/IrinaVKuznetsova/CirGO.git) *(John O'Neil)*. Size of plot component is dependent upon fold enrichment of the GO term. Table displays the same data organised by p value, along with fold enrichment and number of genes corresponding to each term.

4.3 NDUFA4 is regulated by pro- and anti-inflammatory stimuli in macrophages

As mentioned above, the expression of NDUFA4 in macrophages has not been investigated. Since miR-147b is induced by TLR activation and repressed by glucocorticoids in macrophages (**Figure 3.5**), I studied the regulation of the predicted target NDUFA4 in response to these agonists. I found that NDUFA4 protein is expressed in unstimulated primary human macrophages, and is dramatically downregulated by 24h of LPS treatment (**Figure 4.3A**), with detectable expression (by Western blot) completely disappearing in some instances (**Supplementary Figure S2**). This downregulation could be partially rescued by co-treatment with dexamethasone (**Figure 4.3B**). These results are consistent with the regulation of miR-147b by LPS and Dex and potential targeting of NDUFA4 by this miRNA. The mRNA for human *NDUFA4* is also downregulated by LPS treatment, although to a lesser degree than the protein, and *NDUFA4* mRNA is not rescued by the glucocorticoid (**Figure 4.4**). These differences between mRNA and protein regulation indicate that NDUFA4 expression is regulated post-transcriptionally, at the level of protein synthesis or degradation. This could be attributed to targeting by the miRNA, as miRNA action can result in translational repression without altering mRNA abundance (102), although this is less common than miRNA-mediated mRNA degradation (91, 102).
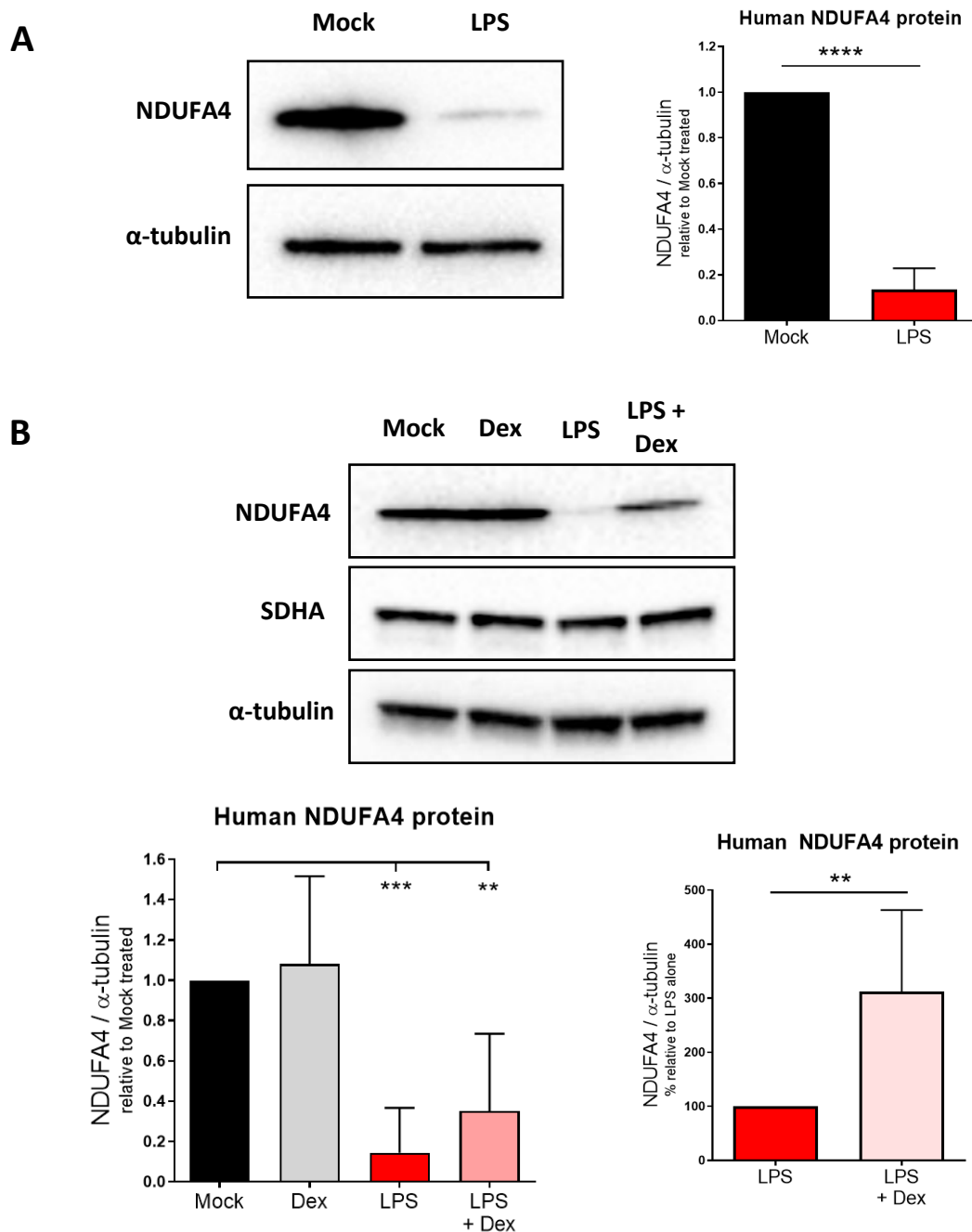
Figure 4.3) Human NDUFA4 protein is downregulated by LPS and partially rescued by dexamethasone

Human monocyte-derived macrophages were stimulated with **A)** LPS (10ng/ml) or **B)** the indicated combination of LPS (10ng/ml) and Dex (100nM) for 24h. NDUFA4 protein was detected by Western blotting and quantified by densitometry, expressed normalised to α-tubulin, relative to Mock treated or as a % of LPS alone; **A)** representative blot of n=6; student's t test; **B)** representative plot of n=6; One-way ANOVA with Dunnett's correction for multiple comparisons, relative to mock treated (left); Unpaired, two-tailed student's t test (right). SDHA was detected as a mitochondrial control. Data presented as mean +SD.
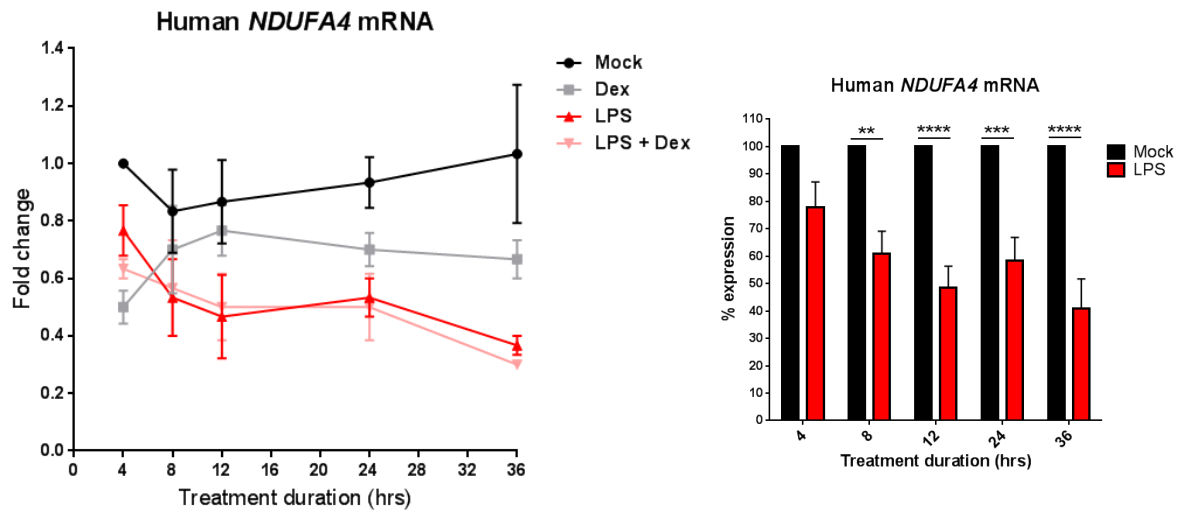
Figure 4.4) Human *NDUFA4* mRNA is downregulated by LPS but not rescued by dexamethasone

Human monocyte-derived macrophages were stimulated with LPS (10ng/ml) and Dex (100nM) for the indicated times. Mature *NDUFA4* mRNA was detected by RT-qPCR. Expressed as fold change (2^-ΔΔCt) normalised to UBC, relative to 4h mock treated control; also as % expression relative to time-matched mock treated; n=3; Two-way ANOVA with Sidak correction for multiple comparisons. Data presented as mean +/-SEM.

The mouse *Ndufa4* gene is also a predicted target of miR-147 based on miRanda target prediction (**Figure 4.1B**). Unlike human *NDUFA4*, mouse *Ndufa4* mRNA was not affected by LPS treatment throughout the time course tested in BMDMs (**Figure 4.5A**). Western blot analysis showed downregulation of mouse NDUFA4 protein at the later time points (**Figure 4.5B**), although this was not to the same dramatic degree as human NDUFA4 protein. This could be a reflection of the lack of downregulation of *Ndufa4* mRNA in mouse macrophages. Dexamethasone also appears to partially rescue mouse NDUFA4 protein in response to LPS, although upon direct comparison of LPS and LPS+Dex conditions this does not reach statistical significance. These observations suggest that human and mouse macrophages may share some common mechanisms for NDUFA4 regulation in response to LPS and GC, for example the conserved miR-147(b), while other mechanisms may be specific to human (*discussed further in Section 4.7*). While many central features are shared between inflammatory responses of mouse and human macrophages, there has been shown to be substantial divergence in transcript regulation in response to LPS, for example certain chemokines, cytokine receptors, and negative feedback mediators have been found to be divergently regulated (360). It is also becoming increasingly evident that important differences in metabolic regulation exist between the two species (*to be addressed in Chapter 5*), therefore it would be interesting to interrogate overall conservation of mitochondrial gene expression patterns between the two species. For the rest of this chapter I have focused on human monocyte-derived macrophages (MoDMs), based on the greater response of human NDUFA4 to LPS treatment.

Liu *et al* reported that miR-147 is induced by activation of TLR2 and TLR3, in addition to LPS-mediated activation of TLR4 (10). I therefore investigated the effect of alternative TLR

agonists on human NDUFA4 expression (**Figure 4.6**). Activation of TLR4 (LPS); TLR2/1 (Pam3CSK4); TLR2 (heat-killed *Listeria monocytogenes*: HKLM); TLR3 (Poly(I:C)); and TLR8 (ssRNA) all resulted in downregulation of NDUFA4 protein in the single donor tested (**Figure 4.6A**). Co-treatment with dexamethasone was able to rescue expression of the protein to varying degrees for each of these agonists (**Figure 4.6A**). Unfortunately, in order to gain enough protein for a Western blot, the majority of the provided reagents from the Invivogen human TLR agonist kit had to be used for a single experiment for several of the agonists. Poly(I:C) and Pam3CSK4 were selected for repeat experiments, since these were used by Liu *et al* in the study of miR-147 (10), and suitable quantities for multiple experiments could be obtained. These agonists also give an indication of the effect of viral or bacterial infection, and signalling through TRIF or MyD88 adapters, respectively (**Figure 1.2**). Pam3CSK4 reproducibly downregulated NDUFA4 protein, and Dex strongly rescued this effect (**Figure 4.6B**). Despite a strong effect of poly(I:C) in the initial experiment (**Figure 4.6A**), repeat experiments showed varied effects of this agonist on NDUFA4 expression (**Supplementary Figure S3**). This may be due to differences between donor responses to this agonist, or due to variation between batches of poly(I:C). Nonetheless, the apparent response of NDUFA4 to multiple different PAMPs indicates that the downregulation of this protein is a general response to infectious challenge, and may be involved in a fundamental function of macrophage inflammatory activity. It would also be interesting to determine whether damage-associated molecular patterns (DAMPS), or inflammatory cytokines are capable of downregulating NDUFA4, or whether the response is specific to infectious stimuli.
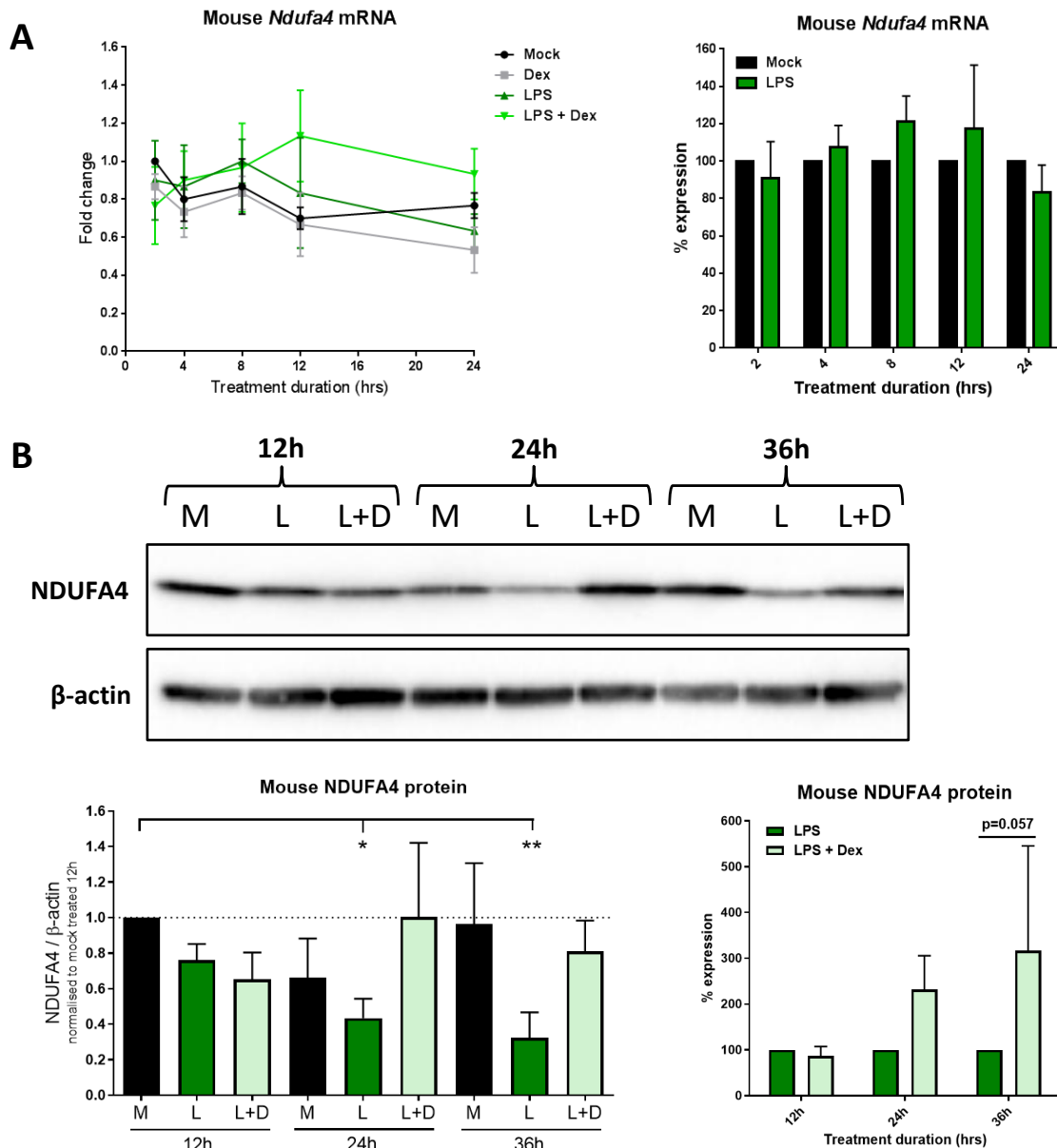
Figure 4.5) Regulation of mouse NDUFA4 in response to LPS and dexamethasone

Western blots were performed by Abbie Lane (MSci student) under my supervision.

WT mouse BMDMs were stimulated with LPS (10ng/ml) and Dex (100nM) for the indicated times.
A) Mature *Ndufa4* mRNA was detected by RT-qPCR. Expressed as fold change (2^-ΔΔCt) normalised to RPL13a, relative to 2h mock treated control; also as % expression relative to time-matched mock treated; n=3; Two-way ANOVA with Sidak correction for multiple comparisons (ns). Data presented as mean +/-SEM.
B) NDUFA4 protein was detected by Western blotting and quantified by densitometry, expressed normalised to β-actin, relative to 12h Mock treated or as a % of time-matched LPS alone; n=3; One-way ANOVA with Dunnett's correction for multiple comparisons, relative to 12h mock treated (left); Two-way ANOVA with Sidak correction for multiple comparisons (right). Data presented as mean +SD.
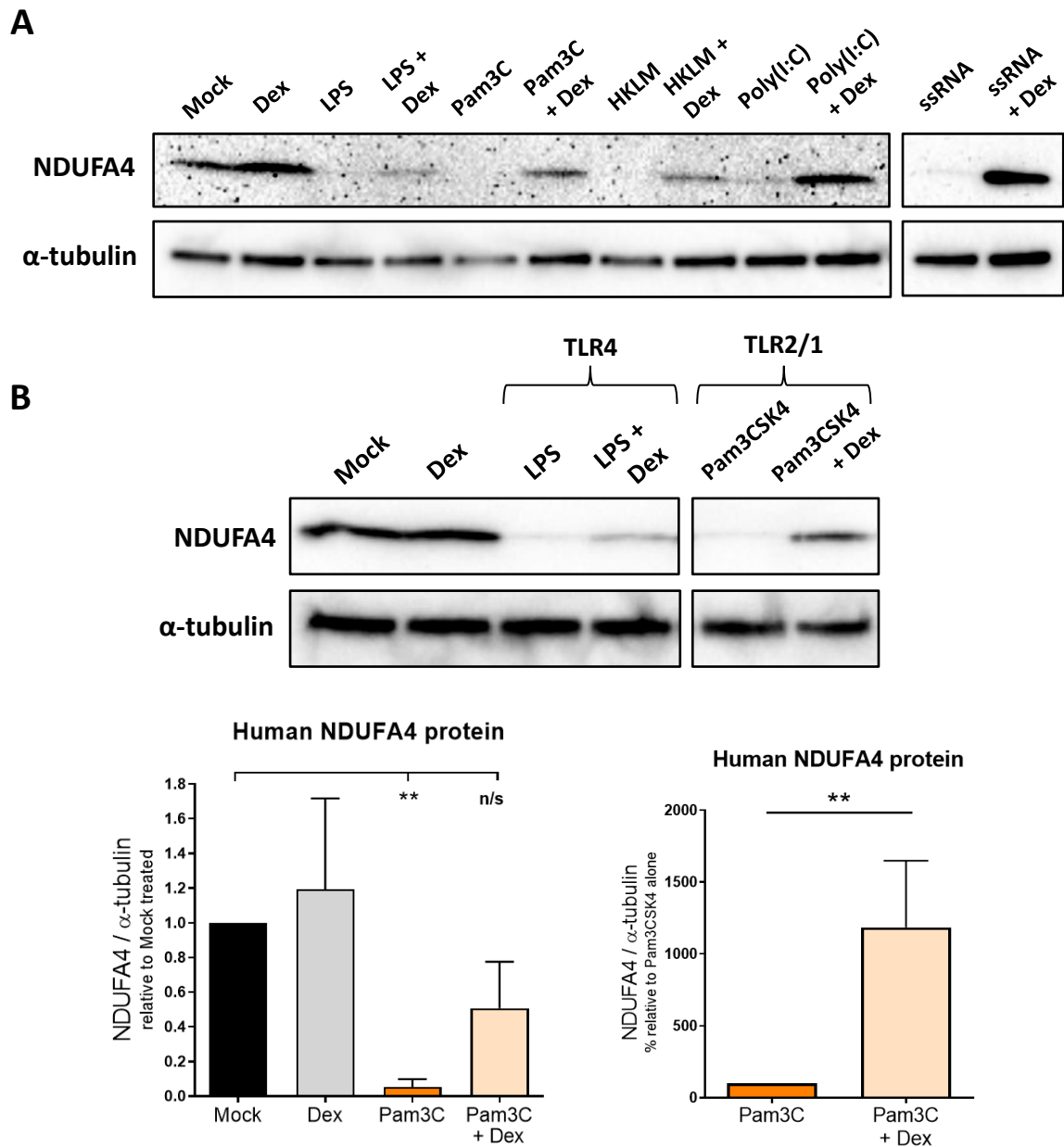
Figure 4.6) Human NDUFA4 protein is downregulated by activation of other TLRs, and this can also be rescued by dexamethasone

Western blots were performed by Abbie Lane (MSci student) under my supervision.

Human monocyte-derived macrophages were stimulated with the following TLR agonists +/- Dex (100nM) for 24h: LPS (10ng/ml); Pam3CSK4 (Pam3C: 1μg/ml); HKLM (10^8cells/ml); Poly(I:C) (10 μg/ml); ssRNA (10 μg/ml). NDUFA4 protein was detected by Western blotting. **A)** n=1; **B)** representative plot of n=4; quantified by densitometry, expressed normalised to α-tubulin, relative to Mock treated or as a % of Pam3CSK4 alone; One-way ANOVA with Dunnett's correction for multiple comparisons, relative to mock treated (left); Unpaired, two-tailed student's t test (right). Data presented as mean +SD.

4.4 Validation of NDUFA4 as a target of miR-147b

4.4.1 The issue with transfection reagents

An established method of validating miRNA targets is cell transfection with synthetic oligonucleotides that either replicate the mature miRNA (miRNA mimics) or antagonise the endogenous miRNA via complementary base pairing (miRNA inhibitors/antogomiRs). I set out to optimise transfection with these species in primary human MoDMs. TransIT-TKO reagent (Mirus) is advertised for efficient delivery of either siRNA or plasmid DNA in a variety of cell types, and has been reported to mediate high transfection efficiency and low toxicity in peritoneal macrophages and macrophage cell lines (361). Whilst I did achieve high transfection efficiency with this reagent in MoDMs (**Figure 2.5**), transfection with the control miRNA mimic (derived from *C. elegans* with minimal sequence identity in the human genome) resulted in an increase in mature miR-147b compared with non-transfected cells treated with OptiMEM media alone, which was detectable by RT-qPCR (**Figure 4.7A**). The primary miR-147b transcript (pri-mir-147b) was also increased compared with non-transfected cells (**Figure 4.7B**), demonstrating that the effect was not at the level of downstream miRNA processing. Measurement of *NDUFA4* mRNA in these samples showed the opposite trend to the miR-147b results (**Figure 4.7C**). While these results were consistent with miR-147b-mediated downregulation of *NDUFA4* mRNA, the non-specific increase in levels of the miRNA in the presence of the control mimic is a confounding factor in their interpretation, and I therefore wished to address this issue.

I compared three different transfection reagents to determine whether any of these could negate the effects demonstrated in **Figure 4.7**. Macrophages possess pattern recognition receptors that respond to foreign nucleic acid (e.g. TLR3, TLR7/8, RIG-1), therefore

in order to establish whether the transfection reagent or the exogenous RNA was mediating the described effects I included samples in which each transfection reagent was used alone, without the addition of RNA. **Figure 4.8A** demonstrates that the TransIT-TKO reagent itself was responsible for the stimulation of miR-147b transcription.

The TransIT-X2 reagent is described as "*an advanced non-liposomal system that comprises of a completely novel class of polymers in addition to other proprietary components that aid in nucleic acid complexation, uptake and endosomal release*" (Mirus). This reagent was able to efficiently deliver the miR-147b mimic, and led to a much smaller increase in levels of miR-147b transcript in the 'no RNA' or control mimic samples compared with TransIT-TKO (**Figure 4.8A**). Lipofectamine 3000 (Invitrogen) also caused minimal change in miR-147b levels in control conditions, but did not effectively deliver the miR-147b mimic under the conditions tested (**Figure 4.8A**). I therefore selected Mirus TransIT-X2 to take forward for the rest of my experiments.

I wanted to optimise transfection with the miRNA mimic in order to replicate the levels of miR-147b induced by LPS treatment of human macrophages, therefore I titrated the mimic concentration and measured miR-147b by RT-qPCR and NDUFA4 by Western blotting. Transfection with 2-5nM mimic caused an increase in cellular levels of miR-147b similar to that caused by treatment of cells with LPS for 12h (**Figure 4.8B**). **Figure 4.8C** demonstrates that 2nM of miR-147b mimic had the greatest silencing effect on NDUFA4 protein expression. These results led me to progress with 2nM mimic concentration and the TransIT-X2 transfection reagent.
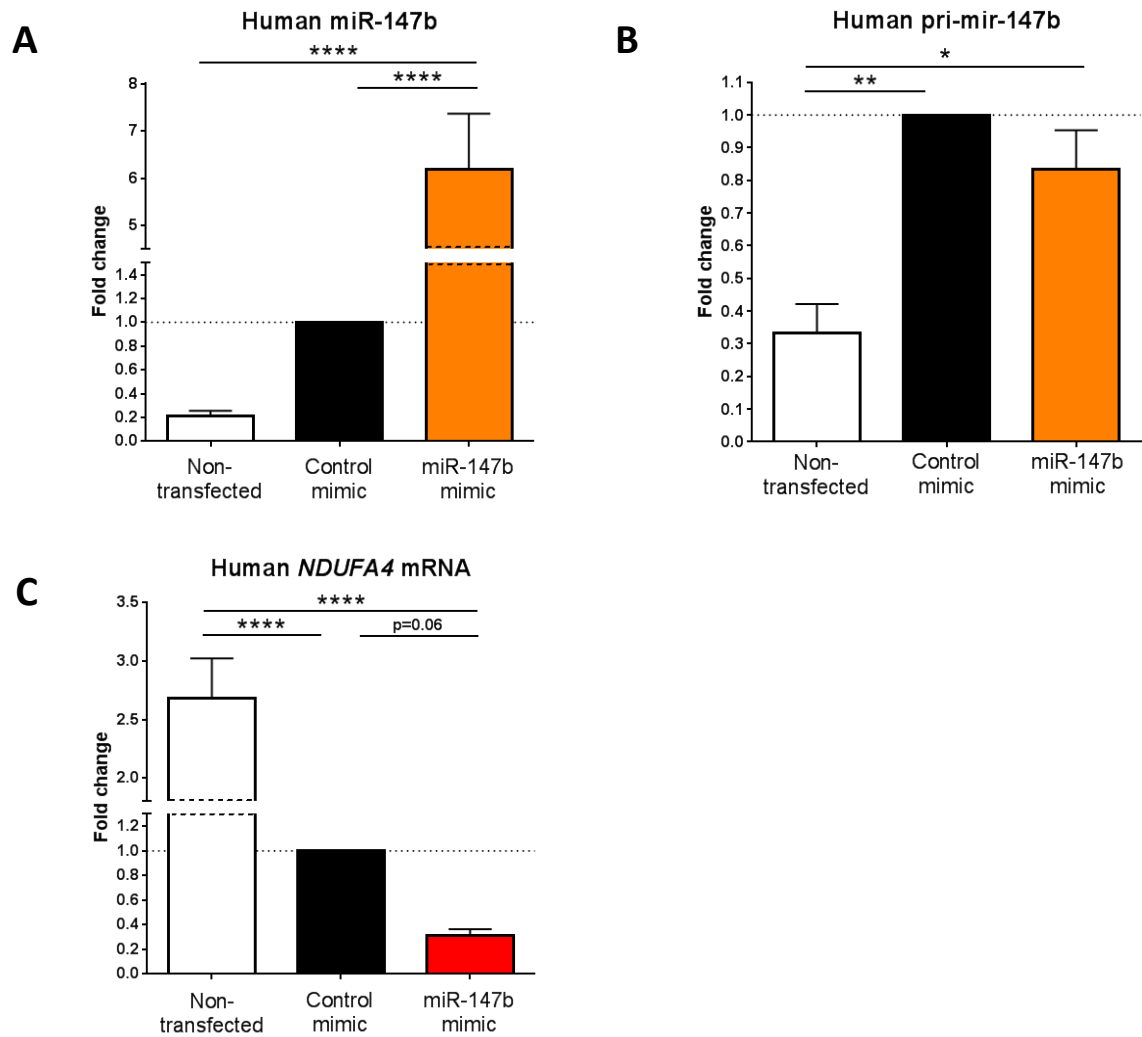
Figure 4.7) Transfection of primary human macrophages induces changes in transcript level

Human macrophages transfected with 2nM of control or miR-147b miRNA mimic using TransIT-TKO reagent or treated with media alone (non-transfected), and harvested for RNA isolation 24h post transfection.

A) hsa-miR-147b; **B)** pri-mir-147b or **C)** *NDUFA4* mRNA was detected by RT-qPCR. Expressed as fold change ($2^{-\Delta\Delta Ct}$) normalised to RNU6-2 (A) or UBC (B,C), relative to control mimic transfected. Data presented as mean +SEM.

A&C) n=8; **B)** n=3; One-way ANOVA with Tukey's correction for multiple comparisons.
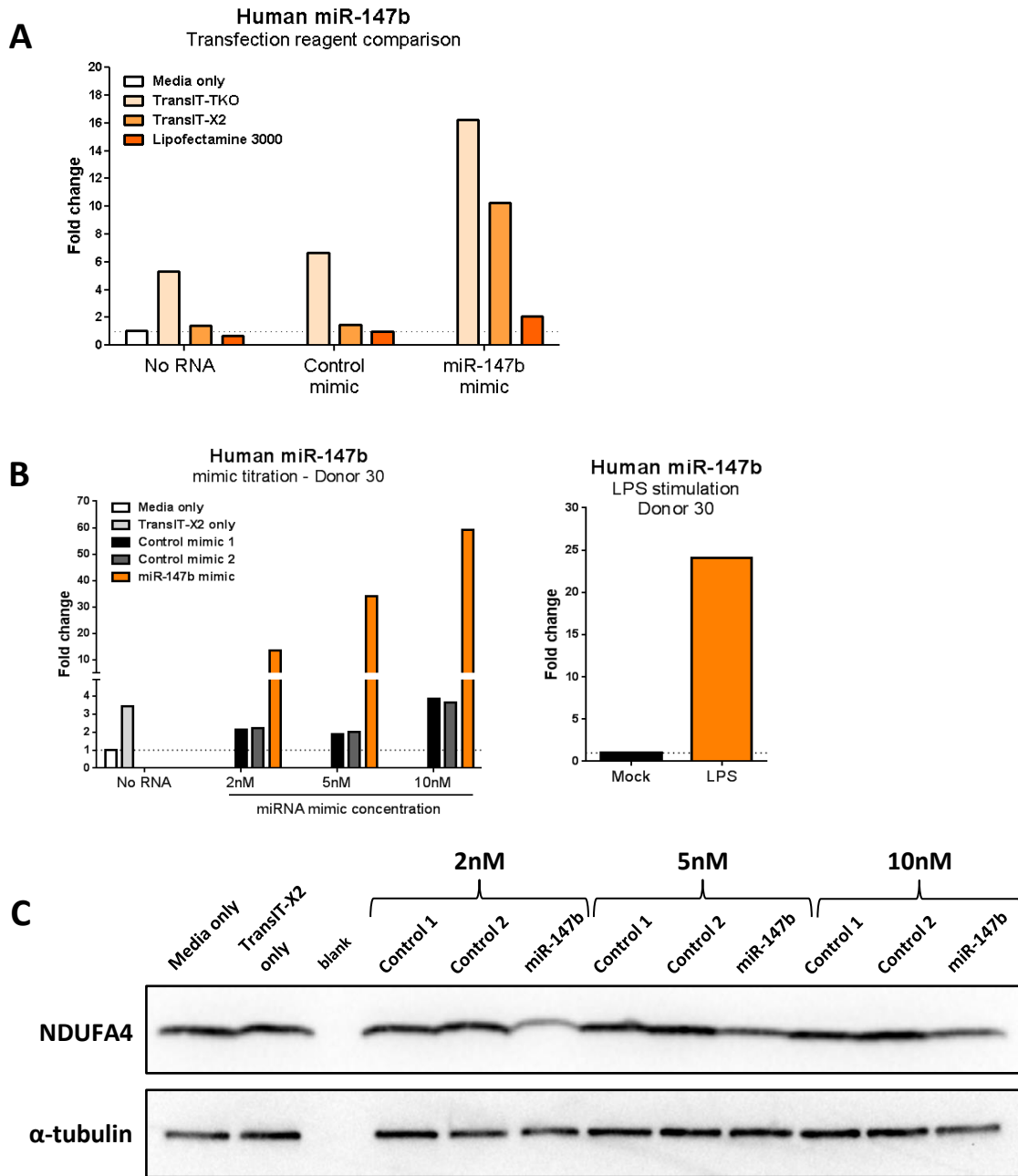
Figure 4.8) Optimisation of transfection with miRNA mimics

A) Human macrophages transfected with 2nM of control or miR-147b miRNA mimic using the indicated transfection reagent or treated with media alone; n=1.

B&C) Human macrophages transfected with the indicated concentration of miRNA mimic using TransIT-X2 reagent; n=1. **A&B)** Cells were harvested for RNA isolation 24h post transfection. Hsa-miR-147b was detected by RT-qPCR. Expressed as fold change ($2^{-\Delta\Delta Ct}$) normalised to RNU6-2 relative to media only sample or mock treated (mean of technical replicates).

C) Cells were harvested for Western blot 48h post transfection; n=1.

B) Induction of miR-147b in the same donor is shown to allow comparison with LPS-induced fold change (12h); n=1 (mean of technical replicates).

4.4.2 MicroRNA mimics and inhibitors

Transfection of primary human macrophages with miR-147b mimic using the optimised conditions resulted in a detectable increase in levels of the mature miRNA compared with the transfection reagent alone or the control mimic (**Figure 4.9A**). This resulted in a significant decrease in the levels of both *NDUFA4* mRNA (**Figure 4.9B**) and NDUFA4 protein (**Figure 4.9C**). This is consistent with the hypothesis that miR-147b targets *NDUFA4* in macrophages.

The inhibition of endogenous miRNA action can support findings obtained using exogenous miRNA mimic delivery. I tested a miR-147b inhibitor supplied by Qiagen (miScript). These inhibitors are reported to result in degradation of the endogenous miRNA by formation of a dsRNA duplex that is recognised by the cellular RNA degradation machinery. While degradation was apparent for the miR-155 inhibitor tested alongside, I saw no downregulation of endogenous miR-147b using the specific antisense miScript miR-147b inhibitor (**Supplementary Figure S4**). A second batch of the inhibitor received from the supplier gave the same result (data not shown). I therefore tried an alternative inhibitor (Qiagen miRCURY power inhibitor), which possesses a locked nucleic acid (LNA) modification as well as phosphorothioate (PS) backbone modification (**Figure 2.6**). The LNA modification locks the sugar moiety into the N-conformation, which is the preferred form for complementary binding (362). It thereby increases the affinity of the oligonucleotide for the miRNA, as well as improving the binding specificity by increasing the difference in melting temperature between a perfect match and a mismatch. The LNA and PS modifications also increase the stability of the oligonucleotide by reducing its susceptibility to endo- and exonucleases (363). This increased stability means that these inhibitors do not cause degradation of the endogenous

miRNA, but instead sequester the miRNA in a high affinity heteroduplex, preventing target binding.

Dose testing of the miRCURY LNA inhibitor showed that inhibition of miR-147b reversed the LPS-induced downregulation of *NDUFA4* mRNA at 25nM inhibitor concentration (**Figure 4.10A right panel**). There was also a trend towards rescue of *NDUFA4* mRNA at lower concentrations of inhibitor, in both LPS-treated and unstimulated (mock treated) conditions (**Figure 4.10A left panel**). When analysing NDUFA4 protein, however, the miR-147b LNA inhibitor was unable to rescue the downregulated protein in the presence of LPS (**Figure 4.10B**). While the mRNA results support the targeting of *NDUFA4* transcript by endogenous miR-147b, the lack of response of the protein to miR-147b inhibition suggests that additional mechanisms are involved in LPS-induced NDUFA4 protein silencing, for example post-translational protein degradation, which shall be addressed later in the chapter.
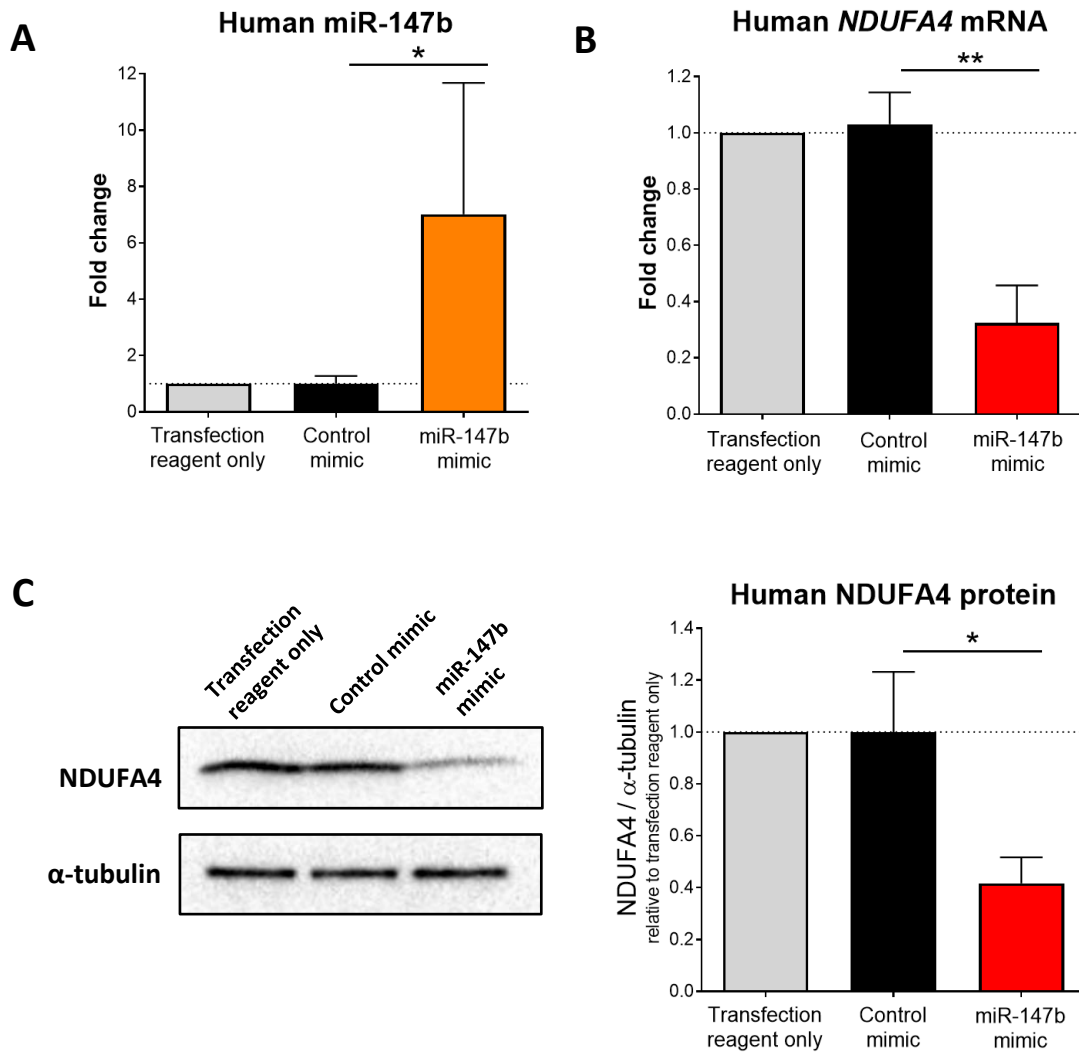
Figure 4.9) Validation of NDUFA4 as a target of miR-147b using miRNA mimics

Human macrophages transfected with 2nM of control or miR-147b miRNA mimic using TransIT-X2 reagent or treated with TransIT-X2 alone (transfection reagent only).

A&B) Cells were harvested for RNA isolation 24h post transfection; **A)** Hsa-miR-147b and **B)** *NDUFA4* mRNA were detected by RT-qPCR. Expressed as fold change (2^-ΔΔCt) normalised to RNU6-2 (A) or UBC (B) relative to transfection reagent only; n=4. Data presented as mean +SEM.

C) Cells were harvested for Western blot 48h post transfection; representative blot of n=3. Data presented as mean +SD. Two-tailed t tests.
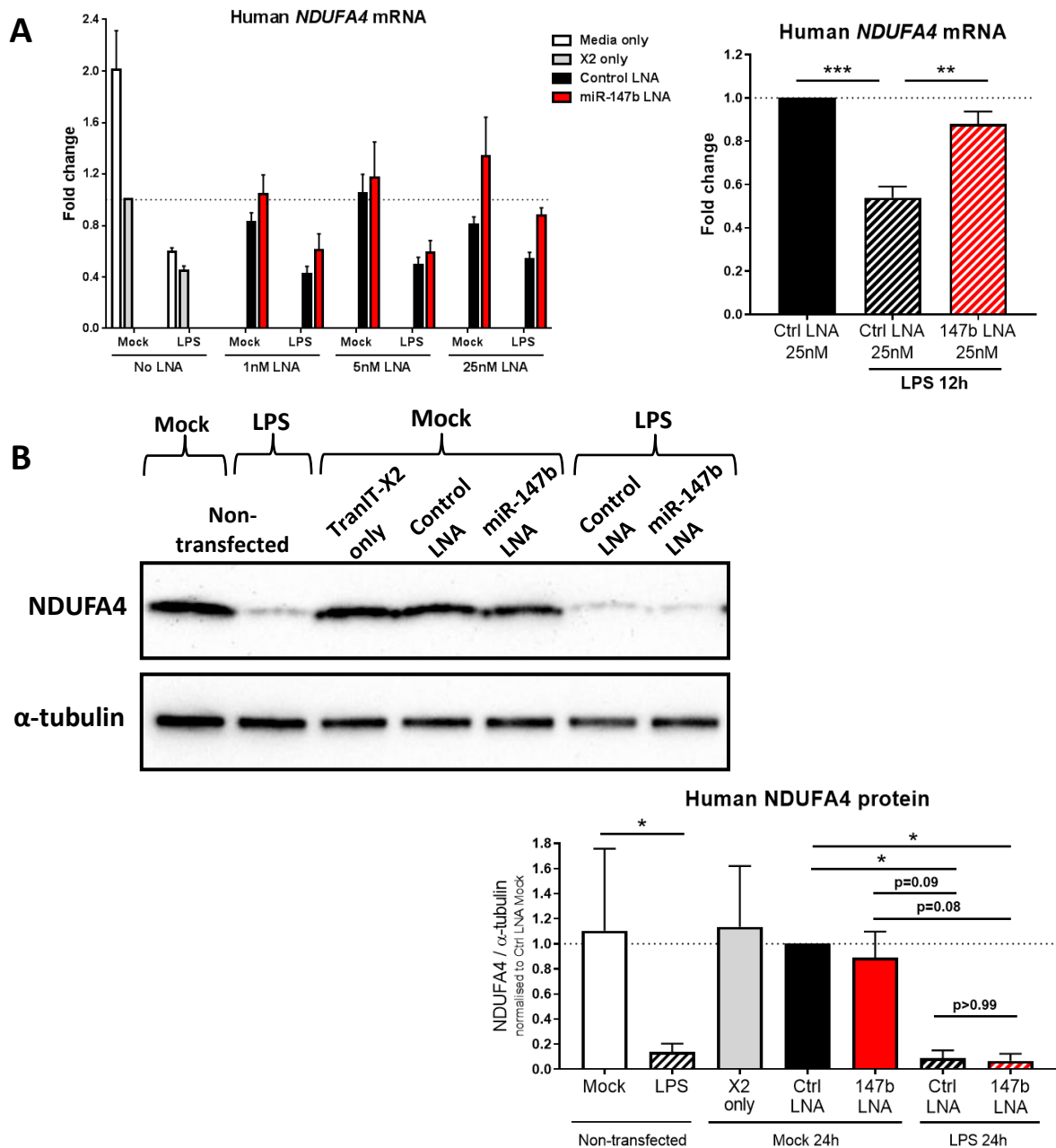
Figure 4.10) Validation of NDUFA4 as a target of miR-147b using miRNA inhibitors

A) Human macrophages transfected with control or miR-147b LNA inhibitor (LNA) at the indicated concentrations using TransIT-X2 reagent. Mock or LPS treatment for 12h, starting 24h post transfection; *NDUFA4* mRNA was detected by RT-qPCR. Expressed as fold change (2^-ΔΔCt) normalised to UBC relative to mock stimulated transfection reagent only (left) or 25nM Ctrl LNA mock (right); n=4; One-way ANOVA with Tukey's correction for multiple comparisons (right). Data presented as mean +SEM.

B) Human macrophages transfected with 25nM control or miR-147b LNA inhibitor (LNA) using TransIT-X2 reagent. Mock or LPS treatment for 24h, starting 24h post transfection; NDUFA4 protein was detected by Western blot; representative blot of n=3; One-way ANOVA with Tukey's correction for multiple comparisons (not all comparisons shown). Data presented as mean +SD.

4.4.3 Reporter assay of miR-147b function

A further method for the validation of miRNA targets is the use of a luciferase reporter assay. I cloned the human *NDUFA4* 3'UTR into a miRNA luciferase reporter plasmid, and also created a mutated plasmid in which three nucleotides of the predicted miR-147b target site seed sequence were altered (*see Section 2.17*). If targeting occurs, co-transfection of cells with the miRNA of interest and the 3'UTR-containing luciferase plasmid results in downregulation of luminescence signal due to silencing of luciferase protein production by the miRNA.

HEK293 cells (human embryonic kidney) were used as a workhorse cell line for this assay. Initially I needed to ensure that I could efficiently co-transfect these cells with both plasmid DNA and mimic RNA. I tested this using a plasmid expressing enhanced green fluorescent protein (EGFP) and a red fluorescently labelled RNA (miRIDIAN hairpin inhibitor Dy547 labelled control), utilising TransIT-X2 transfection reagent, which is advertised for co-transfection of DNA and RNA. **Figure 4.11A** demonstrates that very high efficiency transfection of the RNA was achieved, either in the absence or presence of the plasmid. Transfection efficiency of the plasmid ranged from 59-75% and was not adversely affected by the presence of the RNA. This result is conducive to performing the luciferase assay, since cells that do not contain the plasmid will not produce any luciferase signal so won't skew the result, and the miRNA will be present in nearly all cells. The presence of the Renilla luciferase gene within the plasmid can be used to control for variation in plasmid transfection efficiency between samples. Upon transfection with the miR-147b mimic RNA, I detected a dose-dependent increase in miR-147b levels in the HEK293 cells, which was not adversely affected by the presence of plasmid DNA (**Figure 4.11B**). The miR-147b mimic also suppressed expression of endogenous *NDUFA4* mRNA in these cells (**Figure 4.11C**).

The final luciferase assay results (**Figure 4.12**) show that in the presence of the unmodified luciferase plasmid there is no difference in signal between the control and specific miRNA mimics, as expected. When the luciferase gene is coupled to the wild-type *NDUFA4* 3'UTR, the miR-147b mimic results in strong downregulation of luciferase signal, consistent with 3'UTR targeting by the miRNA resulting in translational inhibition and/or mRNA degradation. When the seed sequence of the predicted target site is mutated, this effect is completely abolished, demonstrating a target site-specific interaction that is dependent upon the seed sequence.

Taken together, the results of the mimic, inhibitor and luciferase assay experiments confirm that human NDUFA4 is a functional target of miRNA-147b, and that this targeting axis occurs in macrophages.
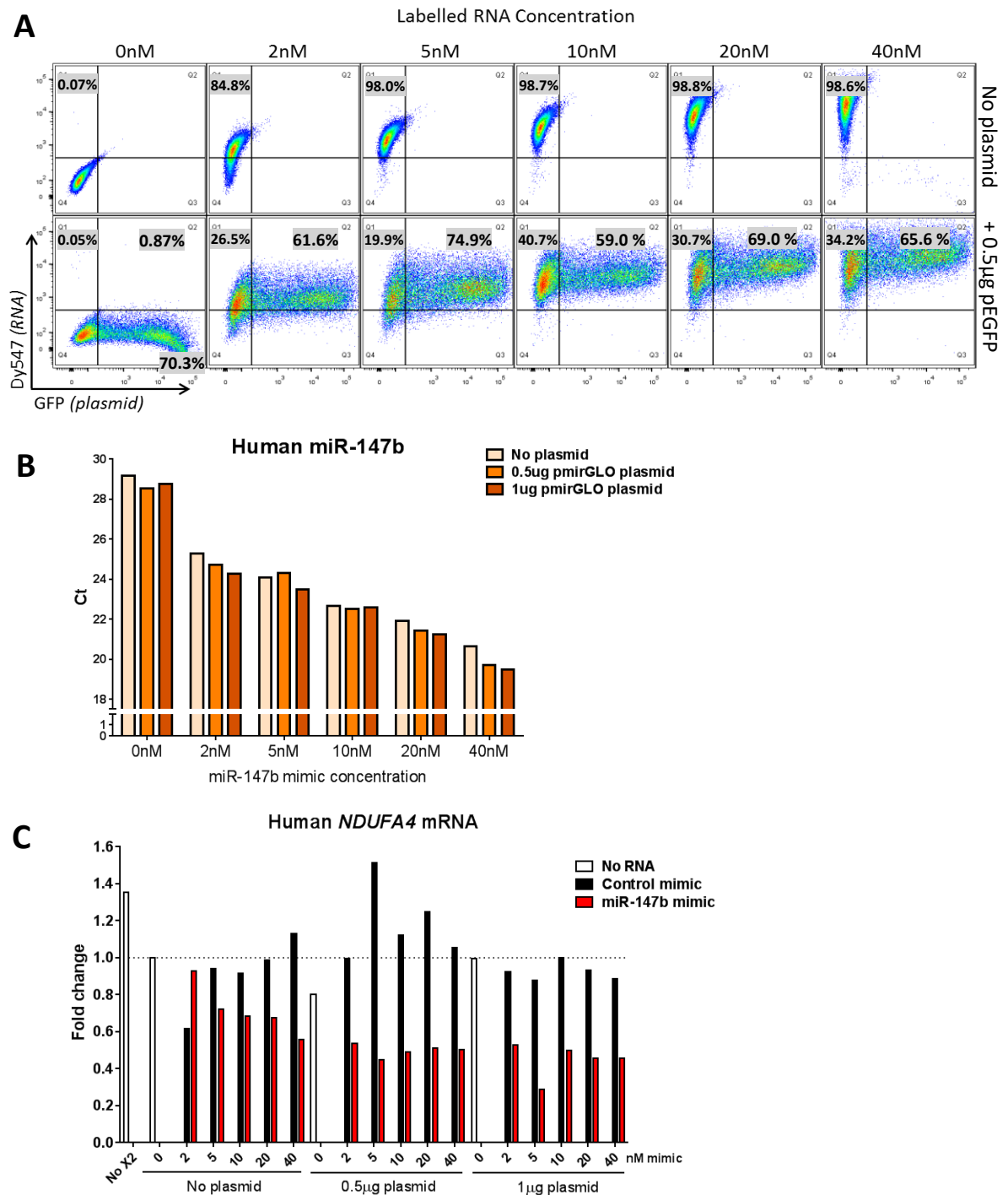
Figure 4.11) Optimisation of transfection for luciferase reporter assay
A) HEK293 cells transfected with the indicated concentrations of Dy547-labelled hairpin RNA +/-
0.5μg pEGFP plasmid using TransIT-X2 reagent. Analysed by flow cytometry; n=1
B&C) HEK293 cells transfected with the indicated concentrations of miR-147b mimic +/-
unmodified pmirGLO plasmid (0.5/1μg) using TransIT-X2 reagent. Cells were harvested for RNA
24h post transfection. **B)** Hsa-miR-147b and **C)** NDUFA4 mRNA were detected by RT-qPCR.
Expressed as raw Ct values (B) or fold change (2^-ΔΔCt) normalised to UBC relative to TransIT-X2
only (0nM RNA) (C); n=1 (mean of technical replicates).
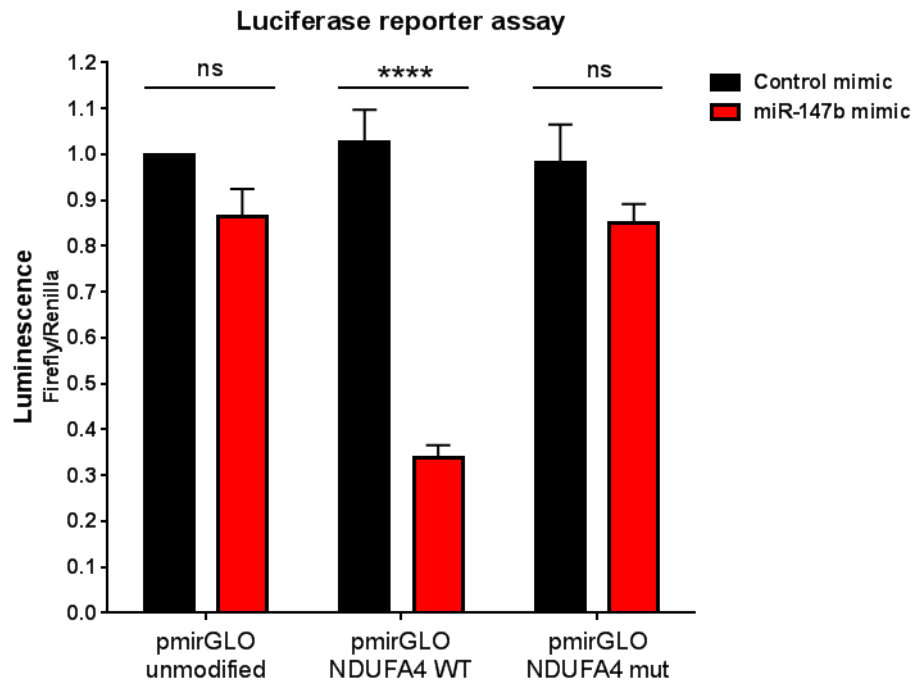
Figure 4.12) Validation of NDUFA4 as a target of miR-147b by luciferase reporter assay
HEK293 cells transfected with 20nM control or miR-147b mimic plus 0.5µg of the indicated pmirGLO plasmid using TransIT-X2 reagent. Cells were harvested for luciferase assay 24h post transfection. Expressed as firefly luciferase luminescence signal normalised to renilla luciferase signal, relative to control mimic + unmodified pmirGLO transfected; n=3; Two-way ANOVA with Sidak correction for multiple comparisons. Data presented as mean +SEM.

4.5 NDUFA4 is regulated post-translationally

Many of the results in this chapter suggest that there are mechanisms in addition to targeting by miR-147b by which macrophages downregulate NDUFA4 protein in response to TLR4 activation (*discussed in Section 4.7*). Cycloheximide (CHX) has been used as an inhibitor of protein synthesis for decades, and inhibits the translocation of mRNA and tRNA along the ribosome during the elongation phase of translation (364, 365). I used cycloheximide to examine the contribution of *de novo* protein synthesis to NDUFA4 levels in unstimulated and LPS stimulated cells (**Figure 4.13**). Since 24 hours of cycloheximide treatment is likely to be toxic to the cells, I initiated the LPS stimulation for 12h and then started the CHX chase for the following 12h to follow the degradation of NDUFA4 protein. In unstimulated (mock treated) cells, there was little effect of cycloheximide treatment, indicating that in this time frame there is no major contribution of new protein synthesis to the NDUFA4 pool. Under LPS treatment there was also no effect of cycloheximide, demonstrating that the reduction in protein level during this period was not due to inhibition of transcription or translation, but that LPS induced post-translational degradation of NDUFA4 protein.

Other complex IV subunits are known to undergo dynamic regulation in conditions such as hypoxia; as well as showing tissue-specific isoform expression (366). HIF-1α has been shown to regulate switching between isoforms of the subunit COXIV under hypoxia. HIF-1α induces transcription of the *COX4-2* isoform, as well as the mitochondrial protease LON (gene *LONP1*). This protease mediates degradation of the COXIV-1 isoform, resulting in a switch between these two isoforms within the cytochrome c oxidase complex (367). NDUFA4 protein has also been shown to be downregulated by hypoxia (359), and LPS is known to induce a state of pseudohypoxia in macrophages, in which HIF-1α is stabilised (207). I therefore

hypothesised that LON protease may be responsible for degradation of NDUFA4 protein in response to LPS. However rather than inducing LON protease transcription, I found that LPS treatment results in a reduction of *LONP1* mRNA (**Figure 4.14**). This suggests that LON is not responsible for the downregulation of NDUFA4 protein, although this is not conclusive. A further experiment that could help to uncover the mechanism of NDUFA4 degradation would be to use a proteasomal inhibitor such as MG132, or to study the expression of alternative mitochondrial proteases (368).
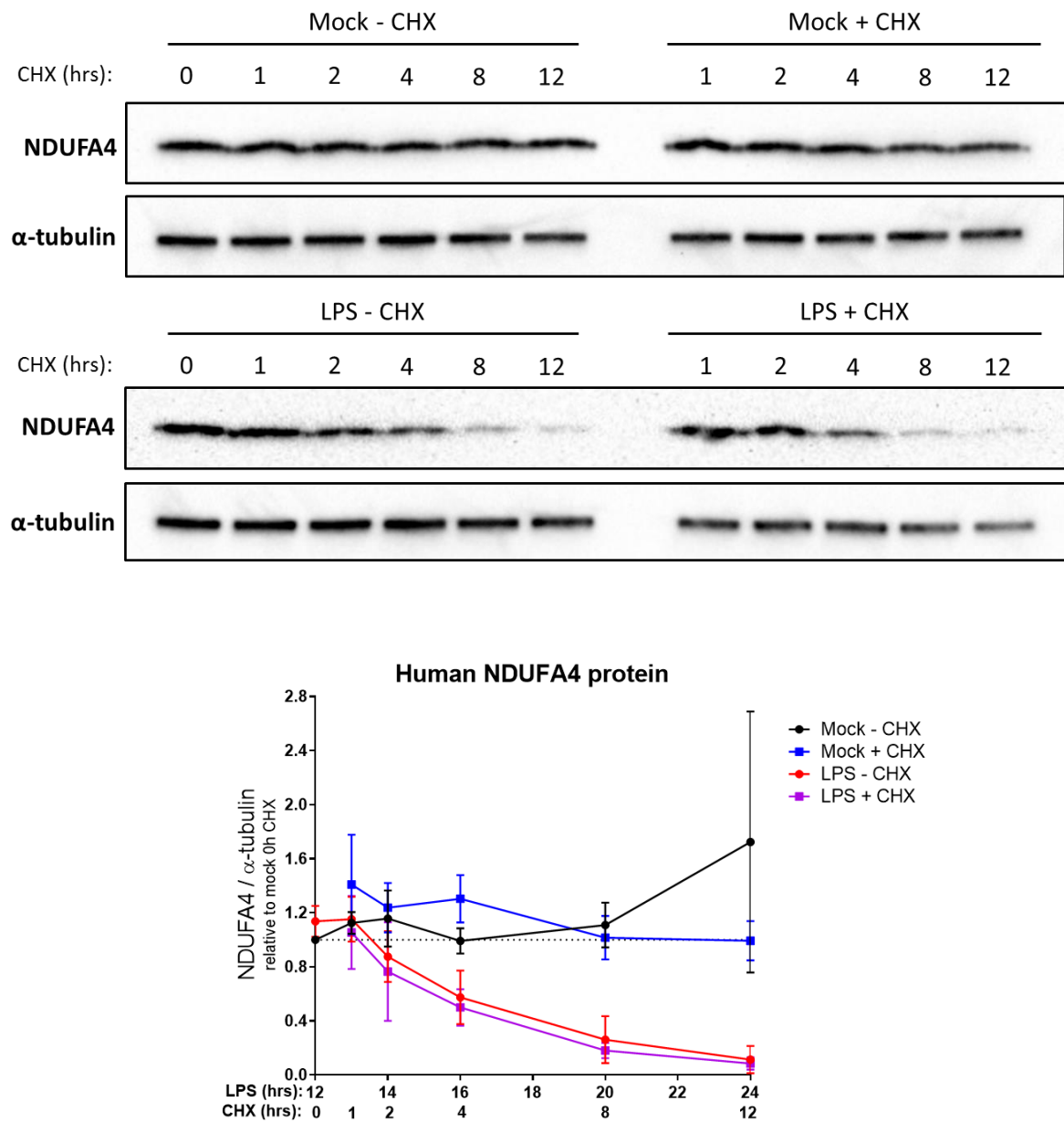
Figure 4.13) Cycloheximide chase

Human macrophages were mock treated or LPS stimulated for 12h before starting chase. Cycloheximide (+CHX) (5µg/ml) or media alone (-CHX) was added for the indicated times and cells were harvested for Western blotting. Expressed relative to 0h CHX Mock treated; n=3. Data presented as mean +/-SD.
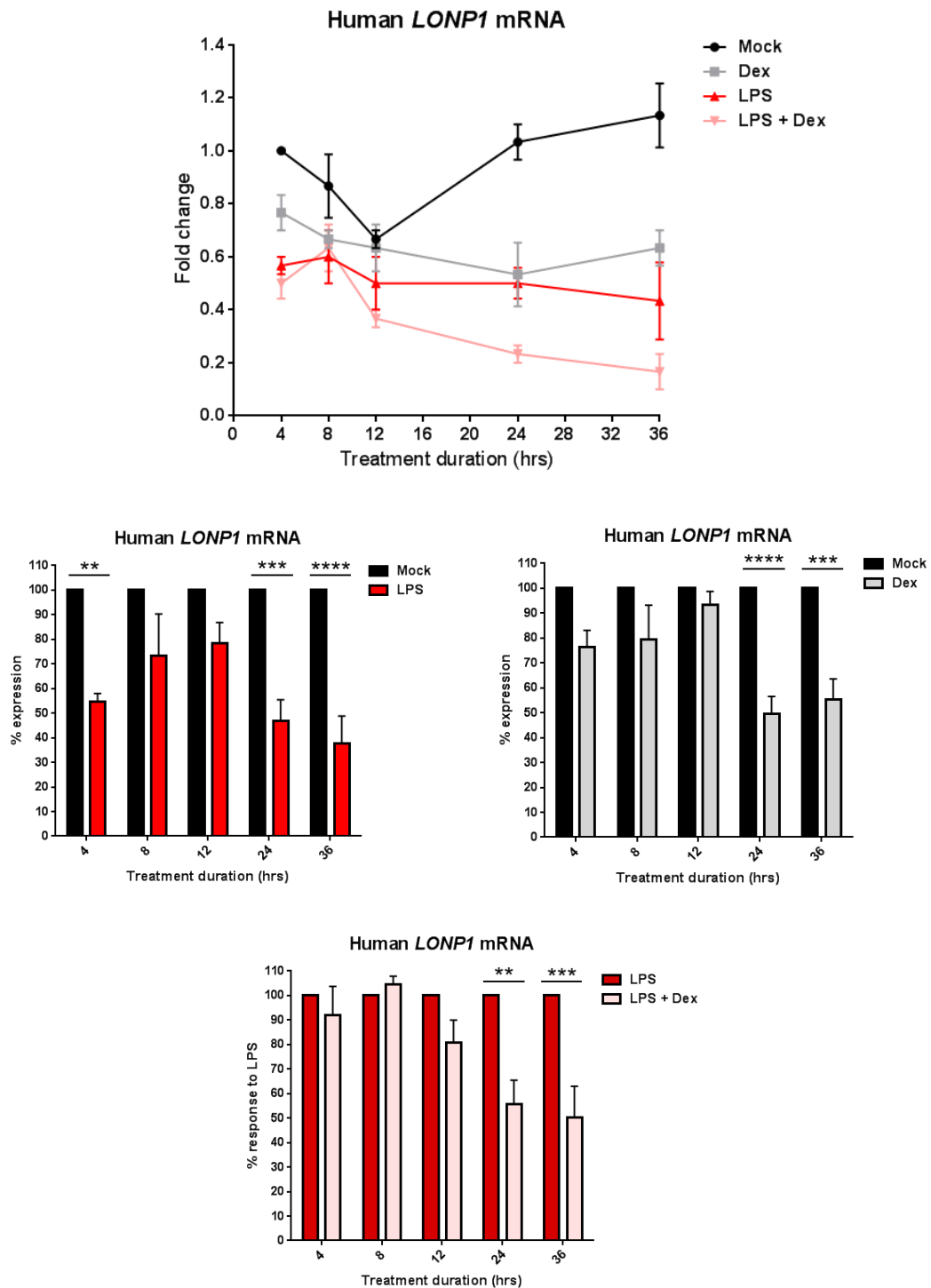
Figure 4.14) Mitochondrial LON protease mRNA is downregulated by LPS and Dex

Human macrophages were stimulated with LPS (10ng/ml) and Dex (100nM) for the indicated times. Mature *LONP1* mRNA was detected by RT-qPCR. Expressed as fold change (2^-ΔΔCt) normalised to UBC, relative to 4h mock treated control; also as % expression relative to time-matched mock treated or LPS treated; n=3; Two-way ANOVA with Sidak correction for multiple comparisons. Data presented as mean +/-SEM.

4.6 Additional predicted metabolic targets of miR-147b

Pathway analysis revealed several predicted targets of miR-147b related to metabolism (**Figure 4.2**). MicroRNAs are known to target multiple different genes and can mediate coordinated pathway regulation, as is evidenced by the control of immune signalling by other miRNAs such a miR-146a (117). I examined the regulation and targeting of a further two of these predicted target genes, which have clear metabolic function and mitochondrial protein localisation: Succinate Dehydrogenase Complex Subunit D (***SDHD***) and Succinate-Semialdehyde Dehydrogenase (otherwise known as Aldehyde Dehydrogenase 5 Family Member A1 – ***ALDH5A1/SSADH***).

SDHD was predicted as a miR-147b target by miRTarBase and miRanda. MiRTarBase predictions take into account published validation, which greatly increases target scoring. Bertero *et al* showed a small but significant decrease in *SDHD* 3'UTR luciferase signal in the presence of miR-147b (323). SDHD is an integral subunit of succinate dehydrogenase - complex II of the electron transport chain - contributing to the ubiquinone binding site (369). Succinate dehydrogenase directly catalyses the conversion of succinate to fumarate and the reduction of FAD^+ (by subunit SDHA), and as such plays a key role in both the TCA cycle and the respiratory chain (190). **Figure 4.15A** illustrates the predicted miR-147b target site in the human *SDHD* 3'UTR based on miRanda, however there is no conserved site within the mouse *Sdhd* gene. Analysis of human *SDHD* mRNA expression showed a small decrease in response to LPS, although this did not reach significance in this experiment (**Figure 4.15B**). There was also no significant change in *SDHD* mRNA expression in response to miR-147b mimic compared with control (**Figure 4.15C**).
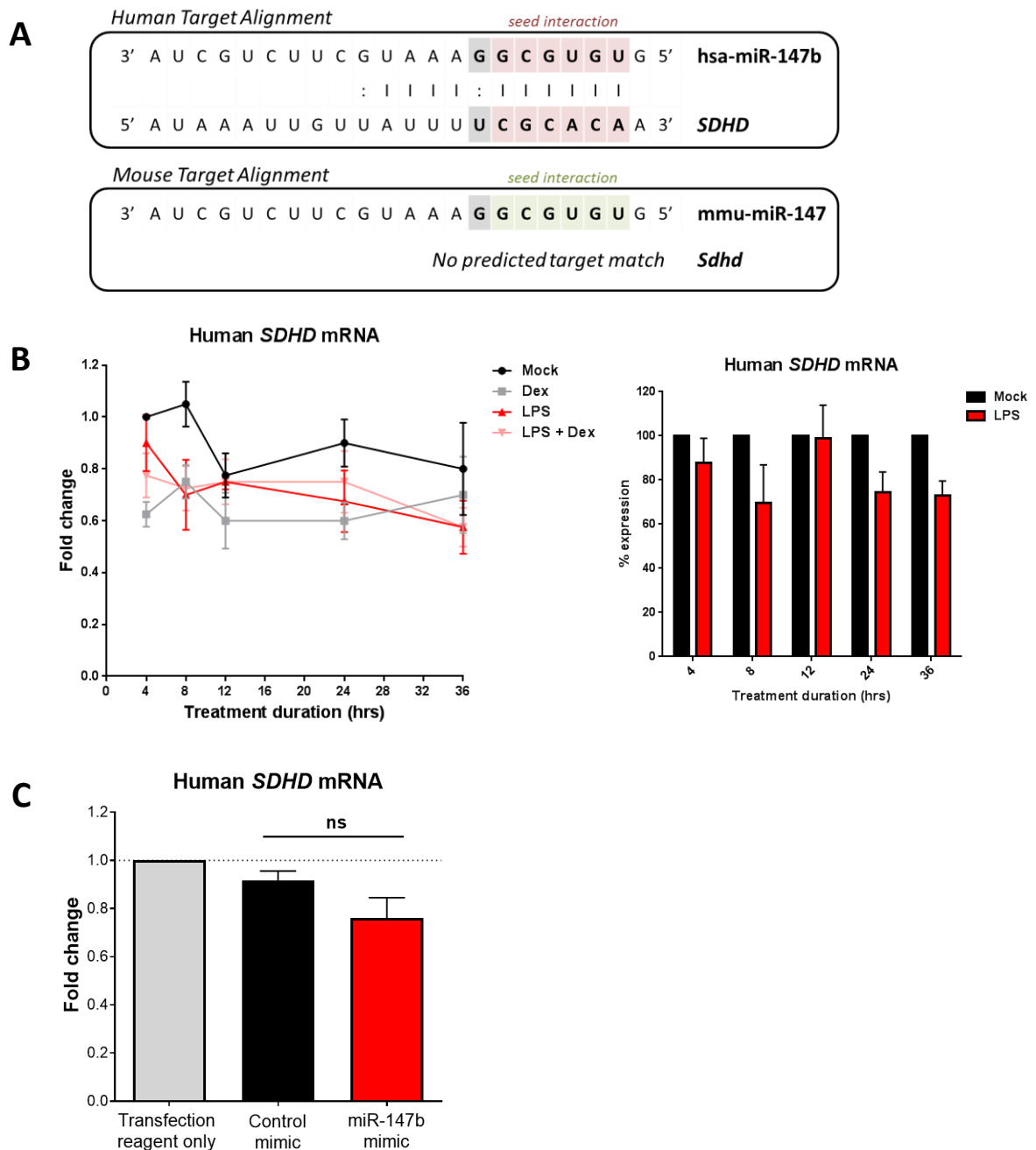
Figure 4.15) *SDHD* **as a predicted target of miR-147b**

A) Human *SDHD* and mouse *Sdhd* 3'UTR predicted target site match to the miR-147(b) sequence. **B)** Human macrophages treated with LPS (10ng/ml) and Dex (100nM) for the indicated times. Mature *SDHD* mRNA was detected by RT-qPCR, normalised to UBC; expressed as fold change (2^-ΔΔCt) relative to 4h mock treated control and as % expression relative to time matched mock treated; n=3; Two-way ANOVA with Sidak correction for multiple comparisons (ns). **C)** Human macrophages transfected with 2nM of control or miR-147b miRNA mimic using TransIT-X2 reagent. Cells were harvested for RNA 24h post transfection. Mature *SDHD* mRNA was detected by RT-qPCR, normalised to UBC; expressed as fold change (2^-ΔΔCt) relative to transfection reagent only; n=3; Two-tailed t test. Data presented as mean +/-SEM.

ALDH5A1 (*SSADH*) was only predicted as a miR-147b target by miRTarBase, though Bertero *et al* showed 40% inhibition by this miRNA by luciferase assay (323). This protein acts in the "GABA shunt" – an anaplerotic pathway that feeds glutamate derived from either glutamine or α-ketoglutarate into the TCA cycle at succinate, via gamma amino butyric acid (GABA) (152). This pathway has been reported to play a role in the accumulation of succinate, which drives pro-inflammatory processes in LPS-stimulated macrophages (191). The predicted miR-147b target site in this gene is conserved between human and mouse, suggesting a functional role, however there is little sequence match to the miRNA other than the 7mer-A1 seed sequence (positions 2-7 with an A opposite position 1) (**Figure 4.16A**). Contradictory to its proposed role in the inflammatory response through succinate, expression of human *ALDH5A1* mRNA was dramatically and reproducibly inhibited by LPS (**Figure 4.16B**). This does not seem to occur through miR-147b, however, as there was no effect of the miR-147b mimic on *ALDH5A1* mRNA (**Figure 4.16C**). While there appears to be fairly low expression of this gene in human macrophages, demonstrated by Ct values around 30 in unstimulated cells (**Figure 4.16C right panel**), the results were highly reproducible across both technical and biological replicates, indicating that they are a true reflection of the *ALDH5A1* mRNA.

The regulation of *ALDH5A1* by LPS is of potential interest with regard to the macrophage metabolic response to LPS. The contradiction of my results to the reported role of the GABA shunt in macrophage inflammatory action are therefore interesting, and may represent a difference between human and mouse macrophages. However, since this regulation does not seem to occur through miR-147b, further investigation was beyond the scope of this project.

A) Human Target Alignment — seed interaction

hsa-miR-147b / ALDH5A1

Mouse Target Alignment — seed interaction

mmu-miR-147 / Aldh5a1

B) Human *ALDH5A1* (*SSADH*) mRNA

Human *ALDH5A1* mRNA

C) Human *ALDH5A1* mRNA

Human *ALDH5A1* mRNA Ct values
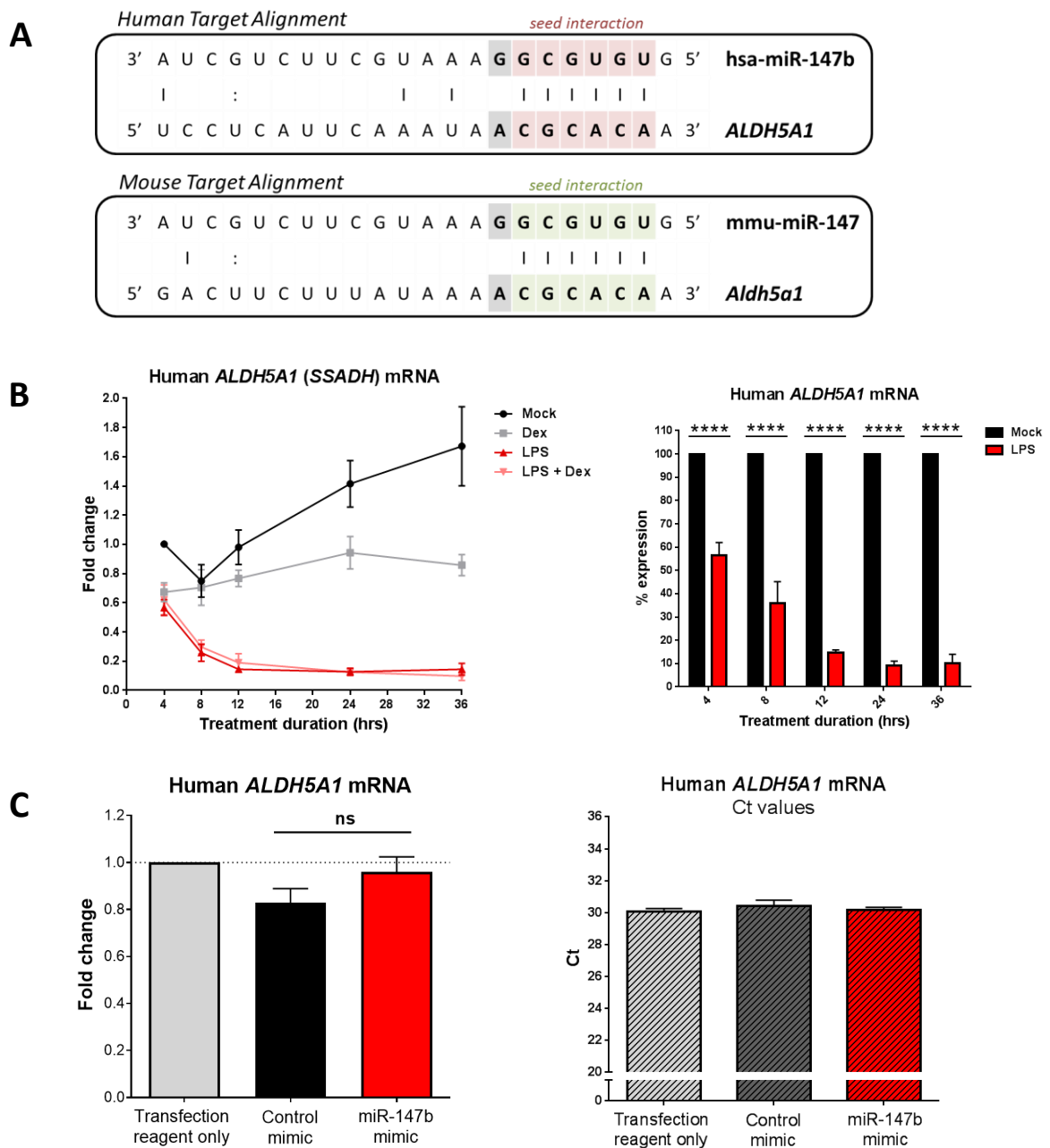
Figure 4.16) *ALDH5A1* (*SSADH*) as a predicted target of miR-147b

A) Human *ALDH5A1* and mouse *Aldh5a1* 3'UTR predicted target site match to the miR-147(b) sequence. **B)** Human macrophages treated with LPS (10ng/ml) and Dex (100nM) for the indicated times. Mature *ALDH5A1* mRNA was detected by RT-qPCR, normalised to UBC; expressed as fold change (2^-ΔΔCt) relative to 4h mock treated control and as % expression relative to time matched mock treated; n=3; Two-way ANOVA with Sidak correction for multiple comparisons. **C)** Human macrophages transfected with 2nM of control or miR-147b miRNA mimic using TransIT-X2 reagent. Cells were harvested for RNA 24h post transfection. Mature *ALDH5A1* mRNA was detected by RT-qPCR, normalised to UBC; expressed as fold change (2^-ΔΔCt) relative to transfection reagent only and as raw Ct values; n=3; Two-tailed t test. Data presented as mean +/-SEM.

4.7 Discussion

Optimisation of miRNA mimic transfection

A reasonable amount of work in this chapter was required to optimise transfection of primary human macrophages, which proved more problematic than originally anticipated. The switch of transfection reagent reduced the confounding effects that I observed, and I also include an additional control of treatment with transfection reagent alone for comparison of miRNA mimic-specific effects. I could also have measured the production of type I interferons in response to synthetic RNA transfection, as these are produced in response to viral infection through the stimulation of TLRs or RIG-like receptors, and would have indicated whether these receptors were activated by the transfected RNA (5).

During this optimisation I thought it important to find a concentration of mimic that replicated the endogenous expression in response to LPS, as excessive ectopic miRNA expression could result in non-physiological effects. An alternative option for the optimisation of concentration would be to measure absolute quantification of the miRNA, utilising known concentrations of synthetic RNA to create a standard curve by RT-qPCR (304). This would allow precise matching of the quantities present in LPS-treated cells. However I believe that approximately matching the fold increase was sufficient for these experiments, as it is likely that cells from different donors show different absolute expression of the miRNA, and it would be unfeasible to optimise the concentration for each donor individually. Using such a low concentration of mimic (2nM), and demonstrating that this concentration gives comparable upregulation to *in vitro* LPS stimulation, are suitable steps to conclude that the results are unlikely to be off-target effects mediated by overexpression. It would, however, be valuable to compare the levels obtained during *in vitro* stimulation with *in vivo* or *ex vivo* miRNA expression levels.

In this chapter I have identified a previously unreported response of the mitochondrial protein NDUFA4 to inflammatory challenge in macrophages, and have proven that this gene is a functional target of the LPS-induced miRNA miR-147b. An alternative approach for the identification of miRNA targets is the analysis of global transcript or protein expression changes in response to miRNA overexpression, for example by RNA-Seq or mass spectrometry-based proteomics. There are several reasons why I didn't go down this route here. Firstly, the issues that I experienced with transfection reagent responses in my cell type meant that I had to increase the number of controls for each experiment (*discussed further in Chapter 6*), which would have greatly increased the costs of these techniques. These issues also highlighted the importance of validating my results by several methods, which I did by performing mimic and inhibitor transfections, as well as luciferase assays. Any subtle changes seen in global expression analyses under mimic transfection could have been confounded by the transfection responses. I also believed that *NDUFA4* was an obvious target to investigate due to the consensus of all prediction tools that this was the highest scoring potential target. Whilst global analysis would have given more data regarding the coordinated regulation of cellular pathways by miR-147b, the combination of the gene enrichment analysis and the high scoring of NDUFA4 indicated that this miRNA may serve in the regulation of macrophage metabolism. Had I carried out RNA-Seq analysis of transcript changes, I would still have wanted to validate which of the observed changes were due to direct targeting by the miRNA. Since *SDHD* showed no significant response to LPS, and both *SDHD* and *ALDH5A1* showed no significant response to miR-147b mimic transfection, I continued to focus on the regulation and role of NDUFA4.

The results in this chapter indicate that there are likely to be multiple mechanisms of regulation of NDUFA4 protein expression in human macrophages. This is demonstrated by the following:

- The discrepancy between NDUFA4 mRNA and protein regulation in response to LPS and dexamethasone (**Figures 4.3 and 4.4**)

- The differences in regulation between human and mouse NDUFA4 (**Figures 4.3, 4.4 & 4.5**)

- The downregulation of NDUFA4 protein by multiple different TLR agonists, which act through varying signalling pathways (**Figure 4.6 and Figure 1.2**)

- The observation that downregulation of NDUFA4 protein by miR-147b mimic is not as complete as LPS-induced downregulation (**Figure 4.9**). This is consistent with our understanding that miRNAs act as fine-tuners of protein expression rather than on/off switches (117).

- The rescue of *NDUFA4* mRNA by the miR-147b inhibitor, but failure in rescue of NDUFA4 protein under LPS treatment (**Figure 4.10**)

- The lack of effect of cycloheximide on NDUFA4 protein expression in the short term (12h treatment), but effective knock down of protein expression by the miRNA mimic in longer experiments (48h post transfection) (**Figures 4.9 & 4.13**).

These observations indicate that NDUFA4 is regulated both post-transcriptionally and post-translationally. Control at the transcriptional level has not been addressed here but is also a possibility, although the lack of response to LPS of mouse *Ndufa4* mRNA suggests that this does not occur in mouse BMDMs. As I did not continue to analyse the responses in mouse macrophages alongside human cells, I cannot conclude with certainty which mechanisms of regulation are shared between the two species, however it is likely that miR-147 also targets *Nduaf4* in the mouse due to conservation of the predicted target site (**Figure 4.1**). It would be interesting to determine the transcription factors responsible for expression of the *NDUFA4* gene in order to better understand its regulation in response to pro- and anti-inflammatory signals. The nuclear respiratory factors NRF-1 and NRF-2/GABPA control expression of multiple nuclear-encoded mitochondrial genes, including electron transport chain subunits.

NRF-2 has been shown to regulate all 10 of the originally-annotated nuclear-encoded cytochrome c oxidase subunits (370). It is worth noting that this is a different gene from Nrf2/NFE2L2 (Nuclear Factor, Erythroid 2 Like 2) which has anti-oxidant activity and has been shown to be regulated by itaconate in LPS-stimulated macrophages (*discussed in Section 1.6*). Nrf2/NFE2L2 has also been shown to regulate mitochondrial biogenesis (potentially through the control of NRF-1 expression) (219, 371). Interestingly, NDUFA4 protein was found to be marginally induced in a breast cancer cell line by treatment with an isothiocyanate that has been reported to enhance Nrf2/NFE2L2 activity. However, genetic KD of the Nrf2/NFE2L2 negative regulator KEAP1 did not recapitulate this result, therefore an alternative mechanism is likely responsible for the observation (372).

The measurement of mRNA levels of the mitochondrial LON protease (*LONP1*) suggest that this protease is not responsible for post-translational downregulation of NDUFA4 in response to LPS, since *LONP1* mRNA was downregulated rather than induced by LPS (**Figure 4.14**). Measurement of LON protein expression could provide further support for this conclusion. LON protease is known to be an important cellular stress response protein, induced by various triggers including oxidative stress. Amongst many described functions, LON acts to proteolytically degrade oxidatively modified proteins within mitochondria, one such target being oxidised mitochondrial aconitase (373). A recent report implicated reduced function of aconitase in the accumulation of citrate in LPS-stimulated macrophages (374), therefore downregulation of LON by LPS as shown here could lead to accumulation of dysfunctional aconitase and contribute to this process. However, the report by Palmieri *et al* describes that iNOS-derived nitric oxide is responsible for the reduced functionality of aconitase in murine macrophages (374), therefore the relevance of this mechanism in human macrophages, which do not produce nitric oxide, is unclear (*to be discussed in Chapter 5*). The regulation of LON may also have implications for cytochrome c oxidase activity. The COXIV-2

isoform, which replaces the COXIV-1 counterpart after LON-mediated degradation of the latter, has been shown to confer lower oxygen affinity, affect ROS production under different oxygen tensions, and alter susceptibility of cytochrome c oxidase to allosteric inhibition by ATP (375).

The culmination of multiple cellular mechanisms to silence NDUFA4 expression in response to TLR activation indicates the existence of evolutionary pressure for the macrophage to silence this protein. This is therefore an exciting novel signalling pathway that links inflammatory signals to the control of mitochondrial protein expression. As NDUFA4 is a fairly poorly studied protein, the role that it plays in macrophages in currently unknown. This led on to the second half of my project, which focused on macrophage metabolism; the effect of glucocorticoids on macrophage metabolic phenotype; and the role of NDUFA4 in the regulation of macrophage metabolic and inflammatory responses.

Chapter 5) The regulation of macrophage metabolism by glucocorticoids

5.1 Introduction – Glucocorticoids and Metabolism

The discovery that the mitochondrial electron transport chain protein NDUFA4 is strongly regulated by inflammatory signals in macrophages brought the topic of macrophage metabolism to the forefront of my attention. As discussed in Chapter 1, macrophage function is underpinned by metabolic regulation, and inflammatory stimuli induce remodelling of metabolic pathways (218). The endogenous glucocorticoid hormone cortisol is well-known to regulate systemic energy homeostasis through its actions on tissues that are broadly termed "metabolic tissues", including the liver, muscle and adipose tissue. In Chapter 1 I highlighted some of the metabolic effects that play major roles in the development of clinical side effects of GC use. These include inhibition of glycolysis and promotion of gluconeogenesis in the liver; stimulation of protein degradation in skeletal muscle; and stimulation of lipolysis in adipose tissue. Some of these metabolic pathways have been shown to be relevant to immune regulation, however the specific role that GCs play in the regulation of immune cell metabolism, in particular in macrophages, is comparatively poorly understood.

5.1.1 Glucocorticoids and lymphocyte metabolism

Glucocorticoids are commonly used for the treatment of lymphocytic malignancies such as acute lymphoblastic leukaemia (ALL), due to their ability to induce apoptosis in lymphoid cells. Resistance to this therapy is an ongoing problem that has sparked interest in studying the mechanisms of apoptosis induction and resistance in these cells (376). GCs have been found to inhibit the high glycolytic flux required for the cancer cells to proliferate and

survive, in part through decreased expression of the glucose transporter GLUT1, as well as decreased expression of glycolytic genes including HK2 (377, 378). It was shown that resistance to GC-induced apoptosis could be overcome by directly inhibiting glycolysis in ALL cells (379).

More recently, Dyczynski *et al* carried out extensive metabolomic and proteomic analysis of GC-treated B-ALL cells (376). Dexamethasone treatment not only brought about a decrease in lactate production, but also decreased glucose and glutamine entry into the TCA cycle, associated with broadly reduced uptake of metabolites from the culture medium. The authors also described an increase in catabolism and autophagy, as well as production of glutamine from intracellular substrates via elevated expression of glutamine synthetase (GS/GLUL). The increased glutamine synthesis was hypothesised to function in reducing intracellular ammonia levels during protein catabolism, in a similar way to atrophic muscle, and to associate with the induction of apoptosis through an unknown mechanism (376).

Glucocorticoids increase production of hydrogen peroxide in immature thymocytes and lymphoma cells. This was shown to arise from mitochondrial superoxide, and may contribute to apoptosis induction (380, 381). Tome *et al* reported that dexamethasone treatment led to inhibition of ETC CI and CIII activities in lymphoma cells, which could explain the elevated mROS production (381). Other studies have suggested that GC resistance is associated with the ability to compensate for reduced glycolytic ATP production through increased oxidative phosphorylation, fuelled either by increased autophagy (378), or fatty acid oxidation (382). It is therefore important to distinguish between GC-mediated effects that directly contribute to lymphocyte apoptosis, and those upregulated pathways that serve to protect against cell death.

5.1.2 Glucocorticoids and myeloid cell metabolism

Myeloid-derived suppressor cells (MDSCs) are a heterogeneous population of immature cells of myeloid origin, which play important roles in immune regulation and have been implicated in the survival of tumours as well as in suppressing inflammatory diseases such as hepatitis (383, 384). GCs have been shown to enhance the suppressive properties of MDSCs - reducing expression of pro-inflammatory cytokines such as TNFα and IL-1β; enhancing expression of anti-inflammatory cytokines such as IL-10; and stimulating the production of NO (385), which plays a key immunosuppressive role in these cells through inhibition of T cell expansion and activity (384). The action of GCs in MDSCs has been linked to the inhibition of glycolysis, mediated through the reduced expression of GLUT1, enolase 1 and MCT4. Specifically, the authors implicated suppression of HIF-1α expression and activity in the reduction of glycolysis and the enhanced immunosuppressive function in response to GCs (385).

In 1992, Bustos and Sobrino studied the activation of PFK-1 and PFK-2 enzymes in activated rat macrophages (386). They reported that treatment of the animals with the synthetic GC triamcinolone acetonide, which is used for asthma management (65), greatly inhibited the activity of both of these glycolytic enzymes in macrophages, associated with a decrease in levels of fructose 2,6-BP and reduced lactate production (386). This has not been further studied in macrophages since, to my knowledge.

5.1.3 Glucocorticoids and HIF-1α

In addition to the reported downregulation of HIF-1α in MDSCs mentioned above, GCs have been demonstrated to inhibit expression or activity of this transcription factor in several other cells types, including colon cancer cell lines and CD4+ T cells (385, 387-390). In contrast,

GCs were reported to potentiate hypoxia-induced gene expression in COS7 and HeLa cell lines through enhancement of HIF-1α transactivatory capacity, without altering HIF-1α protein levels (391). A further contrasting report showed that GCs promote HIF-1α protein stabilisation in normoxia through degradation of Von Hippel Lindau protein in a zebrafish model, as well as in human liver tissue and cultured hepatocytes (392). In addition to these reports of HIF-1α regulation by GCs, the reciprocal regulation has been described. GR expression is elevated during hypoxia exposure, mediated by HIF-1α action. This resulted in a greater cellular response to GC treatment in hypoxic conditions, demonstrated by increased capacity for both transactivation and transrepression of GC-regulated gene expression (393).

The aims of this chapter were to investigate the metabolic effects of GCs in macrophages. This will give a broader context to the regulation of NDUFA4 by these steroids and a better understanding of the underlying mechanisms of anti-inflammatory GC function.

Results

5.2 Differential metabolic responses of mouse and human macrophages

Inflammatory stimulation of macrophages, such as by LPS, results in profound metabolic changes that help to fuel immune responses and contribute to signalling pathway modulation (218). These changes have been extensively studied in murine macrophages (predominantly bone marrow-derived macrophages – BMDMs - differentiated *in vitro*). Due to my interest in metabolic signalling involving NDUFA4 in human macrophages, I wanted to study the effects of pro- and anti-inflammatory signals on the metabolism of primary human monocyte-derived macrophages (MoDMs). I used a Seahorse Metabolic Flux analyser to measure changes in extracellular acidification rate (ECAR) as a readout of glycolytic lactate

production; and oxygen consumption rate (OCR) as a readout of mitochondrial oxidative respiration. Metabolic parameters were calculated after acute injection of fuels or inhibitors as described in **Figures 2.13 & 2.14**.

Consistent with the literature, I found that mouse BMDMs significantly increased their rate of glycolysis in response to 24h LPS treatment (**Figure 5.1A**). This was also true for human MoDMs, which showed a dramatic increase in ECAR compared with unstimulated (Mock) cells (**Figure 5.1B**). This result is in contrast with a recent publication by Vijayan *et al*, which reported a small but significant decrease in basal ECAR after 16h LPS treatment in human macrophages (394). In my experiments, despite differences in the magnitude of the LPS response between different donors, the increase in ECAR was reproducible across all donors tested, including cells derived either from fresh peripheral blood or leukapheresis cones.

Glycolytic capacity is generally calculated from the Seahorse Glyco stress test after additional of the ATP synthase inhibitor oligomycin. However, in my experiments oligomycin treatment did not cause an increase in ECAR in human cells. The glycolytic capacity was therefore calculated using the maximum glycolytic rate (before FCCP injection to avoid contribution of mitochondrial acidification) and this closely mirrored basal glycolytic rate in both mouse and human cells (**Figure 5.1**). Glycolytic reserve describes the difference between maximal glycolytic capacity and the basal glycolytic rate (**Figure 2.13**). Mouse BMDMs showed a small glycolytic reserve that did not change upon LPS treatment, however the glycolytic reserve was absent or negligible for human MoDMs (**Figure 5.1**). These results suggest that the human macrophages consistently act at the maximum possible glycolytic rate when sufficient glucose is present. The slight decrease in ECAR upon oligomycin addition in some instances, particularly in the presence of LPS, are so far unexplained, but could be due to a

reduced pool of oxidised NAD+ during mitochondrial inhibition, which is needed to fuel the high rates of glycolysis (**see Figure 1.7**).

LPS treatment consistently caused an increase in non-glycolytic acidification in human MoDMs, denoted by the ECAR value before glucose injection (**Figure 5.1B**). Interestingly, this was maintained after addition of mitochondrial inhibitors and 2-DG in the final injection, suggesting that TCA cycle CO_2 does not account for this increase. The precise source is not known, but could arise from other cellular decarboxylation reactions, which result in CO_2 release (395). This effect of LPS was not observed in mouse BMDMs (**Figure 5.1A**).

By analysing oxygen consumption rate I showed that LPS-treated mouse BMDMs displayed a dramatically reduced maximal respiratory capacity, which is consistent with the literature (**Figure 5.2A**). This can be demonstrated upon FCCP injection, which dissipates the mitochondrial proton motive force, allowing unrestricted electron flow uncoupled from ATP production. While some researchers report decreases in both basal respiration and maximal capacity in BMDMs in response to LPS (269), others show only loss of maximal capacity, as my results demonstrated (**Figure 5.2A**) (226). It is unclear what causes these differences, but it is possible that different concentrations of LPS used, or different mouse strains, could be responsible. Different mouse strains have been demonstrated to have varying propensities to produce nitric oxide, and NO has been implicated in mitochondrial inhibition (33, 269).

In contrast to the results from mouse macrophages but in agreement with a previous report (394), human MoDMs showed no loss of maximal respiratory capacity following LPS treatment (**Figure 5.2B**). This may be explained by differences in nitric oxide production between mouse and human macrophages – as discussed in Chapter 1. NO is known to inhibit ETC activity and oxygen consumption in mouse BMDMs and dendritic cells (234, 269, 396). We confirmed that in our system we were able to detect significant NO production in mouse

BMDMs, but there was no detectable production from human MoDMs (**Figure 5.3**). This was true either with LPS alone or in the presence of IFNγ, which potentiated the LPS-induced expression in mouse. These results highlighted an important issue of the differences between the two model systems frequently used *in vitro*, which is important to consider for the remainder of my work (*discussed further in Section 5.7*).

Basal respiration in the presence of glucose was increased by LPS in human macrophages (**Figure 5.2B**), however the ATP-linked respiration was not significantly altered (*see Section 2.19 for calculations*). This indicates that the majority of the increase in basal respiration was due to a large LPS-induced increase in proton leak (oxygen consumption in the presence of oligomycin) in human MoDMs. In contrast, proton leak was very slightly reduced by LPS in mouse BMDMs, but while this reached statistical significance, the magnitude may not be a biologically relevant change. Macrophages can express the mitochondrial transporter UCP2, which is related to the brown adipose tissue uncoupling protein (UCP1) that mediates thermogenesis by dissipating the mitochondrial proton gradient (397). Uncoupling such as this could explain the observed increase in proton leak in human macrophages. UCP2 has been shown to be downregulated by LPS treatment of mouse macrophages, resulting in increased ROS production and ROS-mediated activation of inflammatory signalling pathways (398-400). In rat microglia, UCP2 was shown to be increased at 6h but decreased at 24h after LPS treatment (401). It is unclear what impact LPS has on UCP2 expression in human macrophages.

The changes observed in spare respiratory capacity in these experiments reflect the alterations in either maximal capacity or basal respiration in mouse and human cells respectively (**Figure 5.2**). The apparent negative spare capacity in LPS-treated mouse BMDMs

may be a result of the slight downward trend in oxygen consumption rate for these cells throughout the progression of the experiment, and may be an artefact of the assay.

Due to the combination of Mito and Glyco stress tests used (*described in Section 2.19*), the results allowed analysis of oxidative respiration in the absence of glucose (denoted glucose-independent respiration). This parameter was unchanged by LPS in mouse BMDMs, but was significantly enhanced by LPS in human MoDMs (**Figure 5.2**). The portion of this oxygen consumption linked to ATP production was also significantly elevated, suggesting that the increased proton leak does not account for all of this change (NB: this calculation makes the assumption that the proton leak does not change upon addition of glucose). The major fuel present in the assay medium prior to glucose injection is glutamine. Macrophages have been demonstrated to increase their incorporation of glutamine into the TCA cycle in response to LPS stimulation, enabled by upregulation of the glutamine transporter (191). In human macrophages, which do not show inhibited electron transport chain activity, this LPS-induced increase in glutamine utilisation is likely able to drive elevated oxidative respiration to meet cellular energy demands, explaining the observations in Figure 5.2B. This response may also apply for other stimulations, for example glutamine-derived α-ketoglutarate has been shown to be necessary for increased oxidative respiration in response to the M2 stimulus IL-4 (240). The drop in spare respiratory capacity with LPS in mouse BMDMs may explain why this effect is not observed in these cells.

It is also worth noting from these results that both mouse and human cells demonstrate the Crabtree effect (**Figure 5.2C**). This describes the downregulation of oxidative respiration in the presence of a high glycolytic flux, despite the presence of functional mitochondrial machinery, and represents an adaptive and reversible response to nutrient

availability. This is demonstrated upon glucose addition during the Seahorse assay (**Figure 5.2**). The Crabtree effect has also been demonstrated in various cancers, and can impede tumour cell eradication by glycolytic inhibitors. While the precise mechanisms are not known, it has been suggested to occur through competition between the pathways for common substrates such as ADP or phosphate, or through inhibition of mitochondrial respiration by glycolytic intermediates such as fructose 1,6-BP (402). In **Figure 5.2C** this effect is quantified by subtracting the basal OCR after glucose injection from the OCR before glucose injection. The magnitude of the effect is significantly elevated by LPS treatment in both mouse and human macrophages, which likely reflects the enhanced glycolytic rate in stimulated cells in the presence of glucose.
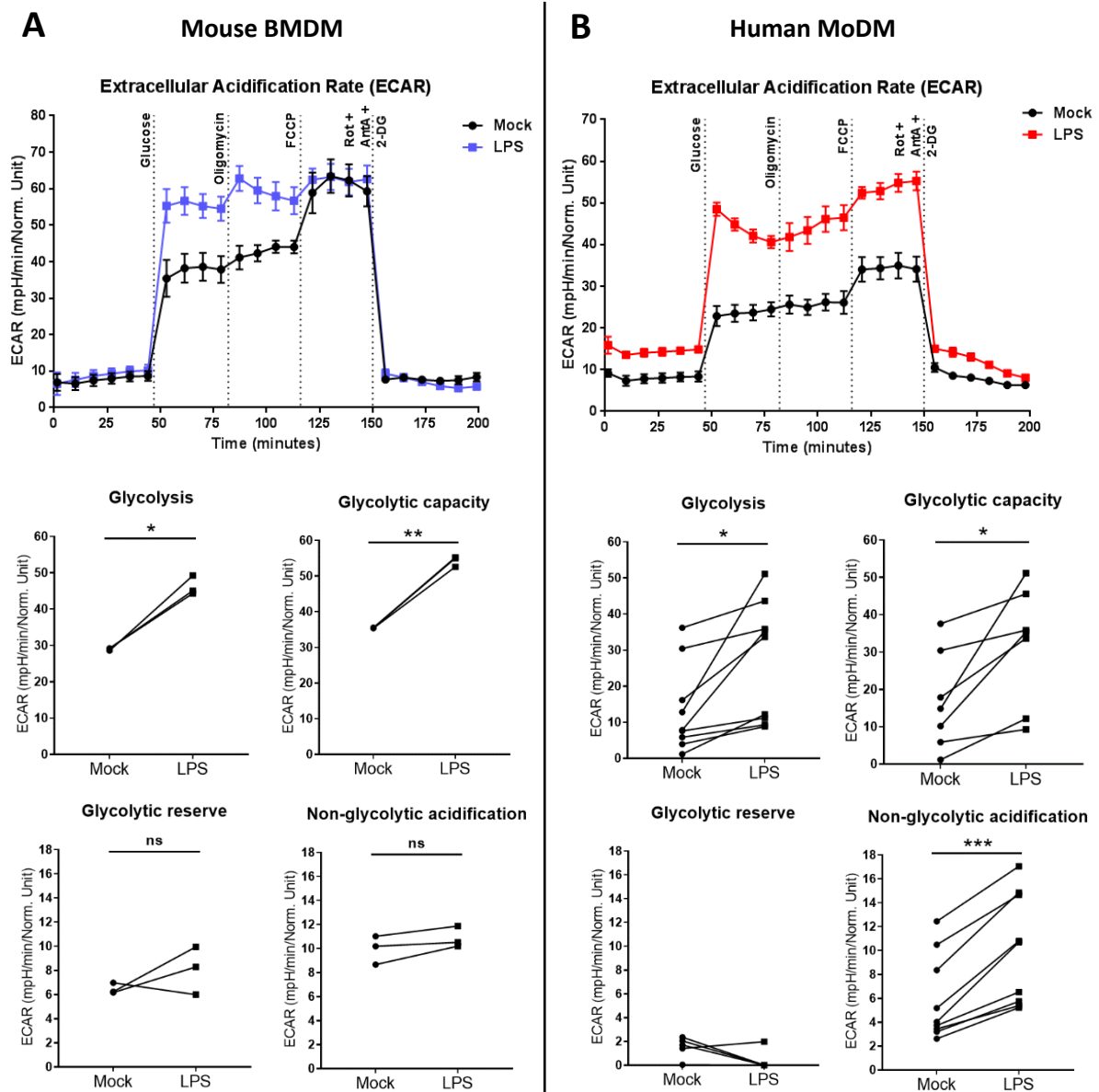
Figure 5.1) LPS treatment causes increased glycolytic metabolism in both mouse and human macrophages

Seahorse extracellular flux analysis of **A)** WT mouse BMDMs or **B)** human monocyte-derived macrophages (MoDMs) treated with LPS (10ng/ml) for 24h. Representative Seahorse traces showing real-time ECAR from combined Mito+Glyco stress test (mean+SD of technical replicates); Normalised to calcein viability assay. Parameters calculated as described in methods.

Paired two-tailed t tests, mouse: n=3; human: n=7-9

A Mouse BMDM
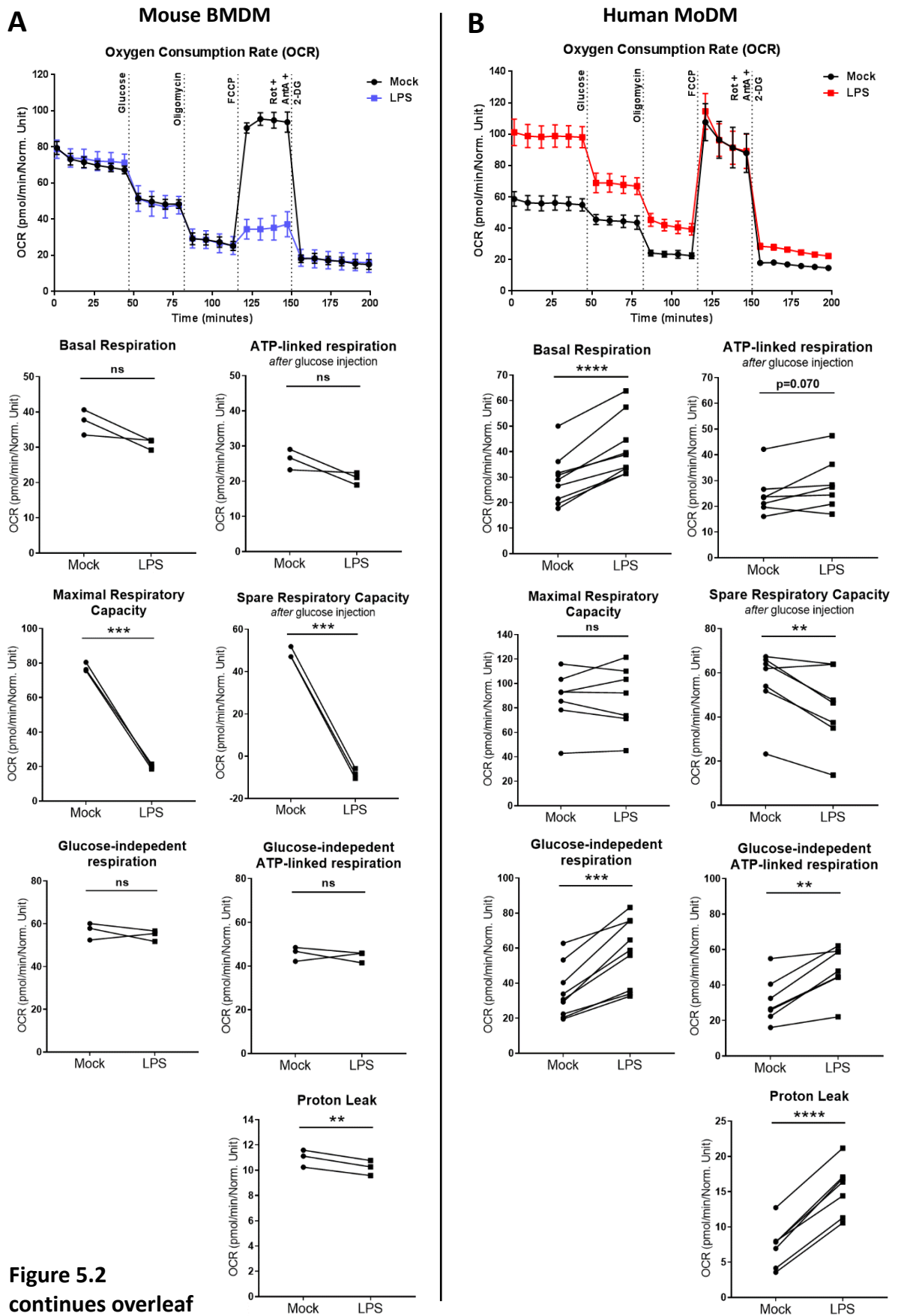
B Human MoDM

Figure 5.2 continues overleaf

C
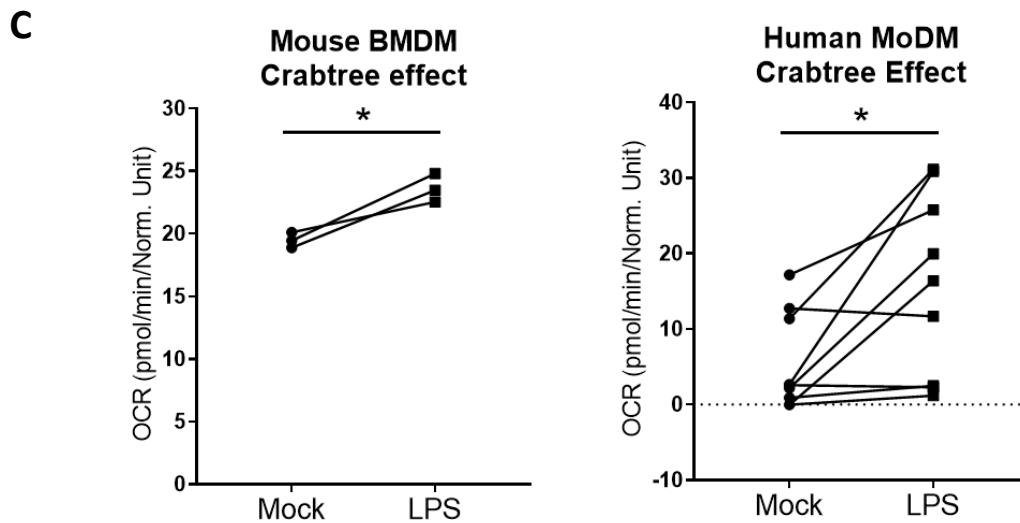
Figure 5.2) Mouse and human macrophages show different oxidative respiratory responses to LPS

Seahorse extracellular flux analysis of **A)** WT mouse BMDMs or **B)** human monocyte-derived macrophages (MoDMs) treated with LPS (10ng/ml) for 24h. Representative Seahorse traces showing real-time OCR from combined Mito+Glyco stress test (mean+SD of technical replicates); Normalised to calcein viability assay. **C)** Crabtree effect analysed from mouse BMDM and human MoDM Seahorse Mito+Glyco stress tests.

Parameters calculated as described in methods; Paired two-tailed t tests, mouse: n=3; human: n=7-9
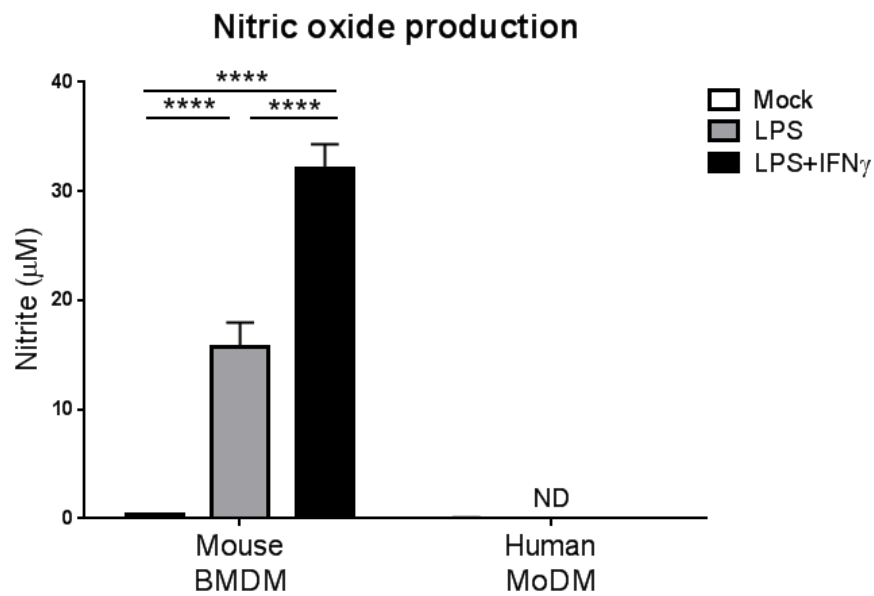
Figure 5.3) Human macrophages show no *in vitro* production of nitric oxide

Data generated by Adeolu Adewoye

WT mouse BMDMs or human monocyte-derived macrophages (MoDMs) treated for 20h with 100ng/ml LPS +/- 100ng/ml of species-specific IFNγ. Nitrite was measured as a read-out of cellular nitric oxide production by Griess reaction; ND = no detectable signal; 3 biological replicate condition per species, assay run simultaneously; Two-way ANOVA with Sidak correction for multiple comparisons. Data presented as mean +SEM.

5.3 Glucocorticoids alter macrophage metabolic responses to LPS

Many of the anti-inflammatory functions of GCs occur through the opposition of inflammatory signalling pathways that are activated by TLRs or cytokine receptors, for example by inhibition of NF-κB, or induction of negative regulators of MAPK signalling (38, 73). Dexamethasone also opposes the downregulation of NDUFA4 by TLR agonists. I was therefore interested to see the effects of GC on the metabolic response of macrophages to LPS. I treated human MoDMs with LPS in the absence or presence of dexamethasone for 24h prior to performing a Seahorse Mito+Glyco stress test. Dex strongly repressed the LPS-induced glycolytic shift in these cells (**Figure 5.4**). This is consistent with studies in lymphocytes, in which glycolytic metabolism is suppressed by GCs, as well as the early results of Bustos and Sobrino in rat macrophages (378, 386). In order to confirm that changes in mitochondrial CO_2 production were not responsible for the observed changes in acidification (ECAR), I performed the standard Seahorse Glyco stress test in the presence of ETC inhibitors rotenone and antimycin A, which gave the same result (**Figure 5.4C**).

As shown in **Figure 5.1**, oligomycin treatment had little effect on glycolytic rate in these primary human macrophages, therefore glycolytic capacity largely paralleled basal glycolysis, and glycolytic reserve was negligible (**Figure 5.4**). Dexamethasone had no effect on these parameters. Dex also had no effect on non-glycolytic acidification rate, which was elevated by LPS in the absence or presence of the glucocorticoid (**Figure 5.4**).

Figure 5.5 recapitulates results of **Figure 5.2** - LPS treatment of human macrophages did not cause loss of mitochondrial respiration, and resulted in a significant increase in oxygen consumption rate in the absence of glucose (glucose-independent respiration). **Figure 5.5** also

demonstrates that the addition of Dex significantly opposed the reduction in oxygen consumption upon glucose injection (Crabtree effect), and LPS+Dex-treated cells maintained a significantly elevated basal respiratory rate relative to unstimulated (**Figure 5.5B**). This suggests that the cellular demands for ATP are still high in the LPS+Dex condition, but due to the GC-mediated inhibition of glycolysis, these extra demands must be met by mitochondria. These results give further evidence for the maintenance of fully functional and adaptable mitochondria in these cells, which can be called upon to meet energetic or biosynthetic demands. Nutrient availability is therefore shown to be an important driver of metabolic activity in these circumstances.

The maximal respiratory capacity did not change under any of the treatment conditions (in contrast to BMDMs shown in **Figure 5.2**). The two spare respiratory capacity calculations represent the reserve capacity that the cells possess to increase respiration rate from the basal state either in the presence or absence of glucose (spare respiratory capacity after/before glucose injection, respectively – *calculations described in Figure 2.14*). Since the maximal respiratory capacity does not change between treatments, these parameters simply reflect the differences in basal respiration (+/- glucose) between treatment conditions (**Figure 5.5B**). The LPS-induced increase in proton leak discussed previously was also not affected by addition of glucocorticoid (**Figure 5.5B**).

A Extracellular Acidification Rate (ECAR)

B Glycolysis / Glycolytic capacity / Glycolytic reserve / Non-glycolytic acidification
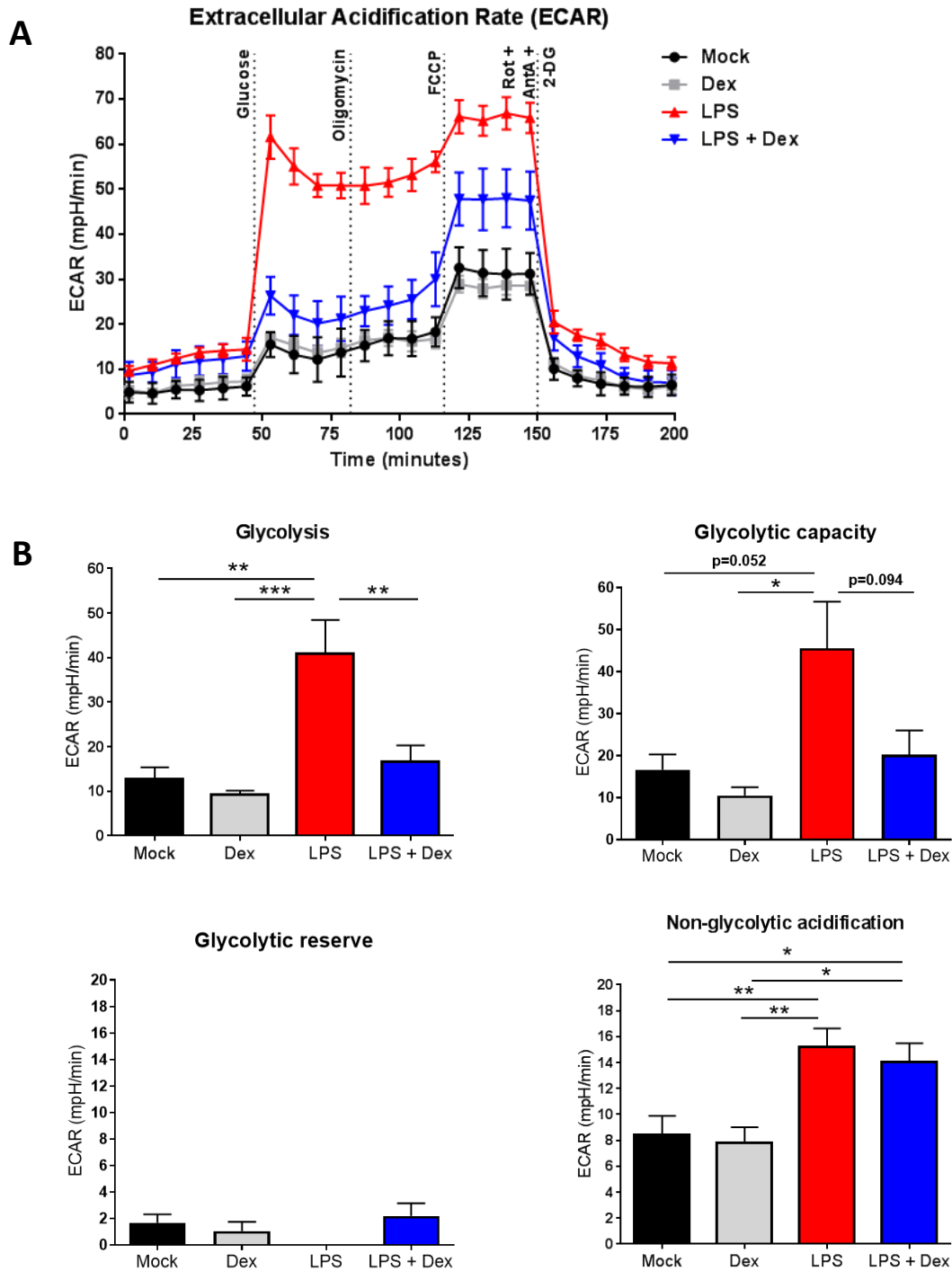
Figure 5.4 continues overleaf
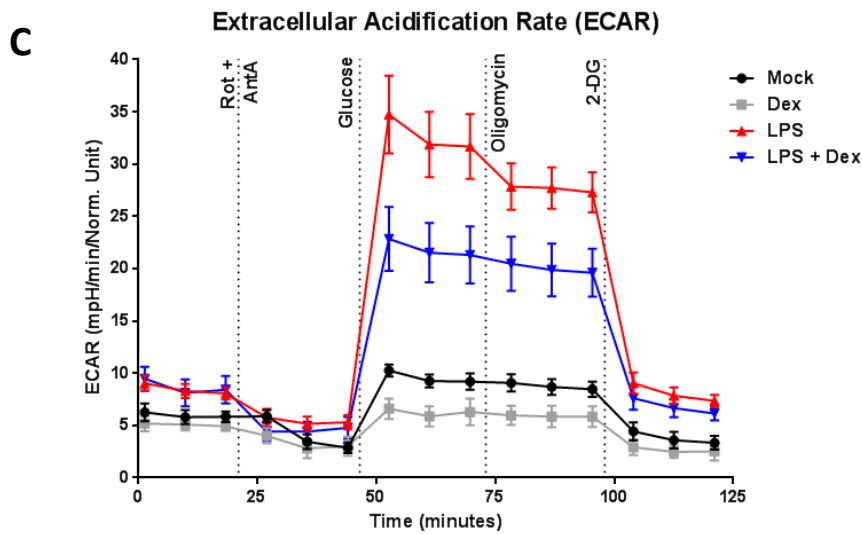
Figure 5.4) Glucocorticoids strongly inhibit the glycolytic shift induced by LPS

Seahorse extracellular flux analysis of human monocyte-derived macrophages treated with LPS (10ng/ml) +/- Dex (100nM) for 24h; **A)** Representative Seahorse trace showing real-time ECAR from combined Mito+Glyco stress test (mean+SD of technical replicates); **B)** Glycolytic parameters calculated as described in methods; n=4-6; One-way ANOVA with Tukey's correction for multiple comparisons; Data presented as mean +SEM; **C)** Glyco Stress test run with initial injection of Rot+AntA to control for mitochondrial acidification; n=1 (mean+SD of technical replicates).
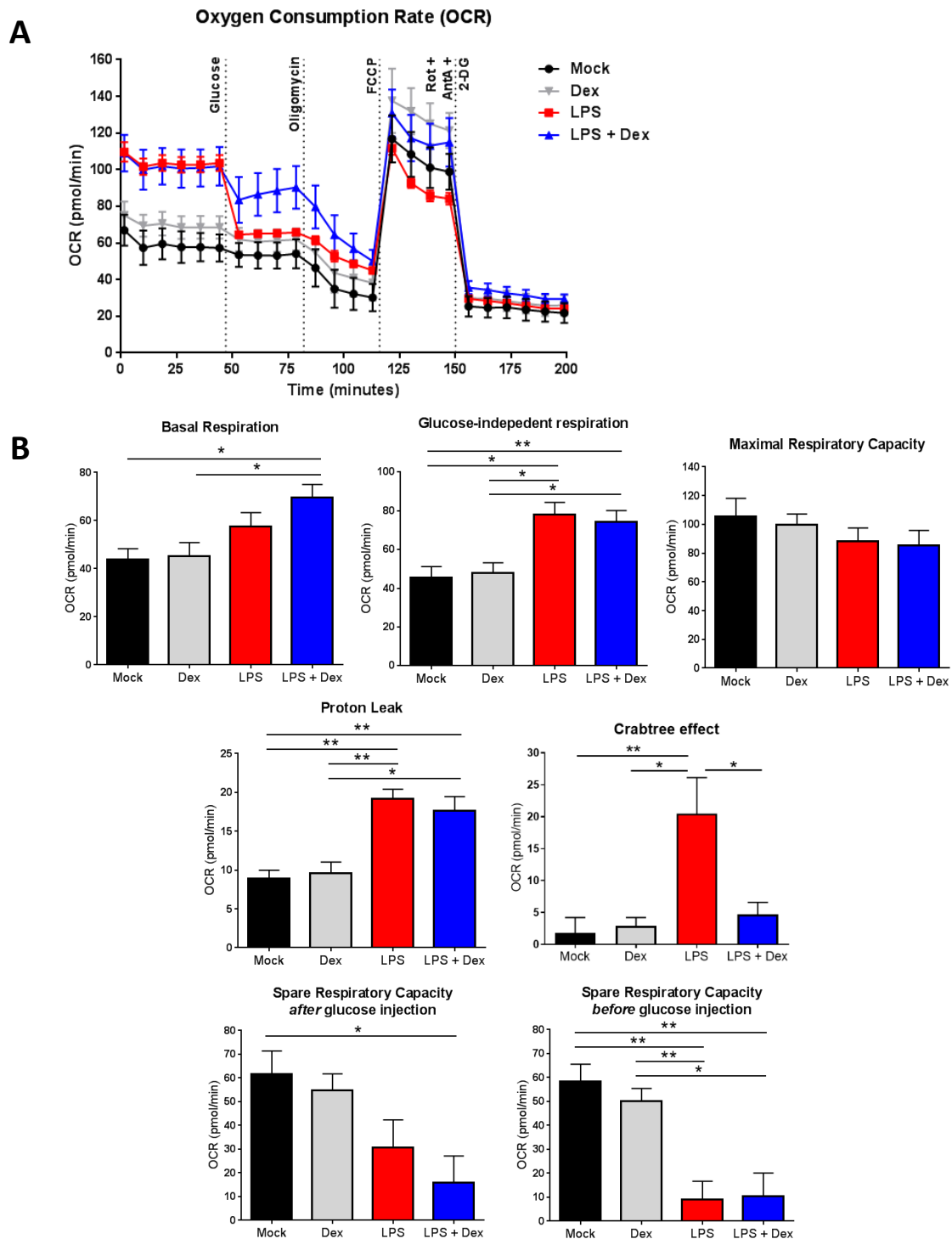
Figure 5.5) Glucocorticoids oppose the Crabtree effect - high oxygen consumption is maintained in the presence of glucose

Seahorse extracellular flux analysis of human monocyte-derived macrophages treated with LPS (10ng/ml) +/- Dex (100nM) for 24h; **A)** Representative Seahorse trace showing real-time OCR from combined Mito+Glyco stress test (mean+SD of technical replicates); **B)** Respiration parameters calculated as described in methods; n=4-6; One-way ANOVA with Tukey's correction for multiple comparisons; Data presented as mean +SEM.

The results discussed above demonstrate that there is strong cross-talk between glycolysis and oxidative respiration in different treatment conditions in human macrophages. In order to confirm that these responses reflect changes in the source of ATP production, I studied the same set of conditions using the Seahorse ATP rate assay. This assay allows calculation of ATP production rates distinctly from glycolytic and mitochondrial origins (*discussed in Section 2.19*). **Figure 5.6A** plots glycolytic vs. mitochondrial ATP production rate, and clearly shows the shifts induced by LPS and dexamethasone. The results from this assay mirrored those from the Mito+Glyco stress test, showing an LPS-induced increase in glycolytic ATP production, which was almost completely abolished by co-treatment with dexamethasone; and combined LPS+Dex treatment significantly enhanced mitochondrial ATP production (**Figure 5.6B**). As a result of these reciprocal changes there was no significant difference in total ATP production in the absence or presence of GC during LPS treatment, despite significantly greater production compared with unstimulated cells. This suggests that the GC-induced changes in oxygen consumption are driven by a requirement to overcome the ATP deficit caused by downregulation of glycolysis.

Interestingly, my results show a much higher rate of ATP production from the mitochondria than from glycolysis, even in the LPS stimulated condition. This reflects the much greater efficiency of ATP generation by oxidative phosphorylation (36 molecules per glucose compared with 2 for glycolysis), and demonstrates the continued requirement for mitochondrial function in these cells.
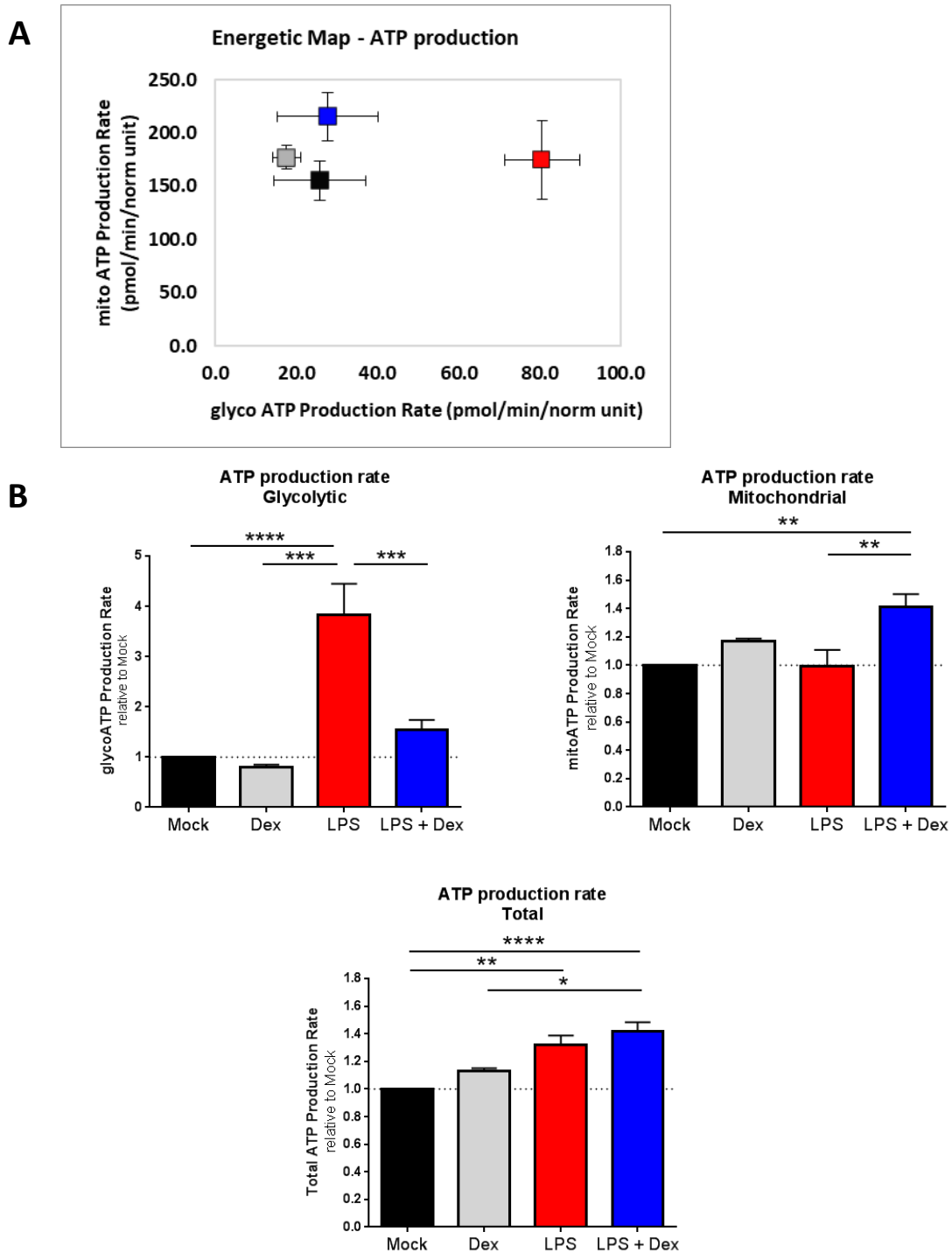
Figure 5.6) Glucocorticoids alter macrophage ATP production
ATP production rates measured by Seahorse ATP rate assay of human monocyte-derived macrophages treated with LPS (10ng/ml) +/- Dex (100nM) for 24h; **A)** Representative energetic map showing glycolytic and mitochondrial ATP production rates (mean+SD of technical replicates); **B)** ATP production rate calculated using Seahorse ATP assay report generator, relative to mock treated control. Normalised to calcein viability assay; n=7; One-way ANOVA with Tukey's correction for multiple comparisons; Data presented as mean +SEM.

5.4 Glucocorticoids decrease expression of HIF-1α and key genes controlling glycolysis

I next wanted to investigate the mechanisms by which GCs inhibit glycolytic metabolism in macrophages. HIF-1α is a key driver of glycolytic metabolism required for the adaptation to hypoxia (403). LPS treatment induces a state of "pseudohypoxia" in macrophages, in which HIF-1α is stabilised in the presence of oxygen (207, 208). Stabilisation of HIF-1α has been shown to be vital for many aspects of pro-inflammatory macrophage function, and drives expression of both inflammatory mediators and glycolytic genes (208, 210). As discussed in Section 5.1, GCs have been shown to impact HIF-1α signalling in several cell types, although the reported outcomes differ between studies (385, 391, 392). I therefore examined the expression of the regulatory HIF-1α subunit in response to LPS and Dex in human MoDMs. *HIF1A* mRNA expression was induced by LPS, and while a small downregulation was seen upon addition of GC, this did not reach significance (**Figure 5.7A**). Inhibition of LPS-induced expression by Dex was seen in 2 out of the 3 donors tested, therefore additional replicates are needed to overcome the variability in primary human samples and reach a conclusive result. Surprisingly, Dex treatment alone led to a significant decrease in *HIF1A* mRNA expression relative to unstimulated (Mock) cells, despite the protein not being detected in these conditions. This suggests that pre-treatment of cells with Dex prior to inflammatory challenge could impart a state of reduced responsiveness through downregulation of *HIF1A* gene expression.
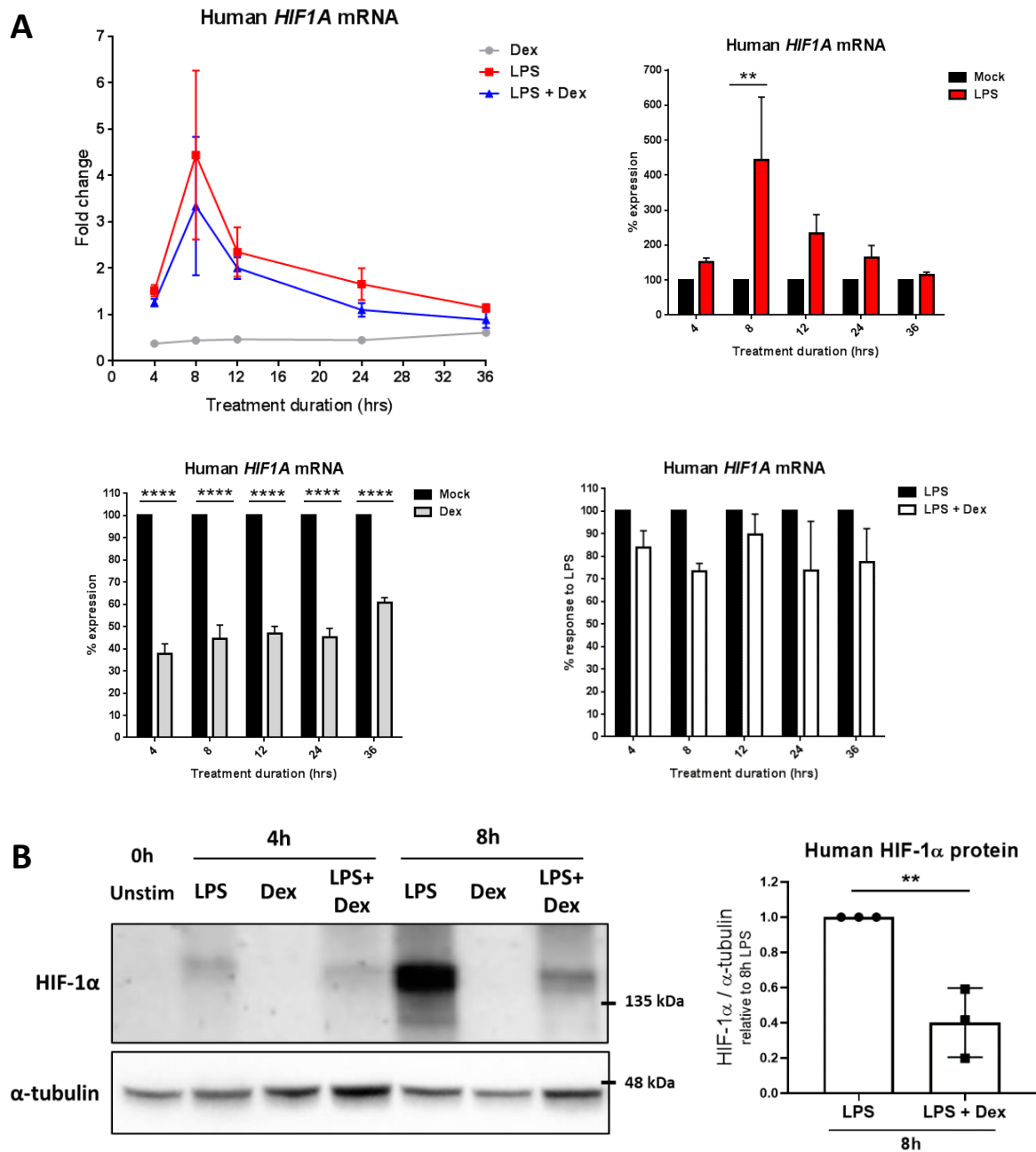
Figure 5.7) Regulation of HIF-1α by glucocorticoids
Human monocyte-derived macrophages were treated with LPS (10ng/ml) +/- Dex (100nM) for the indicated times. **A)** Mature *HIF1A* mRNA was measured by RT-qPCR and expressed as fold change (2^-ΔΔCt) normalised to UBC, relative to time-matched mock treated control; also as % expression relative to time-matched Mock or LPS treated samples; n=3; Two-way ANOVA with Sidak correction for multiple comparisons; Data presented as mean +/-SEM. **B)** HIF-1α protein detected by Western blot; quantification by densitometry of 8h LPS+/-Dex treatment, normalised to α-tubulin, relative to LPS treated only; representative blot of n=3; Unpaired, two-tailed t test; Data presented as mean +/-SD.
Western blot performed by Kalbinder Daley

Study of HIF-1α protein expression is more informative than looking at mRNA levels, as hypoxia and inflammatory stimuli inhibit protein degradation (208). HIF-1α protein was detectable after 4-8h LPS treatment in my experiments (**Figure 5.7B** & **Figure 5.8**). This protein accumulation was significantly reduced in the presence of dexamethasone, although the degree of inhibition was variable between donors tested. These results indicate that a reduction in HIF-mediated transactivation may be responsible for the inhibition of glycolytic flux caused by GC. Further study is required to confirm this.

The most frequently cited inflammatory target of HIF-1α is interleukin-1β (IL-1β), which is produced via a two-step process involving caspase-1 activation by the NLRP3 inflammasome (404). The gene for IL-1β is directly targeted by HIF-1α, inducing expression of this cytokine upon inflammatory stimulation (191), and IL-1β expression has previously been shown to be inhibited by GCs (72, 74, 385, 405). **Figure 5.8** shows the expression of the uncleaved form of IL-1β (pro-IL-1β) in LPS+/-Dex-treated MoDMs. Pro-IL-1β was downregulated by Dex in two out of the three Western blots that I performed, therefore this also requires further repetition. HIF-1α expression in one donor is displayed to demonstrate the relative timing of the expression of these proteins in these experiments, which shall be discussed in Section 5.7.
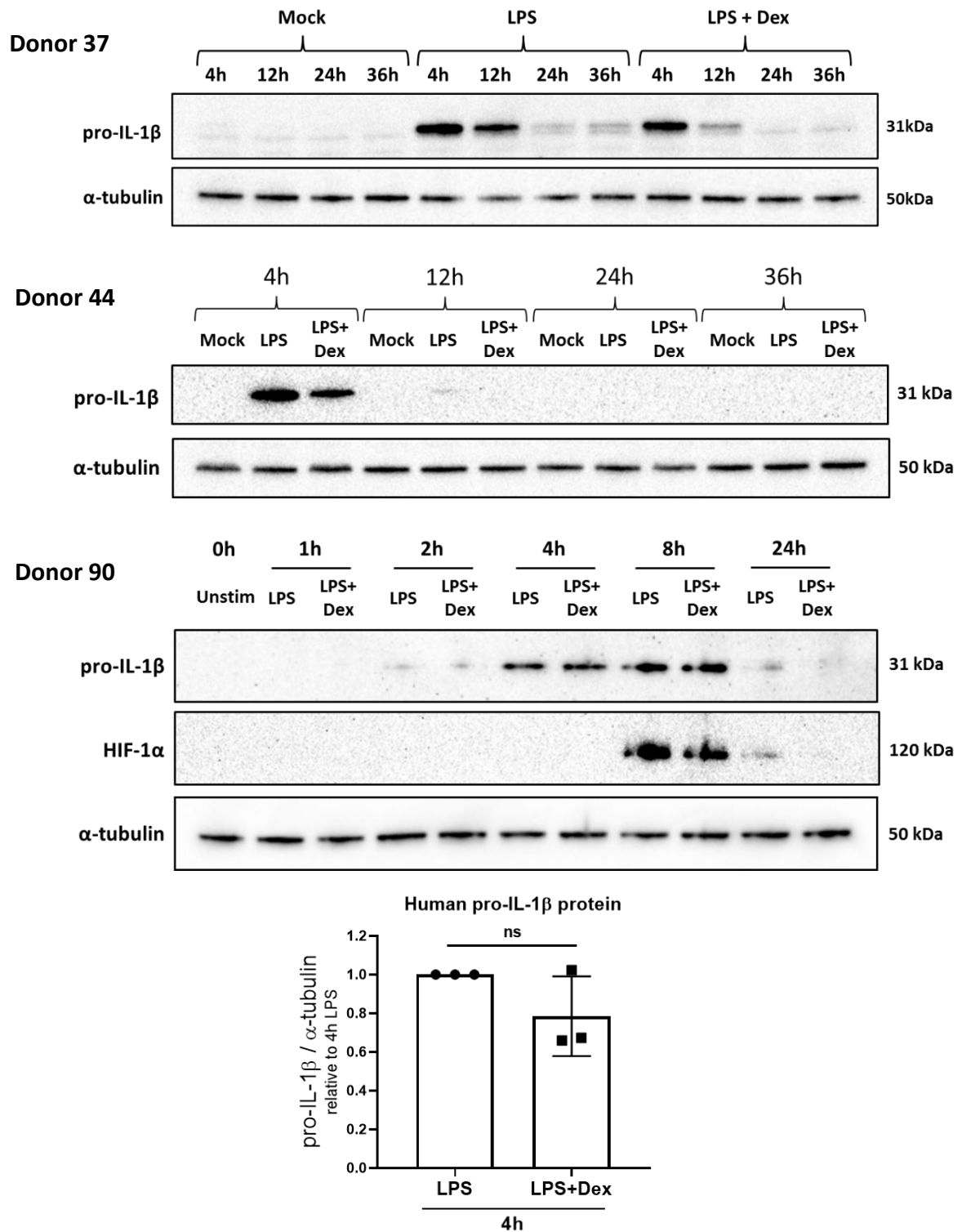
Figure 5.8) Regulation of pro-IL-1β by glucocorticoids

Human monocyte-derived macrophages were stimulated with LPS (10ng/ml) +/- Dex (100nM) for the indicated times. Pro-IL-1β protein (uncleaved) was detected by Western blot. Three blots from separate donors shown to demonstrate different responses of pro-IL-1β to Dex. Quantification by densitometry; two-tailed t test; Data presented as mean +/-SD.

HIF-1α regulates the expression of multiple glycolysis-associated genes, including integral pathway enzymes such as *HK2*, *PFK-1* and enolase, as well as flux-controlling genes such as *SLC2A1* (GLUT1), *PFKFB3*, and *PDK1* (208, 403). I wanted to examine whether these genes show GC sensitivity in human macrophages, which could explain the strong inhibition of glycolytic flux that I observed. Based on the study by Tanner *et al* (*discussed in Section 1.5*), I studied the expression of genes described to control important rate-limiting steps in the glycolytic pathway, which are also HIF-1α targets (**Figure 5.9**) (159). As expected, LPS induced expression of GLUT1, *HK2*, and *PFKFB3* to varying degrees in MoDMs. GC addition significantly inhibited LPS-induced expression of each of these genes at several time points. The most striking response was the complete inhibition of GLUT1 mRNA induction. It would also be pertinent to measure the protein expression of these genes, as mRNA levels don't always reflect protein expression. GLUT1 is also subject to additional regulation by trafficking of the receptor between intracellular vesicles and the plasma membrane, so surface expression would also be interesting to examine (244). Glucose import can also be measured using a fluorescent glucose analogue, which could give a functional readout of GLUT1 expression changes.
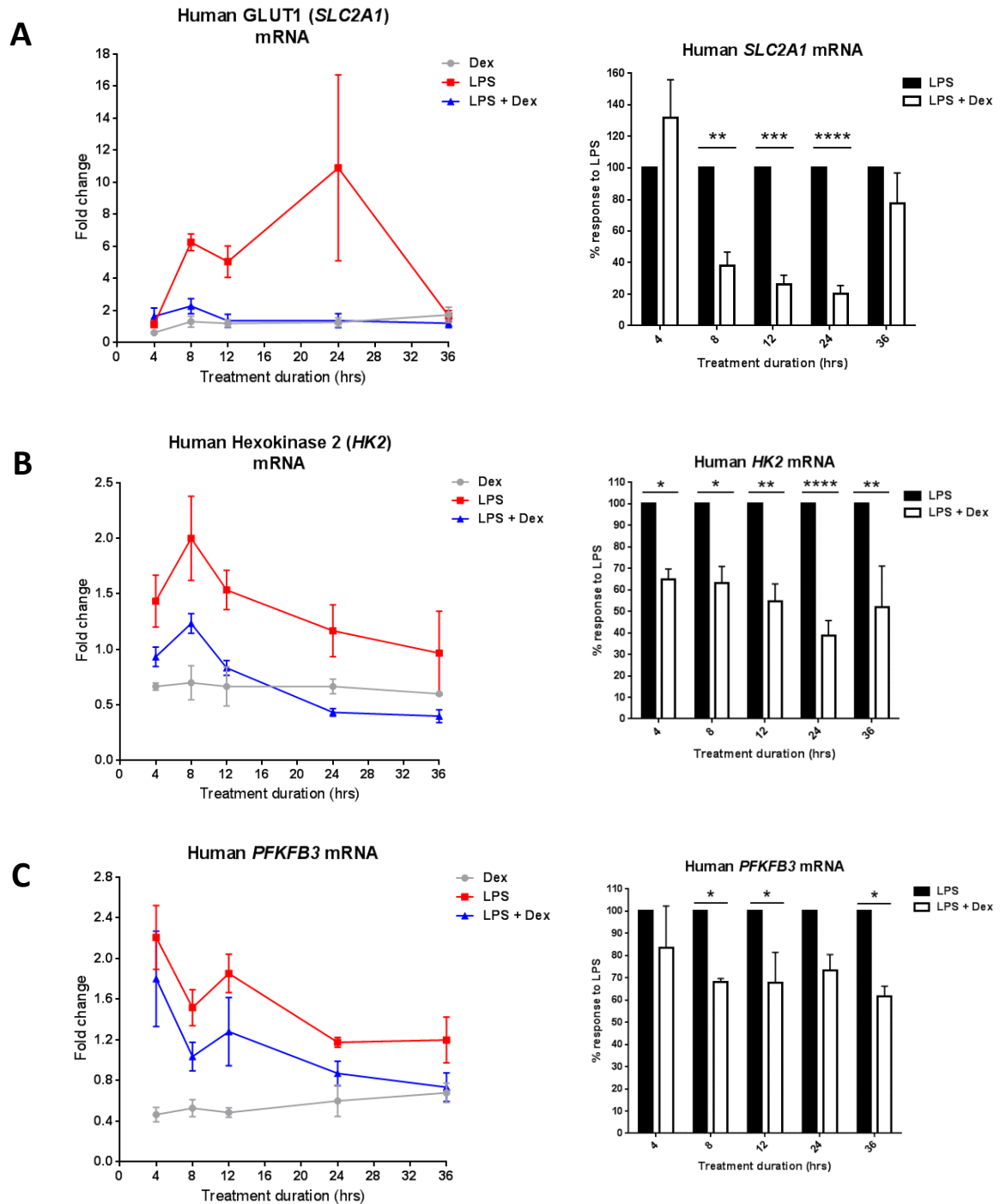
Figure 5.9) Glucocorticoids inhibit expression of key glycolysis rate limiting genes
Human monocyte-derived macrophages were treated with LPS (10ng/ml) +/- Dex (100nM) for the indicated times and harvested for RNA. **A)** GLUT1 (*SLC2A1*); **B)** *HK2* and **C)** *PFKFB3* mature mRNA were measured by RT-qPCR and expressed as fold change (2^-ΔΔCt) normalised to UBC, relative to 4h mock treated control; also as % response to LPS at each time point to show the effect of Dex; **A)** n=4 **B&C)** n=3; Two-way ANOVA with Sidak correction for multiple comparisons; Data presented as mean +/-SEM.
Some replicates performed by Samuel Peters (MSc student) under my supervision

5.5 Altered metabolite profile in response to glucocorticoids

In order to gain a more detailed insight into the effect of glucocorticoids on cellular metabolic pathways, I collected conditioned media samples from 24h-stimulated human MoDMs for analysis by gas chromatography-mass spectrometry (GC-MS). **Figure 5.10** shows the changes in response to LPS and dexamethasone of some of the major metabolites that I have discussed with relation to macrophage metabolic regulation. It should be noted that these data are limited by the lack of matching intracellular metabolite levels, and the inference of intracellular metabolic pathway activity from these data should be approached cautiously.

The addition of GC led to a significant reduction in the levels of extracellular lactate induced by LPS (**Figure 5.10**). This is consistent with the Seahorse results that showed an increase in ECAR with LPS, which was reduced by co-treatment with Dex (**Figure 5.4**), as lactate is considered to be responsible for the majority of the acidification that is detected in the Seahorse. The GC-MS results also show a significant reduction in extracellular pyruvate levels in the LPS+Dex condition compared with LPS alone. Pyruvate can be exported from the cell by monocarboxylate transporters in a similar way to lactate (406). The effect of Dex on extracellular pyruvate levels is complex, however, as addition of the GC is inhibitory in the presence of LPS, but stimulatory compared with the Mock treated condition. The release of pyruvate is dependent upon multiple factors, including the rates of its synthesis from glycolysis, its utilisation to fuel the TCA cycle and its conversion to lactate, as well as the expression of appropriate cell surface transporters. It is likely that LPS and GCs impact several of these factors, culminating in the overall effects shown in Figures 5.10 and 5.11.

The lactate/pyruvate ratio can be used as a readout of cellular redox status, as the drive to convert pyruvate to lactate is the requirement for regeneration of oxidised NAD+ from NADH by lactate dehydrogenase (167). As I only have extracellular metabolite readings, the ratios from my data will only give an indication of redox potential. A more direct way to analyse redox status would be to measure cellular NAD+ and NADH levels. **Figure 5.11A** shows the lactate/pyruvate ratios for each of the four conditions, demonstrating that Dex alone and LPS alone both led to a significant decrease in lactate/pyruvate ratio compared with unstimulated, thus indicating an increase in pyruvate export from the cell. Surprisingly, the effect of Dex was greater than that of LPS, with the GC resulting in roughly a halving of the ratio value compared with the unstimulated condition. As the absolute levels of extracellular lactate were much greater than those of pyruvate under all conditions, the sum of both lactate and pyruvate mirrors the responses of lactate alone (**Figure 5.11A**). As there is no significant different in lactate+pyruvate between mock treated and Dex alone conditions, this suggests that the increased pyruvate export is related to redox control rather than specific diversion of glucose-derived carbon from the TCA cycle. A better way to study this would be by isotope tracing mass spectrometry utilising ^{13}C-labelled glucose. The potential implications of these results shall be discussed further in Section 5.7.

Pyruvate and lactate showed the most pronounced changes in response to the different treatment conditions out of all of the metabolites tested, which may be a reflection of the importance of cellular export of these metabolites, as well as the known regulation of MCT4 and other lactate transporters under inflammatory conditions (407, 408).

The majority of the TCA intermediates were very slightly decreased by GC treatment, which nevertheless reached statistical significance with paired analysis in some cases (**Figure

5.10). It is possible that the intracellular metabolite levels could show more robust changes, as extracellular levels are subject to an additional level of control through the regulation of export or import. The exception to the downregulation is α-ketoglutarate, which was slightly elevated in the presence of Dex, although this does not reach significance. α-ketoglutarate can be generated from the TCA cycle via citrate and isocitrate, or through glutaminolysis, the latter having been shown to be important for fuelling the TCA cycle in both M1 and M2 macrophages (191, 240). The effect of GC treatment on glutamine levels showed great variability in this data set, therefore it cannot reasonably be concluded from what source the increased α-ketoglutarate was derived. The ratio of α-ketoglutarate/succinate has been shown to influence macrophage polarisation, and **Figure 5.11B** shows a decrease in this ratio upon LPS treatment, as has previously been reported (240). Co-treatment with dexamethasone was able to revert this ratio back to comparable with mock treated cells.

A notable result from these data is the observation that LPS led to a significant reduction in citrate levels compared with unstimulated cells, in contrast to the strong LPS-induced accumulation of citrate that has been reported in the literature (217). This was further decreased by co-treatment with Dex (**Figure 5.10**). It is possible that this is a result of measuring extracellular rather than intracellular metabolites. Alternatively, this could be another feature of human macrophages in comparison to mouse BMDMs. A recent publication reported that the accumulation of citrate was dependent upon *Nos2* expression, which the authors explained by the NO-mediated inhibition of mitochondrial aconitase leading to reduced citrate metabolism (374). Interestingly, two groups have reported significantly reduced citrate levels in the synovial fluid of rheumatoid arthritis patients compared with either osteoarthritis patients or healthy controls (409, 410).
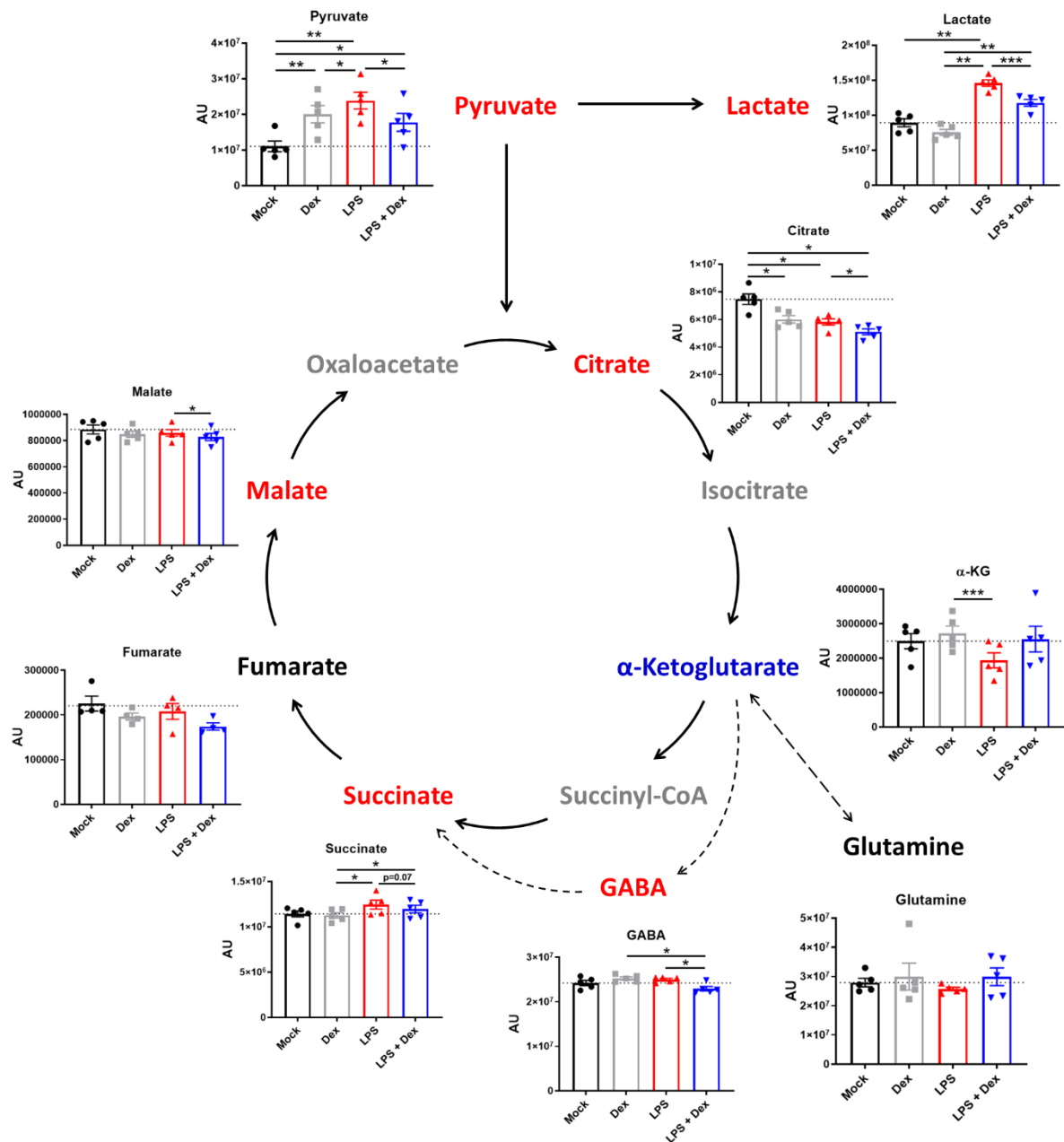
Figure 5.10) Effect of glucocorticoids on extracellular TCA cycle and related metabolites
GC-MS operation and primary data analysis performed by Alpesh Thakker
Human monocyte-derived macrophages were treated with LPS (10ng/ml) +/- Dex (100nM) for
24h. Metabolites were measured by GC-MS from conditioned media samples; raw data were
normalised to glutaric acid internal standard and displayed as ion intensity (arbitrary units); n=5
(n=4 for fumarate); repeated measures one-way ANOVA with Tukey's correction for multiple
comparison; Data presented as mean +/-SD plus individual donor values.
Metabolites that show higher levels in LPS alone conditions are displayed in red, metabolites that
show higher levels in LPS+Dex conditions are displayed in blue.
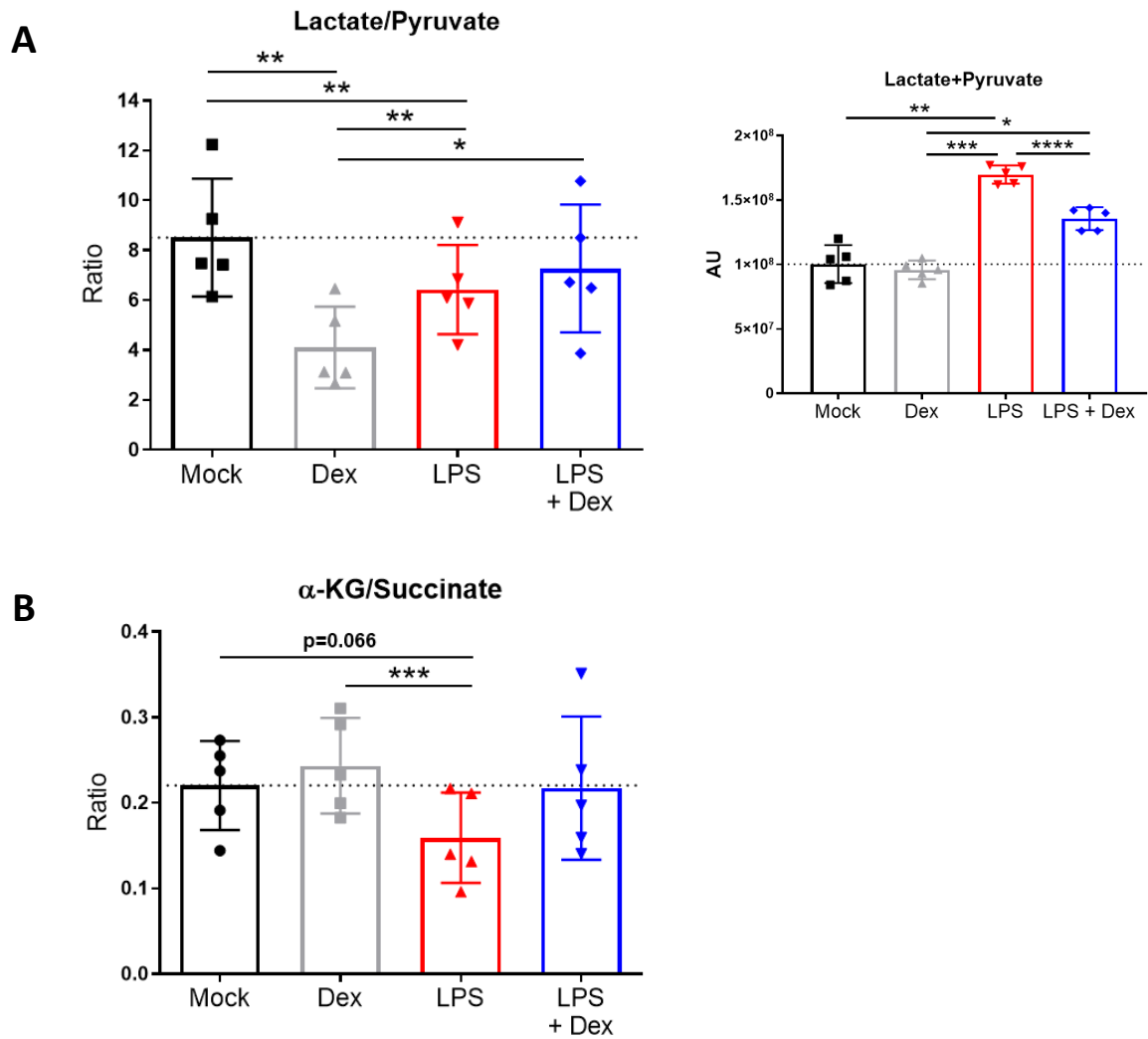
Figure 5.11) LPS and glucocorticoids alter extracellular metabolite ratios
GC-MS operation and primary data analysis performed by Alpesh Thakker
Data from Figure 5.10 were analysed for lactate/pyruvate and α-ketoglurate/succinate ratios, as well as the sum of pyruvate and lactate. Metabolites were measured by GC-MS from conditioned media samples; raw data were normalised to glutaric acid internal standard; n=5; Repeated measures one-way ANOVA with Tukey's correction for multiple comparisons; Data presented as mean +/-SD plus individual donor values.

5.6 Mitochondrial responses to LPS and glucocorticoids in human macrophages

Mitochondria undergo dynamic alterations in response to environmental cues, including shifting the balance of fusion and fission; turnover by mitophagy; and ROS production, all of which can be altered in immune cells by pathogen encounter (177, 411). The mitochondrial membrane potential is the electrical gradient across the inner mitochondrial membrane, created via proton pumping by the respiratory chain complexes. This potential is affected by changes in activity of the ETC or ATP synthase, and in turn influences the production of mROS (*discussed in Section 1.7*). Low membrane potential can be indicative of defective mitochondria, which can be recycled through mitophagy (177, 244). Mitochondrial membrane potential can be measured by staining with lipophilic cationic dyes, the accumulation of which is dependent upon electrical potential (412). An elevated membrane potential is required to drive mROS production by RET (250, 251), and this has been shown to occur upon LPS treatment of BMDMs. Dissipation of this potential led to decreased ROS generation and consequently reduced production of IL-1β (190, 204). However, 24h LPS treatment of mouse bone marrow-derived DCs was shown to decrease membrane potential, associated with NO-mediated inhibition of ETC activity (396). It is likely that membrane potential changes over time after macrophage stimulation, in part through the dynamics of NO and itaconate synthesis and action (225, 396). NDUFA4 is localised within the mitochondrial ETC, and therefore has the potential to influence mitochondrial function and membrane potential. I began by establishing the effects of LPS and Dex on this parameter in human macrophages.

I used MitoTracker Red to study mitochondrial membrane potential by flow cytometry, as well as MitoTracker Green, which stains mitochondria independently of membrane potential and can be used to assess mitochondrial mass and to normalise MitoTracker Red results (**Figure 5.12**). Despite the reported changes in mouse cells, I saw no change in mitochondrial membrane potential after 24h LPS stimulation in human MoDMs. This perhaps wasn't surprising based on my previous observations that human macrophages do not reduce mitochondrial ATP production in response to LPS, therefore the proton gradient is continually dissipated through complex V (**Figure 5.2**). It is also possible that flow cytometry isn't the most appropriate platform to analyse membrane potential by MitoTracker Red staining. It has been reported that a loss of membrane potential results in cytoplasmic staining by this dye, which would not be distinguished from mitochondrial staining by flow cytometry (413). The authors also noted that MitoTracker Red showed some binding to mitochondrial thiol groups, which is the mechanism of MitoTracker Green staining (413). An alternative membrane-sensitive mitochondrial dye, such as TMRE, could be used to validate my results. The only significant changes that I saw in these experiments were a decrease in total mitochondrial mass and an increase in membrane potential per mitochondrial mass unit after treatment with dexamethasone alone (**Figure 5.12**). While these changes were small, they were reproducible across all donors tested.
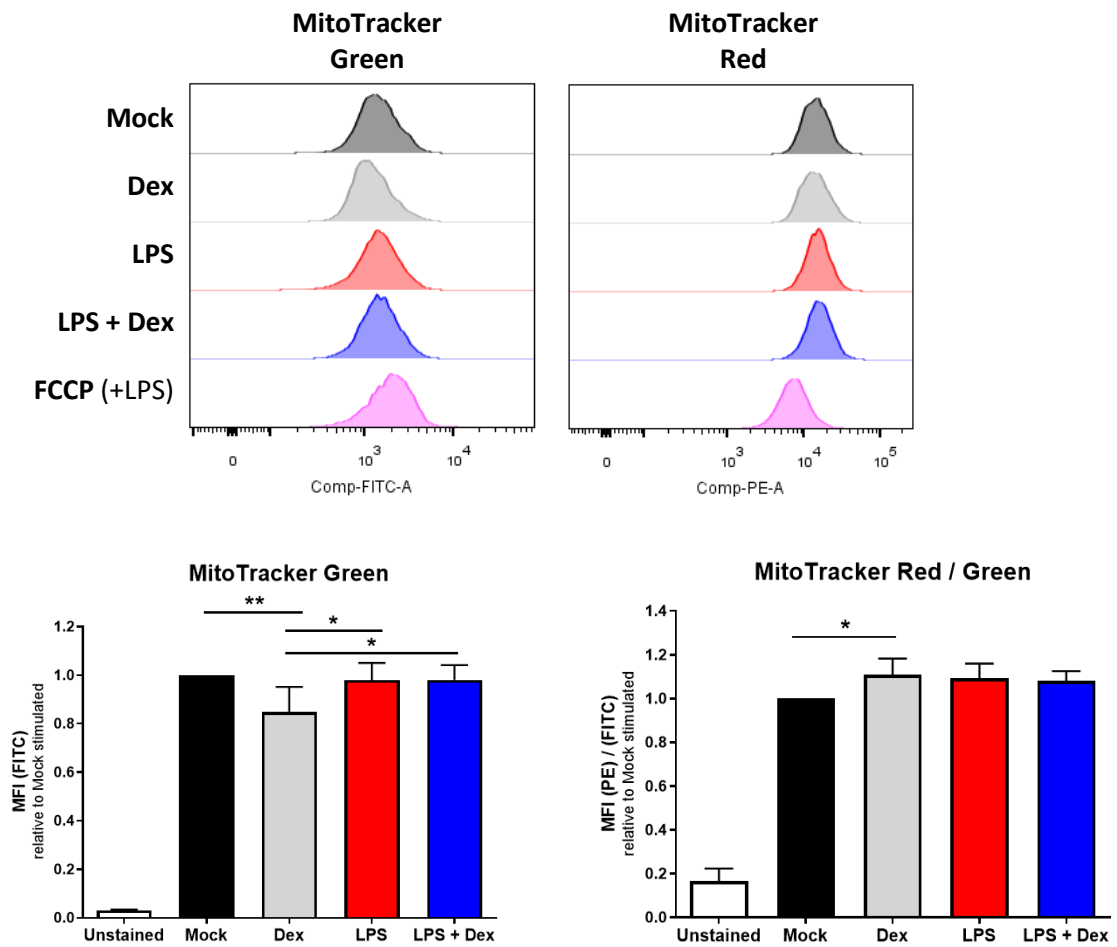
Figure 5.12) Effect of LPS and Dex on mitochondrial mass and membrane potential in human macrophages

Human monocyte-derived macrophages were treated with LPS (10ng/ml) and/or Dex (100nM) for 24h before staining with MitoTracker Green (150nM) and MitoTracker Red CMXRos (200nM) and analysing by flow cytometry. Doublets and dead cells were gated out. FCCP was used as a positive control for membrane depolarisation; median fluorescence intensity was calculated and MitoTracker Red results normalised to MitoTracker Green, displayed relative to mock treated control; representative plot and quantification of n=5; One-way ANOVA with Tukey's correction for multiple comparisons; Data presented as mean +SD.

Mitochondrial ROS production is described as an important part of the macrophage inflammatory response; for example mROS contribute to the stabilisation of HIF-1α and also regulate MAPK activity, affecting production of cytokines including IL-1β and IL-6 (190). NDUFA4 may also play a role in mROS generation, as shall be discussed in Chapter 6. I therefore wanted to examine mROS production in human macrophages in response to pro- and anti-inflammatory stimuli. As shown in **Figure 5.13**, LPS treatment led to very little or no staining by the mitochondrial-specific ROS dye MitoSOX. mROS production was detected using mitochondrial inhibitors as positive controls - antimycin A, which results in Q cycling at CIII, and the CI inhibitor rotenone (**Figure 5.13B**). RPMI medium, used for leukocyte cell culture, contains glutathione - an anti-oxidant that is also produced by cells to protect against oxidative stress. I confirmed that ROS neutralisation by the exogenously supplied glutathione is not responsible for the lack of mROS detection in my experiments by comparing MitoSOX staining in LPS-treated cells cultures in either RPMI or DMEM, which showed no differences (**Supplementary Figure S5**). Vijayan *et al* also reported that human macrophages do not increase mROS production in response to LPS (394). This experiment should be followed up by a side-by-side comparison of MitoSOX staining in mouse and human macrophages to ensure that the published response in mouse BMDMs can be recapitulated in our system. The results shown here suggest that unlike mouse BMDMs, human MoDMs do not engage in reverse electron transport to produce mROS in response to LPS.
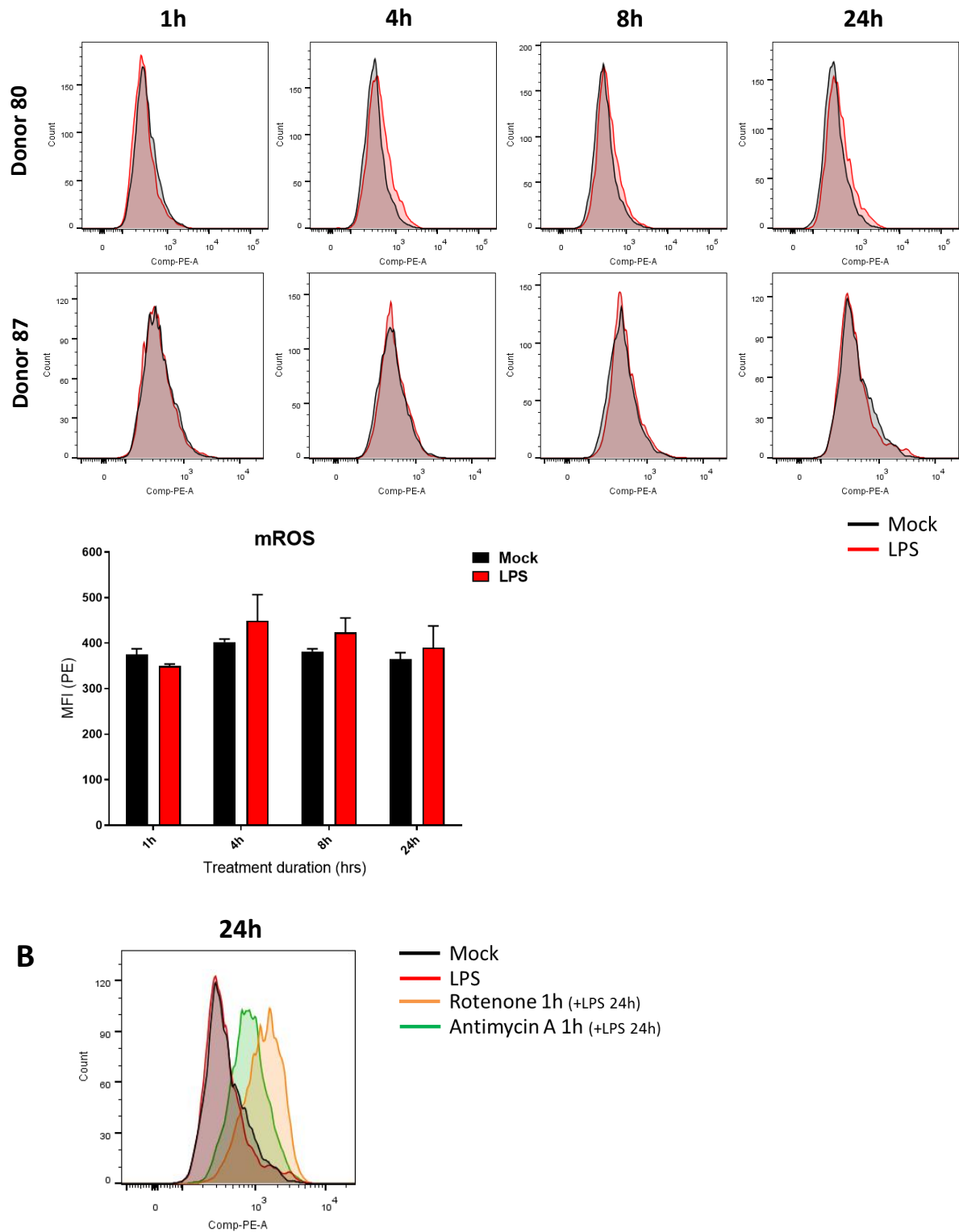
Figure 5.13) Measurement of mitochondrial ROS in human macrophages

Human monocyte-derived macrophages were Mock or LPS stimulated for the indicated times followed by staining with MitoSOX. Doublets and dead cells were gated out. **A)** n=2; Graph shows median fluorescence intensity (MFI) +SD of above plots **B)** Inhibitors added for last hour of stimulation as positive controls for mROS staining; representative plot of n=2.

5.7 Discussion

In this chapter I have begun to characterise the metabolic effects of glucocorticoids in macrophages. While there is still a lot of work to be done on this topic, I have made important findings that will inform the future direction of this work. My main findings are that GCs strongly inhibit glycolytic metabolism in human MoDMs, and are able to almost completely reverse the well-described glycolytic shift that occurs upon LPS treatment. This results in inhibition of glycolytic ATP production and increased oxidative ATP production. I hypothesise that this occurs through the inhibition of HIF-1α protein expression by GCs, resulting in decreased expression of several key glycolytic regulator genes, most notably the glucose transporter GLUT1. I have also identified a regulatory point of the TCA cycle that is potentially involved in GC action, through increased levels of α-ketoglutarate.

I have highlighted some key differences in metabolic regulation between mouse BMDMs and human MoDMs, which are two of the most widely-used *in vitro* model systems to study macrophage function.

5.7.1 Mouse vs human macrophage metabolism

Global gene expression signatures of immune cells are conserved between mouse and human, which has led to the extensive use of mouse models for the study of immune function, however it is well-established that important differences in gene regulation still exist between the two species (360, 414). The differences in metabolic regulation that I observed between mouse BMDMs and human MoDMs complicated the investigations in this chapter, as the current understanding of macrophage metabolism in the literature is predominantly based upon studies in BMDMs. These concepts may not hold true in human cells, and therefore mechanisms of pathway regulation had to be re-addressed in my cell system. The differences

between these cell types has been anecdotally or briefly touched upon in the literature (218, 234), however complete characterisation has not been undertaken. The study by Vijayan *et al* that addresses these differences was published while I was working on this project, however the authors do not report an increase in glycolysis upon LPS treatment of human macrophages, which I reproducibly show (**Figure 5.1**). I have demonstrated some of the ways in which human MoDMs differ from the dogma of macrophage metabolic regulation, including an absence of oxidative respiratory inhibition in response to LPS, as well as little/no detectable mROS generation. It is possible that additional differences exist that are yet to be characterised.

This issue is actually one of two separate parts: 1) differences between species; 2) differences between cell populations of distinct origin. The latter issue was highlighted by Artyomov *et al* (discussed in Chapter 1), who implicated differences in arginine metabolism and consequent NO production in the differential metabolic responses of mouse BMDMs and peritoneal macrophages. The authors hypothesised that this is likely a reflection of gene expression programmes conferred by the extracellular environment during development or differentiation (269).

NO is synthesised in response to inflammatory activation of mouse BMDMs and bone marrow-derived dendritic cells (BM-DCs – differentiated with GM-CSF) (234, 396). NO can inhibit the ETC at several points (259), and inhibition of NO production has been shown to restore oxidative metabolism in LPS-treated BM-DCs or LPS+IFNγ-treated BMDMs (234, 396). Our group have demonstrated that cultured human MoDMs failed to produce any detectable NO in our system, which has been widely reported elsewhere (35, 234, 360). The reasons for this discrepancy are not fully understood, however Gross *et al* showed that the promoter of the human *NOS2* gene contains highly methylated DNA and a repressive chromatin

architecture that is not relieved by *in vitro* stimulation with LPS+IFNγ (264). Thus epigenetic reprogramming by an inflammatory microenvironment may be necessary for *NOS2* transcriptional induction, such as may occur in RA patients or within TB granulomas (35, 265). Evidence that my observations result from species-specific rather than origin-specific differences is given by a study from Everts *et al*, who showed that infection-elicited monocyte-derived DCs isolated from mouse spleen produce NO and show reduced mitochondrial respiration (396); and by a study from Schroder *et al*, who showed that both bone marrow-derived and monocyte-derived macrophages from pig fail to induce *iNOS* expression in response to LPS (360). My results suggest that mitochondrial metabolism is still required in human macrophages exposed to LPS, in particular to adapt to changes in nutrient availability.

Overall, the differences in metabolic responses that I have shown complicate the use of *in vivo* models for this topic, and touch upon the broader issue that macrophages *in vivo* are likely to show different metabolic changes from those imposed by *in vitro* culture conditions, due to the complexity of *in vivo* environmental cues.

5.7.2 Macrophage metabolic regulation by glucocorticoids

My finding that GCs affect macrophage metabolism is perhaps not surprising based on their established role in systemic metabolic control, however metabolic actions of the steroids had not been extensively studied in this cell type. The inhibition of macrophage glycolysis is consistent with much of the literature surrounding the effects of GCs in other cells (79, 378, 385, 386), and my finding of GLUT1 inhibition mirrors the suppression of glucose transporter expression in pancreatic β cells (83) and skeletal muscle (85).

The precise point of inhibition within the glycolytic pathway is important with regard to the regulation of branching pathways and the disruption of inflammatory cytokine

production (discussed in Chapter 1). Inhibition of enzymes downstream of glucose 6-phosphate can result in build-up of early glycolytic intermediates and increased flux through the PPP (164, 415). The inhibition by Dex of GLUT1 and hexokinase, which control early commitment steps in the glycolytic pathway, suggest that GCs downregulate total flux through glycolysis and the PPP. This could be verified by mass spectrometric tracing analysis using ^{13}C-labelled glucose, to study the feeding of various pathways by extracellular glucose. Individual downregulation of certain enzymes could also have cellular effects independent of flux control, for example GAPDH has moonlighting activity by binding to TNFα mRNA and inhibiting its translation (416).

The regulation of HIF-1α could be an important metabolic control point for GCs due to its role in macrophage glycolytic adaptation to inflammatory signals (208). The timing of cellular events is of interest in regard to the regulation of HIF-1α and IL-1β, as pro-IL-1β expression occurred at an earlier time point than HIF-1α protein expression in my experiments (**Figure 5.8**). The *Il-1b* gene has also been shown to be targeted by NF-κB (417), and p38 MAPK signalling (74), which are both sensitive to inhibition by GCs. Interestingly, GCs have been shown to increase expression of NLRP3 mRNA and protein, thereby sensitising cells to activation of the inflammasome by damage-associated cues (418). This would potentiate release of mature IL-1β, in contrast to the reports of beneficial effects of GCs reported in models of sepsis through reduction of IL-1β protein levels (385, 405).

The glycolytic genes measured here are also known targets of HIF-1α, and the direct induction of GLUT1 by HIF-1α is plausible in these experiments due to the delayed GLUT1 kinetic profile (**Figure 5.9A**). Interestingly, an increase in glucose uptake and ECAR by macrophages has been shown to occur very rapidly in response to LPS, reportedly within the first 20mins (199). Nagy & Haschemi outline a time-resolved map of metabolic adaptation to

LPS stimulation based on the literature (199). LPS-induced HIF-1α stabilisation has been shown to rely on an initial increase in glycolytic rate and build-up of succinate (191). Therefore HIF-1α is described as contributing to an amplification loop in the later phases of adaptation, which reinforces the committed metabolic reprogramming (199). An initial rapid increase in glycolysis followed by a sustained commitment phase has also been demonstrated in activated T cells and DCs (419). It would be interesting to determine whether the early phase of increased glycolysis is sensitive to GC; as well as to establish which changes are directly caused by the decrease in HIF-1α protein levels.

The GC-MS results show that glucocorticoids alter TCA cycle dynamics in addition to Warburg-type glycolysis. α-ketoglutarate (α-KG) alters epigenetic reprogramming during macrophage polarisation, and promotes oxidative respiration through fatty acid oxidation. This occurs via co-stimulation by α-KG of Jmjd3 demethylase, which is required for removal of repressive H3K27me3 histone modifications from M2-associated genes in response to IL-4. As succinate is an inhibitor of this demethylase, the α-KG/succinate ratio determines enzyme activity (240). The same is also true for prolyl hydroxylase (PHD) enzymes, which require α-KG as substrate and are inhibited by the reaction product succinate. Thus a high α-KG/succinate ratio can also modulate inflammatory gene expression by promoting hydroxylation of HIF-1α and the NF-κB activator IKKβ. Glutamine-derived α-KG has also been shown to be important in the induction of endotoxin tolerance following LPS stimulation (240). The changes in α-KG/succinate ratio caused by GC treatment can therefore modulate macrophage activity through multiple pathways. The rate of conversion of citrate to α-KG could also impact upon the production of itaconate, and it would be interesting to measure intracellular levels of this metabolite in response to GCs, due to the reported central role for itaconate in macrophage metabolic remodelling (221).

The GC-MS data also highlighted a potential involvement of redox signalling in the action of dexamethasone, indicated by a decrease in lactate/pyruvate ratio. An increase in pyruvate export in response to Dex treatment alone suggests that NAD+ is not limiting in this condition, which could reflect a decreased requirement for NAD+, or increased regeneration by other mechanisms. Alternatively, this could indicate that restriction of NAD+ regeneration is a mechanism of anti-inflammatory function by glucocorticoids, as Haschemi *et al* previously demonstrated that inhibition of pyruvate conversion to lactate led to reduced production of inflammatory cytokines (200). This warrants further investigation. As well as being necessary for continued glycolytic flux, NAD+ is used as a cofactor for histone deacetylases, which have been shown to enhance fatty acid oxidation and inhibit aerobic glycolysis (420). The availability of reducing equivalents in the form of NADH and NADPH are also important for immune signalling in the form of ROS, for example for the production of superoxide and the maintenance of reduced glutathione levels. The reduction in lactate/pyruvate ratio and decreased NAD+ regeneration by Dex or LPS therefore has the potential to impact, or be impacted by, the activity of these processes.

The only changes I saw in mitochondrial parameters under LPS and GC stimulation were a small but significant decrease in mitochondrial mass and concurrent increase in membrane potential in Dex-only treated cells (**Figure 5.12**). Dyczynski *et al* reported that GC treatment of B-ALL cells caused an increase in autophagy (376), and Ip *et al* showed that IL-10 induced the removal of defective mitochondria through increased mitophagy. Loss of IL-10 feedback signalling resulted in accumulation of mitochondria with a low membrane potential during LPS treatment in this study (244). These reports, along with my data, suggest that GCs may function in a similar way to IL-10 with respect to the induction of mitophagy, which may be necessary to maintain a healthy mitochondrial pool for efficient ATP production. However,

this effect was not seen in the LPS+Dex treatment condition, which displayed the highest rate of mitochondrial ATP production (**Figure 5.6**). The mechanism by which IL-10 was shown to induce autophagy was through inhibition of mTOR activity (244). Since GCs have a major role in regulating systemic nutrient homeostasis, it is plausible that they also interact with cellular nutrient sensing machinery such as mTOR complexes. These speculations require further investigation to verify.

Increased mitochondrial ROS production in response to LPS has been reported in mouse BMDMs due to repurposing of the ETC (190), however I did not detect reproducible increases in mROS in my experiments using human MoDMs. Alternative sources of ROS generation include the NADPH oxidase enzyme family, of which the NOX2 isoform is the major ROS-producer in phagocytes (245). This enzyme is also subject to metabolic regulation due to the requirement for NADPH, and cytosol-generated ROS can influence cellular signalling pathways, resulting in the regulation of cytokine production, phagocytosis and apoptotic cell clearance (245). Therefore this system could also be evaluated for its interaction with glucocorticoid signalling. Other methods of mROS measurement could also be used to validate my findings, for example the use of genetically-encoded H_2O_2 sensors targeted to the mitochondria (421).

It has been known for decades that macrophages increase glucose metabolism upon activation, but only in recent years have the precise implications of these metabolic pathways begun to be unravelled. Glycolysis has been shown to be crucial for many aspects of macrophage inflammatory function, therefore the inhibition of glycolytic metabolism by glucocorticoids, which mediate broad repression of inflammatory responses, has the potential to underpin some of the anti-inflammatory effects of these hormones. Therefore my findings may have important implications for our understanding of glucocorticoid action.

Chapter 6) The role of NDUFA4 in macrophage metabolism and inflammatory response

6.1 Introduction

Having established some of the effects of LPS and glucocorticoids on human macrophage metabolism, I next wished to determine how NDUFA4 regulation contributes to these effects. Due to the localisation of NDUFA4 within the ETC, I will begin with a brief introduction surrounding the current literature on ETC regulation in macrophages, followed by discussion of a potential link between NDUFA4 and a related protein.

6.1.1 The ETC and the macrophage inflammatory response

It is becoming increasing clear that complex II (succinate dehydrogenase) plays an important role in the macrophage inflammatory response, and its position in both the TCA cycle and ETC give it a central regulatory function (411). This complex shows a transient increase in activity upon LPS stimulation, leading to elevated membrane potential and mROS production, and its inhibition was shown to have anti-inflammatory effects (190, 204, 411). The LPS-induced production of itaconate is also an important regulatory pathway for determining macrophage activity, and this metabolite is an endogenous inhibitor of CII that facilitates succinate accumulation (221, 225).

Complex I has also been described as important for immune cell mROS production through reverse electron transport (411). The inhibition of CI by the diabetic drug metformin was found to inhibit mROS production, and led to reduced IL-1β and enhanced IL-10 production in BMDMs (422). Treatment of diabetic patients with metformin also resulted in reduced *ex vivo* IL-1β production from the patient MoDMs (423). CI activity has also been

shown to be inhibited by LPS+IFN-γ treatment of BMDMs due to dramatic downregulation of several CI subunits, an effect largely dependent upon NO production in these cells (209). Deletion of the CI subunit Ndufs4, which is essential for complex assembly, was shown to result in systemic inflammation associated with monocyte/macrophage activation. However it is unclear if this was a specific effect of CI deficiency or due to a general loss of mitochondrial oxidative capacity (424). It is likely that the duration of stimulation and production of other signalling mediators such as NO, as well as the precise point of inhibition within CI, dictate the outcome in relation to mROS production.

A more detailed analysis of ETC regulation in macrophages came from Garaude *et al*, who examined the acute effects of *E. coli* on the respiratory chain of BMDMs. The authors reported a decrease in the abundance of CI-containing supercomplexes (I+III$_2$+IV and I+III$_2$) within two hours of infection. This was associated with decreased CI activity and increased CII activity, a response that was dependent upon phagosomal ROS production through NADPH oxidase, and activation of a kinase that targets the SDHA subunit of CII (411, 425). These ETC adaptations facilitated the anti-microbial response and bacterial clearance. Strikingly, the authors found that these adaptations were not recapitulated with heat-killed *E. coli*, and that the detection of bacterial RNA was necessary for the induction of CII activity (425).

6.1.2 NDUFA4 and NDUFA4L2

As discussed in Chapter 4, studies surrounding the function of NDUFA4 are scarce, but the literature has progressed in recent years to establish that this protein resides in ETC CIV and contributes to the activity of this complex in muscle tissue and cell lines (280, 342, 345). More clues as to the function of NDUFA4 can be gained by looking at studies of the related protein NDUFA4L2, which shares 61.7% protein sequence identity with NDUFA4 (**see Figure**

7.2). A dynamic and reciprocal regulation has been reported between these two proteins. NDUFA4L2 is strongly induced by hypoxia at the level of both mRNA and protein in a variety of human and rodent cell types, a response shown to be mediated by HIF-1α (359, 426, 427). Conversely, NDUFA4 protein (but not mRNA) is downregulated by hypoxia in HeLa cells and MEFs, independently of NDUFA4L2 upregulation (359). Deletion of the *Hif1a* gene also restored the expression of NDUFA4 in white adipose tissue of ageing mice, further demonstrating a role for HIF-1α in NDUFA4 regulation (428). It has therefore been proposed that hypoxia induces a switch between these two related proteins - a phenomenon that also occurs between isoforms of other CIV subunits (366).

Tello *et al* found that upregulation of NDUFA4L2 resulted in reduced oxygen consumption through inhibition of CI activity, with the outcome of preventing mitochondrial membrane hyperpolarisation and mROS production in conditions of hypoxia (359). The role that NDUFA4 plays in these responses is unclear, since *Ndufa4l2* KO MEFs showed no loss of CI activity during hypoxia, despite NDUFA4 protein still being downregulated in these cells (359).

NDUFA4L2 expression is protective against oxidative stress in cancer, thereby aiding cancer cell survival, including in non-small cell lung cancer (429); clear cell renal cell carcinoma (ccRCC) (427, 430, 431); colorectal cancer (432); and hepatocellular carcinoma (426). *NDUFA4L2* is one of the most highly differentially expressed genes between ccRCC and normal kidney samples (427). Expression of NDUFA4 has also been measured in some of these tissues, and was found to follow the opposite pattern to NDUFA4L2, with high expression in normal tissue and no detectable expression in cancer samples (426, 427). Studies in these cancers have confirmed the findings of Tello *et al,* that NDUFA4L2 overexpression leads to reduced

oxygen consumption; inhibits ROS production; and drives cellular proliferation (426, 427). Silencing of the *NDUFA4L2* gene brought about an increase in levels of TCA metabolites and decreased PPP metabolites, and the predicted decrease in PPP-fuelled nucleotide synthesis is consistent with the reduced proliferation in KD cells (427). NDUFA4L2-expressing clear cell renal cell carcinoma cells were also shown to have abnormal mitochondrial morphology with disorganised cristae, and showed a decrease in autophagy, though the mechanisms of these changes were not studied (427). NDUFA4L2 expression associates with aggressive features of these tumours, as well as lower overall survival (426, 427, 430-432).

NDUFA4L2 was amongst a panel of genes that were induced in chondrocytes by treatment with rheumatoid arthritis synovial fibroblast conditioned medium, indicating that expression of this gene may be elevated in the diseased state. This effect could be reverted by treatment of the fibroblasts with anti-rheumatic drugs before media collection (433). To my knowledge, this is the only report of NDUFA4L2 regulation in an inflammatory context, but the authors did not study the function of this gene in these conditions.

Building upon my findings that NDUFA4 is regulated by several mechanisms during the macrophage inflammatory response, the aims of this chapter were to assess how the regulation of this protein affects the metabolic processes that govern macrophage phenotype, utilising techniques optimised from the previous chapter. I also wanted to investigate how NDUFA4 regulation impacts the macrophage inflammatory response.

Results

6.2 Loss of NDUFA4 protein in response to LPS is not a result of total complex IV downregulation

A possible explanation for the loss of NDUFA4 protein following TLR stimulation of macrophages would be if this treatment causes a general downregulation of mitochondrial protein or loss of all CIV subunits. I therefore examined the effect of LPS and Dex on other ETC proteins in human macrophages (**Figure 6.1**). MT-COI is one of three mitochondrially-encoded subunits of cytochrome c oxidase. It is the largest of the core catalytic subunits and has been described as the "seed" around which other subunits begin to assemble (434). MT-COI levels were not altered by LPS, indicating that the core complex is not degraded. I also blotted for the COXIV-1 subunit isoform, which is downregulated in hypoxia due to the HIF-mediated upregulation of LON protease. Hypoxia induces a switch to the COXIV-2 isoform, in a similar way to the proposed switching of NDUFA4 and NDUFA4L2 in hypoxia (359, 367). Despite the stabilisation of HIF-1α that I and others have demonstrated in macrophages under LPS stimulation (**Figure 5.7**), there was no detectable change in the level of COXIV-1 protein (**Figure 6.1**). This is consistent with my previous findings that LON mRNA is downregulated, rather than induced, by LPS (**Figure 4.14**). The CII subunit SDHA also showed stable expression across all treatments. These results demonstrate that the striking downregulation in response to LPS is not due to a total loss of mitochondrial protein. This effect may therefore be specific to NDUFA4, although this has not been systematically examined with regard to all ETC subunits.
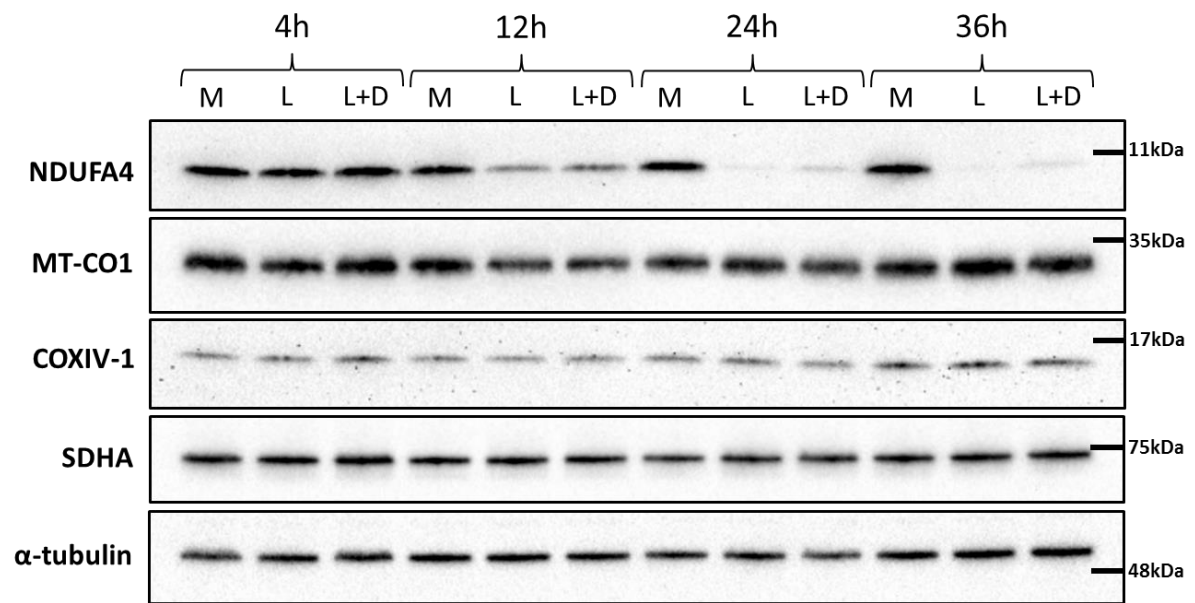
Figure 6.1) Other complex IV subunits are not regulated by LPS

Human monocyte-derived macrophages were Mock treated (M), or treated with LPS (L) or LPS+Dex (L+D) for the indicated times and harvested for Western blotting; Representative blot of n=2.

The potential reciprocal regulation of NDUFA4 and NDUFA4L2 is of obvious interest based on the literature surrounding these two proteins as well as their similar protein sequence. Given the links between inflammatory stimulation and the hypoxic response, this could potentially occur in macrophages under LPS treatment by a similar mechanism. However, our group has thus far been unable to demonstrate expression of NDUFA4L2 in macrophages (*to be discussed in Chapter 7*).

6.3 Optimisation of NDUFA4 silencing by siRNA

In order to study the effect of NDUFA4 downregulation in macrophages independently of other effects of LPS, I wanted to optimise siRNA-mediated knock down (KD). I validated effective silencing of NDUFA4 using a range of concentrations of ON-TARGET*plus* SMARTpool siRNA (Dharmacon), in which four different siRNAs against the target are pooled in order to guarantee knock down, and which includes a proprietary modification to reduce off target effects (**Figure 6.2 A&B**). Both protein and mRNA were downregulated, which was expected since RNA interference by siRNA involves perfect sequence complementarity and consequent mRNA cleavage (91). I also demonstrated that the silencing is maintained for several days after transfection (**Figure 6.2 C&D**).

For protein KD studies it is advisable to demonstrate that functional effects can be replicated using at least two individual siRNA sequences against the target (435). I therefore tested the siRNA from the SMARTpool individually. Only one of these four siRNAs was functional in knocking down NDUFA4 (even at 100nM) (**Figure 6.3**). Therefore I was provided with an alternative set of siRNAs from the Dharmacon siGenome range (these target the gene's coding region rather than the 3'UTR). **Figure 6.4** shows that all four of these siRNAs could functionally knock down NDUFA4 protein and mRNA to varying degrees. NDUFA4 siRNAs 01 and 02 gave the greatest percentage protein knock down, so these were selected for functional evaluation of NDUFA4.
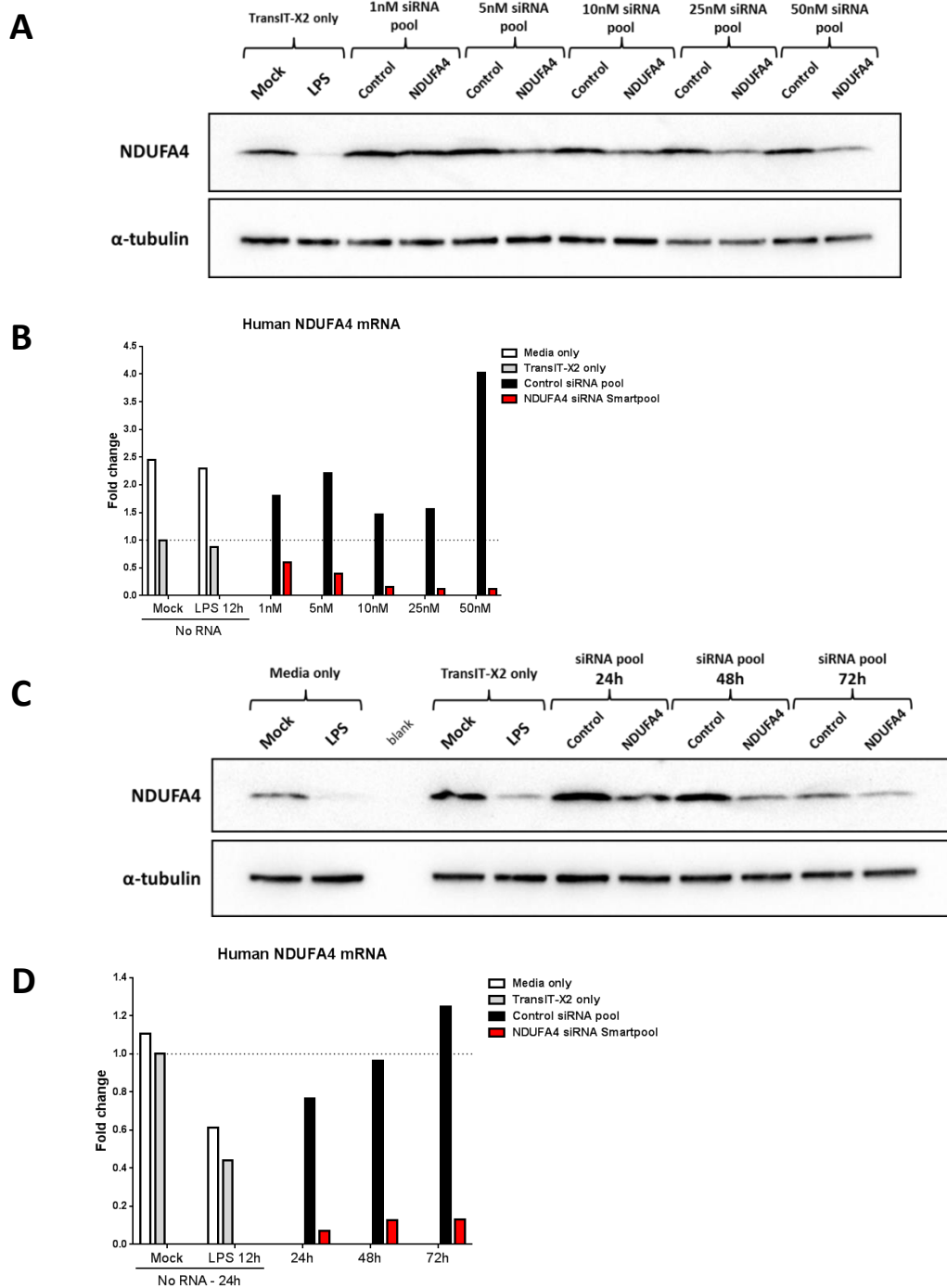
Figure 6.2) Optimisation of ON-TARGET*plus* siRNA SMARTpool transfection
Human monocyte-derived macrophages transfected with Dharmacon ON-TARGET*plus* Control siRNA pool or NDUFA4 siRNA SMARTpool using TransIT-X2 reagent. **A)** Indicated concentrations of siRNA used, cells were harvested for Western blot 48h post transfection, LPS treatment 24h prior to harvest; **B)** Indicated concentrations of siRNA used, cells were harvested for RNA 24h post transfection, LPS applied 12h prior to harvest; **C&D)** cells transfected with 50nM siRNA and harvested after the indicated time; **C)** LPS applied 24h prior to harvest; **D)** LPS applied 12h prior to harvest; **B&D)** expressed as fold change ($2^{-\Delta\Delta Ct}$) normalised to UBC, relative to mock treated X2 only. All n=1 (graphs display mean of technical replicates).
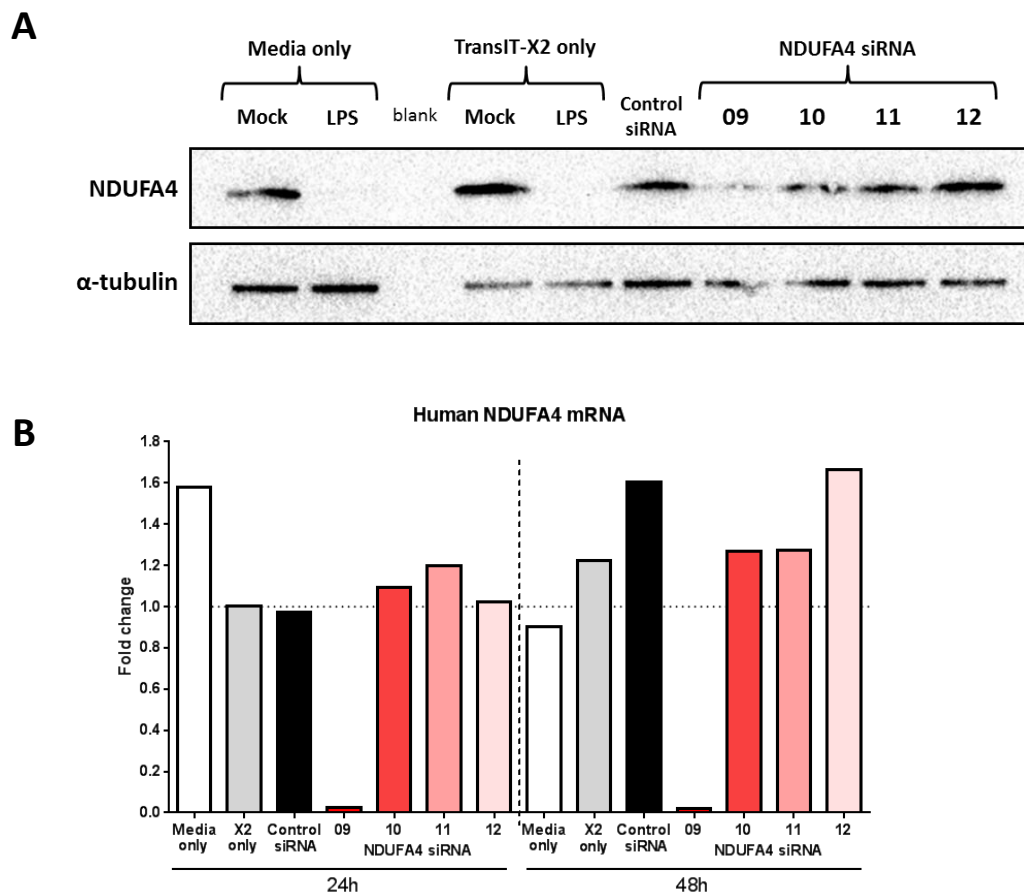
Figure 6.3) Optimisation of ON-TARGET*plus* individual siRNA transfection
Human monocyte-derived macrophages transfected with Dharmacon ON-TARGET*plus* Control siRNA or NDUFA4 siRNAs unlocked from the SMARTpool, using TransIT-X2 transfection reagent. **A)** 25nM of each siRNA used, cells were harvested for Western blot 48h post transfection, LPS applied 24h prior to harvest; **B)** 100nM of each siRNA used, cells were harvested for RNA after the indicated time, expressed as fold change (2^-ΔΔCt) normalised to UBC, relative to mock treated X2 only 24h. All n=1 (graph displays mean of technical replicates).
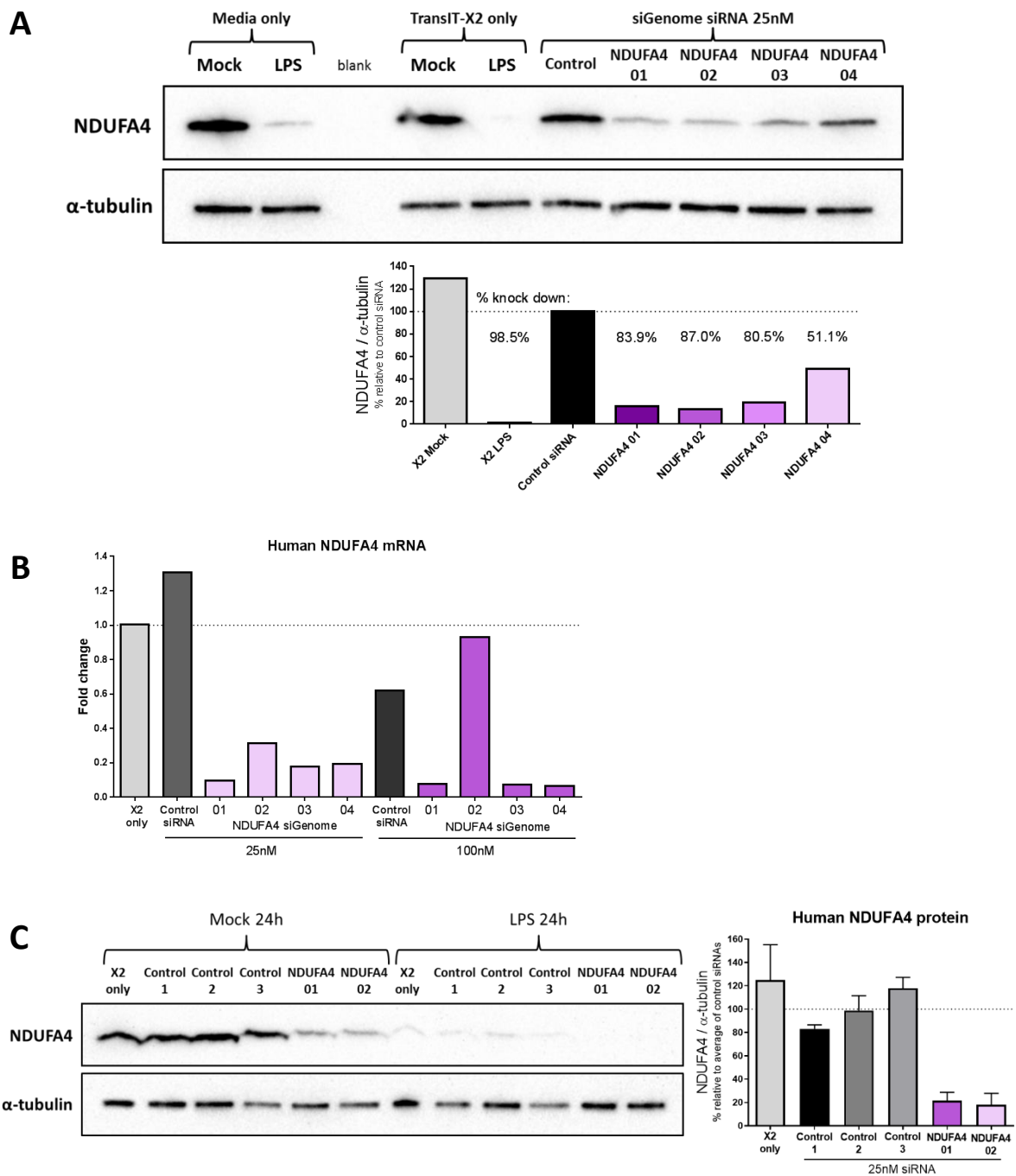
Figure 6.4) siGenome siRNA testing

Human monocyte-derived macrophages transfected with 25nM or 100nM (as indicated) Dharmacon siGenome Control siRNAs or NDUFA4 siRNAs, using TransIT-X2 transfection reagent. **A)** Cells were harvested for Western blot 48h post transfection, LPS applied 24h prior to harvest, quantification by densitometry, n=1; **B)** Cells were harvested for RNA 24h post transfection; expressed as fold change ($2^{-\Delta\Delta Ct}$) normalised to UBC, relative to mock treated X2 only 24h, n=1 (mean of technical replicates); **C)** Cells were harvested for Western blot 48h post transfection, LPS applied 24h prior to harvest, mock treated conditions quantified by densitometry, n=2. Data presented as mean +SD.

6.4 Effects of NDUFA4 KD on cytokine expression

The regulation of NDUFA4 expression by multiple pro-inflammatory stimuli, as well as the anti-inflammatory glucocorticoid, suggest that this protein may influence the macrophage inflammatory response. Liu *et al* reported that miR-147 signalling reduces the production of TNFα and IL-6 in mouse macrophages (10). I therefore wanted to assess changes in cytokine expression mediated by NDUFA4 silencing as an indicator of macrophage function. In order to gain a broad impression of cytokine and chemokine regulation I carried out multiplex measurements by Luminex, including a large range of time points, due to the different temporal regulation of different cytokines. Due to the large number of time points and the requirement for a control and two specific siRNAs, the Luminex could only be performed on a single biological replicate, and was therefore used to gauge appropriate time points and cytokines for further detailed analysis. Knock down of NDUFA4 alone (without LPS stimulation) was not sufficient to induce cytokine production (data not shown). The most interesting cytokine and chemokine results from this experiment are shown in **Figure 6.5**, and the remaining results in **Supplementary Figure S6**. Based on these initial data, it appeared that in comparison to the control siRNA, NDUFA4 silencing resulted in elevated expression of IL-10 and CCL2; downregulated expression of IL-6, IFN-β and CCL7; and had a complex effect on TNFα (**Figure 6.5**). However this experiment was intended merely as a guide for further experimental design, and will not be over-interpreted.
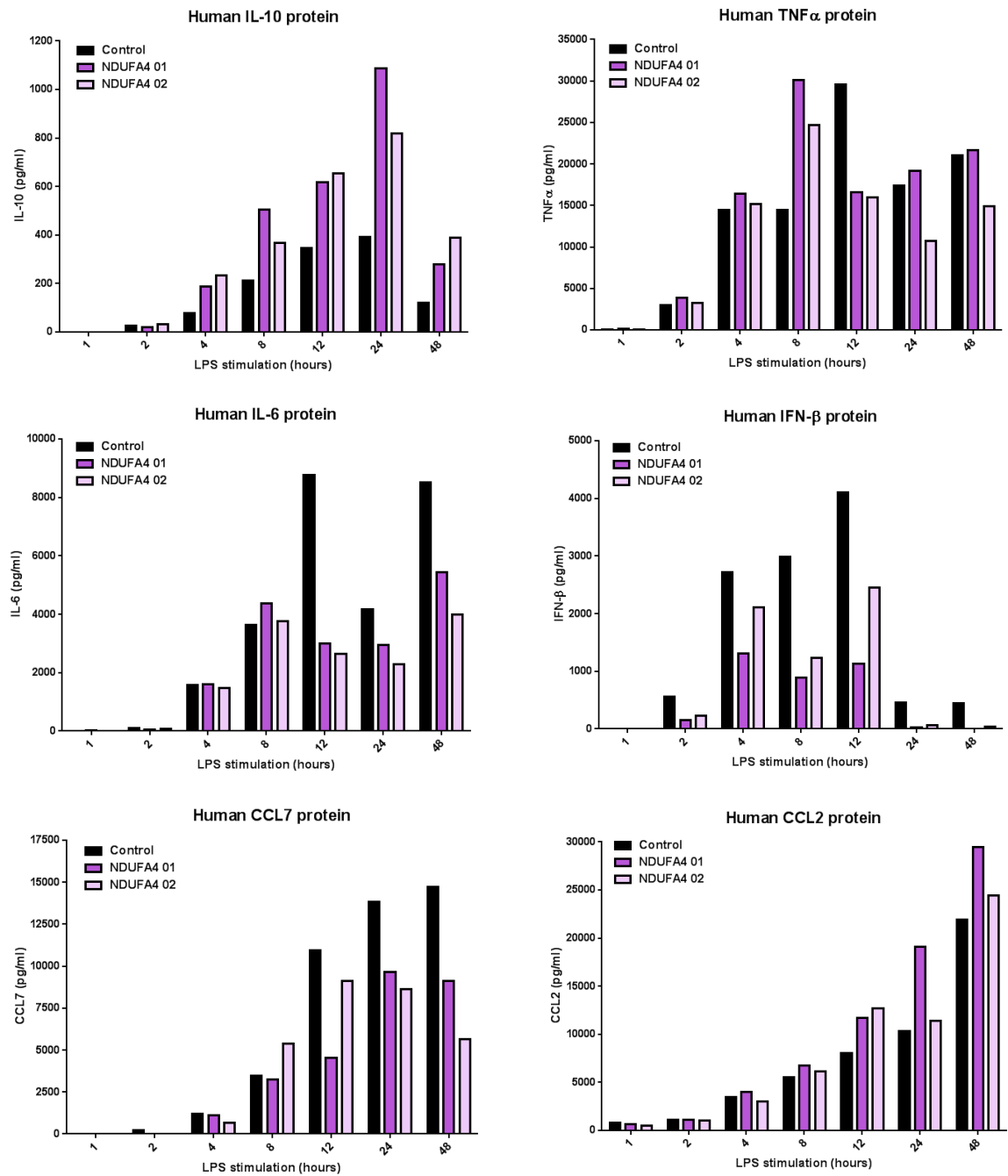
Figure 6.5) Luminex analysis of cytokine expression upon NDUFA4 KD
Human monocyte-derived macrophages transfected with 25nM Dharmacon siGenome Control siRNA or NDUFA4 siRNAs, using TransIT-X2 transfection reagent. LPS stimulation commenced 48h post transfection. Conditioned medium was collected at the indicated times and subjected to cytokine analysis by Luminex multiplex assay. See **Supplementary Figure S6** for additional cytokines; n=1. Data presented as mean of technical replicates.

I repeated the experiment in two further donors, restricting the time points to 8h, 12h and 24h. Interleukin-10 gave the greatest differential response between control and NDUFA4 siRNAs in the Luminex results, so I began by measuring IL-10 in these repeats by ELISA. However, this assay showed that the transfection reagent control (X2 only) gave comparable IL-10 expression to the NDUFA4 siRNA samples. It therefore appears from these results that it is the control siRNA that is having an effect on IL-10 production, rather than specific KD of NDUAF4 (**Figure 6.6**). Treatment of cells with transfection reagent in the absence of nucleic acid can provoke strange effects in cells, which cannot be ruled out here, therefore I repeated the experiment with an additional two non-targeting control siRNAs. These controls have been validated by the supplier to cause minimal targeting by genomewide microarray analysis of cell lines, and I confirmed that they do not alter NDUFA4 expression (**Figure 6.4C**). It is worth noting that control siRNA 1 has been reported to reduce expression of EGFR in certain cell types (stated on supplier webpage). EGFR has been shown to regulate macrophage activation and function, which could account for the apparent effect of this siRNA on IL-10 production (436). **Figures 6.7, 6.8 and 6.9** show mRNA and protein expression of TNFα, IL-6 and IL-10 from these extended experiments, and **Supplementary Figures S7, S8 and S9** show additional time points. Replicate donors are displayed separately in order to demonstrate the great variability.

These experiments highlighted not only transfection reagent effects, as demonstrated in Chapter 4, but also cytokine-, donor- and sequence-specific variability in the behaviour of negative control siRNAs. To briefly summarise the results, the transfection reagent TransIT-X2 (X2) consistently decreased the LPS-induced expression of IL-10 mRNA and protein, but almost invariably increased the expression of the pro-inflammatory mediators TNFα and IL-6.

Although the best of the reagents tested (Chapter 4), it is not neutral, and clearly has some effects on macrophage immune functions. In comparison with X2 alone, control siRNA 1 strikingly increased mRNA and protein levels of IL-6, as well as increasing TNFα and decreasing IL-10 expression to some extent. The other siRNA controls displayed highly inconsistent effects on cytokine expression. Against this background of variability, specific effects of siRNAs targeted against NDUFA4 were difficult to discern. The one possible exception was that the expression of IL-10 protein was increased by both NDUFA4-targeting siRNAs in comparison with controls. This is illustrated in **Figure 6.9C**, where IL-10 levels are normalised to the mean of the three negative controls to take account of the variation in absolute quantities of cytokine produced by macrophages from the three donors.
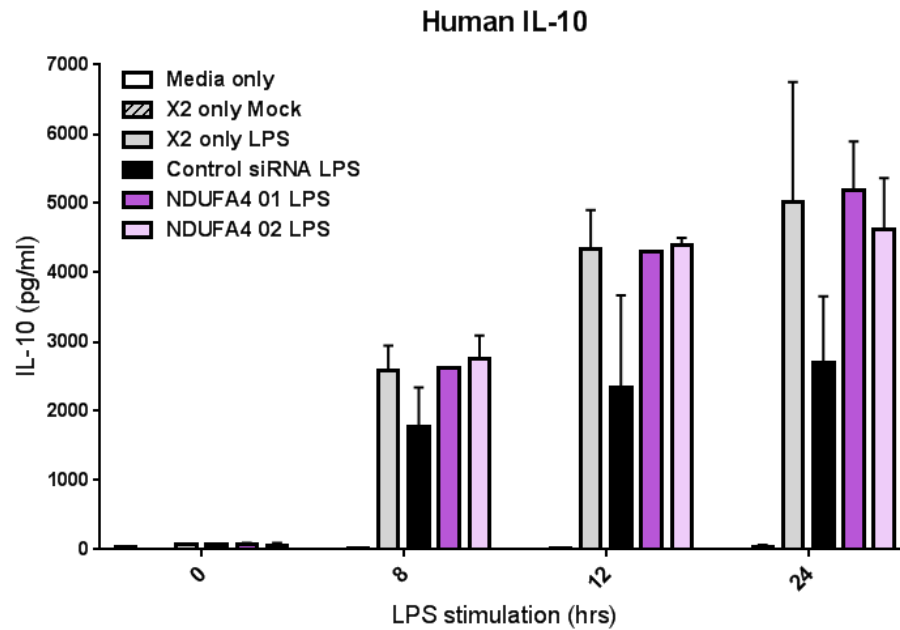
Figure 6.6) ELISA analysis of cytokine expression upon NDUFA4 KD

Human monocyte-derived macrophages transfected with 25nM Dharmacon siGenome Control siRNA or NDUFA4 siRNAs, using TransIT-X2 transfection reagent. LPS stimulation was commenced 48h post transfection. Conditioned medium was collected at the indicated times and IL-10 protein was measured by ELISA; n=2; Data presented as mean +SEM.

A

Donor 58
TNFA mRNA - 8h

Donor 60
TNFA mRNA - 8h

B

Donor 58
TNFα protein - 24h

Donor 60
TNFα protein - 24h

Donor 61
TNFα protein - 24h
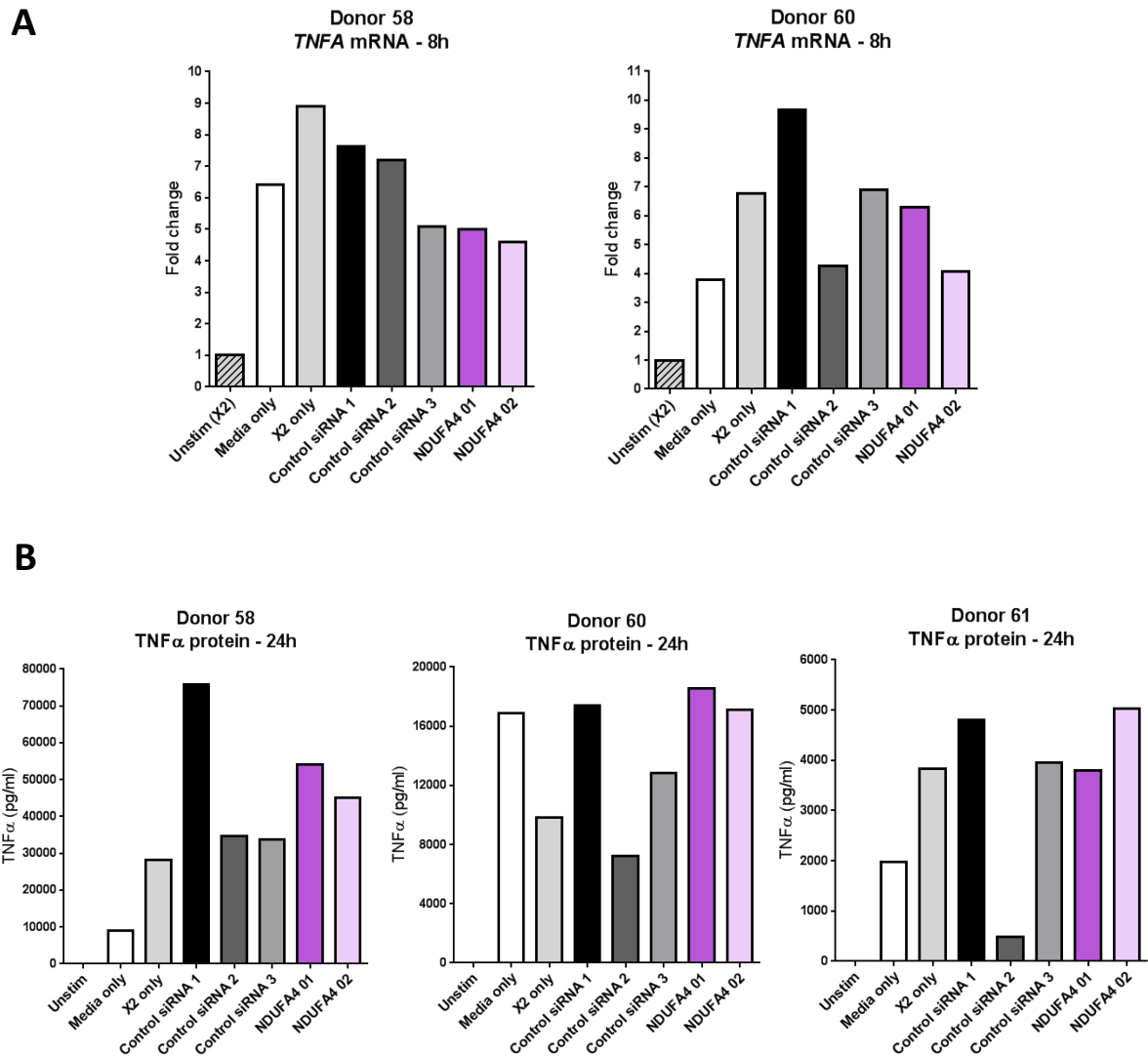
Figure 6.7) TNFα expression in response to siRNA transfection

Human monocyte-derived macrophages transfected with 25nM Control or NDUFA4 siRNAs using TransIT-X2 reagent for 48h followed by LPS stimulation for the indicated time.

A) Human TNFα mRNA was measured by RT-qPCR; expressed as fold change (2^-ΔΔCt) normalised to UBC, relative to X2 transfected unstimulated. **B)** Human TNFα protein was measured by ELISA from conditioned medium.

n=2/3 donors presented separately. Data presented as mean of technical replicates.

See supplementary figure S7 for additional time points

Figure 6.8) Interleukin-6 expression in response to siRNA transfection

Human monocyte-derived macrophages transfected with 25nM Control or NDUFA4 siRNAs using TransIT-X2 reagent for 48h followed by LPS stimulation for the indicated time.

A) Human IL-6 mRNA was measured by RT-qPCR; expressed as fold change ($2^{-\Delta\Delta Ct}$) normalised to UBC, relative to X2 transfected 8h LPS stimulated (no message detected in unstimulated samples). **B)** Human IL-6 protein was measured by ELISA from conditioned medium.

n=2/3 donors presented separately. Data presented as mean of technical replicates.

See supplementary figure S8 for additional time points

A

Donor 58
IL-10 mRNA - 8h

Donor 60
IL-10 mRNA - 8h

B

Donor 58
IL-10 protein - 24h

Donor 60
IL-10 protein - 24h

Donor 61
IL-10 protein - 24h

C

Human IL-10
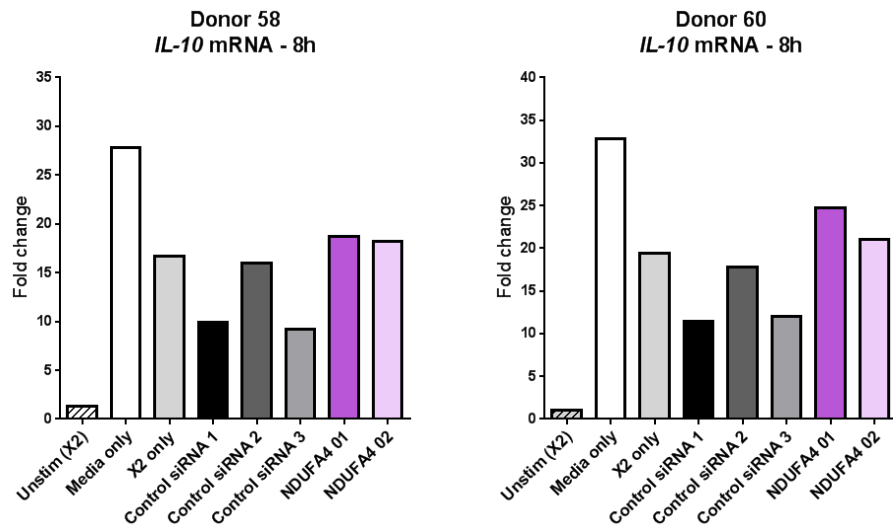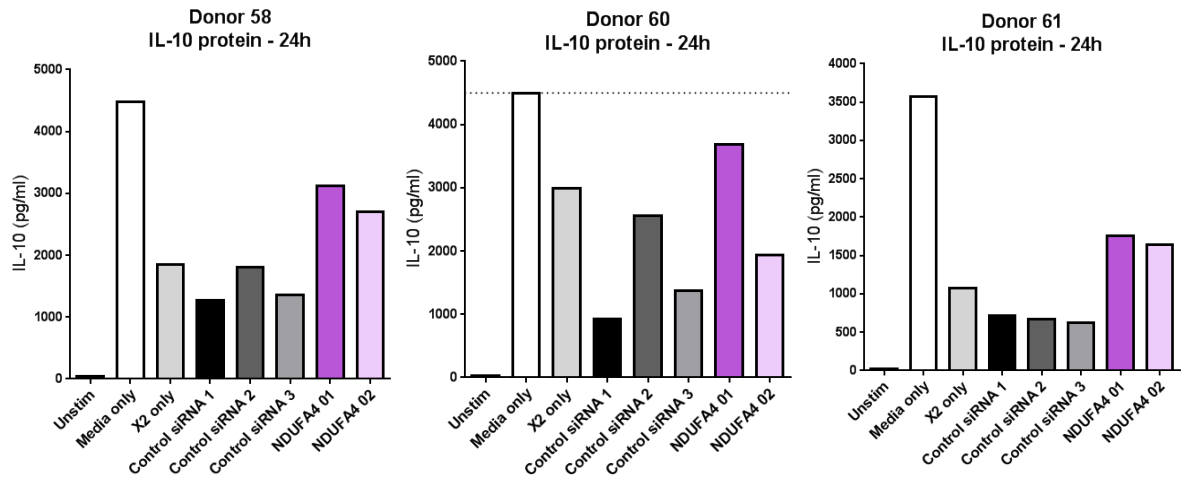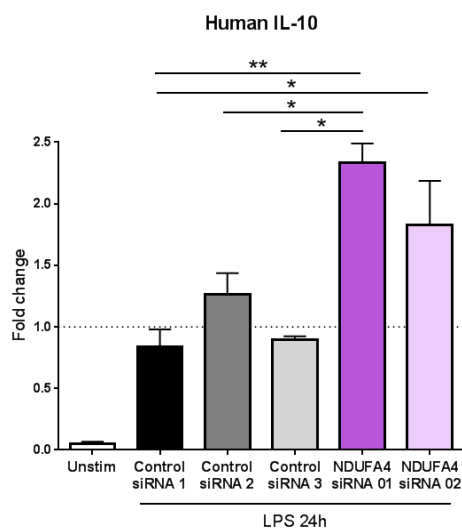
Figure 6.9) See overleaf for figure legend

Figure 6.9) Interleukin-10 production in response to siRNA transfection – additional controls

Human monocyte-derived macrophages transfected with 25nM Control or NDUFA4 siRNAs using TransIT-X2 reagent for 48h followed by LPS stimulation for the indicated time. **A)** Human IL-10 mRNA was measured by RT-qPCR; expressed as fold change (2^-ΔΔCt) normalised to UBC, relative to X2 transfected unstimulated. **B&C)** Human IL-10 protein was measured by ELISA from conditioned medium.

A&B) n=2/3 donors presented separately. Data presented as mean of technical replicates.

C) ELISA data from B combined for all 3 donors and presented relative to the average of control siRNA samples for each donor; One-way ANOVA with Tukey's correction for multiple comparisons; Data presented as mean +SEM.

Note) Donor 60 Media only sample above top standard of IL-10 ELISA (4500pg/ml)

See supplementary figure S9 for additional time points

I also examined IL-10 production upon overexpression of miR-147b. The miR-147b mimic brought about a small increase in IL-10 protein level, but this was significant relative to only one of the control mimics (**Figure 6.10**). These results give some support to the regulation of IL-10 by NDUFA4 silencing, as the lesser response to mimic transfection may be a reflection of the lesser degree of NDUFA4 KD compared with the siRNAs (compare **Figures 4.9 and 6.4**). It is also likely that miR-147b targets additional genes, which may themselves have varying effects on cytokine production. Despite the significant result for IL-10, it is difficult to conclude much with regard to the inflammatory function of NDUFA4 from these experiments due to the lack of reliable controls.
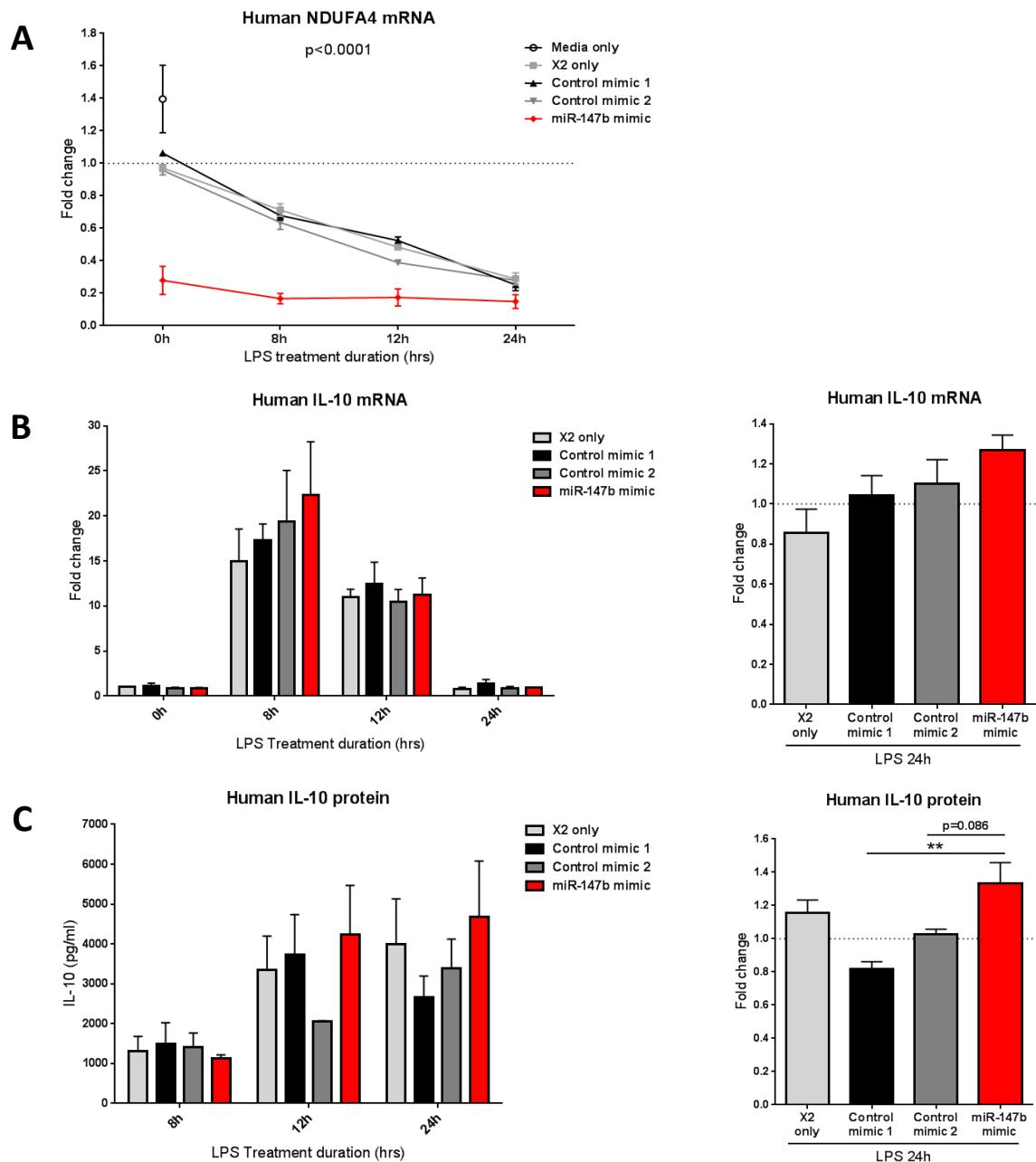
Figure 6.10) Interleukin-10 production in response to miR-147b mimic transfection
Human monocyte-derived macrophages transfected with 2nM Control mimics or miR-147b
mimic using TransIT-X2 for 48h followed by LPS stimulation for the indicated time. **A)** NDUFA4
mRNA measured by RT-qPCR, expressed as fold change (2^-ΔΔCt) normalised to UBC, relative to
the average on control transfected unstimulated samples; n=3; Two-way ANOVA, column factor
(treatment) p<0.0001. **B)** IL-10 mRNA measured by RT-qPCR, expressed as fold change (2^-ΔΔCt)
normalised to UBC, relative to X2 only unstim, and as fold change relative to average of control
mimics 8h LPS treated; n=3; One-way ANOVA with Tukey's correction for multiple comparisons
(ns). **C)** IL-10 protein measured by ELISA from conditioned medium, expressed as pg/ml and as
fold change relative to average of control conditions 24h LPS treated; n=3; One-way ANOVA with
Tukey's correction for multiple comparisons. Data presented as mean +SEM.

6.5 Metabolic effects of NDUFA4 KD

In addition to my aim of understanding the inflammatory consequences of NDUFA4 regulation, I wished to examine the precise role of NDUFA4 in macrophage metabolic regulation, which is likely to underlie any inflammatory effects. Previous studies have reported that NDUFA4 loss reduces cytochrome c oxidase activity, which contributed to the revised understanding of NDUFA4 localisation (280, 342). I therefore optimised measurement of individual respiratory chain complex activity using the Seahorse flux analyser (*discussed in Section 2.19*). In contrast to the literature, I saw no effect of NDUFA4-specific siRNAs on the activity of CIV by this assay (**Figure 6.11**). It is unclear whether this reflects cell type-specific differences in the functionality of this protein, or whether the effects are too minor to be detected using this system. LPS treatment did result in a small but significant reduction in CIV activity (**Supplementary Figure S10A**). As LPS stimulation leads to more complete loss of NDUFA4 protein than the siRNA, it is possible that this result is related to NDUFA4 regulation, however as the effect was not recapitulated by NDUFA4 KD this cannot be confirmed. This is also an interesting result considering that overall oxidative respiration is not decreased by LPS treatment in human MoDMs, and could warrant further study (**Figures 5.2 & 5.5**). Complex I-mediated respiration did not show a significant response to LPS in these studies, although this may require further repetition due to donor variability (**Supplementary Figure S10B**). Alternative methods of measuring CIV activity include the use of more sensitive respirometry such as Oroboros oxygraph; or biochemical assessment of enzymatic activity. These methods could be used to validate my results.

I also analysed the effects of NDUFA4 KD on metabolic parameters of intact human macrophages using the Mito+Glyco stress test. In agreement with the results of CIV activity, I saw no effect of NDUFA4 KD on mitochondrial respiratory parameters, including basal

respiration rate and maximal respiratory capacity, in unstimulated or LPS-treated macrophages (**Figure 6.12**). Unexpectedly, the difference that I did see in this assay was in the rate of glycolysis (ECAR) (**Figure 6.13**). In unstimulated cells NDUFA4 KD did not have a reproducible effect between the two different NDUFA4-specific siRNAs on basal glycolysis or glycolytic capacity. Differences in glycolytic capacity between control siRNAs and between NDUFA4-specific siRNAs in these cells suggest that non-specific alterations in metabolism may occur upon siRNA transfection, similarly to the cytokine measurements. However in LPS-treated cells there was a reproducible effect of NDUFA4 KD on glycolysis. Pre-silencing of NDUFA4 prior to LPS stimulation for 24h resulted in significantly enhanced glycolytic rate and glycolytic capacity in both NDUFA4 siRNA conditions compared with controls. Therefore LPS-mediated silencing of NDUFA4 may act to facilitate the glycolytic shift that occurs in inflammatory macrophages. Similarly to **Figures 5.1** & **5.4**, the glycolytic reserve was negligible in these experiments (**Figure 6.13**).
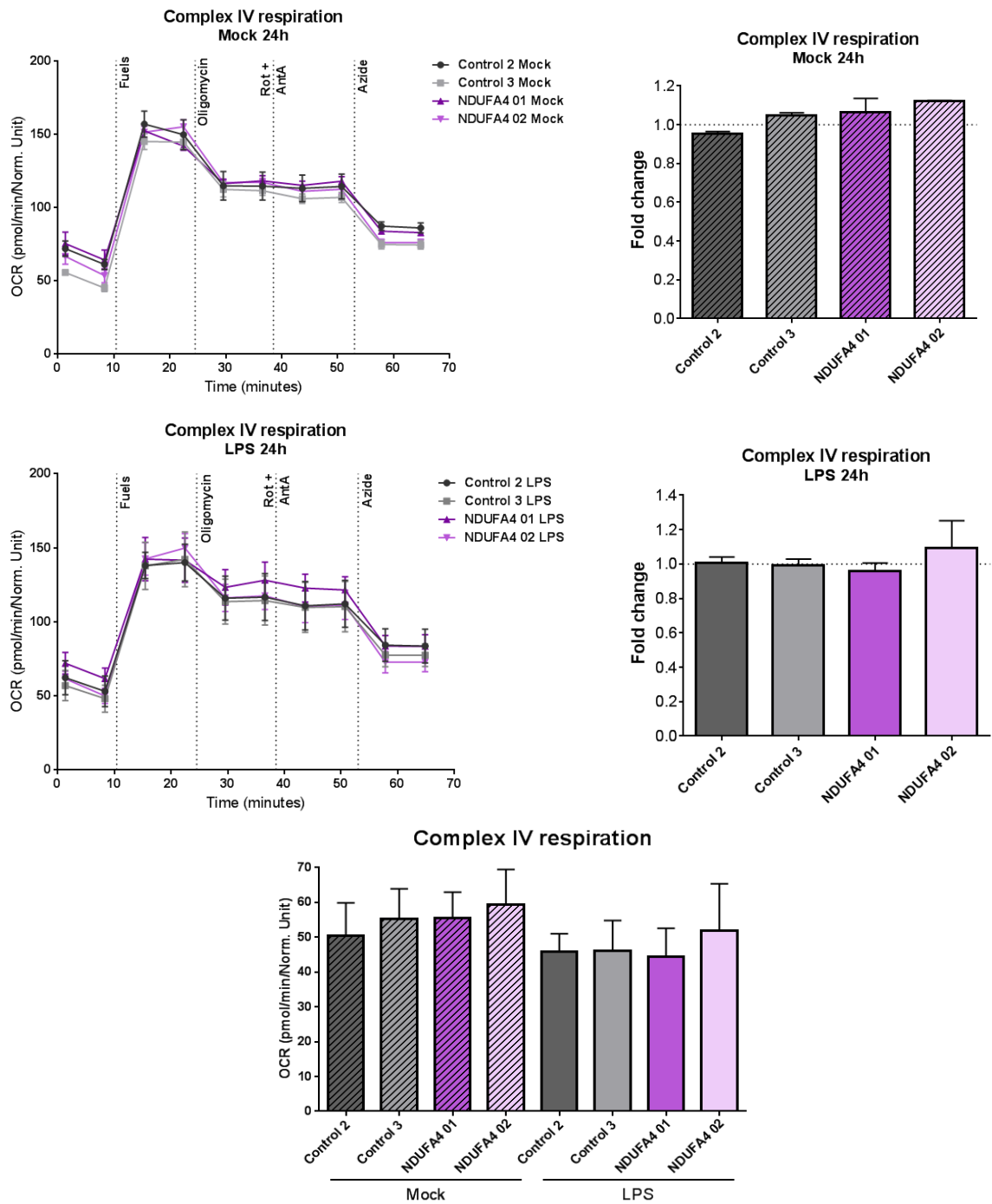
Figure 6.11) Complex IV respiration is not altered by NDUFA4 KD

Human monocyte-derived macrophages transfected with 25nM Control or NDUFA4 siRNAs using TransIT-X2 reagent for 48h prior to seeding into 96well Seahorse plate (35,000 cells/well). Mock treatment or LPS stimulation for 24h prior to permeabilisation and complex IV activity measurement by Seahorse XFe96 analyser; OCR normalised to Picogreen assay ratio. Representative Seahorse traces (mean+SD of technical replicates) and calculated complex IV activity expressed as OCR/norm unit and as fold change relative to average of control siRNAs; n=3; One-way ANOVA with Tukey's correction for multiple comparisons (ns); Data presented as mean +SEM.
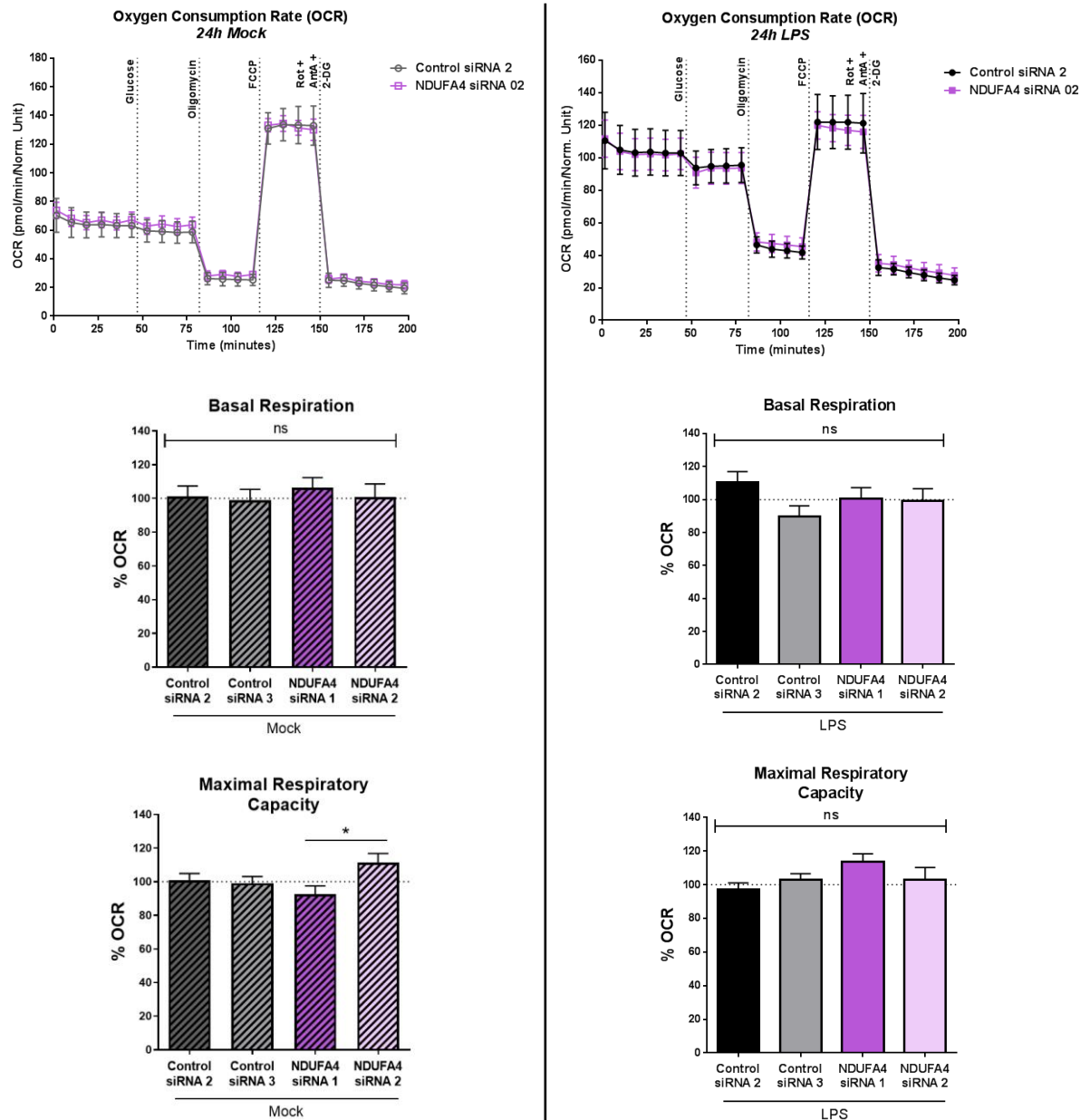
Figure 6.12) Mitochondrial respiration is not altered by NDUFA4 KD

Human monocyte-derived macrophages transfected with 25nM Control or NDUFA4 siRNAs using TransIT-X2 reagent for 48h prior to seeding into 96well Seahorse plate at 50,000 cells/well. Mock treatment or LPS stimulation for 24h prior to performing Mito+Glyco stress test using Seahorse XFe96 analyser; OCR normalised to calcein viability assay ratio. Representative Seahorse traces (mean+SD of technical replicates) and calculated parameters expressed as % OCR relative to average of control siRNAs; n=7; One-way ANOVA with Tukey's correction for multiple comparisons; Data presented as mean +SEM.
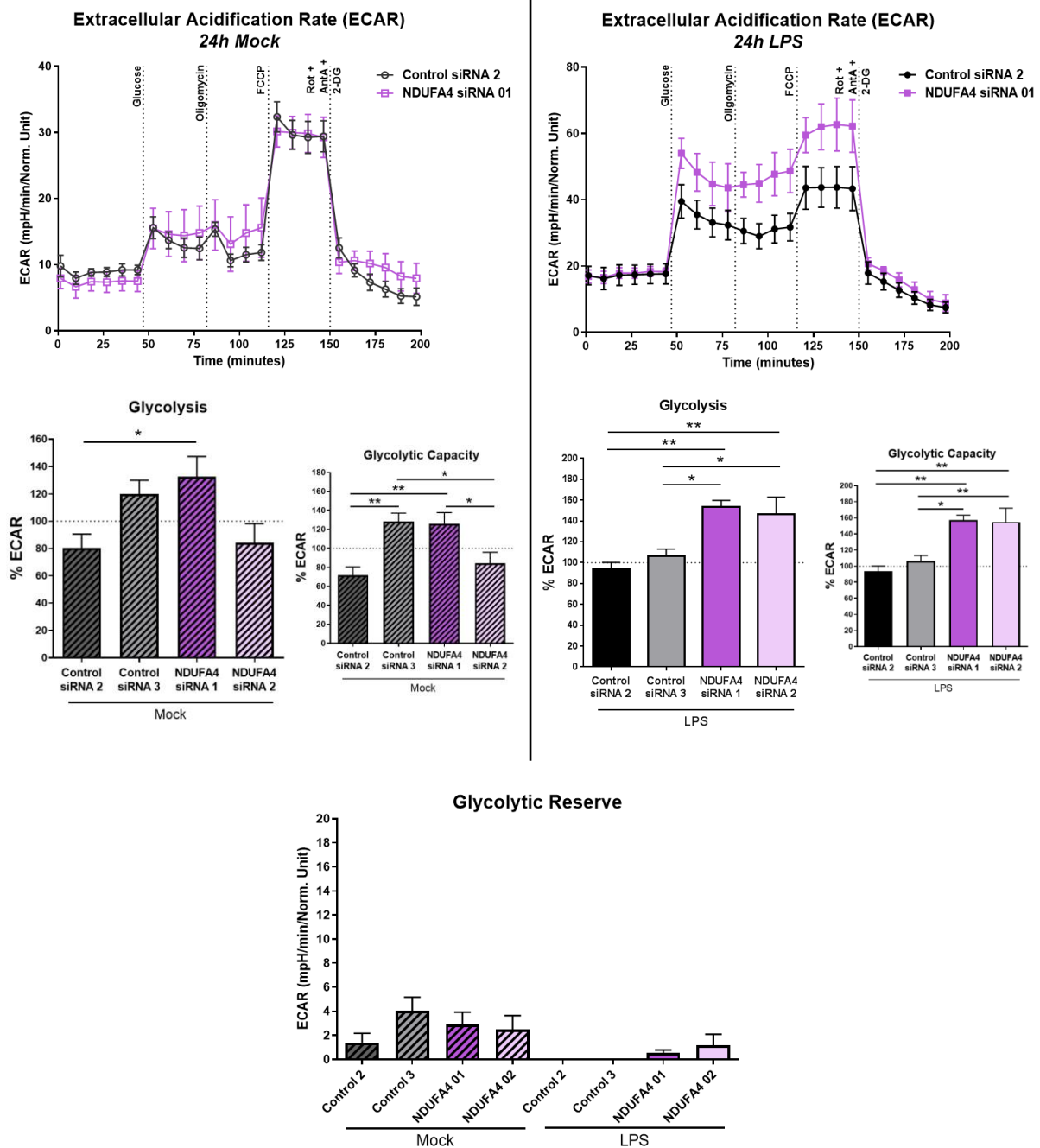
Figure 6.13) LPS-induced glycolytic shift is enhanced by NDUFA4 KD

Human monocyte-derived macrophages transfected with 25nM Control or NDUFA4 siRNAs using TransIT-X2 reagent for 48h prior to seeding into 96well Seahorse plate at 50,000 cells/well. Mock treatment or LPS stimulation for 24h prior to performing Mito+Glyco stress test using Seahorse XFe96 analyser; ECAR normalised to calcein viability assay ratio. Representative Seahorse traces (mean+SD of technical replicates) and calculated parameters expressed as ECAR or % ECAR relative to average of control siRNAs; n=7; One-way ANOVA with Tukey's correction for multiple comparisons; Data presented as mean +SEM.

This effect on glycolysis was surprising, especially given the apparent lack of mitochondrial response to NDUFA4 silencing, due to the mitochondrial localisation of this protein. One possible explanation is a compensatory regulation of glycolytic and oxidative respiratory pathways in order to maintain ATP production. As previously discussed, oxidative phosphorylation via the ETC results in much more efficient ATP synthesis than does glycolysis, and therefore a much greater increase in glycolytic rate would be required to compensate for a small decrease in the rate of oxidative phosphorylation. As the Seahorse ATP rate assay allows determination of the individual contributions of mitochondrial and glycolytic ATP production, I used this assay to investigate this hypothesis. The results show a trend towards an increased glycolytic ATP production rate in the NDUFA4-KD conditions, supporting the results of the Mito+Glyco stress test. However there was no detectable change in mitochondrial ATP production rate (**Figure 6.14**).

Another possible mechanism of glycolytic regulation is through mitochondrial ROS production. ROS can signal throughout the cell and alter protein function, thereby regulating signalling pathway activation, which could include direct or indirect regulation of glycolysis. Due to the reported association between NDUFA4L2 and ROS, I wanted to assess whether NDUFA4 KD also affects mROS production. Despite my previous results showing a lack of reproducible mROS induction by LPS in human macrophages (**Figure 5.13**), I reasoned that an LPS-induced switch between NDUFA4 and an alternative protein, such as NDUFA4L2, may obscure any effects of outright NDUFA4 loss from the ETC. I therefore performed MitoSOX and MitoTracker Green staining in siRNA-transfected human macrophages (**Figure 6.15**). In this experiment I did see an increase in mROS staining with LPS stimulation, which increased throughout the time course (**Figure 6.15** and **Supplementary Figure S11**), however I saw no effect of NDUFA4 KD. This may also have been confounded by inconsistent results for the control siRNAs, similarly to the cytokine measurements.
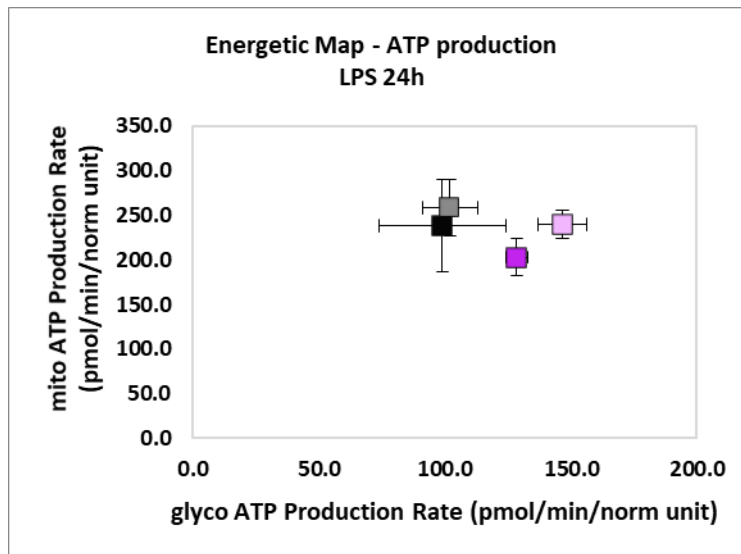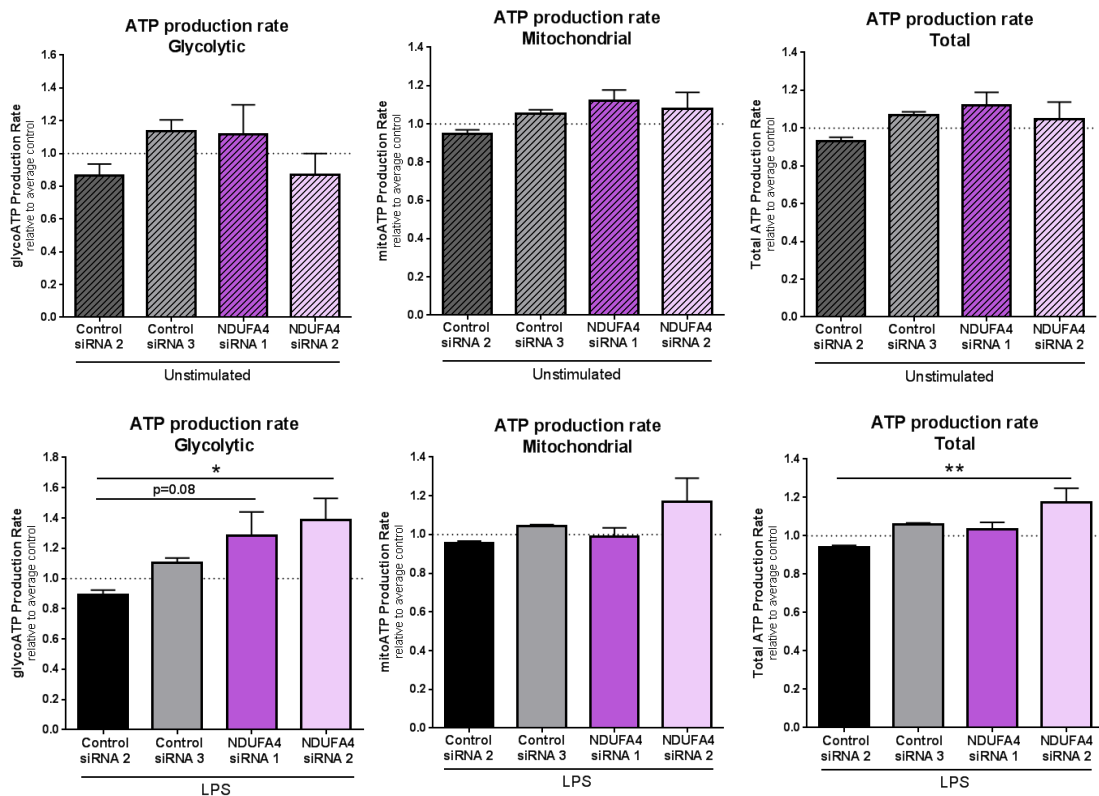
Figure 6.14) ATP production upon NDUFA4 KD
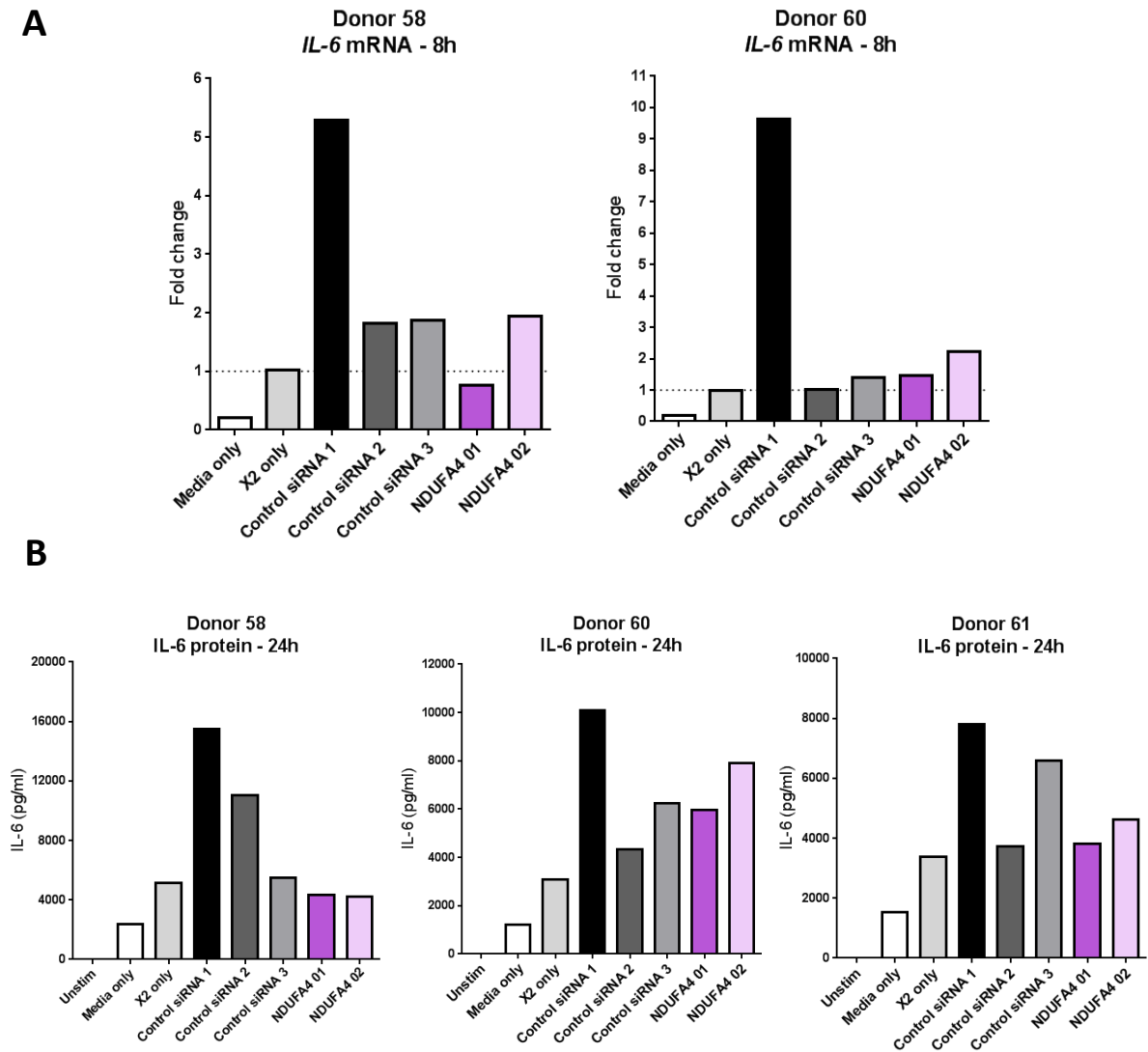
Human monocyte-derived macrophages transfected with 25nM Control or NDUFA4 siRNAs using TransIT-X2 reagent for 48h prior to seeding into 96well Seahorse plate. Mock treatment or LPS stimulation for 24h prior to performing ATP rate assay using Seahorse XFe96 analyser. **A)** Representative energetic map showing glycolytic and mitochondrial ATP production rates of LPS treated conditions (mean+SD of technical replicates); **B)** ATP production rate calculated using Seahorse ATP assay report generator, relative to average of control siRNAs. Normalised to calcein viability assay; n=5; One-way ANOVA with Tukey's correction for multiple comparisons; Data presented as mean +SEM.
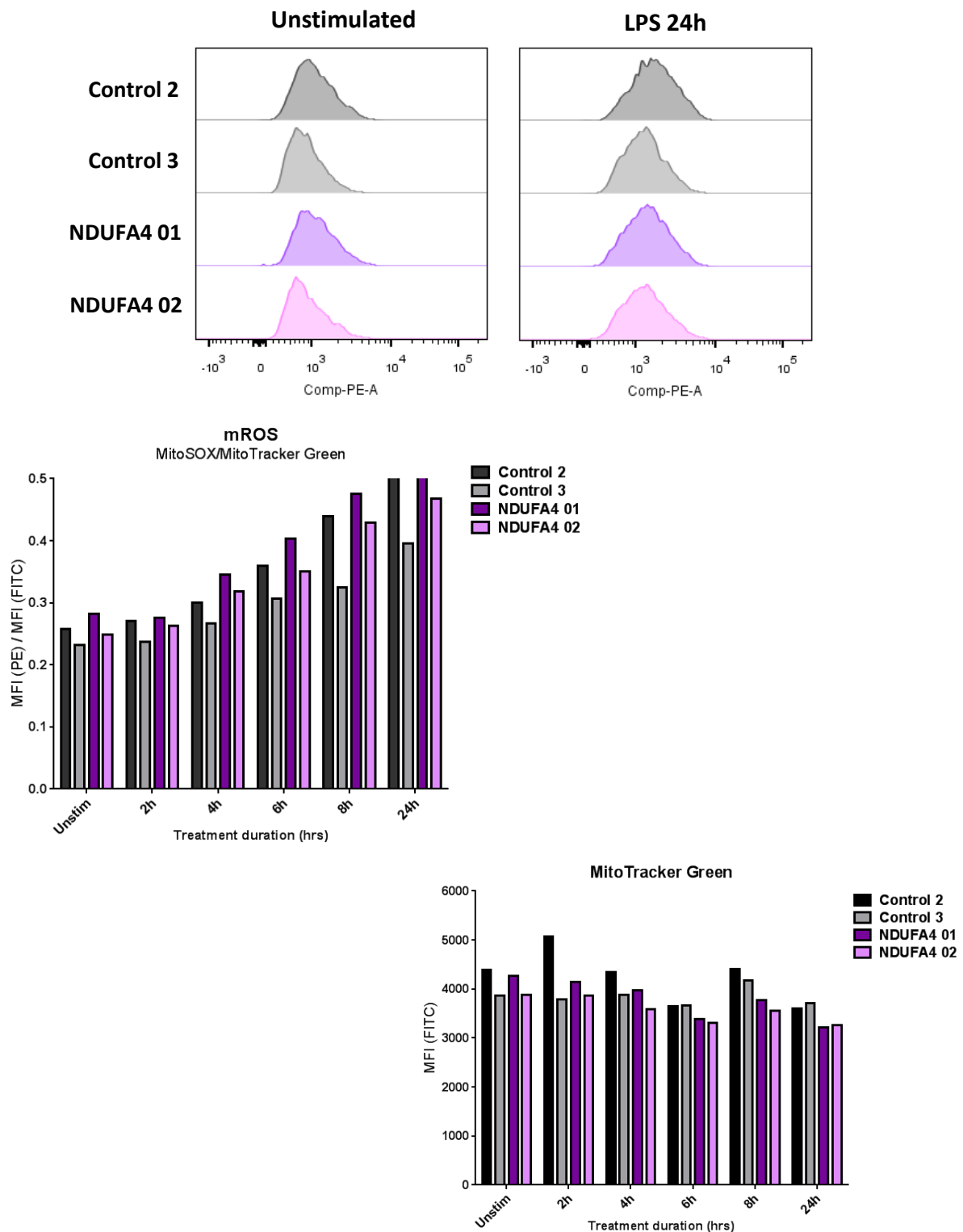
Figure 6.15) mROS measurements upon NDUFA4 KD
Human monocyte-derived macrophages transfected with 25nM Control or NDUFA4 siRNAs using TransIT-X2 reagent for 48h. LPS stimulation for the indicated times followed by staining with MitoSOX. Doublets and dead cells were gated out; n=1. Graphs show median fluorescence intensity (MFI) of MitoSOX normalised to MitoTracker Green, and MitoTracker Green alone

6.6 Study of NDUFA4 patient macrophage function

In Chapter 4 I described a study by Pitceathly *et al* in which the authors found a mutation within the *NDUFA4* gene to underlie a debilitating neuromuscular condition with Leigh syndrome characteristics (280). We were able to obtain blood samples from three such affected individuals, and generated patient monocyte-derived macrophages *in vitro*. This avoids the need to transfect with siRNAs to assess the role of NDUFA4, but was limited by the cell number obtained from the patient samples, and by the small number of patients.

The macrophages of these individuals lack any expression of NDUFA4 protein detectable by Western blot, as expected (**Figure 6.16**). In contrast, the healthy controls show the expected LPS-induced loss of the protein. All subjects display comparable expression of the CIV subunits MT-COI and COXIV-1. These results give further evidence that absence of NDUFA4 does not result in loss of total CIV, although it is possible that compensatory mechanisms could have arisen in these patients, as dramatic loss of CIV activity is likely to be embryonically lethal.
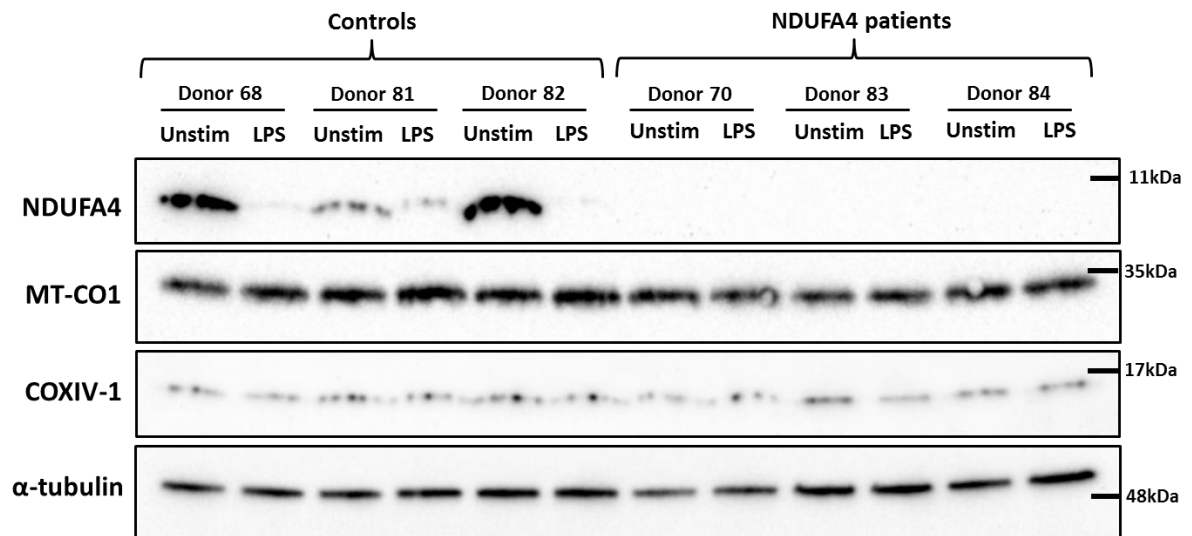
Figure 6.16) NDUFA4 patients show no detectable expression of NDUFA4 protein
Human monocyte-derived macrophages from controls or NDUFA4 patients were mock treated or
LPS stimulated for 24h prior to harvesting for Western blot. 20µg protein per sample.

Pitceathly *et al* reported that muscle tissue from these patients showed decreased activity of CIV, but maintained CI activity comparable to controls. I measured respiration mediated either through CI or directly via CIV in patient macrophages, using the respiratory chain Seahorse assay. I saw no difference in CI-mediated respiration between patients and controls (**Figure 6.17**). The measured CIV activities were slightly reduced in the patient cells compared with controls under mock treated conditions, but due to the variation between individuals, the lack of replicates, and the small magnitude of this effect, I cannot conclude whether this is a true difference.

I also performed the Seahorse ATP assay on the macrophages from these patients, as this assay gives a good overall representation of cellular metabolic activity (**Figure 6.18**). In contrast to my results using NDUFA4 siRNA, the NDUFA4 patient cells did not show an elevated rate of LPS-induced glycolysis compared with controls. There were also no significant differences in mitochondrial or total ATP production between subject groups. This could be a reflection of the large variability between individuals in these assays. What can be concluded from these experiments is that the rescue of NDUFA4 protein is not necessary for the inhibition of LPS-induced glycolytic ATP production by glucocorticoids, as this also occurred in the patient cells (**Figure 6.18**).

A
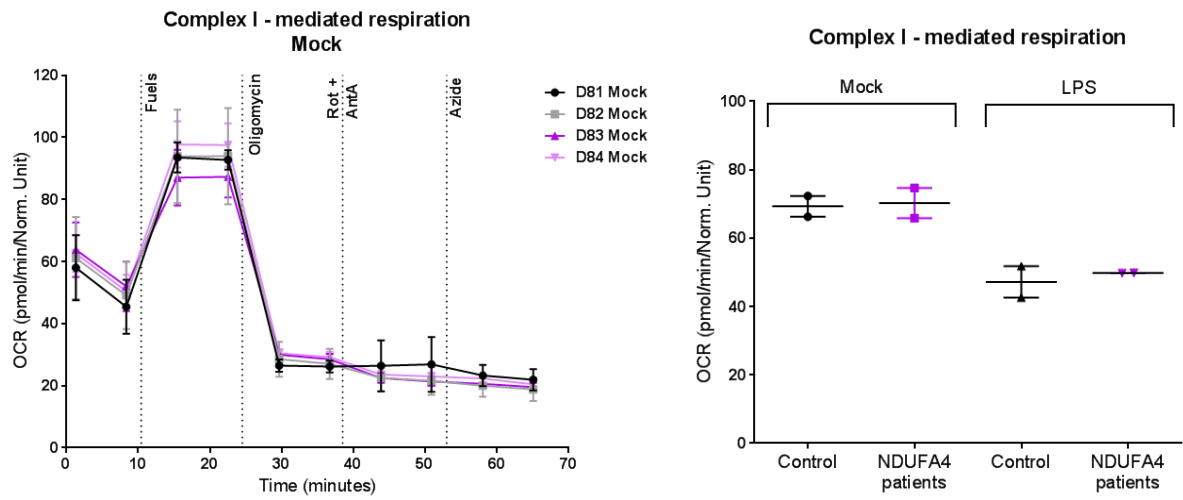
B
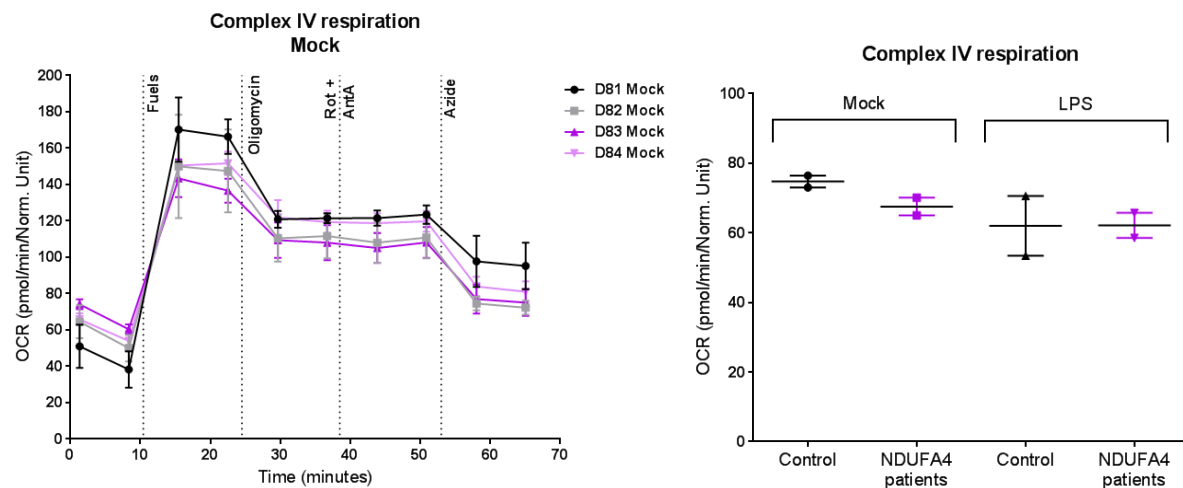
Figure 6.17) Respiratory chain activity in NDUFA4 patients

Human monocyte-derived macrophages from controls or NDUFA4 patients were seeded into 96well Seahorse plate at 35,000 cells/well. Mock treatment or LPS stimulation for 24h prior to permeabilisation and measurement of respiratory chain activity using a Seahorse XFe96 analyser; OCR normalised to Picogreen DNA content assay ratio. Representative Seahorse traces (mean+SD of technical replicates) and calculated respiration mediated from **A)** complex I or **B)** complex IV (displayed as individual values and mean).
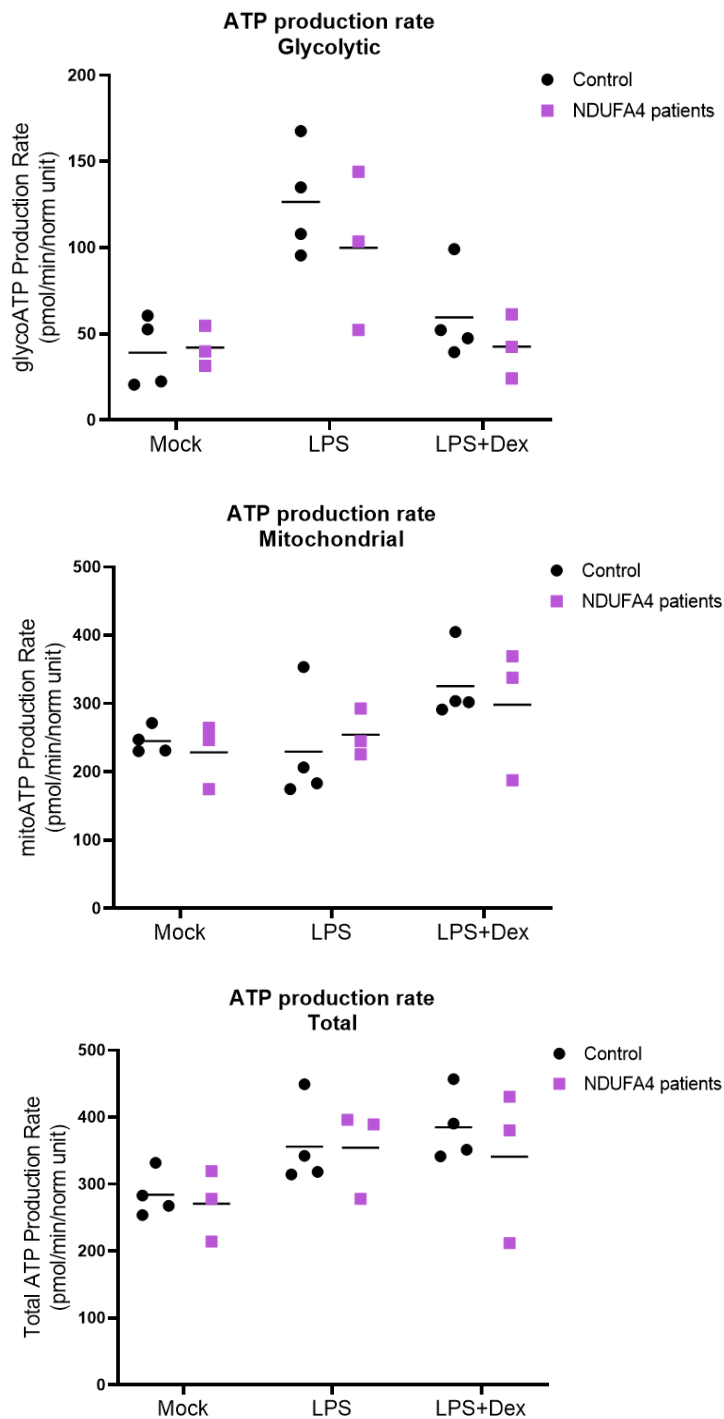
Figure 6.18) ATP production in NDUFA4 patients

Human monocyte-derived macrophages from controls or NDUFA4 patients were seeded into 96well Seahorse plate at 50,000 cells/well. Mock treatment or LPS stimulation for 24h prior to performing ATP rate assay using Seahorse XFe96 analyser; normalised to calcein viability assay ratio (displayed as individual values and mean). Controls were processed and analysed alongside patient samples in two independent experiments.

6.7 Discussion

6.7.1 Limitations and additional experimental approaches

In this chapter I have investigated the metabolic and inflammatory consequences of NDUFA4 downregulation using siRNA-mediated knock down and samples from patients lacking NDUFA4 protein. I focused on the use of primary human macrophages for these experiments due to the striking response of NDUFA4 protein to LPS treatment, and since we did not have an *Ndufa4*-KO mouse available. I came across many challenges over the course of this body of work, most notably due to the effects of siRNA transfection on these sensitive immune cells.

Issues with siRNAs

Exogenous RNA is detected by immune and other cell types, either through cytosolic recognition involving RIG1-like receptors (RLRs) or protein kinase R (PKR); or through endosomal or cell surface detection by PRRs (437). Baum *et al* tested several commercially available control siRNA species for their off target effects in fibroblast cell lines, finding that siRNAs from the same manufacturer induced similar global expression patterns, likely due to specific chemical modifications (438). The authors also demonstrated variations in IL-8 production caused by siRNAs from the same manufacturer, which implicates sequence-specific activity. The impact of siRNA transfection in this study was also highly dependent upon cell type (438).

TLR7/8 have been shown to be activated by GU-rich sequences (439), and Judge *et al* identified a specific RNA motif (UGUGU) that greatly increased production of IFNα from DCs (440). Upon examination of the siRNA sequences used in my experiments, I found that control siRNA 3 does contain several GU motifs (Table 6.1). However this alone does not explain the

differential responses of the controls. Hornung *et al* found an alternative siRNA motif that also strongly stimulates interferon production in DCs, and this motif is not rich in GU dinucleotides (441). Therefore it is likely that there are many sequence-specific characteristics of siRNAs that dictate their immunogenic potential, and we are yet to fully understand these effects. More rigorous controls for these experiments would be mismatch-containing or scrambled versions of the on-target sequences (435). Incorporation of 2'-O-methyl modifications has also been shown to combat activation of anti-viral responses via TLR7/8 (442). This modification does not prevent the activation of TLR3, but this receptor has been reported to require at least 21nt length RNA for activation (443).

Table 6.1) Comparison of siGenome siRNA sequences

	Sequence	GC content (%)	Length
Control siRNA 1	UAGCGACUAAACACAUCAA	36.84	19
Control siRNA 2	UAAGGCUA**UG**AAGAGAUAC	36.84	19
Control siRNA 3	A**UGU**AU**UG**GCC**UGU**AUUAG	36.84	19
NDUFA4 01	GAUCAUCG**GU**CAGGCCAAG	57.89	19
NDUFA4 02	CAC**UGU**AUCUCUUGC**GU**CU	47.37	19

I also saw variations in detection of mROS between the different control siRNA-transfected samples, although this experiment was only n=1. Another inconsistency was the fact that in this instance (**Figure 6.15 and Supplementary Figure S11**) I saw a detectable increase in MitoSOX staining with LPS treatment, while in **Figure 5.13** the response was minor or absent. This may be explained by the transfection process resulting in a cellular state that is more conducive to LPS-induced mROS production. Garaude *et al* reported that activation of RNA sensing pathways was necessary for increased activity of CII during bacterial challenge (425). SiRNA delivery could replicate this effect, mediating elevated CII activity and mitochondrial hyperpolarisation, thereby priming cells for ROS production. These

measurements require replication, and would benefit from the use of additional ROS detection methods (*discussed in Chapter 5*).

Overall, my results using RNA interference highlight the important of rigorous controls during siRNA experiments, and question the suitability of such techniques in macrophages. The immunostimulatory actions of siRNAs have previously led to misinterpretation of results during RNAi treatment in various animal models. Beneficial effects in certain studies were later found to be conferred by non-specific activation of cytokine production by the RNA, rather than specific target-related effects (442, 443). It can be concluded that cytokine and ROS analysis would be better performed in a stable knock out cell line, as this would overcome the need for acute transfection. However it is unclear how metabolic adaptation, including NDUFA4 regulation and role, would differ in a transformed cell line.

An alternative to siRNA transfection or a KO cell line was the use of samples from the NDUFA4-associated Leigh syndrome patients who lack expression of this protein. Whilst I was fortunate to have the opportunity to obtain these samples, the experiments were limited by the rarity of this mutation (there being only three known individuals globally who are homozygous for an NDUFA4 mutation), meaning that many of the results were inconclusive. Other caveats include the possibility that chronic lack of NDUFA4 does not recapitulate acute downregulation, and that compensatory mechanisms may have developed within these patients. Future plans for use of these samples include cytokine analysis and metabolomic profiling, however due to the lack of detection of any robust changes in mitochondrial activity, it may be expected that there will be no differences in other parameters.

Replacement of glucose with galactose

Despite several reports of the importance of NDUFA4 for full activity of CIV, I saw no defects in the activity of this complex, or reduction of overall oxygen consumption rate, in either siRNA-transfected cells or NDUFA4 patient macrophages. It is possible that these results are due to an over-reliance on glycolysis, induced by the presence of high glucose concentrations during cell culture. RPMI1640 medium used to maintain macrophages *in vitro* contains 11.1mM glucose, whereas *in vivo* glucose concentration in healthy human serum is around 5mM, with concentrations in tissues falling much lower during substrate competition (444). Cells may switch off oxidative metabolic pathways in favour of glycolytic metabolism when glucose is plentiful, including changes in respiratory capacity (445). It has been reported that cells increase expression of ETC proteins when cultured with galactose rather than glucose, including the CIV subunit COXVa (445, 446). I have also demonstrated the acute suppressive effect of high glucose concentration on oxidative metabolism (the Crabtree effect) in cultured macrophages (**Figures 5.2 & 5.5**).

Galactose is a simple sugar that can be used in cell culture as an alternative to glucose in order to highlight mitochondrial dysfunction. Galactose is converted to glucose 1-phosphate via the Leloir pathway, which involves an epimerisation reaction between UDP-galactose and UDP-glucose (447). Glucose 1-phosphate is converted to glucose 6-phosphate and enters the glycolytic pathway. The Leloir pathway requires the consumption of ATP, both for initial phosphorylation of galactose, and for the production of UDP (447). Conversion of galactose to pyruvate therefore results in no net ATP production, and as a result cellular reliance on oxidative respiration for energy generation is increased. It is also suggested that the kinetics of galactose metabolism are slower than those of glucose, resulting in a shift

towards glutaminolysis to fuel respiration (198, 448). The use of galactose is a good alternative to 2-DG for studying the impact of glycolytic inhibition. 2-DG treatment has been shown to inhibit oxidative metabolism in addition to glycolytic, resulting in reduced cell viability; whereas BMDMs grown in galactose retain full mitochondrial function and viability (197, 198). Cells with severe mitochondrial defects fail to survive culture in galactose medium due to an inability to generate energy through oxidative phosphorylation (448).

It would therefore be interesting to evaluate the effect of NDUFA4 loss in cells cultured in galactose rather than glucose, as this may highlight any respiratory deficiency caused by absence of the protein. Macrophages cultured in galactose show reduced IL-1β expression in response to bacterial infection or IFNγ treatment, consistent with results using 2-DG (197, 449). Wang *et al* also showed that glucose replacement with galactose severely impairs IFNγ-induced mROS production, HIF-1α activity, iNOS expression and NO generation (197). Unlike 2-DG treatment, glycolytic inhibition by galactose doesn't impair M2 macrophage differentiation (198). Substrate availability is an important consideration when studying metabolic processes, and is highly relevant to *in vivo* cellular regulation due to competition for metabolites between different cell populations within the tissue niche (163).

Complex IV activity

The activity of cytochrome c oxidase is highly regulated, and this complex shows developmental-, tissue- and condition-specific subunit isoform expression (366). Interestingly, NDUFA4L2 is the only hypoxia-regulated ETC subunit described to associate with complex I (366). Due to the high similarity between NDUFA4 and NDUFA4L2, and their reported reciprocal regulation, it seems unlikely that they should reside in different complexes. It is

possible that NDUFA4L2 also belongs to CIV, however upregulation of NDUFA4L2 was found to inhibit CI activity, not CIV (359).

The exquisite regulation of CIV is suggested to occur owing to its importance as the rate-limiting enzymatic step of the ETC (366). In intact cells, CIV activity is repressed by many different factors, including mitochondrial membrane potential, and as a result this complex acts as the rate-limiter of the respiratory chain under most physiological conditions (450). CIV activity is also allosterically inhibited by binding of ATP to COXIV-1, which increases the K_m of the complex for cytochrome c, and is dependent upon phosphorylation of MT-CO1 (450-452). *In vitro* measurement of CIV activity using TMPD, as I performed using the Seahorse, overcomes this inhibition by ATP, as electron transfer occurs without dissociation of cytochrome c from the complex (450, 451). Therefore if NDUFA4 affects the allosteric regulation of CIV by ATP, this would not be detected in my assays. The updated structure of CIV published by Zong *et al* shows NDUFA4 positioned adjacent to MT-CO1. This includes a close association with Tyr-304 in MT-CO1, which has been shown to be phosphorylated in response to TNFα in hepatocytes (345, 453). Therefore NDUFA4 has the potential to impact phosphorylation of this subunit, and these findings also raise the question of whether inflammatory signals regulate NDUFA4 expression in other cell types.

Another limitation of using the Seahorse to study respiratory chain activity is that, other than CIV itself, the measurements do not show individual complex activity, but instead give a readout of electron transport starting from the indicated complex, with final electron transfer to oxygen still occurring at CIV. Thus if CIV activity is rate-limiting, a treatment or condition that alters CIV function would also be expected to impact upon respiration mediated from the other three complexes. Spectrophotometric analysis of individual complex activity

would not be subject to this limitation. However this technique would require careful optimisation of cell disruption to ensure that NDUFA4 is not displaced from CIV, which has been reported upon salt treatment (347) or use of harsh detergents such as high concentrations of *n*-dodecyl-D-maltopyranoside (DDM) (280, 342, 345).

There are multiple further experiments that could be performed in order to confirm and expand upon my results on the function of NDUFA4 in macrophages, and several of these have been discussed throughout this section. In addition, I would like to verify my findings by taking the opposite approach to NDUFA4 KD, using lentiviral-mediated overexpression. Knock down of NDUFA4 alone had no effect in my assays, meaning that LPS treatment was required to stimulate cytokine production or glycolytic flux. Therefore an overexpression approach is more intuitive, given that LPS results in NDUFA4 downregulation. During this approach, it must be verified that the exogenous NDUFA4 protein is not degraded in response to LPS, as I've shown that endogenous NDUFA4 downregulation occurs in part through protein destabilisation (**Figure 4.13**).

6.7.2 Conclusions and implications

Despite the discussed caveats of the work described in this chapter, my results bring us closer to understanding the role of NDUFA4 in macrophages and the consequences of its regulation. In agreement with the known model of CIV assembly (434), but in contrast to the findings of Balsa *et al* (342), I showed that NDUFA4 is not necessary for full expression of CIV, demonstrated in NDUFA4 patient macrophages and LPS-treated controls (**Figures 6.1 & 6.16**). It would be interesting to measure the expression of other CIV subunits, including COXVI,

which was shown to be increased upon upregulation of NDUFA4 in gastric cancer cells (351), and sits in close proximity to NDUFA4 in the CIV crystal structure (345).

My finding that downregulation of NDUFA4 leads to enhanced production of IL-10 suggests a potential role for NDUFA4 in the resolution of inflammation. From a whole organism or tissue perspective, inflammatory resolution can involve the clearance of pro-inflammatory cells, which helps to restore overall homeostasis (39). On a cellular level, particularly in highly plastic macrophages, an important response downstream of an inflammatory stimulus is the activation of intrinsic anti-inflammatory/pro-resolution signalling pathways and downregulation of inflammatory gene expression. This response prevents damage caused by excessive or chronic inflammation, and is mediated by multiple negative feedback systems (39). A role in the resolution of an inflammatory response would fit with the relatively late regulation of NDUFA4 in response to TLR activation (12h onwards), however this function for NDUFA4 cannot be definitively concluded from my results due to the confounding effects of siRNA transfection on cytokine expression. It is also possible that control of cytokine production is not the major outcome of the regulation of NDUFA4 in macrophages, as there are multiple other functions that could be altered by mitochondrial remodelling. As discussed in the context of NDUFA4L2, the regulation of ROS generation is one potential consequence, however I failed to detect a robust effect of NDUFA4 KD on mROS production (**Figure 6.15**).

In contrast to a supposed role in resolution, the increase in glycolysis that occurred upon NDUFA4 KD would typically be associated with a pro-inflammatory macrophage response. However, we know that the macrophage metabolic response is not so clear cut and binary, for example macrophages also increase glucose uptake upon IL-4 stimulation (235). As

previously discussed, the precise control point of glycolysis is important for the impact on flux through branching pathways and ultimate cellular outcome, and this would also be interesting to investigate here. The mechanism by which silencing of the mitochondrial protein NDUFA4 regulates the cytoplasmic glycolytic pathway is still unknown. Despite the lack of a detectable change in mitochondrial ATP production rate (**Figure 6.14**), it is still possible that an ATP deficit from the mitochondria is the driving force for this effect, since oxidative phosphorylation is capable of generating 18x more ATP per glucose molecule than glycolysis. The technology used in these assays may not be sensitive enough to pick up such small changes in mitochondrial activity. Cellular ATP levels can also be measured more directly, for example by its use as a substrate for a luciferase or kinase reaction, producing luminescence or a colour change, respectively. However, unlike the Seahorse ATP rate assay, these methods do not distinguish the different sources of cellular ATP, thus if compensation were occurring between mitochondrial and glycolytic production, this would not be detected. Another consideration is that measurement of ATP level gives a single snapshot rather than a dynamic measure of production rates, and thus is affected by both synthesis and consumption of ATP. As ATP generation is a dynamic process that responds to cellular ATP demand as well as other environmental factors such as nutrient availability and oxygen levels, measurement of production rates is likely to give a more informative output (277).

MicroRNA-147 signalling has been reported to reduce levels of phosphorylated Akt in cancer cells (320, 454), as has the miRNA miR-7 (355), each associated with inhibition of cell growth and proliferation. The effects of miR-7 were attributed to downregulation of NDUFA4 (355). However a decrease in Akt phosphorylation and activity would be expected to cause downregulation of glycolysis, as this kinase phosphorylates and activates HK2, and also

promotes glucose uptake through endosomal trafficking of glucose transporters (455). PI3K/Akt signalling was shown to be necessary for the glycolytic shift in LPS-stimulated DCs that is required for their maturation (194). This is in contrast to the increase in glycolysis that I observed upon NDUFA4 KD, but supports the results of Cui *et al*, who reported that rescue of NDUFA4 expression increased Warburg metabolism in colorectal cancer (319). It is therefore important to confirm my observations by other methods, and it would be interesting to measure phosphoAkt in these cells. The role of Akt signalling in macrophage polarisation and function is incompletely understood, with different studies reporting differing effects of Akt modulation on M1 polarisation and inflammatory mediator production (455).

An important finding from the study of the NDUFA4 patient cells is that glucocorticoids were able to inhibit glycolytic metabolism in the absence of NDUFA4, and there was a trend towards increased mitochondrial ATP production in response to GC in all subjects, including patients (**Figure 6.18**). It is likely that NDUFA4 regulation by GCs forms only a small part of the metabolic response to the steroids, as indicated in Chapter 5. The potential contribution of NDUFA4 rescue to the metabolic action of GCs cannot be ascertained by the small sample size available from these patients.

In summary, while there is still much work to be done to ascertain the precise function of NFUFA4 in macrophages, my results have highlighted interesting areas for future focus, such as determining whether NDUFA4 plays a role in resolution of inflammation, and understanding the mechanism of glycolytic stimulation in response to silencing of this protein. The negative results that I obtained are also informative, telling us that any possible respiratory defect upon loss of NDUFA4 in macrophages is likely to be subtle, as it was not detected in my assays and culture conditions.

Chapter 7) DISCUSSION

Figure 7.1 displays a summary of the major findings of my project, during which I have outlined a molecular pathway starting from the identification of a miRNA that is regulated by glucocorticoids, to the functional consequences of the regulation of a validated miRNA target – NDUFA4. I have also begun to characterise the metabolic effects of glucocorticoids in macrophages, and have highlighted some of the differences in metabolic response that exist between human and mouse macrophages, which I believe should be more widely acknowledged within the field.

Throughout this chapter I have highlighted in bold areas of research that are ongoing or planned.
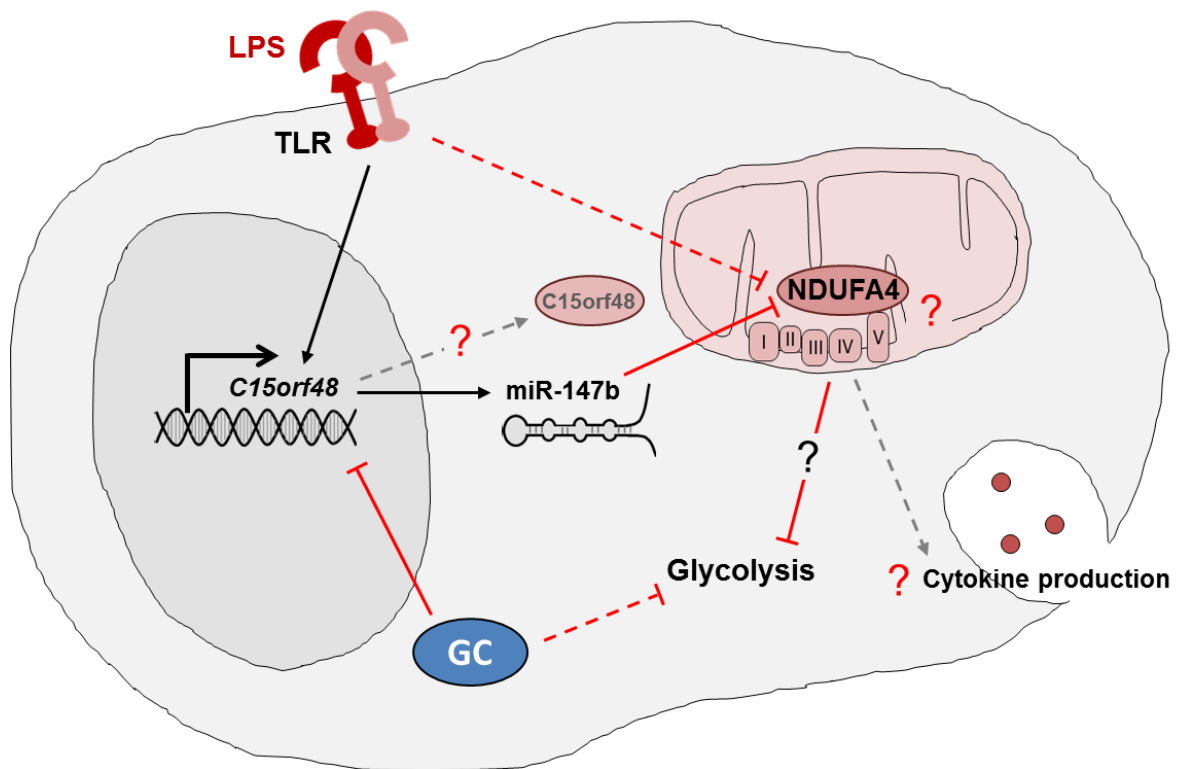
Figure 7.1) Summary: A novel microRNA signalling pathway in macrophages linking glucocorticoids and cellular metabolism

In summary, I have shown that the miRNA miR-147b, which is expressed from within the *C15orf48* gene in response to LPS, is strongly inhibited by the anti-inflammatory therapeutic glucocorticoid in macrophages. This miRNA functionally targets and downregulates NDUFA4, which is also post-translationally degraded in response to TLR activation. While the precise function of NDUFA4 within the mitochondrial electron transport chain is still incompletely understood, I have shown that silencing of NDUFA4 facilitates the macrophage glycolytic shift in response to LPS, by an as yet unknown mechanism. Silencing of NDUFA4 may also contribute to the regulation of cytokine production (for example IL-10), though this is yet to be fully characterised.

I have also shown that glucocorticoids regulate macrophage cellular metabolism, of which the rescue of NDUFA4 protein expression is likely to be just one of many mechanisms. Glucocorticoids strongly inhibit aerobic glycolysis, a function that may be related to downregulation of HIF-1α protein expression and inhibition of the GLUT1 glucose transporter.

Another intriguing twist in this story is the potential role of C15orf48 protein, which shall be discussed in this chapter.

7.1 Addressing aims and hypotheses

The original aims and hypotheses of my project are outlined in Section 1.8. I have successfully addressed the aims of Chapters 3 and 4: by identifying miRNAs regulated by glucocorticoids, validating functional targeting by miR-147b and investigating regulation of target genes. I have not exhaustively interrogated these areas, as it is highly likely that many more miRNAs are regulated by GCs in macrophages, and that there are additional functional targets of miR-147b. The microarrays that I analysed to identify miRNA targets of GCs were not designed for miRNA detection, and this meant that the number of miRNA hits was limited. I considered carrying out RNA sequencing or a miRNA-focused screen for full characterisation of the miRNA response to GC, however the identification of miR-147 as a GC target, which showed a strong and reproducible response to the steroid, gave a good lead to follow up without the additional expense of a screening experiment.

I have gone some way to fully addressing the aims of Chapters 5 and 6: to understand the metabolic regulation of macrophages by GC, and the metabolic and inflammatory roles of NDUFA4. While I have made progress in these areas, there are still many unanswered questions, which were highlighted in the relevant chapters – including elucidating the precise role of NDUFA4, and whether HIF-1α regulation is responsible for the metabolic effects of GCs. I have identified several areas of interest, which will guide future work for the interrogation of these topics.

Below I outline how I have addressed my origin hypotheses and what remains to be undertaken in order to fully prove/disprove them:

Hypothesis 1: I have shown that GCs regulate the expression of miRNAs in macrophages. I have not directly shown that this contributes to the anti-inflammatory action of GCs, due to the issues with cytokine measurement upon transfection of primary macrophages. Liu *et al* reported that miR-147 negatively regulates TNFα and IL-6 production in mouse peritoneal macrophages (10). This would suggest that miR-147 inhibition by GCs would increase expression of these pro-inflammatory cytokines. However the authors do not show reciprocal responses to miR-147 mimic and inhibitor for both cytokines under each TLR stimulation condition (10). This may be related to my results showing that inhibition of miR-147b is not sufficient to rescue NDUFA4 protein expression (**Figure 4.10B**), or the variable effects of transfection on macrophage cytokine expression.

Hypothesis 2: I have proven that GCs regulate cellular metabolism in macrophages. While I have not directly shown that this contributes to the anti-inflammatory function of GCs, it is established in the literature that glycolytic flux is important for several pro-inflammatory actions of macrophages (218), therefore glycolytic inhibition by GCs is likely to serve an anti-inflammatory function. **Understanding which aspects of GC activity are mediated through metabolic effects requires further investigation, as well as the mechanisms of this metabolic regulation.**

Hypothesis 3: I have shown that miR-147b targets and downregulates NDUFA4, and have begun to uncover the metabolic effects of NDUFA4 regulation in macrophages. **Future work to address this hypothesis would be to study the metabolic effects of miR-147b up- or down-regulation and compare these results with the regulation of NDUFA4 alone, to assess the influence of potential miR-147b-mediated targeting of additional metabolism-related genes (Figure 4.2).**

7.2 NDUFA4 and related proteins

As discussed in Chapter 6, the protein NDUFA4L2 has high sequence similarity with NDUFA4 (**Figure 7.2**), and these two proteins have been shown to be reciprocally regulated in several cell lines and cancers. NDUFA4L2 is upregulated by hypoxia and in tumour tissue, where it functions by reducing oxidative respiration and preventing ROS production and oxidative stress; while NDUFA4 is strongly downregulated in these circumstances (359, 426, 427). Despite these reports, we have found no evidence of NDUFA4L2 expression in macrophages in basal conditions, under hypoxia or upon LPS stimulation. Using HeLa cells subjected to hypoxia as the positive control based on reported expression in these cells (359), we observed no detectable expression of *NDUFA4L2* mRNA by RT-qPCR using two distinct primer sets (**Figure 7.3A**). The detection of NDUFA4L2 protein is complicated by the high similarity between this and NDUFA4, meaning that most commercial antibodies cannot discriminate between the two proteins. **Figure 7.3B** shows antibody testing for NDUFA4L2 in NDUFA4 siRNA-transfected samples. This blot suggests that only NDUFA4 is detected by both NDUFA4L2 antibodies in human macrophages. **More rigorous testing to confirm this is underway.**

A potentially intriguing twist to this story is the finding that the protein product of the gene *C15orf48* (aka NMES1), which encodes miR-147 from its 3'UTR, also shows sequence similarity to NDUFA4 (**Figure 7.2**). A study from Floyd *et al* characterised protein-protein interactions of a number of mitochondrial proteins that lack functional annotation. One such protein was C15orf48, and they reported that this protein interacts with subunits of complexes I, III, and IV (456) – a result strikingly similar to our knowledge of NDUFA4. These revelations only became known to us while I was in the final stages of my project, and until

then we were working under the knowledge of limited known function for the protein product of this gene, other than its downregulation in some cancers (309-312).

The transcript of *C15orf48* is highly induced upon inflammatory stimulation of macrophages (**Figure 3.5C** – pri-mir-147b); in astrocytes upon treatment with IL-1β (308); in whole blood of patients infected with dengue virus (307); and in bronchial epithelial cells upon rhinovirus infection (306). We have also found it to be highly induced in RA synovial fibroblasts upon treatment with TNFα (**Figure 7.4**). Antibody testing for C15orf48 detection is also being performed. Preliminary results are promising (**Figure 7.3B**), showing low basal expression and induction by LPS in macrophages. **Once detection is fully validated, we will interrogate the regulation, localisation and function of this protein alongside NDUFA4. The effects of GCs on this protein should also be examined, based on the known inhibition of *C15orf48* mRNA and miR-147 expression.**

A CLUSTAL O(1.2.4) multiple sequence alignment

```
NDUFA4      -----MLRQIIGQAKKHPSLIPLFVFIGTGATGATLYLLRLALFNPDVCWDR-NNPEPWN      54
NDUFA4L2    MAGASLGARFYRQIKRHPGIIPMIGLICLGMGSAALYLLRLALRSPDVCWDRKNNPEPWN      60
                :    ::   * *:**.:**:: :*   *   .*:.******** .******* *******

NDUFA4      KLGPNDQYKFYSVNVDYSKLKKERPDF      81
NDUFA4L2    RLSPNDQYKFLAVSTDYKKLKKDRPDF      87
            :*.******* :*..**.****:****
```

B CLUSTAL O(1.2.4) multiple sequence alignment

```
NDUFA4      MLRQIIGQAKKHPSLIPLFVFIGTGATGATLYLLRLALFNPDVCW-DRNNPEPWNKLGPN      59
C15orf48    --MSFFQLLMKRKELIPLVVFMTVAAGGASSFAV-YSLWKTDVILDRKKNPEPWETVDPT      57
              .::     *: .****.**: ..* **: : :  :*:: **   :.*****:...*.

NDUFA4      DQYKFYSVNVDYSKLKKERPDF----      81
C15orf48    VPQKLITINQQWKPIEELQNVQRVTK      83
            *: ::* ::. ::: :
```

C CLUSTAL O(1.2.4) multiple sequence alignment

```
C15orf48    -------MSFFQLLMKRKELIPLVVFMTVAAGGASSFA-VYSLWKTDVILDRKKNPEPWE      52
NDUFA4      -----MLRQIIGQAKKHPSLIPLFVFIGTGATGATLYLLRLALFNPDVCWDR-NNPEPWN      54
NDUFA4L2    MAGASLGARFYRQIKRHPGIIPMIGLICLGMGSAALYLLRLALRSPDVCWDRKNNPEPWN      60
                 :      ::  :**:. ::   . .*: :    :* . **   ** :*****:

C15orf48    TVDPTVPQKLITINQQWKPIEELQNVQRVTK   83
NDUFA4      KLGPNDQYKFYSVNVDYSKLKKERPDF----   81
NDUFA4L2    RLSPNDQYKFLAVSTDYKKLKKDRPDF----   87
            ::*.   *: ::. ::. ::: :
```

D
```
1: C15orf48     100.00    29.49    24.05
2: NDUFA4        29.49   100.00    61.73
3: NDUFA4L2      24.05    61.73   100.00
```

Figure 7.2) NDUFA4, NDUFA4L2 and C15orf48 amino acid sequence alignment

Run using Clustal Omega v1.2.4 Multiple Sequence Alignment; **A)** NDUFA4 vs NDUFA4L2; **B)** NDUFA4 vs C15orf48; **C)** NDUFA4 vs NDUFA4L2 vs C15orf48; **D)** Percentage sequence identity matrix.

Symbol and colour definitions from Clustal Omega: * (asterisk) indicates positions which have a single, fully conserved residue; : (colon) indicates conservation between groups of strongly similar properties; . (period) indicates conservation between groups of weakly similar properties; RED: Small (small+ hydrophobic (incl.aromatic -Y)); BLUE: Acidic; MAGENTA: Basic – H; GREEN: Hydroxyl + sulfhydryl + amine + G.
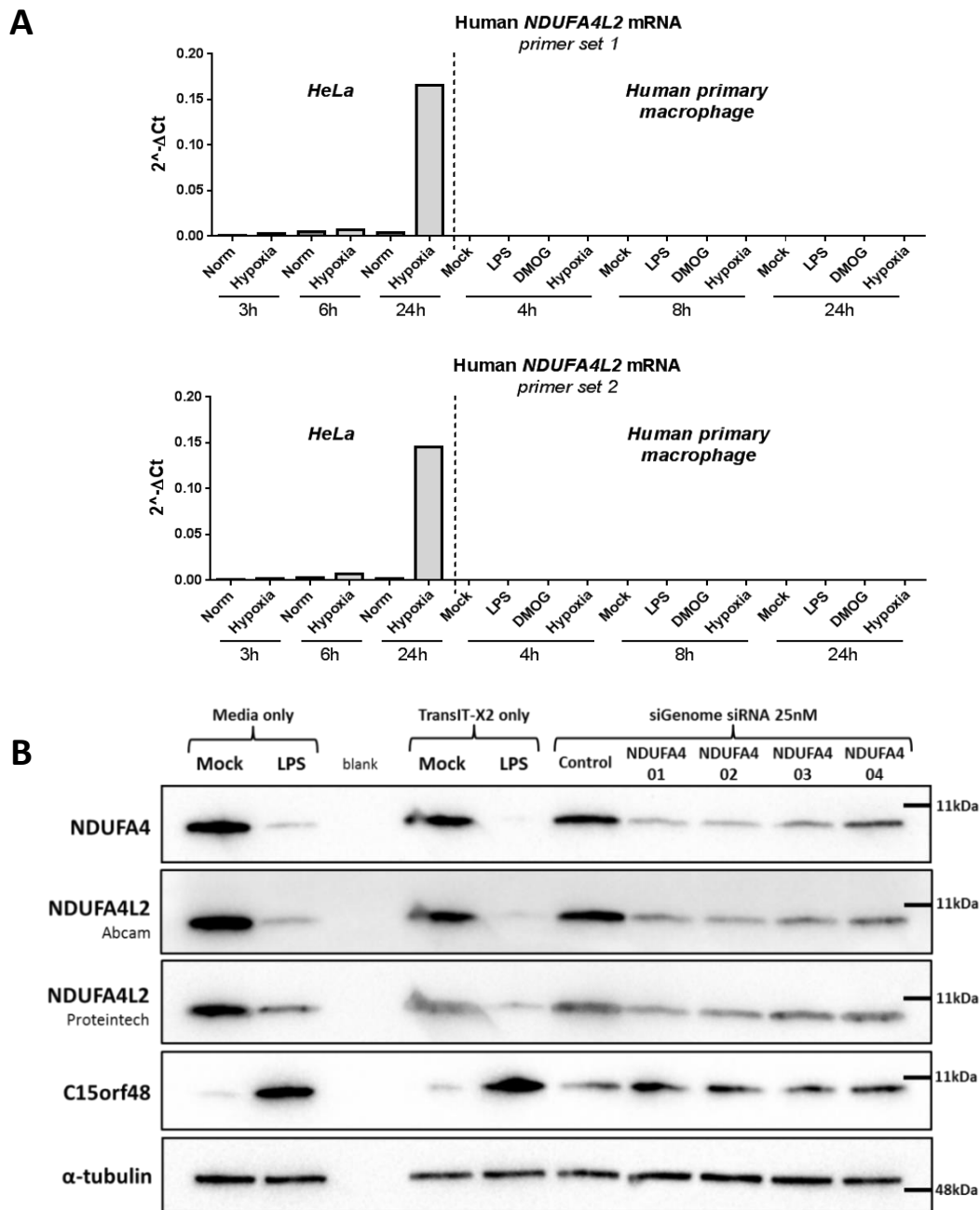
Figure 7.3) Reagent testing for NDUFA4L2 and C15orf48

Data generated by myself, Kalbinder Daley and John O'Neil

A) HeLa cells were cultured in normoxia (norm) or hypoxia (1% O_2) for the indicated times. Human monocyte-derived macrophages were mock, LPS or DMOG-treated (under normoxia), or subjected to hypoxia (1% O_2) for the indicated times. *NDUFA4L2* mRNA was detected using two different primer sets by RT-qPCR; displayed as 2^-ΔCt normalised to UBC; n=1 (mean of technical replicates).

B) Antibodies against NDUFA4L2 and C15orf48 were tested by Western blot in samples from NDUFA4 siRNA-transfected human monocyte-derived macrophages (**see Figure 6.4**); 25nM siRNA, TransIT-X2, cells were harvested 48h after transfection; LPS stimulation applied 24h prior to harvest; n=1.
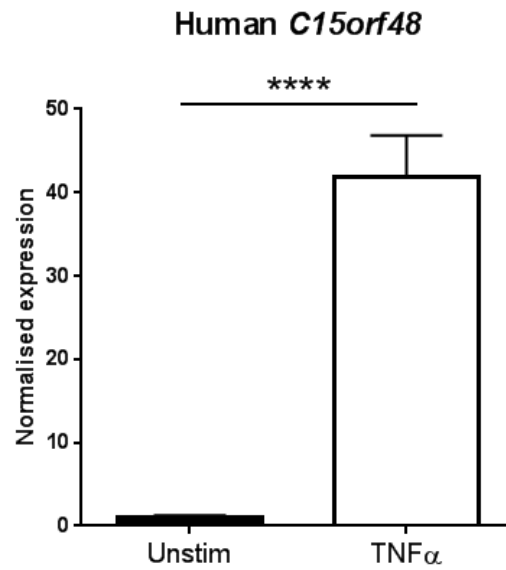
Figure 7.4) Induction of *C15orf48* mRNA in rheumatoid arthritis FLS

Data generated by Maria Juarez, Andrew Filer & Jason Turner

Microarray data of *C15orf48* expression in rheumatoid arthritis fibroblast-like synoviocytes (FLS) either unstimulated or treated with TNFα in culture for 24h. Expression data normalised to internal control and displayed relative to the unstimulated samples; Unstim n=48, TNFα n=45; Two-tailed t test; Data presented as mean +SEM.

Analysis of publicly available single cell RNA sequencing data generated by Zhang *et al* from osteoarthritis (OA) and rheumatoid arthritis (RA) synovial biopsies allowed us to map the expression of *NDUFA4, NDUFA4L2* and *C15orf48* in cell populations of the joint (**Figure 7.5**) (4). *NDUFA4* is broadly expressed across all cell types, including the monocyte/macrophage cluster. *NDUFA4L2* expression is restricted almost exclusively to the fibroblast cluster, while *C15orf48* is primarily expressed in the monocyte/macrophage cluster. These results were confirmed by analysis of bulk RNAseq from the same study (**Figure 7.6**). Single cell RNAseq identified *C15orf48* to be most highly expressed in two particular monocyte subsets in both disease types, which were characterised by either IL-1β expression or an IFN-stimulated gene signature. These populations were generally considered to be pro-inflammatory-type macrophages, but the role of *C15orf48* in these cells cannot be concluded from these data. The caveat of this analysis is that the study of transcript levels does not take into account post-translational regulation, which I and others have shown is highly relevant for determining NDUFA4 protein levels (*Chapter 4*) (359).

The combination of these findings, along with my data, alludes to an elegant system in which inflammatory stimulation triggers expression of the *C15orf48* gene, encoding both a protein product and miR-147. The miRNA then mediates downregulation of NDUFA4, allowing the C15orf48 protein product to replace it. This is still speculative, and ongoing work will address this hypothesis. These suppositions also bring into question the use of simple NDUFA4 KD/KO experiments, as replacement with a related protein (NDUFA4L2 or C15orf48) may be necessary to witness the functionality that occurs in response to inflammatory challenge.
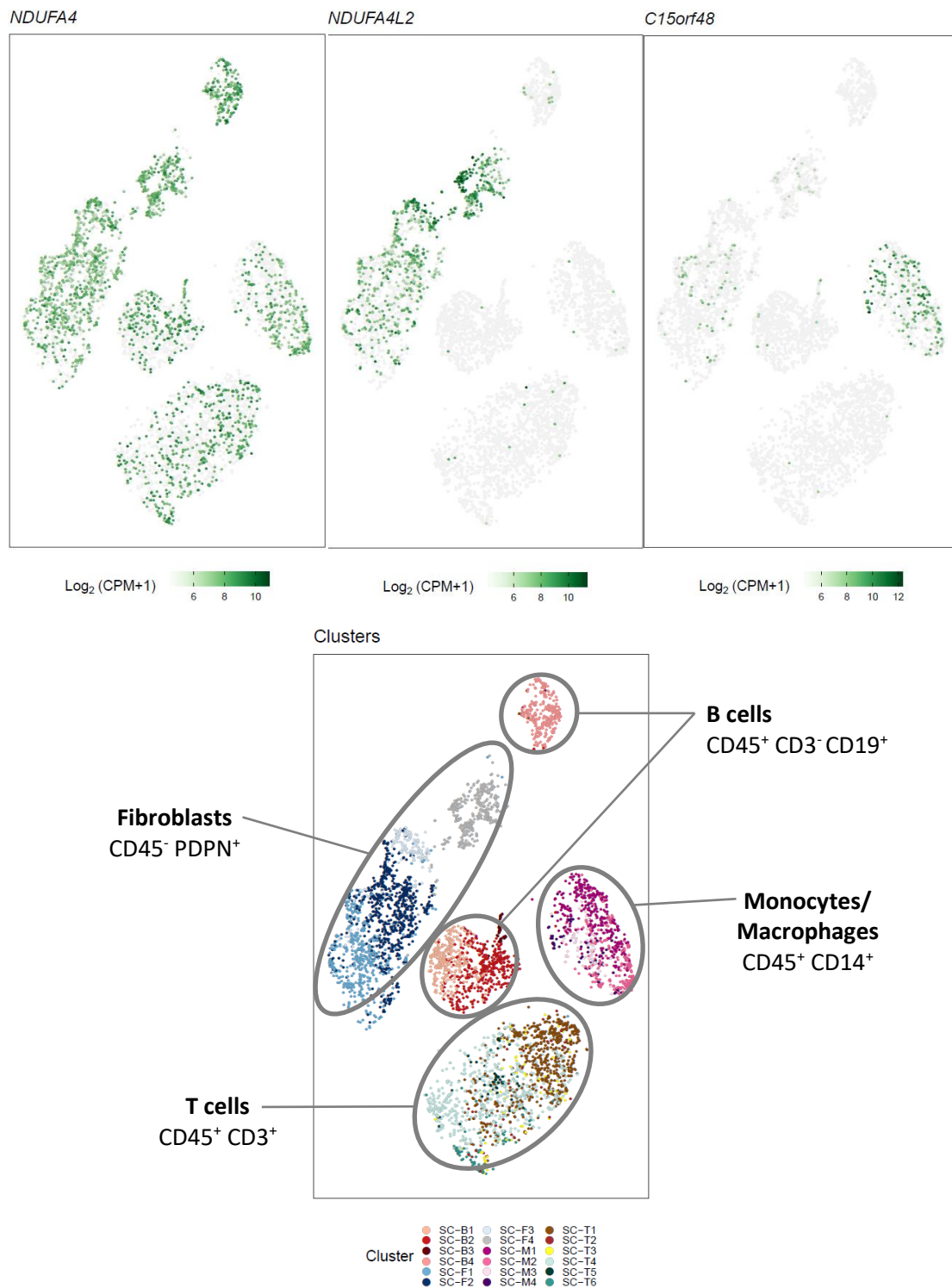
Figure 7.5) scRNA-Seq of arthritis synovial biopsies – *NDUFA4*, *NDUFA4L2* & *C15orf48*

Data generated by Zhang et al (4); Data mining and figure production performed by Jason Turner using modified scripts from Zhang et al.

The indicated cell types were sorted from 51 osteoarthritis and rheumatoid arthritis synovial biopsies and subjected to single cell RNA sequencing, identifying unique cell populations. Data were analysed for expression of *NDUFA4* and the related genes *NDUFA4L2* and *C15orf48*.
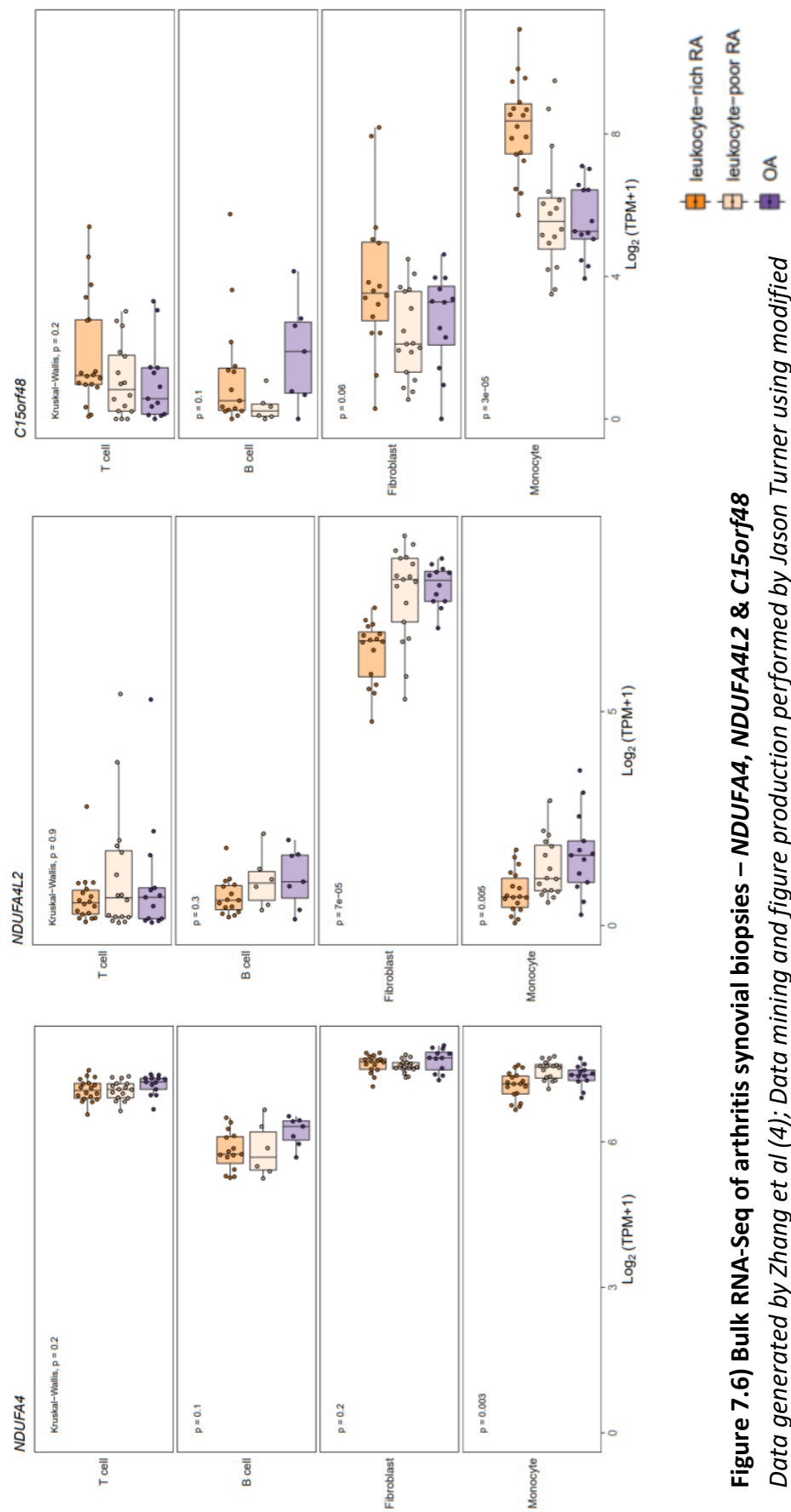
Figure 7.6) Bulk RNA-Seq of arthritis synovial biopsies – *NDUFA4, NDUFA4L2 & C15orf48*

Data generated by Zhang et al (4); Data mining and figure production performed by Jason Turner using modified scripts from Zhang et al.

The indicated cell types were sorted from synovial biopsies of osteoarthritis patients (OA, n=15) and rheumatoid arthritis (RA) patients classified as leukocyte-rich (n=19) and leukocyte-poor (n=17). Cell populations were classified based on the expression markers indicated in **Figure 7.4**. The cells were subjected to bulk RNA sequencing. Data were analysed for expression of *NDUFA4* and the related genes *NDUFA4L2* and *C15orf48*.

7.3 The role of NDUFA4 and broader implications

As discussed, NDUFA4 is a poorly studied gene, which has only recently been re-assigned as a component of CIV instead of CI (342). Understanding the role of this protein in the macrophage response to inflammatory challenge became a major focus of my project after its validation as a target of miR-147b. I found that downregulation of NDUFA4 leads to enhanced glycolytic flux and IL-10 production in response to LPS. However regulation of this protein is not required for the LPS-induced glycolytic shift in macrophages, as demonstrated in the patient samples.

7.3.1 NDUFA4 in inflammatory disease

Published report of NDUFA4 regulation in inflammatory diseases is limited to the single study showing that lower pre-treatment *NDUFA4* mRNA in circulating cells was associated with better response to the biologic therapy abatacept in RA patients (353). The analysis of RNAseq data from Zhang *et al* (**Figure 7.5**) showed that the *NDUFA4* transcript is expressed in all studied cell clusters from the joint (4). However it would be interesting to examine NDUFA4 protein levels in synovial tissue, as I saw almost complete loss of NDUFA4 protein with only a 50-60% decrease in mRNA levels in LPS-treated macrophages (Chapter 4). Activation of TLRs has been shown to occur in RA, instigated by DAMPs including endogenous nucleic acids from necrotic cells, or degraded extracellular matrix components; or instigated by microbial components, which have been detected in rheumatoid joints and can precipitate disease or flare (1, 457). NDUFA4 is downregulated by stimulation of multiple different TLRs, therefore this could occur within the rheumatoid synovium. It is also well-established that the inflamed joint is a highly hypoxic environment, which drives HIF-1α expression in synovial cells including fibroblasts, macrophages and T cells, and precipitates a glycolytic, pro-inflammatory state

(202, 419). This further suggests that NDUFA4 protein may be downregulated in RA, as loss of this protein is induced by hypoxia (359).

Figure 7.6 displays additional analysis of data from Zhang *et al* (4), and shows a small but statistically significant decrease in *NDUFA4* transcript levels in synovial monocytes from patients with leukocyte-rich RA (defined by high numbers of T and B cells and high inflammation scores) compared with leukocyte-poor RA or OA. The same cell population showed a significant increase in levels of *C15orf48* transcript. These results provide a possible pathophysiological context for the hypothesis of switching between these proteins in myeloid cells. **In addition to examining the expression of NDUFA4 and C15orf48 proteins in RA patients, it would be interesting to study the effects of steroid treatment on the levels of these proteins (for example in circulating monocytes), as this would be a clinically relevant progression from my *in vitro* work.**

The targeting of metabolic pathways in inflammatory conditions such as RA has showed therapeutic value in disease models, and also through our increased understanding of the metabolic effects of current therapies (419, 458). Therefore a greater knowledge of the metabolic alterations that occur during disease processes will enhance our understanding of how to appropriately treat patients.

7.3.2 A role in supercomplexes?

One specific function that has been suggested for NDUFA4 is in the formation of supercomplexes, due to its apparent association with several individual respiratory chain complexes (343). While the precise physiological function of supercomplex formation is not definitively known, proposed roles include increasing efficiency of electron flow by decreasing

diffusion distances for electron carriers or through electron carrier "channelling"; reducing ROS production at the ETC due to the increased electron flow efficiency; and assisting in stabilisation and assembly of individual complexes, particularly CI (459). Supercomplex formation has also been shown to regulate relative use of different substrates, for example by favouring electron transfer via CI (from NADH) or CII (from $FADH_2$). It has therefore been demonstrated that fasting can alter the relative assembly of supercomplexes (460). This could have implications for the use of alternative fuel sources for *in vitro* cell culture with relation to NDUFA4 and supercomplex study. Decreases in supercomplex abundance and increased ROS production have been associated with disease processes including heart failure and ischemia-reperfusion injury, although the precise contribution of supercomplex loss has not been fully determined (459).

Very little work has been carried out to look at supercomplex dynamics in immune cells. As discussed in Chapter 6, Garaude *et al* report that treatment of macrophages with *E. coli* reduced the abundance of CI-containing supercomplexes, but this was only examined soon after infection (within 2h), so does not indicate a role for NDUFA4. **A future plan is to examine the role of NDUFA4 in macrophage supercomplexes**. A complicating factor for this investigation is the finding that C57BL/6J and Balb/cJ mice possess a shortened form of the supercomplex assembly factor COX7A2L (also known as SCAFI), and as a result these mice do not incorporate CIV into their supercomplexes (460). This will have to be taken into consideration for experimental assessment of supercomplexes. If NDUFA4 does play a role in supercomplex formation or stability, this could have potential implications for macrophage mROS production, and therefore microbial killing and inflammatory signalling.

7.3.3 Resolution, tolerance and trained immunity

The relatively late regulation of NDUFA4, and its effect on IL-10 production, point towards a potential role in the intrinsic resolution phase that follows pro-inflammatory macrophage activation. This field lacks a complete understanding of metabolic adaptations and drivers that underlie these resolution processes, and establishing whether NDUFA4 contributes to these adaptations could help in the understanding of why the switch to resolution is often deficient in chronic inflammatory conditions (39).

The macrophage inflammatory response has been described to progress from an early initiation phase, driven by glycolysis, to a late adaptation phase, in which glycolysis is replaced by fatty acid oxidation (420). These phases are mediated by HIF-1α-dependent GLUT1 expression, and PGC1-dependent fatty acid uptake, respectively, and regulated by NAD+-dependent deacetylates (420). Further understanding of metabolic contribution to resolution includes the lipid metabolism for the production of pro-resolution signalling mediators such as lipoxins (461); and the action of itaconate, which is produced following TLR activation and has anti-inflammatory properties (219, 224, 225).

Itaconate has also been implicated in the development of endotoxin tolerance - a state of reduced responsiveness to secondary stimulation (228, 462). The distinction between resolution of inflammation and induction of tolerance is not very clearly defined, and many of the mechanisms are likely to be mutual, but tolerance involves persistence of the anti-inflammatory programming. Another related phenomenon that also relies upon metabolic adaptation is trained immunity, which involves an enhanced response to a second stimulus following an initial immunostimulatory encounter (463). The induction of the functionally opposing programs of tolerance or training is dependent upon the nature of the initial

stimulant. For example, LPS induces the production of itaconate and subsequent immune tolerance, while β-glucan inhibits itaconate synthesis and thereby promotes a trained phenotype. Due to this balance, itaconate has been described as a central node in long-term immune cell reprogramming (229).

Both tolerance and trained immunity involve interplay between metabolic and epigenetic adaptations. For example fumarate, produced in the TCA cycle from glutamine, inhibits histone demethylation at promoters of inflammation-associated genes; and acetylCoA, produced from glycolytic or TCA cycle metabolites, is an important substrate for histone acetylation. Therefore disruption of either glutaminolysis or glycolysis was found to reverse training-associated epigenetic marks and attenuate the secondary response (463, 464). HIF-1α signalling has also been shown to be important for innate immune training, driving glycolytic metabolism and inflammatory gene expression (465). **It would be interesting to determine the effects of glucocorticoids on the induction of trained immunity, given their metabolic impact.**

The NDUFA4-KD experiments that I performed better simulate a repeat infection model such as those used for the study of trained immunity or tolerance, rather than informing of the acute effect of NDUFA4 loss, since the initial silencing of NDUFA4 was followed by LPS challenge. The increased IL-10 production observed in these experiments (**Figure 6.9**) could represent either a trained or tolerant phenotype of the NDUFA4-KD cells, as trained immunity is associated with a general increase in responsiveness, including both pro- and anti-inflammatory cytokines (463). Enhanced glycolytic response to secondary stimulation, such as I saw after NDUFA4 KD, is also a hallmark of trained immunity. **Reliable measurement of additional cytokines would be useful to support this theory, and it would**

be interesting to establish the impact of known training stimuli such as β-glucan on the expression of NDUFA4 (and C15orf48).

7.3.4 Metabolic basis of sepsis

Related to the development of immune tolerance, and perhaps a more obvious clinical association to TLR activation, is sepsis - a serious condition involving a dysregulated systemic inflammatory response to infection, resulting in multi-organ dysfunction and risk of mortality (466). The immune response to infection in sepsis comprises a complex two-phase pathology. An initial exaggerated inflammatory response is followed by a prolonged period of immune paralysis, resulting in an increased susceptibility to secondary infection, which is often the cause of mortality (467, 468). The precise cause of the chronic immunosuppression is unclear, but potential contributing mechanisms include apoptosis of inflammatory cells, as reported for T cells (469); and an extended period of endotoxin tolerance, mediated in part by elevated *Irg1* expression and itaconate synthesis (228). The most widely reported cytokines involved in sepsis are TNFα and IL-1β, however the direct targeting of these cytokines is not clinically beneficial (467).

Metabolic alterations, particularly in monocytes, are pivotal to the dysregulated immune response in sepsis (207, 468). HIF-1α has been shown to be critical for the excessive inflammatory response, and macrophage deletion of HIF-1α protected mice against LPS-induced sepsis (207). AMPK is also an important regulator of immune metabolism in sepsis, and pharmacological activation of AMPK was shown to protect mice from lethal endotoxic shock (470, 471). Metabolic alterations associated with endotoxin tolerance have been demonstrated in blood monocytes from late-stage sepsis patients (228, 420, 468, 472).

Ongoing work on the study of NDUFA4 in the immune response involves the collection of blood samples from sepsis patients, enabling measurement of NDUFA4 (and C15orf48) protein in blood monocytes. The results may be complicated by the intricate two-stage nature of the immune response during sepsis, but will give an indication of the regulation of these proteins in response to infection and inflammation *in vivo.*

Glucocorticoids have been used to treat septic shock since the early 1950s (473, 474), however a number of recent studies have reported adverse effects of GC use in sepsis, including increased risk of superinfection (474). My results regarding the metabolic effects of GCs could explain some of the beneficial effects, as the HIF-1α inhibition that I observed may replicate the protective effect of *Hif1a*-deletion in mouse models (207). However these reports also highlight the differences between preventative measures and treatment approaches, *i.e.* deletion of the *Hif1a* gene prior to immune challenge was successful for preventing disease, but inhibition of HIF-1α by GCs after the establishment of sepsis may pose a major threat by contributing to immunosuppression.

7.3.5 Immune phenotype of NDUFA4 patients

The patients suffering from a debilitating neuromuscular condition due to mutation of the *NDUFA4* gene have not been reported to exhibit immunological or inflammatory dysfunction. This observation brings into question the importance of this protein in immune cell function, despite the dramatic response to TLR stimulation that I have demonstrated. There are several possible explanations, including the potential differences between acute and chronic loss of the protein. Another possible explanation is that the C15orf48 protein may compensate for the loss of NDUFA4 in immune cells of these patients - assuming the speculation for a related function is correct. **I therefore plan to measure expression of**

C15orf48 in samples from NDUFA4 patient macrophages. The expression of *C15orf48* RNA is more tissue-restricted than NDUFA4, and global expression analysis shows no/very little expression in the brain or muscle, which could explain the lack of compensatory mechanisms for NDUFA4 loss in these tissues (280, 475, 476).

Alternatively, it is possible that some of the symptoms of the NDUFA4-linked Leigh syndrome have underlying inflammatory drivers. One of the major symptoms is severe and debilitating seizures, and epileptic seizures have been related to the presence of neuroinflammation, mediated in part by cytokines such as IL-1β and IL-6. Inflammatory signalling pathways in the brain are being explored as potential biomarkers or targets for the treatment of epilepsy (477). This implicates the resident brain macrophage population, microglia, in the symptoms of NDUFA4-linked Leigh syndrome. These tissue-resident macrophages, which are established *in utero* (discussed in Chapter 1), serve a number of functions for the maintenance of neuronal health and function, as well as CNS development (478). If NDUFA4 protein loss skews microglia to a more hyper-responsive inflammatory phenotype, the resulting neuroinflammation could underlie the severe seizures, and possibly other symptoms, of the patients. **It would therefore be interesting to establish whether microglia express NDUFA4, how it is regulated in these cells, and how cellular function is affected by NDUFA4 loss.** Monocytes can also infiltrate the CNS during pathology, which would supply an alternative or additional source of neuroinflammation, however the precise contribution and persistence of these cells is poorly studied (478).

Microglia have also been demonstrated to exhibit immune memory in the form of either training or tolerance, which had opposing effects on disease severity in models of neuropathology, including Alzheimer's disease (479). Therefore, if NDUFA4 regulation

contributes to the development of innate memory in myeloid cells, this could impact the development of neurodegenerative disorders, with which NDUFA4 downregulation has been linked (182, 350, 351).

7.3.6 NDUFA4 in other cell types

NDUFA4 is ubiquitously expressed, and shows highest RNA expression in the heart and skeletal muscle, likely due to the high mitochondrial content of these tissues. *NDUFA4* RNA is also highly expressed in most regions of the brain, and in most types of blood leukocyte - particularly basophils and eosinophils, dendritic cells, all classes of monocyte, and T cells (highest in CD4+ and Treg populations) (475, 476). We know from my results that the mRNA and protein expression of NDUFA4 are differentially regulated, but thorough expression mapping of this protein is currently lacking (475). A draft human proteome map published by Kim *et al* in 2014 analysed 17 adult tissues, 7 fetal tissues, and 6 haematopoietic cell types. This showed highest expression of NDUFA4 protein in the heart, liver, kidney, frontal cortex, testis and monocytes (480, 481).

Despite the global expression of this protein, knowledge of its regulation in various cell types is generally lacking. As discussed, NDUFA4 is known to be downregulated by hypoxia in various cell types in culture (359), which could have relevance to many physiological processes, and may be the driver of NDUFA4 downregulation reported in certain cancers (*discussed in Section 6.1.2*) (426, 427). Conversely, NDUFA4 was reported to be upregulated in gastric cancer (351), and colorectal cancer (319), with complex regulation in these tumours involving antagonistic actions of lncRNA and miRNA species. Neither of these papers addressed the topic of the similarity between NDUFA4 and NDUFA4L2 and their reported reciprocal regulation, however they demonstrated downregulation of the measured protein

by miR-147b or miR-212, neither of which is predicted to target NDUFA4L2. Studies of these proteins in cancer cell lines *in vitro* should be approached with caution, however, as cell culture is generally performed at normoxia, while the tumour *in situ* may be subject to hypoxia, which alters the expression of both NDUFA4 and NDUFA4L2 (359).

The reported downregulation of NDUFA4 in blood and brain of Alzheimer's disease patients (182, 350, 351), as well as the neurological symptoms of the NDUFA4-related Leigh syndrome (280), indicate that this protein plays an important role in maintaining proper brain function and homeostasis. Mitochondrial dysfunction is being increasingly implicated in the development and progression of neurodegenerative diseases (482). Of relevance is the finding that *in vitro* LPS+IFN-γ treatment of mouse astrocytes (another important subset of glial cells in the CNS that contributes to neuronal survival and function) leads to upregulated expression of miR-147 (483). This suggests that NDUFA4 may be downregulated in several different cell types within the CNS, and it may be pertinent to understand which of these cell types contributed to the results of Adav *et al*, who reported downregulation of NDUFA4 protein in the medial frontal gyrus (frontal cortex) of Alzheimer's disease patients (182).

Therapeutic targeting of mitochondrial components is being studied for the treatment of diseases including cancer and neurodegenerative diseases (482, 484). The ubiquitous expression of NDUFA4 means that any potential therapeutic manipulation of this protein would have to be highly targeted in order to prevent unwanted side effects in numerous other tissues. Such effects in the heart and brain would be particularly undesirable. The high similarity between NDUFA4 and related proteins would also make specific targeting of one of these proteins difficult. However, understanding how this protein contributes to mitochondrial function and immune cell activity will help to advance our knowledge of how

these systems can become dysregulated during disease development. The involvement of mitochondrial dysfunction in immune disorders is a rapidly growing area of research, linking the fields of mitochondrial biology and immunology (457). Continued collaboration between experts in these fields, as well as the training of cross-discipline researchers will be important for progressing our understanding of complex physiological processes and diseases.

7.4 Implications of the metabolic effects of glucocorticoids

I have already addressed some of the implications of GC-mediated targeting of macrophage metabolic processes, for example for the effects of these steroids in sepsis. In terms of our broader aims to be able to uncouple the beneficial anti-inflammatory properties of GCs from their unwanted side effects, my findings in this area suggest some potentially very important but unwelcome implications. During the ongoing quest to dissociate these aspects of GC action, we have come to understand that a complete separation of transactivatory and transrepressive activity of the GR is unlikely to achieve the desired results (56). However, the opinion has endured that separate on- and off-target effects are mediated by separate targeting events of the receptor, *i.e.* due to regulation of disparate gene targets. My results bring this into question, suggesting that many of the anti-inflammatory actions of GCs, in addition to the side effects in metabolic tissues, occur due to the targeting of metabolic components.

These assumptions appear to make sense with regard to the evolution of the endogenous GC hormone cortisol, which functions to regulate systemic homeostasis during times of stress. From an evolutionary perspective, a major stress factor that needs to be counteracted is nutrient deprivation, resulting in the pleiotropic effects of GCs on metabolic

tissues. The immune response is highly energy-demanding, driven primarily by anabolic processes that fuel biosynthesis of effector molecules and leukocyte proliferation. Therefore during times of nutrient deprivation it may be detrimental to mount a significant immune response at the expense of other vital physiological processes. Thus a single hormone evolved that is responsible for the suppression of inflammation, in addition to the upregulation of catabolic processes, such as glycogenolysis in muscle and lipolysis in adipose tissue, and simultaneous suppression of nutrient storage. In a recent review article, Wang *et al* postulated that cellular control of metabolism, such as in immune cells, mirrors systemic metabolic regulation and evolutionary life history. This dictates that organisms and cells favour either growth and reproduction (proliferation) or maintenance (quiescence), depending upon the environment (485). These concepts particularly resonate with the study of glucocorticoids, which control metabolic processes on both cellular and systemic levels, and are central regulators of maintenance pathways and stress resistance.

In addition to systemic regulation of cortisol synthesis and release, which involve multiple negative feedback systems, cells are also able to control their own exposure to cortisol through regulated and tissue-specific expression of the GC-activating enzyme 11β-HSD1 (60, 486). Cells also control their sensitivity to activated GC by regulated expression of the GR, for example by miRNAs (2). These mechanisms likely enable the cell to fine tune its response to systemic GC release based on the local microenvironment. My experiments did not address the action of 11β-HSD1, as dexamethasone doesn't require activation. However it would be interesting to see if this enzyme is controlled by the cellular metabolic state in macrophages, as it has previously been shown to be inhibited by HIF-1α in adipose tissue (487). This could identify a system of two-way communication between macrophage

metabolism and GC signalling, similar to the increasingly described cross-talk between metabolic pathways and the pro-inflammatory response.

Overall, a metabolic role for glucocorticoids in macrophages is not surprising, based on what we now know about macrophage inflammatory regulation through metabolic pathways, and the well-established role of GCs in systemic metabolism. However, if these metabolic effects are found to be necessary for the anti-inflammatory function of GCs, the separation of beneficial and unwanted effects is likely to be even more difficult than previously thought. Therefore continued work is needed on cell type-specific effects of GCs to identify novel mechanisms of therapeutic intervention, or methods to more efficiently and selectively target GCs to the effector cells of inflammation. In the meantime it is likely that we will continue to utilise these antique therapeutics due to their highly effective nature, while being mindful of the note of caution that continues to accompany their use.

REFERENCES

1.   Joosten LAB, Abdollahi-Roodsaz S, Dinarello CA, O'Neill L, Netea MG. Toll-like receptors and chronic inflammation in rheumatic diseases: new developments. Nat Rev Rheumatol. 2016;12(6):344-57.

2.   Clayton SA, Jones SW, Kurowska-Stolarska M, Clark AR. The role of microRNAs in glucocorticoid action. J Biol Chem. 2018;293(6):1865-74.

3.   Udalova IA, Mantovani A, Feldmann M. Macrophage heterogeneity in the context of rheumatoid arthritis. Nat Rev Rheumatol. 2016;12(8):472-85.

4.   Zhang F, Wei K, Slowikowski K, Fonseka CY, Rao DA, Kelly S, et al. Defining inflammatory cell states in rheumatoid arthritis joint synovial tissues by integrating single-cell transcriptomics and mass cytometry. Nat Immunol. 2019;20(7):928-+.

5.   Takeuchi O, Akira S. Pattern Recognition Receptors and Inflammation. Cell. 2010;140(6):805-20.

6.   Kramer MF. Stem-loop RT-qPCR for miRNAs. Curr Protoc Mol Biol. 2011;Chapter 15:Unit 15.0.

7.   Oosting M, Cheng SC, Bolscher JM, Vestering-Stenger R, Plantinga TS, Verschueren IC, et al. Human TLR10 is an anti-inflammatory pattern-recognition receptor. Proc Natl Acad Sci U S A. 2014;111(42):E4478-E84.

8.   Cain DW, Cidlowski JA. Immune regulation by glucocorticoids. Nature Reviews Immunology. 2017;17(4):233-47.

9.   Astakhova IK, Wengel J. Scaffolding along Nucleic Acid Duplexes Using 2 '-Amino-Locked Nucleic Acids. Accounts Chem Res. 2014;47(6):1768-77.

10.   Liu G, Friggeri A, Yang YP, Park YJ, Tsuruta Y, Abraham E. miR-147, a microRNA that is induced upon Toll-like receptor stimulation, regulates murine macrophage inflammatory responses. Proc Natl Acad Sci U S A. 2009;106(37):15819-24.

11.   Murphy K, Weaver C. Janeway's immunobiology2017.

12.   Wynn TA, Chawla A, Pollard JW. Macrophage biology in development, homeostasis and disease. Nature. 2013;496(7446):445-55.

13.   Hume DA. Macrophages as APC and the dendritic cell myth. J Immunol. 2008;181(9):5829-35.

14.   Gautier EL, Shay T, Miller J, Greter M, Jakubzick C, Ivanov S, et al. Gene-expression profiles and transcriptional regulatory pathways that underlie the identity and diversity of mouse tissue macrophages. Nat Immunol. 2012;13(11):1118-28.

15.   Davies LC, Jenkins SJ, Allen JE, Taylor PR. Tissue-resident macrophages. Nat Immunol. 2013;14(10):986-95.

16.   Ginhoux F, Guilliams M. Tissue-Resident Macrophage Ontogeny and Homeostasis. Immunity. 2016;44(3):439-49.

17.   Ginhoux F, Greter M, Leboeuf M, Nandi S, See P, Gokhan S, et al. Fate Mapping Analysis Reveals That Adult Microglia Derive from Primitive Macrophages. Science. 2010;330(6005):841-5.

18.   Yona S, Kim KW, Wolf Y, Mildner A, Varol D, Breker M, et al. Fate Mapping Reveals Origins and Dynamics of Monocytes and Tissue Macrophages under Homeostasis. Immunity. 2013;38(1):79-91.

19.   Lavin Y, Winter D, Blecher-Gonen R, David E, Keren-Shaul H, Merad M, et al. Tissue-Resident Macrophage Enhancer Landscapes Are Shaped by the Local Microenvironment. Cell. 2014;159(6):1312-26.

20.   van de Laar L, Saelens W, De Prijck S, Martens L, Scott CL, Van Isterdael G, et al. Yolk Sac Macrophages, Fetal Liver, and Adult Monocytes Can Colonize an Empty Niche and Develop into Functional Tissue-Resident Macrophages. Immunity. 2016;44(4):755-68.

21.   Gordon S, Taylor PR. Monocyte and macrophage heterogeneity. Nat Rev Immunol. 2005;5(12):953-64.

22.   Misharin AV, Cuda CM, Saber R, Turner JD, Gierut AK, Haines GK, et al. Nonclassical Ly6C(-) Monocytes Drive the Development of Inflammatory Arthritis in Mice. Cell Reports. 2014;9(2):591-604.

23.   Cane S, Ugel S, Trovato R, Marigo I, De Sanctis F, Sartoris S, et al. The Endless Saga of Monocyte Diversity. Front Immunol. 2019;10:18.

24.   Ziegler-Heitbrock L. Monocyte subsets in man and other species. Cell Immunol. 2014;289(1-2):135-9.

25.   Kawai T, Akira S. Signaling to NF-kappa B by Toll-like receptors. Trends Mol Med. 2007;13(11):460-9.

26.   Arthur JSC, Ley SC. Mitogen-activated protein kinases in innate immunity. Nat Rev Immunol. 2013;13(9):679-92.

27.   Ivashkiv LB, Donlin LT. Regulation of type I interferon responses. Nat Rev Immunol. 2014;14(1):36-49.

28.   Mesev EV, LeDesma RA, Ploss A. Decoding type I and III interferon signalling during viral infection. Nat Microbiol. 2019;4(6):914-24.

29.   Levy DE, Darnell JE. STATs: Transcriptional control and biological impact. Nat Rev Mol Cell Biol. 2002;3(9):651-62.

30.   Schneider WM, Chevillotte MD, Rice CM. Interferon-Stimulated Genes: A Complex Web of Host Defenses. In: Littman DR, Yokoyama WM, editors. Annual Review of Immunology, Vol 32. Annual Review of Immunology. 32. Palo Alto: Annual Reviews; 2014. p. 513-45.

31.   Dixon DR, Darveau RP. Lipopolysaccharide heterogeneity: Innate host responses to bacterial modification of lipid A structure. J Dent Res. 2005;84(7):584-95.

32.   Murray PJ, Allen JE, Biswas SK, Fisher EA, Gilroy DW, Goerdt S, et al. Macrophage activation and polarization: nomenclature and experimental guidelines. Immunity. 2014;41(1):14-20.

33.   Mills CD, Kincaid K, Alt JM, Heilman MJ, Hill AM. M-1/M-2 macrophages and the Th1/Th2 paradigm. J Immunol. 2000;164(12):6166-73.

34.   Fleetwood AJ, Lawrence T, Hamilton JA, Cook AD. Granulocyte-macrophage colony-stimulating factor (CSF) and macrophage CSF-dependent macrophage phenotypes display differences in cytokine profiles and transcription factor activities: Implications for CSF blockade in inflammation. J Immunol. 2007;178(8):5245-52.

35.   Thomas AC, Mattila JT. "Of mice and men": arginine metabolism in macrophages. Front Immunol. 2014;5:7.

36.   Mosser DM, Edwards JP. Exploring the full spectrum of macrophage activation. Nat Rev Immunol. 2008;8(12):958-69.

37.   Xue J, Schmidt SV, Sander J, Draffehn A, Krebs W, Quester I, et al. Transcriptome-Based Network Analysis Reveals a Spectrum Model of Human Macrophage Activation. Immunity. 2014;40(2):274-88.

38.   Abraham SM, Clark AR. Dual-specificity phosphatase 1: a critical regulator of innate immune responses. Biochem Soc Trans. 2006;34:1018-23.

39.   Gilroy D, De Maeyer R. New insights into the resolution of inflammation. Semin Immunol. 2015;27(3):161-8.

40.   Pineda-Torra I, Gage M, de Juan A, Pello OM. Isolation, Culture, and Polarization of Murine Bone Marrow-Derived and Peritoneal Macrophages. In: Andres V, Dorado B, editors. Methods in Mouse Atherosclerosis. Methods in Molecular Biology. 1339. Totowa: Humana Press Inc; 2015. p. 101-9.

41.   Nayak DK, Mendez O, Bowen S, Mohanakumar T. Isolation and In Vitro Culture of Murine and Human Alveolar Macrophages. J Vis Exp. 2018(134):8.

42.   Daigneault M, Preston JA, Marriott HM, Whyte MKB, Dockrell DH. The Identification of Markers of Macrophage Differentiation in PMA-Stimulated THP-1 Cells and Monocyte-Derived Macrophages. PLoS One. 2010;5(1):10.

43.   Bosshart H, Heinzelmann M. THP-1 cells as a model for human monocytes. Ann Transl Med. 2016;4(21):4.

44.   Chu CQ, Field M, Feldmann M, Maini RN. LOCALIZATION OF TUMOR-NECROSIS-FACTOR-ALPHA IN SYNOVIAL TISSUES AND AT THE CARTILAGE PANNUS JUNCTION IN PATIENTS WITH RHEUMATOID-ARTHRITIS. Arthritis Rheum. 1991;34(9):1125-32.

45.   Maini R, St Clair EW, Breedveld F, Furst D, Kalden J, Weisman M, et al. Infliximab (chimeric anti-tumour necrosis factor alpha monoclonal antibody) versus placebo in rheumatoid arthritis patients receiving concomitant methotrexate: a randomised phase III trial. Lancet. 1999;354(9194):1932-9.

46.   Alivernini S, Tolusso B, Ferraccioli G, Gremese E, Kurowska-Stolarska M, McInnes IB. Driving chronicity in rheumatoid arthritis: perpetuating role of myeloid cells. Clin Exp Immunol. 2018.

47.   Feldmann M, Williams RO, Paleolog E. What have we learnt from targeted anti-TNF therapy? Ann Rheum Dis. 2010;69 Suppl 1:i97-9.

48.   McInnes IB, Schett G. Cytokines in the pathogenesis of rheumatoid arthritis. Nat Rev Immunol. 2007;7(6):429-42.

49.   Gregersen PK, Silver J, Winchester RJ. THE SHARED EPITOPE HYPOTHESIS - AN APPROACH TO UNDERSTANDING THE MOLECULAR-GENETICS OF SUSCEPTIBILITY TO RHEUMATOID-ARTHRITIS. Arthritis Rheum. 1987;30(11):1205-13.

50.   Ireland JM, Unanue ER. Autophagy in antigen-presenting cells results in presentation of citrullinated peptides to CD4 T cells. J Exp Med. 2011;208(13):2625-32.

51.   Kurowska-Stolarska M, Alivernini S. Synovial tissue macrophages: friend or foe? RMD Open. 2017;3(2):e000527.

52.   Culemann S, Gruneboom A, Nicolas-Avila JA, Weidner D, Lammle KF, Rothe T, et al. Locally renewing resident synovial macrophages provide a protective barrier for the joint. Nature. 2019;572(7771):670-+.

53.   Liddiard K, Taylor PR. Understanding Local Macrophage Phenotypes In Disease: Shape-shifting macrophages. Nat Med. 2015;21(2):119-20.

54.   Wynn TA, Barron L. Macrophages: Master Regulators of Inflammation and Fibrosis. Semin Liver Dis. 2010;30(3):245-57.

55.   Murray PJ, Wynn TA. Protective and pathogenic functions of macrophage subsets. Nat Rev Immunol. 2011;11(11):723-37.

56.   Clark AR, Belvisi MG. Maps and legends: The quest for dissociated ligands of the glucocorticoid receptor. Pharmacol Ther. 2012;134(1):54-67.

57.   Patel R, Williams-Dautovich J, Cummins CL. Minireview: New Molecular Mediators of Glucocorticoid Receptor Activity in Metabolic Tissues. Mol Endocrinol. 2014;28(7):999-1011.

58.   Barnes PJ. Corticosteroids: The drugs to beat. Eur J Pharmacol. 2006;533(1-3):2-14.

59.   Biddie SC, Conway-Campbell BL, Lightman SL. Dynamic regulation of glucocorticoid signalling in health and disease. Rheumatology. 2012;51(3):403-12.

60.   Hardy RS, Raza K, Cooper MS. Glucocorticoid metabolism in rheumatoid arthritis. AnnNY AcadSci. 2014;1318:18-26.

61.   Gagliardi L, Ho JT, Torpy DJ. Corticosteroid-binding globulin: The clinical significance of altered levels and heritable mutations. Mol Cell Endocrinol. 2010;316(1):24-34.

62.   Morgan SA, Hassan-Smith ZK, Lavery GG. Tissue-specific activation of cortisol in Cushing's syndrome. Eur J Endocrinol. 2016;175(2):R81-R7.

63.   Kadmiel M, Cidlowski JA. Glucocorticoid receptor signaling in health and disease. Trends Pharmacol Sci. 2013;34(9):518-30.

64.   Schacke H, Docke WD, Asadullah K. Mechanisms involved in the side effects of glucocorticoids. Pharmacol Ther. 2002;96(1):23-43.

65.   Daley-Yates PT. Inhaled corticosteroids: potency, dose equivalence and therapeutic index. Br J Clin Pharmacol. 2015;80(3):372-80.

66.   Paragliola RM, Papi G, Pontecorvi A, Corsello SM. Treatment with Synthetic Glucocorticoids and the Hypothalamus-Pituitary-Adrenal Axis. Int J Mol Sci. 2017;18(10):17.

67.   Ramamoorthy S, Cidlowski JA. Corticosteroids Mechanisms of Action in Health and Disease. Rheum Dis Clin North Am. 2016;42(1):15-+.

68.   Kovacs JJ, Murphy PJM, Gaillard S, Zhao XA, Wu JT, Nicchitta CV, et al. HDAC6 regulates Hsp90 acetylation and chaperone-dependent activation of glucocorticoid receptor. Mol Cell. 2005;18(5):601-7.

69.   De Iudicibus S, Lucafo M, Martelossi S, Pierobon C, Ventura A, Decorti G. MicroRNAs as tools to predict glucocorticoid response in inflammatory bowel diseases. World J Gastroenterol. 2013;19(44):7947-54.

70.   Oakley RH, Cidlowski JA. Cellular Processing of the Glucocorticoid Receptor Gene and Protein: New Mechanisms for Generating Tissue-specific Actions of Glucocorticoids. J Biol Chem. 2011;286(5):3177-84.

71.   Oppong E, Cato ACB. Effects of Glucocorticoids in the Immune System. In: Wang JC, Harris C, editors. Glucocorticoid Signaling: from Molecules to Mice to Man. Advances in Experimental Medicine and Biology. 872. Berlin: Springer-Verlag Berlin; 2015. p. 217-33.

72.   Reichardt HM, Tuckermann JP, Gottlicher M, Vujic M, Weih F, Angel P, et al. Repression of inflammatory responses in the absence of DNA binding by the glucocorticoid receptor. Embo Journal. 2001;20(24):7168-73.

73.   Clark AR. Anti-inflammatory functions of glucocorticoid-induced genes. Mol Cell Endocrinol. 2007;275(1-2):79-97.

74.   Abraham SM, Lawrence T, Kleiman A, Warden P, Medghalchi M, Tuckermann J, et al. Antiinflammatory effects of dexamethasone are partly dependent on induction of dual specificity phosphatase 1. J Exp Med. 2006;203(8):1883-9.

75.   Nissen RM, Yamamoto KR. The glucocorticoid receptor inhibits NF kappa B by interfering with serine-2 phosphorylation of the RNA polymerase II carboxy-terminal domain. Genes Dev. 2000;14(18):2314-29.

76.   Auphan N, Didonato JA, Rosette C, Helmberg A, Karin M. IMMUNOSUPPRESSION BY GLUCOCORTICOIDS - INHIBITION OF NF-KAPPA-B ACTIVITY THROUGH INDUCTION OF I-KAPPA-B SYNTHESIS. Science. 1995;270(5234):286-90.

77.   Ayroldi E, Riccardi C. Glucocorticoid-induced leucine zipper (GILZ): a new important mediator of glucocorticoid action. Faseb J. 2009;23(11):3649-58.

78.   Moisan MP, Castanon N. Emerging Role of Corticosteroid-Binding Globulin in Glucocorticoid-Driven Metabolic Disorders. Front Endocrinol. 2016;7.

79.   Rose AJ, Herzig S. Metabolic control through glucocorticoid hormones: An update. Mol Cell Endocrinol. 2013;380(1-2):65-78.

80.   Rabasa C, Dickson SL. Impact of stress on metabolism and energy balance. Current Opinion in Behavioral Sciences. 2016;9:71-7.

81.   Opherk C, Tronche F, Kellendonk C, Kohlmuller D, Schulze A, Schmid W, et al. Inactivation of the glucocorticoid receptor in hepatocytes leads to fasting hypoglycemia and ameliorates hyperglycemia in streptozotocin-induced diabetes mellitus. Mol Endocrinol. 2004;18(6):1346-53.

82.   Ma RH, Zhang WG, Tang K, Zhang HF, Zhang Y, Li DP, et al. Switch of glycolysis to gluconeogenesis by dexamethasone for treatment of hepatocarcinoma. Nat Commun. 2013;4.

83.   Gremlich S, Roduit R, Thorens B. Dexamethasone induces posttranslational degradation of GLUT2 and inhibition of insulin secretion in isolated pancreatic beta cells - Comparison with the effects of fatty acids. J Biol Chem. 1997;272(6):3216-22.

84.   Rafacho A, Ortsater H, Nadal A, Quesada I. Glucocorticoid treatment and endocrine pancreas function: implications for glucose homeostasis, insulin resistance and diabetes. J Endocrinol. 2014;223(3):R49-R62.

85.   Weinstein SP, Wilson CM, Pritsker A, Cushman SW. Dexamethasone inhibits insulin-stimulated recruitment of GLUT4 to the cell surface in rat skeletal muscle. Metabolism-Clinical and Experimental. 1998;47(1):3-6.

86.   Ekstrand A, SchalinJantti C, Lofman M, Parkkonen M, Widen E, FranssilaKallunki A, et al. The effect of (steroid) immunosuppression on skeletal muscle glycogen metabolism in patients after kidney transplantation. Transplantation. 1996;61(6):889-93.

87.   Falduto MT, Hickson RC, Young AP. ANTAGONISM BY GLUCOCORTICOIDS AND EXERCISE ON EXPRESSION OF GLUTAMINE-SYNTHETASE IN SKELETAL-MUSCLE. Faseb J. 1989;3(14):2623-8.

88.   Luijten IHN, Cannon B, Nedergaard J. Glucocorticoids and Brown Adipose Tissue: Do glucocorticoids really inhibit thermogenesis? Mol Asp Med. 2019;68:42-59.

89.   Friedman RC, Farh KKH, Burge CB, Bartel DP. Most mammalian mRNAs are conserved targets of microRNAs. Genome Res. 2009;19(1):92-105.

90.   Fabian MR, Sonenberg N. The mechanics of miRNA-mediated gene silencing: a look under the hood of miRISC. Nat Struct Mol Biol. 2012;19(6):586-93.

91.   Iwakawa HO, Tomari Y. The Functions of MicroRNAs: mRNA Decay and Translational Repression. Trends Cell Biol. 2015;25(11):651-65.

92.   Baulcombe D. RNA silencing in plants. Nature. 2004;431(7006):356-63.

93.   Orellana E, Kasinski A. MicroRNAs in Cancer: A Historical Perspective on the Path from Discovery to Therapy. Cancers. 2015;7(3):1388-405.

94.   Ceribelli A, Nahid MA, Satoh M, Chan EKL. MicroRNAs in rheumatoid arthritis. FEBS Lett. 2011;585(23):3667-74.

95.   Ha M, Kim VN. Regulation of microRNA biogenesis. Nat Rev Mol Cell Biol. 2014;15(8):509-24.

96.   Filipowicz W, Bhattacharyya SN, Sonenberg N. Mechanisms of post-transcriptional regulation by microRNAs: are the answers in sight? Nat Rev Genet. 2008;9(2):102-14.

97.   Su H, Trombly MI, Chen J, Wang XZ. Essential and overlapping functions for mammalian Argonautes in microRNA silencing. Genes Dev. 2009;23(3):304-17.

98.   Liu JD, Rivas FV, Wohlschlegel J, Yates JR, Parker R, Hannon GJ. A role for the P-body component GW182 in microRNA function. Nat Cell Biol. 2005;7(12):1261-6.

99.   Lytle JR, Yario TA, Steitz JA. Target mRNAs are repressed as efficiently by microRNA-binding sites in the 5 ' UTR as in the 3 ' UTR. Proc Natl Acad Sci U S A. 2007;104(23):9667-72.

100.   Tay Y, Zhang JQ, Thomson AM, Lim B, Rigoutsos I. MicroRNAs to Nanog, Oct4 and Sox2 coding regions modulate embryonic stem cell differentiation. Nature. 2008;455(7216):1124-U12.

101.   Liu JD, Carmell MA, Rivas FV, Marsden CG, Thomson JM, Song JJ, et al. Argonaute2 is the catalytic engine of mammalian RNAi. Science. 2004;305(5689):1437-41.

102.   Gu S, Kay MA. How do miRNAs mediate translational repression? Silence. 2010;1(1):11.

103.   Agarwal V, Bell GW, Nam JW, Bartel DP. Predicting effective microRNA target sites in mammalian mRNAs. eLife. 2015;4:38.

104.   Humphreys DT, Westman BJ, Martin DIK, Preiss T. MicroRNAs control translation initiation by inhibiting eukaryotic initiation factor 4E/cap and poly(A) tail function. Proc Natl Acad Sci U S A. 2005;102(47):16961-6.

105.   Guo HL, Ingolia NT, Weissman JS, Bartel DP. Mammalian microRNAs predominantly act to decrease target mRNA levels. Nature. 2010;466(7308):835-U66.

106.   Braun JE, Huntzinger E, Fauser M, Izaurralde E. GW182 Proteins Directly Recruit Cytoplasmic Deadenylase Complexes to miRNA Targets. Mol Cell. 2011;44(1):120-33.

107.   Behm-Ansmant I, Rehwinkel J, Doerks T, Stark A, Bork P, Izaurralde E. MRNA degradation by miRNAs and GW182 requires both CCR4 : NOT deadenylase and DCP1 : DCP2 decapping complexes. Genes Dev. 2006;20(14):1885-98.

108.   Zekri L, Huntzinger E, Heimstadt S, Izaurralde E. The Silencing Domain of GW182 Interacts with PABPC1 To Promote Translational Repression and Degradation of MicroRNA Targets and Is Required for Target Release. Mol Cell Biol. 2009;29(23):6220-31.

109. Fukao A, Mishima Y, Takizawa N, Oka S, Imataka H, Pelletier J, et al. MicroRNAs Trigger Dissociation of eIF4AI and eIF4AII from Target mRNAs in Humans. Mol Cell. 2014;56(1):79-89.

110. Muljo SA, Ansel KM, Kanellopoulou C, Livingston DM, Rao A, Rajewsky K. Aberrant T cell differentiation in the absence of Dicer. J Exp Med. 2005;202(2):261-9.

111. Danger R, Braze F, Giral M, Soulillou JP, Brouard S. MicroRNAs, major players in B cells homeostasis and function. Front Immunol. 2014;5.

112. Meinzinger J, Jack HM, Pracht K. miRNA meets plasma cells "How tiny RNAs control antibody responses". Clinical Immunology. 2018;186:3-8.

113. Baltimore D, Boldin MP, O'Connell RM, Rao DS, Taganov KD. MicroRNAs: new regulators of immune cell development and function. Nat Immunol. 2008;9(8):839-45.

114. Xiao CC, Rajewsky K. MicroRNA Control in the Immune System: Basic Principles. Cell. 2009;136(1):26-36.

115. Lu Q, Wu R, Zhao M, Garcia-Gomez A, Ballestar E. miRNAs as Therapeutic Targets in Inflammatory Disease. Trends Pharmacol Sci. 2019;40(11):853-65.

116. Quinn SR, O'Neill LA. A trio of microRNAs that control Toll-like receptor signalling. International Immunology. 2011;23(7):421-5.

117. O'Connell RM, Rao DS, Baltimore D. microRNA Regulation of Inflammatory Responses. In: Paul WE, editor. Annual Review of Immunology, Vol 30. Annual Review of Immunology. 30. Palo Alto: Annual Reviews; 2012. p. 295-312.

118. Frixa T, Donzelli S, Blandino G. Oncogenic MicroRNAs: Key Players in Malignant Transformation. Cancers. 2015;7(4):2466-85.

119. Schmidt MF. Drug target miRNAs: chances and challenges. Trends Biotechnol. 2014;32(11):578-85.

120. Dowdy SF. Overcoming cellular barriers for RNA therapeutics. Nat Biotechnol. 2017;35(3):222-9.

121. Stein CA, Castanotto D. FDA-Approved Oligonucleotide Therapies in 2017. Mol Ther. 2017;25(5):1069-75.

122. Miller CM, Tanowitz M, Donner AJ, Prakash TP, Swayze EE, Harris EN, et al. Receptor-Mediated Uptake of Phosphorothioate Antisense Oligonucleotides in Different Cell Types of the Liver. Nucleic Acid Therapeutics. 2018;28(3):119-27.

123. Janssen HLA, Reesink HW, Lawitz EJ, Zeuzem S, Rodriguez-Torres M, Patel K, et al. Treatment of HCV Infection by Targeting MicroRNA. N Engl J Med. 2013;368(18):1685-94.

124. Seto AG, Beatty X, Lynch JM, Hermreck M, Tetzlaff M, Duvic M, et al. Cobomarsen, an oligonucleotide inhibitor of miR-155, co-ordinately regulates multiple survival pathways to reduce cellular proliferation and survival in cutaneous T-cell lymphoma. Br J Haematol. 2018;183(3):428-44.

125. miRagen Therapeutics, Inc. http://www.miragen.com/2019 [

126. Butovsky O, Jedrychowski MP, Cialic R, Krasemann S, Murugaiyan G, Fanek Z, et al. Targeting miR-155 Restores Abnormal Microglia and Attenuates Disease in SOD1 Mice. Ann Neurol. 2015;77(1):75-99.

127. Sousa AR, Lane SJ, Cidlowski JA, Staynov DZ, Lee TH. Glucocorticoid resistance in asthma is associated with elevated in vivo expression of the glucocorticoid receptor beta-isoform. J Allergy Clin Immunol. 2000;105(5):943-50.

128. Vreugdenhil E, Verissimo CSL, Mariman R, Kamphorst JT, Barbosa JS, Zweers T, et al. MicroRNA 18 and 124a Down-Regulate the Glucocorticoid Receptor: Implications for Glucocorticoid Responsiveness in the Brain. Endocrinology. 2009;150(5):2220-8.

129. Liang YN, Tang YL, Ke ZY, Chen YQ, Luo XQ, Zhang H, et al. MiR-124 contributes to glucocorticoid resistance in acute lymphoblastic leukemia by promoting proliferation, inhibiting apoptosis and targeting the glucocorticoid receptor. J Steroid Biochem Mol Biol. 2017;172:62-8.

130.   Reichardt HM, Umland T, Bauer A, Kretz O, Schutz G. Mice with an increased glucocorticoid receptor gene dosage show enhanced resistance to stress and endotoxic shock. Mol Cell Biol. 2000;20(23):9009-17.

131.   de Kloet ER, Fitzsimons CP, Datson NA, Meijer OC, Vreugdenhil E. Glucocorticoid signaling and stress-related limbic susceptibility pathway: About receptors, transcription machinery and microRNA. Brain Res. 2009;1293:129-41.

132.   Xu J, Wang R, Liu Y, Liu D, Jiang H, Pan F. FKBP5 and specific microRNAs via glucocorticoid receptor in the basolateral amygdala involved in the susceptibility to depressive disorder in early adolescent stressed rats. Journal of Psychiatric Research. 2017;95:102-13.

133.   Zheng YJ, Xiong SD, Jiang P, Liu RH, Liu XM, Qian J, et al. Glucocorticoids inhibit lipopolysaccharide-mediated inflammatory response by downregulating microRNA-155: a novel anti-inflammation mechanism. Free Radic Biol Med. 2012;52(8):1307-17.

134.   Davis TE, Kis-Toth K, Szanto A, Tsokos GC. Glucocorticoids Suppress T Cell Function by Up-Regulating MicroRNA-98. Arthritis Rheum. 2013;65(7):1882-90.

135.   Chen Y, Wang G, Liu ZM, Wang SJ, Wang YS. Glucocorticoids regulate the proliferation of T cells via miRNA-155 in septic shock. Exp Ther Med. 2016;12(6):3723-8.

136.   Wang ZH, Liang YB, Tang H, Chen ZB, Li ZY, Hu XC, et al. Dexamethasone Down-Regulates the Expression of microRNA-155 in the Livers of Septic Mice. PLoS One. 2013;8(11):7.

137.   Curtale G, Renzi T, Drufuca L, Rubino M, Locati M. Glucocorticoids downregulate TLR4 signaling activity via its direct targeting by miR-511-5p. Eur J Immunol. 2017.

138.   Puimege L, Van Hauwermeiren F, Steeland S, Van Ryckeghem S, Vandewalle J, Lodens S, et al. Glucocorticoid-induced microRNA-511 protects against TNF by down-regulating TNFR1. EMBO Mol Med. 2015;7(8):1004-17.

139.   Zhu QY, Liu Q, Chen JX, Lan K, Ge BX. MicroRNA-101 Targets MAPK Phosphatase-1 To Regulate the Activation of MAPKs in Macrophages. J Immunol. 2010;185(12):7435-42.

140.   Kumar M, Ahmad T, Sharma A, Mabalirajan U, Kulshreshtha A, Agrawal A, et al. Let-7 microRNA-mediated regulation of IL-13 and allergic airway inflammation. J Allergy Clin Immunol. 2011;128(5):1077-U545.

141.   Smith LK, Shah RR, Cidlowski JA. Glucocorticoids Modulate MicroRNA Expression and Processing during Lymphocyte Apoptosis. J Biol Chem. 2010;285(47):36698-708.

142.   Molitoris JK, McColl KS, Distelhorst CW. Glucocorticoid-Mediated Repression of the Oncogenic microRNA Cluster miR-17 similar to 92 Contributes to the Induction of Bim and Initiation of Apoptosis. Mol Endocrinol. 2011;25(3):409-20.

143.   Harada M, Pokrovskaja-Tamm K, Soderhall S, Heyman M, Grander D, Corcoran M. Involvement of miR17 pathway in glucocorticoid-induced cell death in pediatric acute lymphoblastic leukemia. Leuk Lymphoma. 2012;53(10):2041-50.

144.   Mogilyansky E, Rigoutsos I. The miR-17/92 cluster: a comprehensive update on its genomics, genetics, functions and increasingly important and numerous roles in health and disease. Cell Death Differ. 2013;20(12):1603-14.

145.   Wade SM, Ohnesorge N, McLoughlin H, Biniecka M, Carter SP, Trenkman M, et al. Dysregulated miR-125a promotes angiogenesis through enhanced glycolysis. EBioMedicine. 2019;47:402-13.

146.   Duroux-Richard I, Roubert C, Ammari M, Presumey J, Grun JR, Haupl T, et al. miR-125b controls monocyte adaptation to inflammation through mitochondrial metabolism and dynamics. Blood. 2016;128(26):3125-36.

147.   Aschrafi A, Kar AN, Natera-Naranjo O, MacGibeny MA, Gioio AE, Kaplan BB. MicroRNA-338 regulates the axonal expression of multiple nuclear-encoded mitochondrial mRNAs encoding subunits of the oxidative phosphorylation machinery. Cell Mol Life Sci. 2012;69(23):4017-27.

148.   Chan SY, Zhang YY, Hemann C, Mahoney CE, Zweier JL, Loscalzo J. MicroRNA-210 Controls Mitochondrial Metabolism during Hypoxia by Repressing the Iron-Sulfur Cluster Assembly Proteins ISCU1/2. Cell Metab. 2009;10(4):273-84.

149. Geiger J, Dalgaard LT. Interplay of mitochondrial metabolism and microRNAs. Cell Mol Life Sci. 2017;74(4):631-46.

150. Zhuang X, Chen Y, Wu Z, Xu Q, Chen M, Shao M, et al. Mitochondrial miR-181a-5p promotes glucose metabolism reprogramming in liver cancer by regulating the electron transport chain. Carcinogenesis. 2019.

151. O'Neill LAJ, Kishton RJ, Rathmell J. A guide to immunometabolism for immunologists. Nat Rev Immunol. 2016;16(9):553-65.

152. Ren WK, Xia YY, Chen SY, Wu GY, Bazer FW, Zhou BY, et al. Glutamine Metabolism in Macrophages: A Novel Target for Obesity/Type 2 Diabetes. Advances in Nutrition. 2019;10(2):321-30.

153. Chandel NS, Jeffs P. Navigating metabolism2015.

154. Liberti MV, Locasale JW. The Warburg Effect: How Does it Benefit Cancer Cells? Trends BiochemSci. 2016;41(3):211-8.

155. Locasale JW, Cantley LC. Metabolic Flux and the Regulation of Mammalian Cell Growth. Cell Metab. 2011;14(4):443-51.

156. Doherty JR, Yang CY, Scott KEN, Cameron MD, Fallahi M, Li WM, et al. Blocking Lactate Export by Inhibiting the Myc Target MCT1 Disables Glycolysis and Glutathione Synthesis. Cancer Res. 2014;74(3):908-20.

157. Halestrap AP. Monocarboxylic Acid Transport. Compr Physiol. 2013;3(4):1611-43.

158. Buck MD, Sowell RT, Kaech SM, Pearce EL. Metabolic Instruction of Immunity. Cell. 2017;169(4):570-86.

159. Tanner LB, Goglia AG, Wei MH, Sehgal T, Parsons LR, Park JO, et al. Four Key Steps Control Glycolytic Flux in Mammalian Cells. Cell Syst. 2018;7(1):49-62.e8.

160. Rodriguez-Prados JC, Traves PG, Cuenca J, Rico D, Aragones J, Martin-Sanz P, et al. Substrate Fate in Activated Macrophages: A Comparison between Innate, Classic, and Alternative Activation. J Immunol. 2010;185(1):605-14.

161. Mathupala SP, Ko YH, Pedersen PL. Hexokinase II: Cancer's double-edged sword acting as both facilitator and gatekeeper of malignancy when bound to mitochondria. Oncogene. 2006;25(34):4777-86.

162. Marin-Hernandez A, Rodriguez-Enriquez S, Vital-Gonzalez PA, Flores-Rodriguez FL, Macias-Silva M, Sosa-Garrocho M, et al. Determining and understanding the control of glycolysis in fast-growth tumor cells - Flux control by an over-expressed but strongly product-inhibited hexokinase. Febs Journal. 2006;273(9):1975-88.

163. Chang CH, Qiu J, O'Sullivan D, Buck MD, Noguchi T, Curtis JD, et al. Metabolic Competition in the Tumor Microenvironment Is a Driver of Cancer Progression. Cell. 2015;162(6):1229-41.

164. Palsson-McDermott EM, Curtis AM, Goel G, Lauterbach MAR, Sheedy FJ, Gleeson LE, et al. Pyruvate Kinase M2 Regulates Hif-1 alpha Activity and IL-1 beta Induction and Is a Critical Determinant of the Warburg Effect in LPS-Activated Macrophages. Cell Metab. 2015;21(1):65-80.

165. Dayton TL, Jacks T, Vander Heiden MG. PKM2, cancer metabolism, and the road ahead. EMBO Rep. 2016;17(12):1721-30.

166. Shestov AA, Liu XJ, Ser Z, Cluntun AA, Hung YP, Huang L, et al. Quantitative determinants of aerobic glycolysis identify flux through the enzyme GAPDH as a limiting step. eLife. 2014;3:18.

167. DeBerardinis RJ, Lum JJ, Hatzivassiliou G, Thompson CB. The biology of cancer: Metabolic reprogramming fuels cell growth and proliferation. Cell Metab. 2008;7(1):11-20.

168. Potter M, Newport E, Morten KJ. The Warburg effect: 80 years on. Biochem Soc Trans. 2016;44:1499-505.

169. Hanahan D, Weinberg RA. Hallmarks of Cancer: The Next Generation. Cell. 2011;144(5):646-74.

170. Buck MD, O'Sullivan D, Pearce EL. T cell metabolism drives immunity. J Exp Med. 2015;212(9):1345-60.

171.   Patra KC, Hay N. The pentose phosphate pathway and cancer. Trends BiochemSci. 2014;39(8):347-54.

172.   Jha AK, Huang SCC, Sergushichev A, Lampropoulou V, Ivanova Y, Loginicheva E, et al. Network Integration of Parallel Metabolic and Transcriptional Data Reveals Metabolic Modules that Regulate Macrophage Polarization. Immunity. 2015;42(3):419-30.

173.   Andersson SG, Karlberg O, Canbäck B, Kurland CG. On the origin of mitochondria: a genomics perspective. Philos Trans R Soc Lond B Biol Sci. 2003;358(1429):165-77; discussion 77-9.

174.   Gray MW. Mitochondrial evolution. Cold Spring Harb Perspect Biol. 2012;4(9):a011403.

175.   Newsholme P, Cruzat VF, Keane KN, Carlessi R, de Bittencourt PIH. Molecular mechanisms of ROS production and oxidative stress in diabetes. Biochem J. 2016;473:4527-50.

176.   Krebs HA, Johnson WA. The role of citric acid in intermediate metabolism in animal tissues. FEBS Lett. 1980;117 Suppl:K1-10.

177.   van der Bliek AM, Sedensky MM, Morgan PG. Cell Biology of the Mitochondrion. Genetics. 2017;207(3):843-71.

178.   Mitchell P. COUPLING OF PHOSPHORYLATION TO ELECTRON AND HYDROGEN TRANSFER BY A CHEMI-OSMOTIC TYPE OF MECHANISM. Nature. 1961;191(478):144-&.

179.   Abrahams JP, Leslie AG, Lutter R, Walker JE. Structure at 2.8 A resolution of F1-ATPase from bovine heart mitochondria. Nature. 1994;370(6491):621-8.

180.   Chan DC. Mitochondria: Dynamic organelles in disease, aging, and development. Cell. 2006;125(7):1241-52.

181.   Lake NJ, Compton AG, Rahman S, Thorburn DR. Leigh syndrome: One disorder, more than 75 monogenic causes. Ann Neurol. 2016;79(2):190-203.

182.   Adav SS, Park JE, Sze SK. Quantitative profiling brain proteomes revealed mitochondrial dysfunction in Alzheimer's disease. Mol Brain. 2019;12:12.

183.   Moodley D, Mody G, Patel N, Chuturgoon AA. Mitochondrial depolarisation and oxidative stress in rheumatoid arthritis patients. Clinical Biochemistry. 2008;41(16-17):1396-401.

184.   Fearon U, Canavan M, Biniecka M, Veale DJ. Hypoxia, mitochondrial dysfunction and synovial invasiveness in rheumatoid arthritis. Nat Rev Rheumatol. 2016;12(7):385-97.

185.   Iyer A, Brown L, Whitehead JP, Prins JB, Fairlie DP. Nutrient and immune sensing are obligate pathways in metabolism, immunity, and disease. Faseb J. 2015;29(9):3612-25.

186.   Chawla A. Control of Macrophage Activation and Function by PPARs. CircRes. 2010;106(10):1559-69.

187.   O'Neill LAJ, Hardie DG. Metabolism of inflammation limited by AMPK and pseudo-starvation. Nature. 2013;493(7432):346-55.

188.   Weichhart T, Hengstschlager M, Linke M. Regulation of innate immune cell function by mTOR. Nat Rev Immunol. 2015;15(10):599-614.

189.   Namgaladze D, Brune B. Macrophage fatty acid oxidation and its roles in macrophage polarization and fatty acid-induced inflammation. Biochimica Et Biophysica Acta-Molecular and Cell Biology of Lipids. 2016;1861(11):1796-807.

190.   Mills EL, O'Neill LA. Reprogramming mitochondrial metabolism in macrophages as an anti-inflammatory signal. Eur J Immunol. 2016;46(1):13-21.

191.   Tannahill GM, Curtis AM, Adamik J, Palsson-McDermott EM, McGettrick AF, Goel G, et al. Succinate is an inflammatory signal that induces IL-1 beta through HIF-1 alpha. Nature. 2013;496(7444):238-+.

192.   Fukuzumi M, Shinomiya H, Shimizu Y, Ohishi F, Utsumi S. Endotoxin-induced enhancement of glucose influx into murine peritoneal macrophages via GLUT1. Infect Immun. 1996;64(1):108-12.

193.   Gamelli RL, Liu H, He LK, Hofmann CA. Augmentations of glucose uptake and glucose transporter-1 in macrophages following thermal injury and sepsis in mice. J Leukoc Biol. 1996;59(5):639-47.

194.   Krawczyk CM, Holowka T, Sun J, Blagih J, Amiel E, DeBerardinis RJ, et al. Toll-like receptor-induced changes in glycolytic metabolism regulate dendritic cell activation. Blood. 2010;115(23):4742-9.

195.   Wick AN, Drury DR, Nakada HI, Wolfe JB. LOCALIZATION OF THE PRIMARY METABOLIC BLOCK PRODUCED BY 2-DEOXYGLUCOSE. J Biol Chem. 1957;224(2):963-9.

196.   Shirai T, Nazarewicz RR, Wallis BB, Yanes RE, Watanabe R, Hilhorst M, et al. The glycolytic enzyme PKM2 bridges metabolic and inflammatory dysfunction in coronary artery disease. J Exp Med. 2016;213(3):337-54.

197.   Wang FL, Zhang S, Jeon R, Vuckovic I, Jiang XT, Lerman A, et al. Interferon Gamma Induces Reversible Metabolic Reprogramming of M1 Macrophages to Sustain Cell Viability and Pro-Inflammatory Activity. EBioMedicine. 2018;30:303-16.

198.   Wang F, Zhang S, Vuckovic I, Jeon R, Lerman A, Folmes CD, et al. Glycolytic Stimulation Is Not a Requirement for M2 Macrophage Differentiation. Cell Metab. 2018;28:463-75.

199.   Nagy C, Haschemi A. Time and demand are two critical dimensions of immunometabolism: the process of macrophage activation and the pentose phosphate pathway. Front Immunol. 2015;6.

200.   Haschemi A, Kosma P, Gille L, Evans CR, Burant CF, Starkl P, et al. The Sedoheptulose Kinase CARKL Directs Macrophage Polarization through Control of Glucose Metabolism. Cell Metab. 2012;15(6):813-26.

201.   van Diepen JA, Robben JH, Hooiveld GJ, Carmone C, Alsady M, Boutens L, et al. SUCNR1-mediated chemotaxis of macrophages aggravates obesity-induced inflammation and diabetes. Diabetologia. 2017;60(7):1304-13.

202.   Biniecka M, Canavan M, McGarry T, Gao W, McCormick J, Cregan S, et al. Dysregulated bioenergetics: a key regulator of joint inflammation. Ann Rheum Dis. 2016;75(12):2192-200.

203.   Li Y, Liu Y, Wang C, Xia WR, Zheng JY, Yang J, et al. Succinate induces synovial angiogenesis in rheumatoid arthritis through metabolic remodeling and HIF-1 alpha/VEGF axis. Free Radic Biol Med. 2018;126:1-14.

204.   Mills EL, Kelly B, Logan A, Costa ASH, Varma M, Bryant CE, et al. Succinate Dehydrogenase Supports Metabolic Repurposing of Mitochondria to Drive Inflammatory Macrophages. Cell. 2016;167(2):457-+.

205.   Semenza GL. Targeting HIF-1 for cancer therapy. Nature Reviews Cancer. 2003;3(10):721-32.

206.   Taylor CT. Mitochondria and cellular oxygen sensing in the HIF pathway. Biochem J. 2008;409:19-26.

207.   Peyssonnaux C, Cejudo-Martin P, Doedens A, Zinkernagel AS, Johnson RS, Nizet V. Cutting edge: Essential role of hypoxia inducible factor-1 alpha in development of lipopolysaccharide-induced sepsis. J Immunol. 2007;178(12):7516-9.

208.   Corcoran SE, O'Neill LAJ. HIF1 alpha and metabolic reprogramming in inflammation. J Clin Invest. 2016;126(10):3699-707.

209.   Bailey JD, Diotallevi M, Nicol T, McNeill E, Shaw A, Chuaiphichai S, et al. Nitric Oxide Modulates Metabolic Remodeling in Inflammatory Macrophages through TCA Cycle Regulation and Itaconate Accumulation. Cell Reports. 2019;28(1):218-+.

210.   Cramer T, Yamanishi Y, Clausen BE, Forster I, Pawlinski R, Mackman N, et al. HIF-1 alpha is essential for myeloid cell-mediated inflammation. Cell. 2003;112(5):645-57.

211.   Peyssonnaux C, Datta V, Cramer T, Doedens A, Theodorakis EA, Gallo RL, et al. HIF-1 alpha expression regulates the bactericidal capacity of phagocytes. J Clin Invest. 2005;115(7):1806-15.

212.   Anand RJ, Gribar SC, Li J, Kohler JW, Branca MF, Dubowski T, et al. Hypoxia causes an increase in phagocytosis by macrophages in a HIF-1 alpha-dependent manner. J Leukoc Biol. 2007;82(5):1257-65.

213.   Semba H, Takeda N, Isagawa T, Sugiura Y, Honda K, Wake M, et al. HIF-1 alpha-PDK1 axis-induced active glycolysis plays an essential role in macrophage migratory capacity. Nat Commun. 2016;7.

214.   Frede S, Stockmann C, Freitag P, Fandrey J. Bacterial lipopolysaccharide induces HIF-1 activation in human monocytes via p44/42 MAPK and NF-kappa B. Biochem J. 2006;396:517-27.

215.   Rius J, Guma M, Schachtrup C, Akassoglou K, Zinkernagel AS, Nizet V, et al. NF-kappa B links innate immunity to the hypoxic response through transcriptional regulation of HIF-1 alpha. Nature. 2008;453(7196):807-U9.

216.   Lee G, Won HS, Lee YM, Choi JW, Oh TI, Jang JH, et al. Oxidative Dimerization of PHD2 is Responsible for its Inactivation and Contributes to Metabolic Reprogramming via HIF-1 alpha Activation. Sci Rep. 2016;6:12.

217.   O'Neill LAJ, Pearce EJ. Immunometabolism governs dendritic cell and macrophage function. J Exp Med. 2016;213(1):15-23.

218.   Van den Bossche J, O'Neill LA, Menon D. Macrophage Immunometabolism: Where Are We (Going)? Trends Immunol. 2017;38(6):395-406.

219.   Mills EL, Ryan DG, Prag HA, Dikovskaya D, Menon D, Zaslona Z, et al. Itaconate is an anti-inflammatory metabolite that activates Nrf2 via alkylation of KEAP1. Nature. 2018;556(7699):113-+.

220.   Michelucci A, Cordes T, Ghelfi J, Pailot A, Reiling N, Goldmann O, et al. Immune-responsive gene 1 protein links metabolism to immunity by catalyzing itaconic acid production. Proc Natl Acad Sci U S A. 2013;110(19):7820-5.

221.   O'Neill LAJ, Artyomov MN. Itaconate: the poster child of metabolic reprogramming in macrophage function. Nat Rev Immunol. 2019;19(5):273-81.

222.   Bambouskova M, Gorvel L, Lampropoulou V, Sergushichev A, Loginicheva E, Johnson K, et al. Electrophilic properties of itaconate and derivatives regulate the I kappa B zeta-ATF3 inflammatory axis. Nature. 2018;556(7702):501-+.

223.   Liao ST, Han C, Xu DQ, Fu XW, Wang JS, Kong LY. 4-Octyl itaconate inhibits aerobic glycolysis by targeting GAPDH to exert anti-inflammatory effects. Nat Commun. 2019;10(1):5091.

224.   Cordes T, Wallace M, Michelucci A, Divakaruni AS, Sapcariu SC, Sousa C, et al. Immunoresponsive Gene 1 and Itaconate Inhibit Succinate Dehydrogenase to Modulate Intracellular Succinate Levels. J Biol Chem. 2016;291(27):14274-84.

225.   Lampropoulou V, Sergushichev A, Bambouskova M, Nair S, Vincent EE, Loginicheva E, et al. Itaconate Links Inhibition of Succinate Dehydrogenase with Macrophage Metabolic Remodeling and Regulation of Inflammation. Cell Metab. 2016;24(1):158-66.

226.   De Souza DP, Achuthan A, Lee MK, Binger KJ, Lee MC, Davidson S, et al. Autocrine IFN-I inhibits isocitrate dehydrogenase in the TCA cycle of LPS-stimulated macrophages. J Clin Invest. 2019;129(10):4239-44.

227.   Nair S, Huynh JP, Lampropoulou V, Loginicheva E, Esaulova E, Gounder AP, et al. Irg1 expression in myeloid cells prevents immunopathology during M-tuberculosis infection. J Exp Med. 2018;215(4):1035-45.

228.   Li YK, Zhang P, Wang CC, Han CF, Meng J, Liu XG, et al. Immune Responsive Gene 1 (IRG1) Promotes Endotoxin Tolerance by Increasing A20 Expression in Macrophages through Reactive Oxygen Species. J Biol Chem. 2013;288(23):16225-34.

229.   Dominguez-Andres J, Novakovic B, Li Y, Scicluna BP, Gresnigt MS, Arts RJW, et al. The Itaconate Pathway Is a Central Regulatory Node Linking Innate Immune Tolerance and Trained Immunity. Cell Metab. 2019;29(1):211-+.

230.   Hooftman A, O'Neill LAJ. The Immunomodulatory Potential of the Metabolite Itaconate. Trends Immunol. 2019;40(8):687-98.

231.   Mantuano NR, Oliveira-Nunes MC, Alisson-Silva F, Dias WB, Todeschini AR. Emerging role of glycosylation in the polarization of tumor-associated macrophages. Pharmacological Research. 2019;146.

232.   Fritsch SD, Weichhart T. Effects of Interferons and Viruses on Metabolism. Front Immunol. 2016;7:13.

233.   Pantel A, Teixeira A, Haddad E, Wood EG, Steinman RM, Longhi MP. Direct Type I IFN but Not MDA5/TLR3 Activation of Dendritic Cells Is Required for Maturation and Metabolic Shift to Glycolysis after Poly IC Stimulation. PLoS Biol. 2014;12(1):11.

234.   Van den Bossche J, Baardman J, Otto NA, van der Velden S, Neele AE, van den Berg SM, et al. Mitochondrial Dysfunction Prevents Repolarization of Inflammatory Macrophages. Cell Rep. 2016;17(3):684-96.

235.   Huang SCC, Smith AM, Everts B, Colonna M, Pearce EL, Schilling JD, et al. Metabolic Reprogramming Mediated by the mTORC2-IRF4 Signaling Axis Is Essential for Macrophage Alternative Activation. Immunity. 2016;45(4):817-30.

236.   Huang SCC, Everts B, Ivanova Y, O'Sullivan D, Nascimento M, Smith AM, et al. Cell-intrinsic lysosomal lipolysis is essential for alternative activation of macrophages. Nat Immunol. 2014;15(9):846-55.

237.   Vats D, Mukundan L, Odegaard JI, Zhang L, Smith KL, Morel CR, et al. Oxidative metabolism and PGC-1 beta attenuate macrophage-mediated inflammation. Cell Metab. 2006;4(3):255-.

238.   Divakaruni AS, Hsieh WY, Minarrieta L, Duong TN, Kim KKO, Desousa BR, et al. Etomoxir Inhibits Macrophage Polarization by Disrupting CoA Homeostasis. Cell Metab. 2018;28(3):490-+.

239.   O'Connor RS, Guo LL, Ghassemi S, Snyder NW, Worth AJ, Weng L, et al. The CPT1a inhibitor, etomoxir induces severe oxidative stress at commonly used concentrations. Sci Rep. 2018;8.

240.   Liu PS, Wang HP, Li XY, Chao T, Christen TTS, Christen S, et al. alpha-ketoglutarate orchestrates macrophage activation through metabolic and epigenetic reprogramming. Nat Immunol. 2017;18(9):985-+.

241.   Palmieri EM, Menga A, Martin-Perez R, Quinto A, Riera-Domingo C, De Tullio G, et al. Pharmacologic or Genetic Targeting of Glutamine Synthetase Skews Macrophages toward an M1-like Phenotype and Inhibits Tumor Metastasis. Cell Reports. 2017;20(7):1654-66.

242.   Palmieri EM, Menga A, Lebrun A, Hooper DC, Butterfield DA, Mazzone M, et al. Blockade of Glutamine Synthetase Enhances Inflammatory Response in Microglial Cells. Antioxid Redox Signal. 2017;26(8):351-63.

243.   Gordon S. Alternative activation of macrophages. Nat Rev Immunol. 2003;3(1):23-35.

244.   Ip WKE, Hoshi N, Shouval DS, Snapper S, Medzhitov R. Anti-inflammatory effect of IL-10 mediated by metabolic reprogramming of macrophages. Science. 2017;356(6337):513-9.

245.   Brune B, Dehne N, Grossmann N, Jung M, Namgaladze D, Schmid T, et al. Redox Control of Inflammation in Macrophages. Antioxid Redox Signal. 2013;19(6):595-637.

246.   Vega A, Chacon P, Monteseirin J, El Bekay R, Alvarez M, Alba G, et al. A new role for monoamine oxidases in the modulation of macrophage-inducible nitric oxide synthase gene expression. J Leukoc Biol. 2004;75(6):1093-101.

247.   Di Lisa F, Kaludercic N, Carpi A, Menabo R, Giorgio M. Mitochondrial pathways for ROS formation and myocardial injury: the relevance of p66(Shc) and monoamine oxidase. Basic Res Cardiol. 2009;104(2):131-9.

248.   Nunes P, Demaurex N, Dinauer MC. Regulation of the NADPH Oxidase and Associated Ion Fluxes During Phagocytosis. Traffic. 2013;14(11):1118-31.

249.   Liu YB, Fiskum G, Schubert D. Generation of reactive oxygen species by the mitochondrial electron transport chain. J Neurochem. 2002;80(5):780-7.

250.   Murphy MP. How mitochondria produce reactive oxygen species. Biochem J. 2009;417:1-13.

251.   Chouchani ET, Pell VR, James AM, Work LM, Saeb-Parsy K, Frezza C, et al. A Unifying Mechanism for Mitochondrial Superoxide Production during Ischemia-Reperfusion Injury. Cell Metab. 2016;23(2):254-63.

252.   West AP, Brodsky IE, Rahner C, Woo DK, Erdjument-Bromage H, Tempst P, et al. TLR signalling augments macrophage bactericidal activity through mitochondrial ROS. Nature. 2011;472(7344):476-U543.

253. Kamata H, Honda S, Maeda S, Chang LF, Hirata H, Karin M. Reactive oxygen species promote TNF alpha-induced death and sustained JNK activation by inhibiting MAP kinase phosphatases. Cell. 2005;120(5):649-61.

254. Bulua AC, Simon A, Maddipati R, Pelletier M, Park H, Kim KY, et al. Mitochondrial reactive oxygen species promote production of proinflammatory cytokines and are elevated in TNFR1-associated periodic syndrome (TRAPS). J Exp Med. 2011;208(3):519-33.

255. Zhou RB, Yazdi AS, Menu P, Tschopp J. A role for mitochondria in NLRP3 inflammasome activation. Nature. 2011;469(7329):221-5.

256. Brown GC. Regulation of mitochondrial respiration by nitric oxide inhibition of cytochrome c oxidase. Biochim Biophys Acta-Bioenerg. 2001;1504(1):46-57.

257. Hibbs JB, Taintor RR, Vavrin Z. MACROPHAGE CYTOTOXICITY - ROLE FOR L-ARGININE DEIMINASE AND IMINO-NITROGEN OXIDATION TO NITRITE. Science. 1987;235(4787):473-6.

258. Nathan CF, Hibbs JB. ROLE OF NITRIC-OXIDE SYNTHESIS IN MACROPHAGE ANTIMICROBIAL ACTIVITY. Curr Opin Immunol. 1991;3(1):65-70.

259. Poderoso JJ, Helfenberger K, Poderoso C. The effect of nitric oxide on mitochondrial respiration. Nitric Oxide-Biol Chem. 2019;88:61-72.

260. Clementi E, Brown GC, Feelisch M, Moncada S. Persistent inhibition of cell respiration by nitric oxide: Crucial role of S-nitrosylation of mitochondrial complex I and protective action of glutathione. Proc Natl Acad Sci U S A. 1998;95(13):7631-6.

261. Kasuno K, Takabuchi S, Fukuda K, Kizaka-Kondoh S, Yodoi J, Adachi T, et al. Nitric oxide induces hypoxia-inducible factor 1 activation that is dependent on MAPK and phosphatidylinositol 3-kinase signaling. J Biol Chem. 2004;279(4):2550-8.

262. Yasinska IM, Sumbayev VV. S-nitrosation of Cys-800 of HIF-1 alpha protein activates its interaction with p300 and stimulates its transcriptional activity. FEBS Lett. 2003;549(1-3):105-9.

263. Mishra BB, Rathinam VAK, Martens GW, Martinot AJ, Kornfeld H, Fitzgerald KA, et al. Nitric oxide controls the immunopathology of tuberculosis by inhibiting NLRP3 inflammasome-dependent processing of IL-1 beta. Nat Immunol. 2013;14(1):52-60.

264. Gross TJ, Kremens K, Powers LS, Brink B, Knutson T, Domann FE, et al. Epigenetic Silencing of the Human NOS2 Gene: Rethinking the Role of Nitric Oxide in Human Macrophage Inflammatory Responses. J Immunol. 2014;192(5):2326-38.

265. Fang FC, Vazquez-Torres AS. Nitric oxide production by human macrophages: there's NO doubt about it. Am J Physiol-Lung Cell Mol Physiol. 2002;282(5):L941-L3.

266. Jung JY, Madan-Lala R, Georgieva M, Rengarajan J, Sohaskey CD, Bange FC, et al. The Intracellular Environment of Human Macrophages That Produce Nitric Oxide Promotes Growth of Mycobacteria. Infect Immun. 2013;81(9):3198-209.

267. Weinberg JB. Nitric oxide production and nitric oxide synthase type 2 expression by human mononuclear phagocytes: A review. Mol Med. 1998;4(9):557-91.

268. StClair EW, Wilkinson WE, Lang T, Sanders L, Misukonis MA, Gilkeson GS, et al. Increased expression of blood mononuclear cell nitric oxide synthase type 2 in rheumatoid arthritis patients. J Exp Med. 1996;184(3):1173-8.

269. Artyomov MN, Sergushichev A, Schilling JD. Integrating immunometabolism and macrophage diversity. Semin Immunol. 2016;28(5):417-24.

270. Huang dW, Sherman BT, Lempicki RA. Bioinformatics enrichment tools: paths toward the comprehensive functional analysis of large gene lists. Nucleic Acids Res. 2009;37(1):1-13.

271. Huang DW, Sherman BT, Lempicki RA. Systematic and integrative analysis of large gene lists using DAVID bioinformatics resources. Nat Protoc. 2009;4(1):44-57.

272. Kuznetsova I, Lugmayr A, Siira SJ, Rackham O, Filipovska A. CirGO: an alternative circular way of visualising gene ontology terms. BMC Bioinformatics. 2019;20(1):84.

273. Ryan BC, Werner TS, Howard PL, Chow RL. ImiRP: a computational approach to microRNA target site mutation. BMC Bioinformatics. 2016;17:12.

274. Nielsen CB, Shomron N, Sandberg R, Hornstein E, Kitzman J, Burge CB. Determinants of targeting by endogenous and exogenous microRNAs and siRNAs. Rna. 2007;13(11):1894-910.

275. Bratosin D, Mitrofan L, Palii C, Estaquier J, Montreuil J. Novel fluorescence assay using calcein-AM for the determination of human erythrocyte viability and aging. Cytom Part A. 2005;66A(1):78-84.

276. Van den Bossche J, Baardman J, de Winther MP. Metabolic Characterization of Polarized M1 and M2 Bone Marrow-derived Macrophages Using Real-time Extracellular Flux Analysis. J Vis Exp. 2015(105).

277. Romero N, Rogers G, Neilson A, Dranka BP. Quantifying Cellular ATP Production Rate Using Agilent Seahorse XF Technology2018 5th Dec 2019.

278. Salabei JK, Gibb AA, Hill BG. Comprehensive measurement of respiratory activity in permeabilized cells using extracellular flux analysis. Nat Protoc. 2014;9(2):421-38.

279. Hiller K, Hangebrauk J, Jager C, Spura J, Schreiber K, Schomburg D. MetaboliteDetector: Comprehensive Analysis Tool for Targeted and Nontargeted GC/MS Based Metabolome Analysis. Anal Chem. 2009;81(9):3429-39.

280. Pitceathly RDS, Rahman S, Wedatilake Y, Polke JM, Cirak S, Foley AR, et al. NDUFA4 Mutations Underlie Dysfunction of a Cytochrome c Oxidase Subunit Linked to Human Neurological Disease. Cell Reports. 2013;3(6):1795-805.

281. Taganov KD, Boldin MP, Chang KJ, Baltimore D. NF-kappa B-dependent induction of microRNA miR-146, an inhibitor targeted to signaling proteins of innate immune responses. Proc Natl Acad Sci U S A. 2006;103(33):12481-6.

282. Nahid MA, Pauley KM, Satoh M, Chan EKL. miR-146a Is Critical for Endotoxin-induced Tolerance IMPLICATION IN INNATE IMMUNITY. J Biol Chem. 2009;284(50):34590-9.

283. Boldin MP, Taganov KD, Rao DS, Yang LL, Zhao JL, Kalwani M, et al. miR-146a is a significant brake on autoimmunity, myeloproliferation, and cancer in mice. J Exp Med. 2011;208(6):1189-201.

284. So AYL, Zhao JL, Baltimore D. The Yin and Yang of microRNAs: leukemia and immunity. Immunol Rev. 2013;253:129-45.

285. Stanczyk J, Pedrioli DAL, Brentano F, Sanchez-Pernaute O, Kolling C, Gay RE, et al. Altered expression of microRNA in synovial fibroblasts and synovial tissue in rheumatoid arthritis. Arthritis Rheum. 2008;58(4):1001-9.

286. Abou-Zeid A, Saad M, Soliman E. MicroRNA 146a Expression in Rheumatoid Arthritis: Association with Tumor Necrosis Factor-Alpha and Disease Activity. Genet Test Mol Biomark. 2011;15(11):807-12.

287. Feng MJ, Shi F, Qiu C, Peng WK. MicroRNA-181a, -146a and -146b in spleen CD4+ T lymphocytes play proinflammatory roles in a murine model of asthma. Int Immunopharmacol. 2012;13(3):347-53.

288. Tsitsiou E, Williams AE, Moschos SA, Patel K, Rossios C, Jiang XY, et al. Transcriptome analysis shows activation of circulating CD8(+) T cells in patients with severe asthma. J Allergy Clin Immunol. 2012;129(1):95-103.

289. Iliopoulos D, Jaeger SA, Hirsch HA, Bulyk ML, Struhl K. STAT3 Activation of miR-21 and miR-181b-1 via PTEN and CYLD Are Part of the Epigenetic Switch Linking Inflammation to Cancer. Mol Cell. 2010;39(4):493-506.

290. Sheedy FJ, Palsson-McDermott E, Hennessy EJ, Martin C, O'Leary JJ, Ruan QG, et al. Negative regulation of TLR4 via targeting of the proinflammatory tumor suppressor PDCD4 by the microRNA miR-21. Nat Immunol. 2010;11(2):141-U59.

291. Lu TX, Munitz A, Rothenberg ME. MicroRNA-21 Is Up-Regulated in Allergic Airway Inflammation and Regulates IL-12p35 Expression. J Immunol. 2009;182(8):4994-5002.

292. Lee HY, Choi JY, Hur J, Kim IK, Kim YK, Kang JY, et al. Inhibition of MicroRNA-21 by an antagomir ameliorates allergic inflammation in a mouse model of asthma. Exp Lung Res. 2017;43(3):109-19.

293. Wu XB, Wang MY, Zhu HY, Tang SQ, You YD, Xie YQ. Overexpression of microRNA-21 and microRNA-126 in the patients of bronchial asthma. Int J Clin Exp Med. 2014;7(5):1307-12.

294.   Clurman BE, Hayward WS. MULTIPLE PROTO-ONCOGENE ACTIVATIONS IN AVIAN-LEUKOSIS VIRUS-INDUCED LYMPHOMAS - EVIDENCE FOR STAGE-SPECIFIC EVENTS. Mol Cell Biol. 1989;9(6):2657-64.

295.   Tam W, BenYehuda D, Hayward WS. bic, a novel gene activated by proviral insertions in avian leukosis virus-induced lymphomas, is likely to function through its noncoding RNA. Mol Cell Biol. 1997;17(3):1490-502.

296.   Eis PS, Tam W, Sun LP, Chadburn A, Li ZD, Gomez MF, et al. Accumulation of miR-155 and BIC RNA in human B cell lymphomas. Proc Natl Acad Sci U S A. 2005;102(10):3627-32.

297.   Rodriguez A, Vigorito E, Clare S, Warren MV, Couttet P, Soond DR, et al. Requirement of bic/microRNA-155 for normal immune function. Science. 2007;316(5824):608-11.

298.   O'Connell RM, Taganov KD, Boldin MP, Cheng GH, Baltimore D. MicroRNA-155 is induced during the macrophage inflammatory response. Proceedings of the National Academy of Sciences of the United States of America. 2007;104(5):1604-9.

299.   Wang P, Hou J, Lin L, Wang CM, Liu XG, Li D, et al. Inducible microRNA-155 Feedback Promotes Type I IFN Signaling in Antiviral Innate Immunity by Targeting Suppressor of Cytokine Signaling 1. Journal of Immunology. 2010;185(10):6226-33.

300.   O'Connell RM, Chaudhuri AA, Rao DS, Baltimore D. Inositol phosphatase SHIP1 is a primary target of miR-155. Proc Natl Acad Sci U S A. 2009;106(17):7113-8.

301.   Kurowska-Stolarska M, Alivernini S, Ballantine LE, Asquith DL, Millar NL, Gilchrist DS, et al. MicroRNA-155 as a proinflammatory regulator in clinical and experimental arthritis. Proceedings of the National Academy of Sciences of the United States of America. 2011;108(27):11193-8.

302.   Kurowska-Stolarska M, Ballantine L, Stolarski B, Hunter J, Hueber A, Gracie JA, et al. MIR-155 AND MIR-34A REGULATE PROINFLAMMATORY CYTOKINE PRODUCTION BY HUMAN MONOCYTES. Ann Rheum Dis. 2010;69:A30-A.

303.   Elmesmari A, Gilchrist DG, Kurowska-Stolarska M, McInnes IB. Mir-155 Expression Correlates with Clinical Disease Activity and Has Effector Function in Rheumatoid Arthritis. Arthritis Rheumatol. 2014;66:S1069-S.

304.   Elmesmari A, Fraser AR, Wood C, Gilchrist D, Vaughan D, Stewart L, et al. MicroRNA-155 regulates monocyte chemokine and chemokine receptor expression in Rheumatoid Arthritis. Rheumatology. 2016;55(11):2056-65.

305.   Ceppi M, Pereira PM, Dunand-Sauthier I, Barras E, Reith W, Santos MA, et al. MicroRNA-155 modulates the interleukin-1 signaling pathway in activated human monocyte-derived dendritic cells. Proc Natl Acad Sci U S A. 2009;106(8):2735-40.

306.   Bochkov YA, Hanson KM, Keles S, Brockman-Schneider RA, Jarjour NN, Gern JE. Rhinovirus-induced modulation of gene expression in bronchial epithelial cells from subjects with asthma. Mucosal Immunol. 2010;3(1):69-80.

307.   Tolfvenstam T, Lindblom A, Schreiber MJ, Ling L, Chow A, Ooi EE, et al. Characterization of early host responses in adults with dengue disease. BMC Infect Dis. 2011;11:7.

308.   Teh DBL, Prasad A, Jiang WX, Ariffin MZ, Khanna S, Belorkar A, et al. Transcriptome Analysis Reveals Neuroprotective aspects of Human Reactive Astrocytes induced by Interleukin 1 beta. Sci Rep. 2017;7:12.

309.   Zhou J, Wang HX, Lu AL, Hu GX, Luo AP, Ding F, et al. A novel gene, NMES1, downregulated in human esophageal squamous cell carcinoma. Int J Cancer. 2002;101(4):311-6.

310.   Sova P, Feng QH, Geiss G, Wood T, Strauss R, Rudolf V, et al. Discovery of novel methylation biomarkers in cervical carcinoma by global demethylation and microarray analysis. Cancer Epidemiology Biomarkers & Prevention. 2006;15(1):114-23.

311.   Spisak S, Kalmar A, Galamb O, Wichmann B, Sipos F, Peterfia B, et al. Genome-Wide Screening of Genes Regulated by DNA Methylation in Colon Cancer Development. PLoS One. 2012;7(10).

312.   Kim DS, Lee WK, Park JY. Hypermethylation of normal mucosa of esophagus-specific 1 is associated with an unfavorable prognosis in patients with non-small cell lung cancer. Oncol Lett. 2018;16(2):2409-15.

313.   Lu LQ, McCurdy S, Huang SJ, Zhu X, Peplowska K, Tiirikainen M, et al. Time Series miRNA-mRNA integrated analysis reveals critical miRNAs and targets in macrophage polarization. Sci Rep. 2016;6:14.

314.   Xu R, Zeng G, Wang SY, Tao H, Ren L, Zhang Z, et al. Periodontitis promotes the diabetic development of obese rat via miR-147 induced classical macrophage activation. Biomed Pharmacother. 2016;83:892-7.

315.   Choi EJ, Kim HB, Baek YH, Kim EH, Pascua PNQ, Park SJ, et al. Differential microRNA expression following infection with a mouse-adapted, highly virulent avian H5N2 virus. BMC Microbiol. 2014;14:13.

316.   Hicks JA, Yoo D, Liu HC. Characterization of the microRNAome in Porcine Reproductive and Respiratory Syndrome Virus Infected Macrophages. PLoS One. 2013;8(12):12.

317.   Sui CJ, Xu F, Shen WF, Dai BH, Lu JJ, Zhang MF, et al. MicroRNA-147 suppresses human hepatocellular carcinoma proliferation migration and chemosensitivity by inhibiting HOXC6. Am J Cancer Res. 2016;6(12):2787-98.

318.   Ning X, Wang C, Zhang M, Wang K. Ectopic expression of miR-147 inhibits stem cell marker and epithelial-mesenchymal transition (EMT)-related protein expression in colon cancer cells. Oncol Res. 2018.

319.   Cui S, Yang X, Zhang L, Zhao Y, Yan W. LncRNA MAFG-AS1 promotes the progression of colorectal cancer by sponging miR-147b and activation of NDUFA4. Biochem Biophys Res Commun. 2018;506(1):251-8.

320.   Lee CG, McCarthy S, Gruidl M, Timme C, Yeatman TJ. MicroRNA-147 Induces a Mesenchymal-To-Epithelial Transition (MET) and Reverses EGFR Inhibitor Resistance. PLoS One. 2014;9(1):12.

321.   Ranade AR, Cherba D, Sridhar S, Richardson P, Webb C, Paripati A, et al. MicroRNA 92a-2 A Biomarker Predictive for Chemoresistance and Prognostic for Survival in Patients with Small Cell Lung Cancer. J Thorac Oncol. 2010;5(8):1273-8.

322.   Chu GM, Zhang JB, Chen XB. Serum level of microRNA-147 as diagnostic biomarker in human non-small cell lung cancer. J Drug Target. 2016;24(7):613-7.

323.   Bertero T, Grosso S, Robbe-Sermesant K, Lebrigand K, Henaoui IS, Puissegur MP, et al. "Seed-Milarity" Confers to hsa-miR-210 and hsa-miR-147b Similar Functional Activity. PLoS One. 2012;7(9):14.

324.   Shen H, Liu T, Fu LL, Zhao SH, Fan B, Cao JH, et al. Identification of microRNAs involved in dexamethasone-induced muscle atrophy. Mol Cell Biochem. 2013;381(1-2):105-13.

325.   Liston A, Papadopoulou AS, Danso-Abeam D, Dooley J. MicroRNA-29 in the adaptive immune system: setting the threshold. Cell Mol Life Sci. 2012;69(21):3533-41.

326.   Amodio N, Rossi M, Raimondi L, Pitari MR, Botta C, Tagliaferri P, et al. miR-29s: a family of epi-miRNAs with therapeutic implications in hematologic malignancies. Oncotarget. 2015;6(15):12837-61.

327.   Hong YF, Wu JX, Zhao JP, Wang HP, Liu Y, Chen TP, et al. miR-29b and miR-29c Are Involved in Toll-Like Receptor Control of Glucocorticoid-Induced Apoptosis in Human Plasmacytoid Dendritic Cells. PLoS One. 2013;8(7):8.

328.   McCoy CE, Carpenter S, Palsson-McDermott EM, Gearing LJ, O'Neill LAJ. Glucocorticoids inhibit IRF3 phosphorylation in response to toll-like receptor-3 and-4 by targeting TBK1 activation. J Biol Chem. 2008;283(21):14277-85.

329.   Flammer JR, Dobrovolna J, Kennedy MA, Chinenov Y, Glass CK, Ivashkiv LB, et al. The Type I Interferon Signaling Pathway Is a Target for Glucocorticoid Inhibition. Mol Cell Biol. 2010;30(19):4564-74.

330.   Bhattacharyya S, Zhao YX, Kay TWH, Muglia LJ. Glucocorticoids target suppressor of cytokine signaling 1 (SOCS1) and type 1 interferons to regulate Toll-like receptor-induced STAT1 activation. Proc Natl Acad Sci U S A. 2011;108(23):9554-9.

331.	Vettorazzi S, Bode C, Dejager L, Frappart L, Shelest E, Klassen C, et al. Glucocorticoids limit acute lung inflammation in concert with inflammatory stimuli by induction of SphK1. Nature Communications. 2015;6:12.

332.	Zhang ZX, Jones S, Hagood JS, Fuentes NL, Fuller GM. STAT3 acts as a co-activator of glucocorticoid receptor signaling. Journal of Biological Chemistry. 1997;272(49):30607-10.

333.	Sun XX, Zhang J, Hou ZH, Han QJ, Zhang C, Tian ZG. miR-146a is directly regulated by STAT3 in human hepatocellular carcinoma cells and involved in anti-tumor immune suppression. Cell Cycle. 2015;14(2):243-52.

334.	Appelmelk BJ, Shiberu B, Trinks C, Tapsi N, Zheng PY, Verboom T, et al. Phase variation in Helicobacter pylori lipopolysaccharide. Infect Immun. 1998;66(1):70-6.

335.	Visser J, van Boxel-Dezaire A, Methorst D, Brunt T, de Kloet ER, Nagelkerken L. Differential regulation of interleukin-10 (IL-10) and IL-12 by glucocorticoids in vitro. Blood. 1998;91(11):4255-64.

336.	Platanias LC. Mechanisms of type-I- and type-II-interferon-mediated signalling. Nat Rev Immunol. 2005;5(5):375-86.

337.	Felten R, Scher F, Sibilia J, Chasset F, Arnaud L. Advances in the treatment of systemic lupus erythematosus: From back to the future, to the future and beyond. Joint Bone Spine. 2019;86(4):429-36.

338.	Chen HL, Shen LJ, Hsu PN, Shen CY, Hall SA, Hsiao FY. Cumulative Burden of Glucocorticoid-related Adverse Events in Patients with Systemic Lupus Erythematosus: Findings from a 12-year Longitudinal Study. J Rheumatol. 2018;45(1):83-9.

339.	Fanouriakis A, Kostopoulou M, Alunno A, Aringer M, Bajema I, Boletis JN, et al. 2019 update of the EULAR recommendations for the management of systemic lupus erythematosus. Ann Rheum Dis. 2019;78(6):736-45.

340.	Hirst J, Carroll J, Fearnley IM, Shannon RJ, Walker JE. The nuclear encoded subunits of complex I from bovine heart mitochondria. Biochim Biophys Acta-Bioenerg. 2003;1604(3):135-50.

341.	Carroll J, Fearnley IM, Skehel JM, Shannon RJ, Hirst J, Walker JE. Bovine complex I is a complex of 45 different subunits. J Biol Chem. 2006;281(43):32724-7.

342.	Balsa E, Marco R, Pereles-Clemente E, Szklarczyk R, Calvo E, Landazuri MO, et al. NDUFA4 Is a Subunit of Complex IV of the Mammalian Electron Transport Chain. Cell Metab. 2012;16(3):378-86.

343.	Kadenbach B. Regulation of Mammalian 13-Subunit Cytochrome c Oxidase and Binding of other Proteins: Role of NDUFA4. Trends Endocrinol Metab. 2017;28(11):761-70.

344.	Letts JA, Sazanov LA. Clarifying the supercomplex: the higher-order organization of the mitochondrial electron transport chain. Nat Struct Mol Biol. 2017;24(10):800-8.

345.	Zong S, Wu M, Gu J, Liu T, Guo R, Yang M. Structure of the intact 14-subunit human cytochrome c oxidase. Cell Res. 2018.

346.	Ren MD, Phoon CKL, Schlame M. Metabolism and function of mitochondrial cardiolipin. Progress in Lipid Research. 2014;55:1-16.

347.	Liu F, Lossl P, Rabbitts BM, Balaban RS, Heck AJR. The interactome of intact mitochondria by cross-linking mass spectrometry provides evidence for coexisting respiratory supercomplexes. Molecular & Cellular Proteomics. 2018;17(2):216-32.

348.	Pitceathly RDS, Taanman JW. NDUFA4 (Renamed COXFA4) Is a Cytochrome-c Oxidase Subunit. Trends Endocrinol Metab. 2018;29(7):452-4.

349.	Yagil C, Varadi-Levi R, Yagil Y. A novel mutation in the NADH dehydrogenase (ubiquinone) 1 alpha subcomplex 4 (Ndufa4) gene links mitochondrial dysfunction to the development of diabetes in a rodent model. Dis Model Mech. 2018;11(11):9.

350.	Chang WS, Wang YH, Zhu XT, Wu CJ. Genome-Wide Profiling of miRNA and mRNA Expression in Alzheimer's Disease. Med Sci Monitor. 2017;23:2721-31.

351.	Bi R, Zhang W, Zhang DF, Xu M, Fan Y, Hu QX, et al. Genetic association of the cytochrome c oxidase-related genes with Alzheimer's disease in Han Chinese. Neuropsychopharmacology. 2018;43(11):2264-76.

352.	Fu F, Li Y, Li R, Lei TY, Wang D, Yang X, et al. NDUFA4 enhances neuron growth by triggering growth factors and inhibiting neuron apoptosis through Bcl-2 and cytochrome C mediated signaling pathway. Am J Transl Res. 2018;10(1):164-74.

353.	Derambure C, Dzangue-Tchoupou G, Berard C, Vergne N, Hiron M, D'Agostino MA, et al. Pre-silencing of genes involved in the electron transport chain (ETC) pathway is associated with responsiveness to abatacept in rheumatoid arthritis. Arthritis Res Ther. 2017;19:13.

354.	Bonelli M, Scheinecker C. How does abatacept really work in rheumatoid arthritis? Curr Opin Rheumatol. 2018;30(3):295-300.

355.	Lei LY, Chen C, Zhao JJ, Wang HR, Guo MM, Zhou Y, et al. Targeted Expression of miR-7 Operated by TTF-1 Promoter Inhibited the Growth ofHumanLungCancer through theNDUFA4Pathway. Mol Ther-Nucl Acids. 2017;6:183-97.

356.	Puissegur MP, Mazure NM, Bertero T, Pradelli L, Grosso S, Robbe-Sermesant K, et al. miR-210 is overexpressed in late stages of lung cancer and mediates mitochondrial alterations associated with modulation of HIF-1 activity. Cell Death Differ. 2011;18(3):465-78.

357.	Yang C, Wu D, Gao L, Liu X, Jin YJ, Wang D, et al. Competing endogenous RNA networks in human cancer: hypothesis, validation, and perspectives. Oncotarget. 2016;7(12):13479-90.

358.	Kumar V, Gabrilovich DI. Hypoxia-inducible factors in regulation of immune responses in tumour microenvironment. Immunology. 2014;143(4):512-9.

359.	Tello D, Balsa E, Acosta-Iborra B, Fuertes-Yebra E, Elorza A, Ordonez A, et al. Induction of the Mitochondrial NDUFA4L2 Protein by HIF-1 alpha Decreases Oxygen Consumption by Inhibiting Complex I Activity. Cell Metab. 2011;14(6):768-79.

360.	Schroder K, Irvine KM, Taylor MS, Bokil NJ, Cao KAL, Masterman KA, et al. Conservation and divergence in Toll-like receptor 4-regulated gene expression in primary human versus mouse macrophages. Proc Natl Acad Sci U S A. 2012;109(16):E944-E53.

361.	Amarzguioui M, Lundberg P, Cantin E, Hagstrom J, Behlke MA, Rossi JJ. Rational design and in vitro and in vivo delivery of Dicer substrate siRNA. Nat Protoc. 2006;1(2):508-17.

362.	Petersen M, Bondensgaard K, Wengel J, Jacobsen JP. Locked nucleic acid (LNA) recognition of RNA: NMR solution structures of LNA : RNA hybrids. J Am Chem Soc. 2002;124(21):5974-82.

363.	Lima JF, Cerqueira L, Figueiredo C, Oliveira C, Azevedo NF. Anti-miRNA oligonucleotides: A comprehensive guide for design. Rna Biology. 2018;15(3):338-52.

364.	Baliga BS, Pronczuk AW, Munro HN. MECHANISM OF CYCLOHEXIMIDE INHIBITION OF PROTEIN SYNTHESIS IN A CELL-FREE SYSTEM PREPARED FROM RAT LIVER. J Biol Chem. 1969;244(16):4480-&.

365.	Schneider-Poetsch T, Ju JH, Eyler DE, Dang YJ, Bhat S, Merrick WC, et al. Inhibition of eukaryotic translation elongation by cycloheximide and lactimidomycin. Nature Chemical Biology. 2010;6(3):209-17.

366.	Sinkler CA, Kalpage H, Shay J, Lee I, Malek MH, Grossman LI, et al. Tissue-and Condition-Specific Isoforms of Mammalian Cytochrome c Oxidase Subunits: From Function to Human Disease. Oxidative Med Cell Longev. 2017:19.

367.	Fukuda R, Zhang HF, Kim JW, Shimoda L, Dang CV, Semenza GL. HIF-1 regulates cytochrome oxidase subunits to optimize efficiency of respiration in hypoxic cells. Cell. 2007;129(1):111-22.

368.	Deshwal S, Fiedler KU, Langer T. Mitochondrial Proteases: Multifaceted Regulators of Mitochondrial Plasticity. Annu Rev Biochem. 2020.

369.	Horsefield R, Yankovskaya V, Sexton G, Whittingham W, Shiomi K, Omura S, et al. Structural and computational analysis of the quinone-binding site of complex II (succinate-ubiquinone oxidoreductase) - A mechanism of electron transfer and proton conduction during ubiquinone reduction. J Biol Chem. 2006;281(11):7309-16.

370.	Scarpulla RC. Nuclear Control of Respiratory Chain Expression by Nuclear Respiratory Factors and PGC-1-Related Coactivator. Mitochondria and Oxidative Stress in Neurodegenerative Disorders. 2008;1147:321-34.

371.   Dinkova-Kostova AT, Abramov AY. The emerging role of Nrf2 in mitochondrial function. Free Radical Biology and Medicine. 2015;88:179-88.

372.   Agyeman AS, Chaerkady R, Shaw PG, Davidson NE, Visvanathan K, Pandey A, et al. Transcriptomic and proteomic profiling of KEAP1 disrupted and sulforaphane-treated human breast epithelial cells reveals common expression profiles. Breast Cancer Research and Treatment. 2012;132(1):175-87.

373.   Bota DA, Davies KJA. Mitochondrial Lon protease in human disease and aging: Including an etiologic classification of Lon -related diseases and disorders. Free Radical Biology and Medicine. 2016;100:188-98.

374.   Palmieri EM, Gonzalez-Cotto M, Baseler WA, Davies LC, Ghesquière B, Maio N, et al. Nitric oxide orchestrates metabolic rewiring in M1 macrophages by targeting aconitase 2 and pyruvate dehydrogenase. Nat Commun. 2020;11(1):698.

375.   Pajuelo Reguera D, Čunátová K, Vrbacký M, Pecinová A, Houštěk J, Mráček T, et al. Cytochrome c Oxidase Subunit 4 Isoform Exchange Results in Modulation of Oxygen Affinity. Cells. 2020;9(2).

376.   Dyczynski M, Vesterlund M, Bjorklund AC, Zachariadis V, Janssen J, Gallart-Ayala H, et al. Metabolic reprogramming of acute lymphoblastic leukemia cells in response to glucocorticoid treatment. Cell Death Dis. 2018;9:13.

377.   Buentke E, Nordstrom A, Lin H, Bjorklund AC, Laane E, Harada M, et al. Glucocorticoid-induced cell death is mediated through reduced glucose metabolism in lymphoid leukemia cells. Blood Cancer J. 2011;1:9.

378.   Aoki S, Morita M, Hirao T, Yamaguchi M, Shiratori R, Kikuya M, et al. Shift in energy metabolism caused by glucocorticoids enhances the effect of cytotoxic anti-cancer drugs against acute lymphoblastic leukemia cells. Oncotarget. 2017;8(55):94271-85.

379.   Hulleman E, Kazemier KM, Holleman A, VanderWeele DJ, Rudin CM, Broekhuis MJC, et al. Inhibition of glycolysis modulates prednisolone resistance in acute lymphoblastic leukemia cells. Blood. 2009;113(9):2014-21.

380.   Tonomura N, McLaughlin K, Grimm L, Goldsby RA, Osborne BA. Glucocorticoid-induced apoptosis of thymocytes: Requirement of proteasome-dependent mitochondrial activity. J Immunol. 2003;170(5):2469-78.

381.   Tome ME, Lee K, Jaramillo MC, Briehl MM. Mitochondria are the primary source of the H2O2 signal for glucocorticoid-induced apoptosis of lymphoma cells. Exp Ther Med. 2012;4(2):237-42.

382.   Tung S, Shi YH, Wong K, Zhu F, Gorczynski R, Laister RC, et al. PPAR alpha and fatty acid oxidation mediate glucocorticoid resistance in chronic lymphocytic leukemia. Blood. 2013;122(6):969-80.

383.   Zhao Y, Wu TT, Shao S, Shi BY. Phenotype, development, and biological function of myeloid-derived suppressor cells. OncoImmunology. 2016;5(2):12.

384.   Tamadaho RSE, Hoerauf A, Layland LE. Immunomodulatory effects of myeloid-derived suppressor cells in diseases: Role in cancer and infections. Immunobiology. 2018;223(4-5):432-42.

385.   Lu Y, Liu H, Bi Y, Yang H, Li Y, Wang J, et al. Glucocorticoid receptor promotes the function of myeloid-derived suppressor cells by suppressing HIF1α-dependent glycolysis. Cell Mol Immunol. 2018;15(6):618-29.

386.   Bustos R, Sobrino F. STIMULATION OF GLYCOLYSIS AS AN ACTIVATION SIGNAL IN RAT PERITONEAL-MACROPHAGES - EFFECT OF GLUCOCORTICOIDS ON THIS PROCESS. Biochem J. 1992;282:299-303.

387.   Gaber T, Schellmann S, Erekul KB, Fangradt M, Tykwinska K, Hahne M, et al. Macrophage Migration Inhibitory Factor Counterregulates Dexamethasone-Mediated Suppression of Hypoxia-Inducible Factor-1 alpha Function and Differentially Influences Human CD4(+) T Cell Proliferation under Hypoxia. J Immunol. 2011;186(2):764-74.

388. Lim W, Park C, Shim MK, Lee YH, Lee YM, Lee Y. Glucocorticoids suppress hypoxia-induced COX-2 and hypoxia inducible factor-1 alpha expression through the induction of glucocorticoid-induced leucine zipper. Br J Pharmacol. 2014;171(3):735-45.

389. Wang WH, Wang P, Li SY, Yang JW, Liang XJ, Tang Y, et al. Methylprednisolone inhibits the proliferation and affects the differentiation of rat spinal cord-derived neural progenitor cells cultured in low oxygen conditions by inhibiting HIF-1 alpha and Hes1 in vitro. International Journal of Molecular Medicine. 2014;34(3):788-95.

390. Kim JH, Hwang YJ, Han SH, Lee YE, Kim S, Kim YJ, et al. Dexamethasone inhibits hypoxia-induced epithelial-mesenchymal transition in colon cancer. World J Gastroenterol. 2015;21(34):9887-99.

391. Kodama T, Shimizu N, Yoshikawa N, Makino Y, Ouchida R, Okamoto K, et al. Role of the glucocorticoid receptor for regulation of hypoxia-dependent gene expression. J Biol Chem. 2003;278(35):33384-91.

392. Vettori A, Greenald D, Wilson GK, Peron M, Facchinello N, Markham E, et al. Glucocorticoids promote Von Hippel Lindau degradation and Hif-1 alpha stabilization. Proc Natl Acad Sci U S A. 2017;114(37):9948-53.

393. Leonard MO, Godson C, Brady HR, Taylor CT. Potentiation of glucocorticoid activity in hypoxia through induction of the glucocorticoid receptor. J Immunol. 2005;174(4):2250-7.

394. Vijayan V, Pradhan P, Braud L, Fuchs HR, Gueler F, Motterlini R, et al. Human and murine macrophages exhibit differential metabolic responses to lipopolysaccharide - A divergent role for glycolysis. Redox Biol. 2019;22:9.

395. Winer LSP, Wu M. Rapid Analysis of Glycolytic and Oxidative Substrate Flux of Cancer Cells in a Microplate. PLoS One. 2014;9(10).

396. Everts B, Amiel E, van der Windt GJW, Freitas TC, Chott R, Yarasheski KE, et al. Commitment to glycolysis sustains survival of NO-producing inflammatory dendritic cells. Blood. 2012;120(7):1422-31.

397. Bouillaud F, Alves-Guerra MC, Ricquier D. UCPs, at the interface between bioenergetics and metabolism. Biochim Biophys Acta-Mol Cell Res. 2016;1863(10):2443-56.

398. Kizaki T, Suzuki K, Hitomi Y, Taniguchi N, Saitoh D, Watanabe K, et al. Uncoupling protein 2 plays an important role in nitric oxide production of lipopolysaccharide-stimulated macrophages. Proc Natl Acad Sci U S A. 2002;99(14):9392-7.

399. Emre Y, Hurtaud C, Nubel T, Criscuolo F, Ricquier D, Cassard-Doulcier AM. Mitochondria contribute to LPS-induced MAPK activation via uncoupling protein UCP2 in macrophages. Biochem J. 2007;402:271-8.

400. Emre Y, Nubel T. Uncoupling protein UCP2: When mitochondrial activity meets immunity. FEBS Lett. 2010;584(8):1437-42.

401. De Simone R, Ajmone-Cat MA, Pandolfi M, Bernardo A, De Nuccio C, Minghetti L, et al. The mitochondrial uncoupling protein-20 is a master regulator of both M1 and M2 microglial responses. J Neurochem. 2015;135(1):147-56.

402. Diaz-Ruiz R, Rigoulet M, Devin A. The Warburg and Crabtree effects: On the origin of cancer cell energy metabolism and of yeast glucose repression. Biochim Biophys Acta-Bioenerg. 2011;1807(6):568-76.

403. Marin-Hernandez A, Gallardo-Perez JC, Ralph SJ, Rodriguez-Enriquez S, Moreno-Sanchez R. HIF-1 alpha Modulates Energy Metabolism in Cancer Cells by Inducing Over-Expression of Specific Glycolytic Isoforms. Mini-Reviews in Medicinal Chemistry. 2009;9(9):1084-101.

404. Haneklaus M, O'Neill LAJ. NLRP3 at the interface of metabolism and inflammation. Immunol Rev. 2015;265(1):53-62.

405. Kleiman A, Hubner S, Parkitna JMR, Neumann A, Hofer S, Weigand MA, et al. Glucocorticoid receptor dimerization is required for survival in septic shock via suppression of interleukin-1 in macrophages. Faseb J. 2012;26(2):722-9.

406. Contreras-Baeza Y, Sandoval PY, Alarcón R, Galaz A, Cortés-Molina F, Alegría K, et al. Monocarboxylate transporter 4 (MCT4) is a high affinity transporter capable of exporting lactate in high-lactate microenvironments. J Biol Chem. 2019.

407. Tan Z, Xie N, Banerjee S, Cui HC, Fu MG, Thannickal VJ, et al. The Monocarboxylate Transporter 4 Is Required for Glycolytic Reprogramming and Inflammatory Response in Macrophages. Journal of Biological Chemistry. 2015;290(1):46-55.

408. Pucino V, Bombardieri M, Pitzalis C, Mauro C. Lactate at the crossroads of metabolism, inflammation, and autoimmunity. Eur J Immunol. 2017;47(1):14-21.

409. Anderson JR, Chokesuwattanaskul S, Phelan MM, Welting TJM, Lian LY, Peffers MJ, et al. H-1 NMR Metabolomics Identifies Underlying Inflammatory Pathology in Osteoarthritis and Rheumatoid Arthritis Synovial Joints. Journal of Proteome Research. 2018;17(11):3780-90.

410. Carlson AK, Rawle RA, Adams E, Greenwood MC, Bothner B, June RK. Application of global metabolomic profiling of synovial fluid for osteoarthritis biomarkers. Biochemical and Biophysical Research Communications. 2018;499(2):182-8.

411. Garaude J. Reprogramming of mitochondrial metabolism by innate immunity. Curr Opin Immunol. 2019;56:17-23.

412. Scaduto RC, Grotyohann LW. Measurement of mitochondrial membrane potential using fluorescent rhodamine derivatives. Biophysical Journal. 1999;76(1):469-77.

413. Buravkov SV, Pogodina MV, Buravkova LB. Comparison of Mitochondrial Fluorescent Dyes in Stromal Cells. Bull Exp Biol Med. 2014;157(5):654-8.

414. Shay T, Jojic V, Zuk O, Rothamel K, Puyraimond-Zemmour D, Feng T, et al. Conservation and divergence in the transcriptional programs of the human and mouse immune systems. Proc Natl Acad Sci U S A. 2013;110(8):2946-51.

415. Yang Z, Fujii H, Mohan SV, Goronzy JJ, Weyand CM. Phosphofructokinase deficiency impairs ATP generation, autophagy, and redox balance in rheumatoid arthritis T cells. J Exp Med. 2013;210(10):2119-34.

416. Millet P, Vachharajani V, McPhail L, Yoza B, McCall CE. GAPDH Binding to TNF-α mRNA Contributes to Posttranscriptional Repression in Monocytes: A Novel Mechanism of Communication between Inflammation and Metabolism. J Immunol. 2016;196(6):2541-51.

417. Hiscott J, Marois J, Garoufalis J, Daddario M, Roulston A, Kwan I, et al. CHARACTERIZATION OF A FUNCTIONAL NF-KAPPA-B SITE IN THE HUMAN INTERLEUKIN-1-BETA PROMOTER - EVIDENCE FOR A POSITIVE AUTOREGULATORY LOOP. Mol Cell Biol. 1993;13(10):6231-40.

418. Busillo JM, Azzam KM, Cidlowski JA. Glucocorticoids Sensitize the Innate Immune System through Regulation of the NLRP3 Inflammasome. J Biol Chem. 2011;286(44):38703-13.

419. Fearon U, Hanlon MM, Wade SM, Fletcher JM. Altered metabolic pathways regulate synovial inflammation in rheumatoid arthritis. Clin Exp Immunol. 2019;197(2):170-80.

420. Liu TF, Vachharajani VT, Yoza BK, McCall CE. NAD(+)-dependent Sirtuin 1 and 6 Proteins Coordinate a Switch from Glucose to Fatty Acid Oxidation during the Acute Inflammatory Response. J Biol Chem. 2012;287(31):25758-69.

421. Deshwal S, Antonucci S, Kaludercic N, Di Lisa F. Measurement of Mitochondrial ROS Formation. In: Palmeira CM, Moreno AJ, editors. Mitochondrial Bioenergetics: Methods and Protocols, 2nd Edition. Methods in Molecular Biology. 1782. Totowa: Humana Press Inc; 2018. p. 403-18.

422. Kelly B, Tannahill GM, Murphy MP, O'Neill LAJ. Metformin Inhibits the Production of Reactive Oxygen Species from NADH:Ubiquinone Oxidoreductase to Limit Induction of Interleukin-1 beta (IL-1 beta) and Boosts Interleukin-10 (IL-10) in Lipopolysaccharide (LPS)-activated Macrophages. J Biol Chem. 2015;290(33):20348-59.

423. Lee HM, Kim JJ, Kim HJ, Shong M, Ku BJ, Jo EK. Upregulated NLRP3 Inflammasome Activation in Patients With Type 2 Diabetes. Diabetes. 2013;62(1):194-204.

424.	Jin ZX, Wei W, Yang M, Du Y, Wan YH. Mitochondrial Complex I Activity Suppresses Inflammation and Enhances Bone Resorption by Shifting Macrophage-Osteoclast Polarization. Cell Metab. 2014;20(3):483-98.

425.	Garaude J, Acin-Perez R, Martinez-Cano S, Enamorado M, Ugolini M, Nistal-Villan E, et al. Mitochondrial respiratory-chain adaptations in macrophages contribute to antibacterial host defense. Nat Immunol. 2016;17(9):1037-45.

426.	Lai RKH, Xu IMJ, Chiu DKC, Tse APW, Wei LL, Law CT, et al. NDUFA4L2 Fine-tunes Oxidative Stress in Hepatocellular Carcinoma. Clin Cancer Res. 2016;22(12):3105-17.

427.	Minton DR, Fu LP, Mongan NP, Shevchuk MM, Nanus DM, Gudas LJ. Role of NADH Dehydrogenase (Ubiquinone) 1 Alpha Subcomplex 4-Like 2 in Clear Cell Renal Cell Carcinoma. Clin Cancer Res. 2016;22(11):2791-801.

428.	Soro-Arnaiz I, Li QOY, Torres-Capelli M, Melendez-Rodriguez F, Veiga S, Veys K, et al. Role of Mitochondrial Complex IV in Age-Dependent Obesity. Cell Reports. 2016;16(11):2991-3002.

429.	Meng LF, Yang XH, Xie X, Wang MS. Mitochondrial NDUFA4L2 protein promotes the vitality of lung cancer cells by repressing oxidative stress. Thorac Cancer. 2019;10(4):676-85.

430.	Liu L, Lan G, Peng L, Xie X, Peng F, Yu S, et al. NDUFA4L2 expression predicts poor prognosis in clear cell renal cell carcinoma patients. Ren Fail. 2016;38(8):1199-205.

431.	Wang L, Peng ZQ, Wang KZ, Qi YJ, Yang Y, Zhang Y, et al. NDUFA4L2 is associated with clear cell renal cell carcinoma malignancy and is regulated by ELK1. PeerJ. 2017;5:15.

432.	Lv Y, Nie SL, Zhou JM, Liu F, Hu YB, Jiang JR, et al. Overexpression of NDUFA4L2 is associated with poor prognosis in patients with colorectal cancer. ANZ J Surg. 2017;87(12):E251-E5.

433.	Andreas K, Haupl T, Lubke C, Ringe J, Morawietz L, Wachtel A, et al. Antirheumatic drug response signatures in human chondrocytes: potential molecular targets to stimulate cartilage regeneration. Arthritis Res Ther. 2009;11(1).

434.	Signes A, Fernandez-Vizarra E. Assembly of mammalian oxidative phosphorylation complexes I-V and supercomplexes. Mitochondrial Diseases. 2018;62(3):255-70.

435.	Gagnon KT, Corey DR. Guidelines for Experiments Using Antisense Oligonucleotides and Double-Stranded RNAs. Nucleic Acid Therapeutics. 2019;29(3):116-22.

436.	Hardbower DM, Singh K, Asim M, Verriere TG, Olivares-Villagomez D, Barry DP, et al. EGFR regulates macrophage activation and function in bacterial infection. J Clin Invest. 2016;126(9):3296-312.

437.	Tan XJ, Sun LJ, Chen JQ, Chen ZJJ. Detection of Microbial Infections Through Innate Immune Sensing of Nucleic Acids. In: Gottesman S, editor. Annual Review of Microbiology, Vol 72. Annual Review of Microbiology. 72. Palo Alto: Annual Reviews; 2018. p. 447-78.

438.	Baum P, Fundel-Clemens K, Kreuz S, Kontermann RE, Weith A, Mennerich D, et al. Off-Target Analysis of Control siRNA Molecules Reveals Important Differences in the Cytokine Profile and Inflammation Response of Human Fibroblasts. Oligonucleotides. 2010;20(1):17-25.

439.	Heil F, Hemmi H, Hochrein H, Ampenberger F, Kirschning C, Akira S, et al. Species-specific recognition of single-stranded RNA via toll-like receptor 7 and 8. Science. 2004;303(5663):1526-9.

440.	Judge AD, Sood V, Shaw JR, Fang D, McClintock K, MacLachlan I. Sequence-dependent stimulation of the mammalian innate immune response by synthetic siRNA. Nat Biotechnol. 2005;23(4):457-62.

441.	Hornung V, Guenthner-Biller M, Bourquin C, Ablasser A, Schlee M, Uematsu S, et al. Sequence-specific potent induction of IFN-alpha by short interfering RNA in plasmacytoid dendritic cells through TLR7. Nat Med. 2005;11(3):263-70.

442.	Robbins M, Judge A, Ambegia E, Choi C, Yaworski E, Palmer L, et al. Misinterpreting the Therapeutic Effects of Small Interfering RNA Caused by Immune Stimulation. Hum Gene Ther. 2008;19(10):991-9.

443.	Kleinman ME, Yamada K, Takeda A, Chandrasekaran V, Nozaki M, Baffi JZ, et al. Sequence- and target-independent angiogenesis suppression by siRNA via TLR3. Nature. 2008;452(7187):591-U1.

444.   Cantor JR, Abu-Remaileh M, Kanarek N, Freinkman E, Gao X, Louissaint A, et al. Physiologic Medium Rewires Cellular Metabolism and Reveals Uric Acid as an Endogenous Inhibitor of UMP Synthase. Cell. 2017;169(2):258-72.

445.   Aguer C, Gambarotta D, Mailloux RJ, Moffat C, Dent R, McPherson R, et al. Galactose Enhances Oxidative Metabolism and Reveals Mitochondrial Dysfunction in Human Primary Muscle Cells. PLoS One. 2011;6(12):11.

446.   Rossignol R, Gilkerson R, Aggeler R, Yamagata K, Remington SJ, Capaldi RA. Energy substrate modulates mitochondrial structure and oxidative capacity in cancer cells. Cancer Res. 2004;64(3):985-93.

447.   Holden HM, Rayment I, Thoden JB. Structure and function of enzymes of the Leloir pathway for galactose metabolism. J Biol Chem. 2003;278(45):43885-8.

448.   Robinson BH, Petrovabenedict R, Buncic JR, Wallace DC. NONVIABILITY OF CELLS WITH OXIDATIVE DEFECTS IN GALACTOSE MEDIUM - A SCREENING-TEST FOR AFFECTED PATIENT FIBROBLASTS. Biochemical Medicine and Metabolic Biology. 1992;48(2):122-6.

449.   Gleeson LE, Sheedy FJ, Palsson-McDermott EM, Triglia D, O'Leary SM, O'Sullivan MP, et al. Cutting Edge: Mycobacterium tuberculosis Induces Aerobic Glycolysis in Human Alveolar Macrophages That Is Required for Control of Intracellular Bacillary Replication. J Immunol. 2016;196(6):2444-9.

450.   Kadenbach B, Huttemann M. The subunit composition and function of mammalian cytochrome c oxidase. Mitochondrion. 2015;24:64-76.

451.   Arnold S, Kadenbach B. Cell respiration is controlled by ATP, an allosteric inhibitor of cytochrome-c oxidase. Eur J Biochem. 1997;249(1):350-4.

452.   Lee I, Bender E, Kadenbach B. Control of mitochondrial membrane potential and ROS formation by reversible phosphorylation of cytochrome c oxidase. Mol Cell Biochem. 2002;234(1):63-70.

453.   Samavati L, Lee I, Mathes I, Lottspeich F, Huttemann M. Tumor necrosis factor alpha inhibits oxidative phosphorylation through tyrosine phosphorylation at subunit I of cytochrome c oxidase. J Biol Chem. 2008;283(30):21134-44.

454.   Zhang YL, Zhang H, Liu Z. MicroRNA-147 suppresses proliferation, invasion and migration through the AKT/mTOR signaling pathway in breast cancer. Oncol Lett. 2016;11(1):405-10.

455.   Covarrubias AJ, Aksoylar HI, Horng T. Control of macrophage metabolism and activation by mTOR and Akt signaling. Semin Immunol. 2015;27(4):286-96.

456.   Floyd BJ, Wilkerson EM, Veling MT, Minogue CE, Xia CW, Beebe ET, et al. Mitochondrial Protein Interaction Mapping Identifies Regulators of Respiratory Chain Function. Mol Cell. 2016;63(4):621-32.

457.   McGarry T, Biniecka M, Veale DJ, Fearon U. Hypoxia, oxidative stress and inflammation. Free Radic Biol Med. 2018;125:15-24.

458.   McGarry T, Fearon U. Cell metabolism as a potentially targetable pathway in RA. Nat Rev Rheumatol. 2019;15(2):70-2.

459.   Ramirez-Camacho I, Flores-Herrera O, Zazueta C. The relevance of the supramolecular arrangements of the respiratory chain complexes in human diseases and aging. Mitochondrion. 2019;47:266-72.

460.   Lapuente-Brun E, Moreno-Loshuertos R, Acin-Perez R, Latorre-Pellicer A, Colas C, Balsa E, et al. Supercomplex Assembly Determines Electron Flux in the Mitochondrial Electron Transport Chain. Science. 2013;340(6140):1567-70.

461.   Buckley CD, Gilroy DW, Serhan CN. Proresolving Lipid Mediators and Mechanisms in the Resolution of Acute Inflammation. Immunity. 2014;40(3):315-27.

462.   Seeley JJ, Ghosh S. Molecular mechanisms of innate memory and tolerance to LPS. J Leukoc Biol. 2017;101(1):107-19.

463.   Dominguez-Andres J, Netea MG. Long-term reprogramming of the innate immune system. J Leukoc Biol. 2019;105(2):329-38.

464.   Arts RJW, Novakovic B, ter Horst R, Carvalho A, Bekkering S, Lachmandas E, et al. Glutaminolysis and Fumarate Accumulation Integrate Immunometabolic and Epigenetic Programs in Trained Immunity. Cell Metab. 2016;24(6):807-19.

465.   Cheng SC, Quintin J, Cramer RA, Shepardson KM, Saeed S, Kumar V, et al. mTOR- and HIF-1 alpha-mediated aerobic glycolysis as metabolic basis for trained immunity. Science. 2014;345(6204):1579-+.

466.   Gyawali B, Ramakrishna K, Dhamoon AS. Sepsis: The evolution in definition, pathophysiology, and management. SAGE Open Med. 2019;7:13.

467.   Wiersinga WJ, Leopold SJ, Cranendonk DR, van der Poll T. Host innate immune responses to sepsis. Virulence. 2014;5(1):36-44.

468.   Shalova IN, Lim JY, Chittezhath M, Zinkernagel AS, Beasley F, Hernandez-Jimenez E, et al. Human Monocytes Undergo Functional Re-programming during Sepsis Mediated by Hypoxia-Inducible Factor-1 alpha. Immunity. 2015;42(3):484-98.

469.   Kumar V. Targeting macrophage immunometabolism: Dawn in the darkness of sepsis. Int Immunopharmacol. 2018;58:173-85.

470.   Escobar DA, Botero-Quintero AM, Kautza BC, Luciano J, Loughran P, Darwiche S, et al. Adenosine monophosphate-activated protein kinase activation protects against sepsis-induced organ injury and inflammation. J Surg Res. 2015;194(1):262-72.

471.   Huang J, Liu K, Zhu S, Xie M, Kang R, Cao LZ, et al. AMPK regulates immunometabolism in sepsis. Brain Behav Immun. 2018;72:89-100.

472.   Liu TF, Yoza BK, El Gazzar M, Vachharajani VT, McCall CE. NAD(+)-dependent SIRT1 Deacetylase Participates in Epigenetic Reprogramming during Endotoxin Tolerance. J Biol Chem. 2011;286(11):9856-64.

473.   Abraham E, Evans T. Corticosteroids and septic shock. JAMA-J Am Med Assoc. 2002;288(7):886-7.

474.   Long B, Koyfman A. CONTROVERSIES IN CORTICOSTEROID USE FOR SEPSIS. J Emerg Med. 2017;53(5):653-61.

475.   The Human Protein Atlas https://www.proteinatlas.org/2019 [19:[

476.   Uhlen M, Fagerberg L, Hallstrom BM, Lindskog C, Oksvold P, Mardinoglu A, et al. Tissue-based map of the human proteome. Science. 2015;347(6220):10.

477.   Rana A, Musto AE. The role of inflammation in the development of epilepsy. J Neuroinflamm. 2018;15:12.

478.   Prinz M, Jung S, Priller J. Microglia Biology: One Century of Evolving Concepts. Cell. 2019;179(2):292-311.

479.   Wendeln AC, Degenhardt K, Kaurani L, Gertig M, Ulas T, Jain G, et al. Innate immune memory in the brain shapes neurological disease hallmarks. Nature. 2018;556(7701):332-+.

480.   Kim MS, Pinto SM, Getnet D, Nirujogi RS, Manda SS, Chaerkady R, et al. A draft map of the human proteome. Nature. 2014;509(7502):575-+.

481.   Petryszak R, Keays M, Tang YA, Fonseca NA, Barrera E, Burdett T, et al. Expression Atlas update-an integrated database of gene and protein expression in humans, animals and plants. Nucleic Acids Res. 2016;44(D1):D746-D52.

482.   Lee J. Mitochondrial drug targets in neurodegenerative diseases. Bioorg Med Chem Lett. 2016;26(3):714-20.

483.   Mor E, Cabilly Y, Goldshmit Y, Zalts H, Modai S, Edry L, et al. Species-specific microRNA roles elucidated following astrocyte activation. Nucleic Acids Res. 2011;39(9):3710-23.

484.   Bachmann M, Costa R, Peruzzo R, Prosdocimi E, Checchetto V, Leanza L. Targeting Mitochondrial Ion Channels to Fight Cancer. Int J Mol Sci. 2018;19(7):25.

485.   Wang A, Luan HH, Medzhitov R. An evolutionary perspective on immunometabolism. Science. 2019;363(6423):140-.

486. Morgan SA, McCabe EL, Gathercole LL, Hassan-Smith ZK, Larner DP, Bujalska IJ, et al. 11 beta-HSD1 is the major regulator of the tissue-specific effects of circulating glucocorticoid excess. Proc Natl Acad Sci U S A. 2014;111(24):E2482-E91.

487. Lee JH, Gao ZG, Ye JP. Regulation of 11 beta-HSD1 expression during adipose tissue expansion by hypoxia through different activities of NF-kappa B and HIF-1 alpha. Am J Physiol-Endocrinol Metab. 2013;304(10):E1035-E41.

SUPPLEMENTARY MATERIAL

Supplementary Table S1) miR-147b predicted targets and pathway analysis results. DAVID functional annotation tool gene ontology pathway analysis results of hsa-miR-147b predicted targets. Combined results of Targetscan7.1, miRDB and miRTarBase (replicates removed), organised according to third tier Gene Ontology Biological Process allocations. Note: genes can feature in multiple GO terms.

Regulation of cellular component size	
BDNF	brain derived neurotrophic factor
CAPZB	capping actin protein of muscle Z-line beta subunit
CLCN6	chloride voltage-gated channel 6
DEPTOR	DEP domain containing MTOR-interacting protein
WIPF1	WAS/WASL interacting protein family member 1
Energy Derivation by oxidation of organic compounds	
NDUFA4	NDUFA4, mitochondrial complex associated
SDHD	succinate dehydrogenase complex subunit D
ALDH5A1	aldehyde dehydrogenase 5 family member A1
DYRK2	dual specificity tyrosine phosphorylation regulated kinase 2
Regulation of anatomical structure size	
CLCN6	chloride voltage-gated channel 6
BDNF	brain derived neurotrophic factor
DEPTOR	DEP domain containing MTOR-interacting protein
WIPF1	WAS/WASL interacting protein family member 1
CAPZB	capping actin protein of muscle Z-line beta subunit
Electron transport chain	
NDUFA4	NDUFA4, mitochondrial complex associated
SDHD	succinate dehydrogenase complex subunit D
ALDH5A1	aldehyde dehydrogenase 5 family member A1
Regulation of signal transduction	
SUPT16H	SPT16 homolog, facilitates chromatin remodeling subunit
FOLR1	folate receptor 1
GPR27	G protein-coupled receptor 27
BDNF	brain derived neurotrophic factor
SEC14L1	SEC14 like lipid binding 1
DEPTOR	DEP domain containing MTOR-interacting protein
NDRG4	NDRG family member 4
UBE2N	ubiquitin conjugating enzyme E2 N
KMT2D	lysine methyltransferase 2D
CAPZB	capping actin protein of muscle Z-line beta subunit
DYRK2	dual specificity tyrosine phosphorylation regulated kinase 2
SYNGAP1	synaptic Ras GTPase activating protein 1

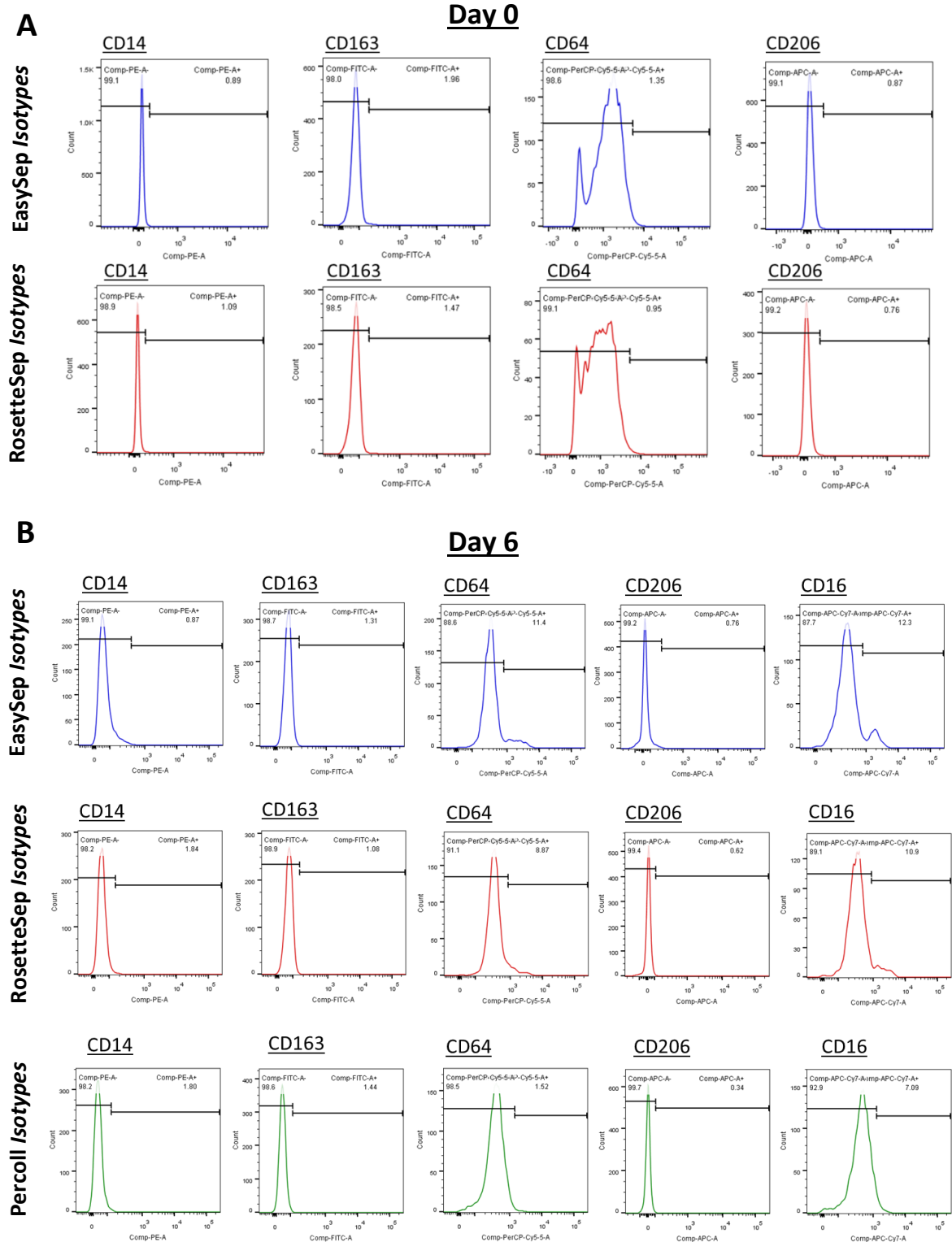**Supplementary Table S1 continues overleaf**

Table S1 continued

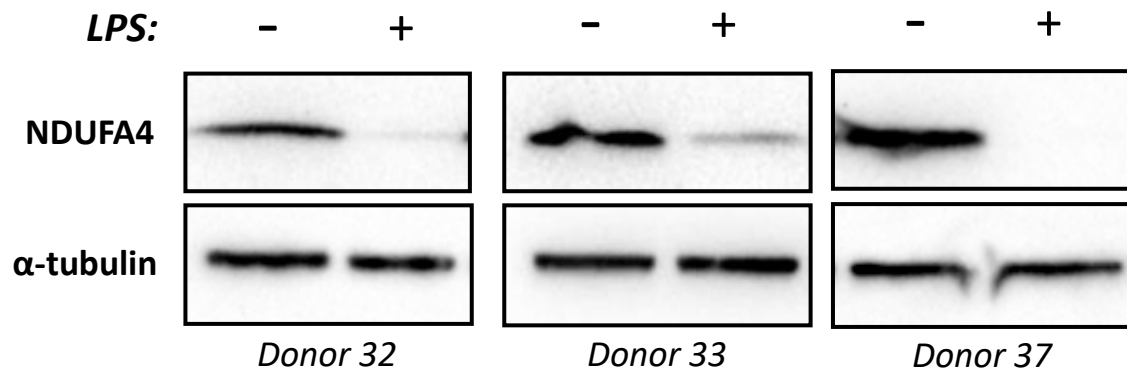|	
Phosphorus metabolic process	
PPTC7	PTC7 protein phosphatase homolog
SEPHS1	selenophosphate synthetase 1
MEF2A	myocyte enhancer factor 2A
MLLT1	MLLT1, super elongation complex subunit
NDUFA4	NDUFA4, mitochondrial complex associated
PKIA	protein kinase (cAMP-dependent, catalytic) inhibitor alpha
RAP2B	RAP2B, member of RAS oncogene family
SDHD	succinate dehydrogenase complex subunit D
DEPTOR	DEP domain containing MTOR-interacting protein
NDRG4	NDRG family member 4
ALDH5A1	aldehyde dehydrogenase 5 family member A1
DYRK2	dual specificity tyrosine phosphorylation regulated kinase 2
SYNGAP1	synaptic Ras GTPase activating protein 1
Protein complex biosynthesis	
FOLR1	folate receptor 1
KCNA3	potassium voltage-gated channel subfamily A member 3
MITF	melanogenesis associated transcription factor
MID1IP1	MID1 interacting protein 1
WIPF1	WAS/WASL interacting protein family member 1
ALDH5A1	aldehyde dehydrogenase 5 family member A1
KMT2D	lysine methyltransferase 2D
CAPZB	capping actin protein of muscle Z-line beta subunit
Generation of precursor metabolites and energy	
NDUFA4	NDUFA4, mitochondrial complex associated
SDHD	succinate dehydrogenase complex subunit D
ALDH5A1	aldehyde dehydrogenase 5 family member A1
DYRK2	dual specificity tyrosine phosphorylation regulated kinase 2
Cellular component assembly	
FOLR1	folate receptor 1
KCNA3	potassium voltage-gated channel subfamily A member 3
MEF2A	myocyte enhancer factor 2A
MITF	melanogenesis associated transcription factor
MID1IP1	MID1 interacting protein 1
RAP2B	RAP2B, member of RAS oncogene family
BDNF	brain derived neurotrophic factor
WIPF1	WAS/WASL interacting protein family member 1
ALDH5A1	aldehyde dehydrogenase 5 family member A1
KMT2D	lysine methyltransferase 2D
CAPZB	capping actin protein of muscle Z-line beta subunit

Supplementary Table S1 continues overleaf

Table S1 continued

| Cell projection organization	
FOLR1	folate receptor 1
MEF2A	myocyte enhancer factor 2A
RAP2B	RAP2B, member of RAS oncogene family
BDNF	brain derived neurotrophic factor
NDRG4	NDRG family member 4
CAPZB	capping actin protein of muscle Z-line beta subunit
SYNGAP1	synaptic Ras GTPase activating protein 1
Pattern specification process	
FOLR1	folate receptor 1
HOXA9	homeobox A9
NDRG4	NDRG family member 4
SYNGAP1	synaptic Ras GTPase activating protein 1
Regulation of cell communication	
SUPT16H	SPT16 homolog, facilitates chromatin remodeling subunit
FOLR1	folate receptor 1
GPR27	G protein-coupled receptor 27
BDNF	brain derived neurotrophic factor
SEC14L1	SEC14 like lipid binding 1
DEPTOR	DEP domain containing MTOR-interacting protein
NDRG4	NDRG family member 4
UBE2N	ubiquitin conjugating enzyme E2 N
KMT2D	lysine methyltransferase 2D
CAPZB	capping actin protein of muscle Z-line beta subunit
DYRK2	dual specificity tyrosine phosphorylation regulated kinase 2
SYNGAP1	synaptic Ras GTPase activating protein 1

Supplementary Figure S1) Isotype staining for monocyte isolation kit comparison
Related to Figure 2.3

Human monocytes were isolated using the indicated techniques. Matched isotope control antibodies for monocyte/macrophage marker antibodies (Figure 2.3). Cells stained **A)** directly after isolation (Day 0) or **B)** after 6 days of differentiation with 50ng/ml M-CSF (Day 6).

LPS: − +   − +   − +

NDUFA4

α-tubulin

Donor 32   Donor 33   Donor 37

Supplementary Figure S2) Dramatic downregulation of human NDUFA4 protein by LPS
Related to Figure 4.3
Human monocyte-derived macrophages were stimulated with LPS (10ng/ml) for 24h. Additional example Western blots demonstrating NDUFA4 downregulation by LPS.

Donor 52

Donor 54

Donor 61
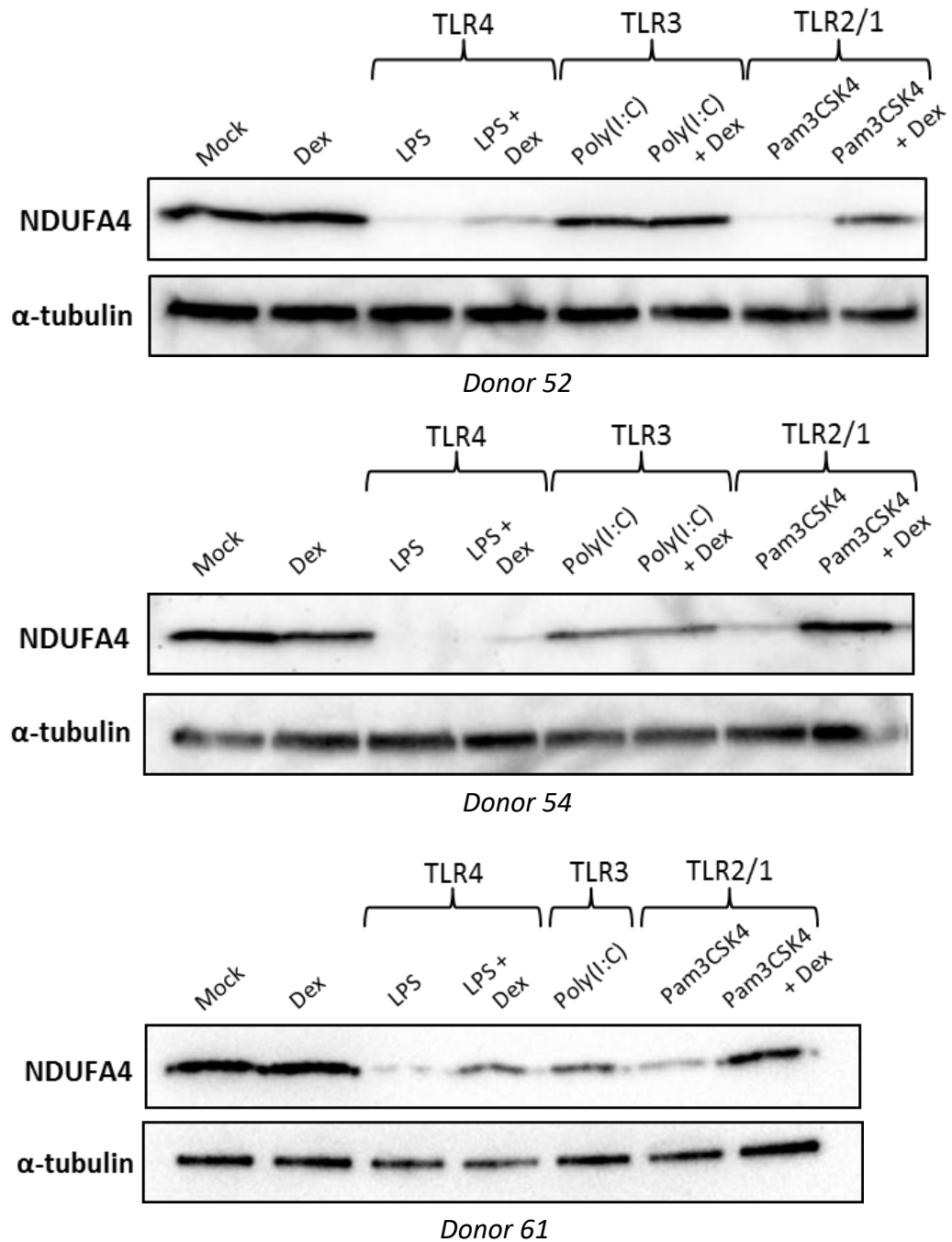
Supplementary Figure S3) Inconsistent responses of NDUFA4 protein to poly(I:C)

Related to Figure 4.6

Human monocyte-derived macrophages were stimulated with LPS (10ng/ml); Poly(I:C) (10 µg/ml); or Pam3CSK4 (Pam3C: 1µg/ml) +/- Dex (100nM) for 24h and harvested for Western blot. *Donor 52 and 54 Western blots were performed by Abbie Lane (MSci student) under my supervision.*

A Human miR-147b
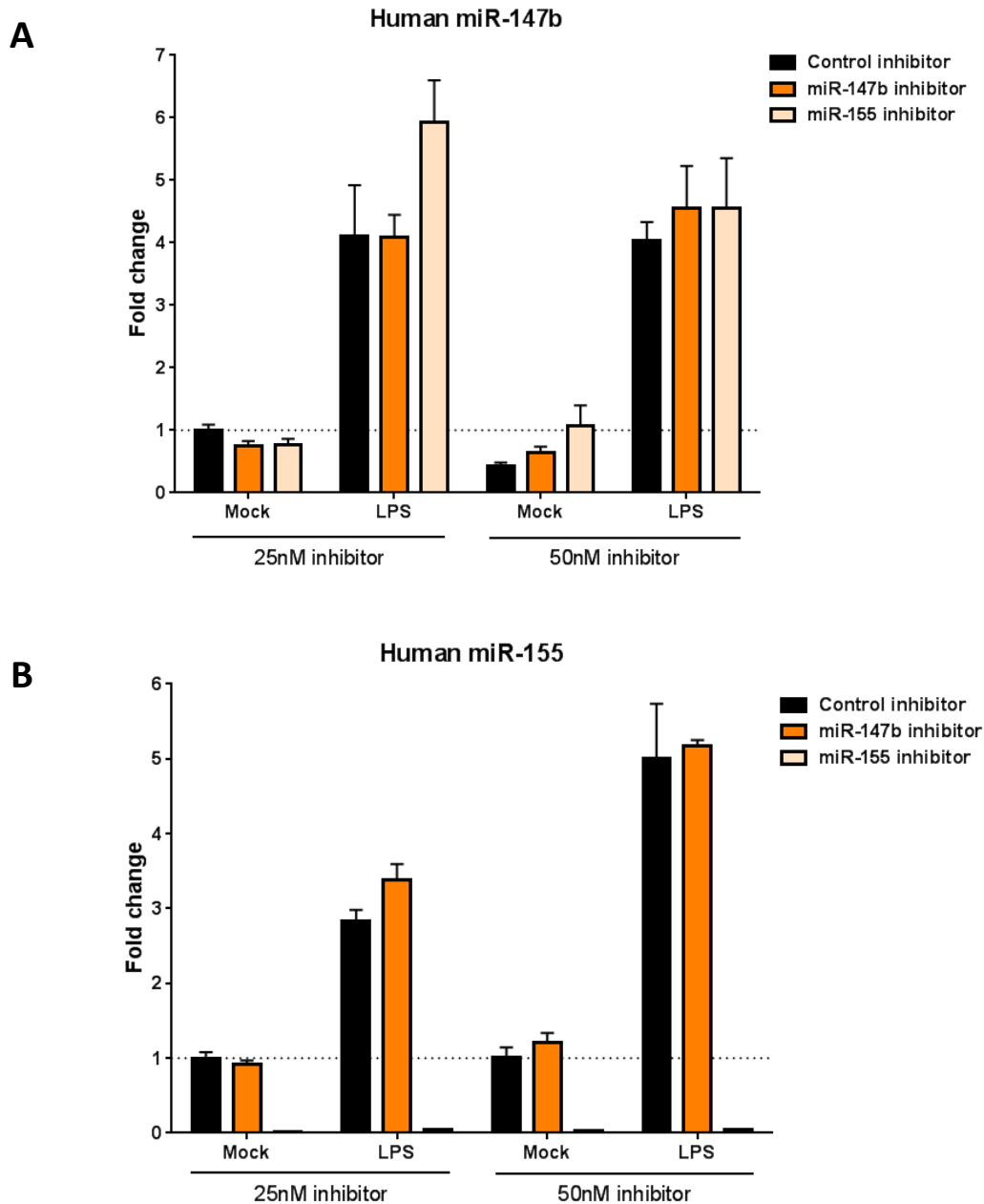
B Human miR-155

Supplementary Figure S4) Lack of function of Qiagen miScript miR-147b inhibitor

Related to Figure 4.10

Human monocyte-derived macrophages were transfected with 25nM or 50nM miScript control inhibitor or specific Hsa-miR-147b or Hsa-miR-155 antisense inhibitor using TransIT-X2 reagent. 24h post transfection cells were Mock or LPS stimulated for 12h and harvested for RNA. **A)** Hsa-miR-147b or **B)** Hsa-miR-155 were measured by RT-qPCR and expressed as fold change ($2^{-\Delta\Delta Ct}$) normalised to RNU6-2, relative to 25nM transfected Mock stimulated control; one representative experiments of n=2 (mean+SD of technical replicates).

A

B
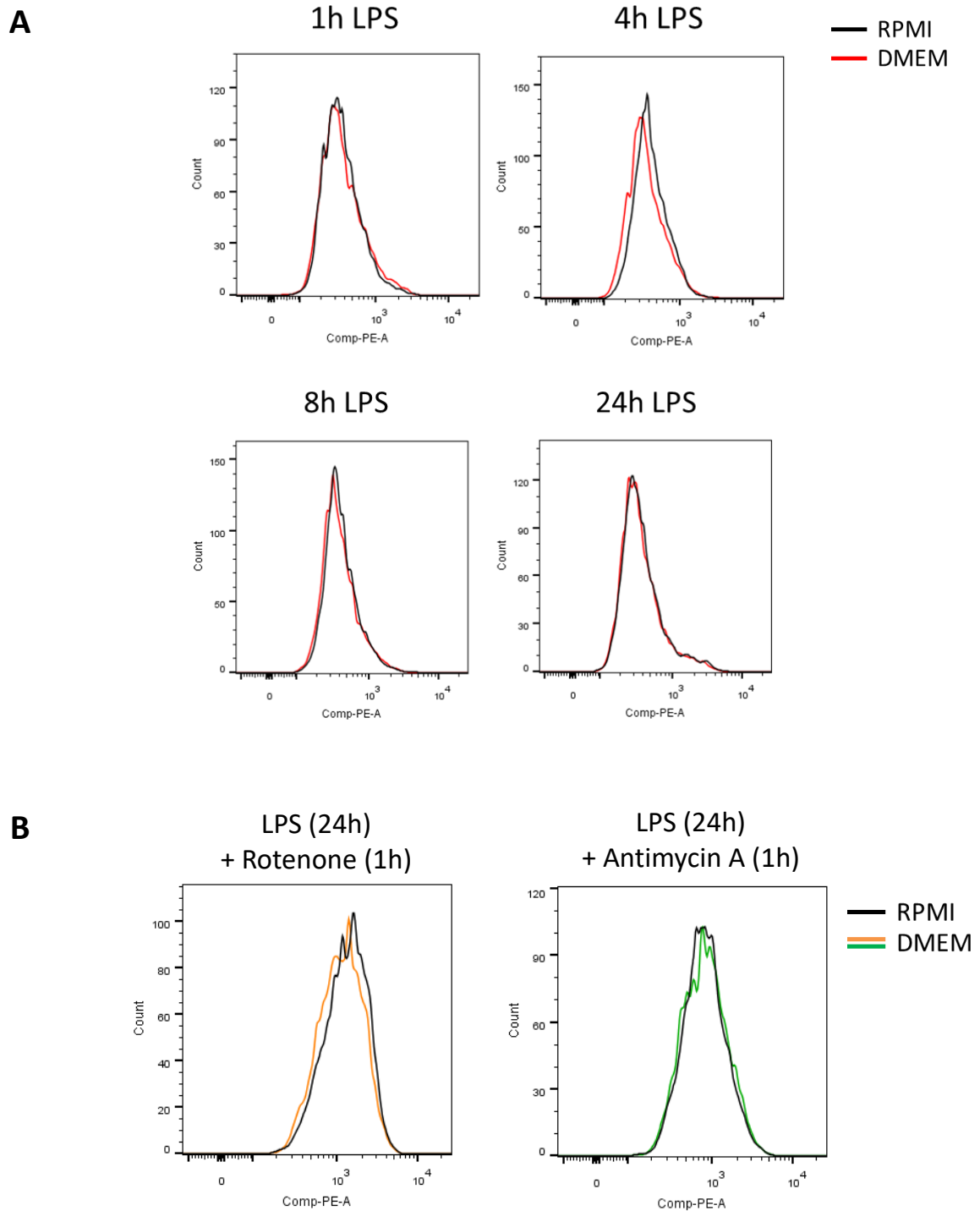
Supplementary Figure S5) mROS detection: RPMI vs DMEM

Related to Figure 5.13

A&B) Human monocyte-derived macrophages were Mock or LPS stimulated for the indicated times in either RPMI or DMEM (both + 5% HI-FCS) followed by staining with MitoSox. Doublets and dead cells were gated out; n=1.

B) Inhibitors added for last hour of LPS stimulation as positive controls for mROS staining
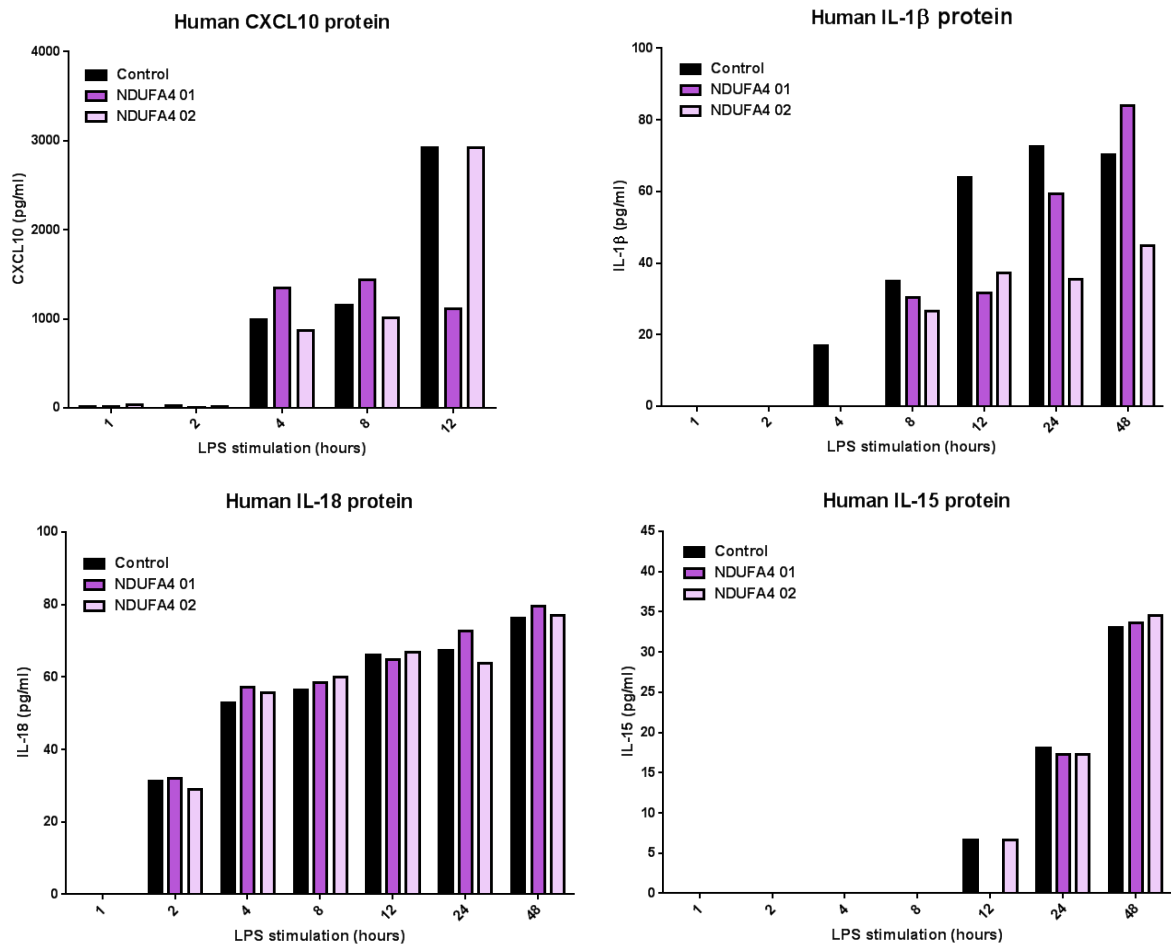
Supplementary Figure S6) Luminex analysis of cytokine expression upon NDUFA4 KD – additional cytokines

Related to Figure 6.5

Human monocyte-derived macrophages transfected with 25nM Dharmacon siGenome Control siRNA or NDUFA4 siRNAs, using TransIT-X2 transfection reagent. LPS stimulation commenced 48h post transfection. Conditioned medium was collected at the indicated times and subjected to cytokine analysis by Luminex multiplex assay; n=1 (mean of technical replicates).
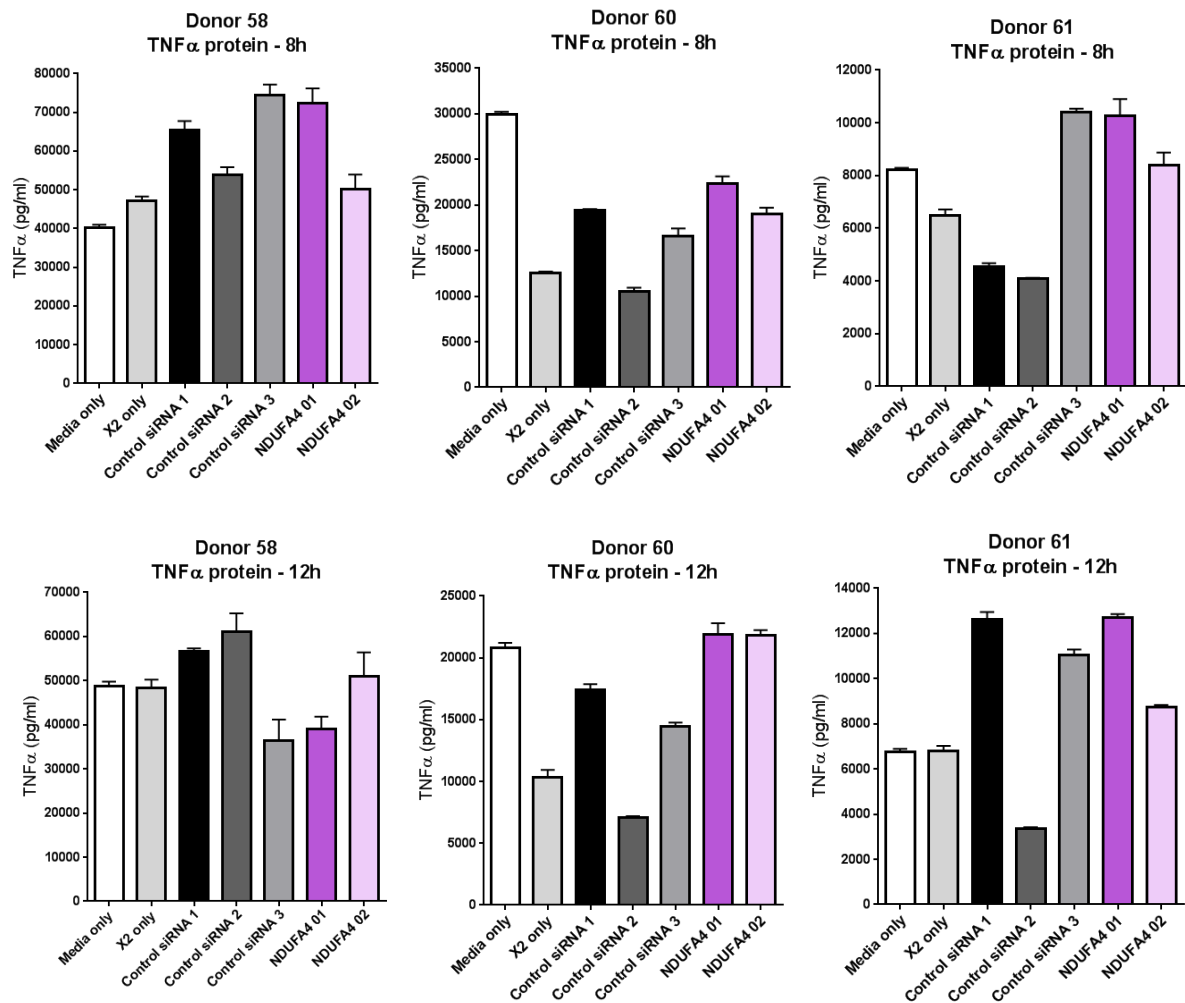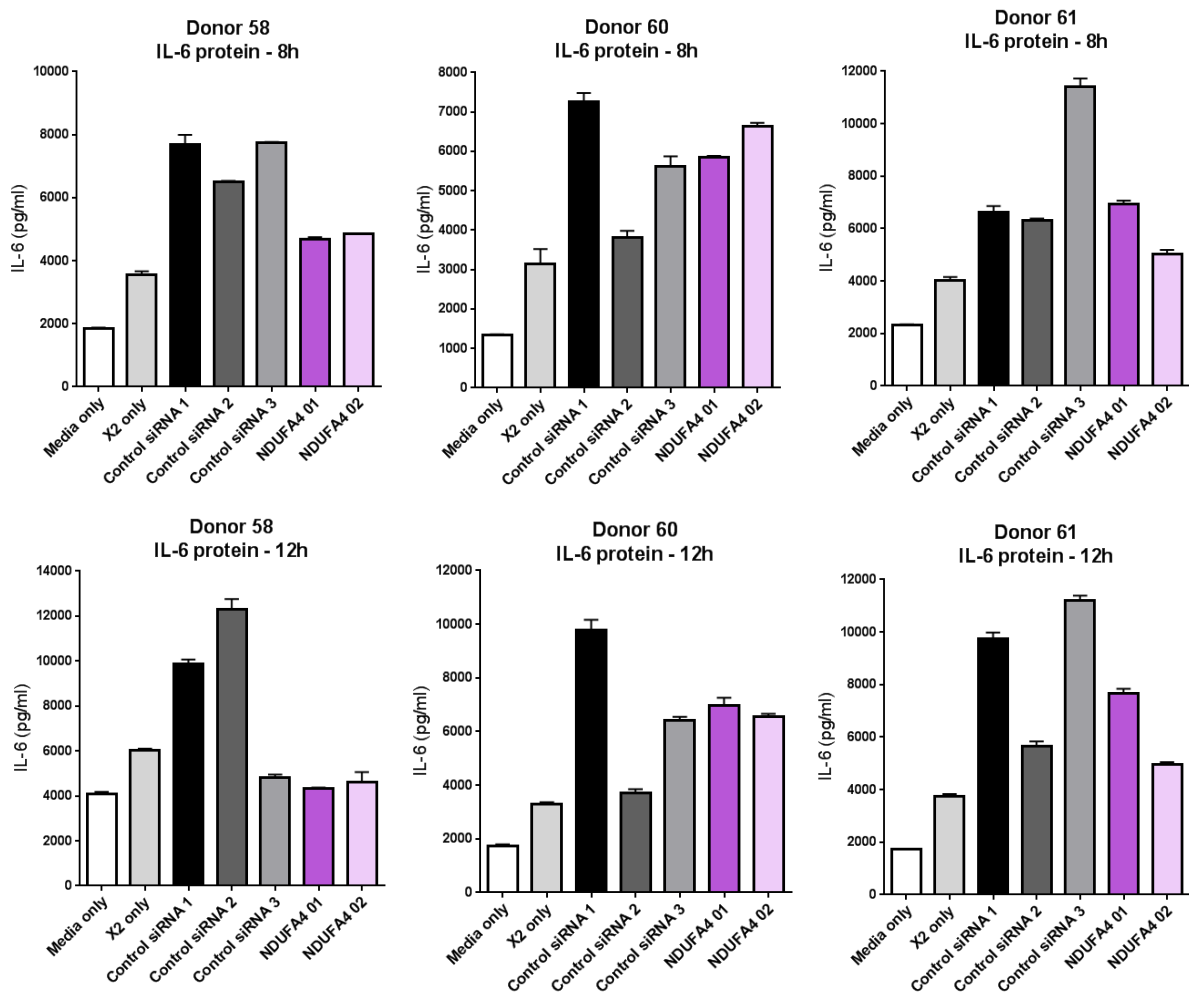
Supplementary Figure S7) TNFα expression in response to siRNA transfection – additional time points

Related to Figure 6.7

Human monocyte-derived macrophages transfected with 25nM Control or NDUFA4 siRNAs using TransIT-X2 reagent for 48h followed by LPS stimulation for the indicated time. Human TNFα protein was measured by ELISA from conditioned medium.

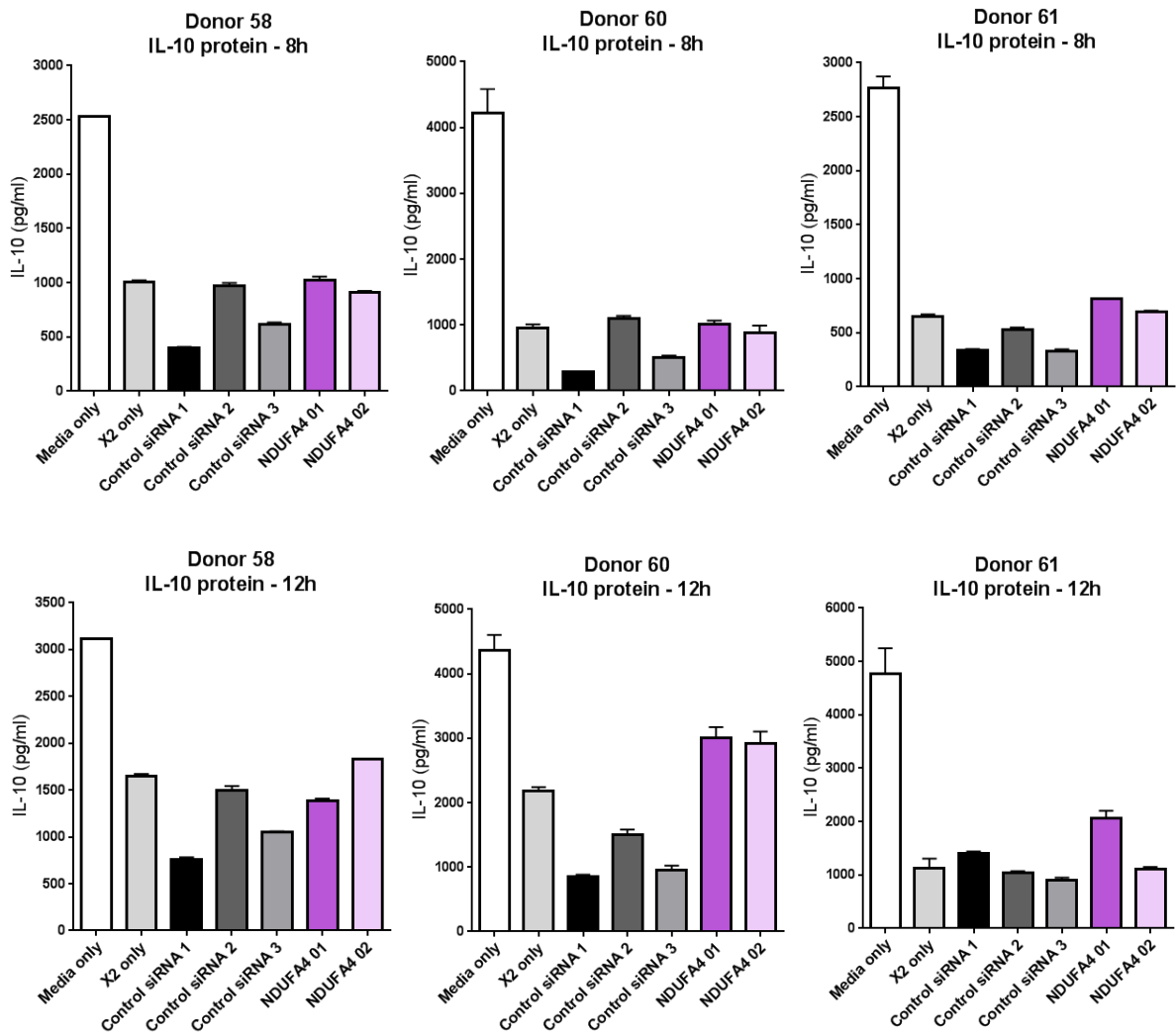n=3 donors presented separately; Data presented as mean +SD of technical replicates.

Supplementary Figure S8) IL-6 expression in response to siRNA transfection – additional time points

Related to Figure 6.8

Human monocyte-derived macrophages transfected with 25nM Control or NDUFA4 siRNAs using TransIT-X2 reagent for 48h followed by LPS stimulation for the indicated time. Human IL-6 protein was measured by ELISA from conditioned medium.

n=3 donors presented separately; Data presented as mean +SD of technical replicates.
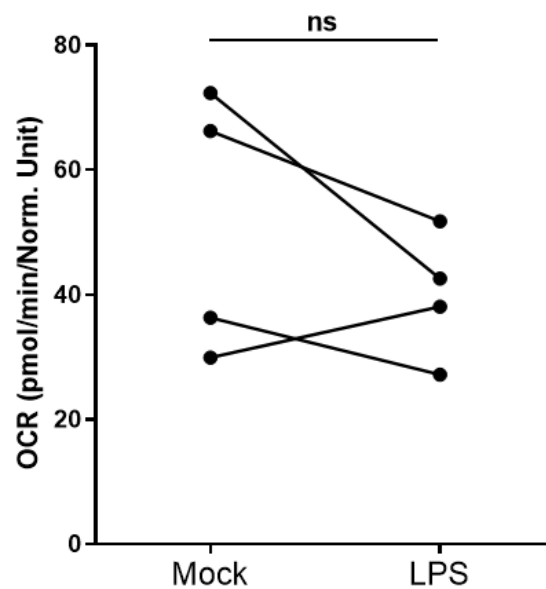
Supplementary Figure S9) IL-10 expression in response to siRNA transfection – additional
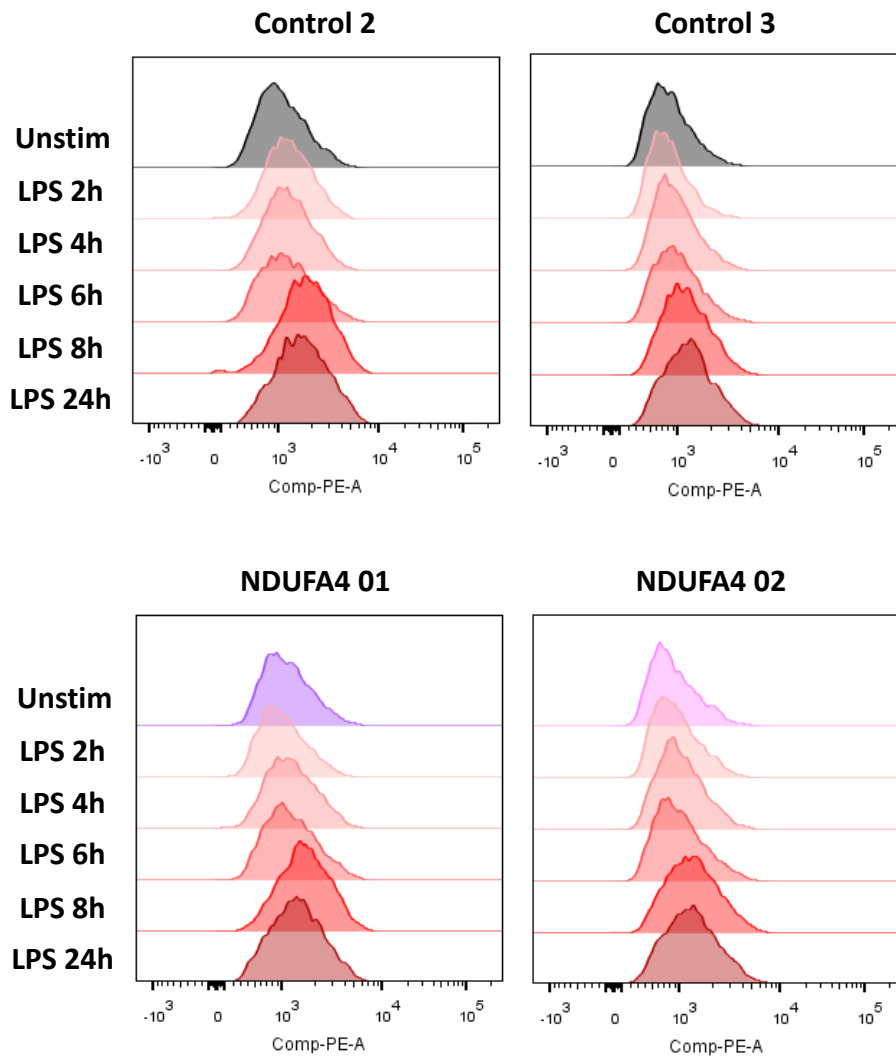time points

Related to Figure 6.9

Human monocyte-derived macrophages transfected with 25nM Control or NDUFA4 siRNAs using
TransIT-X2 reagent for 48h followed by LPS stimulation for the indicated time. Human IL-10
protein was measured by ELISA from conditioned medium.

n=3 donors presented separately; Data presented as mean +SD of technical replicates.

A

B
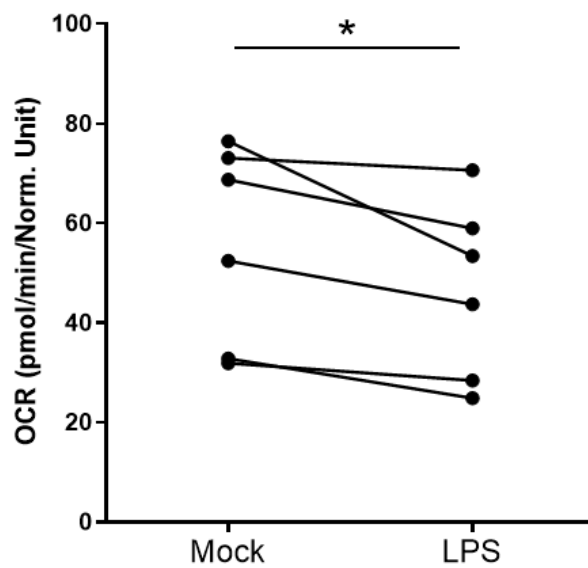
Supplementary Figure S10) Effect of LPS on ETC complex IV and complex I-mediated respiration

Related to Figures 6.11 & 6.17

Human monocyte-derived macrophages were Mock or LPS-treated for 24h. **A)** Complex IV-specific or **B)** complex I-mediated respiration was measured by Seahorse extracellular flux analysis using complex-specific fuels as described in methods. A) n=6; B) n=4. Mix of peripheral blood and blood cone-derived cells. Paired two-tailed t test.

Supplementary Figure S11) Effect of LPS on mROS staining in siRNA-transfected cells (Donor 80)

Related to Figure 6.15

Human monocyte-derived macrophages transfected with 25nM Control or NDUFA4 siRNA using TransIT-X2 reagent for 48h. LPS stimulation for the indicated times followed by staining with MitoSOX. Doublets and dead cells were gated out; n=1.